MicroRNA SIGNALING

EDITED BY: Dragos Cretoiu, Junjie Xiao and Saumya Das

PUBLISHED IN: Frontiers in Cell and Developmental Biology and Frontiers in Genetics

frontiers Research Topics

frontiers

ISSN 1664-8714
ISBN 978-2-88966-289-0
DOI 10.3389/978-2-88966-289-0

About Frontiers

Frontiers is more than just an open-access publisher of scholarly articles: it is a pioneering approach to the world of academia, radically improving the way scholarly research is managed. The grand vision of Frontiers is a world where all people have an equal opportunity to seek, share and generate knowledge. Frontiers provides immediate and permanent online open access to all its publications, but this alone is not enough to realize our grand goals.

Frontiers Journal Series

The Frontiers Journal Series is a multi-tier and interdisciplinary set of open-access, online journals, promising a paradigm shift from the current review, selection and dissemination processes in academic publishing. All Frontiers journals are driven by researchers for researchers; therefore, they constitute a service to the scholarly community. At the same time, the Frontiers Journal Series operates on a revolutionary invention, the tiered publishing system, initially addressing specific communities of scholars, and gradually climbing up to broader public understanding, thus serving the interests of the lay society, too.

Dedication to Quality

Each Frontiers article is a landmark of the highest quality, thanks to genuinely collaborative interactions between authors and review editors, who include some of the world's best academicians. Research must be certified by peers before entering a stream of knowledge that may eventually reach the public - and shape society; therefore, Frontiers only applies the most rigorous and unbiased reviews.
Frontiers revolutionizes research publishing by freely delivering the most outstanding research, evaluated with no bias from both the academic and social point of view. By applying the most advanced information technologies, Frontiers is catapulting scholarly publishing into a new generation.

What are Frontiers Research Topics?

Frontiers Research Topics are very popular trademarks of the Frontiers Journals Series: they are collections of at least ten articles, all centered on a particular subject. With their unique mix of varied contributions from Original Research to Review Articles, Frontiers Research Topics unify the most influential researchers, the latest key findings and historical advances in a hot research area! Find out more on how to host your own Frontiers Research Topic or contribute to one as an author by contacting the Frontiers Editorial Office: researchtopics@frontiersin.org

MicroRNA SIGNALING

Topic Editors:
Dragos Cretoiu, Carol Davila University of Medicine and Pharmacy, Romania
Junjie Xiao, Shanghai University, China
Saumya Das, Harvard Medical School, United States

Citation: Cretoiu, D., Xiao, J., Das, S., eds. (2020). MicroRNA Signaling. Lausanne: Frontiers Media SA. doi: 10.3389/978-2-88966-289-0

Table of Contents

frontiers in Cell and Developmental Biology

EDITORIAL
published: 30 October 2020
doi: 10.3389/fcell.2020.612425

Editorial: MicroRNA Signaling

Lijun Wang[1,2], *Carmen Elena Condrat*[3], *Saumya Das*[4]*, *Junjie Xiao*[1,2]* and *Dragos Crețoiu*[3,5]*

[1] Cardiac Regeneration and Ageing Lab, Institute of Cardiovascular Sciences, School of Life Science, Shanghai University, Shanghai, China, [2] School of Medicine, Shanghai University, Shanghai, China, [3] Alessandrescu-Rusescu National Institute of Mother and Child Health, Fetal Medicine Excellence Research Center, Bucharest, Romania, [4] Cardiovascular Division of the Massachusetts General Hospital and Harvard Medical School, Boston, MA, United States, [5] Department of Cell and Molecular Biology and Histology, Carol Davila University of Medicine and Pharmacy, Bucharest, Romania

Keywords: microRNA, signaling, disease, circulating microRNA, hypertrophy

Editorial on the Research Topic

MicroRNA Signaling

MicroRNAs (miRNAs, miRs) are a class of non-coding small RNA molecules composed of 21–25 nucleotides. Recent studies have shown that miRNAs play important regulatory roles in various physiological and pathological processes. MicroRNAs (notably present in biofluids) also have value as biomarkers of disease, and can be therapeutic targets in certain diseases. This Research Topic entitled "MicroRNA Signaling" highlights the disease-related molecular pathways where miRNAs play an important role. The 21 selected papers in this special Research Topic cover the role of miRNAs in both physiological and pathological processes, including embryonic development, cancers, cardiovascular diseases, neurological disorders. Additionally, they discuss the emerging role of circulating miRNAs as potential biomarkers with a possible role as novel mediators of intercellular communication and gene expression regulation.

Research papers from this topic were all directed toward a better understanding of miRNA regulation of signal transduction networks in various diseases and incorporated a wide range of methods. Altered expression of miRNAs and their function as a major contributor of various cellular pathways in cancers have been widely implicated. In this topic, Neagu et al. provided an outstanding overview about the miRNAs in the diagnosis and prognosis of skin cancer, as well as putative future therapeutic targets. In addition, the main miRNA detection technologies that are used to evaluate miRNAs in tissues and body fluids were also summarized, along with their advantages and limitations. Xia et al. explored the role of miR-486 in pancreatic cancer. They found that miR-486 promoted proliferation and cell cycle progression of Capan-2 pancreatic cancer cells via targeting PTEN and inhibition of miR-486 was proposed as a novel therapy for pancreatic cancer. Interestingly, Wang H. et al. investigated the mechanism of SHU00238, which is an isoxazole derivative, and has been reported to inhibit colorectal tumor growth. They found that SHU00238 promotes colorectal cancer cell apoptosis through regulating miR-4701-3p and miR-4793-3p, and provides a potential drug target and therapeutic strategy for colorectal cancer. Also, Wang X. et al. demonstrated that lncRNA LINC00319/miR-3127/RAP2A plays an important role in cell growth and invasion of bladder cancer. Thus, enhancing the expression of miR-3127 or inhibition of LINC00319 might represent a promising therapeutic strategy for bladder cancer treatment. In addition, Yusof et al. provided a comprehensive dataset of human miRNAs and (PIWI)-interacting RNAs expression derived from next-generation sequencing in papillary thyroid carcinoma. In addition, the utility of extracellular vesicles derived miR-21-5p and miR-92a-3p for hepatocellular carcinoma diagnosis was explored by Sorop et al.

Five original research papers and one review in this topic focusing on the role of miRNAs involved in regulating the cardiovascular system. Zhang et al. gave an outstanding review of the

OPEN ACCESS

Edited and reviewed by:
Ana Cuenda,
Consejo Superior de Investigaciones Científicas (CSIC), Spain

***Correspondence:**
Saumya Das
sdas@mgh.harvard.edu
Junjie Xiao
junjiexiao@live.cn
Dragos Crețoiu
dragos@cretoiu.ro

Specialty section:
This article was submitted to Signaling, a section of the journal Frontiers in Cell and Developmental Biology

Received: *30 September 2020*
Accepted: *06 October 2020*
Published: *30 October 2020*

Citation:
Wang L, Condrat CE, Das S, Xiao J and Crețoiu D (2020) Editorial: MicroRNA Signaling. Front. Cell Dev. Biol. 8:612425. doi: 10.3389/fcell.2020.612425

regulatory effects of non-coding RNAs in exercise-mediated cardiac protection, highlighting the regulation of miRNAs in adaptive cardiovascular changes after exercise and discussing future perspectives. Autophagy is required for exercise-induced beneficial adaptive changes. Qi et al. explored the mechanism of autophagy in exercise-induced physiological cardiac hypertrophy and found that miR-26b-5p, miR-204-5p, and miR-497-3p were involved in modulating physiological cardiac hypertrophy by targeting their respective autophagy genes. Interestingly, Zhu et al. reported that a circular RNA circNFIB attenuated cardiac fibrosis via sponging miR-433, and the circNFIB–miR-433 axis might represent a novel therapeutic approach for the treatment of fibrotic diseases. Cheng et al. demonstrated that inhibition of long non-coding RNA H19 protects the endothelium against high glucose-induced inflammation and oxidative stress by means of regulation of the H19/miR-29b/VEGFA signaling pathways. Tesovnik et al. explored the function of extracellular vehicles (EVs) derived human miRNAs in type 1 diabetes, describing the importance of EVs-derived miRNAs in the regulation of the immune system and treatment of type 1 diabetes. Finally, Zhou et al. profiled the circulating miRNAs in response to cardiopulmonary exercise testing and acute exercise training in healthy adults and found changes of serum circulating miRNAs miR-20a and miR-21.

MiRNAs contribution to other physiological and pathological processes was also explored in this topic. Lin et al. studied the embryo-secreted miR-10b in bovine embryos and found that miR-10b promotes embryonic cells apoptosis via HOXA1. Zhu et al. sequenced the small RNAs at the epiboly stage in MZdgcr8 mutant embryos and investigated the role of Dgcr8 in miRNA processing. The contribution of miR-216 in bovine primary muscle cells proliferation and differentiation, and the elderly plasma circulating miRNAs regulation in response to sarcopenia were examined by Yang et al. and He et al., respectively. Gao et al. studied neurogenic differentiation from amniotic epithelial cells and found that lncRNA Maternally Expressed 3 (MEG3) could act as a competing endogenous RNA of miR-128-3p that activated the Notch signaling pathway to increase neuronal differentiation. Ma et al. identified Agrin participates in regulating BoNT/A-induced nerve sprouting via miR-144-agrin-Musk signaling, and possibly be a therapeutic target for neurological disorders. Also, Han et al. explored the mechanism that contributed to the dysregulation of miR-384 in T-helper cell 17 (Th17) polarization. They found that the signal transducer and activator of transcription 3 (STAT3) activated miR-384/SOCS3 axes to regulate Th17 polarization. Pang et al. identified and analyzed the miRNA and mRNA expression profiles that were involved in agonistic behavior in Chinese Mitten Crab via a deep sequence method. They found that miRNAs and mRNAs mainly focused on the RAS, cAMP, AMPK, and energy metabolism pathways after a fight. Finally, Barbu et al. gave an outstanding overview about miRNAs that are involved in interacting with various signaling pathways during viral infections, providing insight into further investigations and potential clinical applications.

In conclusion, this Research Topic provided detailed regulatory roles and molecular mechanisms for understanding miRNAs signaling pathways in physiological and pathological processes. The number and range of papers considered within the subject of the microRNA signaling demonstrate the complexity of the topic. The papers comprising this Research Topic greatly contributed to further understanding of the regulatory signaling pathway and potential applications for the diagnosis of miRNAs.

AUTHOR CONTRIBUTIONS

LW drafted the manuscript. CC, SD, JX, and DC significantly contributed to the drafts toward the final product and critically reviewed the manuscript. All authors listed have read this editorial and approved it for publication.

FUNDING

This work was supported by the grants from National Natural Science Foundation of China (82020108002, 81722008, and 81911540486 to JX and 81800358 to LW), Innovation Program of Shanghai Municipal Education Commission (2017-01-07-00-09-E00042 to JX), the grant from Science and Technology Commission of Shanghai Municipality (18410722200 and 17010500100 to JX), National Key Research and Development Project (2018YFE0113500 to JX), the "Dawn" Program of Shanghai Education Commission (19SG34 to JX), and Natural Science Foundation of Shanghai (19ZR1474100 to LW).

Conflict of Interest: The authors declare that the research was conducted in the absence of any commercial or financial relationships that could be construed as a potential conflict of interest.

frontiers in Genetics

ORIGINAL RESEARCH
published: 14 June 2019
doi: 10.3389/fgene.2019.00541

miR-486 Promotes Capan-2 Pancreatic Cancer Cell Proliferation by Targeting Phosphatase and Tensin Homolog Deleted on Chromosome 10 (PTEN)

Lu Xia[1], Meiyi Song[1], Mengxue Sun[1], Wei Chen[2] and Changqing Yang[1]**

[1]Division of Gastroenterology and Hepatology, Digestive Disease Institute, Shanghai Tongji Hospital, Tongji University School of Medicine, Shanghai, China, [2]Emergency Department, Shanghai Tongji Hospital, Tongji University School of Medicine, Shanghai, China

OPEN ACCESS

Edited by:
Dragos Cretoiu,
Carol Davila University of Medicine and Pharmacy, Romania

Reviewed by:
Guoping Li,
Harvard Medical School, United States
Yuan Qinggong,
Hannover Medical School, Germany
Dongchao Lu,
Hannover Medical School, Germany,
in collaboration with reviewer YQ

***Correspondence:**
Wei Chen
chenwei_17@126.com
Changqing Yang
changqingyang_tj@hotmail.com

Specialty section:
This article was submitted to RNA, a section of the journal Frontiers in Genetics

Received: 13 April 2019
Accepted: 21 May 2019
Published: 14 June 2019

Citation:
Xia L, Song M, Sun M, Chen W and Yang C (2019) miR-486 Promotes Capan-2 Pancreatic Cancer Cell Proliferation by Targeting Phosphatase and Tensin Homolog Deleted on Chromosome 10 (PTEN). Front. Genet. 10:541. doi: 10.3389/fgene.2019.00541

Introduction: Pancreatic cancer is one of the most common malignant digestive system tumors. Current treatment options for pancreatic cancer cannot achieve the expected curative effect. MicroRNAs (miRNAs and miRs) participate in many biological and pathological processes. miR-486 has been reported to be involved in diverse types of malignant tumors; however, its role in pancreatic cancer remains unclear.

Material and Methods: miR-486 mimics and inhibitors were transfected into Capan-2 cells to increase or decrease the expression of miR-486. Western blot was used to detect protein expression levels. EdU proliferation assay and flow cytometry were applied to identify changes in proliferation. In combination with a PTEN overexpression plasmid, miR-486 mimics were used to determine whether PTEN upregulation abolished the proliferative effect of miR-486.

Results: Overexpression of miR-486 promoted proliferation and cell cycle progression of Capan-2 cells. Conversely, the proliferation and cell cycle of Capan-2 cells were attenuated after inhibition of miR-486. Using a combination of bioinformatics and Western blot analysis, PTEN was identified as a downstream target gene of miR-486. The effect of miR-486 on Capan-2 cell proliferation could be abolished by PTEN overexpression.

Conclusions: miR-486 promotes the proliferation of Capan-2 cells by targeting PTEN. Inhibition of miR-486 might be a novel therapy for pancreatic cancer.

Keywords: miRNAs, pancreatic cancer, PTEN, proliferation, therapy

INTRODUCTION

Pancreatic cancer is a leading cause of mortality worldwide, with characteristic insidious onset, rapid progression, and low survival rate. The mortality rate of pancreatic cancer ranks fourth among all malignant tumors in the US (Jemal et al., 2003; Siegel et al., 2017, 2018) and is predicted to rank second in Western countries by the year 2030 (Rahib et al., 2014; Kuroczycki-Saniutycz et al., 2017). Surgical resection is the only possible treatment to improve long-term survival rate of patients with pancreatic cancer at present (Ryan et al., 2014; Attiyeh et al., 2016). Thus, novel therapies are desperately needed.

MicroRNAs (miRNAs, miRs) are a class of single-stranded non-coding RNAs that play a regulatory role in different tissues/organs and in different growth stages. They participate in many biological and pathological progresses, including embryo development, cell proliferation and apoptosis, and metabolism (Lee et al., 1993; Ambros, 2004; Lewis et al., 2005; Ksiazek-Winiarek et al., 2013; Eaton et al., 2018; Wang et al., 2018). In addition, multiple miRNAs have been reported to play major roles in the development of tumors. miR-486 has been found to be involved in many malignant tumors such as gastric cancer, lung cancer, liver cancer, cervical cancer, and ovarian cancer (Hang et al., 2009; Braconi et al., 2010; Yujuan et al., 2010; Hue-Kian et al., 2011; Res, 2011; Yong et al., 2013; Parikh et al., 2014; Guo et al., 2015; Hou et al., 2016; Roh and So, 2017; Guan et al., 2018), nevertheless, its role in pancreatic cancer is poorly understood.

Here, we found that miR-486 overexpression promoted the proliferation of human pancreatic cancer cell line Capan-2, while miR-486 inhibitors attenuated proliferation. Phosphatase and tensin homolog deleted on chromosome 10 (PTEN) was identified as a target gene of miR-486 in Capan-2 cells, mediating its pro-proliferation effects. Our results suggest that inhibition of miR-486 might be a novel therapy for pancreatic cancer.

MATERIALS AND METHODS

Cell Culture

Human pancreatic cancer cell line Capan-2 was acquired from the Shanghai Cell Bank of Chinese Academy of Sciences (China). Capan-2 cell was cultured with RPMI-1640 medium (keyGEN, Jiangsu, China) containing 10% fetal bovine serum (Gibco, USA) and 1% penicillin-streptomtcin solution (Solarbio, Beijing). The cell was cultured at 37°C in the incubator containing 5% CO_2 and the morphology was observed by microscope.

miRNA Transfection

Capan-2 cells were transfected with miR-486 mimics (50 nM, RiboBio, Guangzhou, China), miR-486 inhibitors (100 nM, RiboBio, Guangzhou, China), PTEN overexpression plasmid, or the respective negative controls after 6 h of starvation using Lipo2000 (Invitrogen, Carlsbad, CA, USA). Cells were harvested at 48 h after transfection. The cloning primer sequences for PTEN were designed as follows: has-PTEN-F: CGC GGA TCC ATG TTA GAA GTG GTG ACC TCAC; has-PTEN-R: CCG GAA TTC CTA TAG ATA CTC CAG TTC CAGG.

Western Blot

Cells were lysed in RIPA buffer supplied with 1 mM PMSF (Invitrogen, Carlsbad, CA, USA) to obtain cell protein. After 30 min on ice, the supernatant was collected by centrifugation at 12,000 rpm for 15 min. Protein concentration was determined using a BCA assay kit (Takara, Japan), and equivalent amounts of protein were resolved by SDS-PAGE and transferred to PVDF membranes (Roche, USA) using a wet transfer method. Membranes were blocked with 5% (w/v) skim milk powder for 2 h and subsequently incubated with primary antibody overnight at 4°C. Primary antibodies used in this study were PTEN (ABclonal, USA, 1:1,000), and GAPDH (Bioworld, USA, 1:1,000). Membranes were next incubated with appropriate secondary antibody (Jackson, USA, 1:10,000) at 25°C for 2 h. ECL detection reagent (Tanon, Shanghai, China) and a fully automated chemiluminescence image analysis system (Tanon, Shanghai, China) were used to visualize the signals. Image J (National Institutes of Health) was used for gray value measurement and statistics.

Cell Proliferation Assay

Capan-2 cells were incubated with 50 μM 5-ethynyl-2′-deoxyuridine (EdU) for 2 h, and then fixed in 4% (v/v) paraformaldehyde for 30 min. Cells were treated with 2 mg/ml glycine solution and washed with PBS thoroughly to remove paraformaldehyde. After permeabilization, cells were incubated with Apollo dye solution (keyGEN, Jiangsu, China) for 30 min and all nuclei were counterstained with hoechst33342 (keyGEN, Jiangsu, China) for 20 min. An inverted fluorescence microscope (Leica, Germany) was used for obtain florescent images and Image J was used to calculate the ratio of EdU positive cells to total nuclei.

Analysis of Cell Cycle by Flow Cytometry

At the end of experiment, cells suspensions were prepared by trypsinizing for 1–2 min, which were subsequently mixed with absolute ethyl alcohol and fixed at −20°C overnight. The fixed cells were incubated with a 100 μg/ml propidium iodide (Sigma, USA, P4170) solution supplied with 100 μg/ml RNase A (keyGEN, Jiangsu, China). Cell distribution at different fluorescence intensities was analyzed using a Beckman flow cytometer. FlowJo 7.0 was used to calculate the percentage of cells in G1/G0, S, and G2 phase.

Real-Time Quantitative Polymerase Chain Reaction

Total RNA of cells was extracted by Total RNA Extractor (Takara, Japan). Extracted RNA was dissolved in RNase-free water and the concentration was measured using a NanoDrop spectrophotometer. To quantify the expression of miR-486 in cells, cDNA was first synthesized by cDNA synthesis kit (Bio-rad, USA). Then SYBR Green reagent (Bio-Rad, USA) and Bulge-LoopTM miRNA qPCR primers (RiboBio, Guangzhou, China) were used together to determine the expression levels of miR-486 on a Bio-Rad CFX-96 Touch Real-Time PCR Detection System. The expression level of miR-486 was normalized to U6 and quantified by the $2^{-\Delta\Delta CT}$ method. The sequences were as follow: U6 forward: 5-CTCGCTTCGG CAGCACA-3; U6 reverse: 5-AACGCTTCACGAATTTGCGT-3; miR-486 forward: 5-ACACTCCAGCTGGGTC CTGTACTGAG CTGCCC-3; miR-486 reverse: 5-CTCAACTGGTGTCG TGGA GTC GGCAATTCAGTTGAGCCCCGAG-3.

Statistical Analysis

All data were repeated for three times and presented as means ± SEM. The difference between two groups was compared by two-tailed unpaired student's t test, and a significance test of mean difference between two or more samples was conducted by one-way ANOVA followed by Bonferroni test. Differences were considered to be statistically significant when the p was <0.05.

RESULTS

miR-486 Promotes Cell Proliferation and Cell Cycle Progression in Capan-2 Cells

To investigate the role of miR-486 in Capan-2 cell proliferation, miR-486 mimics and inhibitors were used. Real time quantitative PCR confirmed that miR-486 mimics significantly increased the expression of miR-486 (**Figure 1A**), while miR-486 inhibitors decreased its expression (**Figure 1B**). As determined by EdU staining, miR-486 mimics significantly increased the number of EdU positive cells, while miR-486 inhibitors decreased the number of EdU positive cells, indicating that miR-486 mimics could promote the proliferation of Capan-2 cells and miR-486 inhibitors could block it (**Figure 2**). Moreover, flow cytometry revealed that miR-486 mimics promoted cell progression from G1 to S phase, whereas miR-486 inhibitors decreased it (**Figure 3**). Collectively, these data suggested that miR-486 promoted cell proliferation and cell cycle progression in Capan-2 cells.

PTEN Is a Target Gene of miR-486 in Capan-2 Cells

PTEN has been reported to be a target gene of miR-486 in other types of cells (Small et al., 2010; Gao et al., 2018), however, whether PTEN is a target gene of miR-486 in Capan-2 cells has not been confirmed. Capan-2 cells were transfected with miR-486 mimics and inhibitors, and Western blot was used to determine the expression of PTEN at the protein level. It was found that overexpression of miR-486 in Capan-2 decreased the expression of PTEN, while inhibition of miR-486 increased its expression, confirming that miR-486 could regulate PTEN at least at the protein level (**Figure 4; Supplementary Figures 1–4**).

Overexpression of PTEN Reverses the Pro-proliferation Effect of miR-486 in Capan-2 Cells

To determine whether PTEN influences the proliferation effects of miR-486 in Capan-2 cells, a PTEN overexpression plasmid was used to perform a functional rescue experiment in the presence of the miR-486 mimics (**Figure 5A; Supplementary Figures 5, 6**). It was found that overexpression of PTEN reduced the number of EdU positive cells. Compared with the group transfected with miR-486 mimics, the number of EdU positive cells in the group transfected with PTEN overexpression plasmid and miR-486 mimics decreased significantly, indicating that overexpression of PTEN could reduce the pro-proliferation effects of miR-486 in Capan-2 cells (**Figure 5B**). This result confirmed that up-regulation of PTEN mediates the pro-proliferation effects of miR-486 in Capan-2 cells.

DISCUSSION

As a worldwide public health threat, pancreatic cancer has a metastasis rate of 85–95%, which causes approximately 330,000 deaths annually (Siegel et al., 2015). Surgical resection is currently the most effective treatment, but local recurrence and distant metastasis tend to occur after operation and the 5-year survival rate is less than 20% (Oettle et al., 2007). Gemcitabine is the preferred chemotherapy drug for non-surgical treatment of pancreatic cancer. While chemotherapy drugs tend to prolong the survival of patients with advanced stage pancreatic cancer, such drugs have limitations due to their toxicity and adverse reactions (Thota et al., 2014). In the present study, we demonstrated that miR-486 was involved in the regulation of Capan-2 pancreatic cancer cell proliferation by targeting PTEN. Inhibition of miR-486 might be a novel therapeutic strategy for pancreatic cancer.

miR-486 locates to the region sAnk1 on chromosome 8p11, and interestingly, the abnormal changes of genes in this region are closely related to the pathogenesis of various tumors. miR-486 has been reported to inhibit the proliferation and metastasis of lung cancer, but may play a causative role in cervical and prostate cancer (Yong et al., 2013; Ye et al., 2016; Yang et al., 2017). It has been suggested that miR-486 functions as a tumor suppressor in digestive system cancer including colorectal cancer, esophageal and hepatocellular carcinoma and is highly expressed in colorectal cancer (Small et al., 2010; Mosakhani et al., 2012; Youness et al., 2016; Lang and Zhao, 2018). Tumor suppressor PTEN has been reported to be a regulatory target gene of miR-486, and the regulation axis of miR-486/PTEN has been confirmed in non-small cell lung cancer (Gao et al., 2018). MiR-486 is also considered

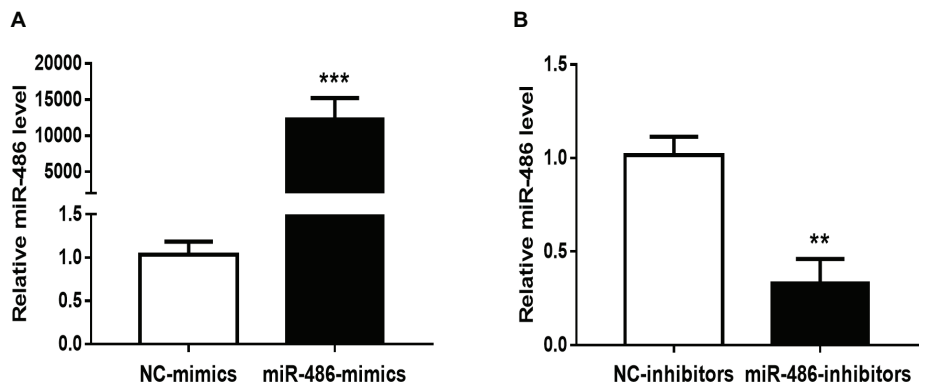

FIGURE 1 | Effects of miR-486 mimics and inhibitors on miR-486 expression in Capan-2 cells. **(A)** miR-486 mimics significantly increase the expression of miR-486 in Capan-2 cells. **(B)** miR-486 inhibitors significantly decrease the expression of miR-486 in Capan-2 cells. $^{**}p < 0.01$; $^{***}p < 0.001$. $n = 4$ per group.

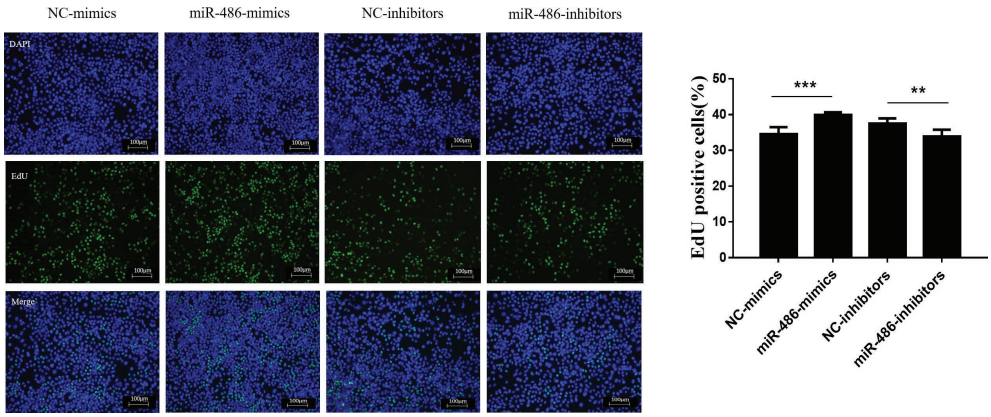

FIGURE 2 | miR-486 promotes the proliferation of Capan-2 cells. EdU proliferation assay shows that miR-486 mimics promote the proliferation of Capan-2 cells, while miR-486 inhibitors inhibit that. Scale bar: 100 μm. $^{**}p < 0.01$; $^{***}p < 0.001$; $n = 6$ per group.

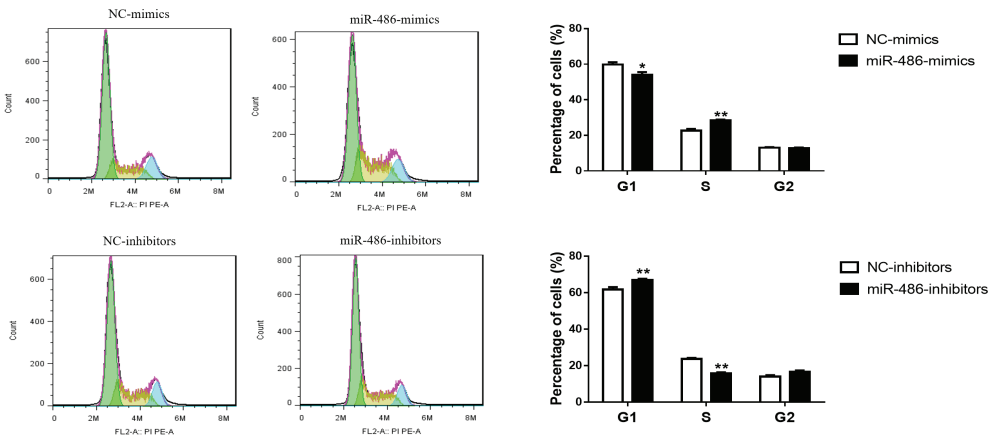

FIGURE 3 | miR-486 promotes the cell cycle progression of Capan-2 cells. PI cell cycle assay shows that miR-486 mimics promote the progression of Capan-2 cells from G1 to S phase while miR-486 inhibitors inhibit it. $^{*}p < 0.05$; $^{**}p < 0.01$; $n = 6$ per group.

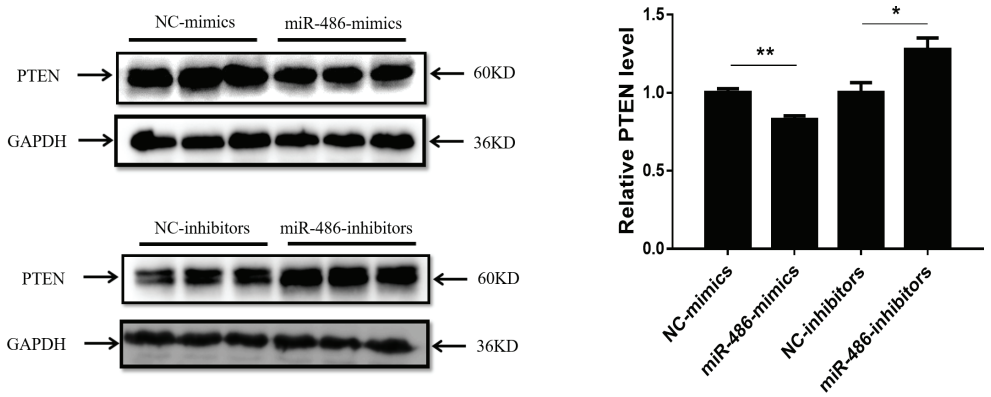

FIGURE 4 | PTEN is negatively regulated by miR-486 in Capan-2 cells. Western blot shows that miR-486 mimics downregulate the expression of PTEN in Capan-2 cells while miR-486 inhibitors upregulate it (Relative to GAPDH). $^{*}p < 0.05$; $^{**}p < 0.01$; $n = 3$ per group.

as the biomarker for the diagnosis and prognosis of multiple tumors (Li et al., 2015, 2018; Jiang et al., 2018). Recently, the expression level of circulating miR-486 was found to be increased in the patients with pancreatic cancer and exhibited good diagnostic value for this disease (Xu et al., 2016). However, the role of miR-486 in pancreatic cancer was to this point less clear. Here,

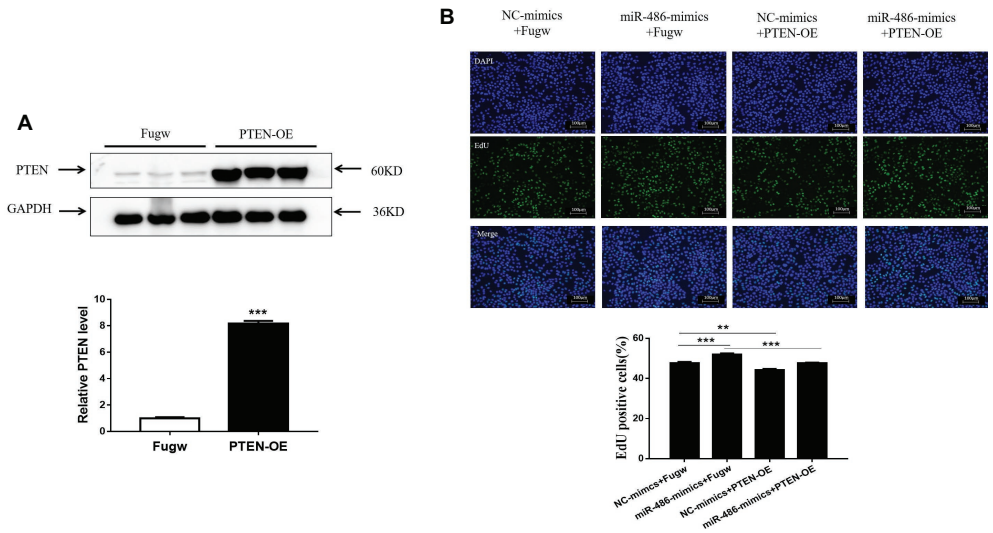

FIGURE 5 | Down-regulation of PTEN mediates the pro-proliferation effects of miR-486 in Capan-2 cells. **(A)** Western blot confirmed that PTEN overexpression (PTEN-OE) plasmid significantly increases PTEN in Capan-2 cells. **, $p < 0.01$. $n = 3$ per group. **(B)** PTEN overexpression reverse the pro-proliferation effect of miR-486 in Capan-2 cells. Scale bar: 100 μm. **$p < 0.01$; ***$p < 0.001$; $n = 6$ per group.

we found that miR-486 overexpression promoted the proliferation of human pancreatic cancer Capan-2 cell line while miR-486 inhibition attenuated such proliferation as determined by EdU staining and flow cytometry cell cycle analysis.

PTEN was the first tumor suppressor gene found to have phosphatase activity. Located on human chromosome 10q23, it can promote the dephosphorylation of the second messenger PIP3, and functions in maintaining cell structure and signal transduction. PTEN is necessary for the body to maintain normal biological processes and to exert anti-cancer effects. A variety of tumors including glioblastoma, prostate cancer, breast cancer, lung cancer, melanoma, and digestive system cancer are associated with the inactivation of PTEN (Furnari et al., 1997; Myers et al., 1997; Maehama and Dixon, 1998; Zhang et al., 2004). PTEN was reported to be down-regulated in pancreatic cancer cell lines and targets NF-kappaB and c-Myc by activating PI3K/Akt signaling pathway, thereby exerting a role in inhibiting pancreatic cancer (Asano et al., 2004; Ying et al., 2011). In addition, PTEN is involved in the regulation of angiogenesis in pancreatic cancer cells and may be related to the chemoresistance and cancer stemness (Gu et al., 2016; Wang et al., 2016). PTEN is a well-documented target of miR-486 in other types of cells (Small et al., 2010; Alexander et al., 2014; Gao et al., 2018); however, due to cell specificity, whether PTEN is a target gene of miR-486 in pancreatic cancer was unclear. In this study, we found that miR-486 could negatively regulate the expression of PTEN at least at the protein level. Importantly, overexpression of PTEN abolished the pro-proliferation effects of miR-486 mimics, suggesting that PTEN is a functional target gene of miR-486 in Capan-2 cells.

In conclusion, miR-486 promotes human pancreatic cancer cell line Capan-2 cell proliferation by targeting PTEN. Therefore, targeting miR-486/PTEN is a potential new therapeutic strategy for pancreatic cancer.

DATA AVAILABILITY

The raw data supporting the conclusions of this manuscript will be made available by the authors, without undue reservation, to any qualified researcher.

AUTHOR CONTRIBUTIONS

LX performed the experiments and wrote the manuscript. MSo and MSu performed the experiments and analyzed the data. WC revised the manuscript. CY designed the study. All authors have read and approved the final manuscript.

FUNDING

This work was supported by the grants from the National Natural Science Foundation of China (81670571 and 81370559 to CY), Joint Projects in Major Diseases funding from the Shanghai Municipal Commission of Health and Family Planning (2014ZYJB0201 to CY), Joint Projects for Novel Frontier Technology in Shanghai Municipal Hospital from the Shanghai Municipal Commission of Health and Family Planning (SHDC12014122 to CY), and funds from the Shanghai Innovation Program (12431901002 to CY).

SUPPLEMENTARY MATERIAL

The Supplementary Material for this article can be found online at: https://www.frontiersin.org/articles/10.3389/fgene.2019.00541/full#supplementary-material

REFERENCES

Alexander, M. S., Casar, J. C., Motohashi, N., Vieira, N. M., Eisenberg, I., Marshall, J. L., et al. (2014). MicroRNA-486 dependent modulation of DOCK3/PTEN/AKT signaling pathways improves muscular dystrophy-associated symptoms. *J. Clin. Investig.* 124, 2651–2667. doi: 10.1172/JCI73579

Ambros, V. (2004). The functions of animal microRNAs. *Nature* 431, 350–355. doi: 10.1038/nature02871

Asano, T., Yao, Y. J., Li, D., Abbruzzese, J. L., and Reddy, S. A. (2004). The PI 3-kinase/Akt signaling pathway is activated due to aberrant Pten expression and targets transcription factors NF-kappaB and c-Myc in pancreatic cancer cells. *Oncogene* 23, 8571–8580. doi: 10.1038/sj.onc.1207902

Attiyeh, M. A., Fernández-Del, C. C., Al, E. M., Eaton, A. A., Gönen, M., Batts, R., et al. (2016). Development and validation of a multi-institutional preoperative nomogram for predicting grade of dysplasia in intraductal papillary mucinous neoplasms (IPMNs) of the pancreas: a report from the Pancreatic Surgery Consortium. *Ann. Surg.* 1, 157–163. doi: 10.1097/SLA.0000000000002015

Braconi, C., Huang, N., and Patel, T. (2010). MicroRNA dependent regulation of DNMT-1 and tumor suppressor gene expression by Interleukin-6 in human malignant cholangiocytes. *Hepatology* 51, 881–890. doi: 10.1002/hep.23381

Eaton, M., Granata, C., Barry, J., Safdar, A., Bishop, D., and Little, J. P. (2018). Impact of a single bout of high-intensity interval exercise and short-term interval training on interleukin-6, FNDC5, and METRNL mRNA expression in human skeletal muscle. *J. Sport Health Sci.* 7, 191–196. doi: 10.1016/j.jshs.2017.01.003

Furnari, F. B., Lin, H., Huang, H. J. S., and Cavenee, W. K. (1997). Growth suppression of glioma cells by PTEN requires a functional phosphatase catalytic domain. *Proc. Natl. Acad. Sci. U.S.A.* 94, 12479–12484. doi: 10.1073/pnas.94.23.12479

Gao, Z. J., Yuan, W. D., Yuan, J. Q., Yuan, K., and Wang, Y. (2018). miR-486-5p functions as an oncogene by targeting PTEN in non-small cell lung cancer. *Pathol. Res. Pract.* 214, 700–705. doi: 10.1016/j.prp.2018.03.013

Gu, J., Wang, D., Zhang, J., Zhu, Y., Li, Y., Chen, H., et al. (2016). GFRα2 prompts cell growth and chemoresistance through down-regulating tumor suppressor gene PTEN *via* Mir-17-5p in pancreatic cancer. *Cancer Lett.* 380, 434–441. doi: 10.1016/j.canlet.2016.06.016

Guan, Z., Tan, J., Gao, W., Li, X., Yang, Y., Li, X., et al. (2018). Circular RNA hsa_circ_0016788 regulates hepatocellular carcinoma tumorigenesis through miR-486/CDK4 pathway. *J. Cell. Physiol.* 234, v500–v508. doi: 10.1002/jcp.26612

Guo, Q., Zhang, H., Zhang, L., He, Y., Weng, S., Dong, Z., et al. (2015). MicroRNA-21 regulates non-small cell lung cancer cell proliferation by affecting cell apoptosis *via* COX-19. *Int. J. Clin. Exp. Med.* 8, 8835–8841.

Hang, S., Jian-Rong, Y., Teng, X., Jun, H., Li, X., Yunfei, Y., et al. (2009). MicroRNA-101, down-regulated in hepatocellular carcinoma, promotes apoptosis and suppresses tumorigenicity. *Cancer Res.* 69, 1135–1142. doi: 10.1158/0008-5472.CAN-08-2886

Hou, L., Jian, C., Zheng, Y., and Wu, C. (2016). Critical role of miR-155/FoxO1/ROS axis in the regulation of non-small cell lung carcinomas. *Tumor Biol.* 37, 5185–5192. doi: 10.1007/s13277-015-4335-9

Hue-Kian, O., Angie Lay-Keng, T., Kakoli, D., Chia-Huey, O., Nian-Tao, D., Iain Beehuat, T., et al. (2011). Genomic loss of miR-486 regulates tumor progression and the OLFM4 antiapoptotic factor in gastric cancer. *Clin. Cancer Res.* 17, 2657–2667. doi: 10.1158/1078-0432.CCR-10-3152

Jemal, A., Siegel, R., Ward, E., Murray, T., Xu, J., and Thun, M. J. (2003). Cancer statistics, 2009. *CA Cancer J. Clin.* 53, 5–26. doi: 10.3322/canjclin.53.1.5

Jiang, M., Li, X., Quan, X., Yang, X., Zheng, C., Hao, X., et al. (2018). MiR-486 as an effective biomarker in cancer diagnosis and prognosis: a systematic review and meta-analysis. *Oncotarget* 9, 13948–13958. doi: 10.18632/oncotarget.24189

Ksiazek-Winiarek, D. J., Kacperska, M. J., and Glabinski, A. (2013). MicroRNAs as novel regulators of neuroinflammation. *Mediat. Inflamm.* 2013:172351. doi: 10.1155/2013/172351

Kuroczycki-Saniutycz, S., Grzeszczuk, A., Zwierz, Z. W., Kołodziejczyk, P., Szczesiul, J., Zalewska-Szajda, B., et al. (2017). Prevention of pancreatic cancer. *Contemp. Oncol.* 21, 30–34. doi: 10.5114/wo.2016.63043

Lang, B. P., and Zhao, S. (2018). miR-486 functions as a tumor suppressor in esophageal cancer by targeting CDK4/BCAS2. *Oncol. Rep.* 39, 71–80. doi: 10.3892/or.2017.6064

Lee, R. C., Feinbaum, R. L., and Ambros, V. (1993). The C. elegans heterochronic gene lin-4 encodes small RNAs with antisense complementarity to lin-14. *Cell* 75, 843–854. doi: 10.1016/0092-8674(93)90529-Y

Lewis, B. P., Burge, C. B., and Bartel, D. P. (2005). Conserved seed pairing, often flanked by adenosines, indicates that thousands of human genes are microRNA targets. *Cell* 120, 15–20. doi: 10.1016/j.cell.2004.12.035

Li, W., Wang, Y., Zhang, Q., Tang, L., Liu, X., Dai, Y., et al. (2015). MicroRNA-486 as a biomarker for early diagnosis and recurrence of non-small cell lung cancer. *PLoS One* 11:e0148589. doi: 10.1371/journal.pone.0148589

Li, C., Zheng, X., Li, W., Bai, F., Lyu, J., and Meng, Q. H. (2018). Serum miR-486-5p as a diagnostic marker in cervical cancer: with investigation of potential mechanisms. *BMC Cancer* 18:61. doi: 10.1186/s12885-017-3753-z

Maehama, T., and Dixon, J. E. (1998). The tumor suppressor, PTEN/MMAC1, dephosphorylates the lipid second messenger, phosphatidylinositol 3,4,5-trisphosphate. *J. Biol. Chem.* 273, 13375–13378. doi: 10.1074/jbc.273.22.13375

Mosakhani, N., Sarhadi, V. K., Borze, I., Karjalainen-Lindsberg, M. L., Sundstrom, J., Ristamaki, R., et al. (2012). MicroRNA profiling differentiates colorectal cancer according to KRAS status. *Genes Chromosom. Cancer* 51, 1–9. doi: 10.1002/gcc.20925

Myers, M. P., Stolarov, J. P., Eng, C., Li, J., Wang, S. I., Wigler, M. H., et al. (1997). P-TEN, the tumor suppressor from human chromosome 10q23, is a dual-specificity phosphatase. *Proc. Natl. Acad. Sci. U.S.A.* 94, 9052–9057. doi: 10.1073/pnas.94.17.9052

Oettle, H., Post, S., Neuhaus, P., Gellert, K., Langrehr, J., Ridwelski, K., et al. (2007). Adjuvant chemotherapy with gemcitabine vs observation in patients undergoing curative-intent resection of pancreatic cancer - A randomized controlled trial. *JAMA* 297, 267–277. doi: 10.1001/jama.297.3.267

Parikh, A., Lee, C., Joseph, P., Marchini, S., Baccarini, A., Kolev, V., et al. (2014). microRNA-181a has a critical role in ovarian cancer progression through the regulation of the epithelial–mesenchymal transition. *Nat. Commun.* 5, 149–168. doi: 10.1038/ncomms3977

Rahib, L., Smith, B. D., Aizenberg, R., Rosenzweig, A. B., Fleshman, J. M., and Matrisian, L. M. (2014). Projecting cancer incidence and deaths to 2030: the unexpected burden of thyroid, liver, and pancreas cancers in the United States. *Cancer Res.* 74, 2913–2921. doi: 10.1158/0008-5472.CAN-14-0155

Res, C. (2011). Correction: serum microRNA profiles serve as novel biomarkers for HBV infection and diagnosis of HBV-positive hepatocarcinoma. *Cancer Res.* 71, 9798–9807. doi: 10.1158/0008-5472

Roh, H. T., and So, W. Y. (2017). The effects of aerobic exercise training on oxidant-antioxidant balance, neurotrophic factor levels, and blood-brain barrier function in obese and nonobese men. *J. Sport Health Sci.* 6, 447–453. doi: 10.1016/j.jshs.2016.07.006

Ryan, D. P., Hong, T. S., and Bardeesy, N. (2014). Pancreatic adenocarcinoma. *N. Engl. J. Med.* 371, 1039–1049. doi: 10.1056/NEJMra1404198

Siegel, R. L., Miller, K. D., and Dvm, A. J. (2017). Cancer statistics, 2017. *CA Cancer J.Clin.* 67, 7–30. doi: 10.3322/caac.21387

Siegel, R. L., Miller, K. D., and Jemal, A. (2015). Cancer statistics, 2015. *CA Cancer J. Clin.* 65, 5–29. doi: 10.3322/caac.21254

Siegel, R. L., Miller, K. D., and Jemal, A. (2018). Cancer statistics, 2018. *CA Cancer J. Clin.* 60, 277–300. doi: 10.3322/caac.21442

Small, E. M., O'Rourke, J. R., Moresi, V., Sutherland, L. B., McAnally, J., Gerard, R. D., et al. (2010). Regulation of PI3-kinase/Akt signaling by muscle-enriched microRNA-486. *Proc. Natl. Acad. Sci. U.S.A.* 107, 4218–4223. doi: 10.1073/pnas.1000300107

Thota, R., Pauff, J. M., and Berlin, J. D. (2014). Treatment of metastatic pancreatic adenocarcinoma: a review. *Oncology* 28, 70–74. doi: 10.3892/ol.2013.1655

Wang, L., Lv, Y., Li, G., and Xiao, J. (2018). MicroRNAs in heart and circulation during physical exercise. *J. Sport Health Sci.* 7, 433–441. doi: 10.1016/j.jshs.2018.09.008

Wang, M. C., Min, J., Tao, W., Li, J., Jie, C., Hui, G., et al. (2016). Polycomb complex protein BMI-1 promotes invasion and metastasis of pancreatic cancer stem cells by activating PI3K/AKT signaling, anex vivo,in vitro, andin vivostudy. *Oncotarget* 7, 9586–9599. doi: 10.18632/oncotarget.7078

Xu, J. W., Cao, Z., Liu, W. J., You, L., Zhou, L., Wang, C. Y., et al. (2016). Plasma miRNAs effectively distinguish patients with pancreatic cancer from controls: a multicenter study. *Ann. Surg.* 263, 1173–1179. doi: 10.1097/SLA.0000000000001345

Yang, Y., Ji, C. W., Guo, S. H., Su, X., Zhao, X. Z., Zhang, S. W., et al. (2017). The miR-486-5p plays a causative role in prostate cancer through negative regulation of multiple tumor suppressor pathways. *Oncotarget* 8, 72835–72846. doi: 10.18632/oncotarget.20427

Ye, H., Yu, X., Xia, J., Tang, X., Tang, L., and Chen, F. (2016). MiR-486-3p targeting ECM1 represses cell proliferation and metastasis in cervical cancer. *Biomed. Pharmacother.* 80, 109–114. doi: 10.1016/j.biopha.2016.02.019

Ying, H., Elpek, K. G., Vinjamoori, A., Zimmerman, S. M., Chu, G. C., Yan, H., et al. (2011). PTEN is a major tumor suppressor in pancreatic ductal adenocarcinoma and regulates an NF-κB–cytokine network. *Cancer Discov.* 1, 158–169. doi: 10.1158/2159-8290.CD-11-0031

Yong, P., Yuntao, D., Charles, H., Xiaojuan, Y., Kassis, E. S., Lunxu, L., et al. (2013). Insulin growth factor signaling is regulated by microRNA-486, an underexpressed microRNA in lung cancer. *Proc. Natl. Acad. Sci. U.S.A.* 110, 15043–15048. doi: 10.1073/pnas.1307107110

Youness, R. A., El-Tayebi, H. M., Assal, R. A., Hosny, K., Esmat, G., and Abdelaziz, A. I. (2016). MicroRNA-486-5p enhances hepatocellular carcinoma tumor suppression through repression of IGF-1R and its downstream mTOR, STAT3 and c-Myc. *Oncol. Lett.* 12, 2567–2573. doi: 10.3892/ol.2016.4914

Yujuan, X., Jian-Hong, F., Jing-Ping, Y., Jine, Y., Ying, Z., Wei-Hua, J., et al. (2010). Effects of microRNA-29 on apoptosis, tumorigenicity, and prognosis of hepatocellular carcinoma. *Hepatology* 51, 836–845. doi: 10.1002/hep.23380

Zhang, L., Yu, Q., He, J., and Zha, X. (2004). Study of the PTEN gene expression and FAK phosphorylation in human hepatocarcinoma tissues and cell lines. *Mol. Cell. Biochem.* 262, 25–33. doi: 10.1023/B:MCBI.0000038212.78008.7f

Conflict of Interest Statement: The authors declare that the research was conducted in the absence of any commercial or financial relationships that could be construed as a potential conflict of interest.

frontiers in Genetics

ORIGINAL RESEARCH
published: 20 June 2019
doi: 10.3389/fgene.2019.00564

Upregulation of Circular RNA CircNFIB Attenuates Cardiac Fibrosis by Sponging miR-433

Yujiao Zhu[1†], Wen Pan[1†], Tingting Yang[1], Xiangmin Meng[1], Zheyi Jiang[1], Lichan Tao[2] and Lijun Wang[1*]*

[1] Cardiac Regeneration and Ageing Lab, Institute of Cardiovascular Sciences, School of Life Sciences, Shanghai University, Shanghai, China, [2] Department of Cardiology, The Third Affiliated Hospital of Soochow University, Changzhou, China

OPEN ACCESS

Edited by:
Dragos Cretoiu, Carol Davila University of Medicine and Pharmacy, Romania

Reviewed by:
Ke Xiao, Hannover Medical School, Germany
Chen Liu, First Affiliated Hospital of Sun Yat-sen University, China

***Correspondence:**
Lichan Tao
sherry0019@126.com
Lijun Wang
lijunwang@shu.edu.cn

† These authors have contributed equally to this work

Specialty section:
This article was submitted to RNA, a section of the journal Frontiers in Genetics

Received: *18 April 2019*
Accepted: *29 May 2019*
Published: *20 June 2019*

Citation:
Zhu Y, Pan W, Yang T, Meng X, Jiang Z, Tao L and Wang L (2019) Upregulation of Circular RNA CircNFIB Attenuates Cardiac Fibrosis by Sponging miR-433. Front. Genet. 10:564. doi: 10.3389/fgene.2019.00564

Cardiac fibrosis is the pathological consequence of fibroblast proliferation and fibroblast-to-myofibroblast transition. As a new class of endogenous non-coding RNAs, circular RNAs (circRNAs) have been identified in many cardiovascular diseases including fibrosis, generally acting as microRNA (miRNA) sponges. Here, we report that the expression of circRNA–circNFIB was decreased in mice post-myocardial infarction heart samples, as well as in primary adult cardiac fibroblasts treated with TGF-β. Forced expression of circNFIB decreased cell proliferation in both NIH/3T3 cells and primary adult fibroblasts as evidenced by EdU incorporation. Conversely, inhibition of circNFIB promoted adult fibroblast proliferation. Furthermore, circNFIB was identified as a miR-433 endogenous sponge. Overexpression of circNFIB could attenuate pro-proliferative effects induced by the miR-433 mimic while inhibition of circNFIB exhibited opposite results. Finally, upregulation of circNFIB also reversed the expression levels of target genes and downstream signaling pathways of miR-433. In conclusion, circNFIB is critical for protection against cardiac fibrosis. The circNFIB–miR-433 axis may represent a novel therapeutic approach for treatment of fibrotic diseases.

Keywords: cardiac fibrosis, circNFIB, miR-433, primary adult cardiac fibroblasts, transforming growth factor-β

INTRODUCTION

Cardiac fibrosis, defined as the imbalance of extracellular matrix (ECM) production and degradation, which contributes to accumulation of connective tissue proteins in the interstitial and perivascular tissues, plays a crucial role in the development and evolution of heart failure (Weber et al., 2013). Fibrosis is a common pathological feature of most adverse ventricular remodeling, such as myocardial infarction (MI), diabetic cardiomyopathy, hypertrophic, and dilated cardiomyopathy (DCM) (Gyongyosi et al., 2017). It normally includes three overlapping phases: proliferation, granulation, and maturation. Cardiac fibroblasts are the predominant cells involved in each of these phases (Lajiness and Conway, 2014). Under pathological conditions, increased mechanical stress and release of cytokines and growth factors dynamically modulate fibroblast proliferation and *trans*-differentiation into highly proliferative transformed fibroblasts, termed myofibroblasts. The transformation involves subcellular changes such as increased expression of α-smooth muscle actin

(α-SMA) and secretion of extracellular procollagen chains into collagen type I and type III fibrils (Li et al., 2014; Watson et al., 2014; Gyongyosi et al., 2017). The accumulation of excessive diffused collagen results in disruption of myocardial architecture, myofibrils disarray, and mechanical, electrical, and vasomotor dysfunction (Segura et al., 2014).

Clinical studies have shown that cardiac fibrosis is closely related with higher long-term mortality in patients with cardiac diseases, particularly for those with heart failure (Besler et al., 2017; Bacmeister et al., 2019). Thus, detecting, preventing, and treating myocardial fibrosis have critical significance in the strategies of heart failure therapy. Based on microRNA (miRNA) array, we have previously reported different expression of miRNAs during MI remodeling. In particular, miR-433 was highly conserved and was not only significantly increased in MI remodeling samples but also upregulated in a rodent model of doxorubicin-induced cardiomyopathy and human DCM. Furthermore, upregulation of miR-433 increased proliferation and *trans*-differentiation of cardiac fibroblasts into myofibroblasts, whereas knockdown of miR-433 suppressed these responses depending on the stimulation of transforming growth factor-β (TGF-β). More importantly, treatment with miR-433 antagomir or adeno-associated virus 9 (AAV9)-mediated miR-433 sponge reversed cardiac dysfunction and fibrosis induced by MI remodeling (Tao et al., 2016). Thus, inhibition of miR-433 is regarded as a novel strategy for the treatment of cardiac fibrosis.

Circular RNAs (circRNAs) are a new class of endogenous non-coding RNAs with single-stranded, covalently closed structures that are produced by back splicing (Hentze and Preiss, 2013; Chen and Yang, 2015). Lacking 5′- to 3′-polarity and polyadenylated tails, circRNAs are conserved and stable, and numerous circRNAs seem to be specifically expressed in a given cell type or developmental phase (Jeck et al., 2013; Memczak et al., 2013). Natural endogenous circRNAs can contain conserved miRNA target sites, thus functioning as efficient miRNA sponges to play important roles in many physiological and pathological processes (Wang et al., 2016; Hall et al., 2018). Therefore, studies on circRNAs have provided promising new insights into miRNA regulation.

Our previous study showed that miR-433 inhibition could improve post-MI cardiac function and fibrosis. In the current study, we report that circRNA circNFIB (circBase: mmu_circ_0011794) could function as a miR-433 endogenous sponge to regulate cardiac fibrosis. We firstly generated circNFIB overexpression construct and designed siRNA of circNFIB, identifying that knockdown of circNFIB increased proliferation of primary adult cardiac fibroblasts, whereas overexpression of circNFIB reversed cell proliferation in both NIH/3T3 cell lines and adult cardiac fibroblasts upon TGF-β stimulation. Luciferase assay and functional rescue experiments further confirmed that circNFIB regulated cardiac fibrosis by directly targeting miR-433. Collectively, our findings indicate that circNFIB could act as an endogenous miR-433 sponge to inhibit fibroblast proliferation and therefore might be regarded as a potential therapy for the treatment of cardiac fibrosis.

MATERIALS AND METHODS

Construction of circRNA

A double-stranded DNA PCR product was amplified and then cloned into a commercially available circRNA expression vector pLO-ciR vector (Guangzhou Geneseed Biotech Co., China). Plasmid DNA was extracted and subsequently sequenced. To verify the circNFIB overexpression vector (circNFIB OE), we next designed a divergent primer that specifically amplified the back-spliced forms of circNFIB, and the cross-junction fragments were verified by Sanger sequence. After confirming the results of sequence, the circNFIB OE was successfully generated. The empty vector Plo-ciR was used as negative control (NC circNFIB).

Quantitative Real-Time Polymerase Chain Reactions

Total RNAs were extracted from heart samples and cardiac fibroblasts by using RNAiso Plus (Takara) according to the manuscript's instructions. Total RNAs (800 ng, 20 μl system) were reverse transcribed using a cDNA synthesis kit (Bio-Rad, Hercules, CA, United States). Then, quantification of circRNA and mRNA was performed using SYBR Premix Ex TaqTM (Takara) and the Roche Real-Time PCR Detection System (Roche). 18S RNA was used as an internal control for gene expressions. For quantitative miRNA analysis, the Bulge-Loop miRNA qPCR primer kit (RiboBio, Guangzhou, China) was used to determine the expression levels of miRNA, and the levels of small nuclear U6 were used to normalize the miRNA expression level. The primer sequences of circNFIB were as follows—forward: TGAACGAGATCAAGCACCCAT; reverse: CTGCTCGGTGGAGAAGACAG. For 18S: forward: TCAAGAACGAAAGTCGGAGG; reverse: GACATCTAAGGGCATCAC.

Isolation of Mice Cardiac Fibroblasts

Cardiac fibroblasts were isolated for each round of experiments from 8- to 10-week male adult C57BL/6N mice by trypsin-collagenase-based digestion and pooled before pre-plating and culturing. Briefly, heart samples were explanted and washed in ice-cold Hanks medium. After dicing into small pieces and further washing in ice-cold Hanks medium for removal of plasma contaminants, the cardiac pieces were pre-digested for 10 min at 37°C in an enzyme solution (60% trypsin and 40% collagenase dissolved in Hanks medium). After replacement of the enzyme solution, the cardiac pieces were incubated at 37°C for 7 min for 6–7 cycles. Fibroblast-containing supernatants were diluted with HS, centrifuged at 1,000 rpm for 5 min, and pooled together in culture medium [DMEM 4.5 g/l glucose, 10% fetal bovine serum (FBS), 100 U/ml penicillin, and 100 μg/ml streptomycin] in a 5% CO_2 incubator. All the pooled supernatants were filtered through a 100-μm cell strainer and pre-plated at 37°C in a humidified atmosphere of 5% CO_2 for 48 h. Cells at passage 3 were used in all experiments shown.

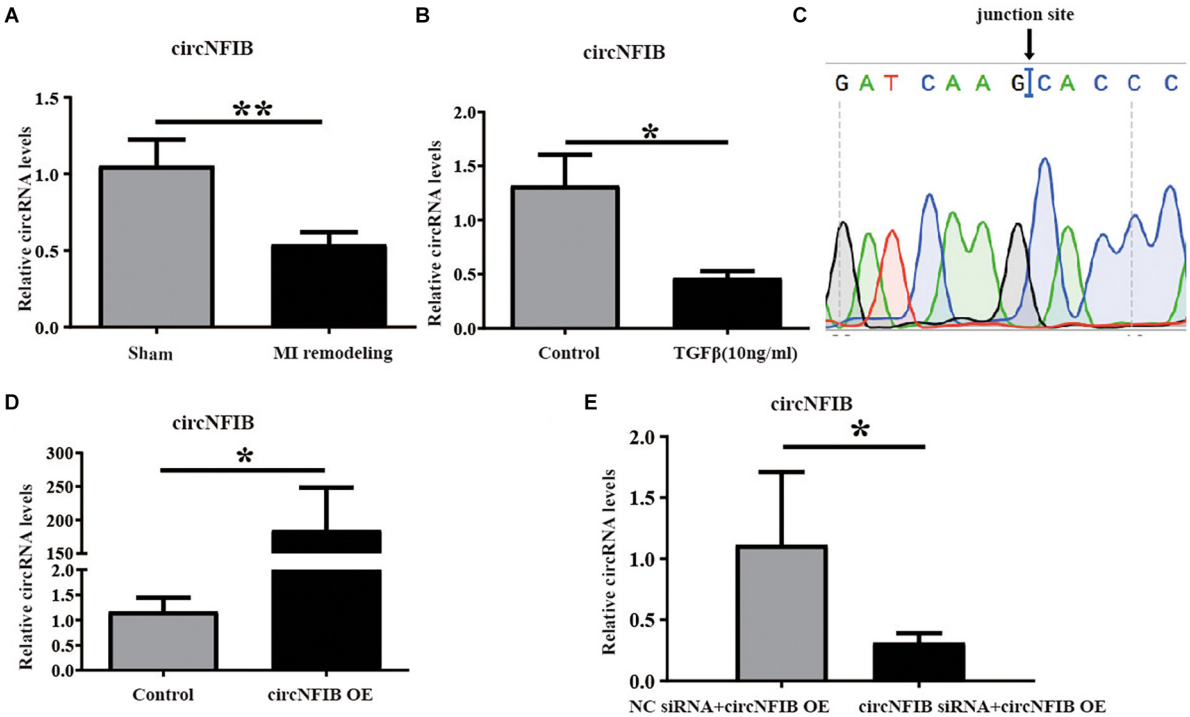

FIGURE 1 | CircNFIB is decreased in cardiac fibrosis. **(A)** CircNFIB is decreased in ventricle samples from 21 days post-myocardial infarction mice (n = 5:6). **(B)** circNFIB is decreased in primary adult cardiac fibroblasts treated by TGF-β (n = 5:6). **(C)** Results of sequencing of divergent PCR products generated from circNFIB confirmed the head-to-tail junction point. **(D)** The transfection efficacy of circNFIB plasmid is confirmed by qRT-PCR (n = 6). **(E)** The transfection efficacy of circNFIB siRNA is confirmed by qRT-PCR (n = 4). *$p < 0.05$, **$p < 0.01$ versus controls.

Transfection of Synthetic circRNA and Small Interfering RNA

All transfections and assays were performed on cardiac fibroblasts at passage 3 or NIH/3T3 cell lines cultured in low serum medium (1% FBS). CircNFIB is knocked down using custom-designed small interfering RNA (siRNA) oligonucleotides and, additionally, a targeting site across the head-to-tail junction. CircNFIB siRNA target sequence is 5′-GAGATCAAGCACCCATAAC-3′ (purchased from Biotend, Shanghai, China). A non-related, scrambled siRNA sequence is used as a control (5′-TTCTCCGAACGTGTCACGT-3′). Cardiac fibroblasts or NIH/3T3 cell lines were exposed to either plasmid overexpressing circNFIB versus empty vector (50 nM) or siRNA for circNFIB versus negative control (NC, 50 nM) for 48 h, and treated with recombinant human TGF-β1 (10 ng/ml, Sino Biological, Beijing, China) for 24 h. Notably, considering the low expression abundance of circNFIB in adult cardiac fibroblast, plasmid overexpressing circNFIB was first transfected and then cells were exposed to circNFIB siRNA versus NC. miR-433 mimic and NC (50 nM) were purchased from RiboBio. All the transfections were carried out by using Lipofectamine RNAiMAX Transfection Reagent (Invitrogen).

Establishment of MI Remodeling Model

Animal procedures were performed in C57BL/6N male mice (8–10 weeks old). Following full anesthesia through the intraperitoneal injection of 3% chloral hydrate, the mice were intubated and placed on a standard rodent ventilator. An incision was made between the third and fourth intercostal space, and MI mode was generated by ligating the left anterior descending coronary artery (LAD) using 7-0 suture. The sham group was created by the same process but without LAD ligation.

Immunofluorescence and EdU Staining

Forty-eight hours after transfection, cardiac fibroblasts or NIH/3T3 cells were fixed with 4% paraformaldehyde (PFA) for 20 min at room temperature. After washing three times with phosphate-buffered saline (PBS), cells were permeabilized with 0.2% Triton X-100 (PBST) for 20 min at room temperature. Then, cardiac fibroblasts were blocked with 10% goat serum in PBST for 1 h at room temperature. Primary antibodies with α-SMA-Cy3 (1:100, Sigma, St. Louis, MO, United States) diluted in 10% goat serum were incubated at 4°C overnight. Click-iT Plus EdU Alexa Fluor 488 Imaging Kit (KeyGEN BioTECH, Nanjing, China) was used to detect proliferation according to the manufacturer's instructions. Nuclei were counterstained with DAPI. The proliferative rate was calculated by the number of EdU-positive cells/DAPI.

Luciferase Reporter Assay

A luciferase reporter vector containing miR-433 binding site was constructed by inserting annealed miR-433 binding site into

the pMIRGLO vector (Promega, Madison, WI, United States) using PmeI and XbaI restriction enzymes. When the cell confluence reached about 80%, the miR-433 mimic (RiboBio) and pMIR-circNFIB-wide type or pMIR-circNFIB-mutant were co-transfected into HEK293T cells using Lipofectamine 2000 (Investigen). After 48 h of co-transfection, the luciferase activity was measured with a dual luciferase reporter assay system (Promega). The relative fold change of luciferase activity normalized with NC.

Western Blot Analysis

The total proteins were extracted from cardiac fibroblasts using protein lysis buffer (RIPA) containing 1 mM PMSF (KeyGEN BioTECH, Nanjing, China). Then, 30 μg of total proteins was loaded and separated on 10% sodium dodecyl sulfate-polyacrylamide gel electrophoresis (SDS-PAGE) gels. After electrophoresis, the proteins were transferred to polyvinylidene fluoride (PVDF) membrane and then blocked with 5% skim milk in tris saline with tween 20 (TBST) for 1 h at room temperature. The PVDF membrane was then incubated with primary antibodies at 4°C overnight. The primary antibodies used were from the following sources: AZIN1 (1:500, cat. NO. 11548, Proteintech), Jnk1 (1:1,000, cat. NO. 3708, Cell Signaling Technology, Boston, MA, United States), p38 (1:1,000, cat. NO. 8690, CST), p-p38 (1:1,000, cat. NO. 4511, CST), ERK (1:1,000, cat. NO. 4695, CST), p-ERK (1:1,000, cat. NO. 4370, CST), Smad3 (1:1,000, cat. NO. 9523, CST), p-Smad3 (1:1,000, cat. NO. 9520, CST), and GAPDH (1:1,000, cat. NO. AP0063, Bioworld). The PVDF membrane was washed three times with TBST and then incubated with a second antibody, which was horseradish peroxidase (HRP)-labeled anti-mouse or anti-rabbit immunoglobulin G (IgG; 1:1,000, CST). All the proteins were visualized by ECL chemiluminescence kit (Thermo Fisher, Waltham, MA, United States), and the quantification of each band was performed using Imagelab Software (Bio-Rad) as compared to GAPDH. Uncropped images of western blots are available in **Supplementary Figure S1**.

Statistical Analysis

Data were presented at mean of independent experiments/independent samples ± SE. Statistical analysis was performed using Prism Software (GraphPad Prism 5). For analysis of two groups, Student's *t*-test was used; for comparison of three or more groups, one-way ANOVA followed by Bonferroni's post test was applied. A *p*-value less than 0.05 was considered to be statistically different.

RESULTS

CircNFIB Is Downregulated in Cardiac Fibrosis *in vivo* and *in vitro*

Previously, we have studied the essential role of miR-433 in regulating cardiac fibrosis (Tao et al., 2016). CircRNAs have been reported to act as miRNA sponges to regulate the function of miRNAs (Wang et al., 2016; Cai et al., 2019). This encourages us to investigate whether circRNAs can function as miR-433 sponge to modulate cardiac fibrosis. Firstly, we identified seven circRNAs (circBase: mmu_circ_0001140, mmu_circ_0004085, mmu_circ_0004087, mmu_circ_0001221, mmu_circ_0011794, mmu_circ_0000377, and mmu_circ_0004047) related to miR-433 in mouse heart samples by bioinformatics analysis. Next, we designed divergent primers for those circRNAs to amplify the back-splicing regions from mouse heart, and PCR products close to the predicted head-to-tail junction size would be subjected to Sanger sequence for further analysis. Then, we found that three out of seven circRNAs (circBase: mmu_circ_0011794, mmu_circ_0000377, and mmu_circ_0004047) had verified junction sites (**Supplementary Figure S2**). Using the Masson's Trichrome staining approach, we have previously reported that heart samples from 3 weeks post-MI exhibited massive fibrosis (Tao et al., 2016). To further confirm which circRNA is involved in cardiac fibrosis, we explored the expression levels of these three circRNAs in heart samples from the 3-week post-MI model. Based on quantitative real-time polymerase chain reaction (qRT-PCR) analysis, we confirmed that only circNFIB (circBase: mmu_circ_0011794) was downregulated in heart samples from the 3-week post-MI mice (**Figure 1A** and **Supplementary Figure S3**). In addition, the expression of circNFIB was significantly reduced in TGF-β-treated cardiac fibroblasts (**Figure 1B**). These findings indicate a strong connection between the expression of circNFIB and cardiac fibrosis both *in vivo* and *in vitro*. The full length of circNFIB was 240 nucleotides and named based on its host gene NFIB, which is located in chromosome 4. Accurate overexpression construction of circNFIB was validated by a divergent primer amplified PCR product following Sanger sequencing (**Figure 1C**).

Overexpression of circNFIB Attenuates Cardiac Fibroblast Proliferation Induced by TGF-β

Over-proliferation of cardiac fibroblasts is an essential process of cardiac fibrosis, contributing to both systolic and diastolic dysfunction during pathological remodeling (Wang et al., 2017; Park et al., 2018). TGF-β signaling is the major mechanism mediating fibroblast proliferation (Dobaczewski et al., 2011; Kong et al., 2014; Khalil et al., 2017; Felisbino and Mckinsey, 2018). In this study, overexpression and downregulation of circNFIB and its related NC were first transfected into primary adult cardiac fibroblasts, and transfection efficacy was confirmed by qRT-PCR (**Figures 1D,E**). Then, to evaluate the function of circNFIB in TGF-β stimulation, overexpression of circNFIB and relative NC were transfected into NIH/3T3 cell lines, and results showed that circNFIB overexpression attenuated cell proliferation as evidenced by the decreased ratio of EdU staining based on TGF-β stimulation (**Figures 2A,B**). To further confirm the role of circNFIB on fibroblast proliferation, primary adult cardiac fibroblasts were isolated from adult C57BL/6N mice and treated with TGF-β and over-proliferation of fibroblasts were induced (**Figures 2C,D**). Moreover, circNFIB overexpression attenuated cardiac fibroblast proliferation based on TGF-β stimulation (**Figures 2E,F**), while inhibition of circNFIB promoted fibroblast proliferation (**Figures 2H,I**).

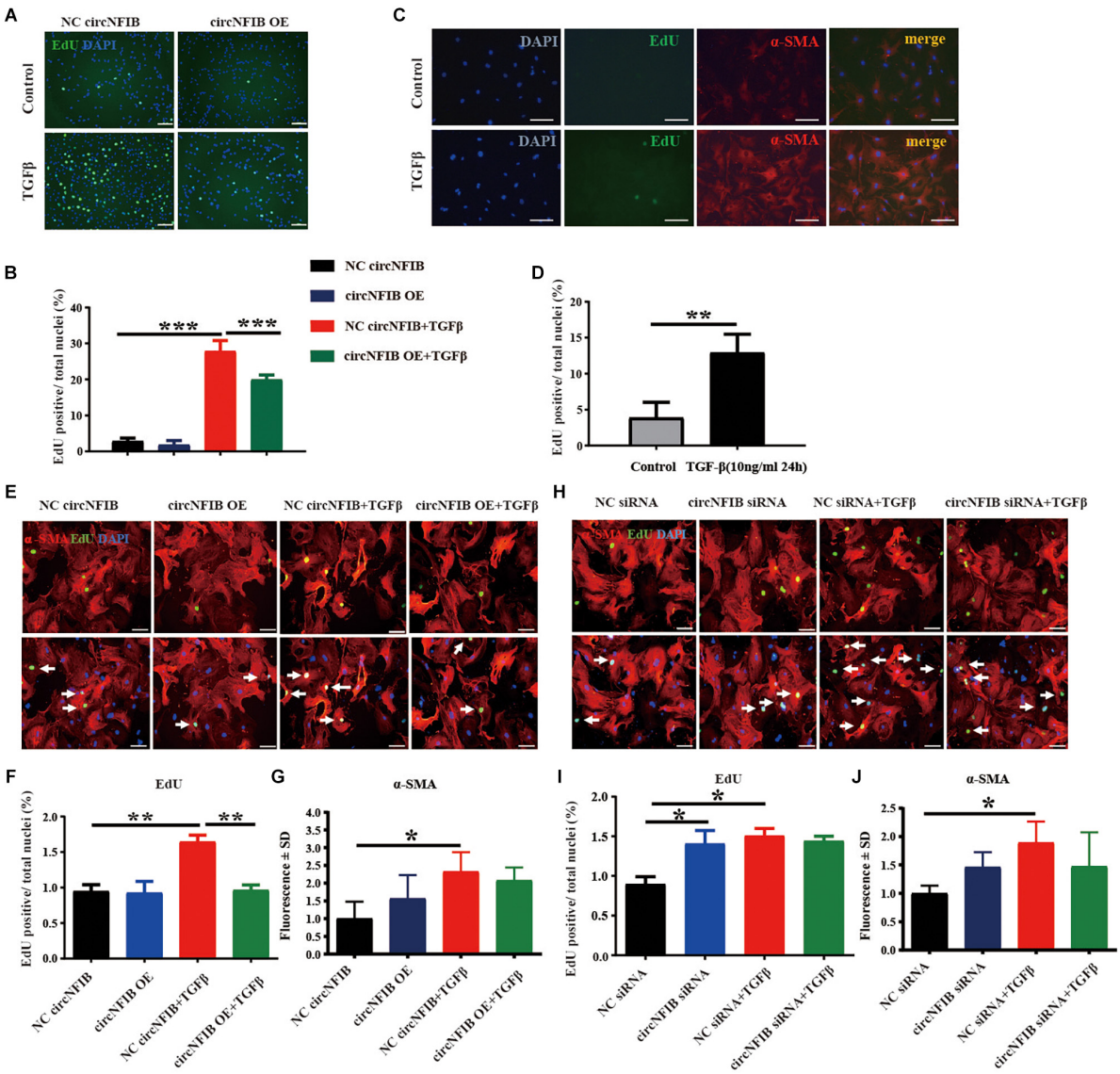

FIGURE 2 | Overexpression of circNFIB attenuates cardiac fibroblast proliferation induced by TGF-β. **(A,B)** Forced expression of circNFIB decreases proliferation of NIH/3T3 cell stimulated by TGF-β, as evidenced EdU/α-SMA staining (n = 4). **(C,D)** Over-proliferation of primary adult fibroblasts is induced by TGF-β, as evidenced EdU/α-SMA staining (n = 5). **(E–G)** Forced expression of circNFIB does not have an effect on fibroblast activation but significantly decreased primary adult cardiac fibroblasts proliferation depending on TGF-β stimulation (n = 5). **(H–J)** Downregulation of circNFIB *via* siRNA promotes cardiac fibroblasts proliferation in the absence of TGF-β stimulation while having no statistical effect on α-SMA expression (n = 5). Scale bar: 50 μm. $^*p < 0.05$, $^{**}p < 0.01$, $^{***}p < 0.001$ versus controls.

Downregulation of circNFIB failed to further enhance cardiac fibroblast proliferation in the presence of TGF-β stimulation (**Figures 2H,I**). In addition, neither upregulation nor inhibition of circNFIB had statistical effects on α-SMA expression (**Figures 2G,J**). Collectively, these data indicate that overexpression of circNFIB abates proliferation but not *trans*-differentiation of cardiac fibroblasts *in vitro*.

CircNFIB Acts as a Competing Endogenous RNA for miR-433

Previously, we have already shown that inhibition of miR-433 attenuated cardiac fibroblast proliferation and myofibroblast differentiation in murine post-MI models and in fibroblasts induced by TGF-β and AngII stimulation. In contrast, upregulation of miR-433 promoted cardiac fibrotic response (Tao et al., 2016). Therefore, we proposed that circNFIB may impact fibroblast proliferation through acting as a competing endogenous RNA for miR-433. RNAhybrid (Kruger and Rehmsmeier, 2006) and TargetScan (Agarwal et al., 2015) were used for miRNA recognition sequences on mouse circNFIB and revealed one putative miR-433 binding site (**Figures 3A,B**). Luciferase reporter assay revealed that miR-433 significantly inhibited luciferase activity for the wild-type 3′UTR construct for circNFIB but had no effect when the miR-433 binding site in the

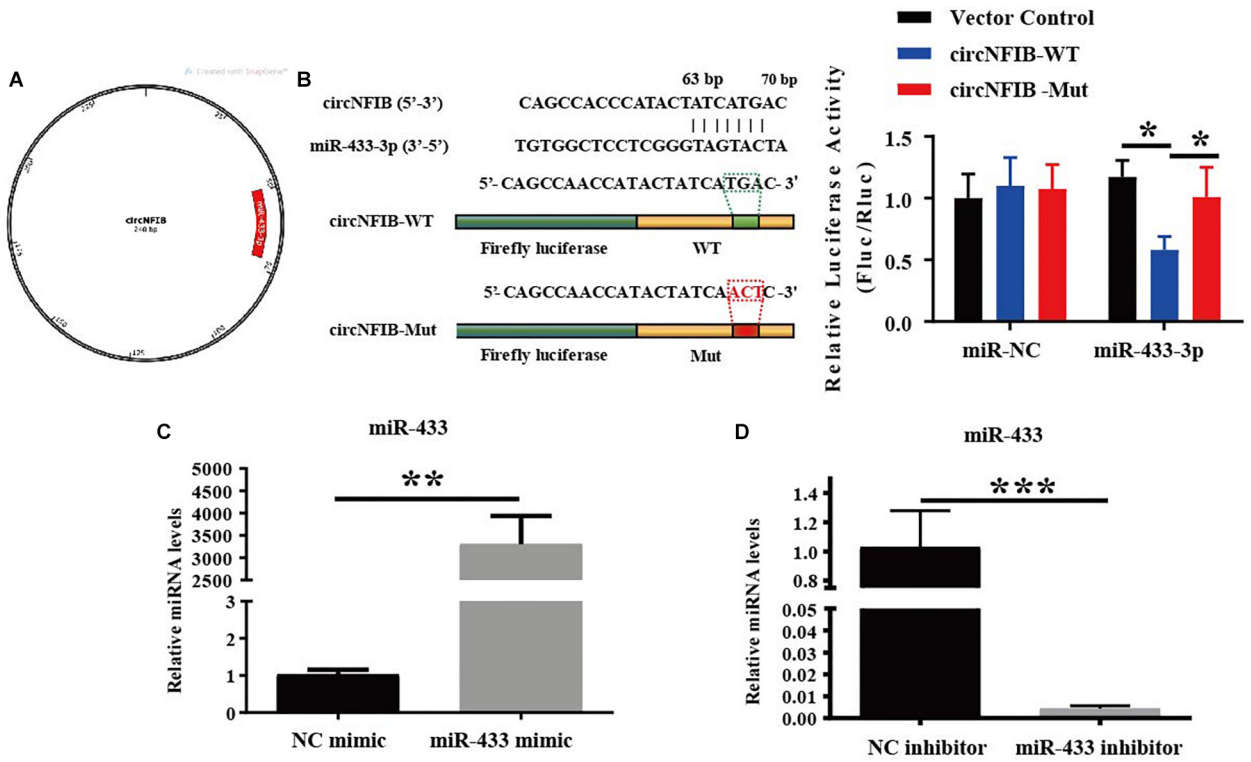

FIGURE 3 | MiR-433 is identified as a direct target of circNFIB. **(A)** A schematic diagram displaying the putative binding site of miR-433 associated with circNFIB (processed using SnapGene). **(B)** Targetscan and Luciferase reporter assays identify miR-433 as a direct target of circNFIB ($n = 6$). **(C,D)** The transfection efficacy of miR-433 mimic ($n = 6$) or inhibitor ($n = 4$) is confirmed by qRT-PCR. $^*p < 0.05$, $^{**}p < 0.01$, $^{***}p < 0.001$ versus controls.

circNFIB was mutated, indicating a direct interaction between miR-433 and circNFIB (**Figure 3B**). To investigate whether the effects of circNFIB on fibroblast proliferation were mediated by miR-433, overexpression or inhibition of circNFIB and miR-433 was co-transfected into primary adult cardiac fibroblasts (**Figures 3C,D**). Our data illustrated that overexpression of circNFIB could abate the pro-proliferative effects of the miR-433 mimic on cardiac fibroblasts as evidenced by decreased EdU-positive cells (**Figures 4A,B**). Furthermore, downregulation of circNFIB *via* siRNA also reversed the anti-proliferative effects of the miR-433 inhibitor as identified by an increase in EdU staining (**Figures 4C,D**).

As AZIN1 and JNK1 were previously confirmed as target genes of miR-433, further researches demonstrated that knockdown of AZIN1 could promote proliferation and differentiation of cardiac fibroblasts into myofibroblasts accompanied by an activation of the TGF-β–Smad3 signaling pathway. Besides AZIN1, reduction of JNK1 was responsible for the pro-fibrotic effects by activation of ERK and p38 kinase, in parallel with the activation of Smad3 (Tao et al., 2016). Therefore, we further examined the modulatory effects of circNFIB on miR-433 target genes and downstream signaling pathways. Our data showed that the inhibition of AZIN1 and JNK1 by the miR-433 mimic was reversed by overexpression of circNFIB (**Figures 5A–C**). Moreover, upregulation of circNFIB also attenuated the activation of p38, ERK kinases, and the Smad3 signaling pathway as evidenced by the decreased ratio of p-p38/p38, p-ERK/ERK, and p-Smad3/Smad3 (**Figures 5D–G**). However, circNFIB failed to have an additive effect on target genes and downstream signaling pathways independent of miR-433 (**Figures 5A–G**). These data suggest that circNFIB is an endogenous competing sponge of miR-433 mediating its effects in cardiac fibrosis.

DISCUSSION

Despite the high incidence of mortality and morbidity related to cardiac fibrosis, no fibrotic strategies are available under the current treatment regimens recommended by the official guidelines such as angiotensin-converting enzyme inhibitors (ACEIs), angiotensin receptor blockers (ARBs), and aldosterone synthase inhibitors (Ghosh et al., 2013; Weber et al., 2013; Xie et al., 2013). Thus, targeting the direct molecular mediators holds promise to develop therapeutic interventions. Recently, novel therapeutic strategies such as non-coding RNAs (ncRNAs) (Wang et al., 2018), exosomes (Bellin et al., 2019), and exercise (Cipryan, 2018; Randers et al., 2018) have been reported to perform beneficial effects against diverse cardiovascular diseases. The roles of circRNAs in cardiovascular diseases including cardiac fibrosis have attracted much attention (Bei et al., 2018).

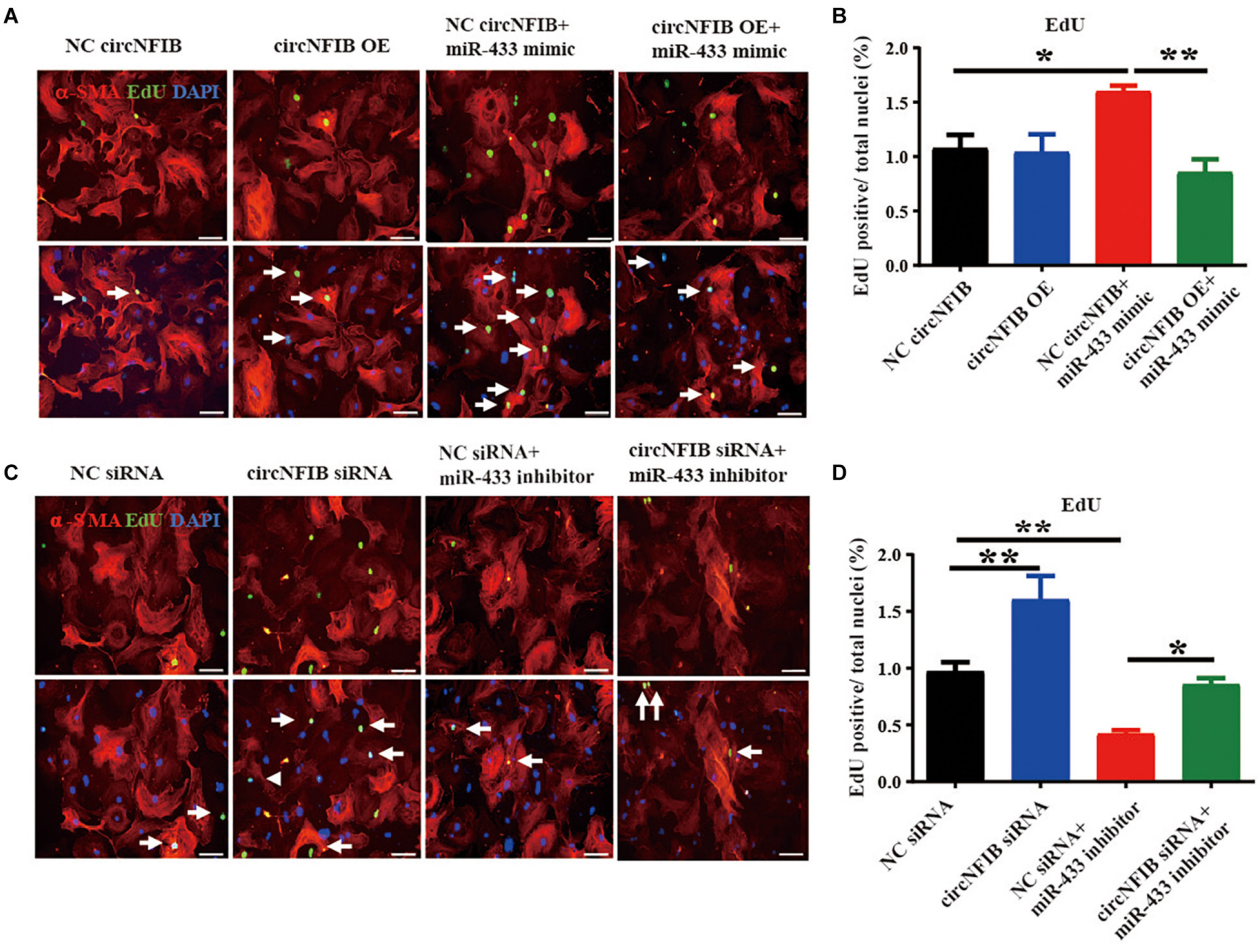

FIGURE 4 | CircNFIB acts as a competing endogenous RNA for miR-433. **(A,B)** Overexpression of circNFIB attenuates the pro-proliferative effects of miR-433 mimic on cardiac fibroblasts, as evidenced EdU/α-SMA staining ($n = 5$). **(C,D)** Downregulation of circNFIB reverses the anti-proliferative responses of miR-433 inhibitor on cardiac fibroblasts, as evidenced EdU/α-SMA staining. Scale bar: 50 μm. $^{*}p < 0.05$, $^{**}p < 0.01$, versus controls.

CircRNAs are endogenous, abundant, and stable ncRNAs with diverse action modes formed by back-splicing events (Zeng et al., 2017). The mechanisms for circRNA function in the physiological or pathological heart have not been well elucidated clearly, especially in cardiac fibrosis. The most reported function pattern for circRNA is acting as a miRNA sponge and forming the circRNA–miRNA–mRNA axis (Chen, 2016; Du et al., 2017). It has been suggested that dysregulated circRNAs, such as circRNA_010567 and circRNA_000203, contribute to cardiac fibrosis by sponging miR-141 and miR-26b-5p, respectively (Tang et al., 2017; Zhou and Yu, 2017). Our previous data revealed that overexpression of miR-433 promoted cardiac fibroblast proliferation and their differentiation into myofibroblasts both *in vivo* and *in vitro*, while knockdown of miR-433 inhibited fibrotic effects by targeting AZIN1 and JNK1. Moreover, the protective effects of miR-433 inhibition against cardiac fibrosis were confirmed by administration of exogenous miR-433 sponge *via* cardiotropic AAV9. Therefore, we hypothesized that circNFIB may act as a miR-433 endogenous competing sponge regulating cardiac fibrosis. CircNFIB was derived from the exon regions of the *Nfib* gene. *Nfib*-encoded protein nuclear factor 1 B-type (NF1-B) belongs to the CTF/NF-I family and is relatively highly expressed in mouse heart[1]. However, it has no relevant reports in the heart field so far. As a CCAAT-box-binding transcription factor, NF1-B is involved in the biological process of DNA replication, transcription, and transcription regulation. Therefore, it is possible that NF1-B itself takes an important part in the heart, and we cannot rule out the possibility that circNFIB and Nfib mRNA, even protein NF1-B, may have functional relevance, but we have not studied it here. Of course, further efforts to explore the functional difference and correlation between NFIB mRNA and circ-NFIB should be of great significance.

Activation of multiple key fibrogenic pathways has been shown to contribute to the progression of fibrosis (Piccoli et al., 2017; Xie et al., 2018; Martinez-Martinez et al., 2019). Proliferation of the resident fibroblasts is one of the major

[1]https://www.ncbi.nlm.nih.gov/gene/18028

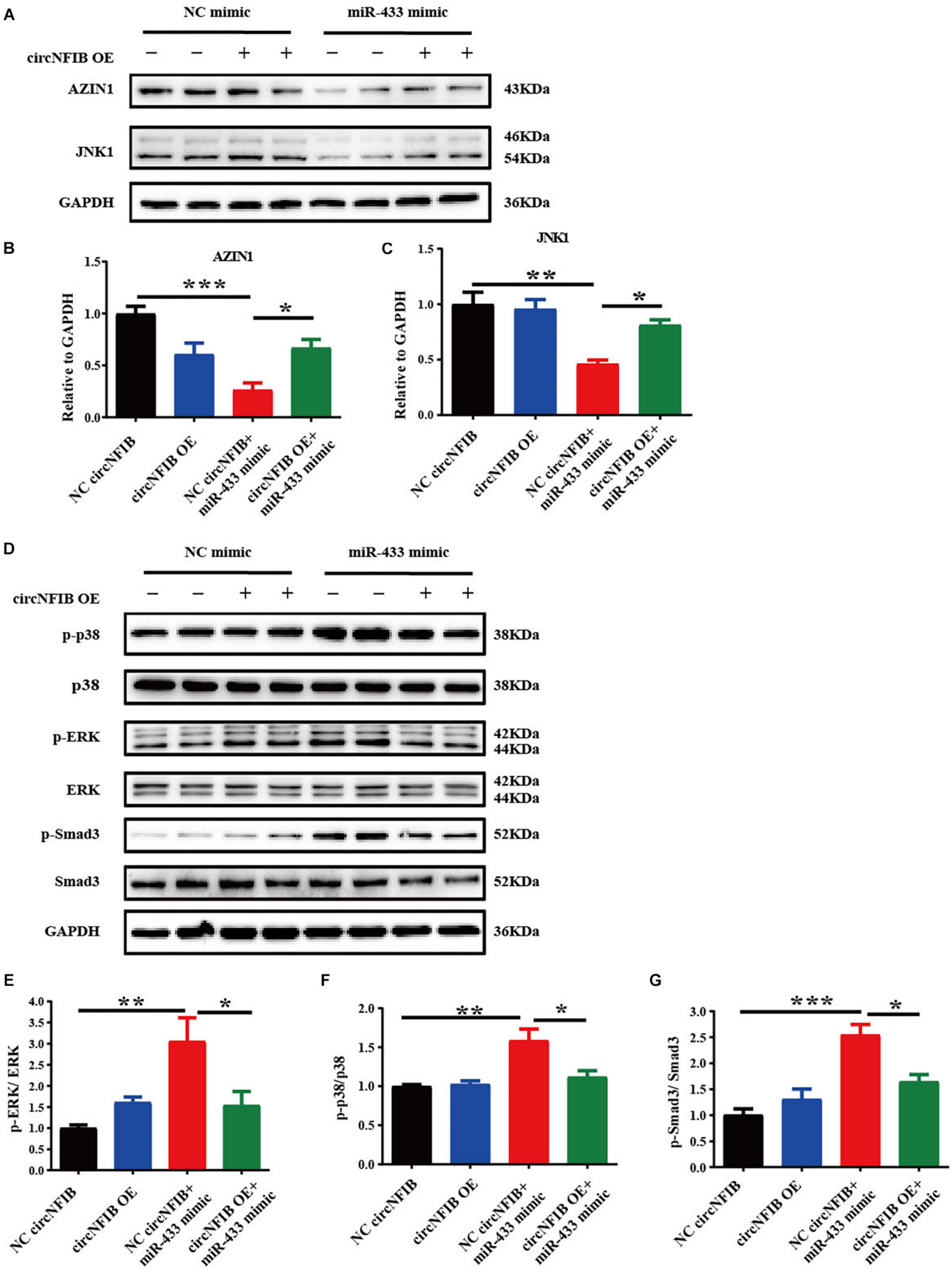

FIGURE 5 | Continued

FIGURE 5 | CircNFIB reverses the expression level of target genes and downstream signaling pathways of miR-433. **(A–C)** Overexpression of circNFIB reverses expression level of miR-433 target genes AZIN1 and JNK1 by Western blot analysis ($n = 4$). **(D–G)** Overexpression of circNFIB reverses downstream signaling pathways of miR-433, as evidenced by ratio of p-ERK/ERK, p-p38/p38, and p-Smad3/Smad3 by Western blot analysis ($n = 4$). $^{*}p < 0.05$, $^{**}p < 0.01$, $^{***}p < 0.001$ versus controls.

mechanisms. This concept is supported by a recent fate mapping study that revealed that the excessive proliferation of fibroblasts may result in fibroblast accumulation after pressure overload (Moore-Morris et al., 2014). In our present study, knockdown of circNFIB promoted cardiac fibroblast proliferation as exhibited by the increased number of EdU-positive cells. Notably, the overexpression of circNFIB prevents the increase in cell proliferation in TGF-β induced fibrosis in both NIH/3T3 cell lines and primary adult cardiac fibroblasts. However, neither overexpression nor inhibition of circNFIB has an additional role on α-SMA expression, indicating that circNFIB may act as a novel anti-proliferative effector *in vitro*; however, its role in cardiac fibrosis *in vivo* remains largely unknown. In addition, the function of circNFIB in different models of cardiac fibrosis is still uncertain and necessitates future study.

In the present study, miR-433 was confirmed to be a direct target of circNFIB by luciferase reporter assay. Functional analysis showed that upregulation of circNFIB attenuated the proliferation of cardiac fibroblasts while downregulation of circNFIB reversed the anti-proliferative effects of the miR-433 inhibitor. Our previous research demonstrated that miR-433 performs pro-fibrotic effects by inhibiting its target genes AZIN1 and JNK1. Knockdown of AZIN1 could promote proliferation and differentiation of cardiac fibroblasts into myofibroblasts accompanied by an activation of the TGF-β–Smad3 signaling pathway. Furthermore, reduction of another target gene JNK1 was also responsible for the pro-fibrotic effects of miR-433 in cardiac fibroblasts accompanied by activation of ERK and p38 kinase signaling pathways (Tao et al., 2016). Currently, we suggest that overexpression of circNFIB reversed the effects of AZIN1 and JNK1 and downstream signaling pathways including ERK, p38, and Smad3 by the miR-433 mimic, suggesting that circNFIB may serve as an endogenous competing sponge of miR-433 regulating cardiac fibrosis. However, there are still some questions that need to be answered in future studies. As our results show, overexpression of circNFIB fails to influence fibroblast proliferation independent of TGF-β and circNFIB also fails to have an additive effect on target genes and downstream signaling pathways independent of miR-433. Furthermore, neither overexpression nor inhibition of circNFIB has additional roles on cardiac fibroblast *trans*-differentiation. However, in our previous study, inhibition of miR-433 attenuated both proliferation and differentiation of cardiac fibroblasts. This inconsistent role observed between circNFIB and miR-433 on cardiac fibrosis could be attributed to two points. First, a single miRNA can be regulated by multiple factors, such as circRNAs, long ncRNAs, or other proteins (Pu et al., 2019). In this case, circNFIB may act as only one regulator of miR-433. There should be other upstream factors modulating the function of miR-433. Second, although our research here is limited to studying the regulatory role of the circNFIB–miR-433 axis, circRNAs may act as sponges of different miRNAs as previous studies demonstrated (Zheng et al., 2016). Besides miRNA sponges, circRNAs are also found to bind to RNA-binding proteins (RBPs) or regulate gene transcription (Li et al., 2015; Du et al., 2017). The diversity regulatory mechanisms of circRNAs indicate that circNFIB may also have other potential functioning mechanisms that need further in-depth investigation in the future.

CONCLUSION

We have discovered that circNFIB expression is significantly decreased in heart samples from mice post-MI and TGF-β-treated cardiac fibroblasts. Functionally and mechanistically, overexpression of circNFIB attenuates cardiac fibroblast proliferation depending on TGF-β stimulation. Furthermore, miR-433 is identified as a direct target of circNFIB, and circNFIB could rescue the effects of target genes and downstream signaling pathways of miR-433. Taken together, our study indicates that the circNFIB–miR-433 axis may function as a novel therapy for cardiac fibrosis.

DATA AVAILABILITY

The raw data supporting the conclusions of this manuscript will be made available by the authors, without undue reservation, to any qualified researcher.

ETHICS STATEMENT

All animals were purchased from the Cavens Laboratory Animal (Changzhou, China) and raised at the Experimental Animal Center of Shanghai University (Shanghai, China). All the procedures with animals were in accordance with the guidelines of the National Institutes of Health (No. 85-23, revised in 1996). The protocols in this study were approved by the ethical committees of School of Life Sciences, Shanghai University.

AUTHOR CONTRIBUTIONS

LW and LT designed the study, conducted all the experiments, and drafted the manuscript. YZ, WP, TY, XM, and ZJ conducted the experiments and analyzed the data.

FUNDING

This work was supported by grants from the National Natural Science Foundation of China (81700343 to LT and 81800358

to LW), the Natural Science Foundation of Jiangsu Province (BK20170296 to LT), the China Postdoctoral Science Foundation (2018M642317 to LT), the Post-doctoral Foundation of Jiangsu Province (2018K095B to LT), and the Six Talent Peaks Project of Jiangsu Province (WSN-202 to LT).

SUPPLEMENTARY MATERIAL

The Supplementary Material for this article can be found online at: https://www.frontiersin.org/articles/10.3389/fgene.2019.00564/full#supplementary-material

REFERENCES

Agarwal, V., Bell, G. W., Nam, J. W., and Bartel, D. P. (2015). Predicting effective microRNA target sites in mammalian mRNAs. *eLife* 4:e05005. doi: 10.7554/eLife.05005

Bacmeister, L., Schwarzl, M., Warnke, S., Stoffers, B., Blankenberg, S., Westermann, D., et al. (2019). Inflammation and fibrosis in murine models of heart failure. *Basic Res. Cardiol.* 114:19. doi: 10.1007/s00395-019-0722-5

Bellin, G., Gardin, C., Ferroni, L., Chachques, J. C., Rogante, M., Mitrečić, D., et al. (2019). Exosome in cardiovascular diseases: a complex world full of hope. *Cells* 8:166. doi: 10.3390/cells8020166

Bei, Y., Yang, T., Wang, L., Holvoet, P., Das, S., Sluijter, J. P. G., et al. (2018). Circular RNAs as potential theranostics in the cardiovascular system. *Mol. Ther. Nucleic Acids.* 13, 407–418. doi: 10.1016/j.omtn.2018.09.022

Besler, C., Lang, D., Urban, D., Rommel, K. P., Von Roeder, M., Fengler, K., et al. (2017). Plasma and cardiac galectin-3 in patients with heart failure reflects both inflammation and fibrosis: implications for Its use as a biomarker. *Circ. Heart Fail* 10:e003804. doi: 10.1161/CIRCHEARTFAILURE.116.003804

Cai, L., Qi, B., Wu, X., Peng, S., Zhou, G., Wei, Y., et al. (2019). Circular RNA Ttc3 regulates cardiac function after myocardial infarction by sponging miR-15b. *J. Mol. Cell. Cardiol.* 130, 10–22. doi: 10.1016/j.yjmcc.2019.03.007

Chen, L. L. (2016). The biogenesis and emerging roles of circular RNAs. *Nat. Rev. Mol. Cell. Biol.* 17, 205–211. doi: 10.1038/nrm.2015.32

Chen, L. L., and Yang, L. (2015). Regulation of circRNA biogenesis. *RNA Biol.* 12, 381–388. doi: 10.1080/15476286.2015.1020271

Cipryan, L. (2018). The effect of fitness level on cardiac autonomic regulation, IL-6, total antioxidant capacity, and muscle damage responses to a single bout of high-intensity interval training. *J. Sport Health Sci.* 7, 363–371. doi: 10.1016/j.jshs.2016.11.001

Dobaczewski, M., Chen, W., and Frangogiannis, N. G. (2011). Transforming growth factor (TGF)-β signaling in cardiac remodeling. *J. Mol. Cell. Cardiol.* 51, 600–606. doi: 10.1016/j.yjmcc.2010.10.033

Du, W. W., Zhang, C., Yang, W., Yong, T., Awan, F. M., and Yang, B. B. (2017). Identifying and characterizing circRNA–protein interaction. *Theranostics* 7, 4183–4191. doi: 10.7150/thno.21299

Felisbino, M. B., and Mckinsey, T. A. (2018). Epigenetics in cardiac fibrosis: emphasis on inflammation and fibroblast activation. *JACC Basic Transl. Sci.* 3, 704–715. doi: 10.1016/j.jacbts.2018.05.003

Ghosh, A. K., Quaggin, S. E., and Vaughan, D. E. (2013). Molecular basis of organ fibrosis: potential therapeutic approaches. *Exp. Biol. Med.* 238, 461–481. doi: 10.1177/1535370213489441

Gyongyosi, M., Winkler, J., Ramos, I., Do, Q. T., Firat, H., Mcdonald, K., et al. (2017). Myocardial fibrosis: biomedical research from bench to bedside. *Eur. J. Heart Fail.* 19, 177–191. doi: 10.1002/ejhf.696

Hall, I. F., Climent-Salarich, M., Quintavalle, M., Farina, F. M., Schorn, T., Zani, S. M., et al. (2018). Circ_Lrp6, a circular RNA enriched in vascular smooth muscle cells, acts as a sponge regulating miRNA-145 function. *Circ. Res.* 124, 498–510. doi: 10.1161/CIRCRESAHA.118.314240

Hentze, M. W., and Preiss, T. (2013). Circular RNAs: splicing's enigma variations. *Embo. J.* 32, 923–925. doi: 10.1038/emboj.2013.53

Jeck, W. R., Sorrentino, J. A., Wang, K., Slevin, M. K., Burd, C. E., Liu, J., et al. (2013). Circular RNAs are abundant, conserved, and associated with ALU repeats. *Rna* 19, 141–157. doi: 10.1261/rna.035667.112

Khalil, H., Kanisicak, O., Prasad, V., Correll, R. N., Fu, X., Schips, T., et al. (2017). Fibroblast-specific TGF-beta-Smad2/3 signaling underlies cardiac fibrosis. *J. Clin. Invest.* 127, 3770–3783. doi: 10.1172/JCI94753

Kong, P., Christia, P., and Frangogiannis, N. G. (2014). The pathogenesis of cardiac fibrosis. *Cell. Mol. Life Sci.* 71, 549–574. doi: 10.1007/s00018-013-1349-6

Kruger, J., and Rehmsmeier, M. (2006). RNAhybrid: microRNA target prediction easy, fast and flexible. *Nucleic Acids Res.* 34, W451–W454. doi: 10.1093/nar/gkl243

Lajiness, J. D., and Conway, S. J. (2014). Origin, development, and differentiation of cardiac fibroblasts. *J. Mol. Cell. Cardiol.* 70, 2–8. doi: 10.1016/j.yjmcc.2013.11.003

Li, A. H., Liu, P. P., Villarreal, F. J., and Garcia, R. A. (2014). Dynamic changes in myocardial matrix and relevance to disease: translational perspectives. *Circ. Res.* 114, 916–927. doi: 10.1161/CIRCRESAHA

Li, Z., Huang, C., Bao, C., Chen, L., Lin, M., Wang, X., et al. (2015). Exon–intron circular RNAs regulate transcription in the nucleus. *Nat. Struct. Mol. Biol.* 22, 256–264. doi: 10.1038/nsmb.2959

Martinez-Martinez, E., Brugnolaro, C., Ibarrola, J., Ravassa, S., Buonafine, M., Lopez, B., et al. (2019). CT-1 (Cardiotrophin-1)–Gal-3 (Galectin-3) axis in cardiac fibrosis and inflammation. *Hypertension* 73, 602–611. doi: 10.1161/HYPERTENSIONAHA

Memczak, S., Jens, M., Elefsinioti, A., Torti, F., Krueger, J., Rybak, A., et al. (2013). Circular RNAs are a large class of animal RNAs with regulatory potency. *Nature* 495, 333–338. doi: 10.1038/nature11928

Moore-Morris, T., Guimaraes-Camboa, N., Banerjee, I., Zambon, A. C., Kisseleva, T., Velayoudon, A., et al. (2014). Resident fibroblast lineages mediate pressure overload-induced cardiac fibrosis. *J. Clin. Invest.* 124, 2921–2934. doi: 10.1172/JCI74783

Park, S., Ranjbarvaziri, S., Lay, F. D., Zhao, P., Miller, M. J., Dhaliwal, J. S., et al. (2018). Genetic regulation of fibroblast activation and proliferation in cardiac fibrosis. *Circulation* 138, 1224–1235. doi: 10.1161/CIRCULATIONAHA

Piccoli, M. T., Gupta, S. K., Viereck, J., Foinquinos, A., Samolovac, S., Kramer, F. L., et al. (2017). Inhibition of the cardiac fibroblast-enriched lncRNA Meg3 prevents cardiac fibrosis and diastolic dysfunction. *Circ. Res.* 121, 575–583. doi: 10.1161/CIRCRESAHA

Pu, M., Chen, J., Tao, Z., Miao, L., Qi, X., Wang, Y., et al. (2019). Regulatory network of miRNA on its target: coordination between transcriptional and post-transcriptional regulation of gene expression. *Cell. Mol. Life Sci.* 76, 441–451. doi: 10.1007/s00018-018-2940-7

Randers, M. B., Hagman, M., Brix, J., Christensen, J. F., Pedersen, M. T., Nielsen, J. J., et al. (2018). Effects of 3 months of full-court and half-court street basketball training on health profile in untrained men. *J. Sport Health Sci.* 7, 132–138. doi: 10.1016/j.jshs.2017.09.004

Segura, A. M., Frazier, O. H., and Buja, L. M. (2014). Fibrosis and heart failure. *Heart Fail. Rev.* 19, 173–185. doi: 10.1007/s10741-012-9365-4

Tang, C. M., Zhang, M., Huang, L., Hu, Z. Q., Zhu, J. N., Xiao, Z., et al. (2017). CircRNA_000203 enhances the expression of fibrosis-associated genes by derepressing targets of miR-26b-5p, Col1a2 and CTGF, in cardiac fibroblasts. *Sci. Rep.* 7:40342. doi: 10.1038/srep40342

Tao, L., Bei, Y., Chen, P., Lei, Z., Fu, S., Zhang, H., et al. (2016). Crucial role of miR-433 in regulating cardiac fibrosis. *Theranostics* 6, 2068–2083. doi: 10.7150/thno.15007

Wang, J., Guo, L., Shen, D., Xu, X., Wang, J., Han, S., et al. (2017). The role of c-SKI in regulation of TGFbeta-induced human cardiac fibroblast proliferation and ECM protein expression. *J. Cell. Biochem.* 118, 1911–1920. doi: 10.1002/jcb.25935

Wang, K., Long, B., Liu, F., Wang, J. X., Liu, C. Y., Zhao, B., et al. (2016). A circular RNA protects the heart from pathological hypertrophy and heart failure by targeting miR-223. *Eur. Heart J.* 37, 2602–2611. doi: 10.1093/eurheartj/ehv713

Wang, L., Lv, Y., Li, G., and Xiao, J. (2018). MicroRNAs in heart and circulation during physical exercise. *J. Sport. Health. Sci.* 7, 433–441. doi: 10.1016/j.jshs.2018.09.008

Watson, C. J., Phelan, D., Collier, P., Horgan, S., Glezeva, N., Cooke, G., et al. (2014). Extracellular matrix sub-types and mechanical stretch impact human cardiac fibroblast responses to transforming growth factor beta. *Connect. Tissue Res.* 55, 248–256. doi: 10.3109/03008207.2014.904856

Weber, K. T., Sun, Y., Bhattacharya, S. K., Ahokas, R. A., and Gerling, I. C. (2013). Myofibroblast-mediated mechanisms of pathological remodelling of the heart. *Nat. Rev. Cardiol.* 10, 15–26. doi:10.1038/nrcardio.2012.158

Xie, M., Burchfield, J. S., and Hill, J. A. (2013). Pathological ventricular remodeling: therapies: Part 2 of 2. *Circulation* 128, 1021–1030. doi: 10.1161/CIRCULATIONAHA

Xie, Y., Ostriker, A. C., Jin, Y., Hu, H., Sizer, A. J., Peng, G., et al. (2018). LMO7 is a negative feedback regulator of TGF-beta signaling and fibrosis. *Circulation* 139, 679–693. doi: 10.1161/CIRCULATIONAHA

Zeng, X., Lin, W., Guo, M., and Zou, Q. (2017). A comprehensive overview and evaluation of circular RNA detection tools. *PLoS Comput. Biol.* 13:e1005420. doi: 10.1371/journal.pcbi.1005420

Zheng, Q., Bao, C., Guo, W., Li, S., Chen, J., Chen, B., et al. (2016). Circular RNA profiling reveals an abundant circHIPK3 that regulates cell growth by sponging multiple miRNAs. *Nat. Commun.* 7:11215. doi: 10.1038/ncomms11215

Zhou, B., and Yu, J. W. (2017). A novel identified circular RNA, circRNA_010567, promotes myocardial fibrosis via suppressing miR-141 by targeting TGF-beta1. *Biochem. Biophys. Res. Commun.* 487, 769–775. doi: 10.1016/j.bbrc.2017.04.044

Conflict of Interest Statement: The authors declare that the research was conducted in the absence of any commercial or financial relationships that could be construed as a potential conflict of interest.

The handling Editor declared a past co-authorship with one of the authors LT.

frontiers in Genetics

ORIGINAL RESEARCH
published: 22 August 2019
doi: 10.3389/fgene.2019.00757

Bta-miR-10b Secreted by Bovine Embryos Negatively Impacts Preimplantation Embryo Quality

*Xiaoyuan Lin[1], Krishna Chaitanya Pavani[2], Katrien Smits[2], Dieter Deforce[3], Björn Heindryckx[4], Ann Van Soom[2] and Luc Peelman[1]**

[1] Department of Nutrition, Genetics and Ethology, Faculty of Veterinary Medicine, Ghent University, Ghent, Belgium, [2] Reproduction, Obstetrics and Herd Health, Ghent University, Ghent, Belgium, [3] Laboratory for Pharmaceutical Biotechnology, Faculty of Pharmaceutical Sciences, Ghent University, Ghent, Belgium, [4] Department for Reproductive Medicine, Ghent University Hospital, Ghent, Belgium

In a previous study, we found miR-10b to be more abundant in a conditioned culture medium of degenerate embryos compared to that of blastocysts. Here, we show that miR-10b mimics added to the culture medium can be taken up by embryos. This uptake results in an increase in embryonic cell apoptosis and aberrant expression of DNA methyltransferases (*DNMTs*). Using several algorithms, Homeobox A1 (*HOXA1*) was identified as one of the potential miR-10b target genes and dual-luciferase assay confirmed *HOXA1* as a direct target of miR-10b. Microinjection of si-*HOXA1* into embryos also resulted in an increase in embryonic cell apoptosis and downregulation of *DNMTs*. Cell progression analysis using Madin–Darby bovine kidney cells (MDBKs) showed that miR-10b overexpression and *HOXA1* knockdown results in suppressed cell cycle progression and decreased cell viability. Overall, this work demonstrates that miR-10b negatively influences embryo quality and might do this through targeting *HOXA1* and/or influencing DNA methylation.

Keywords: bovine embryos, secreted miRNAs, miR-10b, *HOXA1*, DNA methylation, apoptosis

OPEN ACCESS

Edited by:
Junjie Xiao,
Shanghai University, China

Reviewed by:
Dušan Fabian,
Institute of Animal Physiology (SAS), Slovakia
Xue-Ming Zhang,
Jilin University, China

****Correspondence:***
Luc Peelman
Luc.Peelman@UGent.be

Specialty section:
This article was submitted to RNA, a section of the journal Frontiers in Genetics

Received: *13 May 2019*
Accepted: *17 July 2019*
Published: *22 August 2019*

Citation:
Lin X, Pavani KC, Smits K, Deforce D, Heindryckx B, Van Soom A and Peelman L (2019) Bta-miR-10b Secreted by Bovine Embryos Negatively Impacts Preimplantation Embryo Quality. Front. Genet. 10:757. doi: 10.3389/fgene.2019.00757

INTRODUCTION

MiRNAs, small non-coding RNAs, function as crucial (epigenetic) regulators that can be transferred between cells (Valadi et al., 2007). MiRNAs' selective secretion and high stability (resistant to RNase digestion and other harsh conditions) (Luo et al., 2009; Donker et al., 2012) make them good candidates as non-invasive biomarkers for preimplantation embryo quality assessment and thus increase efficiency and reduce both the risks and the costs associated with assisted reproductive treatment (ART) (Homer et al., 2017).

In a previous study, we identified 114 known and 180 novel secreted miRNAs present in bovine embryo culture media (CM). Of these miRNAs, miR-30c and miR-10b were much more abundant in CM of slow-cleaving embryos compared to intermediate-cleaving embryos. We further demonstrated that miR-30c directly targets Cyclin-dependent kinase 12 mRNA and downregulates several DNA damage response (DDR) genes (Lin et al., 2019). MiR-10b was also shown to be more abundant in the culture medium of degenerate embryos compared with that of blastocysts, and more abundant in the culture medium of slow-cleaving embryos compared with that of intermediate-cleaving embryos, indicating that overexpression of miR-10b has a negative influence on preimplantation embryo development in cattle (Lin et al., 2019). Previously, miR-10b has been shown to regulate cell

invasion, apoptosis, viability, and migration in multiple cell lines in human, mouse, and goat (Chen et al., 2016; Li et al., 2016; Peng et al., 2016; Zhen et al., 2016; Zhu et al., 2016; Tan et al., 2018).

Among the possible miR-10b target genes we identified using several computational methods, *HOXA1* stood out as it was previously shown to be involved in cell proliferation in human epithelial cells (Bitu et al., 2012) and cell growth, invasion, and migration in esophageal cancer cells (Li et al., 2017). MiR-10b is located within an intron of *HOXD4* (Homeobox D4) in bovine (NC_037329.1) and mouse (NC_000068.7), and between *HOXD4* and *HOXD8* (Homeobox D8) in human (NC_000002.12). Human miR-10b has also been shown to target *HOX* genes (homeobox transcription factor) such as *HOXD10* (Liu et al., 2012; Nakayama et al., 2013) and *HOXB3* (Chen et al., 2016), thus regulating cell invasion, migration, proliferation, and apoptosis. *HOXA1* is a conserved member of the HOX family, which regulates cell fate, early development patterns, and organogenesis (Shah and Sukumar, 2010; Rezsohazy et al., 2015). As the first HOX gene to be expressed in connection with gastrulation during embryogenesis, *HOXA1* plays important roles in modulation of cell proliferation, metastasis, and invasion (Bitu et al., 2012; Zha et al., 2012; Wardwell-Ozgo et al., 2014; Taminiau et al., 2016). These diverse functional roles of *HOXA1* appear to be at least partially related to its ability to influence key signaling pathways involved in regulating the cell cycle.

In addition to miRNAs, DNA methylation, a major component of the epigenome, is also a regulator of mammalian embryogenesis (Santos et al., 2002; Zhang et al., 2016). It was previously reported that there might be a possible synergy between miRNA and DNA methylation of cancer-related genes (Shivakumar et al., 2017). To be more specific, miRNAs regulate DNA methylation by modulating *DNMTs* or methylation-related proteins (Wang et al., 2017). DNA methylation involves the covalent addition of a methyl group to the 5-carbon position of cytosine by *DNMTs* and regulates gene transcription without changing the DNA sequence (Wu and Zhang, 2014). There are three major *DNMTs*: *DNMT3a*, *DNMT3b*, and *DNMT1*. *DNMT3a* and *DNMT3b* are *de novo* methyltransferases that establish the initial DNA methylation patterns, while *DNMT1* is the maintenance DNA methyltransferase that is the most abundant DNMT in various cell types (Jeltsch, 2002; Jin and Robertson, 2013). DNA methylation plays important roles in mammalian development, X chromosome inactivation, genomic integrity, and genomic imprinting. Aberrant DNA methylation has been implicated in a lot of disease conditions, such as neurological disease, cancer, and cardiovascular diseases (Robertson, 2005; Kanai and Hirohashi, 2007; Stenvinkel et al., 2007; Bergman and Cedar, 2013). DNA methylation status has also been linked to cell apoptosis and cell proliferation (Wang et al., 2016; Loginov et al., 2017). However, possible mechanisms of synergistic interactions between miRNA and DNA methylation on transcriptomic changes in bovine embryos and its association with pregnancy outcome are so far unknown.

For this study, we hypothesized that miR-10b would exert its detrimental effect on embryo development through influencing DNA methylation and/or directly targeting certain genes such as *HOXA1*. To test this hypothesis, we supplemented culture medium with miR-10b mimics and microinjected si*HOXA1* into embryos during *in vitro* bovine preimplantation embryo development and measured *DNMTs* mRNA levels.

METHODS AND MATERIALS

Experiment Design

In this study, miR-10b mimics were supplemented into presumed zygotes *in vitro* and embryos were cultured until day 8. Blastocysts were evaluated by morphological assessment and apoptosis staining. RT-qPCR was performed to determine the uptake of mimics by embryos and the expression of *DNMTs*. *HOXA1* was validated to be a direct target of miR-10b with dual-luciferase assay in embryos and MDBKs. To functionally study HOXA1, siHOXA1 was microinjected into presumed zygotes and embryos were cultured until day 8. Blastocysts were evaluated using similar parameters to miR-10b functional analysis. In addition, MDBKs were transfected with miR-10b mimics or siHOXA1. Cell viability and cell cycle were analyzed using WST-1 assay and PI staining.

MiR-10b Mimics Supplementation

All animal handlings were approved by the Ethical Committee of the Faculty of Veterinary Medicine (EC2013/118) of Ghent University. All methods were performed in accordance with the relevant guidelines and regulations. The rationale behind this experiment was to investigate whether miR-10b present in the culture medium can effectively be taken up by embryos and thus affect early embryo development. To this end, bovine embryos were produced according to the previously used routine *in vitro* fertilization (IVF) methods in our lab (Wydooghe et al., 2014). Briefly, to obtain cumulus oocyte complexes from 4- to 8-mm-diameter follicles, ovaries were collected from a slaughterhouse and aspirated with a needle and fluid was pooled. Cumulus oocyte complexes were then cultured in groups of 60 in 500-µl maturation media-containing TCM199 (Life Technologies, Ghent, Belgium) supplemented with 20% heat-inactivated fetal bovine serum (FBS) (Biochrom AG, Berlin, Germany) at 38.5°C in 5% CO_2 in the air. After 22 h, frozen–thawed bovine spermatozoa were separated using a Percoll gradient (GE Healthcare Biosciences, Uppsala, Sweden). The final sperm concentration for fertilization was 1×10^6 spermatozoa/ml. After 21 h, presumed zygotes were transferred to 50-µl drops of synthetic oviductal fluid (SOF) supplemented with ITS (5 µg/ml insulin + 5 µg/ml transferrin + 5 ng/ml selenium) and 4 mg/ml BSA. MiRNA mimics (double-stranded, chemically synthesized RNAs that mimic mature endogenous miR-10b) or control mimics (double-stranded, chemically synthesized RNAs that have no homology to any known microRNA or mRNA sequences) were purchased from Qiagen (Germantown, USA) and supplemented into the culture medium of presumed zygotes with a final concentration of 1 µM. Culture occurred in groups of 25, covered with mineral oil at 38.5°C in 5% CO_2, 5% O_2, and 90% N_2. Embryo quality was assessed during development and all blastocysts (day 8) were collected for RNA and immunofluorescence analysis.

TUNEL Staining

TUNEL staining was performed using a previously described protocol (Ortiz-Escribano et al., 2017) with a commercial *in situ* cell death detection kit (Sigma, St. Louis, USA). Blastocysts were fixed in neutral buffered 4% paraformaldehyde at room temperature (RT) for 1 h, and then permeabilized with 0.1% Triton X-100 at RT for 10 min. Afterwards, blastocysts were incubated with 20 µl of TUNEL mixture for 1 h at 37°C and subsequently washed three times in phosphate-buffered saline (PBS) and finally stained with 10 µg/ml 4′,6-diamidino-2-phenylindool (DAPI) for 10 min. Slides were examined using a 20× water immersion objective on a Leica TCS-SP8 X confocal microscope (Leica Microsystems, Wetzlar, Germany). The apoptosis ratio was expressed as the total number of TUNEL-positive cells relative to the total number of the cells per blastocyst.

Microinjection

The microinjection was performed using the previously described protocol (Goossens et al., 2010; Vandenberghe et al., 2018). Briefly, bovine zygotes were produced *in vitro* and randomly divided into three groups: (Valadi et al., 2007) a control group of zygotes that was not manipulated (Donker et al., 2012), a test group of zygotes that were injected with the short-interfering RNA (siRNA) targeting *HOXA1* (Luo et al., 2009), and zygotes injected with a non-target control siRNA (siNTC) (Qiagen, Germantown, USA). The injections were performed on an inverted microscope (Olympus, Tokyo, Japan) using piezo drill assisted micromanipulation (Narishige, London, UK). During injection, zygotes were kept at 38°C in 5-µl droplets of Hepes-buffered TCM-199 covered with mineral oil. Ten picoliters of siRNA (20 µM) was injected into the cytoplasm of zygotes 21 h post insemination (hpi). Subsequently, zygotes were washed with SOF and then cultured in groups of 25 in 50-µl droplets of SOF covered with mineral oil at 38.5°C in 5% CO_2, 5% O_2, and 90% N_2. Embryo survival was checked after injection, and the cleavage rate (48 hpi) and the percentage of blastocysts [8 days post insemination (dpi)] were determined. Blastocysts were collected for RNA and for immunofluorescence analysis. Three replicates (n = 25 each) were performed.

RNA Isolation and RT-qPCR

The expression patterns of *HOXA1* and *DNMTs* were analyzed using RT-qPCR. Total RNA was isolated from three pools of five blastocysts each using the RNeasy Micro kit (Qiagen, Germantown, USA) and reverse transcribed using the iScript cDNA synthesis kit (BioRad, Brussels, Belgium). RT-qPCR was performed on a BioRad CFX 96 PCR detection system by mixing 2.5 µl of template cDNA with 5 µl of Sso Advanced SYBR Green Supermix (BioRad, Brussels, Belgium) and 300 nM of each primer in a 10-µl total volume. The PCR program consisted of an initial denaturation step at 95°C for 3 min, followed by 40 cycles of denaturation at 95°C for 5 s and a combined primer annealing-extension step at specific primer annealing temperatures for 30 s. A melting curve was produced afterwards by heating samples from 70°C to 95°C in 0.5°C increments for 5 s to confirm a single specific peak for each pair of primers (**Supplementary Table S1**). *GAPDH* and *YWHAZ*, previously shown to be stable in bovine embryos (Goossens et al., 2005), were quantified to normalize mRNA expression levels using geNorm (Vandesompele et al., 2002). RT-qPCR reactions were performed in triplicate, and the $2^{-\Delta\Delta Ct}$ method was used to analyze the data. The primer sequences used for RT-qPCR are listed in **Supplementary Table S1**.

The expression pattern of miR-10b was analyzed using RT-qPCR. MiRNA was isolated from three pools of five blastocysts each using the miRNeasy Mini kit (Qiagen, Germantown, USA) and reverse transcribed using a miScript II RT kit (Qiagen, Germantown, USA). The miRNA levels were quantified with a miScript SYBR Green Kit containing 10 × miScript Universal Primer (Qiagen, Germantown, USA). The RT-qPCR was performed by mixing 1 µl of template cDNA with 5 µl of 2 × QuantiTect SYBR Green PCR Master Mix (Qiagen, Germantown, USA), 10 × miScript Primer assay, and 10 × miScript Universal Primer in 10 µl of final volume. The PCR program consisted of an initial denaturation step at 95°C for 15 min, followed by 40 cycles of denaturation at 94°C for 15 s, a combined primer annealing-extension step at specific primer annealing temperatures for 30 s and then at 70°C for 30 s. A melting curve was produced afterwards by heating samples from 70°C to 95°C in 0.5°C increments for 5 s to confirm a single specific peak for each pair of primers. *U6* (Mondou et al., 2012; Abd El Naby et al., 2013) and *SNORD61* (Qiagen, Germantown, USA), previously shown to be stable in bovine embryos, were quantified to normalized mRNA expression levels using geNorm (Vandesompele et al., 2002).

Cell Culture and Transfection

HEK293Ts or MDBKs were thawed and resuspended in Dulbecco Modified Eagle Media (DMEM) (Thermo Fisher Scientific, Waltham, USA) containing penicillin/streptomycin (100 U/ml) and 10% FBS (VWR, Radnor, USA). Culture occurred at 37°C, 5% CO_2 in an incubator. MiR-10b mimics or control mimics were delivered into MDBKs using Hiperfect reagent (Qiagen, Germantown, USA) in Opti-MEM media (with a final concentration of 50 nM). SiRNA or siNTC was transfected into MDBKs using Lipofectamine 2000 (Invitrogen, Carlsbad, USA) according to the manufacturer's instructions (with a final concentration of 500 nM). Twenty-four or 48 h after transfection, total RNA or protein was extracted for RT-qPCR or Western blotting (WB).

Validation of *HOXA1* as a Target of miR-10b

To understand the mechanisms by which miR-10b induces apoptosis of embryonic cells, we used three computational algorithms, Targetscan, PicTar, and Miranda, to identify putative miR-10b targets in cattle. If a target was identified by all three algorithms, it was considered likely to be a miRNA target. Of the putative target genes identified in this way, *HOXA1* was chosen for further analysis because it was previously shown to be implicated in cell proliferation in human epithelial cells (Bitu et al., 2012) and cell growth, invasion, and migration in esophageal cancer cells (Li et al., 2017), which makes it of particular interest. The

wild-type 3′UTR of *HOXA1* (594 bp) (NC_037331.1) containing the predicted miR-10b binding site was amplified and ligated into the psiCHECK2 vector (Promega, Madison, USA) *via* NotI and XhoI sites and subsequently confirmed by sequencing. To test whether the predicted miR-10b target site in the *HOXA1* 3′UTR is critical for the miR-10b-mediated repression of *HOXA1* expression, the seed sequence of the predicted miR-10b's binding site was mutated. The primer sequences used for vector construction are listed in **Supplementary Table S1**.

HEK293T cells (70–80% confluency) were co-transfected with 500 ng of plasmid harboring wild-type or mutant sequences of the 3′UTR of *HOXA1* and 5 nM miR-10b mimics/control mimics using Lipofectamine 2000 in Opti-MEM media. Transfected cells were collected 24 h post-transfection and assayed using the Dual Luciferase reporter Kit (Promega, Madison, USA).

Protein Isolation and Western Blot

Western blot was carried out using standard methods. Briefly, total protein was extracted from cultured cells 48 h after transfection using radioimmunoprecipitation lysis buffer consisting of 50 mM Tris–HCl (pH 7.5), 1% NP-40, 0.1% SDS, 0.5% sodium deoxycholate, 150 mM NaCl, and protease inhibitors. Before being loaded onto 10% SDS-polyacrylamide gels, the samples were denatured for 10 min at 100°C. Separated proteins were then transferred onto nitrocellulose membranes and subsequently blocked overnight with 5% non-fat milk in PBS with 0.1% Tween-20. Afterwards, membranes were incubated overnight with 1/1,000 rabbit anti-HOXA1 (Novus Biologicals, Abingdon, UK) or 1/1,000 rabbit anti-β-actin. After three washes, the membranes were incubated with HRP-conjugated goat anti-rabbit IgG (H+L) at room temperature for 2 h. Signals were detected by autograph using SuperSignal West Femto Maximum Sensitivity Substrate (Thermo Fisher Scientific, Waltham, USA).

Cell Cycle Assays: PI Staining and Flow Cytometry

Forty-eight hours after transfection, MDBKs were collected by centrifugation, followed by fixation in ice-cold 70% ethanol at 4°C overnight. Then, the cells were stained with a final concentration of 50 μg/ml propidium iodide PI and 100 μg/ml RNase A in PBS. After 30 min in the dark, the stained cells were analyzed using Accuri™ C6 flow cytometry (BD, Erembodegem, Belgium).

Cell Viability Assays: WST-1 Colorimetric Assay

Cell viability was determined using the WST-1(4-(3-(4-iodophenyl)-2-(4-nitrophenyl)-2H-5-tetrazolio)-1,3-benzene disulfonate) (Merck, Kenilworth, USA). The assay was performed with ~20,000 cells using 96-well plates. Forty-eight hours after transfection, 10 μl of WST-1 was added to 90-μl samples. The samples were then measured at 450 nm wavelength (570 nm as a reference wavelength) on an EZ read 400 microplate reader (Biochrom, Holliston, USA). After background subtraction, the viability was determined by comparing the absorbance values of samples.

STATISTICAL ANALYSIS

The statistical analyses were performed using Student's *t* test or ANOVA followed by Tukey's test using GraphPad prism version 5. For each analysis, $P < 0.05$ was considered significant. The data are presented as mean ± S.D. and derived from at least three independent experiments.

RESULTS

MiR-10b Mimics Can Be Taken Up by Bovine Embryos and Increase Apoptosis of Embryonic Cells

RT-qPCR results showed that miR-10b is indeed taken up by the embryos as its levels were noticeably higher (approximately 70 times) in the miR-10b mimics supplemented group compared with the control mimics group (**Figure 1A**). No significant difference was found in cleavage or blastocyst rate between the miR-10b mimics group and the control mimics group (**Figures 1B**, **C**). However, TUNEL staining showed a higher apoptosis rate in the miR-10b mimics group (10.52%) than in the control mimics group (4.88%) (**Figures 1D**, **E**).

MiR-10b Regulates the Expression of HOXA1 Protein

The *HOXA1*-encoded mRNA contains a 3′UTR element that is complementary to the miR-10b seed sequence (**Figure 2A**). To evaluate whether miR-10b directly targets *HOXA1*, we constructed luciferase reporter plasmids with wild-type (psiCHECK2-*HOXA1*-WT-3′UTR) and a mutated 3′UTR (psiCHECK2-*HOXA1*-MUT-3′UTR). After co-transfecting the reporters with miR-10b mimics into HEK293T cells, we observed a clear reduction in the activity of the luciferase reporter gene fused to the wild-type *HOXA1* 3′UTR (63.5% reduction, **Figure 2B**).

After miR-10b mimics supplementation into embryo culture medium, no significant mRNA difference could be observed (**Figure 2C**), but a reduction of the endogenous HOXA1 protein was clear (**Figure 2D**). This indicates that miR-10b directly targets *HOXA1* and inhibits translation of the mRNA.

Since further functional analysis of miR-10b and *HOXA1* was out of practical necessity, performed using a bovine cell line (MDBK), the direct relationship between miR-10b and *HOXA1* was also analyzed on MDBKs. MiR-10b mimics were delivered into MDBKs with Lipofectamine 2000 and the expression of *HOXA1* was examined using RT-qPCR and WB. No significant differences were found at the mRNA level (**Figure 2E**), while HOXA1 protein levels were reduced in the miR-10b mimics group compared with the control mimics group (**Figure 2F**), in agreement with the results obtained on embryos. Other potential targets of miR-10b are listed in **Supplementary Table S2**. Among these potential target genes, *HOXD10* has been already proven to be a direct target of miR-10b and regulates cell proliferation in human glioblastoma cells and hepatocellular carcinoma cells (Su et al., 2001; Chisaka and Kameda, 2005).

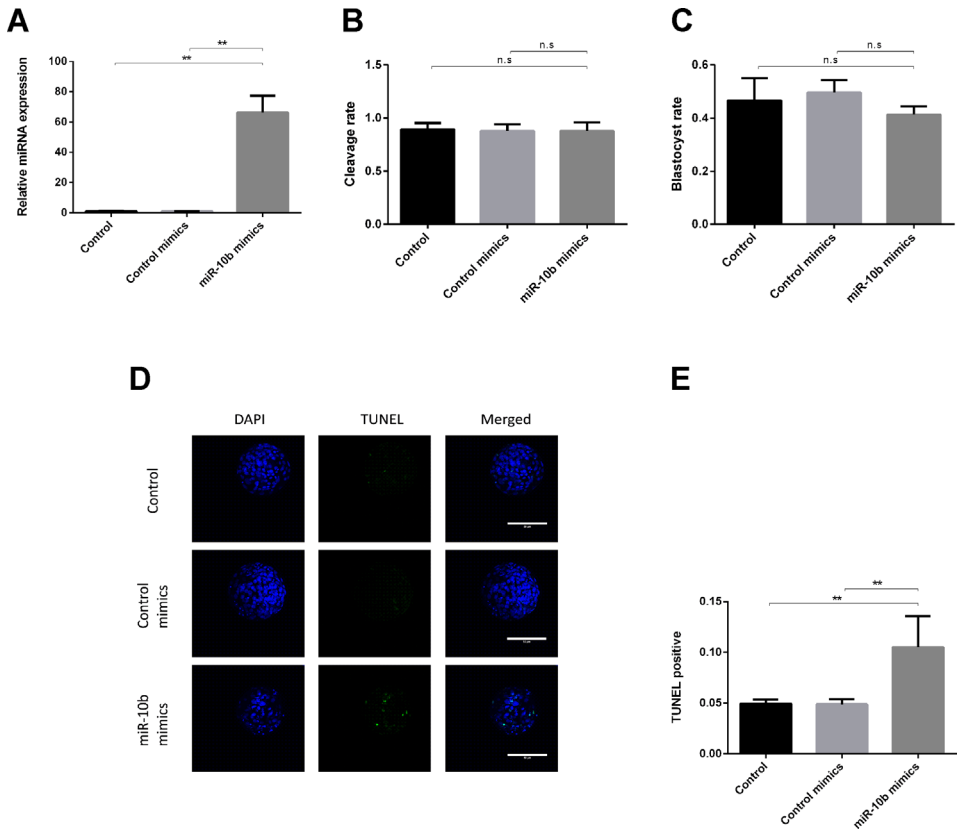

FIGURE 1 | Effects of miR-10b mimics on embryo growth and apoptosis. **(A)** Embryos were treated with miR-10b mimics and the relative expression level of miR-10b was detected using RT-qPCR at 8 dpi. **(B** and **C)** Cleavage and blastocyst rate of embryos treated with miRNA mimics or control mimics were assessed. **(D** and **E)** Apoptosis rate of embryos was determined by TUNEL staining. The statistical analyses were performed using one-way ANOVA and data are presented as mean ± SD of three experiments (**$P < 0.01$; ns, no significance).

HOXA3, another member of the HOX family, was reported to regulate cell proliferation in mouse thymic epithelial cells and neural crest cells (Su et al., 2001; Chisaka and Kameda, 2005) and differentiation in human hematopoietic progenitor cells (Mahdipour et al., 2011).

MiR-10b Mimics Result in Aberrant *DNMTs* Expression in Bovine Embryos

Recent studies have shown that epigenetic changes such as DNA methylation and miRNAs play crucial roles in embryonic development (Greenberg et al., 2016; Liu et al., 2016; Okada and Yamaguchi, 2017). However, the interaction mechanisms between miRNAs and DNA methylation have remained largely unexplored. In this study, we examined expression of *DNMTs* after supplementation of miR-10b mimics into embryo culture media. The expression of *DNMT1* was significantly lower in the miR-10b mimics-treated group compared with the control mimics group, while *DNMT3b* expression was significantly higher in the miR-10b mimics group compared with the control mimics group. No significant differences were found in *DNMT3a* for embryos cultured with miR-10b mimics versus control mimics (**Figure 3**).

Microinjection of si*HOXA1* Increases Apoptosis of Embryonic Cells and Downregulates *DNMTs* in Bovine Embryos

To investigate the possible mechanisms of *HOXA1*'s function on embryos, blastocyst formation was determined and the expression of *DNMTs* in embryos was validated after si*HOXA1* microinjection. As presented in **Figure 4A**, the cleavage rate showed no significant difference between the si*HOXA1*-injected group and the siNTC-injected group, while the blastocyst rate was decreased in the si*HOXA1*-injected group compared with the siNTC-injected group, but the change did not reach statistical significance (**Figure 4B**). TUNEL staining showed that the apoptosis rate in the si*HOXA1*-injected group was 18.06%, while it was 4.07% in the siNTC-injected group (**Figures 4C**, **D**), meaning that the injection of si*HOXA1* increased apoptosis of embryonic cells.

We also examined expression of *HOXA1* mRNA and *DNMTs* mRNA after injecting si*HOXA1* into embryos. The expression of *HOXA1* was 10.8 times lower in the si*HOXA1*-injected group than in the siNTC-injected group (**Figure 4E**). The expression of *DNMT1* (5.2 times), *DNMT3a* (8.7 times), and *DNMT3b* (5.2 times) was found to be significantly decreased in the si*HOXA1* injected group compared to the siNTC group (**Figure 4E**).

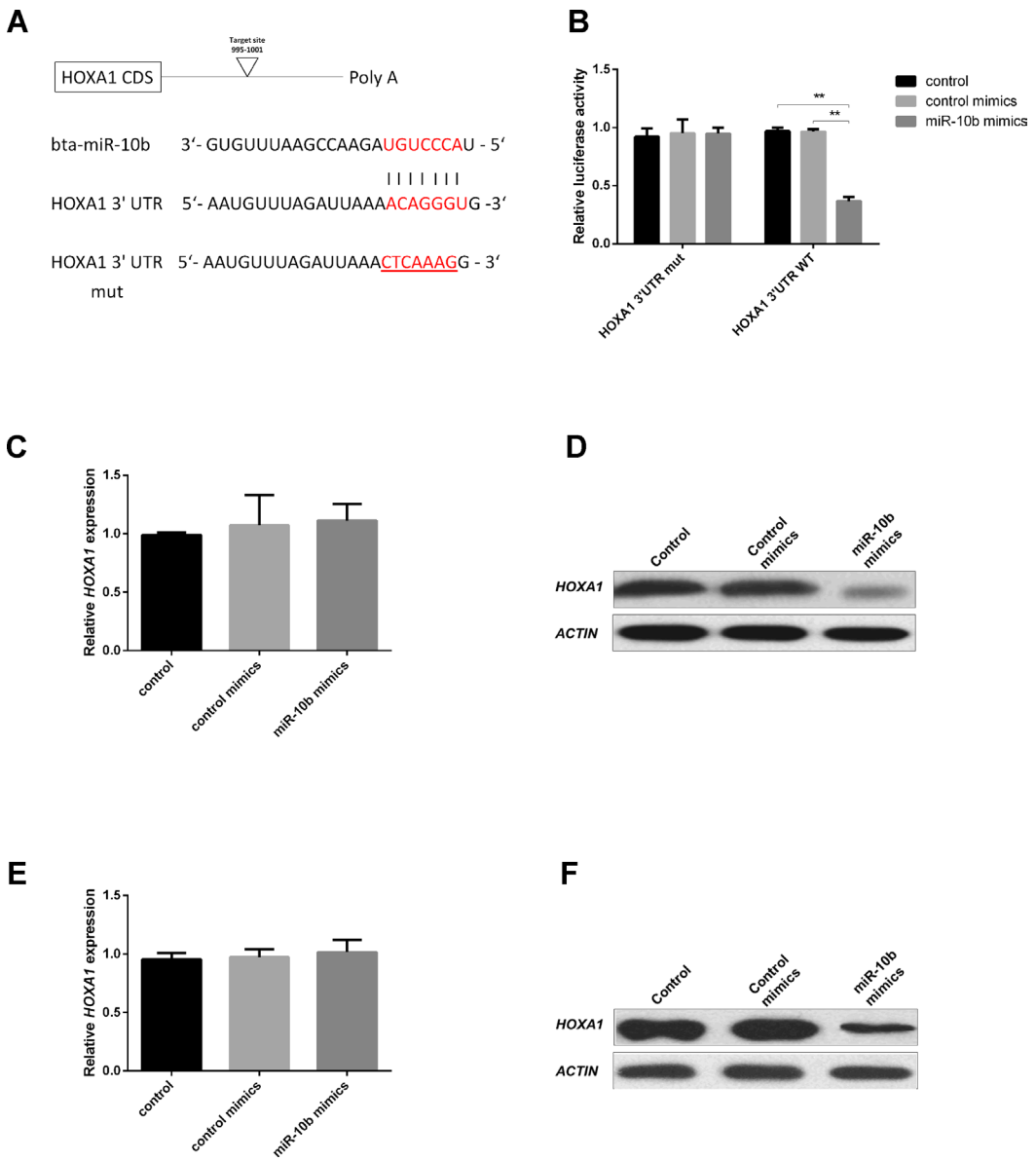

FIGURE 2 | *HOXA1* is a direct target of miR-10b. **(A)** 3′UTR analysis of *HOXA1* containing putative regions that match the seed sequence of miR-10b, and the mutated nucleotides are underlined. **(B)** Overexpression of miR-10b inhibited Renilla luciferase activities. HEK-293T cells were cotransfected with 500 ng of reporter plasmid containing the MUT or WT-type UTRs and 5 nM miR-10b mimics. After 24 h, Renilla luciferase was normalized against firefly luciferase and then presented. **(C** and **D)** Embryos were treated with miR-10b mimics or control mimics and the relative levels of *HOXA1* were detected with RT-qPCR and WB. **(E** and **F)** MiR-10b mimics were transfected into MDBKs. After 48 h or 24 h, cells were harvested for RT-qPCR or WB. The statistical analyses were performed using ANOVA and data are presented as mean ± SD of three experiments (**$P < 0.01$).

MiR-10b Overexpression and *HOXA1* Knockdown in MDBKs Decrease Cell Viability

Although miR-10b has been shown to regulate cell progression in human and mouse, the regulatory relationship is still unclear in bovine. To further verify the above results, we explored the effect of miR-10b overexpression and *HOXA1* knockdown on cell progression using the bovine cell line MDBK. MDBKs were transfected with miR-10b mimics or si*HOXA1*, and their expression was assessed using RT-qPCR. As presented in **Figures 5A**, **B**, the expression of miR-10b was successfully increased in MDBKs by delivery of miR-10b mimics and *HOXA1* expression was significantly knocked down in MDBKs by transfection with si*HOXA1*.

The cellular metabolic activity, which indicates cell viability, was monitored using the WST-1 assay. As shown in **Figure 5C**, cell viability was reduced in miR-10b mimics-delivered cells (28%) compared with control mimics-delivered cells. Similarly, the inhibition of *HOXA1* significantly decreased the cell viability (34%).

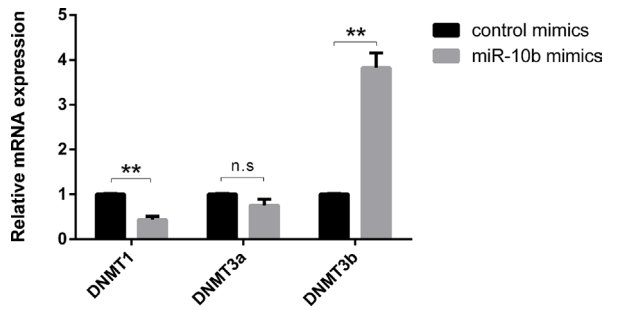

FIGURE 3 | Effects of miR-10b mimics on *DNMTs* expression. Embryos were treated with miR-10b mimics and the relative expression levels of *DNMTs* were detected using RT-qPCR at 8 dpi. The statistical analyses were performed using two-way ANOVA, and data are presented as mean ± SD of three experiments (**$P < 0.01$; ns, no significance).

MiR-10b Overexpression and *HOXA1* Knockdown in MDBKs Slow Down the Cell Cycle

To elucidate the mechanism of growth inhibition by miR-10b overexpression and *HOXA1* downregulation, flow cytometry was used to analyze the cell cycle in MDBKs. The intensity of PI staining has a positive correlation with the number of cells. A higher proportion of cells in G1 indicates the slowing down of the cell cycle, while a higher proportion of cells in G2 and S stages indicates the promoting of the cell cycle. As shown in **Figure 5D**, cell cycle phase displayed a 7.66% increase of treated cells in the G1 phase and an 8.13% decrease in the S phase after the delivery of miR-10b mimics, indicating cell growth suppression. Similarly, knockdown of *HOXA1* resulted in a 10.86% increase in cell number in the G1 phase and an 11.48% decrease in the S phase compared with the siNTC-transfected group.

DISCUSSION

In our previous study (Lin et al., 2019), we have reported that several miRNAs were differentially released into conditioned media from bovine embryos with different developmental competence. One of those, miR-10b, was previously shown to be expressed in bovine embryos (Goossens et al., 2013), oocytes (Abd El Naby et al., 2013), follicles, and ovarian tissues (Huang et al., 2011; Gebremedhn et al., 2015). Several studies have shown that miR-10b plays important roles in cell apoptosis, cell proliferation, cell migration, and invasion in

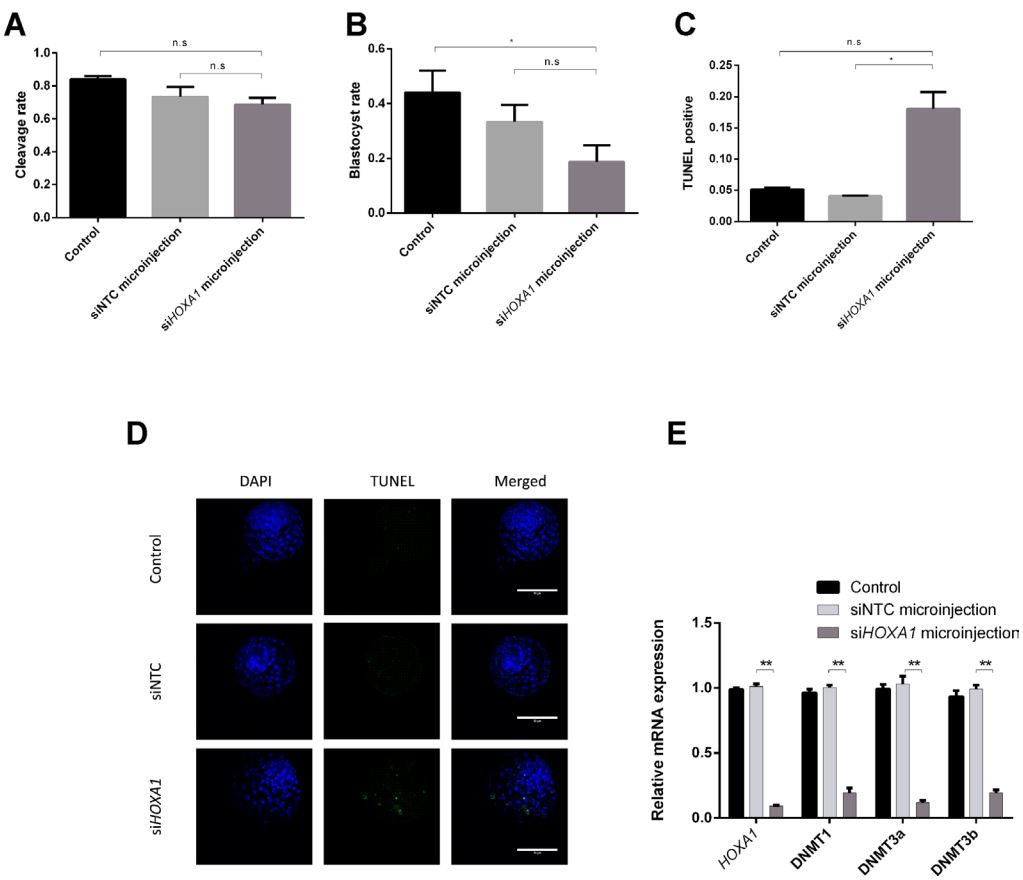

FIGURE 4 | Effects of *HOXA1* in embryo growth, apoptosis, and *DNMTs*. Embryos were injected with si*HOXA1* and the cleavage rate **(A)** and blastocyst rate were assessed **(B)**; cell apoptosis was determined by TUNEL staining **(C** and **D)**; *HOXA1* and *DNMTs* expressions were evaluated using RT-qPCR **(E)**. The statistical analyses were performed using ANOVA and data are presented as mean ± SD of three experiments (*$P < 0.05$, **$P < 0.01$; ns, no significance).

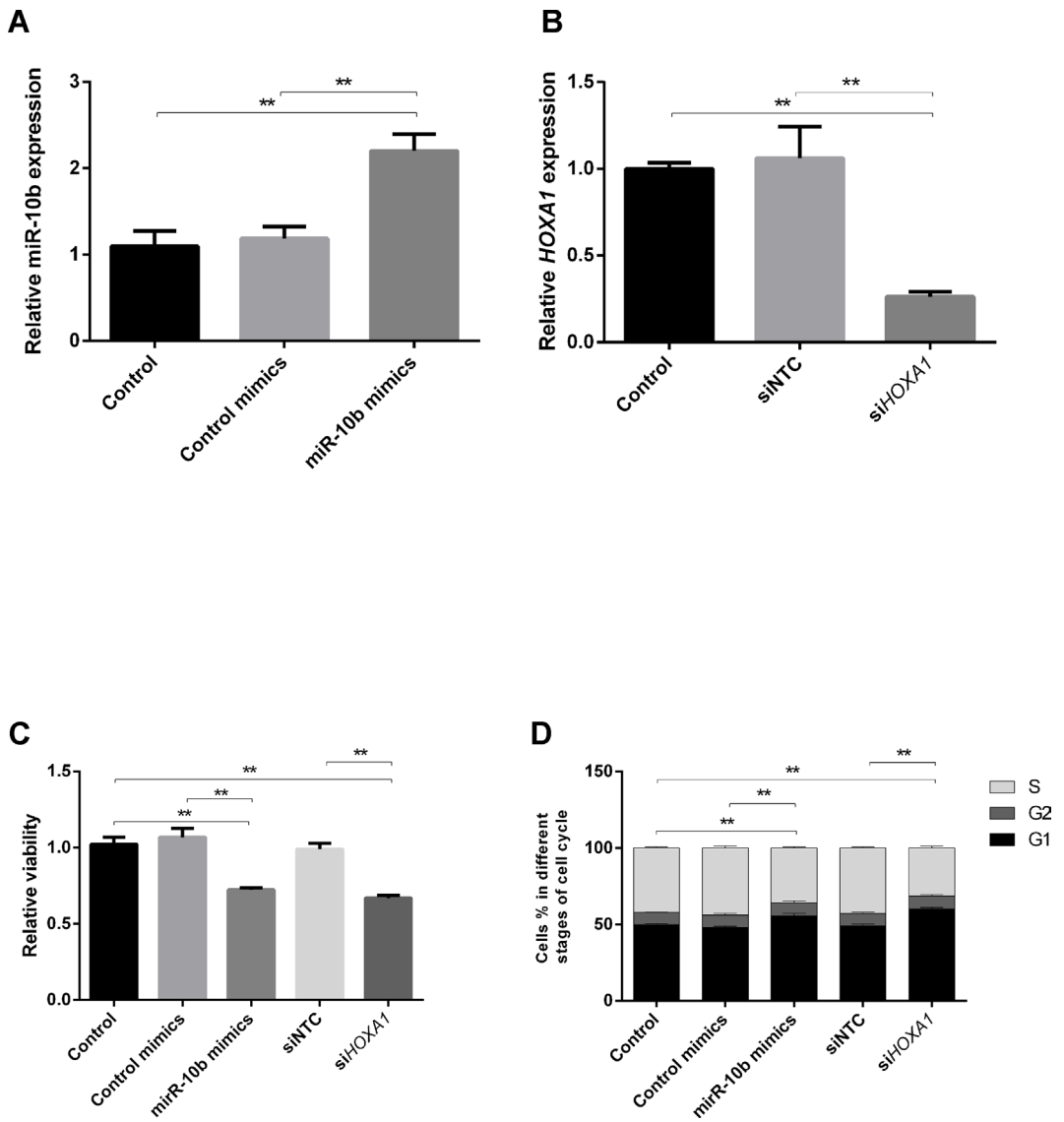

FIGURE 5 | Effects of miR-10b overexpression and *HOXA1* knockdown on cell progression**. (A** and **B)** MDBKs were reverse transfected with miR-10b mimics or si*HOXA1* for 48 h. RT-qPCR was then performed to assess the expression of miR-10b and *HOXA1*. **(C** and **D)** MDBKs were reverse transfected with miR-10b mimics or si*HOXA1* for 48 h. **(C)** Cell viability was measured using the WST-1 assay, and **(D)** cell cycle assay by PI staining. Data are presented as mean ± SD of three experiments (**$P < 0.01$).

human cancer cells (Wang et al., 2007; Liao et al., 2014; Chen et al., 2016; Zhen et al., 2016; Zhu et al., 2016; Guan et al., 2018), mouse cells (Tan et al., 2018), and goat granulosa cells (Peng et al., 2016).

To further investigate how miR-10b negatively impacts bovine preimplantation bovine quality, we tested two possible mechanisms based on target gene prediction and literature.

Firstly, we tested *HOXA1* and verified it as a direct target of miR-10b. As one of the HOX family members, *HOXA1* is involved in various biological processes, including cell apoptosis and growth (Zhang et al., 2018). For instance, it was demonstrated that *HOXA1* can inhibit the migration, invasion and growth of HepG2 cells (Zha et al., 2012). Besides, forced expression of *HOXA1* in human mammary carcinoma cells resulted in increased proliferation and decreased apoptotic cell death in a Bcl-2-dependent manner (Zhang et al., 2003). In addition, *HOXA1* was found to enhance cell invasion, proliferation, and metastasis of prostate cancer cells (Wang et al., 2015). By microinjecting si*HOXA1* into zygotes, we found increased apoptosis in bovine embryos, an effect similar to after adding miR-10b mimics. The combination of these results with the observation that the HOXA1 protein level was decreased after supplementing miR-10b mimics into culture medium of embryos gives an indication that miR-10b might induce apoptosis of embryonic cells *via* targeting *HOXA1*. This could be in a Bcl-2-dependent manner as mentioned above, or through regulating other proteins involved

in the apoptotic process, such as Bax, Bak, Bcl-xL, Fas, and FADD (Zhang et al., 2003).

Secondly, we tested if miR-10b exerts its negative effect on embryo development by interacting with the DNA methylation status. Since *DNMTs* are known to be involved in the maintenance of methylation patterns of genes (*DNMT1*) and de novo methylation (*DNMT3a* and *DNMT3b*), we investigated the mRNA levels of all three members after miR-10b mimics supplementation in culture medium. This resulted in a decrease in *DNMT1* expression, an increase of *DNMT3b* expression, and no effect on *DNMT3a*. The maintenance of methylation and de novo methylation are two distinct processes that are required for the establishment and mitotic inheritance of tissue-specific methylation patterns. *DNMT1* is recognized as the maintenance *DNMT* that copies methylation patterns after DNA replication as it has a preference for hemimethylated, rather than unmethylated DNA (Talbot et al., 1997). Loss of *Dnmt1* in mice has been reported to cause global DNA methylation loss and embryonic death (Tsumura et al., 2006). Moreover, loss of *DNMT1* in human colon cancer cell lines contributes to growth impairment (Rhee et al., 2002). *DNMT3b* is essential for early embryonic development and responsible for de novo methylation (Watanabe et al., 2002; Uysal et al., 2017). In fact, overexpression of *DNMT3b* was shown to result in aberrant DNA methylation in T-cell acute lymphoblastic leukemia (Poole et al., 2017) and to be significantly correlated with unfavorable prognosis in various human malignancies (Kim et al., 2006; Park et al., 2006; Vallböhmer et al., 2006; Wang et al., 2006; Lin et al., 2007; Xing et al., 2008).

Our data indicate an interaction between miRNA expression and DNA methylation, which is in agreement with other studies (Kim et al., 2014; Shivakumar et al., 2017; Wang et al., 2017). Taken together, the *DNMT1* downregulation and *DNMT3b* overexpression after overexpressing miR-10b found in the present study points to a link between aberrant DNA methylation and hampered development in bovine embryos. To our knowledge, this is the first study focusing on miRNAs regulation of DNA methylation in bovine embryos.

Since our results outlined above showed that miR-10b regulates both *HOXA1* and *DNMTs*, we further investigated the possible relationship between *HOXA1* and DNA methylation. Microinjection of si*HOXA1* clearly downregulated all three *DNMTs*, indicating that miR-10b may exert its inhibitory effect on *DNMT1* by regulating *HOXA1*, as *DNMT1* mRNA has no binding site for miR-10b (according to three computational methods: Targetscan, PicTar and Miranda) and hence is not a direct target of miR-10b. In a similar way, *DNMT3b* mRNA also has no binding site for miR-10b, which indicates that the upregulation of *DNMT3b* by miR-10b could be an indirect effect mediated by one or multiple other targets of miR-10b. Moreover, miR-10b overexpression and HOXA1 knockdown resulted in aberrant DNMT expression and an increased embryo apoptosis ratio. Previous findings in human cancer cells have shown that cell apoptosis and cell proliferation are related to DNA methylation, and DNA methylation can help inactivate apoptotic pathways at several points (Cho et al., 2011; Ye et al., 2016; Costa et al., 2017; Loginov et al., 2017).

Considering the fact that the compaction of embryos makes it difficult to use them for flow cytometry analysis, a complementary study regarding the effect of miR-10b overexpression and *HOXA1* knockdown on cell cycle was performed using the bovine cell line MDBK. The delivery of miR-10b mimics to MDBKs resulted in reduced cell viability and a high proportion at G1 stage. Similarly, the transfection of si*HOXA1* also led to reduced cell viability and a high proportion at G1 stage, indicating that miR-10b suppresses cell growth by targeting *HOXA1* and thus complementing the results obtained in the embryos.

Given the above results, bovine embryo-secreted miR-10b can be regarded as a potential biomarker for suppressed preimplantation developmental competence. miRNAs are gaining interest as potential biomarkers for diseases (Mitchell et al., 2008; Qu et al., 2017; Ma, 2018), embryo development in cattle (Kropp and Khatib, 2015), and embryo viability in human (Rosenbluth et al., 2014). According to the majority of studies, miRNAs are stable biomarkers. For instance, it was shown that miRNA levels remain remarkably stable when plasma is freeze–thawed multiple times or subjected to prolonged room temperature incubation (Mitchell et al., 2008). Besides, it was reported that miRNAs were stable frozen or refrigerated for 72 h and at room temperature for 24 h (McDonald et al., 2011). Apart from the stability, a biomarker should be easily detected. We have found miR-10b to be significantly higher expressed in the conditioned media of degenerate embryos compared to blastocysts in a previous study (Lin et al., 2019).

In this study, we examined the effects of embryo-secreted miR-10b on apoptosis and DNA methylation in bovine embryos. We conclude that miR-10b enhances apoptosis of embryonic cells *via* targeting *HOXA1*. Additionally, we found aberrant *DNMTs* expression after miR-10b mimics supplementation into embryo culture medium. As *DNMTs* are not direct targets of miR-10b, it probably exerts its effect on these genes through a network of other genes, among which is *HOXA1*.

DATA AVAILABILITY

All data generated or analyzed during this study are included in this published article and its Supplementary Information file.

ETHICS STATEMENT

All animal handlings were approved by the Ethical Committee of the Faculty of Veterinary Medicine (EC2013/118) of Ghent University. All methods were performed in accordance with the relevant guidelines and regulations.

AUTHOR CONTRIBUTIONS

XL performed the experiment and wrote the manuscript. KP helped to produce and stain embryos. KS contributed to the microinjection experiments. DD, BH, AS, and LP participated in the study design. All authors reviewed the manuscript.

ACKNOWLEDGMENTS

This work was supported by Ghent University (BOF GOA project 01G01112). The authors thank Petra Van Damme for her excellent technical assistance.

SUPPLEMENTARY MATERIAL

The Supplementary Material for this article can be found online at: https://www.frontiersin.org/articles/10.3389/fgene.2019.00757/full#supplementary-material

REFERENCES

Abd El Naby, W. S., Hagos, T. H., Hossain, M. M., Salilew-Wondim, D., Gad, A. Y., Rings, F., et al. (2013). Expression analysis of regulatory microRNAs in bovine cumulus oocyte complex and preimplantation embryos. *Zygote* 21, 31–51. doi: 10.1017/S0967199411000566

Bergman, Y., and Cedar, H. (2013). DNA methylation dynamics in health and disease. *Nat. Struct. Mol. Biol.* 20, 274. doi: 10.1038/nsmb.2518

Bitu, C. C., Destro, M. F., Carrera, M., da Silva, S. D., et al. (2012). HOXA1 is overexpressed in oral squamous cell carcinomas and its expression is correlated with poor prognosis. *BMC Cancer* 12, 146. doi: 10.1186/1471-2407-12-146

Chen, H., Fan, Y., Xu, W., Chen, J., Xu, C., Wei, X., et al. (2016). miR-10b inhibits apoptosis and promotes proliferation and invasion of endometrial cancer cells via targeting HOXB3. *Cancer Biother. Radiopharm.* 31, 225–231. doi: 10.1089/cbr.2016.1998

Chisaka, O., and Kameda, Y. (2005). Hoxa3 regulates the proliferation and differentiation of the third pharyngeal arch mesenchyme in mice. *Cell Tissue Res.* 320, 77. doi: 10.1007/s00441-004-1042-z

Cho, H.-S., Kelly, J. D., Hayami, S., Toyokawa, G., Takawa, M., Yoshimatsu, M., et al. (2011). Enhanced expression of EHMT2 is involved in the proliferation of cancer cells through negative regulation of SIAH1. *Neoplasia* 13, 676–IN10. doi: 10.1593/neo.11512

Costa, S. F. S., Pereira, N. B., Pereira, K. M. A., Campos, K., de Castro, W. H., Diniz, M. G., et al. (2017). DNA methylation pattern of apoptosis-related genes in ameloblastoma. *Oral Dis.* 23, 779–783. doi: 10.1111/odi.12661

Donker, R. B., Mouillet, J. F., Chu, T., Hubel, C. A., Stolz, D. B., Morelli, A. E., et al. (2012). The expression profile of C19MC microRNAs in primary human trophoblast cells and exosomes. *Mol. Hum Reprod.* 18, 417–424. doi: 10.1093/molehr/gas013

Gebremedhn, S., Salilew-Wondim, D., Ahmad, I., Sahadevan, S., Hossain, M. M., Hoelker, M., et al. (2015). MicroRNA expression profile in bovine granulosa cells of preovulatory dominant and subordinate follicles during the late follicular phase of the estrous cycle. *PLOS One* 10, e0125912. doi: 10.1371/journal.pone.0125912

Goossens, K., Van Poucke, M., Van Soom, A., Vandesompele, J., Van Zeveren, A., and Peelman, L. J. (2005). Selection of reference genes for quantitative real-time PCR in bovine preimplantation embryos. *BMC Dev. Biol.* 5, 27. doi: 10.1186/1471-213X-5-27

Goossens, K., Mestdagh, P., Lefever, S., Van Poucke, M., Van Zeveren, A., Van Soom, A., et al. (2013). Regulatory microRNA network identification in bovine blastocyst development. *Stem Cells Dev.* 22, 1907–1920. doi: 10.1089/scd.2012.0708

Goossens, K., Tesfaye, D., Rings, F., Schellander, K., Holker, M., Van Poucke, M., et al. (2010). Suppression of keratin 18 gene expression in bovine blastocysts by RNA interference. *Reprod. Fer. Develop* 22, 395–404. doi: 10.1071/RD09080

Greenberg, M. V. C., Glaser, J., Borsos, M., Marjou, F. E., Walter, M., Teissandier, A., et al. (2016). Transient transcription in the early embryo sets an epigenetic state that programs postnatal growth. *Nat. Genet.* 49, 110. doi: 10.1038/ng.3718

Guan, L., Ji, D., Liang, N., Li, S., and Sun, B. (2018). Up-regulation of miR-10b-3p promotes the progression of hepatocellular carcinoma cells via targeting CMTM5. *J. Cell. Mol. Med.* 22, 3434–3441. doi: 10.1111/jcmm.13620

Homer, H., Rice, G. E., and Salomon, C. (2017). Review: embryo- and endometrium-derived exosomes and their potential role in assisted reproductive treatments—Liquid biopsies for endometrial receptivity. *Placenta* 54, 89–94. doi: 10.1016/j.placenta.2016.12.011

Huang, J., Ju, Z., Li, Q., Hou, Q., Wang, C., Li, J., et al. (2011). Solexa sequencing of novel and differentially expressed microRNAs in testicular and ovarian tissues in Holstein cattle. *Int. J. Biol. Sci.* 7, 1016–1026. doi: 10.7150/ijbs.7.1016

Jeltsch, A. (2002). Beyond Watson and Crick: DNA methylation and molecular enzymology of DNA methyltransferases. *Chembiochem* 3 (4), 274–293. doi: 10.1002/1439-7633(20020402)3:4<274::AID-CBIC274>3.0.CO;2-S

Jin, B., and Robertson, K. D. (2013). DNA methyltransferases, DNA damage repair, and cancer. *Adv. Exp. Med. Biol.* 754, 3–29. doi: 10.1007/978-1-4419-9967-2_1

Kanai, Y., and Hirohashi, S. (2007). Alterations of DNA methylation associated with abnormalities of DNA methyltransferases in human cancers during transition from a precancerous to a malignant state. *Carcinogenesis* 28, 2434–2442. doi: 10.1093/carcin/bgm206

Kim, H., Kwon, Y. M., Kim, J. S., Han, J., Shim, Y. M., Park, J., et al. (2006). Elevated mRNA levels of DNA methyltransferase-1 as an independent prognostic factor in primary nonsmall cell lung cancer. *Cancer* 107, 1042–1049. doi: 10.1002/cncr.22087

Kim, D., Shin, H., Sohn, K.-A., Verma, A., Ritchie, M. D., and Kim, J. H. (2014). Incorporating inter-relationships between different levels of genomic data into cancer clinical outcome prediction. *Methods (San Diego, Calif.)* 67, 344–353. doi: 10.1016/j.ymeth.2014.02.003

Kropp, J., and Khatib, H. (2015). Characterization of microRNA in bovine in vitro culture media associated with embryo quality and development. *J. Dairy Sci.* 98, 6552–6563. doi: 10.3168/jds.2015-9510

Li, Q., Zhang, X., Li, N., Liu, Q., and Chen, D. (2017). miR-30b inhibits cancer cell growth, migration, and invasion by targeting homeobox A1 in esophageal cancer. *Biochem. Biophys. Res. Commun.* 485, 506–512. doi: 10.1016/j.bbrc.2017.02.016

Li, Y., Li, Y., Liu, J., Fan, Y., Li, X., Dong, M., et al. (2016). Expression levels of microRNA-145 and microRNA-10b are associated with metastasis in non-small cell lung cancer. *Cancer Boil. Ther.* 17, 272–279. doi: 10.1080/15384047.2016.1139242

Liao, C.-G., Kong, L.-M., Zhou, P., Yang, X.-l., Huang, J.-G., Zhang, H.-l., et al. (2014). miR-10b is overexpressed in hepatocellular carcinoma and promotes cell proliferation, migration and invasion through RhoC, uPAR and MMPs. *J. Transl. Med.* 12, 234. doi: 10.1186/s12967-014-0234-x

Lin, R.-K., Hsu, H.-S., Chang, J.-W., Chen, C.-Y., Chen, J.-T., and Wang, Y.-C. (2007). Alteration of DNA methyltransferases contributes to 5′CpG methylation and poor prognosis in lung cancer. *Lung Cancer* 55, 205–213. doi: 10.1016/j.lungcan.2006.10.022

Lin, X., Beckers, E., Mc Cafferty, S., Gansemans, Y., Joanna Szymańska, K., Chaitanya Pavani, K., et al. (2019). Bovine embryo-secreted microRNA-30c is a potential non-invasive biomarker for hampered preimplantation developmental competence. *Front. Genet.* 10, 315. doi: 10.3389/fgene.2019.00315

Liu, Z., Zhu, J., Cao, H., Ren, H., and Fang, X. (2012). miR-10b promotes cell invasion through RhoC-AKT signaling pathway by targeting HOXD10 in gastric cancer. *Int. J. Oncol.* 40, 1553–1560. doi: 10.3892/ijo.2012.1342

Liu, W., Niu, Z., Li, Q., Pang, R. T. K., Chiu, P. C. N., and Yeung, W. S.-B. (2016). MicroRNA and embryo implantation. *Am. J. Reprod. Immunol.* 75, 263–271. doi: 10.1111/aji.12470

Loginov, V. I., Pronina, I. V., Burdennyi, A. M., Pereyaslova, E. A., Braga, E. A., Kazubskaya, T. P., et al. (2017). Role of methylation in the regulation of apoptosis genes APAF1, DAPK1, and BCL2 in breast cancer. *Bull. Exp. Boil. Med.* 162, 797–800. doi: 10.1007/s10517-017-3716-z

Luo, S.-S., Ishibashi, O., Ishikawa, G., Ishikawa, T., Katayama, A., Mishima, T., et al. (2009). Human villous trophoblasts express and secrete placenta-specific microRNAs into maternal circulation via exosomes. *Biol. Reprod.* 81, 717–729. doi: 10.1095/biolreprod.108.075481

Ma, Y. (2018). The challenge of microRNA as a biomarker of epilepsy. *Curr. Neuropharmacol.* 16, 37–42. doi: 10.2174/1570159X15666170703102410

Mahdipour, E., Charnock, J. C., and Mace, K. A. (2011). Hoxa3 promotes the differentiation of hematopoietic progenitor cells into proangiogenic Gr-1+CD11b+ myeloid cells. *Blood* 117, 815. doi: 10.1182/blood-2009-12-259549

McDonald, J. S., Milosevic, D., Reddi, H. V., Grebe, S. K., and Algeciras-Schimnich, A. (2011). Analysis of circulating microRNA: preanalytical and analytical challenges. *Clin. Chem.* 57, 833. doi: 10.1373/clinchem.2010.157198

Mitchell, P. S., Parkin, R. K., Kroh, E. M., Fritz, B. R., Wyman, S. K., Pogosova-Agadjanyan, E. L., et al. (2008). Circulating microRNAs as stable blood-based markers for cancer detection. *Proc. Natl. Acad. Sci.* 105, 10513. doi: 10.1073/pnas.0804549105

Mondou, E., Dufort, I., Gohin, M., Fournier, E., and Sirard, M. A. (2012). Analysis of microRNAs and their precursors in bovine early embryonic development. *MHR Basic Sci. Reprod. Med.* 18, 425–434. doi: 10.1093/molehr/gas015

Nakayama, I., Shibazaki, M., Yashima-Abo, A., Miura, F., Sugiyama, T., Masuda, T., et al. (2013). Loss of HOXD10 expression induced by upregulation of miR-10b accelerates the migration and invasion activities of ovarian cancer cells. *Int. J. Oncol.* 43, 63–71. doi: 10.3892/ijo.2013.1935

Okada, Y., and Yamaguchi, K. (2017). Epigenetic modifications and reprogramming in paternal pronucleus: sperm, preimplantation embryo, and beyond. *Cell. Mol. Life Sci.* 74, 1957–1967. doi: 10.1007/s00018-016-2447-z

Ortiz-Escribano, N., Szymańska, K. J., Bol, M., Vandenberghe, L., Decrock, E., Van Poucke, M., et al. (2017). Blocking connexin channels improves embryo development of vitrified bovine blastocysts. *Biol. Reprod.* 96, 288–301. doi: 10.1095/biolreprod.116.144121

Park, H.-J., Yu, E., and Shim, Y.-H. (2006). DNA methyltransferase expression and DNA hypermethylation in human hepatocellular carcinoma. *Cancer Lett.* 233, 271–278. doi: 10.1016/j.canlet.2005.03.017

Peng, J. Y., An, X. P., Fang, F., Gao, K. X., Xin, H. Y., Han, P., et al. (2016). MicroRNA-10b suppresses goat granulosa cell proliferation by targeting brain-derived neurotropic factor. *Domest. Anim. Endocrinol.* 54, 60–67. doi: 10.1016/j.domaniend.2015.09.005

Poole, C. J., Zheng, W., Lodh, A., Yevtodiyenko, A., Liefwalker, D., Li, H., et al. (2017). DNMT3B overexpression contributes to aberrant DNA methylation and MYC-driven tumor maintenance in T-ALL and Burkitt's lymphoma. *Oncotarget* 8, 76898–76920. doi: 10.18632/oncotarget.20176

Qu, K., Zhang, X., Lin, T., Liu, T., Wang, Z., Liu, S., et al. (2017). Circulating miRNA-21-5p as a diagnostic biomarker for pancreatic cancer: evidence from comprehensive miRNA expression profiling analysis and clinical validation. *Sci. Rep.* 7, 1692. doi: 10.1038/s41598-017-01904-z

Rezsohazy, R., Saurin, A. J., Maurel-Zaffran, C., and Graba, Y. (2015). Cellular and molecular insights into Hox protein action. *Development* 142, 1212. doi: 10.1242/dev.109785

Rhee, I., Bachman, K. E., Park, B. H., Jair, K.-W., Yen, R.-W. C., Schuebel, K. E., et al. (2002). DNMT1 and DNMT3b cooperate to silence genes in human cancer cells. *Nature* 416, 552–556. doi: 10.1038/416552a

Robertson, K. D. (2005). DNA methylation and human disease. *Nat. Rev. Genet.* 6, 597. doi: 10.1038/nrg1655

Rosenbluth, E. M., Shelton, D. N., Wells, L. M., Sparks, A. E. T., and Van Voorhis, B. J. (2014). Human embryos secrete microRNAs into culture media—a potential biomarker for implantation. *Fertil. Sterility* 101, 1493–1500. doi: 10.1016/j.fertnstert.2014.01.058

Santos, F., Hendrich, B., Reik, W., and Dean, W. (2002). Dynamic reprogramming of DNA methylation in the early mouse embryo. *Dev. Biol.* 241, 172–182. doi: 10.1006/dbio.2001.0501

Shah, N., and Sukumar, S. (2010). The Hox genes and their roles in oncogenesis. *Nat. Rev. Cancer* 10, 361. doi: 10.1038/nrc2826

Shivakumar, M., Lee, Y., Bang, L., Garg, T., Sohn, K.-A., and Kim, D. (2017). Identification of epigenetic interactions between miRNA and DNA methylation associated with gene expression as potential prognostic markers in bladder cancer. *BMC Med. Genomics* 10, 30–30. doi: 10.1186/s12920-017-0269-y

Stenvinkel, P., Karimi, M., Johansson, S., Axelsson, J., Suliman, M., Lindholm, B., et al. (2007). Impact of inflammation on epigenetic DNA methylation—a novel risk factor for cardiovascular disease? *J. Internal Med.* 261, 488–499. doi: 10.1111/j.1365-2796.2007.01777.x

Su, D.-M., Ellis, S., Napier, A., Lee, K., and Manley, N. R. (2001). Hoxa3 and Pax1 regulate epithelial cell death and proliferation during thymus and parathyroid organogenesis. *Dev. Biol.* 236, 316–329. doi: 10.1006/dbio.2001.0342

Talbot, D., Jaenisch, R., Sha, M., Li, E., Benner, J., Hornstra, L., et al. (1997). Baculovirus-mediated expression and characterization of the full-length murine DNA methyltransferase. *Nucleic Acids Res.* 25, 4666–4673. doi: 10.1093/nar/25.22.4666

Taminiau, A., Draime, A., Tys, J., Lambert, B., Vandeputte, J., Nguyen, N., et al. (2016). HOXA1 binds RBCK1/HOIL-1 and TRAF2 and modulates the TNF/NF-κB pathway in a transcription-independent manner. *Nucleic Acids Res.* 44, 7331–7349. doi: 10.1093/nar/gkw606

Tan, Y., Gan, M., Fan, Y., Li, L., Zhong, Z., Li, X., et al. (2018). miR-10b-5p regulates 3T3-L1 cells differentiation by targeting Apol6. *Gene* 687, 36–49. doi: 10.1016/j.gene.2018.11.028

Tsumura, A., Hayakawa, T., Kumaki, Y., Takebayashi, S.-I., Sakaue, M., Matsuoka, C., et al. (2006). Maintenance of self-renewal ability of mouse embryonic stem cells in the absence of DNA methyltransferases Dnmt1, Dnmt3a and Dnmt3b. *Genes Cells* 11, 805–814. doi: 10.1111/j.1365-2443.2006.00984.x

Uysal, F., Ozturk, S., and Akkoyunlu, G. (2017). DNMT1, DNMT3A and DNMT3B proteins are differently expressed in mouse oocytes and early embryos. *J. Mol. Histol.* 48, 417–426. doi: 10.1007/s10735-017-9739-y

Valadi, H., Ekstrom, K., Bossios, A., Sjostrand, M., Lee, J. J., and Lotvall, J. O. (2007). Exosome-mediated transfer of mRNAs and microRNAs is a novel mechanism of genetic exchange between cells. *Nat. Cell Biol.* 9, 654–659. doi: 10.1038/ncb1596

Vallböhmer, D., Brabender, J., Yang, D., Schneider, P. M., Metzger, R., Danenberg, K. D., et al. (2006). DNA methyltransferases messenger RNA expression and aberrant methylation of CpG islands in non-small-cell lung cancer: association and prognostic value. *Clin. Lung Cancer* 8, 39–44. doi: 10.3816/CLC.2006.n.031

Vandenberghe, L. T. M., Heindryckx, B., Smits, K., Szymanska, K., Ortiz-Escribano, N., Ferrer-Buitrago, M., et al. (2018). Platelet-activating factor acetylhydrolase 1B3 (PAFAH1B3) is required for the formation of the meiotic spindle during in vitro oocyte maturation. *Reprod. Fer. Develop* 30, 1739–1750. doi: 10.1071/RD18019

Vandesompele, J., De Preter, K., Pattyn, F., Poppe, B., Van Roy, N., De Paepe, A., et al. (2002). Accurate normalization of real-time quantitative RT-PCR data by geometric averaging of multiple internal control genes. *Genome Biol.* 3. research0034.1. doi: 10.1186/gb-2002-3-7-research0034

Wang, J., Walsh, G., Liu, D. D., Lee, J. J., and Mao, L. (2006). Expression of DDNMT3B variants and its association with promoter methylation of p16 and RASSF1A in primary non–small cell lung cancer. *Cancer Res.* 66, 8361. doi: 10.1158/0008-5472.CAN-06-2031

Wang, G. G., Cai, L., Pasillas, M. P., and Kamps, M. P. (2007). NUP98–NSD1 links H3K36 methylation to Hox-A gene activation and leukaemogenesis. *Nat. Cell Biol.* 9, 804. doi: 10.1038/ncb1608

Wang, H., Liu, G., Shen, D., Ye, H., Huang, J., Jiao, L., et al. (2015). HOXA1 enhances the cell proliferation, invasion and metastasis of prostate cancer cells. *Oncol. Rep.* 34, 1203–1210. doi: 10.3892/or.2015.4085

Wang, Y., Zhang, Z.-X., Chen, S., Qiu, G.-B., Xu, Z.-M., and Fu, W.-N. (2016). Methylation status of SP1 sites within miR-23a-27a-24-2 promoter region influences laryngeal cancer cell proliferation and apoptosis. *Biomed Res. Int.* 2016, 2061248–2061248. doi: 10.1155/2016/2061248

Wang, S., Wu, W., and Claret, F. X. (2017). Mutual regulation of microRNAs and DNA methylation in human cancers. *Epigenetics* 12, 187–197. doi: 10.1080/15592294.2016.1273308

Wardwell-Ozgo, J., Dogruluk, T., Gifford, A., Zhang, Y., Heffernan, T. P., van Doorn, R., et al. (2014). HOXA1 drives melanoma tumor growth and metastasis and elicits an invasion gene expression signature that prognosticates clinical outcome. *Oncogene* 33, 1017–1026. doi: 10.1038/onc.2013.30

Watanabe, D., Suetake, I., Tada, T., and Tajima, S. (2002). Stage- and cell-specific expression of Dnmt3a and Dnmt3b during embryogenesis. *Mech. Dev.* 118, 187–190. doi: 10.1016/S0925-4773(02)00242-3

Wu, H., and Zhang, Y. (2014). Reversing DNA methylation: mechanisms, genomics, and biological functions. *Cell* 156, 45–68. doi: 10.1016/j.cell.2013.12.019

Wydooghe, E., Heras, S., Dewulf, J., Piepers, S., Van den Abbeel, E., De Sutter, P., et al. (2014). Replacing serum in culture medium with albumin and insulin, transferrin and selenium is the key to successful bovine embryo development in individual culture. *Reprod. Fer. Develop* 26, 717–724. doi: 10.1071/RD13043

Xing, J., Stewart, D. J., Gu, J., Lu, C., Spitz, M. R., and Wu, X. (2008). Expression of methylation-related genes is associated with overall survival in patients with non-small cell lung cancer. *Br. J. Cancer.* 98, 1716. doi: 10.1038/sj.bjc.6604343

Ye, K., Wang, S., Wang, J., Han, H., Ma, B., and Yang, Y. (2016). Zebularine enhances apoptosis of human osteosarcoma cells by suppressing methylation of ARHI. *Cancer Sci.* 107, 1851–1857. doi: 10.1111/cas.13088

Zha, T.-Z., Hu, B.-S., Yu, H.-F., Tan, Y.-F., Zhang, Y., and Zhang, K. (2012). Overexpression of HOXA1 correlates with poor prognosis in patients with hepatocellular carcinoma. *Tumor Biol.* 33, 2125–2134. doi: 10.1007/s13277-012-0472-6

Zhang, X., Zhu, T., Chen, Y., Mertani, H. C., Lee, K. O., and Lobie, P. E. (2003). Human growth hormone-regulated HOXA1 is a human mammary epithelial oncogene. *J. Biol. Chem.* 278, 7580–7590. doi: 10.1074/jbc.M212050200

Zhang, Y., Fang, J., Zhao, H., Yu, Y., Cao, X., and Zhang, B. (2018). Downregulation of microRNA-1469 promotes the development of breast cancer via targeting HOXA1 and activating PTEN/PI3K/AKT and Wnt/β-catenin pathways. *J. Cell. Biochem.* 120, 5097–5107. doi: 10.1002/jcb.27786

Zhang, S., Chen, X., Wang, F., An, X., Tang, B., Zhang, X., et al. (2016). Aberrant DNA methylation reprogramming in bovine SCNT preimplantation embryos. *Sci. Rep.* 6, 30345–30345. doi: 10.1038/srep30345

Zhen, L., Li, J., Zhang, M., and Yang, K. (2016). MiR-10b decreases sensitivity of glioblastoma cells to radiation by targeting AKT. *J. Boil. Res. Thessalonike Greece* 23, 14–14. doi: 10.1186/s40709-016-0051-x

Zhu, Q., Gong, L., Wang, J., Tu, Q., Yao, L., Zhang, J.-R., et al. (2016). miR-10b exerts oncogenic activity in human hepatocellular carcinoma cells by targeting expression of CUB and sushi multiple domains 1 (CSMD1). *BMC Cancer* 16, 806–806. doi: 10.1186/s12885-016-2801-4

Conflict of Interest Statement: The authors declare that the research was conducted in the absence of any commercial or financial relationships that could be construed as a potential conflict of interest.

frontiers in Genetics

DATA REPORT
published: 08 October 2019
doi: 10.3389/fgene.2019.00941

Deep Small RNA Sequencing of *BRAF* V600E Mutated Papillary Thyroid Carcinoma With Lymph Node Metastasis

*Azliana Mohamad Yusof[1], Rahman Jamal[2], Sazuita Saidin[2], Rohaizak Muhammad[3], Shahrun Niza Abdullah Suhaimi[3], Isa Mohamed Rose[4], Wan Fahmi Wan Nazarie[2], Francis Tieng Yew Fu[5] and Nurul-Syakima Ab Mutalib[2]**

[1] Cytogenetics and Molecular Diagnostics Laboratory, Pantai Premier Pathology Sdn Bhd, Kuala Lumpur, Malaysia, [2] UKM Medical Molecular Biology Institute (UMBI), Universiti Kebangsaan Malaysia, Kuala Lumpur, Malaysia, [3] Department of Surgery, Faculty of Medicine, Universiti Kebangsaan Malaysia, Kuala Lumpur, Malaysia, [4] Department of Pathology, Faculty of Medicine, Universiti Kebangsaan Malaysia, Kuala Lumpur, Malaysia, [5] Institute of Bioscience (IBS), Universiti Putra Malaysia, UPM Serdang, Selangor, Malaysia

Keywords: small RNA sequencing, papillary thyroid cancer, lymph node metastasis, *BRAF* V600E, microRNAs, Piwi-interacting RNA

OPEN ACCESS

Edited by:
Junjie Xiao,
Shanghai University, China

Reviewed by:
Dominic C. Voon,
Kanazawa University, Japan
Elton J. R. Vasconcelos,
University of Leeds,
United Kingdom

****Correspondence:***
Nurul-Syakima Ab Mutalib
syakima@ppukm.ukm.edu.my

Specialty section:
This article was submitted to RNA, a section of the journal Frontiers in Genetics

Received: *23 May 2019*
Accepted: *05 September 2019*
Published: *08 October 2019*

Citation:
Yusof AM, Jamal R, Saidin S, Muhammad R, Suhaimi SNA, Rose IM, Nazarie WFW, Fu FTY and Mutalib N-SA (2019) Deep Small RNA Sequencing of BRAF V600E Mutated Papillary Thyroid Carcinoma With Lymph Node Metastasis. Front. Genet. 10:941. doi: 10.3389/fgene.2019.00941

INTRODUCTION

Papillary thyroid carcinoma (PTC) is the most predominant subtype of thyroid cancer, contributing to more than 80% of all thyroid or endocrine malignancies. Its prognosis is relatively good compared to other cancers, with more than 90% overall 10-year survival rate (Haugen et al., 2016). However, despite the favorable prognosis, some cases exhibit aggressive phenotype. On average, 50% of the patients are presented with lymph node metastases (LNM) at diagnosis (Saiselet et al., 2015). LNM in PTC confers various poor prognostic indicators; it increases recurrence risk and decreases long term survival predominantly in patients older than 45 years old (Lundgren et al., 2006; Xing, 2013). Treating recurrent PTCs is still a challenge (Pasternak and Shen, 2017) and one of the important issues yet to be solved in PTC patient management is the mortality and morbidity associated with the recurrent disease (Lee et al., 2013).

MicroRNAs (miRNAs) are short, endogenous noncoding RNAs first identified in *Caenorhabditis elegans* which regulate gene expression by binding to the 3′-UTR of target messenger RNA (mRNAs). Their post-transcriptional regulatory functions are involved in controlling the level of proteins involved in numerous biological processes, including embryogenesis, organogenesis, tissue homeostasis, immune system function and cell cycle control (Tafrihi and Hasheminasab, 2019). Relationship between miRNAs and tumor growth, tumor progression and metastasis has been demonstrated by many studies, indicating the ability of these molecules to be used as biomarkers for diagnosis and prognosis (Iorio and Croce, 2012). MiRNA also plays a role as biomarker in predicting lymph nodes metastasis (LNM) in thyroid cancer (Ab Mutalib et al., 2016; Mutalib et al., 2016; Mohamad Yusof et al., 2018).

P-element-induced wimpy testis (PIWI)-interacting RNAs (piRNAs) are a quite recently discovered class of RNAs and more than 30,000 piRNA genes been identified within the human genome (Zhang et al., 2014; Wang et al., 2019). Originally described as key regulators for the germline maintenance and transposon silencing, these short RNAs were disregarded for a long time due to our limited knowledge regarding their function (Weng et al., 2019). However, emergent of new data reveals that unusual expression of piRNAs is a distinct feature Fin many diseases, including

cancers (Weng et al., 2019). This has changed our perspectives on their significance in various diseases. Epigenetically, piRNAs are also the post-transcriptional regulators of the expression of specific downstream target genes (Watanabe and Lin, 2014), and accumulating evidence demonstrates that similarly to miRNAs, piRNAs also possess both oncogenic and tumor-suppressive roles (Weng et al., 2019).

BRAF is a serine-threonine kinase that is activated by RAS binding and protein recruitment to the cell membrane. Activation of MEK along with the MAPK signaling pathway is activated by BRAF phosphorylation (Nikiforov and Nikiforova, 2011). The most frequent genetic changes in PTC are point mutations of *BRAF* which are observed in 35 to 70% of PTC cases (Li et al., 2012; Xing, 2013). More than 95% of *BRAF* mutations in thyroid cancers are thymine to adenine transversion at position 1799 (T1799A) which result in the substitution of glutamate from valine at residue 600 (V600E) (Xing et al., 2015). Various studies have also shown that the *BRAF* V600E mutation is related to LNM, as further presented by a meta-analysis by Song et al. (2018).

In the past years, the evolution of next-generation sequencing technologies has enabled global transcriptome expression profiling and the discovery of novel human miRNAs (Kozomara and Griffiths-Jones, 2011; Kozomara and Griffiths-Jones, 2014; Kozomara et al., 2019) and piRNAs (Weng et al., 2019). Coincidentally, PTC has a relatively lower overall mutation burden hence termed as quiet genome (Cancer Genome Atlas Research Network, 2014; Siraj et al., 2016), therefore investigating the regulatory molecules such as the miRNAs and piRNAs has the potential to deepen our understanding of this cancer. This Data Report aims to provide the readers a comprehensive dataset of small RNAs expression derived from next-generation sequencing in an unbiased manner. For detailed analysis of this dataset focusing on miRNAs with biological insights in PTC, please refer to our original article published in Frontiers of Endocrinology (Mohamad Yusof et al., 2018).

METHODS

Clinical Specimens

Five pairs of tumor-adjacent normal fresh frozen thyroid tissues (n = 10) were collected from PTC patients with lymph node metastasis (N stage = N1, N1a or N1b) from the UKM Medical Centre (UKMMC). Only the thyroid specimens were collected and there was no metastatic lymph node included for several reasons. Firstly, we would like to study the source of the metastasis, which is from the cancer cells at the primary origin (the thyroid itself). Another reason was that the metastatic lymph nodes were unavailable from our Biobank. The resected lymph nodes were all sent to the Pathology Laboratory for diagnostic confirmation. Henceforth, the nodes are fixed in formalin which renders the specimens unsuitable for next-generation sequencing experiment due to RNA degradation. This study was approved by the Universiti Kebangsaan Malaysia Research Ethics Committee (UKMREC; UKM 1.5.3.5/244/UMBI-2015-002). Informed consent was obtained from all the study participants. The tissues were dissected, snap-frozen and stored in liquid nitrogen. All samples were cryosectioned and stained with hematoxylin and eosin and the percentage of tumor cells and normal cells contents were confirmed by a pathologist. The representative figures of the staining at 200× magnification were provided in **Figure 1A** (left: PTC, right: normal adjacent thyroid). Only tumor samples with at least 80% cancerous cells and normal adjacent thyroid tissues with less than 20% necrosis were selected for small RNA sequencing. The tissues were subjected to nucleic acids extraction using Allprep DNA/RNA/miRNA Universal Kit (Qiagen, Valencia, CA, USA) according to manufacturer's recommendations. The integrity of RNA was assessed using Agilent Bioanalyzer 2100 (Agilent Technologies, Santa Clara, CA, USA) while the quantity and purity of RNA were assessed using Qubit 2.0 fluorometer and Nanodrop 2000c Spectrometer (Thermo Fisher Scientific, Pittsburgh, PA, USA), respectively.

BRAF V600E Genotyping

BRAF V600E genotyping was performed using forward primer 5′-TGCTTGCTCTGATAGGAAAATG-3′ and reverse primer 5′-AGCATCTCAGGGCCAAAAAT-3′ (Monti et al., 2015). The DNA sequencing was performed on ABI Prism 3130xl Genetic Analyzer (Applied Biosystem, USA).

Libraries Preparation

RNA from tumor and their adjacent normal tissues were processed into libraries using TruSeq Small RNA Sample Prep Kit (Illumina, San Diego, CA, USA). Briefly, 3′ and 5′ adapters were sequentially ligated to the ends of small RNAs fractionated from 2 μg of total RNA, and reverse transcribed to generate cDNA. The cDNA was amplified using a common primer complementary to the 3′ adapter, and a primer containing 1 of 48 index sequences. Samples were size-selected (140–160 bp fragments) on a 6% polyacrylamide gel, purified, quantified and pooled for multiplexed sequencing.

Small RNA Sequencing

The resulting pooled libraries were normalized to 2 nM and were hybridized to oligonucleotide-coated single-read flow cells for cluster generation using HiSeq® Rapid SR Cluster Kit v2 on Hiseq 2500 (Illumina, San Diego, CA, USA). Subsequently, the clustered pooled microRNA libraries were sequenced on the HiSeq 2500 for 50 sequencing cycles using HiSeq® Rapid SBS Kit v2 (50 Cycle) (Illumina, San Diego, CA, USA). The sequencing run was completed on December 18, 2015.

Bioinformatics and Statistical Analyses

Pre- and post-processing of data were executed in BaseSpace software (Illumina, San Diego, CA, USA). Illumina Sequence Integration Software (Isis) version 2.5.52.11 processed raw data from Illumina sequencers into FASTQ files. Subsequently, Small RNA Analysis app version 1.0.0.0 was used for determination of differentially expressed small RNAs. Differential expression analysis is performed for the following marker types; miRNA family, precursor group, miRNAs (include mature miRNAs and isomiRs) and piRNAs. Briefly, this workflow uses Bowtie version

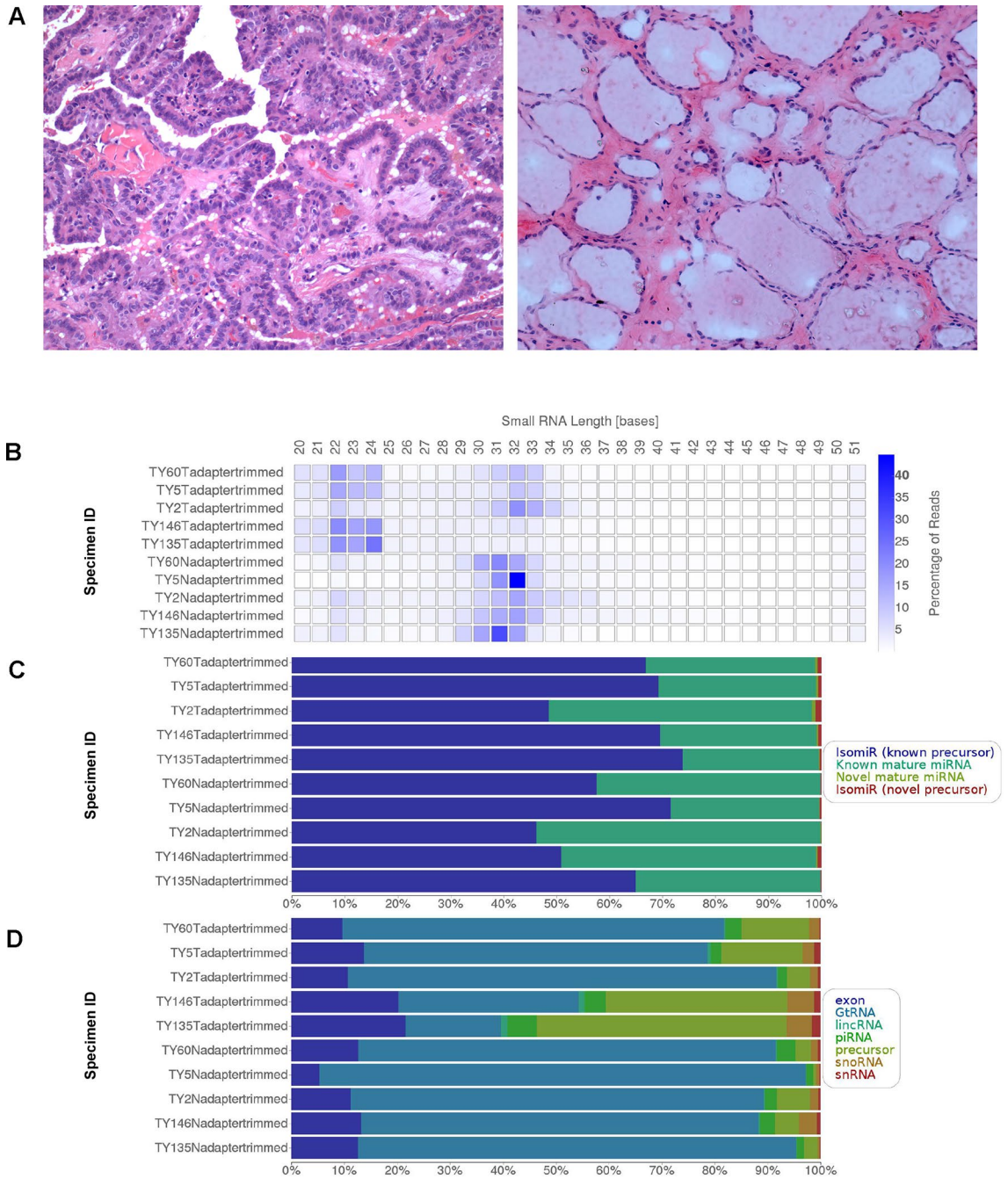

FIGURE 1 | (A) Representative H&E staining of the PTC (left) and adjacent normal thyroid (right) under 200× magnification. **(B)** Small RNA length distribution **(C)** miRNA hits by category and **(D)** other RNA hits by category.

0.12.8 to align each cluster against abundant, mature miRNA, other RNA, and genomic reference databases (Langmead et al., 2009). The reference genome used for the alignment was Homo sapiens maskedPAR (UCSC hg19). The output from Bowtie was then processed by SAMtools 0.1.19-isis-1.0.2 (Li et al., 2009), annotated to miRBase v21 (Kozomara and Griffiths-Jones, 2014; Kozomara et al., 2019) and performed differential analysis using DESeq2 (Love et al., 2014). DESeq2 removed low expressed markers with normalized mean count < 10 before testing. The DESeq2 variance model is used to detect and exclude outliers based on the extreme variation between replicates. The status (filtered or passed) and the result of the analysis (mean expression, fold change, standard error, p-value, q-value, etc.) were reported for each marker and will be available upon request. Additionally,

novel miRNA and precursor discovery are performed for each sample group using miRDeep* version 3.2 (An et al., 2013).

DESCRIPTION OF ANALYSIS OUTPUT

Small RNA Sequencing Yield

The deep sequencing of small RNA libraries derived from PTC tissues and adjacent normal thyroid yielded 130,459,076 reads with 122,182,874 reads passing filters (93.3%) and 96.25% reads had Phred score of ≥Q30. The total reads that passed filter per sample range from 8,331,660 to 16,629,882 reads, generating comprehensive digital profiles of small RNAs expression in PTC. Summary of small RNA sequencing results is provided in **Table 1**. **Figure 1** illustrates the small RNA length distribution, miRNA hits by category and other RNA hits by category. In the cancer specimens, the size distribution was mainly 22–24 bases and/or 30–34 bases (**Figure 1B**). Interestingly, the size distribution of small RNA in normal thyroid appeared bigger and more consistent, which is in the range of 30 to 33 bases. Focusing on only the miRNAs, our alignment resulted in average more than 50% of the reads were mapped to isomiR of known precursors, followed by known mature miRNAs (**Figure 1C**). Additionally, small percentage of the reads were mapped to the novel mature miRNAs and isomiRs from novel precursor. In **Figure 1D**, we present the outcome of the alignment from other coding and noncoding RNA species, including the exonic RNAs, genomic transfer RNAs (GtRNA), long intergenic noncoding RNAs (lincRNA), piRNAs, precursors, small nucleolar RNAs (snoRNAs) and small nuclear RNAs (snRNAs). The lincRNAs gained wide attention in cancer research lately and with our deep sequencing data, the expression profiles of lincRNAs can be subjected to future research. Meanwhile, the roles of GtRNA, snoRNA and snRNA in cancers are also emerging.

Mature miRNAs and isomiRs

Expression profiles for 4,662 previously annotated miRNAs were delineated and 1,079 miRNAs passed the filter and subjected to differential analysis. A set of 252 miRNAs were significantly differentially expressed (q value < 0.05) in cancer versus normal thyroid tissues. There were 134 upregulated miRNAs and 118 downregulated miRNAs.

Novel miRNAs

Expression profiles for 173 novel miRNAs predicted by miRDeep* were described; 26 novel miRNAs passed the filter and subjected to differential analysis. Sixteen novel miRNAs were significantly differentially expressed (adjusted p-value < 0.05) in cancer versus normal thyroid tissues; 11 novel miRNAs were upregulated while five were downregulated.

Precursor Group

There were 971 precursors detected in this dataset, with 219 precursors passed the filter and subjected to differential analysis. A set of 58 precursor miRNAs were significantly differentially expressed (q value < 0.05) in cancer versus normal thyroid tissues. There were 33 upregulated and 25 downregulated precursor miRNAs, respectively.

Novel Precursor miRNAs

There were 95 novel precursors predicted from this dataset, with 36 novel precursors passed the filter and subjected to differential analysis. A set of 16 novel precursor miRNAs were significantly differentially expressed (q value < 0.05) in cancer versus normal thyroid tissues. There were 4 upregulated and 12 downregulated novel precursor miRNAs, respectively.

miRNA Family

Expression profiles for 418 previously annotated miRNA families were detected and 150 families passed the filter and subjected to differential analysis. A set of 36 miRNA families were significantly differentially expressed (q value < 0.05) in cancer versus normal thyroid tissues. There were 17 upregulated and 19 downregulated miRNA families, respectively. The workflow does not predict novel miRNA families.

piRNA

Expression profiles for 848 previously annotated piRNAs were detected and 110 piRNAs passed the filter and subjected to differential analysis. A set of 19 piRNAs were significantly differentially expressed (q value < 0.05) in cancer versus normal thyroid tissues. There were 8 upregulated piRNAs and 11 downregulated piRNAs. The workflow does not predict novel piRNAs.

Direct Link to Deposited Data and Information to Users

The small RNA sequencing data in fastq. format was deposited at the NCBI Sequence Read Archive (SRA) at http://www.ncbi.nlm.nih.gov/sra with accession number PRJNA378313 (SRP101463). The sample IDs are TY135, TY 146, TY2, TY5 and

TABLE 1 | Summary of small RNA sequencing results.

	Known	Novel	Total
miRNAs			
Total miRNAs	4,662	173	4,835
Tested miRNAs	1,079	26	1,105
Differentially expressed miRNAs	252	16	268
Precursors			
Total Precursor Groups	971	95	1,066
Tested Precursor Groups	219	36	255
Differentially Expressed Precursor Groups	58	16	74
miRNA families			
Total miRNA Families	418	0	418
Tested miRNA Families	150	0	150
Differentially expressed miRNA families	36	0	36
piRNAs			
Total piRNAs	848	0	848
Tested piRNAs	110	0	110
Differentially expressed piRNAs	19	0	19

Tested markers are those that pass the low-count filter and are tested for statistical significance. Novel markers (when applicable) are predicted by miRDeep.*

TY60. This raw data will enable other researchers to perform mapping and differential expression analysis according to their specific objectives.

DATA AVAILABILITY STATEMENT

The datasets generated for this study can be found in the NCBI Sequence Read Archive (SRA), PRJNA378313 (SRP101463).

ETHICS STATEMENT

The studies involving human participants were reviewed and approved by Universiti Kebangsaan Malaysia Research Ethics Committee. The patients/participants provided their written informed consent to participate in this study.

AUTHOR CONTRIBUTIONS

AMY and N-SAM involved in the specimen collections, libraries preparation and sequencing, data analyses, acquisition of data and drafting the manuscript. RJ provides a critical review of the manuscript. SS performed *BRAF* V600E genotyping, cryosectioning and staining of the fresh frozen tissues. RM and SNAS are thyroid surgeons involved in specimen retrieval. IMR assessed tumor percentage of the tissues. FTYF was involved in the initial draft. WFWN is the bioinformatician partly involved in data analysis. All authors read and approved the final manuscript.

FUNDING

This research was funded by the Fundamental Research Grant Scheme (FRGS) from the Ministry of Education Malaysia (FRGS/1/2014/SKK01/UKM/03/1).

ACKNOWLEDGMENTS

The authors thanks Miss Chin Minning, the former Field Application Specialist from Science Vision Sdn Bhd for her extensive support during library preparation and next-generation sequencing.

REFERENCES

Ab Mutalib, N.-S., Othman, S. N., Mohamad Yusof, A., Abdullah Suhaimi, S. N., Muhammad, R., and Jamal, R. (2016). Integrated microRNA, gene expression and transcription factors signature in papillary thyroid cancer with lymph node metastasis. *PeerJ* 4, e2119. doi: 10.7717/peerj.2119.

An, J., Lai, J., Lehman, M. L., and Nelson, C. C. (2013). miRDeep*: an integrated application tool for miRNA identification from RNA sequencing data. *Nucleic Acids Res.* 41, 727–737. doi: 10.1093/nar/gks1187.

Cancer Genome Atlas Research Network. (2014). Integrated genomic characterization of papillary thyroid carcinoma. *Cell* 159, 676–690. doi: 10.1016/j.cell.2014.09.050.

Haugen, B. R., Alexander, E. K., Bible, K. C., Doherty, G. M., Mandel, S. J., Nikiforov, Y. E., et al. (2016). 2015 American Thyroid Association management guidelines for adult patients with thyroid nodules and differentiated thyroid cancer: the American Thyroid Association Guidelines Task Force on thyroid nodules and differentiated thyroid cancer. *Thyroid Off. J. Am. Thyroid Assoc.* 26, 1–133. doi: 10.1089/thy.2015.0020.

Iorio, M. V., and Croce, C. M. (2012). microRNA involvement in human cancer. *Carcinogenesis* 33, 1126–1133. doi: 10.1093/carcin/bgs140.

Kozomara, A., Birgaoanu, M., and Griffiths-Jones, S. (2019). miRBase: from microRNA sequences to function. *Nucleic Acids Res.* 47, D155–D162. doi: 10.1093/nar/gky1141.

Kozomara, A., and Griffiths-Jones, S. (2014). miRBase: annotating high confidence microRNAs using deep sequencing data. *Nucleic Acids Res.* 42, D68–D73. doi: 10.1093/nar/gkt1181.

Kozomara, A., and Griffiths-Jones, S. (2011). miRBase: integrating microRNA annotation and deep-sequencing data. *Nucleic Acids Res.* 39, D152–D157. doi: 10.1093/nar/gkq1027.

Langmead, B., Trapnell, C., Pop, M., and Salzberg, S. L. (2009). Ultrafast and memory-efficient alignment of short DNA sequences to the human genome. *Genome Biol.* 10, R25. doi: 10.1186/gb-2009-10-3-r25.

Lee, J. C., Zhao, J. T., Clifton-Bligh, R. J., Gill, A., Gundara, J. S., Ip, J. C., et al. (2013). MicroRNA-222 and microRNA-146b are tissue and circulating biomarkers of recurrent papillary thyroid cancer. *Cancer* 119, 4358–4365. doi: 10.1002/cncr.28254.

Li, H., Handsaker, B., Wysoker, A., Fennell, T., Ruan, J., Homer, N., et al. (2009). The sequence alignment/map format and SAMtools. *Bioinforma. Oxf. Engl.* 25, 2078–2079. doi: 10.1093/bioinformatics/btp352.

Li, X., Abdel-Mageed, A. B., and Kandil, E. (2012). BRAF mutation in papillary thyroid carcinoma. *Int. J. Clin. Exp. Med.* 5, 310–315.

Love, M. I., Huber, W., and Anders, S. (2014). Moderated estimation of fold change and dispersion for RNA-seq data with DESeq2. *Genome Biol.* 15, 550. doi: 10.1186/s13059-014-0550-8.

Lundgren, C. I., Hall, P., Dickman, P. W., and Zedenius, J. (2006). Clinically significant prognostic factors for differentiated thyroid carcinoma: a population-based, nested case-control study. *Cancer* 106, 524–531. doi: 10.1002/cncr.21653.

Mohamad Yusof, A., Jamal, R., Muhammad, R., Abdullah Suhaimi, S. N., Mohamed Rose, I., Saidin, S., et al. (2018). Integrated characterization of microRNA and mRNA transcriptome in papillary thyroid carcinoma. *Front. Endocrinol.* 9, 158. doi: 10.3389/fendo.2018.00158.

Monti, E., Bovero, M., Mortara, L., Pera, G., Zupo, S., Gugiatti, E., et al. (2015). BRAF mutations in an Italian regional population: implications for the therapy of thyroid cancer. *Int. J. Endocrinol.* 2015, 138734. doi: 10.1155/2015/138734.

Mutalib, N.-S. A., Yusof, A. M., Mokhtar, N. M., Harun, R., Muhammad, R., and Jamal, R. (2016). MicroRNAs and lymph node metastasis in papillary thyroid cancers. *Asian Pac. J. Cancer Prev. APJCP* 17, 25–35. doi: 10.7314/APJCP.2016.17.1.25.

Nikiforov, Y. E., and Nikiforova, M. N. (2011). Molecular genetics and diagnosis of thyroid cancer. *Nat. Rev. Endocrinol.* 7, 569–580. doi: 10.1038/nrendo.2011.142.

Pasternak, J. D., and Shen, W. T., (2017). "The management of the persistent and recurrent cervical lymph node metastases," in *Management of thyroid nodules and differentiated thyroid cancer: a practical guide*. Eds. Roman, S. A., Sosa, J. A., and Solórzano, C. C. (Cham: Springer International Publishing), 255–262. doi: 10.1007/978-3-319-43618-0_17.

Saiselet, M., Gacquer, D., Spinette, A., Craciun, L., Decaussin-Petrucci, M., Andry, G., et al. (2015). New global analysis of the microRNA transcriptome of primary tumors and lymph node metastases of papillary thyroid cancer. *BMC Genomics* 16, 828. doi: 10.1186/s12864-015-2082-3.

Siraj, A. K., Masoodi, T., Bu, R., Beg, S., Al-Sobhi, S. S., Al-Dayel, F., et al. (2016). Genomic profiling of thyroid cancer reveals a role for thyroglobulin in metastasis. *Am. J. Hum. Genet.* 98, 1170–1180. doi: 10.1016/j.ajhg.2016.04.014.

Song, J.-Y., Sun, S.-R., Dong, F., Huang, T., Wu, B., and Zhou, J. (2018). Predictive value of BRAFV600E mutation for lymph node metastasis in papillary thyroid cancer: a meta-analysis. *Curr. Med. Sci.* 38, 785–797. doi: 10.1007/s11596-018-1945-7.

Tafrihi, M., and Hasheminasab, E. (2019). MiRNAs: biology, biogenesis, their web-based tools, and databases. *MicroRNA Shariqah United Arab Emir.* 8, 4–27. doi: 10.2174/2211536607666180827111633.

Wang, J., Zhang, P., Lu, Y., Li, Y., Zheng, Y., Kan, Y., et al. (2019). piRBase: a comprehensive database of piRNA sequences. *Nucleic Acids Res.* 47, D175–D180. doi: 10.1093/nar/gky1043.

Watanabe, T., and Lin, H. (2014). Posttranscriptional regulation of gene expression by Piwi proteins and piRNAs. *Mol. Cell* 56, 18–27. doi: 10.1016/j.molcel.2014.09.012.

Weng, W., Li, H., and Goel, A. (2019). Piwi-interacting RNAs (piRNAs) and cancer: emerging biological concepts and potential clinical implications. *Biochim. Biophys. Acta Rev. Cancer* 1871, 160–169. doi: 10.1016/j.bbcan.2018.12.005.

Xing, M. (2013). Molecular pathogenesis and mechanisms of thyroid cancer. *Nat. Rev. Cancer* 13, 184–199. doi: 10.1038/nrc3431.

Xing, M., Alzahrani, A. S., Carson, K. A., Shong, Y. K., Kim, T. Y., Viola, D., et al. (2015). Association between BRAF V600E mutation and recurrence of papillary thyroid cancer. *J. Clin. Oncol.* 33, 42–50. doi: 10.1200/JCO.2014.56.8253.

Zhang, P., Si, X., Skogerbø, G., Wang, J., Cui, D., Li, Y., et al. (2014). piRBase: a web resource assisting piRNA functional study. *Database J. Biol.* doi: 10.1093/database/bau110.

Conflict of Interest: The authors declare that the research was conducted in the absence of any commercial or financial relationships that could be construed as a potential conflict of interest.

frontiers in Cell and Developmental Biology

ORIGINAL RESEARCH
published: 01 November 2019
doi: 10.3389/fcell.2019.00263

Long Non-coding RNA H19 Suppression Protects the Endothelium Against Hyperglycemic-Induced Inflammation via Inhibiting Expression of *miR-29b* Target Gene Vascular Endothelial Growth Factor a Through Activation of the Protein Kinase B/Endothelial Nitric Oxide Synthase Pathway

Xiao-wen Cheng[1,2†], Zhen-fei Chen[3†], Yu-feng Wan[4†], Qing Zhou[2], Hua Wang[5] and Hua-qing Zhu[2*]*

[1] Department of Clinical Laboratory, The First Affiliated Hospital, Anhui Medical University, Hefei, China, [2] Laboratory of Molecular Biology, Department of Biochemistry, Anhui Medical University, Hefei, China, [3] Department of Vasculocardiology, Hefei Hospital Affiliated to Anhui Medical University, Hefei, China, [4] Department of Otolaryngology, The Affiliated Chaohu Hospital, Anhui Medical University, Hefei, China, [5] Department of Oncology, The First Affiliated Hospital, Institute for Liver Disease, Anhui Medical University, Hefei, China

It has been shown that non-coding RNAs (ncRNAs) play an important regulatory role in pathophysiological processes involving inflammation. The vascular endothelial growth factor A (*VEGFA*) gene also participates in the inflammatory process. However, the relationships between ncRNAs and VEGFA are currently unclear. Here, this study was designed to determine the relationship between long non-coding RNA (lncRNA) H19, mircoRNA29b (miR-29b), and VEGFA in the development of diabetes mellitus (DM). We demonstrate that H19 is upregulated and miR-29b downregulated in individuals with DM and directly binds miR-29b. VEGFA is the target of miR-29b in the vascular endothelium of individuals with DM. We found that positive modulation of miR29b and inhibition of H19 and VEGFA significantly attenuates high glucose-induced endothelial inflammation and oxidative stress. We also found that the protein kinase B/endothelial nitric oxide synthase (AKT/eNOS) signal pathway in endothelial cells is activated through regulation of miR29b and H19 endogenous RNAs. We conclude that H19 suppression protects the endothelium against high glucose-induced inflammation and oxidative stress in endothelial cells by upregulation of miR-29b and downregulation of *VEGFA*

OPEN ACCESS

Edited by:
Junjie Xiao,
Shanghai University, China

Reviewed by:
Zlyi Liu,
National Institutes of Health (NIH), United States
Huichang Bi,
Sun Yat-sen University, China

****Correspondence:***
Hua Wang
wanghua@ahmu.edu.cn
Hua-qing Zhu
aydzhq@126.com

† These authors have contributed equally to this work

Specialty section:
This article was submitted to Signaling, a section of the journal Frontiers in Cell and Developmental Biology

Received: *12 August 2019*
Accepted: *17 October 2019*
Published: *01 November 2019*

Citation:
Cheng X-w, Chen Z-f, Wan Y-f, Zhou Q, Wang H and Zhu H-q (2019) Long Non-coding RNA H19 Suppression Protects the Endothelium Against Hyperglycemic-Induced Inflammation via Inhibiting Expression of miR-29b Target Gene Vascular Endothelial Growth Factor a Through Activation of the Protein Kinase B/Endothelial Nitric Oxide Synthase Pathway. Front. Cell Dev. Biol. 7:263. doi: 10.3389/fcell.2019.00263

through AKT/eNOS signal pathway activation. These results suggest a novel link between dysregulated ncRNA expression, inflammation, and the signaling pathway in the vascular endothelium of individuals with DM, indicating a promising strategy for preventing cardiovascular disease in such individuals.

Keywords: diabetes, *H19*, inflammation, miRNA-29b, vascular endothelial growth factor A

INTRODUCTION

Impaired vascular remodeling is considered to be involved in the development of cardiovascular disease (CVD) (García-Redondo et al., 2016). It is generally accepted that there is a relationship between CVD and vascular inflammation (Haybar et al., 2019). Vascular inflammation also contributes to the progression of more complex diseases such as atherosclerosis (AS) and diabetes mellitus (DM). There is strong evidence that DM independently increases the risk of CVD and that pro-inflammatory components play a key role in its development (Fishman et al., 2018; Yuan et al., 2019). Brownlee (2001) have proposed that hyperglycemia plays a role in promoting overproduction of reactive oxygen species (ROS) by the mitochondrial electron transport chain and that prolonged production of mitochondrial superoxide contributes to development of diabetes-related vascular damage. ROS are generated in the vascular wall by nicotinamide adenine dinucleotide phosphate (NADPH) oxidase, xanthine oxidase, the mitochondrial electron transport chain, and uncoupled endothelial nitric oxide synthase (eNOS). Therefore, it would be useful to identify new inflammatory factors associated with the development of CVD. In this study, we aimed to investigate whether vascular epithelial growth factor A (VEGFA), a member of the VEGF family that is considered to be pro-inflammatory cytokines, is involved in the pathogenesis of CVD in individuals with DM.

Sequencing experiments have shown that more than 90% of the genome is transcribed into non-coding RNA (ncRNA). ncRNA includes microRNA (miRNA; 18–24 nucleotides) and long ncRNA (lncRNA; >200 nucleotides). miRNAs and lncRNAs have different functions. miRNAs bind to the 3′-UTR of target genes to mediate translational repression, thereby altering the biology of diverse disease states. Meanwhile, lncRNAs have emerged as powerful biological regulators that act by modulating numerous cellular processes. lncRNAs can act as miRNA sponges and inhibit miRNA expression. Numerous studies have suggested that ncRNAs play a key role in regulating pathophysiological processes involved in CVD (Hung et al., 2018; Simion et al., 2019). H19, a paternally imprinted and maternally expressed gene, produces a 2.3-kb spliced, capped, and polyadenylated lncRNA (Yoshimura et al., 2018). H19 is up-regulated in AS and associated with its progression but the underlying regulatory mechanisms have not yet been conclusively established (Bitarafan et al., 2019). H19 expression is chronically increased in individuals with DM but the biological significance of this is not yet understood (Zhang N. et al., 2018). Recent studies have shown that H19 upregulates VEGFA to enhance the survival and angiogenic capacity of mesenchymal stem cells through miR-199a-5p inhibition. This also mediates the antiapoptotic effect of hypoxic postconditioning against hypoxia-reoxygenation-induced injury in aged cardiomyocytes by inhibiting miR-29b-3p expression (Hou et al., 2018; Zhang et al., 2019). In the present study, we explored the interaction between VEGFA and H19 during hyperglycemia-induced inflammation and investigated whether miR-29b is involved in this interaction.

MATERIALS AND METHODS

Patients

The study cohort comprised 30 patients with DM and 30 healthy individuals all of whom attended the First Affiliated Hospital of Anhui Medical University. DM was diagnosed following the 1999 World Health Organization guidelines and classification. Peripheral blood (10 ml; EDTA anticoagulation) was obtained from each participant. Blood samples were centrifuged at 1500 *g* for 10 min to collect plasma. Plasma samples were aliquoted into Eppendorf tubes (500 μl in each), and all samples were stored at −80°C until further analysis. The study protocols were approved by the Ethics Committee of Anhui Medical University. All patients provided written informed consent.

Cell Culture

Human umbilical vein endothelial cells (HUVECs) obtained from the American Type Culture Collection (Manassas, VA, United States) were cultured in Dulbecco's Modified Eagles Media (Thermo Fisher Scientific, Beijing, China) supplemented with 10% fetal bovine serum and 100 IU/ml penicillin/streptomycin (Invitrogen, Carlsbad, CA, United States). Cells were maintained at 37°C with 5% CO_2.

Cell Transfection

MiR-29b mimics and inhibitors (GenePharm Co., Ltd., Shanghai, China) were used to upregulate or downregulate miR-29b expression. Cells were transfected with VEGFA-siRNA (GenePharm), H19-shRNA (GenePharm), or miR-29b mimics, inhibitors, or controls (GenePharm) using Lipofectamine 2000 (Invitrogen; Thermo Fisher Scientific, Inc., Waltham, MA, United States) according to the manufacturer's protocol. A scrambled oligonucleotide (GenePharm) served as a control. Changes in RNA expression were determined by qRT-PCR 24 h after transfection, and changes in protein expression were measured by western blotting 48 h after transfection.

Determination of ROS, Tumor Necrosis Factor-Alpha (TNF-α), and NADPH

Reactive oxygen species production was assessed following the method described by Zhu et al. (2009). The proteins obtained from the HUVECs were incubated with 20 μM 2′,7′-dichlorofluorescin diacetate at 37°C for 3 h. Fluorescence was measured by spectrofluorometry at an excitation of 488 nm and an emission of 525 nm. TNF-α titers were determined by enzyme-linked immunosorbent assay (eBioscience, San Diego, CA, United States). Lucigenin-enhanced chemiluminescence was used to evaluate NADPH oxidase activity in cell lysates using a multilabel counter (VICTOR3; PerkinElmer-Wallac, Waltham, MA, United States) (Li et al., 2009). Light signals were detected every 5 s. NADPH oxidase activity was calculated and is presented as counts per second.

Western Blotting

Cells were then harvested and lysed with 1 × sodium dodecyl sulfate (SDS) lysis buffer containing 50 mM Tris–HCl (pH 6.8), 10% glycerol, and 2% SDS. Cell lysates were boiled for 10 min then centrifuged at 12,000 *g* for 15 min at room temperature. Samples were separated by 12% SDS-PAGE and transferred to a polyvinylidene difluoride membrane (GE Healthcare, Piscataway, NJ, United States). The membranes were blocked in 5% bovine serum albumen for 2 h, followed by a 4°C overnight incubation with primary antibodies. Primary antibodies were detected with corresponding horseradish peroxidase-conjugated secondary antibodies (Zhongshan Jinqiao, Beijing, China) coupled with enhanced chemiluminescence reagents (Engreen, Beijing, China).

Luciferase Assay

The H19 and VEGFA 3′-UTR regions, containing potential miR-29b binding sites, were predicted using TargetScan version 7.1[1]. The predicted 3′-UTR fragments were amplified by PCR. Mutants were then constructed by introducing point mutations into the seed binding site for miR-29b. The wild type and mutant fragments (wt-Luc-H19 and wt-Luc-VEGFA, and mu-Luc-H19 and mu-Luc-VEGFA) were subcloned into the psiCHECK2 vector (Promega Corporation, United States), downstream of the renilla luciferase gene. The vector also contains the firefly luciferase gene. Cells were seeded in 24-well plates and cotransfected with wild-type or mutated luciferase constructs along with miR-29b mimics, miR-29b inhibitors, or controls. The Dual Luciferase Reporter Assay System (Promega) was used 48 h after transfection following the manufacturer's protocol. The relative luciferase activity was calculated using the ratio of firefly luciferase activity to renilla luciferase activity.

RNA Immunoprecipitation (RIP)

We assessed the direct interaction between miR-29b and lncRNA H19 by Argonaute 2 (Ago2)-RNA immunoprecipitation (Ago2-RIP). Anti-Ago2 (Sigma-Aldrich, United States), or control anti-IgG and Dynabeads Protein G (Invitrogen, United States) were incubated at 4°C with rotation a day prior to the experiment. Complete RIP lysis buffer, containing protease inhibitor, phosphatase inhibitor (Roche, Switzerland), and RNase inhibitor (Invitrogen, United States), was used to lyse cells. RNA in Ago2-RIP materials was washed several times with PEB buffer and treated with DNase I and Proteinase K (Promega). RNA was isolated with Trizol (Invitrogen) and precipitated with absolute ethanol overnight at −20°C. After the removal of the proteins and beads, RT-qPCR analysis of the purified RNA, and lncRNA H19 enrichment in Ago2-RIP, was performed.

Reverse Transcription-Quantitative Polymerase Chain Reaction (RT-qPCR)

Total RNA from mouse tissues and GC-1 cells was extracted using TRIzol reagent following the manufacturer's instructions (Invitrogen, Carlsbad, CA, United States). Isolated total RNA (1 μg) was converted to complementary DNA (cDNA) using a First-Strand cDNA Synthesis Kit (Toyobo, Osaka, Japan). Power SYBR green master mix (Applied Biosystems, Foster City, CA, United States) was added to the cDNA samples, which were then subjected to qRT-PCR using a StepOne Real Time PCR system. *GAPDH* and U6 were used as endogenous controls for mRNAs/lncRNAs and for miRNAs, respectively.

The amplification results were calculated using the 2 (−ΔΔCt) method. The PCR primers used were: H19, forward 5′-ATCGGTGCCTCAGCGTTCGG-3′, reverse 5′-CTGTCCTCGCCGTCACACCG-3′; *VEGFA*, forward 5′-TGGCTCACTGGCTTGCTCTA-3′, and reverse 5′-ATCCAACTGCACCGTCACAG-3′; *GAPDH*, forward 5′-GGTGGTCTCCTCTGACTTCAA-3′, and reverse 5′-GTTGCTGTAGCCAAATTCGTTGT-3′; miR-29b, 5′UAGCACCAUUUGAAAUCAGUGUU-3′; and U6, 5′-CGCTTCGGCAGCACATATACTAAAATTGGAAC-3′.

Statistical Analysis

Statistical analysis was performed using SPSS software version 20.0. The data were subjected to one-way ANOVA and parametric *t*-testing and are presented as the mean ± SD. The tests were performed at least in triplicate. $P < 0.05$ was considered to denote statistical significance.

RESULTS

Relationships Between H19, miR-29b, and VEGFA

Expression of H19 was significantly downregulated after treatment with either H19-shRNA1 or H19-shRNA2 ($P < 0.05$, **Figure 1A**). In cases of H19 downregulation, expression of miR-29b was significantly upregulated ($P < 0.05$, **Figure 1B**). Additionally, after H19 downregulation, VEGFA protein expression was also significantly reduced ($P < 0.05$, **Figure 1C**). VEGFA-siRNA1 and VEGFA-siRNA2 transfection significantly downregulated *VEGFA* expression, especially VEGFA-siRNA1

[1]http://www.targetscan.org/vert_71/

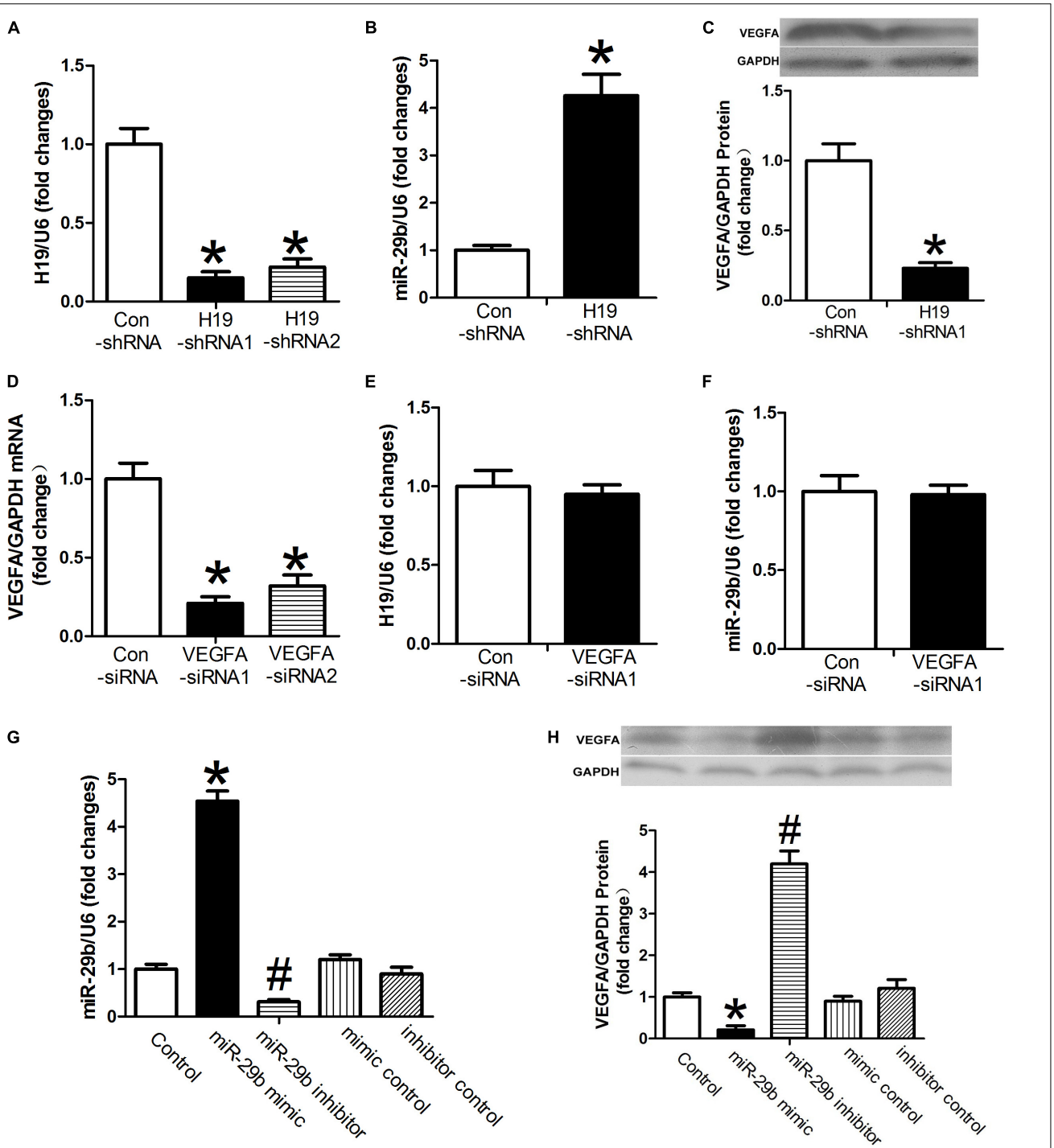

FIGURE 1 | The relationships between H19, miR-29b, and VEGFA. **(A)** The inhibitory effects of H19-shRNA on H19 mRNA expression were determined by RT-PCR. **(B,C)** Human umbilical vein endothelial cells (HUVECs) were transfected with H19-shRNA1. miR29b and VEGFA expression were measured by RT-PCR after 24 h and by western blot after 48 h. **(D)** RT-PCR showed *VEGFA* mRNA expression is downregulated after exposure to VEGFA-siRNA1. **(E,F)** H19 and miR-29b expression was measured following 24 h of exposure to VEGFA-siRNA1. **(G,H)** miR29b and VEGFA expression was measured in the presence of miR-29b mimics. $^{*}P < 0.05$ vs. control group. $^{\#}P < 0.05$ vs. miR-29b inhibitor control group.

($P < 0.05$, **Figure 1D**). VEGFA-siRNA1 transfection did not result in significant changes in H19 or miR-29b expression ($P > 0.05$, **Figures 1E,F**). However, *VEGFA* expression was significantly decreased in the presence of miR-29b mimics (**Figures 1G,H**), implying a potential association between H19, miR-29b, and VEGFA.

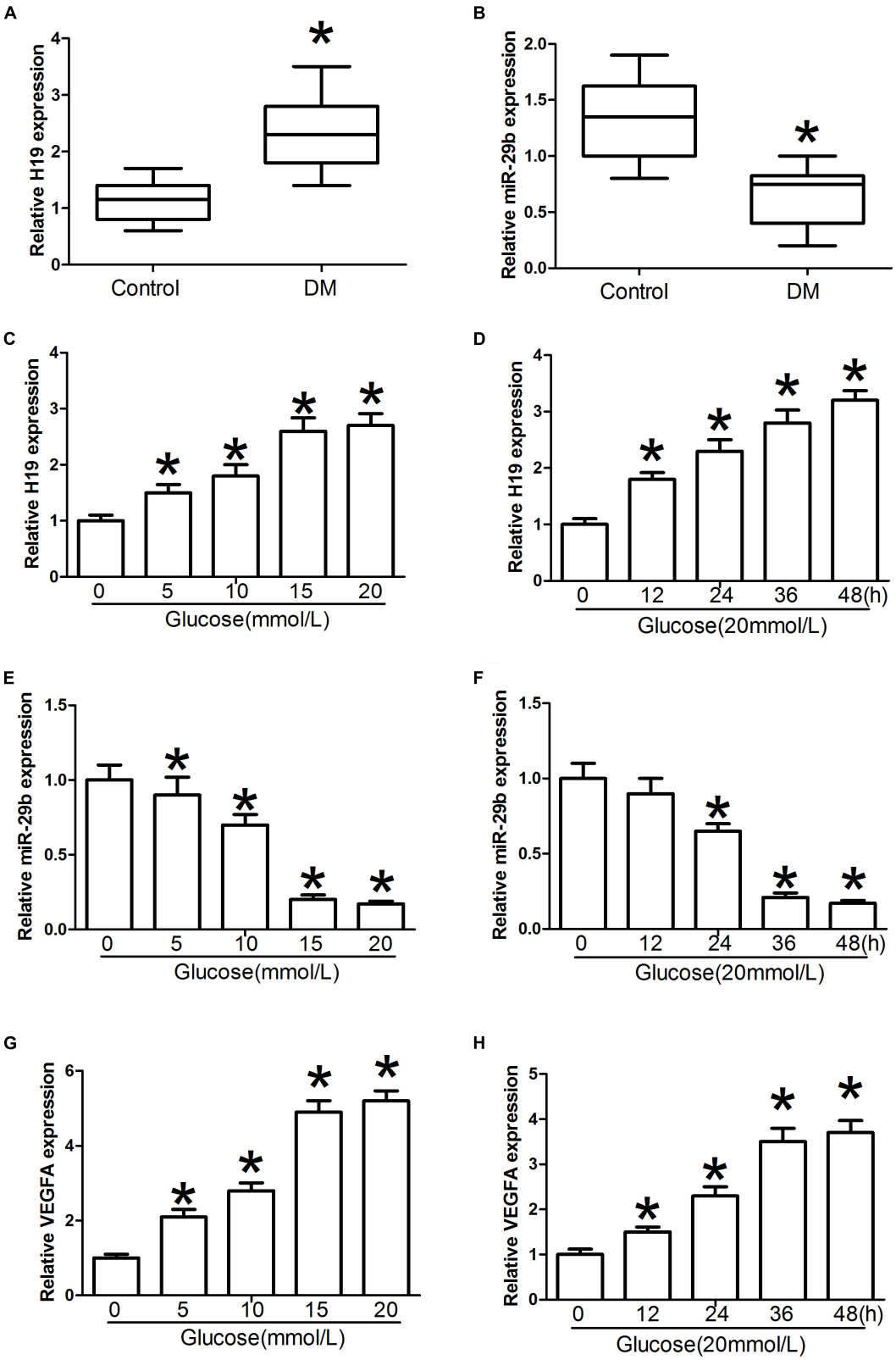

FIGURE 2 | H19 and miR-29b expression in individuals with diabetes mellitus (DM) and in glucose-treated HUVECs. **(A,B)** Circulating lncRNA H19 and miR-29b levels were measured by RT-PCR. **(C–H)** Relative H19, miR-29b, and VEGFA expression about 24 h after exposure to various concentrations of glucose (0, 5, 10, 15, and 20 mmol/l) or treatment with glucose (20 mmol/l) for the indicated times. $^*P < 0.05$ vs. control group.

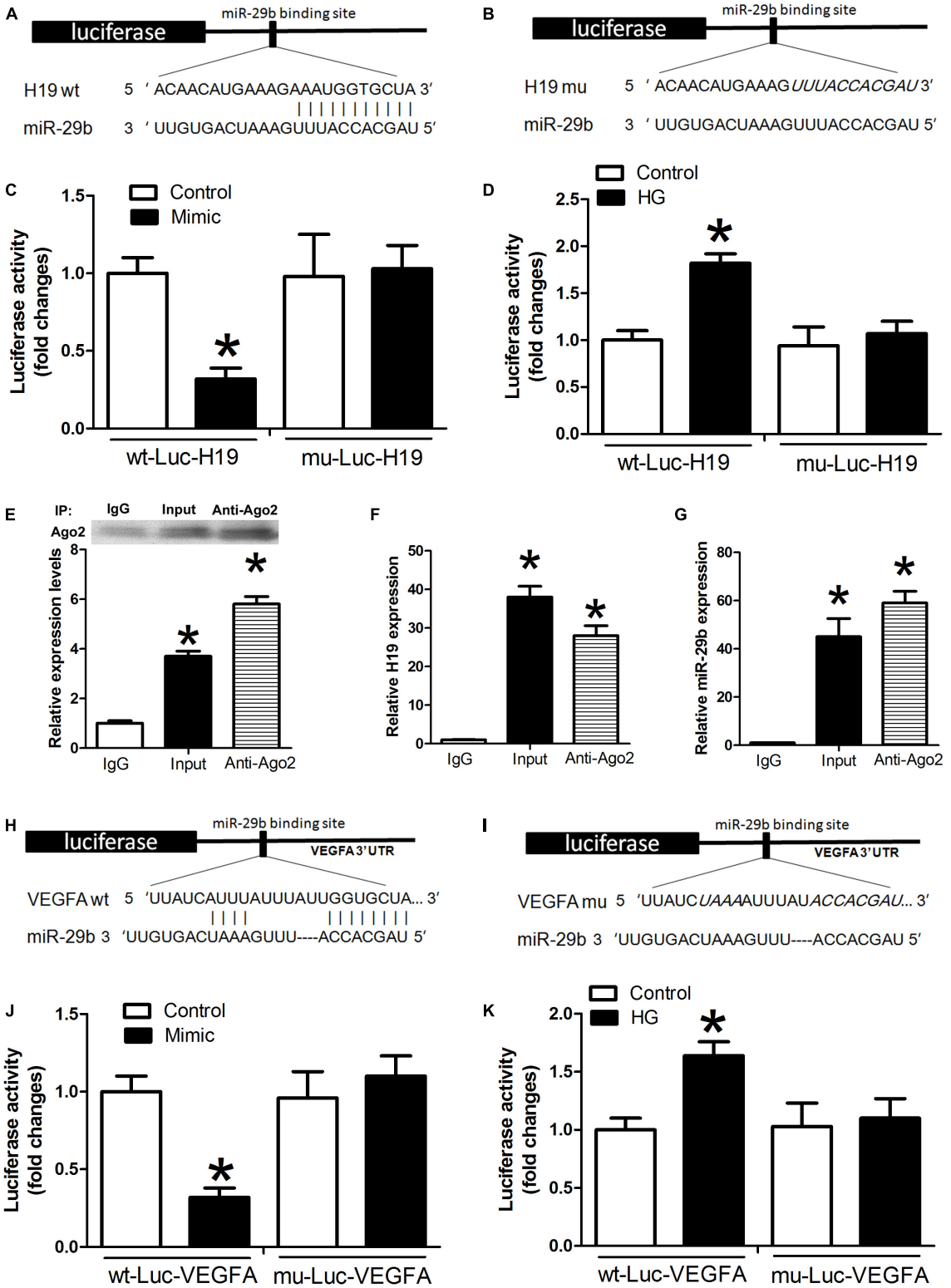

FIGURE 3 | Potential miR-29b binding sites in H19 and VEGFA. **(A,B)** H19 3′-UTR, wild type and mutated miR-29b binding sites. miR-29b mimic and luciferase constructs were co-transfected into HUVECs **(C)** and HUVECs exposed to high glucose concentrations **(D)**. Cellular lysates from HUVECs were used for RNA immunoprecipitation with an Ago2 antibody. Ago2 protein levels were measured by western blotting **(E)**, the amount of H19 **(F)**, and miR-29b **(G)** in the immunoprecipitate was measured by RT-PCR. Wild type **(H)** and mutated miR-29b **(I)** binding sites in the *VEGFA* 3′-UTR are shown in the upper panel. **(J,K)** Luciferase activity of wild type and mutant Luc VEGFA. **P* < 0.05 vs. control group. Mimic:miR29b mimic.

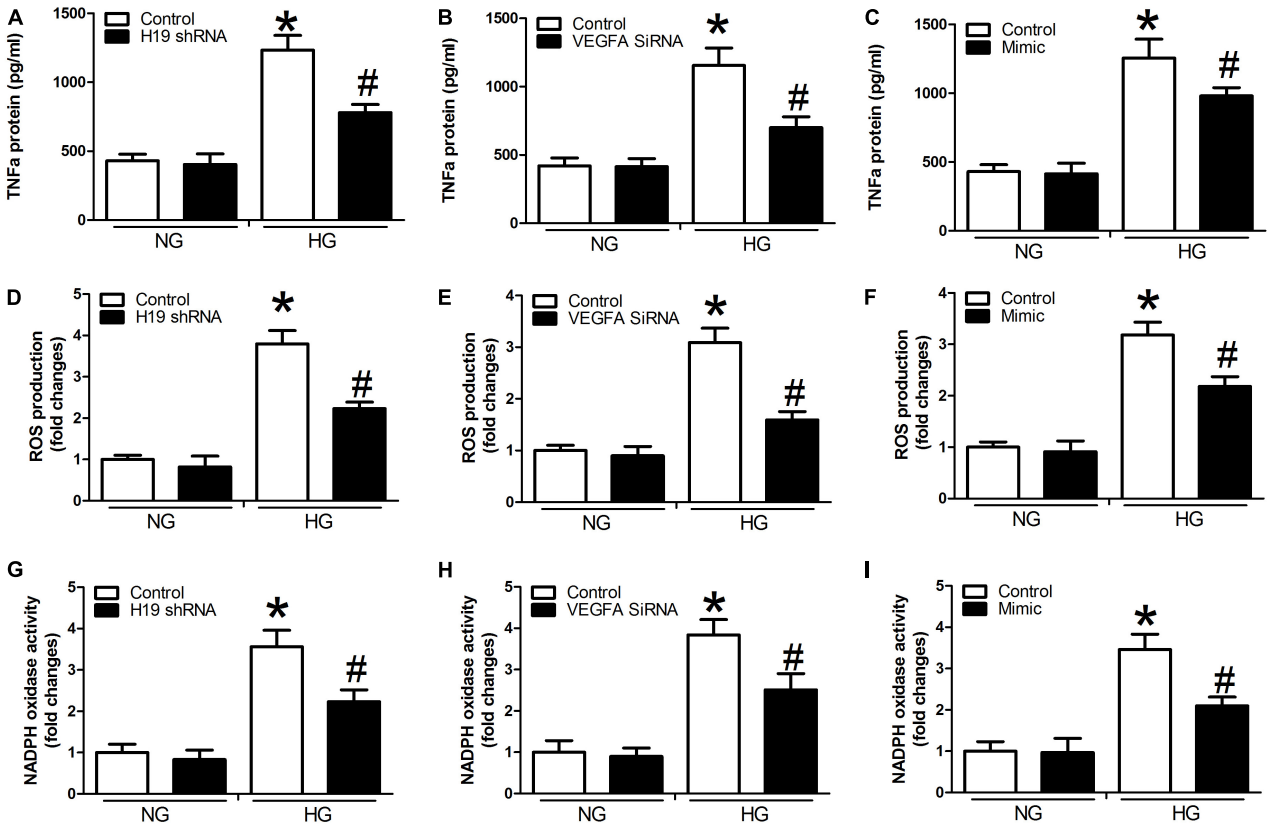

FIGURE 4 | H19, VEGFA, and miR-29b regulate the expression of TNF-α, ROS production, and NADPH oxidase activity under normal glucose (NG: 5 mM) or high glucose (HG: 20 mM) conditions. **(A–C)** TNF-α protein expression was determined after treatment with H19 shRNA, VEGFA siRNA, and miR-29b mimic, as was ROS production **(D–F)**, and NADPH oxidase activity **(G–I)**. $^{*}P < 0.05$, compared with control group in the presence of NG. $^{\#}P < 0.05$, compared with control group in the presence of HG. mimic, miR-29b mimic.

Expression of H19 and miR-29b in Patients With DM and Glucose-Treated HUVECs

H19 levels were significantly higher in blood samples obtained from individuals with DM than in the control individuals ($P < 0.05$, **Figure 2A**). Furthermore, relative miR-29b expression in individuals with DM was significantly weaker than that observed in the control individuals ($P < 0.05$, **Figure 2B**). Treatment with glucose in various doses and timings was associated with significant dose- and time-dependent H19 upregulation ($P < 0.05$, **Figures 2C,D**). In contrast, expression of miR-29b was significantly downregulated after administration of glucose in a dose- and time-dependent manner ($P < 0.05$, **Figures 2E,F**). Treatment with glucose in different doses and timings was also associated with significant dose- and time-dependent increase in VEGFA expression compared with the control group ($P < 0.05$, **Figures 2G,H**).

H19 Binds miR-29b Directly and VEGFA Is a Target of miR-29

Luciferase assay results indicated that miR-29b mimics induced decreases in H19 luciferase activity. However, this effect was not observed with the H19 mutants ($P < 0.05$, **Figures 3A,C**), and there were no statistically significant differences between the miR-29b group and controls ($P > 0.05$, **Figures 3A,C**). Treatment with high glucose levels induced a significant increase in wild type H19 luciferase activity, and this effect was reduced after mutation at certain H19 sites (**Figures 3B,D**). An RNA immunoprecipitation (RIP) experiment was performed to investigate whether H19 and miR-29b are components of the RNA-induced silencing complex. An Ago2 antibody was used to precipitate Ago2 protein from cultured cells (**Figure 3E**). mRNA expression of both H19 and miR-29b was significantly enriched in the immunoprecipitates (**Figures 3F,G**), indicating that there is direct binding between H19 and miR-29b. A luciferase test was performed to identify potential VEGFA miR-29b binding sites. Our results show that miR-29b mimics induce decreases in VEGFA luciferase activity. However, this effect was not observed in the mutant ($P < 0.05$, **Figures 3H,J**) and there were no statistically significant differences between the miR-29b group and the control in VEGFA mutants ($P > 0.05$, **Figures 3F,G**). In the wild type, high glucose treatment induced significant increases in luciferase activity, while this effect was reduced after mutation of certain VEGFA sites (**Figures 3I,K**).

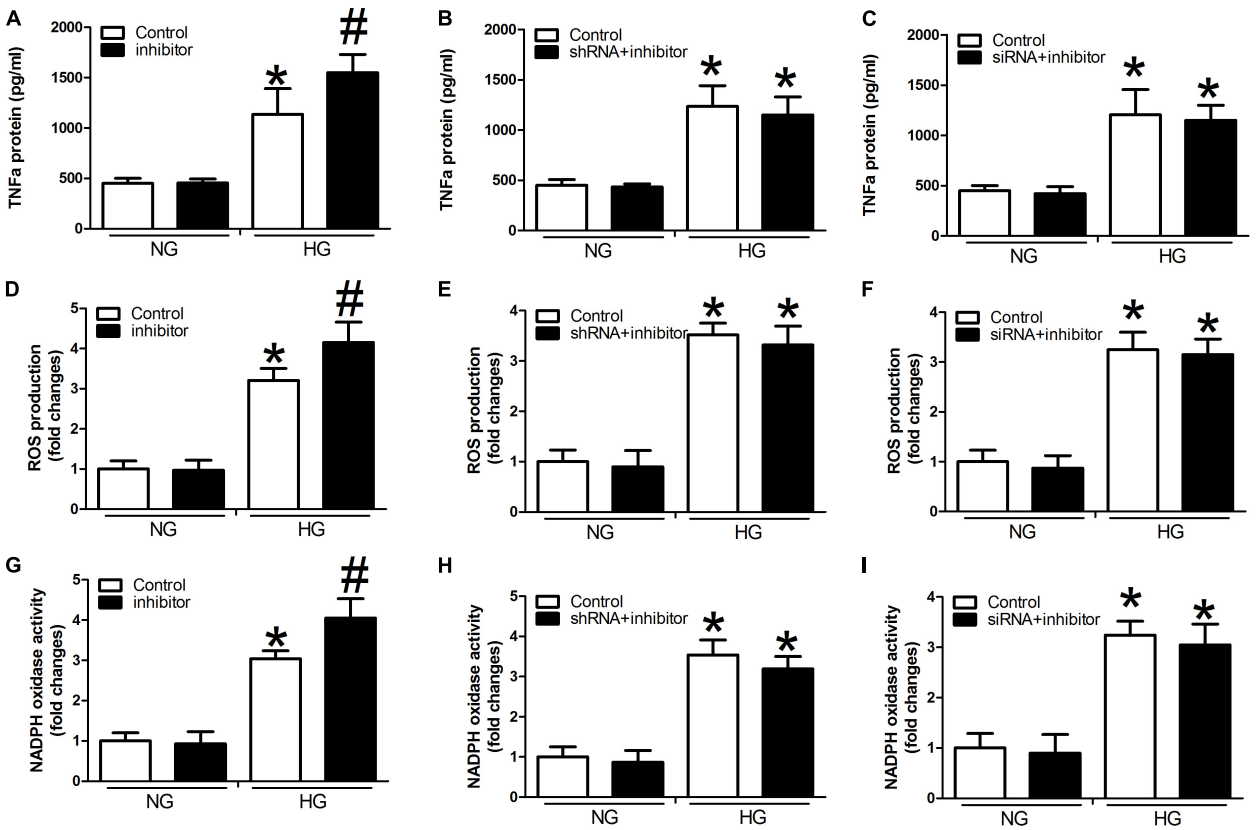

FIGURE 5 | miR-29b inhibitor alone and in combination with H19 shRNA and VEGFA siRNA can regulate the expression of TNF-α, ROS production, and NADPH oxidase activity. Cells were transfected with miR29b inhibitor, or H19-shRNA + miR-29b inhibitor, or VEGFA-siRNA + miR-29b inhibitor and were cultured under normal glucose (NG: 5 mM) or high glucose (HG: 20 mM) conditions. Decreased expression of TNF-α **(A–C)**, ROS **(D–F)**, and NADPH **(G–I)** oxidase activity observed in response to H19 silencing or VEGFA silencing was suppressed by miR-29b inhibitors. $^{*}P < 0.05$, compared with control group in the presence of NG. $^{\#}P < 0.05$ vs. miRNA-29b inhibitor group under normal glucose condition (NG, 5 mM). Inhibitor:miRNA-29b inhibitor; shRNA:H19 shRNA; siRNA:VEGFA siRNA.

Determination of TNF-α Expression, ROS Production, and NADPH Oxidase Activity in HUVECs Treated With High Concentrations of Glucose

Compared with controls, we detected significant activation of TNF-α expression, ROS production, and NADPH oxidase activity in the presence of high glucose concentrations in the miR-29b inhibitor alone group ($P < 0.05$, **Figures 4A,D,G**). We also observed obvious inhibition of TNF-α expression, ROS production, and NADPH oxidase activity in the H19 shRNA, VEGFA siRNA, and miR-29b mimic groups in the presence of high glucose concentrations ($P < 0.05$, **Figures 4B,C,E,F,H,I**). In addition, miR-29b inhibitor treatment reversed the effects of H19 shRNA and VEGFA siRNA on TNF-α expression, ROS production, and NADPH oxidase activity in the presence of high glucose concentrations ($P < 0.05$, **Figure 5**).

Role of H19/miR-29b/VEGFA in the AKT-eNOS Pathway

To test whether the observed changes in endogenous RNAs and inflammatory factors are related to the AKT-eNOS pathway, we assessed the expression of p-eNOS, eNOS, p-AKT, and AKT. p-eNOS, eNOS, and p-AKT expression levels were higher in the H19 shRNA group than those observed in the control group ($P < 0.05$, **Figures 6A,B**). However, this effect was suppressed in the H19shRNA + miR29b inhibitor group ($P < 0.05$, **Figures 6A,B**). Expression of p-eNOS, eNOS, and p-AKT was significantly upregulated the VEGFA siRNA group ($P < 0.05$, **Figures 6C,D**). Decreased p-eNOS, eNOS and p-AKT expression in response to H19 silencing was also suppressed by VEGFA siRNA + miR29b inhibitor treatment ($P < 0.05$, **Figures 6C,D**).

DISCUSSION

Diabetes has become an increasingly serious global health problem. High blood glucose concentrations are an independent risk factor for the development and progression of AS (Bhupathiraju and Hu, 2016; Shah and Brownlee, 2016). Moreover, endothelial cell dysfunction is a leading factor in the development and progression of AS (Haybar et al., 2019). High blood glucose concentrations may induce damage in endothelial cells, mainly through the dual mechanisms of inflammation,

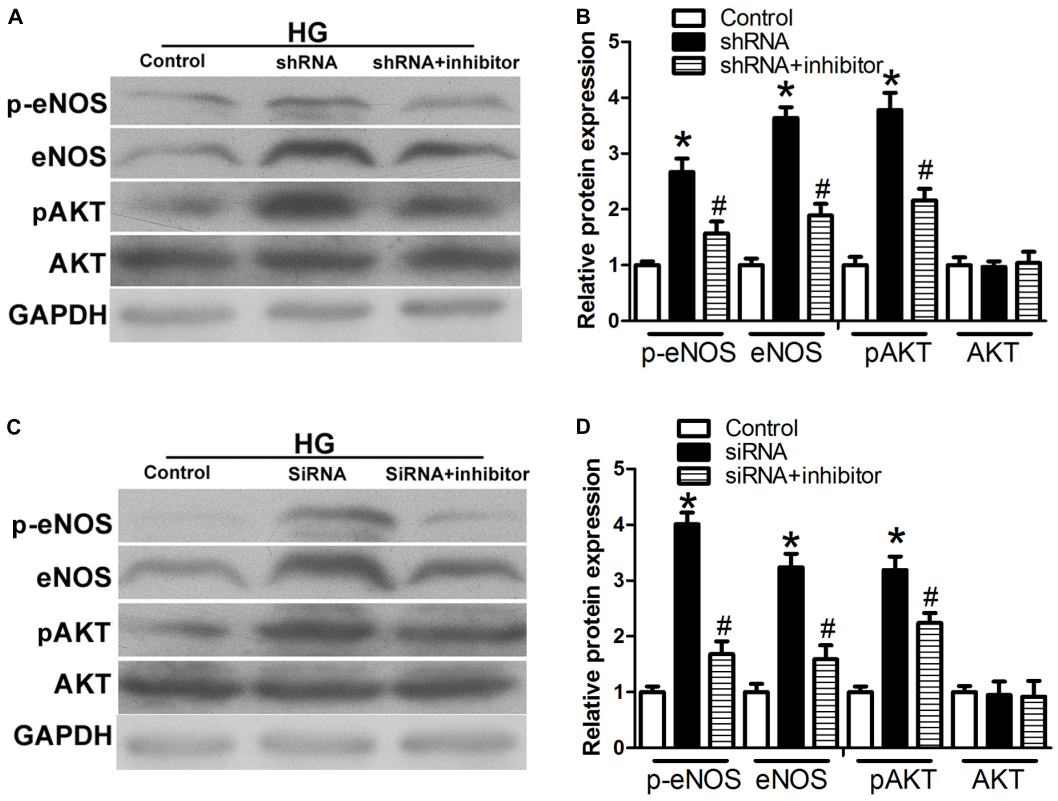

FIGURE 6 | The H19/miR-29b/VEGFA pathway is associated with the AKT–NOS pathway. **(A,B)** Expression of p-eNOS, eNOS, and p-AKT in HUVECs after treatment with H19 shRNA and H19 shRNA + miR-29b inhibitor. $^{*}P < 0.05$ vs. control group. $^{\#}P < 0.05$ vs. shRNA group. **(C,D)** Expression of p-eNOS, eNOS, and p-AKT in HUVECs after treatment with *VEGFA* siRNA and *VEGFA* siRNA + miR-29b inhibitor. $^{*}P < 0.05$ vs. control group. $^{\#}P < 0.05$ vs. siRNA group (HG, 20 mM). Inhibitor:miRNA-29b inhibitor; shRNA:H19 shRNA.

and oxidative stress (Shi and Vanhoutte, 2017). However, the specific molecular mechanisms through which this could occur are unclear. Based on these data, we surmised that regulating vascular inflammation by regulating expression of inflammation-related genes may be a means of preventing and treating CVDs.

In recent years, many studies have confirmed the important role of ncRNA networks in the regulation of gene expression. Furthermore, interactions between lncRNA and miRNA are reportedly involved in a variety of physiological and pathological processes (Abdollahzadeh et al., 2019). One of the first identified lncRNAs, H19, plays a wide range of roles *in vivo*. H19 can function as both a tumor suppressor or oncogene and also as a regulator of growth and development in multiple mammalian embryo tissues (Bai et al., 2016; Yoshimura et al., 2018). A previous study revealed that H19 is up-regulated in AS and is related to AS progression (Pan, 2017), but the underlying regulation mechanism has not yet been determined. Overexpression of miR-222 protects against cardiac injury and miR-17-3p promotes cardiomyocyte proliferation and increased cardiomyocyte size through directly targeting TIMP3 (Wang et al., 2018). miR-29b is one of the first miRNAs that was found to be dysregulated in retinal cells and diabetic rats exposed to high glucose concentrations, suggesting that they are involved in the development of DM (Dantas da Costa E Silva et al., 2019). A recent *in vivo* study showed that miR-29b is involved in regulation of glucose balance and insulin secretion through a variety of target genes and influences the pathogenesis of diabetes (Dooley et al., 2016). The VEGF glycoprotein family has a strong ability to promote vascular endothelial cell division and proliferation and enhance capillary permeability. This family includes VEGFA, VEGFB, VEGFC, VEGFD, and the placenta growth factor. VEGFA has been demonstrated to show prominent activity with vascular endothelial cells (Tan et al., 2018) and VEGFA is a direct target gene for many miRNAs. For instance, miR-9 inhibits retinal neovascularization and tubule formation in diabetic retinitis and promotes apoptosis in retinal microvascular endothelial cells by targeting VEGFA (Liu, 2019). miR-150-5p may function as a tumor suppressor in colorectal cancer, making the miR-150-5p/VEGFA axis a potential therapeutic target in colorectal cancer treatment (Chen et al., 2018). miR-15a-5p acts as a regulator of *VEGFA* mRNA and of subsequent inflammation and fibrosis in peritoneal mesothelial cells (Shang et al., 2019). These data led us to further investigate the potential involvement of H19 miR-29b/VEGFA in the inflammatory response in individuals with DM.

In this study, we show that H19/miR-29b/VEGFA signaling pathway plays a role in hyperglycemic-induced endothelial dysfunction. We found that H19 expression is upregulated

and miR-29b expression downregulated in ECs and blood samples obtained from individuals with DM. It has been widely reported that disease-associated lncRNAs and miRNA are detectable in the blood of patients (Yin et al., 2017; Zhang Y. et al., 2018; Yoffe et al., 2019). Therefore, lncRNA might present a potential biomarker for the dynamic monitoring of DM. In individuals with DM, H19 and miR-29b expression was consistent with the expression changes we observed in endothelial cells following glucose treatment for 48 h. VEGFA expression was consistent with H19 changes in the presence of high glucose concentrations. With increasing glucose concentrations in the growth medium of endothelial cells, H19, and VEGFA expression was significantly upregulated in endothelial cells, while miR-29b expression decreased in a dose-dependent manner. Furthermore, downregulation of H19 increases miR-29b expression and facilitates miR-29b-mediated VEGFA inhibition. The results of luciferase and RIP experiments suggest that H19 and miR-29b directly interact. Luciferase assay results revealed that miR-29b mimics decrease luciferase activity in wt-Luc-H19 transfected cells and that this effect is not observed in mu-Luc-H19-transfected cells. Exposure to high glucose concentrations increased wt-Luc-H19 luciferase activity and this effect was abrogated by the H19 mutant. We found that miR-29b mimics restrain luciferase activity in the wt-Luc-VEGFA reporter vector. However, this phenomenon was completely suppressed by mutation in the 3′-UTR of *VEGFA*. RIP experiments showed that the Ago2 protein was successfully precipitated from the digested cells by the Ago2 antibody. Both H19 and miR-29b were significantly enriched in the immunoprecipitates, suggesting that there is direct binding between H19 and miR-29b. These results indicate that H19 may in part regulate VEGFA expression by competing with miR-29b.

Next, we studied the link between H19/miR-29b/VEGFA and inflammatory factors in the pathogenesis of CVD by investigating TNF-α expression, ROS production, and NADPH oxidase activity. TNF-α, a prototype proinflammatory cytokine, increases endothelial permeability and disrupts endothelial integrity (Cui et al., 2018). ROS is considered to induce impairment of endothelial function in CVD. NADPH oxidase-derived ROS has been implicated in the activation of NF-κB and release of proinflammatory mediators (Yao et al., 2007). We identified significant inhibition of TNF-α expression, ROS production, and NADPH oxidase activity in H19 shRNA, VEGFA siRNA, and miR-29b mimic groups in the presence of high glucose. In addition, the miR-29b inhibitor reversed these effects. These results indicate that regulation of H19, miR-29b, and VEGFA expression modulates the expression of inflammatory factors that may contribute to the pathogenesis of CVD.

The AKT/eNOS signaling pathway is involved in key endothelial cell functions and in central cardiovascular regulation. To the best of our knowledge, the AKT/eNOS pathway plays an important role in improving endothelial function and alleviating AS (Xing et al., 2015). Our data show that phosphorylation of eNOS and AKT significantly increase in the presence of H19 shRNA and VEGFA siRNA and high glucose concentrations, and that these effects are reversed by the miR-29b inhibitor. Therefore, we speculate that H19 downregulates expression of VEGFA, the miR-29b target gene, and through competing with miR-29b. Moreover, modulation of H19/miR-29b/VEGFA may trigger up-regulation of the AKT/eNOS signaling pathway, indicating a potentially promising therapeutic strategy against AS.

We found a novel pathogenic link between lncRNA H19, miR-29b, and VEGFA in hyperglycemic-induced endothelial dysfunction. Suppression of H19 may alleviate inflammation in endothelial cells incubated at high glucose concentrations by upregulating miR-29b and inhibiting expression of VEGFA. These events are closely associated with activation of the AKT/eNOS signaling pathway, and can attenuate the progression of DM-related AS.

DATA AVAILABILITY STATEMENT

The data used to support the findings of this study are available from the corresponding authors upon request.

ETHICS STATEMENT

This study protocols were approved by the Ethics Committee of Anhui Medical University.

AUTHOR CONTRIBUTIONS

H-QZ and HW contributed to the conception and design of the experiments, gave final approval, and agreed to be accountable for all aspects of work ensuring integrity and accuracy. X-WC and Z-FC drafted and critically revised the manuscript. X-WC, Z-FC, and Y-FW completed the human and cell experiments. X-WC, Z-FC, Y-FW, and QZ contributed to the analysis.

FUNDING

This study was supported by the National Natural Science Foundation of China (81570419, 81302150, and 81270372) and Grants for Cultivating Program of National Natural Science Foundation for Young Scholars of the First Affiliated Hospital of Anhui Medical University (Grant No. 2012KJ10).

ACKNOWLEDGMENTS

We thank Dr. Trish Reynolds, MBBS, FRACP, and Rebecca Porter, Ph.D., from Liwen Bianji, Edanz Group China (www.liwenbianji.cn/ac), for editing the English text of a draft of this manuscript.

REFERENCES

Abdollahzadeh, R., Daraei, A., Mansoori, Y., Sepahvand, M., Amoli, M. M., and Tavakkoly-Bazzaz, J. (2019). Competing endogenous RNA (ceRNA) cross talk and language in ceRNA regulatory networks: a new look at hallmarks of breast cancer. *J. Cell. Physiol.* 234, 10080–10100. doi: 10.1002/jcp.27941

Bai, G. Y., Song, S. H., Wang, Z. D., Shan, Z. Y., Sun, R. Z., Liu, C. J., et al. (2016). Embryos aggregation improves development and imprinting gene expression in mouse parthenogenesis. *Dev. Growth Differ.* 58, 270–279. doi: 10.1111/dgd.12271

Bhupathiraju, S. N., and Hu, F. B. (2016). Epidemiology of obesity and diabetes and their cardiovascular complications. *Circ. Res.* 118, 1723–1725. doi: 10.1161/CIRCRESAHA.115.306825

Bitarafan, S., Yari, M., Broumand, M. A., Ghaderian, S. M. H., Rahimi, M., Mirfakhraie, R., et al. (2019). Association of increased levels of lncRNA H19 in PBMCs with risk of coronary artery disease. *Cell J.* 20, 564–568. doi: 10.22074/cellj.2019.5544

Brownlee, M. (2001). Biochemistry and molecular cell biology of diabetic complications. *Nature* 414, 813–820. doi: 10.1038/414813a

Chen, X., Xu, X., Pan, B., Zeng, K., Xu, M., Liu, X., et al. (2018). miR-150-5p suppresses tumor progression by targeting VEGFA in colorectal cancer. *Aging* 10, 3337–3421. doi: 10.18632/aging.101656

Cui, S., Men, L., Li, Y., Zhong, Y., Yu, S., Li, F., et al. (2018). Selenoprotein S attenuates tumor necrosis factor-α-induced dysfunction in endothelial cells. *Mediat. Inflamm.* 2018:1625414. doi: 10.1155/2018/1625414

Dantas da Costa E Silva, M. E., Polina, E. R., Crispim, D., Sbruzzi, R. C., Lavinsky, D., Mallmann, F., et al. (2019). Plasma levels of miR-29b and miR-200b in type 2 diabetic retinopathy. *J. Cell Mol. Med.* 23, 1280–1287. doi: 10.1111/jcmm.14030

Dooley, J., Garcia-Perez, J. E., Sreenivasan, J., Schlenner, S. M., Vangoitsenhoven, R., Papadopoulou, A. S., et al. (2016). The microRNA-29 family dictates the balance between homeostatic and pathological glucose handling in diabetes and obesity. *Diabetes Metab. Res. Rev.* 65, 53–61. doi: 10.2337/db15-0770

Fishman, S. L., Sonmez, H., Basman, C., Singh, V., and Poretsky, L. (2018). The role of advanced glycation end-products in the development of coronary artery disease in patients with and without diabetes mellitus: a review. *Mol. Med.* 24:59. doi: 10.1186/s10020-018-0060-3

García-Redondo, A. B., Aguado, A., Briones, A. M., and Salaices, M. (2016). NADPH oxidases and vascular remodeling in cardiovascular diseases. *Pharmacol. Res.* 114, 110–120. doi: 10.1016/j.phrs.2016.10.015

Haybar, H., Shahrabi, S., Rezaeeyan, H., Shirzad, R., and Saki, N. (2019). Endothelial cells: from dysfunction mechanism to pharmacological effect in cardiovascular disease. *Cardiovasc. Toxicol.* 19, 13–22. doi: 10.1007/s12012-018-9493-8

Hou, J., Wang, L., Wu, Q., Zheng, G., Long, H., Wu, H., et al. (2018). Long noncoding RNA H19 upregulates vascular endothelial growth factor a to enhance mesenchymal stem cells survival and angiogenic capacity by inhibiting miR-199a-5p. *Stem Cell Res. Ther.* 9 :109. doi: 10.1186/s13287-018-0861-x

Hung, J., Miscianinov, V., Sluimer, J. C., Newby, D. E., and Baker, A. H. (2018). Targeting non-coding RNA in vascular biology and disease. *Front. Physiol.* 9:1655. doi: 10.3389/fphys.2018.01655

Li, Y., Arnold, J. M., Pampillo, M., Babwah, A. V., and Peng, T. (2009). Taurine prevents cardiomyocyte death by inhibiting NADPH oxidase-mediated calpain activation. *Free Radic. Biol. Med.* 46, 51–61. doi: 10.1016/j.freeradbiomed.2008.09.025

Liu, W. L. (2019). MicroRNA-9 inhibits retinal neovascularization in rats with diabetic retinopathy by targeting vascular endothelial growth factor A. *J. Cell. Biochem.* 120, 8032–8043. doi: 10.1002/jcb.28081

Pan, J. X. (2017). LncRNA H19 promotes atherosclerosis by regulating MAPK and NF-kB signaling pathway. *Eur. Rev. Med. Pharmacol. Sci.* 21, 322–328.

Shah, M. S., and Brownlee, M. (2016). Molecular and cellular mechanisms of cardiovascular disorders in diabetes. *Circ. Res.* 118, 1808–1829. doi: 10.1161/CIRCRESAHA.116.306923

Shang, J., He, Q., Chen, Y., Yu, D., Sun, L., Cheng, G., et al. (2019). miR-15a-5p suppresses inflammation and fibrosis of peritoneal mesothelial cells induced by peritoneal dialysis via targeting VEGFA. *J. Cell. Physiol.* 234, 9746–9755. doi: 10.1002/jcp.27660

Shi, Y., and Vanhoutte, P. M. (2017). Macro- and microvascular endothelial dysfunction in diabetes. *J. Diabetes* 9, 434–449. doi: 10.1111/1753-0407.12521

Simion, V., Haemmig, S., and Feinberg, M. W. (2019). LncRNAs in vascular biology and disease. *Vascul. Pharmacol.* 114, 145–156. doi: 10.1016/j.vph.2018.01.003

Tan, Z., Chen, K., Wu, W., Zhou, Y., Zhu, J., Wu, G., et al. (2018). Overexpression of HOXC10 promotes angiogenesis in human glioma via interaction with PRMT5 and upregulation of VEGFA expression. *Theranostics* 8, 5143–5158. doi: 10.7150/thno.27310

Wang, L., Lv, Y., Li, G., and Xiao, J. (2018). MicroRNAs in heart and circulation during physical exercise. *J. Sport. Health Sci.* 7, 433–441. doi: 10.1016/j.jshs.2018.09.008

Xing, S. S., Yang, X. Y., Zheng, T., Li, W. J., Wu, D., Chi, J. Y., et al. (2015). Salidroside improves endothelial function and alleviates atherosclerosis by activating a mitochondria-related AMPK/PI3K/Akt/eNOS pathway. *Vascul. Pharmacol.* 72, 141–152. doi: 10.1016/j.vph.2015.07.004

Yao, H., Yang, S. R., Kode, A., Rajendrasozhan, S., Caito, S., Adenuga, D., et al. (2007). Redox regulation of lung inflammation: role of NADPH oxidase and NF-kappaB signaling. *Biochem. Soc. Trans.* 35, 1151–1155. doi: 10.1042/bst0351151

Yin, Q., Wu, A., and Liu, M. (2017). Plasma long non-coding RNA (lncRNA) GAS5 is a new biomarker for coronary artery disease. *Med. Sci. Monit.* 23, 6042–6048. doi: 10.12659/msm.907118

Yoffe, L., Polsky, A., Gilam, A., Raff, C., Mecacci, F., Ognibene, A., et al. (2019). Early Diagnosis of gestational diabetes mellitus using circulating microRNAs. *Eur. J. Endocrinol.* 181, 565–577. doi: 10.1530/eje-19-0206

Yoshimura, H., Matsuda, Y., Yamamoto, M., Kamiya, S., and Ishiwata, T. (2018). Expression and role of long non-coding RNA H19 in carcinogenesis. *Front. Biosci.* 23:614–625. doi: 10.2741/4608

Yuan, T., Yang, T., Chen, H., Fu, D., Hu, Y., Wang, J., et al. (2019). New insights into oxidative stress and inflammation during diabetes mellitus-accelerated atherosclerosis. *Redox. Biol.* 20, 247–260. doi: 10.1016/j.redox.2018.09.025

Zhang, N., Geng, T., Wang, Z., Zhang, R., Cao, T., Camporez, J. P., et al. (2018). Elevated hepatic expression of H19 long noncoding RNA contributes to diabetic hyperglycemia. *JCI Insight* 3:e120304. doi: 10.1172/jci.insight.120304

Zhang, X., Cheng, L., Xu, L., Zhang, Y., Yang, Y., Fu, Q., et al. (2019). The lncrna, h19 mediates the protective effect of hypoxia postconditioning against hypoxia-reoxygenation injury to senescent cardiomyocytes by targeting microRNA-29b-3p. *Shock* 52, 249–256. doi: 10.1097/SHK.0000000000001213

Zhang, Y., Wu, H., Wang, F., Ye, M., Zhu, H., and Bu, S. (2018). Long non-coding RNA MALAT1 expression in patients with gestational diabetes mellitus. *Int. J. Gynaecol. Obstet.* 140, 164–169. doi: 10.1002/ijgo.12384

Zhu, H., Shan, L., and Peng, T. (2009). Rac1 mediates sex difference in cardiac tumor necrosis factor-alpha expression via NADPHoxidase-ERK1/2/p38 MAPK pathway in endotoxemia. *J. Mol. Cell Cardiol.* 47, 264–274. doi: 10.1016/j.yjmcc.2009.05.002

Conflict of Interest: The authors declare that the research was conducted in the absence of any commercial or financial relationships that could be construed as a potential conflict of interest.

frontiers in Cell and Developmental Biology

ORIGINAL RESEARCH
published: 01 November 2019
doi: 10.3389/fcell.2019.00253

STAT3 Regulates miR-384 Transcription During Th17 Polarization

Jingjing Han[1,2†], Yaping Liu[3†], Fei Zhen[1], Wen Yuan[1], Wei Zhang[1], Xiaotao Song[1], Fuxing Dong[1], Ruiqin Yao[1] and Xuebin Qu[1]**

[1] Department of Cell Biology and Neurobiology, Xuzhou Key Laboratory of Neurobiology, Xuzhou Medical University, Xuzhou, China, [2] Department of Neurology, the Affiliated Hospital of Xuzhou Medical University, Xuzhou, China, [3] National Demonstration Center for Experimental Basic Medical Sciences Education, Xuzhou Medical University, Xuzhou, China

MicroRNAs are powerful regulators of gene expression in physiological and pathological conditions. We previously showed that the dysregulation of miR-384 resulted in a T helper cell 17 (Th17) imbalance and contributed to the pathogenesis of experimental autoimmune encephalomyelitis, an animal model of multiple sclerosis. In this study, we evaluated the molecular mechanisms underlying the abnormal increase in miR-384. We did not detect typical CpG islands in the *Mir384* promoter. Based on a bioinformatics analysis of the promoter, we identified three conserved transcription factor binding regions (R_I, R_{II}, and R_{III}), two of which (R_{II} and R_{III}) were *cis*-regulatory elements. Furthermore, we showed that signal transducer and activator of transcription 3 (STAT3) bound to specific sites in R_{II} and R_{III} based on chromatin immunoprecipitation, electrophoretic mobility shift assays, and site-specific mutagenesis. During Th17 polarization *in vitro*, STAT3 activation up-regulated miR-384, while a STAT3 phosphorylation inhibitor decreased miR-384 levels and reduced the percentage of IL-17$^+$ cells, IL-17 secretion, and expression of the Th17 lineage marker Rorγt. Moreover, the simultaneous inhibition of STAT3 and miR-384 could further block Th17 polarization. These results indicate that STAT3, rather than DNA methylation, contributes to the regulation of miR-384 during Th17 polarization.

Keywords: miR-384, STAT3, promoter, CpG island, T helper cell 17

OPEN ACCESS

Edited by:
Junjie Xiao,
Shanghai University, China

Reviewed by:
Jens Staal,
Ghent University, Belgium
Yingqiu Li,
Sun Yat-sen University, China

***Correspondence:**
Ruiqin Yao
wenxi_yao@163.com
Xuebin Qu
100002012036@xzhmu.edu.cn

† These authors have contributed equally to this work

Specialty section:
This article was submitted to Signaling, a section of the journal Frontiers in Cell and Developmental Biology

Received: *05 August 2019*
Accepted: *14 October 2019*
Published: *01 November 2019*

Citation:
Han J, Liu Y, Zhen F, Yuan W, Zhang W, Song X, Dong F, Yao R and Qu X (2019) STAT3 Regulates miR-384 Transcription During Th17 Polarization. Front. Cell Dev. Biol. 7:253. doi: 10.3389/fcell.2019.00253

INTRODUCTION

MicroRNAs (miRNAs) are a class of important small non-coding RNAs that either inhibit the translation of or trigger the degradation of target mRNAs by binding to 3′-untranslated regions (Saliminejad et al., 2019). About 1000 human miRNAs have been identified. They are thought to regulate more than 50% of protein-coding genes in the genome and thereby contribute to a wide array of complex cellular processes, including cell proliferation, differentiation, invasion, metastasis, apoptosis, and cell–cell communication (Selbach et al., 2008; Bayraktar et al., 2017). Furthermore, miRNAs are involved in many diseases, such as cancer, cardiovascular diseases, metabolic diseases, neurodegenerative diseases, and autoimmune diseases (Paul et al., 2018). They are used as diagnostic, prognostic, and predictive biomarkers (Jamali et al., 2018; Petrovic and Ergun, 2018; Salehi and Sharifi, 2018), and miRNA-based therapies have shown promising results

in clinical trials for cancer and viral infections (Beg et al., 2017; van der Ree et al., 2017). However, the upstream mechanisms underlying the regulation of miRNAs are not well understood. In other words, the factors contributing to the disruption of specific miRNAs in certain diseases are unclear.

Most miRNA genes are transcribed by RNA polymerase II as initial stem-loop structured primary miRNAs, cleaved into precursor miRNAs by Drosha (Garcia-Lopez et al., 2013), and processed into small double-stranded RNAs by Dicer (Ha and Kim, 2014). When the miRNA-induced silencing complex is assembled, mature miRNAs are guided to destabilize mRNA and repress translation (Bartel, 2004; Bagga et al., 2005; Krol et al., 2010). Although Drosha and Dicer are indispensable during miRNA biogenesis, they cannot precisely regulate specific miRNAs in a tissue- and developmental stage-specific manner.

Tissue- or developmental stage-specific miRNAs are often associated with diseases related to specific cells and tissues. Transcription profiling of miRNAs in human tissue biopsies of different organs has shown that approximately 17% of miRNAs and miRNA families are predominantly expressed in certain tissues (Ludwig et al., 2016). Emerging evidence now indicates that epigenetic and transcriptional regulation play major roles in controlling the spatial and temporal transcription of miRNAs. In cancer, the altered transcription of many miRNAs is caused in large part by changes in DNA CpG island methylation; approximately 50% of miRNA genes are associated with CpG islands (Wang et al., 2013). For example, DNA methyltransferase (DNMT) inhibitors restore miR-127 transcription (Saito et al., 2006) and the genetic disruption of DNMTs restores the transcription of miR-124a (Lujambio et al., 2007), suggesting that DNA methylation is a major factor in miRNA transcriptional silencing in cancers.

In addition to DNA methylation, transcription factors (TFs) are thought to regulate miRNA genes in a manner similar to the regulation of protein-coding genes (Ozsolak et al., 2008). This is supported by the observation that conventional TF binding sites are located in or near promoter regions lying upstream of many miRNA genes (Turner and Slack, 2009), indicating that the promoters of specific miRNA genes can be positively or negatively controlled by TFs for activation or silencing in a tissue- or developmental stage-specific manner (Krol et al., 2010). For example, Myc activates miR-17-92 and miR-9 but inhibits the transcription of miR-15a during the proliferation and apoptosis of cancer cells (Chang et al., 2008). P53 promotes the transcription of miR-34 and miR-107 (He et al., 2007), while signal transducer and activator of transcription 3 (STAT3) down-regulates miR-520d-5p (Li et al., 2017). During nervous system development, REST is closely related to miR-124 transcription (Conaco et al., 2006).

Recent studies have shown that miR-384 is closely associated with cancer cell proliferation, metastasis, and progression (Zheng et al., 2016; Wang Y. et al., 2018; Wang Y. X. et al., 2018; Yao et al., 2019). We have previously shown that miR-384 levels are abnormally increased in the pathogenesis of experimental autoimmune encephalomyelitis (EAE) (Qu et al., 2017), a central nervous system autoimmune disease caused by inappropriate inflammation and the infiltration of IL-17-producing $CD4^+$ T helper (Th17) cells (Zhu et al., 2017; Zhang et al., 2019). Enforced constitutive expression of miR-384 in $CD4^+$ naïve T cells promotes polarization to the Th17 lineage, leading to severe EAE, by targeting suppressor of cytokine signaling 3 (SOCS3) (Qu et al., 2017). This previous work has clearly established that miR-384 regulates Th17 development and thereby contributes to the pathogenesis of EAE. In this study, we evaluated the upstream molecular mechanisms underlying the regulation of miR-384 and found that miR-384 could be activated by p-STAT3, thus explaining the abnormal increase in this miRNA during Th17 polarization.

MATERIALS AND METHODS

Mice

C57BL/6 wild-type (WT) mice were purchased from SLAC Laboratory Animal Co., Ltd. (Shanghai, China), and housed under specific-pathogen-free conditions in the Xuzhou Medical University animal facility (Xuzhou, China). All experiments were performed in accordance with the Provisions and General Recommendations of the Chinese Experimental Animal Administration Legislation, as well as institutional approval from the Xuzhou Medical University Experimental Animal Ethics Committee.

Cell Isolation, Culture, and Induction

Splenocytes (SPs), isolated from 5- to 6-week-old C57BL/6 mice, were prepared for a single-cell suspension with red blood cells depletion by ACK lysis (Beyotime, Shanghai, China). $CD4^+$ T cells were isolated according to manufacturer's instructions (Miltenyi Biotec, Bergisch Gladbach, Germany). As our previous description (Qu et al., 2016), purification of $CD4^+$ naïve T cells was achieved by depletion of magnetically labeled non-naïve $CD4^+$ T cells and $CD44^+$ memory T cells following kit instructions (Miltenyi Biotec, Bergisch Gladbach, Germany).

For Th17 polarization, purified $CD4^+$ naïve T cells were cultured for 3 days in RPMI-1640 containing 10% FBS, 1 mM glutamine, 0.1 mM β-mercaptoethanol, 1% non-essential amino acids (Sigma-Aldrich, MO, United States), anti-CD3 plus anti-CD28-coated beads (Invitrogen, CA, United States), 5 ng/ml IL-2 (R&D Systems Inc., MN, United States), 20 ng/ml IL-6, 5 ng/ml transforming growth factor-β, 10 ng/ml IL-23, 2 μg/ml anti-IL-4, and 2 μg/ml anti-interferon-γ (BD Bioscience, CA, United States). In some experiments, 10 μM AG490 (MCE, NJ, United States), 200 nM SignalSilence® Stat3 siRNA II (CST, MA, United States) or miR-384 inhibitor (acauugccuaggaauuguuuaca) (Qu et al., 2017) was used.

Flow Cytometric Analyses

Cells were incubated with Cell Stimulation Cocktail (eBioscience, CA, United States) for 5 h, then surface-stained with anti-CD4 antibody (Clone GK1.5, Miltenyi Biotec, Germany), followed by

fix and permeabilization using a Fixation/Permeabilization Kit (BD Biosciences, United States). Subsequently, the cells were washed and stained with anti-IL-17 antibody (Clone TC11-18H10, Miltenyi Biotec, Germany). Tests were proceeded on MACSQuant™ Flow Cytometers (Miltenyi Biotec, Germany) and analyzed with FlowJo software.

ELISA

Quantikine ELISA kit to measure IL-17 concentration was obtained from Westang Biological Technology Co., Ltd (Shanghai, China) and used according to the manufacturer's instructions. All samples were measured in duplicate for five times.

Quantitative RT-PCR

After RNA were extracted using TRIzol (Invitrogen, United States) according to usual protocol, 1 μg total RNA was reverse-transcribed using a Quantscript RT kit (TIANGEN, Beijing, China) and examined with a SYBR Green real-time PCR kit (Roche, Basel, Switzerland) in lightCycler® 480II System (Roche, Switzerland). The primers used were as follows: Rorγt, 5′-TGCAAGACTCATCGACAAGG and 5′-AGGGGATTCAACATCAGTGC; SOCS3, 5′-ATGGTCACCC ACAGCAAGTTT and 5′-TCCAGTAGAATCCGCTCTCCT; β-actin,5′-GAGACCTTCAACACCCCAGCC and 5′-AATGTCA CGCACGATTTCCC. Analyses of miR-384 levels were performed using SYBR Green miRNA assays (Genechem, Shanghai, China) with U6 small RNA as an internal reference for normalization. Relative expression was evaluated using $2^{-\Delta\Delta Ct}$ calculation.

Western Blot

Cells were ultrasonically homogenized in RIPA buffer, and quantified using bicinchoninic acid protein assay kit (Beyotime, Shanghai, China). Protein samples were electrophoresed in an SDS denaturing 10% polyacrylamide gels and transferred to nitrocellulose membranes. Membranes were blocked in 0.01% PBS containing 5% BSA, incubated overnight at 4°C with anti-p-STAT3 (Clone EP2147Y), anti-STAT3 (Clone EPR787Y) and anti-GAPDH (Clone 6C5) primary antibodies (Abcam, Cambridge, United Kingdom), and then incubated in IRDye-conjugated secondary antibodies (LI-COR, CA, United States). Bands were scanned using an Odyssey Infrared Imaging System Scanner (LI-COR, United States) and images were analyzed using ImageJ software.

Dual-Luciferase Reporter Assay

Synthesized DNA sequences (deletion constructs or binding site-mutated fragments) were cloned into the pGL4.20[luc2Puro] vector (Promega, Madison, WI, United States). The recombinant plasmids together with internal control PRL-TK Renilla vector were transfected into Jurkat cells using Lipofectamine 2000 reagent (Invitrogen, United States) following the instructions. Cells were harvested at 48 h post transfection and assayed for luciferase activity using the Dual-Luciferase Reporter Assay System (Promega, United States).

Chromatin Immunoprecipitation Assay

ChIP assays were performed using an EZ-Magna ChIP™ HiSens kit (Millipore, MA, United States) according to the manufacturer's instructions. Chromatin was cross-linked with 1% formaldehyde for 10 min, followed by neutralization with glycine for 5 min at room temperature. Cells were then harvested, lysed, and sonicated 15 times for 4.5 s each with 9 s intervals on ice water using a Scientz-IID (Scientz, Zhejiang, China). An equal amount of chromatin was immunoprecipitated at 4°C overnight with 2 μg of p-STAT3 (Clone EP2147Y) or isotype IgG antibodies (Clone EPR25A, Abcam, United Kingdom) together with Magna ChIP protein A Magnetic Beads. Immunoprecipitated products were collected on the magnetic separator, eluted in ChIP elution buffer, and purified to obtain DNA for PCR test. Primers for PCR were listed as follows: Site 1, 5′-ATGCTATAACCACCACCA and 5′-CTTGGGATATTGTTCTGTAA; Site 2, 5′-TGCTGCCTTC TGCTTTGA and 5′-CAGGCATTGTGAACAATTTCTA; Site 3, 5′-CACTCATAAACTGGCTCG and 5′-ACTGTCTGAAGC AGTCCC.

Electrophoretic Mobility Shift Assay

Cellular nuclear protein was extracted with Nucleoprotein Extraction Kit (Beyotime, China). A total of 12 μg of nuclear protein was added to 0.1 μM Biotin-labeled double-stranded oligonucleotides (Sangon, Shanghai, China) in 1 × EMSA/Gel-Shift binding buffer. In some trials, extra 5 μM unlabeled competitor oligonucleotide or 2 μg of anti-p-STAT3 antibody was used. Mixtures were incubated at 24°C for 20 min, analyzed by electrophoresis in 4% polyacrylamide gels at 10 V/cm, and then transferred to a nylon membrane. Membranes were UV-light cross-linked, incubated with Streptavidin-conjugated HRP, and proceeded with chemiluminescence. The probe sequences were listed as follows: Site 1, 5′-TGACCCCAGGAACTTGTATA***TGCTAGGCAA***GTACTCTATT ACAGAACAAT; Site 2, 5′-TGTATAATGTTGGTAAGTCA***TTC CTAGAAA***TTGTTCACAATGCCTGTAAC. The sequences in bold and italic show the predicted binding sites of STAT3. Site 1 mutation, 5′-TGACCCCAGGAACTTGTATA CCGACTCTTCGTACTCTATTACAGAACAAT; Site 2 mutation, 5′-TGTATAATGTTGGTAAGTCACCGACTCTTCTTGTTCAC AATGCCTGTAAC. The underline marked sequences show the mutated binding sites of STAT3.

Bioinformatics Analysis Websites

MiR-384 and gene promoter sequences were obtained from Mirbase[1] and UCSC[2]. CpG islands prediction was analyzed by EMBOSS Cpgplot[3], MethPrimer[4], and Sequence Manipulation

[1] http://www.mirbase.org/

[2] http://genome.ucsc.edu/ENCODE/

[3] http://www.ebi.ac.uk/emboss/cpgplot/

[4] http://www.urogene.org/methprimer

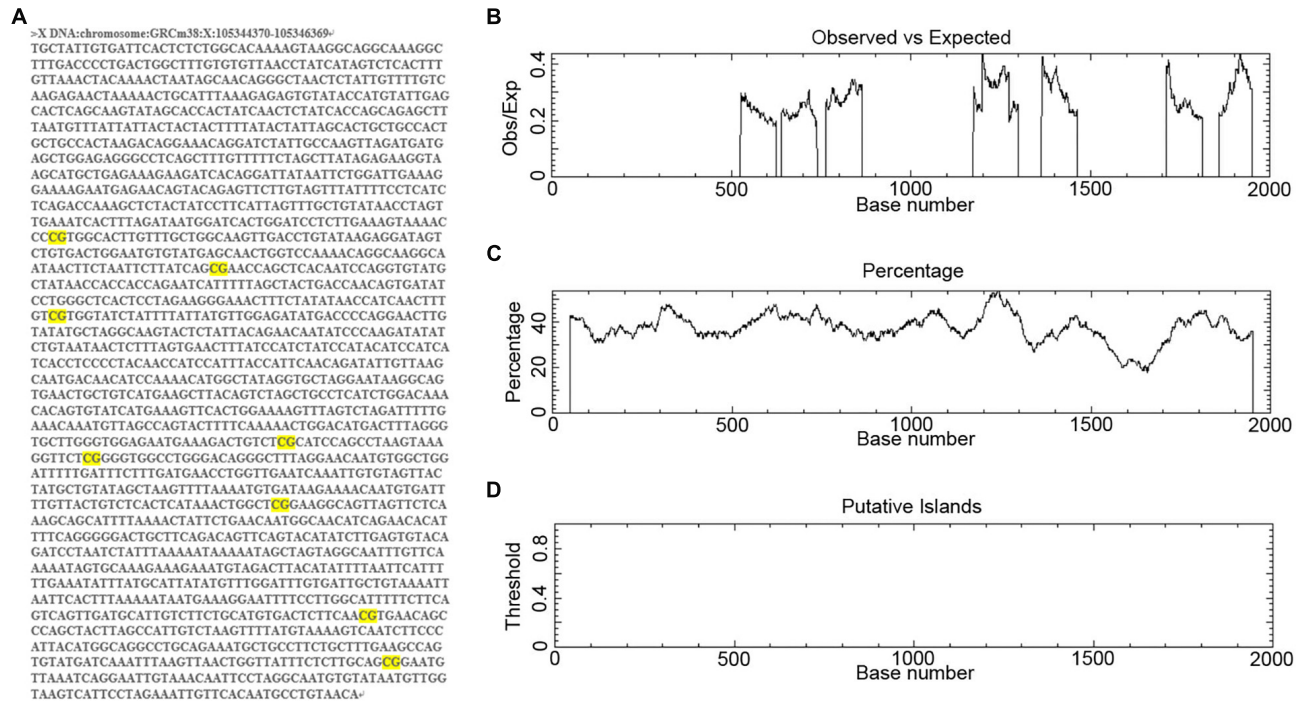

FIGURE 1 | Analysis of CpG islands in *Mir384* promoter. **(A)** The DNA sequence 2000 bp upstream of *Mir384* in chromosome X. CG dinucleotides are marked in bright yellow. **(B–D)** *Mir384* promoter sequence is analyzed by EMBOSS Cpgplot for CpG islands prediction, and the ratio of observed to expected **(B)**, percentage of CG **(C)**, and putative CpG island **(D)** are shown.

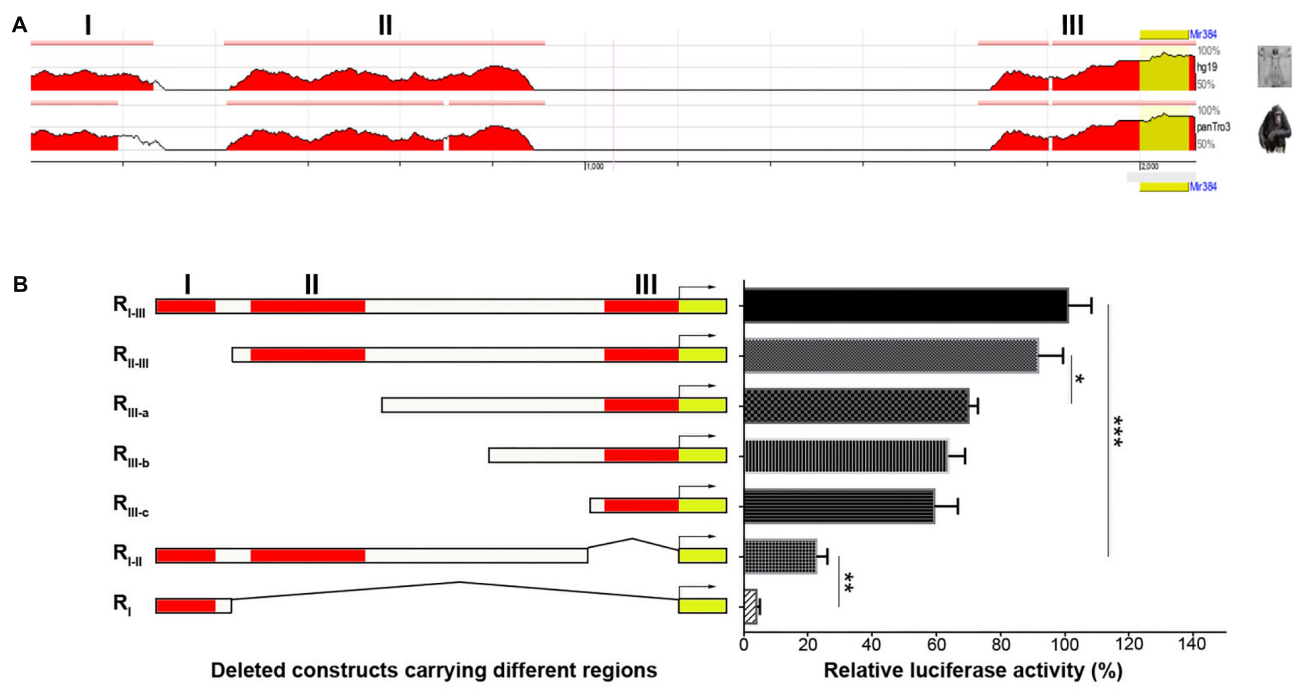

FIGURE 2 | Analysis of TFs binding in different regions of *Mir384* promoter. **(A)** The homologous binding sites of TFs in *Mir384* promoter among the species of mouse, human, and chimp. This sequence is divided into three regions (I, II, and III) according to the binding sites. Peaks represent the level of homology. **(B)** Effects of different binding region deletion on transcriptional activity by luciferase assay. On the left side is a schematic representation of the deleted DNA sequences carrying different regions. The right panel shows luciferase activity normalized to Renilla luciferase activity. Data are presented as mean ± standard deviation. $^{*}P < 0.05$. $^{**}P < 0.01$. $^{***}P < 0.001$. Data are representative of three experiments done in triplicate.

A

Matrix ID	Name	Score	Relative score	Sequence ID	Start	End	Predicted sequence
MA0144.1	Stat3	6.10531	0.800387955698	X	299	308	AGACAGGAAA
MA0144.1	Stat3	6.7854	0.812875295519	X	864	873	TGCTAGGCAA
MA0144.1	Stat3	7.94	0.834075088193	X	1035	1044	TGCTAGGAAT
MA0144.1	Stat3	6.10874	0.800451055218	X	1119	1128	TCACTGGAAA
MA0144.1	Stat3	9.18987	0.857024340665	X	1970	1979	TTCCTAGAAA

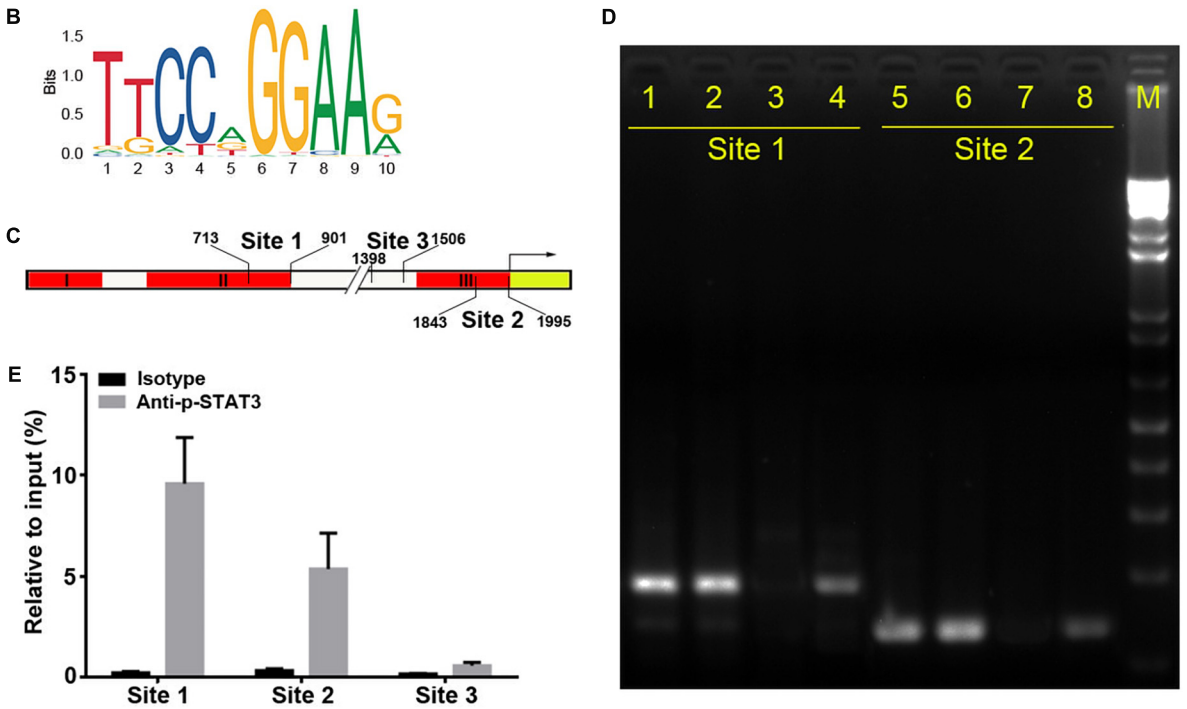

FIGURE 3 | STAT3 binds to *Mir384* promoter. **(A)** Analysis of STAT3 binding sites in the *Mir384* promoter by JASPAR database. **(B)** Sequence logo of STAT3 binding sites. **(C)** Pattern diagram shows the locations of site 1, site 2, site 3, and primers for ChIP-PCR. **(D)** Gel electropherogram of ChIP-PCR products at site 1 and site 2. Lanes 1 and 5, immunoprecipitation by anti-RNA Polymerase II antibody. Lanes 2 and 6, input. Lanes 3 and 7, immunoprecipitation by isotype IgG. Lanes 4 and 8, immunoprecipitation by anti-p-STAT3 antibody. M, DNA marker. **(E)** ChIP-qRT-PCR assay to analyze p-STAT3 binding to the *Mir384* promoter at three sites. DNA isolated from immune-precipitated materials is amplified using qRT-PCR. The values are normalized to the input for each sample.

Suite[5]. Transcription factor binding sites were predicted using the ECR Browser[6] and JASPAR database[7].

Statistical Analyses

The results were expressed as mean ± standard deviation (SD) and analyzed by SPSS 17.0. Independent sample *t* tests were used to evaluate differences between groups. Two-way analysis of variance followed by Bonferroni's *post hoc* test was used for multiple comparisons. A *P* value of 0.05 or less was considered significant.

RESULTS

CpG Islands Are Absent in the *Mir384* Promoter

To determine the regulatory mechanisms controlling miR-384 transcription, we obtained the DNA sequence 2000 bp upstream

[5]http://www.bioinformatics.org/sms2/

[6]https://www.dcode.org/

[7]https://jaspar.genereg.net/

of *Mir384* (**Figure 1A**). We scanned this sequence for promoter methylation, a major mechanism underlying miRNA activation or silencing. We found eight groups of CpG dinucleotides separated from each other (**Figure 1A**). Further analysis using EMBOSS Cpgplot showed that in every 100-nucleotide window, the ratio of observed to expected (Obs/Exp) CpG sites was less than 0.45 (**Figure 1B**) and the percentage of CpG sites was less than 55% (**Figure 1C**). Thus, no putative CpG island was identified in this sequence (**Figure 1D**) according to established criteria (Island size >100 bp, GC percentage >50, and Obs/Exp >0.6). Similarly, no CpG islands were found in this sequence based on analyses using MethPrimer and Sequence Manipulation Suite (data not shown). Based on these results, we hypothesized that miR-384 transcription was not regulated by promoter methylation.

STAT3 Binds Directly to Specific Sites in the *Mir384* Promoter

The lack of CpG islands in the *Mir384* promoter suggests that miR-384 might be regulated by TFs. Using ECR Browser, we identified three predicted TF binding site regions (I, II, and III) in this promoter sequence with high conservation across three closely related mammalian taxa: mice, humans, and chimps (**Figure 2A**). Next, we constructed DNA fragments carrying variant regions (**Figure 2B**, left) for luciferase assays and found that the deletion of region I had no obvious effect on transcriptional activity, while a lack of region II attenuated transcription and the construct lacking region III exhibited only about one-fifth of the total activity observed for the construct carrying all three regions (**Figure 2B**). Moreover, the simultaneous deletion of region II and III resulted in highly decreased transcriptional activity (**Figure 2B**). These data suggest that region II and, to a greater extent, region III, have important roles in transcription.

To identify the precise TFs that bind to regions II and III to regulate miR-384 transcription, we analyzed the *Mir384* promoter sequence using the JASPAR database and identified five STAT3 binding motifs (**Figures 3A,B**), one (864 to 873, site 1) located in region II and another (1970 to 1979, site 2) located in region III (**Figure 3C**). A ChIP analysis showed that the site 1 and site 2 fragments were significantly enriched, while the site 3 fragment with no STAT3 binding motif was underrepresented after p-STAT3 immunoprecipitation (**Figures 3D,E**), suggesting that p-STAT3 binds to both site 1 and 2 but not to site 3.

Supershifted EMSA bands further indicated that p-STAT3 bound to both site 1 and site 2 probes, while these bands disappeared when using unlabeled competitor probes (**Figure 4A**). When mutations were introduced in sites 1 and 2, the supershifted bands disappeared (**Figure 4B**). Furthermore, site-specific mutations in either site 1 or site 2 could significantly decrease transcriptional activity, and simultaneous mutations in both sites further inhibited transcription (**Figure 4C**). Taken together, these data demonstrate that p-STAT3 can bind to conserved sites in *cis*-regulatory elements of the *Mir384* promoter.

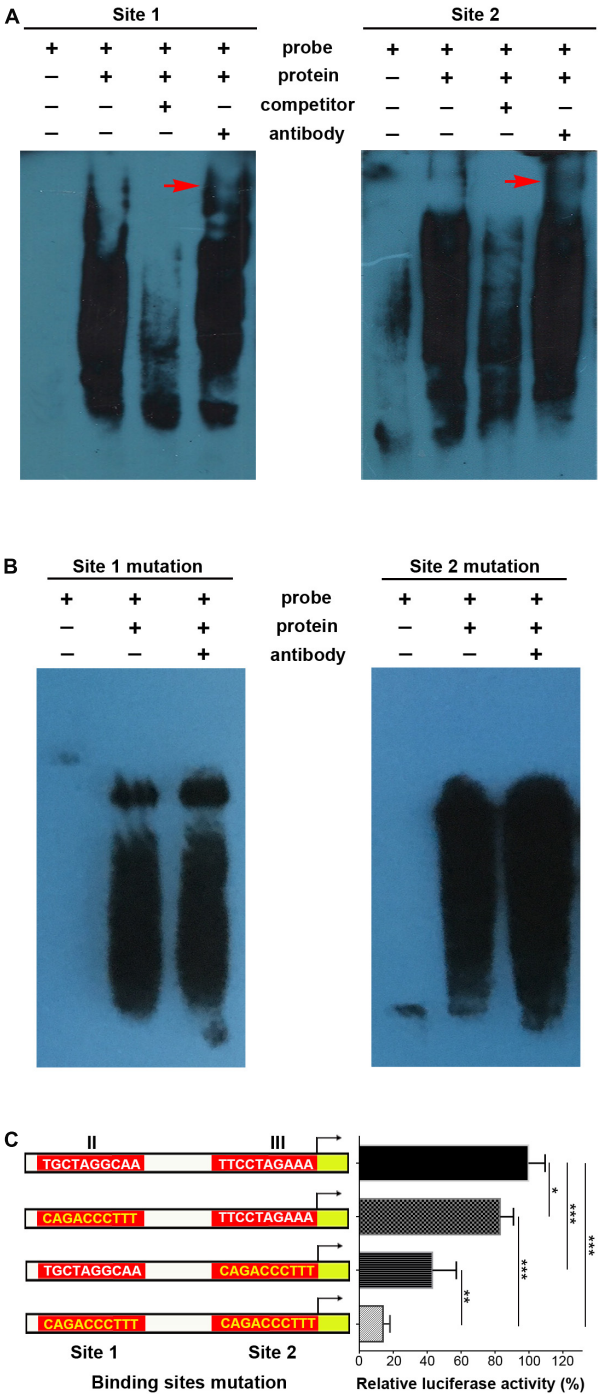

FIGURE 4 | STAT3 binds with special sites in *Mir384* promoter. **(A,B)** EMSA shows the interaction between p-STAT3 and specific probe sequences containing site 1, site 2, mutated site 1, or mutated site 2. Binding complexes are identified by supershifted bands (red arrows) with antibody against p-STAT3. **(C)** Effects of binding site mutagenesis on transcriptional activity by luciferase assay. On the left side is a schematic representation of the WT (white) and special site-directed mutation (yellow) constructs at site 1 in region II and site 2 in region III. The right panel shows the luciferase activity normalized to Renilla luciferase activity. Data are presented as mean ± standard deviation. $^{*}P < 0.05$. $^{**}P < 0.01$. $^{***}P < 0.001$. Data are representative of three experiments done in triplicate.

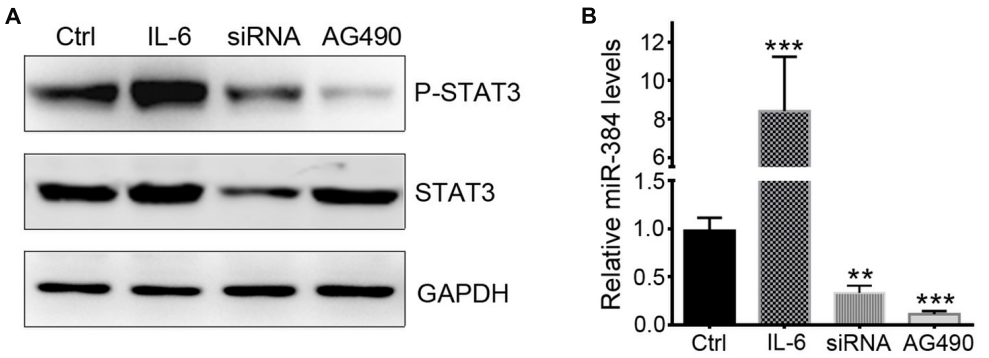

FIGURE 5 | STAT3 regulates miR-384 transcription. CD4$^+$ naïve T cells are cultured with IL-6, siRNA, or AG490, and then p-STAT3 and STAT3 levels are tested by Western blot **(A)**, and miR-384 transcription is measured by qRT-PCR **(B)**. Data are presented as mean ± standard deviation. $^{**}P < 0.01$. $^{***}P < 0.001$. Data are representative of three experiments done in triplicate.

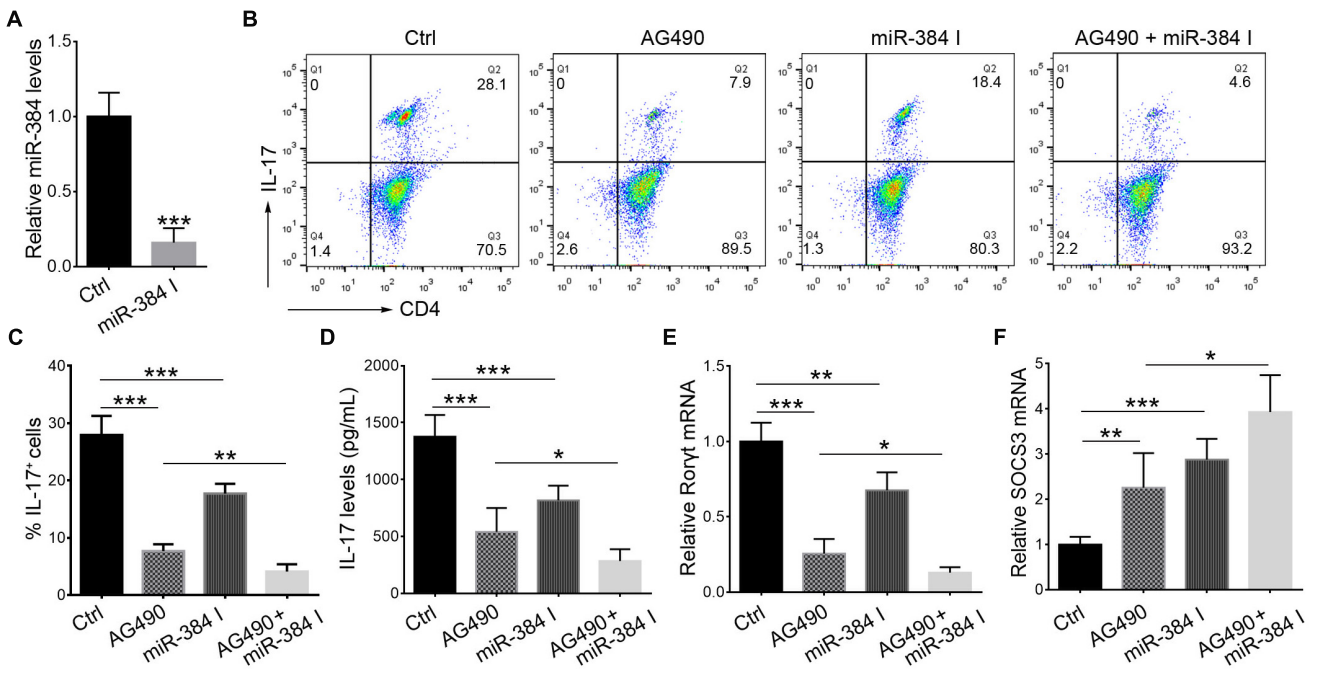

FIGURE 6 | STAT3 and miR-384 mediate Th17 polarization. CD4$^+$ naïve T cells are cultured in Th17 polarizing conditions with AG490 or miR-384 inhibitor (miR-384 I) for 3 days, and then miR-384 transcription is measured by qRT-PCR **(A)**, percentage of stimulated IL-17$^+$ cells is tested by flow cytometry **(B,C)**, dose of IL-17 in culture supernatant is measured by ELISA **(D)**, and Rorγt mRNA **(E)** and SOCS3 mRNA **(F)** levels are analyzed by qRT-PCR. Data are presented as mean ± standard deviation. $^{*}P < 0.05$. $^{**}P < 0.01$. $^{***}P < 0.001$. Data are representative of three experiments done in triplicate.

STAT3 Regulates miR-384 Transcription During Th17 Polarization

To determine whether STAT3 activation could regulate miR-384 transcription, we used IL-6 to activate STAT3, siRNA to knockdown STAT3 expression, or AG490 to inhibit STAT3 phosphorylation with more than 95% selectively by blocking JAK2 with no effect on STAT3 mass and cell viability (Dowlati et al., 2004). In CD4$^+$ naïve T cells, IL-6 could obviously promote the phosphorylation of STAT3, while siRNA and AG490 significantly decreased p-STAT3 levels (**Figure 5A**). A qRT-PCR analysis showed that IL-6 increased miR-384 levels by more than eightfold, while miR-384 levels reduced to one-third or one-sixth of control levels when siRNA or AG490 was used, respectively (**Figure 5B**), suggesting that STAT3 activation mediates miR-384 transcription.

During Th17 polarization *in vitro*, treatment with AG490 or a miR-384 inhibitor (**Figure 6A**) could suppress IL-17$^+$ cell cytopoiesis, with decreased IL-17 secretion and Rorγt expression but up-regulated SOCS3 (**Figures 6B–F**). Moreover, the simultaneous inhibition of STAT3 and miR-384 further reduced IL-17$^+$ cell generation, IL-17 concentrations, and Rorγt expression but increased SOCS3 (**Figures 6B–F**). These data

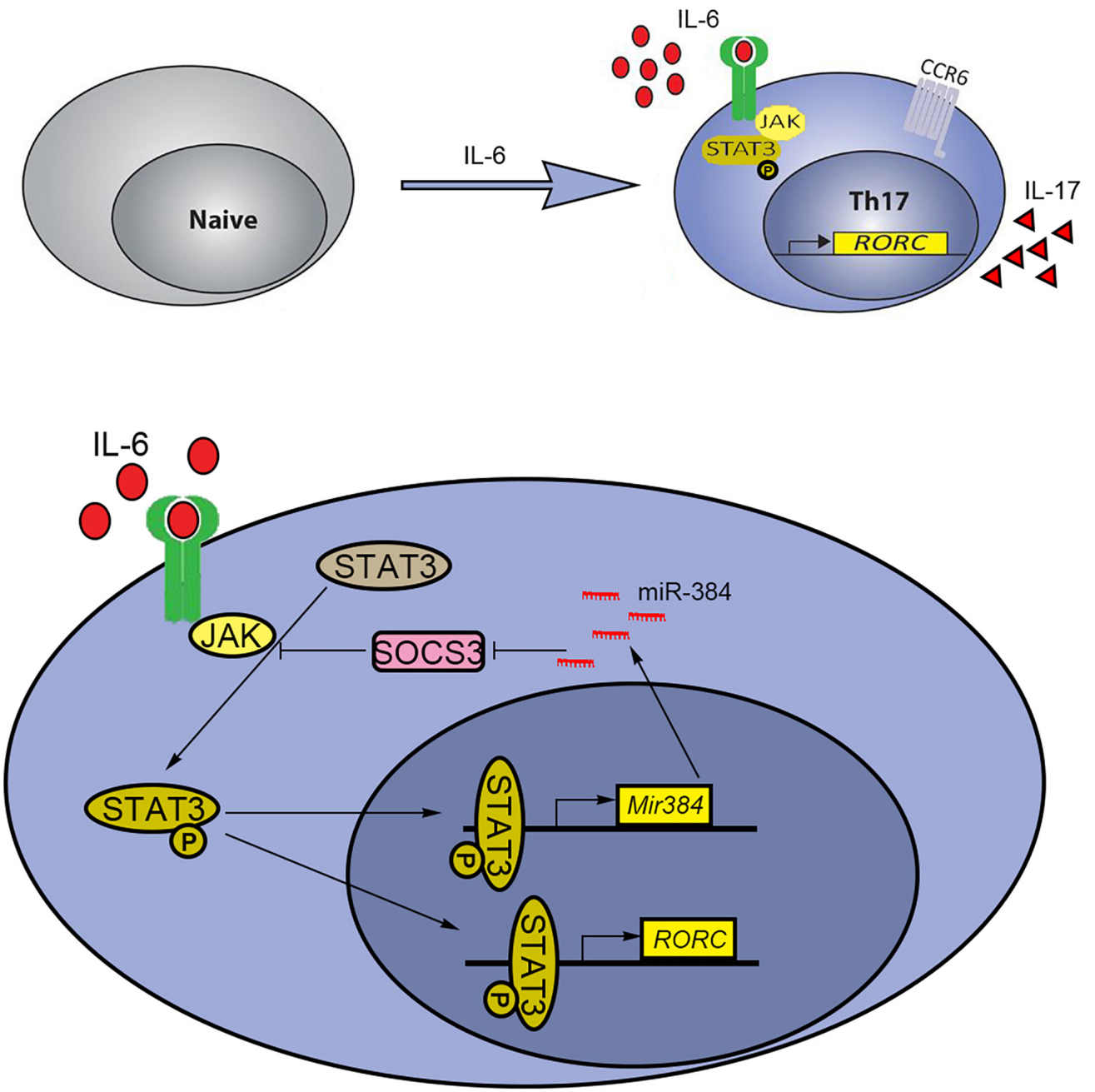

FIGURE 7 | Schematic model of STAT3 and miR-384 regulating Th17 polarization. IL-6-induced activation of STAT3 promotes transcription of miR-384 and Roryt (RORC). The increased miR-384 further activates STAT3 via targeting SOCS3, resulting in promoted Th17 polarization.

indicate that the STAT3-mediated regulation of miR-384 transcription plays a role in Th17 polarization.

DISCUSSION

Tissue- or developmental stage-specific alterations in miRNAs are associated with diseases. Studies of miRNAs in tumors have been fruitful, including the identification of hundreds of thousands of miRNAs related to tumorigenesis (Kulkarni et al., 2019), proliferation, migration (Li et al., 2010), apoptosis, necroptosis (Shirjang et al., 2019), and metabolism (Subramaniam et al., 2019). Recent findings have suggested that the dysregulation of miRNAs is associated with several central neurological disorders, such as Alzheimer's disease (Angelucci et al., 2019), Parkinson's disease (Reddy et al., 2019), and multiple sclerosis (MS) (Marangon et al., 2019). Our previous studies have shown that certain miRNAs are closely related

to the development of EAE, a mouse model of MS. Genome-wide transcription profiling indicates that miR-30a levels are substantially decreased in both patients with MS and mice with EAE, but miR-384 levels are significantly increased. Enforced constitutive expression of miR-30a *in vivo* results in fewer Th17 cells and alleviates EAE via IL-21R, while the expression of miR-384 *in vivo* leads to severe EAE due to SOCS3 inhibition (Qu et al., 2016, 2017). However, these studies have not resolved the factors contributing to the abnormal levels of miR-30a and miR-384 in EAE conditions. Promoter-associated CpG island methylation is a major mechanism underlying miRNA regulation and about 50% of miRNA genes are associated with CpG islands (Wang et al., 2013). However, we did not identify CpG island regions in 2000 bp upstream of *Mir384* using bioinformatics tools, suggesting that promoter methylation status does not explain differences in transcription. Thus, neither methylation-specific PCR nor bisulfite-modified DNA sequencing were performed. We detected potential binding motifs of STAT3, a key TF regulating Th17 polarization, in *cis*-regulatory elements within the *Mir384* promoter. Owing to the high false-positive and false-negative rates for prediction algorithms, we performed an additional ChIP assay, EMSA, and binding site mutagenesis combined with luciferase reporter assays to show that p-STAT3 bound directly to the *Mir384* promoter in regions II and III. Furthermore, STAT3 activation up-regulated miR-384, while a STAT3 phosphorylation inhibitor decreased miR-384, with reductions in the percentage of IL-17$^+$ cells, IL-17 secretion, and expression of the Th17 lineage marker Rorγt, suggesting that STAT3 activation directly regulates miR-384 transcription during Th17 polarization.

STAT3, a member of the STAT family of TFs, is an important constitutive signaling molecule for many key genes involved in multiple biological functions. It targets many miRNAs (Rokavec et al., 2014; Liao et al., 2015). For example, STAT3-induced miR-92a and miR-520d-5p suppression regulate cancer growth and survival (Chen et al., 2017; Li et al., 2017), and the inactivation of the phosphorylation of STAT3 decreases miR-155-5p and its anti-cancer properties (Zheng et al., 2018). Inhibition of the STAT3-associated pathway not only reduces miR-21 levels in cells but also inhibits the release of miR-21-enriched exosomes (Chuang et al., 2019). Using STAT3 cardiomyocyte-deficient mice, STAT3-mediated decreases in miR-34b and miR-337 play key roles in cardio-protection (Pedretti et al., 2019). Mechanistically, p-STAT3 binds to the promoter region of miR-199a-2 for regulation (Zhou et al., 2019). Three functional binding sites of STAT3 in the *Mir21* promoter region mediate angiogenesis (Chen et al., 2019). During Th17 polarization, IL-6-activated STAT3 has particularly important roles in the expression of Rorγt, a Th17 lineage marker. However, it is not clear whether STAT3 regulates Th17-related miRNAs. Our results showed that IL-6 stimulation resulted in the phosphorylation of STAT3 and activation of miR-384, thus potentially explaining the abnormal increase in miR-384 levels in Th17 and EAE.

T helper cell 17 development relies on key cytokines, including IL-6, IL-21, and IL-23, via STAT3 activation for gain of effector Th17 cell functions, such as the expression of the inflammatory cytokines IL-17, IFN-γ, and GM-CSF. Mice with STAT3 knockout in Th17 cells are resistant to the development of EAE because the STAT3 deficiency decreases Th17 counts in lymph nodes and the central nervous system (Yang et al., 2007). Thus, targeting STAT3 signaling is a potential strategy to alleviate Th17-related diseases. Our previous results showed that miR-384 was an upstream factor that directly inhibited SOCS3 during Th17 polarization (Qu et al., 2017). Furthermore, miR-384 is a direct target of STAT3 and is induced by IL-6. However, the repression of Th17 polarization when miR-384 was inhibited was weaker than that observed for STAT3 inhibition, suggesting that miR-384 is not the only downstream target of STAT3, which can directly regulate Rorγt (Qu et al., 2012; Tanaka et al., 2014). Since STAT3 is constitutively expressed in cells, it is possible that miR-384 is co-regulated by other TF complexes under specific cellular contexts or chromatin features; this is supported by our analysis showing that the simultaneous inhibition of STAT3 and miR-384 further blocked Th17 polarization. Based on our findings, we propose a schematic model by which IL-6 induces the STAT3-mediated activation of miR-384 and its downstream target SOCS3 to partially regulate Th17 polarization (**Figure 7**).

DATA AVAILABILITY STATEMENT

All datasets generated for this study are included in the article/supplementary material.

ETHICS STATEMENT

The animal study was reviewed and approved by Xuzhou Medical University Experimental Animal Ethics Committee.

AUTHOR CONTRIBUTIONS

XQ and RY designed the study, performed experiments, analyzed the data, and wrote and reviewed the manuscript. JH, YL, FZ, WY, WZ, XS, and FD performed the experiments. All authors read and approved the final manuscript.

FUNDING

This work was supported by grants from the National Natural Science Foundation of China (81771337 and 81271345), the National Key R&D Program of China (2017YFA0104202), the Natural Science Foundation of Jiangsu Province (BK20161174), the Jiangsu Provincial Undergraduate Training Program for Innovation and Entrepreneurship (201810313098H), the 333 Project of Jiangsu Province, the Xuzhou Basic Research Science and Technology Project (KC19059), and the Xuzhou Medical University Scientific Research Fund for Talents.

REFERENCES

Angelucci, F., Cechova, K., Valis, M., Kuca, K., Zhang, B., and Hort, J. (2019). MicroRNAs in Alzheimer's disease: diagnostic markers or therapeutic agents? *Front. Pharmacol.* 10:665. doi: 10.3389/fphar.2019.00665

Bagga, S., Bracht, J., Hunter, S., Massirer, K., Holtz, J., Eachus, R., et al. (2005). Regulation by let-7 and lin-4 miRNAs results in target mRNA degradation. *Cell* 122, 553–563. doi: 10.1016/j.cell.2005.07.031

Bartel, D. P. (2004). MicroRNAs: genomics, biogenesis, mechanism, and function. *Cell* 116, 281–297.

Bayraktar, R., Van Roosbroeck, K., and Calin, G. A. (2017). Cell-to-cell communication: microRNAs as hormones. *Mol. Oncol.* 11, 1673–1686. doi: 10.1002/1878-0261.12144

Beg, M. S., Brenner, A. J., Sachdev, J., Borad, M., Kang, Y. K., Stoudemire, J., et al. (2017). Phase I study of MRX34, a liposomal miR-34a mimic, administered twice weekly in patients with advanced solid tumors. *Invest. New Drugs* 35, 180–188. doi: 10.1007/s10637-016-0407-y

Chang, T. C., Yu, D., Lee, Y. S., Wentzel, E. A., Arking, D. E., West, K. M., et al. (2008). Widespread microRNA repression by Myc contributes to tumorigenesis. *Nat. Genet.* 40, 43–50. doi: 10.1038/ng.2007.30

Chen, L. Y., Wang, X., Qu, X. L., Pan, L. N., Wang, Z. Y., Lu, Y. H., et al. (2019). Activation of the STAT3/microRNA-21 pathway participates in angiotensin II-induced angiogenesis. *J. Cell Physiol.* 234, 19640–19654. doi: 10.1002/jcp.28564

Chen, M. W., Yang, S. T., Chien, M. H., Hua, K. T., Wu, C. J., Hsiao, S. M., et al. (2017). The STAT3-miRNA-92-wnt signaling pathway regulates spheroid formation and malignant progression in ovarian cancer. *Cancer Res.* 77, 1955–1967. doi: 10.1158/0008-5472.CAN-16-1115

Chuang, H. Y., Su, Y. K., Liu, H. W., Chen, C. H., Chiu, S. C., Cho, D. Y., et al. (2019). Preclinical evidence of STAT3 inhibitor pacritinib overcoming temozolomide resistance via downregulating miR-21-enriched exosomes from M2 glioblastoma-associated macrophages. *J. Clin. Med.* 8:E959. doi: 10.3390/jcm8070959

Conaco, C., Otto, S., Han, J. J., and Mandel, G. (2006). Reciprocal actions of REST and a microRNA promote neuronal identity. *Proc. Natl. Acad. Sci. U.S.A.* 103, 2422–2427. doi: 10.1073/pnas.0511041103

Dowlati, A., Nethery, D., and Kern, J. A. (2004). Combined inhibition of epidermal growth factor receptor and JAK/STAT pathways results in greater growth inhibition in vitro than single agent therapy. *Mol. Cancer Ther.* 3, 459–463.

Garcia-Lopez, J., Brieno-Enriquez, M. A., and Del Mazo, J. (2013). MicroRNA biogenesis and variability. *Biomol. Concepts* 4, 367–380.

Ha, M., and Kim, V. N. (2014). Regulation of microRNA biogenesis. *Nat. Rev. Mol. Cell Biol.* 15, 509–524. doi: 10.1038/nrm3838

He, L., He, X., Lim, L. P., de Stanchina, E., Xuan, Z., Liang, Y., et al. (2007). A microRNA component of the p53 tumour suppressor network. *Nature* 447, 1130–1134. doi: 10.1038/nature05939

Jamali, L., Tofigh, R., Tutunchi, S., Panahi, G., Borhani, F., Akhavan, S., et al. (2018). Circulating microRNAs as diagnostic and therapeutic biomarkers in gastric and esophageal cancers. *J. Cell Physiol.* 233, 8538–8550. doi: 10.1002/jcp.26850

Krol, J., Loedige, I., and Filipowicz, W. (2010). The widespread regulation of microRNA biogenesis, function and decay. *Nat. Rev. Genet.* 11, 597–610. doi: 10.1038/nrg2843

Kulkarni, B., Kirave, P., Gondaliya, P., Jash, K., Jain, A., Tekade, R. K., et al. (2019). Exosomal miRNA in chemoresistance, immune evasion, metastasis and progression of cancer. *Drug Discov. Today* doi: 10.1016/j.drudis.2019.06.010 [Epub ahead of print].

Li, M., Li, J., Ding, X., He, M., and Cheng, S. Y. (2010). microRNA and cancer. *AAPS J.* 12, 309–317.

Li, T., Guo, H., Zhao, X., Jin, J., Zhang, L., Li, H., et al. (2017). Gastric cancer cell proliferation and survival is enabled by a cyclophilin B/STAT3/miR-520d-5p signaling feedback loop. *Cancer Res.* 77, 1227–1240. doi: 10.1158/0008-5472.CAN-16-0357

Liao, X. H., Zheng, L., He, H. P., Zheng, D. L., Wei, Z. Q., Wang, N., et al. (2015). STAT3 regulated ATR via microRNA-383 to control DNA damage to affect apoptosis in A431 cells. *Cell. Signal.* 27, 2285–2295. doi: 10.1016/j.cellsig.2015.08.005

Ludwig, N., Leidinger, P., Becker, K., Backes, C., Fehlmann, T., Pallasch, C., et al. (2016). Distribution of miRNA expression across human tissues. *Nucleic Acids Res.* 44, 3865–3877. doi: 10.1093/nar/gkw116

Lujambio, A., Ropero, S., Ballestar, E., Fraga, M. F., Cerrato, C., Setien, F., et al. (2007). Genetic unmasking of an epigenetically silenced microRNA in human cancer cells. *Cancer Res.* 67, 1424–1429. doi: 10.1158/0008-5472.CAN-06-4218

Marangon, D., Raffaele, S., Fumagalli, M., and Lecca, D. (2019). MicroRNAs change the games in central nervous system pharmacology. *Biochem. Pharmacol.* 168, 162–172. doi: 10.1016/j.bcp.2019.06.019

Ozsolak, F., Poling, L. L., Wang, Z., Liu, H., Liu, X. S., Roeder, R. G., et al. (2008). Chromatin structure analyses identify miRNA promoters. *Genes Dev.* 22, 3172–3183. doi: 10.1101/gad.1706508

Paul, P., Chakraborty, A., Sarkar, D., Langthasa, M., Rahman, M., Bari, M., et al. (2018). Interplay between miRNAs and human diseases. *J. Cell Physiol.* 233, 2007–2018. doi: 10.1002/jcp.25854

Pedretti, S., Brulhart-Meynet, M. C., Montecucco, F., Lecour, S., James, R. W., and Frias, M. A. (2019). HDL protects against myocardial ischemia reperfusion injury via miR-34b and miR-337 expression which requires STAT3. *PLoS One* 14:e0218432. doi: 10.1371/journal.pone.0218432

Petrovic, N., and Ergun, S. (2018). miRNAs as potential treatment targets and treatment options in cancer. *Mol. Diagn. Ther.* 22, 157–168. doi: 10.1007/s40291-017-0314-318

Qu, X., Han, J., Zhang, Y., Wang, Y., Zhou, J., Fan, H., et al. (2017). MiR-384 regulates the Th17/treg ratio during experimental autoimmune encephalomyelitis pathogenesis. *Front. Cell Neurosci.* 11:88. doi: 10.3389/fncel.2017.00088

Qu, X., Liu, X., Cheng, K., Yang, R., and Zhao, R. C. (2012). Mesenchymal stem cells inhibit Th17 cell differentiation by IL-10 secretion. *Exp. Hematol.* 40, 761–770. doi: 10.1016/j.exphem.2012.05.006

Qu, X., Zhou, J., Wang, T., Han, J., Ma, L., Yu, H., et al. (2016). MiR-30a inhibits Th17 differentiation and demyelination of EAE mice by targeting the IL-21R. *Brain Behav. Immun.* 57, 193–199. doi: 10.1016/j.bbi.2016.03.016

Reddy, A. P., Ravichandran, J., and Carcaci-Salli, N. (2019). Neural regeneration therapies for Alzheimer's and Parkinson's disease-related disorders. *Biochim. Biophys. Acta Mol. Basis Dis.* doi: 10.1016/j.bbadis.2019.06.020 [Epub ahead of print].

Rokavec, M., Oner, M. G., Li, H., Jackstadt, R., Jiang, L., Lodygin, D., et al. (2014). IL-6R/STAT3/miR-34a feedback loop promotes EMT-mediated colorectal cancer invasion and metastasis. *J. Clin. Invest.* 124, 1853–1867. doi: 10.1172/JCI73531

Saito, Y., Liang, G., Egger, G., Friedman, J. M., Chuang, J. C., Coetzee, G. A., et al. (2006). Specific activation of microRNA-127 with downregulation of the proto-oncogene BCL6 by chromatin-modifying drugs in human cancer cells. *Cancer Cell* 9, 435–443. doi: 10.1016/j.ccr.2006.04.020

Salehi, M., and Sharifi, M. (2018). Exosomal miRNAs as novel cancer biomarkers: challenges and opportunities. *J. Cell Physiol.* 233, 6370–6380. doi: 10.1002/jcp.26481

Saliminejad, K., Khorram Khorshid, H. R., Soleymani Fard, S., and Ghaffari, S. H. (2019). An overview of microRNAs: biology, functions, therapeutics, and analysis methods. *J. Cell Physiol.* 234, 5451–5465. doi: 10.1002/jcp.27486

Selbach, M., Schwanhausser, B., Thierfelder, N., Fang, Z., Khanin, R., and Rajewsky, N. (2008). Widespread changes in protein synthesis induced by microRNAs. *Nature* 455, 58–63. doi: 10.1038/nature07228

Shirjang, S., Mansoori, B., Asghari, S., Duijf, P. H. G., Mohammadi, A., Gjerstorff, M., et al. (2019). MicroRNAs in cancer cell death pathways: apoptosis and necroptosis. *Free Radic. Biol. Med.* 139, 1–15. doi: 10.1016/j.freeradbiomed.2019.05.017

Subramaniam, S., Jeet, V., Clements, J. A., Gunter, J. H., and Batra, J. (2019). Emergence of MicroRNAs as key players in cancer cell metabolism. *Clin. Chem.* 65, 1090–1101. doi: 10.1373/clinchem.2018.299651

Tanaka, S., Suto, A., Iwamoto, T., Kashiwakuma, D., Kagami, S., Suzuki, K., et al. (2014). Sox5 and c-Maf cooperatively induce Th17 cell differentiation via RORgammat induction as downstream targets of Stat3. *J. Exp. Med.* 211, 1857–1874. doi: 10.1084/jem.20130791

Turner, M. J., and Slack, F. J. (2009). Transcriptional control of microRNA expression in C. elegans: promoting better understanding. *RNA Biol.* 6, 49–53. doi: 10.4161/rna.6.1.7574

van der Ree, M. H., de Vree, J. M., Stelma, F., Willemse, S., van der Valk, M., Rietdijk, S., et al. (2017). Safety, tolerability, and antiviral effect of RG-101 in patients with chronic hepatitis C: a phase 1B, double-blind, randomised controlled trial. *Lancet* 389, 709–717.

Wang, Y., Zhang, Z., and Wang, J. (2018). MicroRNA-384 inhibits the progression of breast cancer by targeting ACVR1. *Oncol. Rep.* 39, 2563–2574. doi: 10.3892/or.2018.6385

Wang, Y. X., Zhu, H. F., Zhang, Z. Y., Ren, F., and Hu, Y. H. (2018). MiR-384 inhibits the proliferation of colorectal cancer by targeting AKT3. *Cancer Cell Int.* 18:124. doi: 10.1186/s12935-018-0628626

Wang, Z., Yao, H., Lin, S., Zhu, X., Shen, Z., Lu, G., et al. (2013). Transcriptional and epigenetic regulation of human microRNAs. *Cancer Lett.* 331, 1–10. doi: 10.1016/j.canlet.2012.12.006

Yang, X. O., Panopoulos, A. D., Nurieva, R., Chang, S. H., Wang, D., Watowich, S. S., et al. (2007). STAT3 regulates cytokine-mediated generation of inflammatory helper T cells. *J. Biol. Chem.* 282, 9358–9363. doi: 10.1074/jbc.C600321200

Yao, Y., Rao, C., Zheng, G., and Wang, S. (2019). Luteolin suppresses colorectal cancer cell metastasis via regulation of the miR384/pleiotrophin axis. *Oncol. Rep.* 42, 131–141. doi: 10.3892/or.2019.7136

Zhang, Y., Han, J., Wu, M., Xu, L., Wang, Y., Yuan, W., et al. (2019). Toll-like receptor 4 promotes Th17 lymphocyte infiltration via CCL25/CCR9 in pathogenesis of experimental autoimmune encephalomyelitis. *J. Neuroimmune Pharmacol.* 14, 493–502.

Zheng, F., Tang, Q., Zheng, X. H., Wu, J., Huang, H., Zhang, H., et al. (2018). Inactivation of STAT3 and crosstalk of miRNA155-5p and FOXO3a contribute to the induction of IGFBP1 expression by beta-elemene in human lung cancer. *Exp. Mol. Med.* 50:121.

Zheng, J., Liu, X., Wang, P., Xue, Y., Ma, J., Qu, C., et al. (2016). CRNDE promotes malignant progression of glioma by attenuating miR-384/PIWIL4/STAT3 axis. *Mol. Ther.* 24, 1199–1215. doi: 10.1038/mt.2016.71

Zhou, Y., Pang, B., Xiao, Y., Zhou, S., He, B., Zhang, F., et al. (2019). The protective microRNA-199a-5p-mediated unfolded protein response in hypoxic cardiomyocytes is regulated by STAT3 pathway. *J. Physiol. Biochem.* 75, 73–81.

Zhu, L., Chen, H., Liu, M., Yuan, Y., Wang, Z., Chen, Y., et al. (2017). Treg/Th17 cell imbalance and IL-6 profile in patients with unexplained recurrent spontaneous abortion. *Reprod. Sci.* 24, 882–890. doi: 10.1177/1933719116670517

Conflict of Interest: The authors declare that the research was conducted in the absence of any commercial or financial relationships that could be construed as a potential conflict of interest.

frontiers in Genetics

ORIGINAL RESEARCH
published: 13 November 2019
doi: 10.3389/fgene.2019.01112

Micro-Ribonucleic Acid-216a Regulates Bovine Primary Muscle Cells Proliferation and Differentiation *via* Targeting *SMAD Nuclear Interacting Protein-1* and *Smad7*

*Zhaoxin Yang†, Chengchuang Song†, Rui Jiang, Yongzhen Huang, Xianyong Lan, Chuzhao Lei and Hong Chen**

Shaanxi Key Laboratory of Animal Genetics, Breeding and Reproduction, College of Animal Science and Technology, Northwest A&F University, Yangling, China

OPEN ACCESS

Edited by:
Junjie Xiao, Shanghai University, China

Reviewed by:
Xiaofei Cong, Eastern Virginia Medical School, United States
Nithyananda Thorenoor, Pennsylvania State University, United States

***Correspondence:**
Hong Chen
chenhong1212@263.net

†These authors have contributed equally to this work

Specialty section:
This article was submitted to RNA, a section of the journal Frontiers in Genetics

Received: *09 July 2019*
Accepted: *16 October 2019*
Published: *13 November 2019*

Citation:
Yang Z, Song C, Jiang R, Huang Y, Lan X, Lei C and Chen H (2019) Micro-Ribonucleic Acid-216a Regulates Bovine Primary Muscle Cells Proliferation and Differentiation via Targeting SMAD Nuclear Interacting Protein-1 and Smad7. Front. Genet. 10:1112. doi: 10.3389/fgene.2019.01112

MicroRNAs (miRNAs), belonging to a class of evolutionarily conserved small noncoding RNA of ~22 nucleotides, are widely involved in skeletal muscle growth and development by regulating gene expression at the post-transcriptional level. While the expression feature and underlying function of miR-216a in mammal skeletal muscle development, especially in cattle, remains to be further elucidated. The aim of this study was to investigate the function and mechanism of miR-216a during bovine primary muscle cells proliferation and differentiation. Herein, we found that the expression level of miR-216a both presented a downward trend during the proliferation and differentiation phases, which suggested that it might have a potential role in the development of bovine skeletal muscle. Functionally, during the cells proliferation phase, overexpression of miR-216a inhibited the expression of proliferation-related genes, reduced the cell proliferation status, and resulted in cells G1 phase arrest. In cells differentiation stages, overexpression of miR-216a suppressed myogenic maker genes mRNA, protein, and myotube formation. Mechanistically, we found that *SNIP1* and *smad7* were the directly targets of miR-216a in regulating bovine primary muscle cells proliferation and differentiation, respectively. Altogether, these findings suggested that miR-216a functions as a suppressive miRNA in development of bovine primary muscle cells *via* targeting *SNIP1* and *smad7*.

Keywords: miR-216a, *SMAD nuclear interacting protein-1*, *smad7*, skeletal muscle, bovine

INTRODUCTION

Skeletal muscle, as an important sports and metabolic organization of animals, accounts for a large proportion of body weight and is directly related to the economic traits such as meat production in cattle. The skeletal muscle development in mammal undergoes two important stages the increase in the number of pre-natal muscle fibers (Russell and Oteruelo, 1981; Hocquette, 2010) and the increase in the volume of muscle fibers after birth (Zhu et al., 2006). Therefore, it is of great value to study the intrinsic mechanism of muscle formation. Skeletal muscle development originates from the embryonic stage, which is derived from the paraxial mesoderm structures in the vertebrate (Christ and Ordahl, 1995). Here, the dorsal somite forms the dermomyotome which can further

form the myotome (Tajbakhsh and Buckingham, 2000). Then, the muscle progenitor cells will form and migrate from the myotome. Myotome quickly differentiates into primary myoblasts. Finally, these primary muscle progenitor cells undergo proliferate and differentiate to form skeletal muscle (Buckingham et al., 2003). Orchestral molecules mechanisms are involved in the process of myogenesis, which are mainly regulated by transcription factors likely paired box transcription factors *Pax3/Pax7* (Relaix et al., 2006; Lagha et al., 2008; Buckingham and Relaix, 2015), *myogenic regulatory factors (MRFs)* (Ott et al., 1991), and *myocyte enhancer factor 2 family (MEF2)* (Edmondson et al., 1994). It's worth noting that these key transfection factors are also regulated by other multiple regulatory factors, including protein coding gene such as *transforming growth factor-beta (TGF-β)* (Liu et al., 2001; Gardner et al., 2011) and noncoding RNA likely microRNAs (miRNAs) (Chen et al., 2006).

MiRNAs are a variety of evolutionarily conserved short noncoding RNA. The function and molecular mechanism of miRNAs has been extensively studied in almost all biological processes. The mature sequence of miRNA could complete or partial complementary pair with the 3' UTR of mRNA, which cause mRNA decay or impede protein translation (Bartel, 2004; Bartel, 2009). MiRNAs, as an integral part of skeletal muscle development, can regulate skeletal muscle proliferation, differentiation, and regeneration by targeting the key factors of the myogenic regulatory network during the different stages of skeletal muscle development process (Chen et al., 2006; Crist et al., 2009; Cheung et al., 2012; Alexander et al., 2013; Diniz and Wang, 2016). Studies have shown that dicer knock-out mice in embryonic skeletal muscle resulted in embryonic lethality, skeletal muscle hypoplasia, myofiber morphogenesis defects, and increased apoptosis (O'Rourke et al., 2007). So far, large numbers of miRNAs have been report to affect skeletal muscle development (Ge and Chen, 2011). Some of them are muscle specific expression miRNAs (myomiRs), including miR-1 (Chen et al., 2006; Sluijter et al., 2010), miR-133 (Chen et al., 2006; Feng et al., 2013), miR-206 (McCarthy, 2008; Dey et al., 2011), etc. miR-1 could promote myogenic cells differentiation by targeting *HDAC4* (Chen et al., 2006). miR-133 could promote myoblast proliferation by repressing the expression of *SRF* (Chen et al., 2006). In the differentiation stage of satellite cells, the expression of miR-206 is upregulated, which can enhance satellite cell differentiation by targeting *Pax7* (Dey et al., 2011). Besides that, numerous non-muscle-specific miRNAs (non-myomiRs) also play important role in the regulation of myogenesis (Ju et al., 2015). For example, miR-26a can promote myogenesis by targeting transcription factors *Smad1, Smad4,* and *Ezh2 (enhancer of zeste homologue 2)*, a negative regulator of myogenesis (Wong and Tellam, 2008; Dey et al., 2012). miR-486 can promote muscle differentiation by activating *PI3K/AKT* pathway or targets *Pax7* directly (Small et al., 2010; Dey et al., 2011). MiR-22 can inhibit proliferation and enhances differentiation of C2C12 myoblasts by targeting *TGF-βR1* (Wang et al., 2018b). Although the research of miRNAs is receiving considerable, there are still many miRNAs to be further investigated in skeletal muscle.

miR-216a is a widely expressed miRNA that involved in disease and tumorigenesis by targeting different target genes (Ji et al., 2017; Tao et al., 2017; Wang et al., 2017a). However, little is known about the function of miR-216a in regulation of bovine skeletal muscle development. Therefore, the purpose of current study was to explore the function and mechanism of miR-216a for bovine primary muscle cells proliferation and differentiation. Here, the expression level of miR-216a presented a downward trend both in the proliferation and differentiation phases of bovine skeletal muscle cell. Functional analysis found that miR-216a could inhibit the proliferation and differentiation of bovine skeletal muscle cell by directly targeting *SNIP1* and *smad7* respectively.

MATERIALS AND METHODS

Animals and Tissue Sample Collection

Three months old fetal Qinchuan cattle from Shaanxi Kingbull Livestock Co., Ltd. (Baoji, China) were used in this research. The heart, liver, spleen, lung, kidney, stomach, gut, and leg muscle were collected and kept at -80°C until RNA isolation. Animal care and study protocols were approved by the Animal Care Commission of the College of Veterinary Medicine, Northwest A&F University (permit number: NWAFAC1019).

Cell Culture

Bovine skeletal muscle cells are derived from the longissimus muscle or hind limbs of the 3-month-old fetus. The stripped muscle tissue is cut and then digested with collagenase I. The specific separation steps refer to the previous description (Miyake et al., 2012). The growth stage bovine skeletal muscle cells were cultured in DMEM with 20% FBS and 1% penicillin/streptomycin. When inducing skeletal muscle cells differentiation, replace 20% FBS in the medium with 2% horse serum. HEK293T cells (ATCC, USA) were cultured in DMEM with 10% FBS and 1% penicillin/streptomycin. All these cells were cultured at 37°C in a 5% CO2 atmosphere.

Plasmid Construction and Cell Transfection

The wild-type and mutant-type sequences of *smad7* or *SNIP1* 3'UTR were inserted into the psi-check2 reporter vector, respectively. The mutant type 3'UTR sequences of *smad7* or *SNIP1* each contained four nucleotide mutations at the miR-216a targeting site. The precursor sequences of miR-216a were cloned into pcDNA3.1 (+) expression vector. The mimic and inhibitor of miR-216a were purchased from Ribobio (Guangzhou, China). The primers used in this study were listed in **Supplementary Table 1**.

The proliferated bovine primary muscle cells were transfected with miR-216a mimic, inhibitor, and control when the cell density reached 60–70% and collected at 24 h after transfection in 12-well plates. The differentiated bovine primary muscle cells were transfected when the cell density reached 70–80% confluence and 20% FBS medium was changed to 2% horse serum to induce cells differentiation at 24 h after transfection. Cells were collected at three days after induced differentiation. The bovine primary muscle cells used in CCk-8, 5-ethynyl-2′-deoxyuridine (EdU) experiment, and HEK293T cells were cultured in 96-well plates, and they were collected at 24 h after transfection. Thermo transfection reagent

was used in this study. The detail procedure of transfection was performed according to the manufacturer's instructions.

Real-Time Quantitative Polymerase Chain Reaction

Total RNA of tissues and cells was extracted with TRIzol Reagent (Takara) according to the manufacturer's instruction. Total RNA was reverse transcribed by using the PrimeScript™ RT Reagent Kit with gDNA Eraser (Takara). Real-time quantitative PCR (RT-qPCR) was performed with the SYBR Green Kit (Genestar, Beijing, China) on a CFX96 system (Bio-Rad, Hercules, CA, USA) with three biological replicates each time. Relative expression levels of mRNAs and miRNAs were calculated with the $2^{-\Delta\Delta Ct}$ method (Livak and Schmittgen, 2001). *U6* and *GAPDH* gene was used as reference gene for the expression of miRNA and all genes. The primers used in this study were listed in **Supplementary Table 1**.

Western Blot

Total proteins were extracted from cells by using radio immunoprecipitation assay buffer with 1% PMSF (Solarbio, Beijing, China). The protein concentration was measured by using the BCA Protein Assay Kit (Beyotime, Shanghai, China) and denatured with 5× protein loading buffer at 98°C for 10 min. The specific operation process of WB was described previously (Li et al., 2018). In short, the target proteins were separated by sodium dodecyl sulfate polyacrylamide gel electrophoresis and transferred to a methanol-activated polyvinylidene fluoride (PVDF) membrane. The corresponding primary antibody was added to incubate PVDF membrane for overnight at 4°C. At room temperature, the PVDF membrane was re-incubated with the corresponding secondary antibody for 2 h. The protein signal strength was detected using enhanced chemiluminescence reagent. The primary antibodies and secondary antibodies were listed in **Supplementary Table 2**. The quantified of the protein was performed by the ImageJ program (National Institutes of Health).

Cell Proliferation Assay

For the CCK-8 assay, the bovine primary muscle cells were transfected with the negative control (NC), mimics, and inhibitor when the cell densities were 50–60%. After transfection for 24 h, the culture medium containing 10% CCK-8 reagent was changed and incubated the cells for 2 h. The CCK-8 Reagent Kit (Tiandz, Beijing, China) was performed to measure cell proliferation index at 450 nm by using Microplate Reader (Tecan, Switzerland) and repeated five times for each independent experiment. The Cell-Light EdU DNA Cell Proliferation Kit (Ribobio, Guangzhou, China) was used to measure S phase positive cell according to the manufacturer's instructions. The EdU positive cells was observed by using fluorescence microscope (AMG EVOS, USA) and each treatment group had three independent replicates.

Cell Cycle Assay

The muscle cells were seeded into 60 mm diameter petri dish and transfected with the NC, mimics, and inhibitor when the cell densities were 60%. After transfection for 24 h, muscle cells were fixed in PBS containing 70% ethanol, and cell cycle assays were performed with cell cycle staining kit (MultiSciences Biotech Co., Ltd, Hangzhou, China) by using a flow cytometry. The experimental procedure is based on our previous research (Song et al., 2015).

Dual-Luciferase Activity Assay

The target genes of miR-216a were predicted with the online software TargetScan (http://www.targetscan.org). The 3' untranslated region (3'UTR) (wild-type or mutant-type) sequences of the genes SNIP1 and smad7 mRNA was cloned into the psi-Check2 reporter vector, respectively. To confirm their targeting relationship, miR-216a expression plasmid and the psi-Check2 reporter vector (wild or mutant) were co-transfected into HEK293T cells. After transfection for 24 h, the relative luciferase activity was measured by using a Dual-Luciferase® Reporter DLR™Assay System Kit (Promega, USA) according to the manufacturer's protocols.

Immunofluorescence Staining

Immunofluorescence staining was used to detect the number of *MyHC*-positive myotubes. After transfection and induction of differentiation for 4 days, the bovine primary muscle cells were fixed with 4% paraformaldehyde in PBS for 20 min. After permeabilized with 0.5% Triton X-100 for 10 min and blocked with 5% BSA at 4°C for 30 min, the cells were incubated with primary antibody-*MyHC* diluted 1:200 with 5% bovine serum albumin (BSA) in PBS at 4°C overnight. Then the cells were incubated with the corresponding fluorescent secondary antibody [goat anti-mouse immunoglobulin G (IgG) H&L] diluted 1:400 with 5% BSA at 37°C for 2 h. Then cells were stained with 5 mg/ml 4′,6-diamidino-2-phenylindole. The cells were washed three times with PBS for 5 min before each procedure. All images were observed on a fluorescence microscope (DM5000B, Leica, Germany). The antibodies source information was listed in **Supplementary Table 2**.

Statistical Analysis

Results were presented as mean ± SEM. The data statistical analysis was performed using one-way analysis of variance (ANOVA) or student's t test. The significance of differences between the groups were considered significant at $P < 0.05$ (* $P < 0.05$; ** $P < 0.01$).

RESULT

The Expression Feature of miR-216a in Bovine Tissues and Primary Muscle Cells

To investigate the expression feature of miR-216a in various tissues (heart, liver, spleen, lung, kidney, stomach, gut, and skeletal muscle) during embryonic stage, RT-qPCR analysis data demonstrated that miR-216a was found to be mainly expressed in the heart, but relatively low in skeletal muscle (**Figure 1A**). During the growth stage (-24, -12, and 0 h) of bovine primary muscle cells, the expression level of miR-216a showed a downward

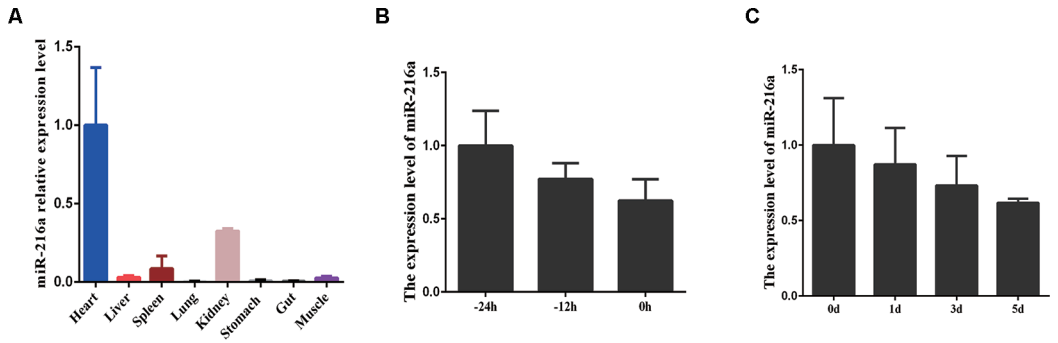

FIGURE 1 | The expression feature of miR-216a in bovine tissues and primary muscle cells. **(A)** RT-qPCR analysis of relative miR-216a levels in different tissues (heart, liver, spleen, lung, kidneys, stomach, gut, and muscle) of Qinchuan cattle at embryonic stage. **(B)** RT-qPCR analysis the relative expression level of miR-216a during the growth stage (-24, -12, and 0 h) of bovine primary muscle cells. **(C)** Real-time quantitative PCR analysis the relative expression level of miR-216a during the differentiation stage (0, 1, 3, and 5 days) of bovine primary muscle cells. Data are presented as the mean ± SEM; n = 3.

trend (**Figure 1B**). During the differentiated stage (0, 1, 3, and 5 days) of bovine primary muscle cells, the expression level of miR-216a also showed a downward trend (**Figure 1C**). Together, the expression characteristics of miR-216a suggested that it might play a negative factor in the proliferation and differentiation of bovine primary muscle cells.

miR-216a Inhibits Bovine Primary Muscle Cells Proliferation

To verify the function of miR-216a for bovine primary muscle cells proliferation, miR-216a mimic was transfected into cells to enhance its expression level. After transfection for 24 h, RT-qPCR detection data showed that the relative expression of miR-216a was significantly higher than that of the control group (**Figure 2A**). At the molecular level, RT-qPCR was used to detect cell proliferation key genes (*CyclinD1*, *PCNA*, and *CDK2*) mRNA expression level. The analysis data demonstrated that the expression of *CyclinD1* and *CDK2* was significantly lower than that of the control group, but not *PCNA* (**Figure 2B**). Western blot analysis showed that the expression level of *PCNA* and *CDK2* protein decreased significantly and the expression level of *p53* protein increased significantly (**Figures 2C, D**). Inhibition of endogenous miR-216a expression was induced by its inhibitor (**Figure 2E**). Unfortunately, loss of miR-216a did not significantly affect the mRNA levels of the cell proliferation key genes (**Figure 2F**). But the protein levels of the cell proliferation key genes are significantly affected which consisted with overexpression (**Figures 2G, H**). At the cellular level, overexpression of miR-216a reduced the number of EdU positive cells, while no significant changes were observed after inhibition of miR-216a (**Figure 3A**). The results of CCK-8 assay showed that the overexpression of

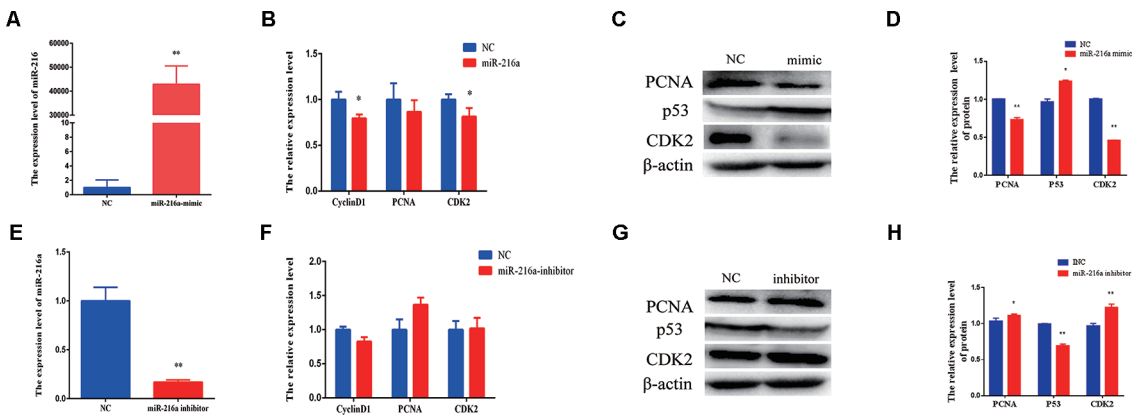

FIGURE 2 | miR-216a regulates bovine primary muscle cells proliferation at the molecular level. **(A)** The detection of expression efficiency of miR-216a after transfection miR-216a mimic. **(B)** Gain of miR-216a, cell proliferation key genes *(CyclinD1, PCNA,* and *CDK2*) messenger RNA (mRNA) were detected by RT-qPCR. **(C)** Gain of miR-216a, western blot was used to detect the protein expression level of *PCNA*, *CDK2,* and *p53*. **(D)** Protein quantitative analysis of *PCNA*, *p53,* and *CDK2* for **(C)**. **(E)** The detection of expression level of miR-216a after transfection miR-216a inhibitor. **(F)** The mRNA expression of cell proliferation genes *CyclinD1*, *PCNA,* and *CDK2* were detected by real-time quantitative PCR after loss of miR-216a. **(G)** Western blot was used to detect the protein expression level of *PCNA*, *CDK2,* and *p53* after loss of miR-216a. **(H)** Protein quantitative analysis of *PCNA*, *p53,* and *CDK2* for **(G)**. Data are presented as the mean ± SEM; n = 3; $^{*}P < 0.05$ and $^{**}P < 0.01$.

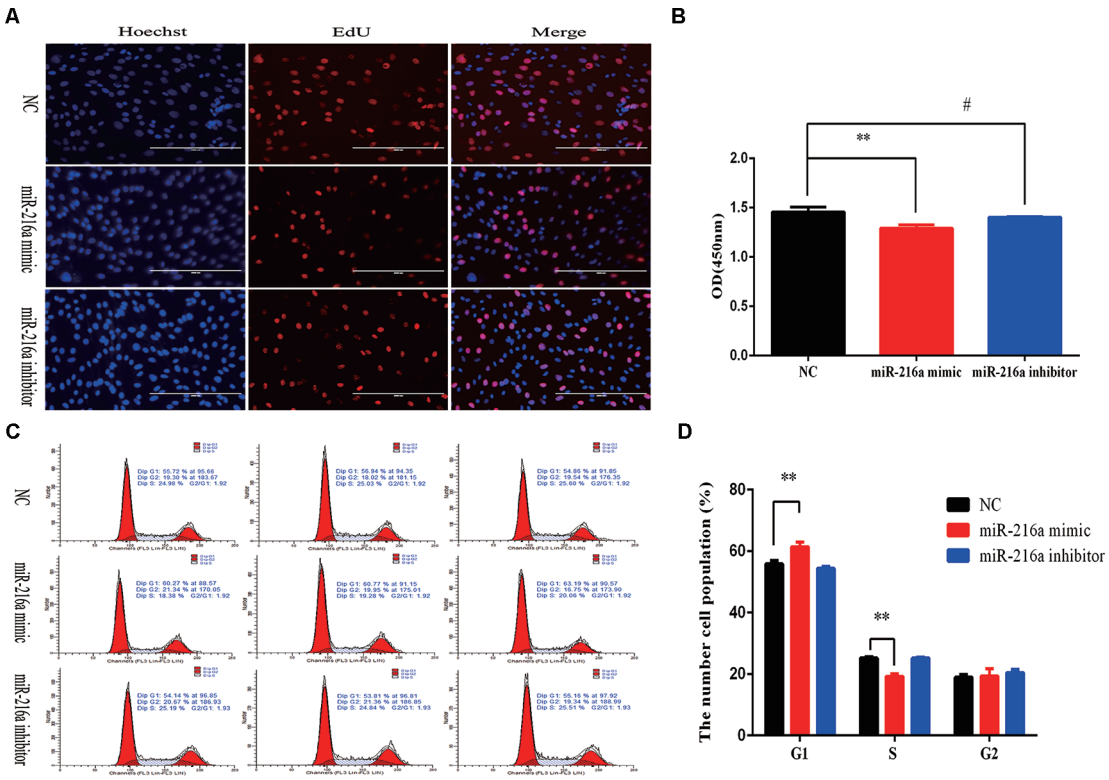

FIGURE 3 | miR-216a regulates bovine primary muscle cells proliferation at the cellular level.**(A)** Bovine primary muscle cells in the S-phase were stained with 5-ethynyl-2′-deoxyuridine in red, and the cell nuclei were dyed with Hoechst in blue after transfection miR-216a mimic or inhibitor, respectively. **(B)** During bovine primary muscle cells growth stage, CCK-8 analysis was performed after gain or loss miR-216a. **(C)** Bovine primary muscle cells phases were analyzed by flow cytometry after transfected with miR-216a mimic or inhibitor, respectively. **(D)** Statistical results of flow cytometry. Data are presented as the mean ± SEM; n = 3; $^{**}P < 0.01$ and $^{\#}P > 0.05$.

miR-216a resulted in a significant decrease in cell optical density (OD) value, while the cell OD value did not change significantly after interfering with mir-216a (**Figure 3B**). Detection the cell cycle by flow cytometry showed that overexpression of miR-216a increased the number of cells in G1 phase and decreased the number of cells in S phase, while the inhibition of miR-216a had no significant effect on cell cycle (**Figures 3C, D**). Together, the above results indicated that miR-216a inhibited the proliferation of bovine primary muscle cells.

miR-216a Inhibits Bovine Primary Muscle Cells Differentiation

When the confluence of bovine primary cells reached about 100%, horse serum at a low concentration of 2% was used to induce the differentiation into myotube. Since miR-216a regulates the proliferation of bovine primary muscle cells, it is not clear what role miR-216a plays in the differentiation process. After transfection of miR-216a mimic for 3 days, RT-qPCR was used to detect the mRNA expression level of differentiation marker gene (*MyoD1*, *MyoG*, and *MyHC*). It was found that the mRNA expression levels of *MyoD*, *MyoG*, and *MyHC* were all decreased, and the expression level of MyoG decline was significant (**Figure 4A**). Western blot results indicated that the protein expression levels of *MyoD*, *MyoG*, and *MyHC* were significantly decreased compared with the control group (**Figures 4B, C**). Immunofluorescence results showed that overexpression of miR-216a significantly inhibited the formation of myotube (**Figure 4D**). However, inhibition of miR-216a did not significantly affect the mRNA and protein levels of myoblast differentiation marker genes (**Figures 4E–G**). In addition, there was no significant difference in myotube formation after inhibition of miR-216a (**Figure 4H**). All these data demonstrated that overexpression of miR-216a inhibited bovine primary muscle cells differentiation.

SNIP1 and *Smad7* Were the Targets of miR-216a

Further, we explored molecular mechanisms underlying the function of miR-216a in impeding bovine primary muscle cells proliferation and differentiation by investigating its target genes. The mature sequence of miR-216a was highly conservative among different species (bovine, mouse, human, and rat) (**Figure 5A**), which aroused our research interest. To validate the function of miR-216a for bovine muscle cells proliferation and differentiation, predicting and verifying its target genes is essential. Through the online prediction software TargetScan (http://www.Targetscan.org) the seed sequence of miR-216a can

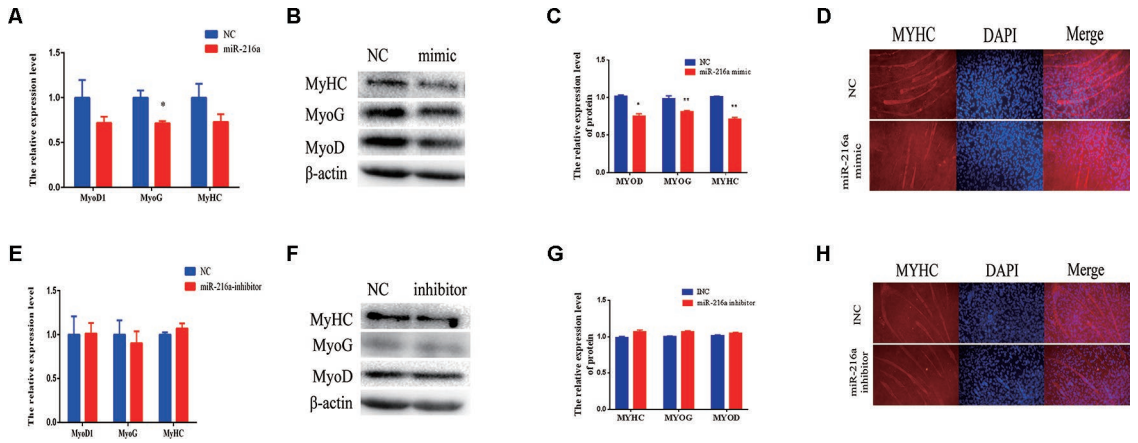

FIGURE 4 | miR-216a regulates bovine primary muscle cells differentiation. **(A)** RT-qPCR was used to detect the messenger RNA (mRNA) expression of myogenic marker genes *MyoD1*, *MyoG*, and *MyHC* after transfection of miR-216a mimic. **(B)** Western blot was used to detect the protein expression level of *MyoD*, *MyoG*, and *MyHC* after transfection miR-216a mimic. **(C)** Protein quantitative analysis of *MYHC*, *MYOG*, and *MYOD* for **(B)**. **(D)** The myotube formation of bovine primary muscle cells was measured by immunofluorescence assay under the 200 times field of microscope after transfection miR-216a mimic. **(E)** After loss of miR-216a, the mRNA expression of myogenic marker genes *MyoD1*, *MyoG*, and *MyHC* were detected by RT-qPCR. **(F)** After loss of miR-216a, the protein level of *MyoD*, *MyoG*, and *MyHC* were detected by western blot. **(G)** Protein quantitative analysis of *MYHC*, *MYOG*, and *MYOD* for **(F)**. **(H)** After loss of miR-216a, the myotube formation of bovine primary muscle cells was measured by immunofluorescence assay under the 200 times field of microscope. Data are presented as the mean ± SEM; n = 3; $^{*}P < 0.05$ and $^{**}P < 0.01$.

target the (3'UTR) of the gene *SNIP1* and *smad7* mRNA (**Figure 5B**). After transfection of miR-216a expression plasmid with *SNIP1* (wild or mutant) and *smad7* (wild or mutant) psi-Check2 reporter vector into HEK293T cells, respectively, the analysis results showed that miR-216a could reduce the luciferase activity of their wild-type reporter vector but has no effect on the mutant reporter vector (**Figures 5C, H**). During the growth stage of bovine skeletal muscle cells, gain of miR-216a could reduce the mRNA and protein levels of *SNIP1* significantly (**Figures 5D, E**). At the same time, miR-216a inhibitor was transfected into the cells, which had significantly enhanced the mRNA and protein levels of *SNIP1* (**Figures 5F, G**). During the differentiated stage of bovine skeletal muscle cells, gain of miR-216a reduced *smad7* mRNA and protein expression level (**Figures 5I, J**), whereas loss of miR-216a enhanced *smad7* mRNA and protein expression level (**Figures 5K, L**). According to the above results, during the proliferation and differentiation stages of bovine primary muscle cells, miR-216a targeted *SNIP1* and *smad7*, respectively.

DISCUSSION

In this study, we found that miR-216a possessed an inhibitory role in the process of proliferation and differentiation of bovine primary muscle cells by targeting *SNIP1* and *smad7*, respectively. Herein, miRNA-216a as a non-muscle-specific miRNA presented a downward trend in the proliferative and differentiation stages of bovine primary muscle cells, which suggested a potential role in the development of bovine skeletal muscle. To evaluate this hypothesis, mimic and inhibitor of miR-216a were used to enhance or block its expression, respectively. The current research found that overexpression of miR-216a can inhibit bovine primary muscle cells proliferation and differentiation. Unfortunately, inhibition of miR-216a expression did not affect the proliferation and differentiation of bovine primary muscle cells. We speculated that this might be caused by the low expression of miR-216a in bovine skeletal muscle or other potential compensation mechanisms. And it has been reported that an individual miRNA might interact with hundreds of mRNA targets while individual mRNAs can be targeted by many different miRNAs (Sassen et al., 2008). It was observed that if one specific miRNA fails, the pathway might be regulated by another miRNA within a complex cross path of miRNA network (Rottiers et al., 2011; Ebert and Sharp, 2012; Lima et al., 2017).

In the current study, we found miR-216a played a significant role in inhibiting skeletal muscle growth and development. According to our prediction and analysis, the mature sequence of miR-216a was found to be highly conserved among different species (bovine, human, mouse, and rat) (**Figure 5A**). Consistent with the research results, in previous studies, miR-216a also mainly played a suppressive role in disease and tumorigenesis. For instance, miR-216a inhibited tumor cells growth by down-regulating the expression level of Janus kinase 2 (*JAK2*) in pancreatic cancer (Siliang et al., 2014; Hou et al., 2016). In colorectal cancer, miR-216a can impede tumor cells invasion *in vitro* and metastasis *in vivo* by down-regulation of *KIAA1199* (Zhang et al., 2017). In gastric cancer, miR-216a restrained tumor cells migration and invasion possibly by targeting *JAK2/STAT3*-mediated epithelial-mesenchymal transition (EMT) (Tao et al., 2017). In osteosarcoma patients, the expression level of miR-216a was downregulated. Gain of miR-216a can inhibit tumor cells proliferation, migration and invasion *in vitro* and *in vivo via* suppressing the expression of *CDK14* (Ji et al., 2017). In renal cell carcinoma, miR-216a exerts tumor-suppressing functions by targeting *TLR4* (Wang et al., 2018c). Based on the above studies, it's worth noting that miR-216a has a broad application prospect in cancer therapy. Besides these, in muscle,

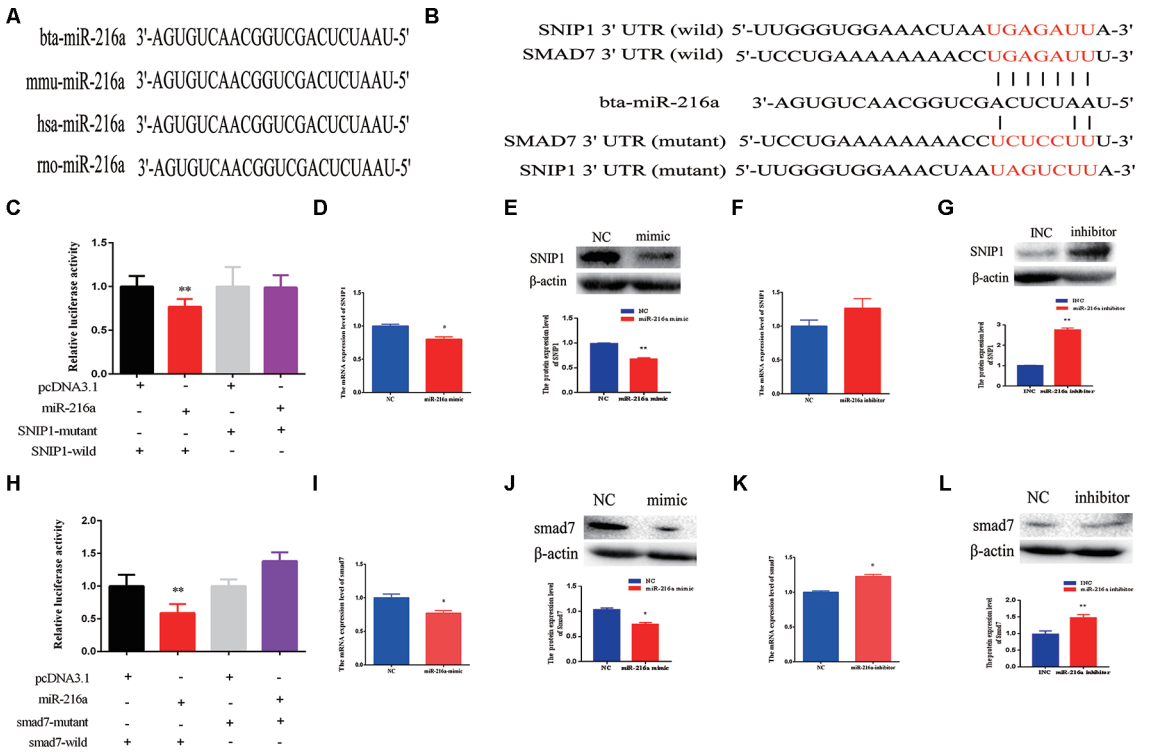

FIGURE 5 | SMAD nuclear interacting protein-1 (*SNIP1*) and *smad7* were the targets of miR-216a. **(A)** Conservative analysis of the mature sequence of miR-216a among different species (bovine, mouse, human, and rat). **(B)** The binding sites of miR-216a in the 3′-UTR of *SNIP1* and *smad7* were predicted by TargetScan software. The sequences in red indicate the target position of the miR-483 seed sequence and certain mutated bases. **(C)** The relative luciferase activity was detected after transfection of miR-216a expression plasmid with *SNIP1* (wild or mutant) psi-Check2 reporter vector into HEK293T cells. **(D, E)** During the growth stage of bovine primary muscle cells, the messenger RNA (mRNA) and protein expression level of *SNIP1* were detected by real-time quantitative PCR (RT-qPCR) and western blot after transfection miR-216a mimic. **(F, G)** During the growth stage of bovine primary muscle cells, the mRNA and protein expression level of *SNIP1* were detected by RT-qPCR and western blot after transfection miR-216a inhibitor. **(H)** The relative luciferase activity was detected after transfection of miR-216a expression plasmid with *smad7* (wild or mutant) psi-Check2 reporter vector into HEK293T cells. **(I, J)** During the differentiation stage of bovine primary muscle cells, the mRNA and protein expression level of *samd7* were detected by RT-qPCR and western blot after transfection miR-216a mimic. **(K, L)** During the differentiation stage of bovine primary muscle cells, the mRNA and protein expression level of *samd7* were detected by RT-qPCR and western blot after transfection miR-216a inhibitor. Data are presented as the mean ± SEM; n = 3; $^{*}P < 0.05$ and $^{**}P < 0.01$.

a certain preliminary study of miR-216a has been reported. For example, miR-216a inhibits proliferation and promotes apoptosis of human airway smooth muscle cells by targeting *JAK2* (Yan et al., 2019). And it can also exacerbate *TGF-β*-induced myofibroblast trans-differentiation *via PTEN/AKT* signaling (Qu et al., 2019). These results suggest that miR-216a has a potentially important role in muscle development. So, it is important to explore its role in skeletal muscle growth and development.

The current study further confirmed that miR-216a regulated the proliferation and differentiation of bovine primary muscle cells by targeting *SNIP1* and *smad7*. Bioinformatics prediction, dual-luciferase reporter assay, and related verification suggested that *SNIP1* and *smad7* were the direct targets of miR-216a. In previous studies, *SMAD nuclear interacting protein-1* (*SNIP1*) had been demonstrated function as an oncogene (Fujii et al., 2006), which can partially regulate *CyclinD1* to accelerate cell cycle progression through G1 (Roche et al., 2004; Etsu et al., 2010). In a variety of cellular contexts, knockdown of *SNIP1* could inhibit the mRNA and protein levels of *CyclinD1* (Roche et al., 2004; Bracken et al., 2008). In the current study, overexpression of mir-216a in the growth stage of bovine primary muscle cells significantly inhibited the mRNA and protein levels of *SNIP1*, and the mRNA expression level of *CyclinD1* also decreased at the same stage. *Smad7*, as a member of the inhibitory Smads (I-Smads) family, can specifically inhibit *TGF-β* pathway as described above and can also inhibit myostatin signaling by competitive combination with the R-Smads (Xiangyang et al., 2004). It has been reported that *TGF-β* signal pathway participated in regulating satellite cells (myoblasts) proliferation and differentiation by a complex regulatory network (Greene and Allen, 1991; Hathaway et al., 1991; Liu et al., 2001; Allen and Boxhorn, 2010). It has been reported that *Smad7* can promotes and enhances skeletal muscle differentiation not only by blocking smad2/3 transcriptional activity but also by physically interacting with *MyoD in vitro* experiments (Kollias et al., 2006). *Smad7-/-* mice have the feature of reducing muscle cells proliferation and differentiation by enhancing *smad2/3* signaling, which impedes muscle growth and regeneration (Cohen et al., 2015).

In summary, the current experimental results indicated that miR-216a suppressed bovine primary muscle cells proliferation and differentiation. Bioinformatics analysis, dual luciferase report

analysis and experimental verification showed that *SNIP1* and *smad7* were the targets of miR-216a regulating the proliferation and differentiation of bovine muscle primary cells, respectively. Therefore, the function and mechanism of miR-216a in bovine primary muscle cells growth might provide theoretical basis for elucidating bovine skeletal muscle development in future experiments.

DATA AVAILABILITY STATEMENT

All datasets generated for this study are included in the article/ **Supplementary Material**.

ETHICS STATEMENT

Animal care and study protocols were approved by the Animal Care Commission of the College of Veterinary Medicine, Northwest A&F University (Permit Number: NWAFAC1019).

AUTHOR CONTRIBUTIONS

ZY and CS contributed equally to this work. ZY conducted the analysis and wrote the manuscript. CS designed the study and finalized the manuscript. RJ carried out the part of experiments. YH, XL, CL, and HC provided experimental guidance.

FUNDING

This work was supported by the National Natural Science Foundation of China No.31772574), the Program of National Beef Cattle and Yak Industrial Technology System (CARS-37).

SUPPLEMENTARY MATERIAL

The Supplementary Material for this article can be found online at: https://www.frontiersin.org/articles/10.3389/fgene.2019.01112/full#supplementary-material

REFERENCES

Alexander, M. S., Kawahara, G., Motohashi, N., Casar, J. C., Eisenberg, I., Myers, J. A., et al. (2013). MicroRNA-199a is induced in dystrophic muscle and affects WNT signaling, cell proliferation, and myogenic differentiation. *Cell Death Differ.* 20 (9), 1194–1208. doi: 10.1038/cdd.2013.62

Allen, R. E., and Boxhorn, L. K. (2010). Regulation of skeletal muscle satellite cell proliferation and differentiation by transforming growth factor-beta, insulin-like growth factor I, and fibroblast growth factor. *J. Cell. Physiol.* 138 (2), 311–315. doi: 10.1002/jcp.1041380213

Bartel, D. P. (2004). MicroRNAs_ Genomics, Review Biogenesis, Mechanism, and Function. *Cell* 116, 281–297. doi: 10.1016/S0092-8674(04)00045-5

Bartel, D. P. (2009). MicroRNAs: target recognition and regulatory functions. *Cell* 136 (2), 215–233. doi: 10.1016/j.cell.2009.01.002

Bracken, C. P., Wall, S. J., Benjamin, B., Panov, K. I., Ajuh, P. M., and Perkins, N. D. (2008). Regulation of cyclin D1 RNA stability by SNIP1. *Cancer Res.* 68 (18), 7621–7628. doi: 10.1158/0008-5472.CAN-08-1217

Buckingham, M., Bajard, L., Chang, T., Daubas, P., Hadchouel, J., Meilhac, S., et al. (2003). The formation of skeletal muscle: from somite to limb. *J. Anat.* 202 (1), 59–68. doi: 10.1046/j.1469-7580.2003.00139.x

Buckingham, M., and Relaix, F. (2015). PAX3 and PAX7 as upstream regulators of myogenesis. *Semin. Cell Dev. Biol.* 44, 115–125. doi: 10.1016/j.semcdb.2015.09.017

Chen, J. F., Mandel, E. M., Thomson, J. M., Wu, Q., Callis, T. E., Hammond, S. M., et al. (2006). The role of microRNA-1 and microRNA-133 in skeletal muscle proliferation and differentiation. *Nat. Genet.* 38 (2), 228–233. doi: 10.1038/ng1725

Cheung, T. H., Quach, N. L., Charville, G. W., Liu, L., Park, L., Edalati, A., et al. (2012). Maintenance of muscle stem-cell quiescence by microRNA-489. *Nature* 482 (7386), 524–528. doi: 10.1038/nature10834

Christ, B., and Ordahl, C. P. (1995). EARLY STAGES OF CHICK SOMITE DEVELOPMENT. *Anat. Embryol.* 191 (5), 381–396. doi: 10.1007/BF00304424

Cohen, T. V., Kollias, H. D., Naili, L., Ward, C. W., and Wagner, K. R. (2015). Genetic disruption of Smad7 impairs skeletal muscle growth and regeneration. *J. Physiol.* 593 (11), 2479–2497. doi: 10.1113/JP270201

Crist, C. G., Montarras, D., Pallafacchina, G., Rocancourt, D., Cumano, A., Conway, S. J., et al. (2009). Muscle stem cell behavior is modified by microRNA-27 regulation of Pax3 expression. *PNAS* 106 (32), 13383–13387. doi: 10.1073/pnas.0900210106

Dey, B. K., Gagan, J., and Dutta, A. (2011). miR-206 and -486 induce myoblast differentiation by downregulating Pax7. *Mol. Cell Biol.* 31 (1), 203–214. doi: 10.1128/MCB.01009-10

Dey, B. K., Gagan, J., Yan, Z., and Dutta, A. (2012). miR-26a is required for skeletal muscle differentiation and regeneration in mice. *Genes Dev.* 26 (19), 2180–2191. doi: 10.1101/gad.198085.112

Diniz, G. P., and Wang, D. Z. (2016). Regulation of Skeletal Muscle by microRNAs. *Compr. Physiol.* 6 (3), 1279–1294. doi: 10.1002/cphy.c150041

Ebert, M. S., and Sharp, P. A. (2012). Roles for MicroRNAs in Conferring Robustness to Biological Processes. *Cell* 149 (3), 515–524. doi: 10.1016/j.cell.2012.04.005

Edmondson, D. G., Lyons, G. E., Martin, J. F., and Olson, E. N. (1994). Mef2 gene expression marks the cardiac and skeletal muscle lineages during mouse embryogenesis. *Development* 120, 1251–1263.

Etsu, T., Ayako, T., and Masaya, I. (2010). Functions of cyclin D1 as an oncogene and regulation of cyclin D1 expression. *Cancer Sci.* 98 (5), 629–635. doi: 10.1111/j.1349-7006.2007.00449.x

Feng, Y., Niu, L. L., Wei, W., Zhang, W. Y., Li, X. Y., Cao, J. H., et al. (2013). A feedback circuit between miR-133 and the ERK1/2 pathway involving an exquisite mechanism for regulating myoblast proliferation and differentiation. *Cell Death Dis.* 4, e934. doi: 10.1038/cddis.2013.462

Fujii, M., Lyakh, L. A., Bracken, C. P., Fukuoka, J., Hayakawa M., Tsukiyama T., et al. (2006). SNIP1 is a candidate modifier of the transcriptional activity of c-Myc on E box-dependent target genes. *Mol. Cell* 24 (5), 771–783. doi: 10.1016/j.molcel.2006.11.006

Gardner, S., Alzhanov, D., Knollman, P., Kuninger, D., and Rotwein, P. (2011). TGF-β Inhibits Muscle Differentiation by Blocking Autocrine Signaling Pathways Initiated by IGF-II. *Mol. Endocrinol.* 25 (1), 128–137. doi: 10.1210/me.2010-0292

Ge, Y., and Chen, J. (2011). MicroRNAs in skeletal myogenesis. *Cell Cycle* 10 (3), 441–448. doi: 10.4161/cc.10.3.14710

Greene, E. A., and Allen, R. E. (1991). Growth factor regulation of bovine satellite cell growth in vitro. *J. Anim. Sci.* 69 (1), 146–152. doi: 10.2527/1991.691146x

Hathaway, M. R., Hembree, J. R., Pampusch, M. S., and Dayton, W. R. (1991). Effect of transforming growth factor beta-1 on ovine satellite cell proliferation and fusion. *J. Cell. Physiol.* 146 (3), 435. doi: 10.1002/jcp.1041460314

Hocquette, J. F. (2010). Endocrine and metabolic regulation of muscle growth and body composition in cattle. *Animal* 4 (11), 1797–1809. doi: 10.1017/S1751731110001448

Hou, B. H., Jian, Z. X., Cui, P., Li, S. J., Tian, R. Q., and Ou, J. R. (2016). miR-216a may inhibit pancreatic tumor growth by targeting JAK2. *FEBS Lett.* 589 (17), 2224–2232. doi: 10.1016/j.febslet.2015.06.036

Ji, Q., Xu, X., Li, L., Goodman, S. B., Bi, W., Xu, M., et al. (2017). miR-216a inhibits osteosarcoma cell proliferation, invasion and metastasis by targeting CDK14. *Cell Death Dis.* 8 (10), e3103. doi: 10.1038/cddis.2017.499

Ju, H., Yang, Y., Sheng, A., and Jiang, X. (2015). Role of microRNAs in skeletal muscle development and rhabdomyosarcoma (review). *Mol. Med. Rep.* 11 (6), 4019–4024. doi: 10.3892/mmr.2015.3275

Kollias, H. D., Perry, R. L., Miyake, T., Aziz, A., and McDermott, J. C. (2006). Smad7 promotes and enhances skeletal muscle differentiation. *Mol. Cell Biol.* 26 (16), 6248–6260. doi: 10.1128/MCB.00384-06

Lagha, M., Kormish, J. D., Rocancourt, D., Manceau, M., Epstein, J. A., Zaret, K. S., et al. (2008). Pax3 regulation of FGF signaling affects the progression of embryonic progenitor cells into the myogenic program. *Genes Dev.* 22 (13), 1828–1837. doi: 10.1101/gad.477908

Li, H., Wei, X., Yang, J., Dong, D., Hao, D., Huang, Y., et al. (2018). circFGFR4 Promotes Differentiation of Myoblasts via Binding miR-107 to Relieve Its Inhibition of Wnt3a 11, *Mol. Ther. Nucleic Acids* 11, 272–283. doi: 10.1016/j.omtn.2018.02.012

Lima, T. I., Araujo, H. N., Menezes, E. S., Sponton, C. H., Araujo, M. B., Bomfim, L. H., et al. (2017). Role of microRNAs on the Regulation of Mitochondrial Biogenesis and Insulin Signaling in Skeletal Muscle. *J. Cell Physiol.* 232 (5), 958–966. doi: 10.1002/jcp.25645

Liu, D., Black, B. L., and Derynck, R. (2001). TGF-beta inhibits muscle differentiation through functional repression of myogenic transcription factors by Smad3. *Genes Dev.* 15 (22), 2950–2966. doi: 10.1101/gad.925901

Livak, K. J., and Schmittgen, T. D. (2001). Analysis of relative gene expression data using real-time quantitative PCR and the 2(-Delta Delta C(T)) *Methods* 25, 402–408. doi: 10.1006/meth.2001.1262

McCarthy, J. J. (2008). MicroRNA-206: the skeletal muscle-specific myomiR. *Biochim. Biophys. Acta* 1779 (11), 682–691. doi: 10.1016/j.bbagrm.2008.03.001

Miyake, M., Takahashi, H., Kitagawa, E., Watanabe, H., Sakurada, T., Aso, H., et al. (2012). AMPK activation by AICAR inhibits myogenic differentiation and myostatin expression in cattle. *Cell Tissue Res.* 349 (2), 615–623. doi: 10.1007/s00441-012-1422-8

O'Rourke, J. R., Georges, S. A., Seay, H. R., Tapscott, S. J., McManus, M. T., Goldhamer, D. J., et al. (2007). Essential role for Dicer during skeletal muscle development. *Dev. Biol.* 311 (2), 359–368. doi: 10.1016/j.ydbio.2007.08.032

Ott, M. O., Bober, E., Lyons, G., Arnold, H., and Buckingham, M. (1991). Early expression of the myogenic regulatory gene, myf-5, in precursor cells of skeletal muscle in the mouse embryo. *Development* 111, 1097–1107.

Qu, C., Liu, X., Ye, T., Wang, L., Liu, S., Zhou, X., et al. (2019). miR216a exacerbates TGFbetainduced myofibroblast transdifferentiation via PTEN/AKT signaling. *Mol. Med. Rep.* 19 (6), 5345–5352. doi: 10.3892/mmr.2019.10200

Relaix, F., Montarras, D., Zaffran, S., Gayraud-Morel, B., Rocancourt, D., Tajbakhsh, S., et al. (2006). Pax3 and Pax7 have distinct and overlapping functions in adult muscle progenitor cells. *J. Cell Biol.* 172 (1), 91–102. doi: 10.1083/jcb.200508044

Roche, K. C., Nicola, W., Tom, O. H., and Perkins, N. D. (2004). The FHA domain protein SNIP1 is a regulator of the cell cycle and cyclin D1 expression. *Oncogene* 23 (50), 8185–8195. doi: 10.1038/sj.onc.1208025

Rottiers, V., Najafi-Shoushtari, S. H., Kristo, F. G., Gurumurthy, S., Zhong, L., Li, Y., et al, (2011). MicroRNAs in Metabolism and Metabolic Diseases-miRNA. *Cold Spring Harbor Symp. Quant. Biol.* 76, 225–233. doi: 10.1101/sqb.2011.76.011049

Russell, R. G., and Oteruelo, F. T. (1981). An Ultrastructural Study of the Differentiation of Skeletal Muscle in the Bovine Fetus. *Anat. Embryol.* 162 (4), 403–417. doi: 10.1007/BF00301866

Sassen, S., Miska, E. A., and Caldas, C. (2008). MicroRNA: implications for cancer. *Virchows Arch.* 452 (1), 1–10. doi: 10.1007/s00428-007-0532-2

Siliang, W., Xiaodong, C., and Meiyue, T. (2014). MicroRNA-216a inhibits pancreatic cancer by directly targeting Janus kinase 2. *Oncol. Rep.* 32 (6), 2824–2830. doi: 10.3892/or.2014.3478

Sluijter, J. P., van Mil, A., van Vliet, P., Metz, C. H., Liu, J., Doevendans, P. A., et al. (2010). MicroRNA-1 and -499 regulate differentiation and proliferation in human-derived cardiomyocyte progenitor cells. *Arterioscler. Thromb. Vasc. Biol.* 30 (4), 859–868. doi: 10.1161/ATVBAHA.109.197434

Small, E. M., O'Rourke, J. R., Moresi, V., Sutherland, L. B., McAnally, J., Gerard, R. D., et al. (2010). Regulation of PI3-kinase/Akt signaling by muscle-enriched microRNA-486. *Proc. Natl. Acad. Sci. U. S. A.* 107 (9), 4218–4223. doi: 10.1073/pnas.1000300107

Song, C., Wu, G., Xiang, A., Zhang, Q., Li, W., Yang, G., et al. (2015). Overexpression of miR-125a-5p inhibits proliferation in C2C12 myoblasts by targeting E2F3. *Acta Biochim. Biophys. Sin. (Shanghai)* 47 (4), 244–249. doi: 10.1093/abbs/gmv006

Tajbakhsh, S., and Buckingham, M. (2000). The birth of muscle progenitor cells in the mouse: Spatiotemporal considerations. *Curr. Topics Dev. Biol. Vol 48* 48, 225–268. doi: 10.1016/S0070-2153(08)60758-9

Tao, Y., Yang, S., Wu, Y., Fang, X., Wang, Y., Song, Y., et al. (2017). MicroRNA-216a inhibits the metastasis of gastric cancer cells by targeting JAK2/STAT3-mediated EMT process. *Oncotarget* 8 (51), 88870–88881. doi: 10.18632/oncotarget.21488

Wang, D., Li, Y., Zhang, C., Li, X., and Yu, J. (2017a). MiR-216a-3p inhibits colorectal cancer cell proliferation through direct targeting COX-2 and ALOX5. *J. Cell. Biochem.* 119 (2), 1755–1766. doi: 10.1002/jcb.26336

Wang, H., Zhang, Q., Wang, B., Wu, W., Wei, J., Li, P., et al. (2018b). miR-22 regulates C2C12 myoblast proliferation and differentiation by targeting TGFBR1. *Eur. J. Cell Biol.* 97 (4), 257–268. doi: 10.1016/j.ejcb.2018.03.006

Wang, W., Zhao, E., Yu, Y., Geng, B., Zhang, W., and Li, X. (2018c). MiR-216a exerts tumor-suppressing functions in renal cell carcinoma by targeting TLR4. *Am. J. Cancer Res.* 8 (3), 476–488.

Wong, C. F., and Tellam, R. L. (2008). MicroRNA-26a targets the histone methyltransferase Enhancer of Zeste homolog 2 during myogenesis. *J. Biol. Chem.* 283 (15), 9836–9843. doi: 10.1074/jbc.M709614200

Xiangyang, Z., Stavros, T., Li-Fang, L., and Stotish, R. L. (2004). Myostatin signaling through Smad2, Smad3 and Smad4 is regulated by the inhibitory Smad7 by a negative feedback mechanism. *Cytokine* 26 (6), 262–272. doi: 10.1016/j.cyto.2004.03.007

Yan, Y. R., Luo, Y., Zhong, M., and Shao, L. (2019). MiR-216a inhibits proliferation and promotes apoptosis of human airway smooth muscle cells by targeting JAK2. *J. Asthma* 56 (9), 938–946. doi: 10.1080/02770903.2018.1509991

Zhang, D., Zhao, L., Shen, Q., Lv, Q., Jin, M., Ma, H., et al. (2017). Down-regulation of KIAA1199/CEMIP by miR-216a suppresses tumor invasion and metastasis in colorectal cancer. *Int. J. Cancer* 140 (10), 2298–2309. doi: 10.1002/ijc.30656

Zhu, M. J., Ford, S. P., Means, W. J., Hess, B. W., Nathanielsz, P. W., and Du, M. (2006). Maternal nutrient restriction affects properties of skeletal muscle in offspring. *J. Physiol.* 575 (Pt 1), 241–250. doi: 10.1113/jphysiol.2006.112110

Conflict of Interest: The authors declare that the research was conducted in the absence of any commercial or financial relationships that could be construed as a potential conflict of interest.

frontiers in Cell and Developmental Biology

ORIGINAL RESEARCH
published: 23 December 2019
doi: 10.3389/fcell.2019.00342

Long Non-coding RNA Maternally Expressed 3 Increases the Expression of Neuron-Specific Genes by Targeting miR-128-3p in All-Trans Retinoic Acid-Induced Neurogenic Differentiation From Amniotic Epithelial Cells

Yuhua Gao[1,2], Ranxi Zhang[3], Guanghe Wei[1], Shanshan Dai[1], Xue Zhang[1], Wancai Yang[1,4], Xiangchen Li[2,5] and Chunyu Bai[1,2]**

[1] Institute of Precision Medicine, School of Clinical Medicine, Jining Medical University, Jining, China, [2] Institute of Animal Sciences, Chinese Academy of Agricultural Sciences, Beijing, China, [3] Department of Spine Surgery, Qingdao Municipal Hospital, Qingdao, China, [4] Department of Pathology, University of Illinois at Chicago, Chicago, IL, United States, [5] College of Animal Science and Technology, College of Veterinary Medicine, Zhejiang A&F University, Lin'an, China

MicroRNA (miR)-128-3p is a brain-enriched miRNA that participates in the regulation of neural cell differentiation and the protection of neurons, but the mechanisms by which miR-128-3p regulates its target and downstream genes to influence cell fate from adult stem cells are poorly understood. In this study, we show down-regulation of miR-128-3p during all-trans retinoic acid (ATRA)-induced neurogenic differentiation from amniotic epithelial cells (AECs). We investigated miR-128-3p in both the Notch pathway and in the expression of neuron-specific genes predicted to be involved in miR-128-3p signaling to elucidate its role in the genetic regulation of downstream neurogenic differentiation. Our results demonstrate that miR-128-3p is a negative regulator for the transcription of the neuron-specific genes β III-tubulin, neuron-specific enolase (NSE), and polysialic acid-neural cell adhesion molecule (PSA-NCAM) via targeting Jagged 1 to inhibit activation of the Notch signaling pathway. We also used bioinformatics algorithms to screen for miR-128-3p interactions with long non-coding (lnc) RNA and circular RNA as competing endogenous RNAs to further elucidate underlying down-regulated molecular mechanisms. The lncRNA maternally expressed 3 is up-regulated by the ATRA/cAMP/CREB pathway, and it, in turn, is directly down-regulated by miR-128-3p to increase the amount of neuron differentiation. Endogenous miRNAs are, therefore, involved in neurogenic differentiation from AECs and should be considered during the development of effective cell transplant therapies for the treatment of neurodegenerative disease.

Keywords: AECs, neurogenic differentiation, ATRA, miRNA, lncRNA

OPEN ACCESS

Edited by:
Oleh Khalimonchuk, University of Nebraska–Lincoln, United States

Reviewed by:
Seiji Yamamoto, University of Toyama, Japan
Xinghui Sun, University of Nebraska System, United States

****Correspondence:***
Xiangchen Li
xcli863@zafu.edu.cn
Chunyu Bai
chunyu_bai@hotmail.com

Specialty section:
This article was submitted to Signaling, a section of the journal Frontiers in Cell and Developmental Biology

Received: *03 July 2019*
Accepted: *03 December 2019*
Published: *23 December 2019*

Citation:
Gao Y, Zhang R, Wei G, Dai S, Zhang X, Yang W, Li X and Bai C (2019) Long Non-coding RNA Maternally Expressed 3 Increases the Expression of Neuron-Specific Genes by Targeting miR-128-3p in All-Trans Retinoic Acid-Induced Neurogenic Differentiation From Amniotic Epithelial Cells. Front. Cell Dev. Biol. 7:342. doi: 10.3389/fcell.2019.00342

INTRODUCTION

Amniotic epithelial cells (AECs) are derived from the epiblast of the amniotic membrane and exhibit biological characteristics similar to embryonic stem cells, which have the capacity for differentiation into all three germ layers, as well as neural cells. Therefore, AECs have potential use in the recovery of injured nervous tissues. All-trans retinoic acid (ATRA) is the active ingredient of Vitamin A and plays an important role in the development of the nervous system by providing trophic effects that support the proliferation, differentiation, and maintenance of neural cells. ATRA affects the differentiation of neural cells derived from stem cells, including embryonic stem cells, mesenchymal stem cells, induced pluripotent stem cells, and AECs (Mark et al., 2015; Samarut et al., 2015; Davenport et al., 2016).

MicroRNAs (miRNAs) are a major group of endogenous, non-coding, small ribonucleotides (18–25 nt long) present in invertebrates, vertebrates, and plants that play important roles in the regulation of gene expression through the 3′-untranslated region (UTR) binding of specific messenger RNAs (mRNAs) to interfere with transcription (Bofill-De Ros et al., 2019). The role of miRNAs in the differentiation and development of the nervous system has received increased attention and importance in recent research, and specific miRNA spatiotemporal expression patterns may be essential for neuron neurogenesis (Volvert et al., 2012; Zhang et al., 2014; Bai et al., 2019). miR-128 is a brain-enriched miRNA that was reported to participate in the regulation of neural cell differentiation. Zhang et al. (2016) demonstrated that miR-128 prevents cortical neural progenitor cells (NPCs) from dividing and supports the specialized development of cells in a mouse model. Removing miR-128 from mouse NPCs enhanced cell division, resulting in less neuron formation (Zhang et al., 2016).

The human miR-128-1 stem-loop sequence contains two mature sequences, miR-128-1-5p and miR-128-3p. miR-128-3p was observed to be neural-protective after Fingolimod (FTY720) (and derivatives) treatment in dopaminergic MN9D cells (Vargas-Medrano et al., 2019). FTY720 is a Food and Drug Administration-approved drug for Parkinson's disease therapeutics. In the present study, we observed significant down-regulation of miR-128-3p in ATRA-induced neural cell differentiation from AECs. Dramatic positive changes were also observed in the expression of β III-tubulin, a specific neural marker. We investigated downstream miR-128-3p-regulated pathways and demonstrated the effects of those pathways on activation of the Notch signaling pathway related to the influence of neuronal marker expression to better illuminate the roles of miR-128-3p in the transcriptional regulation of neural cell differentiation. Additionally, we analyzed the causes of decreased miR-128-3p expression. We identified the long non-coding RNA (lncRNA) maternally expressed 3 (MEG3) as interacting with miR-128-3p, and previous reports of its up-regulation through a series of gene transcriptions after cAMP pathway activation (Zhao et al., 2006; Zhu et al., 2019). This reinforces our current miR-128-3p biological function proposal.

MATERIALS AND METHODS

Cell Culture and Neural Cell Differentiation

Amniotic epithelial cells were obtained from human amniotic membranes using enzyme digestion (Gao et al., 2016) and were cultured in Dulbecco's modified Eagle's medium/Ham's F-12 supplemented with 10% fetal bovine serum (Gibco, Carlsbad, CA, United States), 10 ng/ml epidermal growth factor, 10 ng/ml basic fibroblast growth factor, and 55 μM β-Mercaptoethanol. AECs were plated in six-well plates for neural differentiation and then 5×10^{-5} M ATRA was added to AEC cultures. After culturing for 18 days, the cells were harvested to analyze the expression of specific markers.

Reverse Transcription Quantitative PCR

miR-128-3p transcription levels were analyzed using reverse transcription quantitative (RT-q)PCR after neural differentiation. miRNAs were isolated from induced AECs with the miRcute miRNA Isolation Kit (Tiangen Biotech, Beijing, China), and pure miRNAs were poly(A)-tailed and reverse-transcribed with the miRcute miRNA First-strand cDNA Synthesis Kit (Tiangen Biotech, Beijing, China). qPCR was performed with the SYBR Green-based miRcute miRNA qPCR Detection Kit (Tiangen Biotech, Beijing, China) on an ABI 7500 Real-Time PCR system (Thermo Fisher Scientific, Waltham, MA, United States) according to the manufacturer's instructions. miR-128-3p and U6 primers were obtained from Tiangen Biotech, Beijing, China.

The expression of genes upstream and downstream of miR-128-3p [β III-tubulin, glial fibrillary acidic protein (*GFAP*), Jagged 1 (*JAG1*), and *MEG3*] was also tested using RT-qPCR. Total RNA was isolated from AECs and induced AECs using TRIzol reagent (Gibco, Carlsbad, CA, United States). It was then reverse-transcribed and used for qPCR analysis with the RNA PCR kit version 3.0 (Takara, Dalian, China) on an Applied Biosystems 7500 Real-Time PCR system. Reactions were performed in 20-μl volumes containing 7 μl of dd H_2O, 10 μl of SYBR premix Ex Taq buffer, 0.8 μM each of forward and reverse primers, 0.4 μl of ROX Reference Dye, and 1 μl of template cDNA. PCR conditions were 30 PCR cycles. Each experiment was performed in duplicate in 96-well plates and repeated three times. The mRNA gene expression cycle threshold value from each sample was calculated and normalized to internal controls using glyceraldehyde-3-phosphate dehydrogenase (GAPDH), and relative values were plotted. Primers are listed in **Supplementary Table S1**.

Immunofluorescence

Amniotic epithelial cells and induced AECs were fixed using 4% paraformaldehyde for 15 min and then permeabilized with 0.01% Triton X-100 for 30 min. After rinsing three times with phosphate-buffered saline (PBS), cells were blocked with 4% bovine serum albumin for 1 h and then incubated with primary antibodies [GFAP, 1:500; β III-tubulin, 1:200; Notch intracellular domain (NICD), 1:500; HES5, 1:500; CREB, 1:200] overnight in a humidified chamber at 4°C. All antibodies were purchased

from Abcam (Cambridge, MA, United States). Cells were then incubated with Cy5 or FITC-labeled secondary antibodies at room temperature for 1 h the following day. Immunofluorescent data were obtained using a confocal optical system (Nikon TE2000, Tokyo, Japan).

Flow Cytometry

To determine the level of β III-tubulin and GFAP expression after neural differentiation, cells were analyzed using an FC500 flow cytometer (Beckman Coulter, Atlanta, GA, United States). Briefly, cells were collected, blocked, and labeled with FITC- or Cy5-conjugated antibodies against β III-tubulin or GFAP as per manufacturer instructions. Data were analyzed with CXP software (Beckman Coulter, Atlanta, GA, United States). Mean fluorescence intensity was determined after the subtraction of a negative control (normal AECs).

Western Blotting

The expression of proteins encoded by genes up- and downstream of miR-128-3p was detected by Western blot analysis. Cells were lysed with the NP40 Extraction Reagent (CWBio, Beijing, China) and supplemented with a protease inhibitor (CWBio, Beijing, China). The bicinchoninic acid assay was used to measure protein concentrations. Extracted proteins were mixed with loading buffer and subjected to sodium dodecyl sulfate–polyacrylamide gel electrophoresis, followed by transfer to 0.2-μm nitrocellulose membranes. Primary antibodies (GFAP, 1:500; β III-tubulin, 1:400; NICD, 1:200; HES5, 1:500; CREB, 1:500, GAPDH, 1:5000; and histone, 1:5000) and horseradish peroxidase (HRP)-labeled secondary antibodies (1:10,000) were purchased from Abcam, Cambridge, MA, United States. Proteins were visualized with the Pierce ECL Western blotting substrate (CWBio, Beijing, China) for HRP. GAPDH and histone were used as internal controls.

Site-Directed Mutagenesis

The PCR-based Fast Site-Directed Mutagenesis Kit (Tiangen Biotech, Beijing, China) was used to mutate the base sequence. Primers containing the appropriate base substitutions are listed in **Supplementary Table S1**. PCR products were digested with the restriction enzyme *Dpn*I (Thermo Fisher Scientific, Waltham, MA, United States) at 37°C for 8 h and then transformed into competent *E. coli* cells. Mutation sites were confirmed using Sanger sequencing.

Luciferase Reporter Assays

We constructed a pGL3.0-Luc plasmid with target 3′-UTRs using firefly luciferase reporter vectors to test whether predicted miR-128-3p-binding sites in the 3′-UTR of the target were responsible for silencing expression. A mutation at nucleotide position 4 of the miRNA seed sequence in each 3′-UTR was generated with the Fast Site-Directed Mutagenesis Kit according to the manufacturer's instructions. Constructs containing mutated target (MUT) 3′-UTRs were used as the test group. Lipofectamine 3000 (Gibco, Carlsbad, CA, United States) was used to transfect HEK293T cells with a mixture of firefly luciferase reporter plasmids (wild-type plasmid, WT and mutation plasmid, MUT), the miRNA precursor or control, and the *Renilla reniformis* luciferase-encoding plasmid.

Hes 5-Binding Site Prediction

Putative Hes 5-binding sites within the promoter sequences of neuron-specific enolase (*NSE*), β III-tubulin, and polysialic acid-neural cell adhesion molecule (*PSA-NCAM*) were predicted using JASPAR CORE databases[1] (Khan et al., 2018), which construct specific binding site weight matrices for binding site prediction. The promoter sequences of *NSE*, β III-tubulin, and *PSA-NCAM* were obtained from the UCSC Genome Browser Gateway and were defined based on the location of the GC box and TATA box.

Chromatin Immunoprecipitation Assay-PCR

Chromatin immunoprecipitation (ChIP) was performed using the ChIP assay kit (Beyotime Institute of Biotechnology, Beijing, China) to test whether the transcription factor HES5 binds to the promotor regions of neural genes *NSE*, β III-tubulin, and *PSA-NCAM*. ChIP DNA was extracted with a DNA Purification Kit (Beyotime Institute of Biotechnology, Beijing, China), and the purified sample was subjected to qPCR amplification with primers spanning the protein-binding sites (**Supplementary Table S1**).

Co-immunoprecipitation

To test for interactions between MEG3 and miR-128-3p, an Argonaute 2 (AGO2)-containing plasmid and the miRNA precursor were co-transfected into AECs. After 3 days, cells were lysed in 1 ml of lysis buffer (CWBio, Beijing, China), lysates were centrifuged, and 1 μg of AGO2 antibodies was added to 500 μl of the supernatant. IP was carried out with a Pierce Co-immunoprecipitation (Co-IP) Kit (Thermo Fisher Scientific, Waltham, MA, United States) according to the manufacturer's instructions and then MEG3 expression was analyzed in the IP products using qPCR. The empty plasmid (EV) and miRNA-Let 7a served as experimental controls.

Statistical Analysis

The Student's *t*-test was used to compare data between the two experimental groups. Statistical significance was defined as $^{*}P < 0.05$ and $^{**}P < 0.01$. All studies were performed in three separate experiments, each performed in triplicate. All data are expressed as the mean ± standard deviation (SD).

RESULTS

miR-128-3p Signature in Neurogenic Differentiation From AECs

All-trans retinoic acid affects the differentiation of neural cells from stem cells. The effects of ATRA in neurogenic

[1] http://jaspar.genereg.net/

differentiation from AECs were assessed in this study. AECs induced toward neurogenic differentiation take on a different, elongated neuronal morphology, with apparent large, flat, and multipolar cells. Neurogenic differentiation was evaluated according to the expression level of neuron-specific genes. After treatment with ATRA, expression of the neuron-specific gene β III-tubulin and astrocyte-specific gene *GFAP* was detected using immunofluorescence, flow cytometry, and RT-qPCR. Increased β III-tubulin and GFAP expression levels were detected in ATRA-induced AECs (**Figures 1A–D**) compared with untreated cells.

miR-128 is a brain-enriched miRNA, and miR-128-3p has been shown to be neuroprotective (Zhang et al., 2016). Therefore, we tested the relative expression levels of miR-128-3p, as well as that of JAG1 protein as a putative target of miR-128-3p predicted using TargetScan Human v7.2[2], in normal AECs and induced AECs using RT-qPCR (**Figures 1E,H**). miR-128-3p expression decreased dramatically following neurogenic differentiation, while JAG1 expression was significantly up-regulated. Expression level analysis of miR-128-3p with β III-tubulin showed a significantly negative correlation between normal AECs and induced AECs ($P < 0.05$, **Figures 1F,G**). These results demonstrate that miR-128-3p plays a critical role in the expression of neuron-specific genes.

Notch Pathway Activation and Roles in the Expression of Neuron-Specific Genes

Jagged 1 is the canonical ligand for the receptor of notch 1, which interacts with cell surface transmembrane-spanning receptors of the Notch pathway to release a NICD from the membrane tether. The NICD translocates into the nucleus and associates with the CBF1/RBP-Jk/Suppressor of Hairless/LAG-1 (CSL) family of DNA-binding proteins to form a transcriptional activator. This activates the tissue-specific basic helix–loop–helix hairy and enhancer of split (HES) gene family members HES1 and HES5, which enhances transcription of a set of target genes. In our research, we first tested the regulation of miR-128-3p, JAG1, β III-tubulin, and GFAP. miR-128-3p mimics and inhibitor were added to the induced AECs. The protein levels of the abovementioned genes were tested by Western blot analysis, and JAG1 and β III-tubulin expression was shown to dramatically decrease, while GFAP levels were significantly up-regulated after the overexpression of miR-128-3p in induced AECs; the opposite was observed with the addition of an inhibitor, the effect of overexpressed miR-128 in induced AECs was rescued after JAG1 addition (**Figures 2A,B**).

To determine whether the predicted site in the 3′-UTR of JAG1 is responsible for the silencing of gene expression by miR-128-3p, the AGO2-IP qPCR was used for further analyses. As an essential component of the RNA-induced silencing complex (RISC), the AGO2 protein plays a central role in RNA silencing processes. To determine whether AGO2 serves as a binding platform for JAG1 and miR-128-3p, we performed Myc-AGO2 IP in HEK293T cells containing either an AGO expression vector or an empty vector and transiently co-expressing miR-128-3p or Let-7a (negative control). The binding site of Let-7a was not found in the JAG1 sequence after analysis using bioinformatics algorithms, so Let-7a was used as a negative control in this study. JAG1 levels were analyzed by qPCR of the IP products, and shown to be specifically enriched by more than five- to sevenfold in the presence of AGO2 in miR-128-3p-transfected cells compared with the control (Let-7a-transfected cells, **Figure 2C**). These data suggest that miR-128-3p interacts with JAG1 in the RISC complex. We next cloned WT and MUT versions of the *JAG1* 3′-UTR region downstream of a luciferase reporter gene and then co-transfected one or the other of these vectors into HEK293T cells with either pre-miR-128 or a control. In cells transfected with pre-miR-128 and pRL-JAG1-WT, luciferase activity significantly decreased relative to that in cells co-transfected with the control precursor or mutated versions of the target (**Figure 2D**). These results demonstrate that miR-128 directly suppresses the expression of JAG1 through targeting seed sequences in the 3′-UTR of *JAG1*, in agreement with a previous report (Yi et al., 2018). To test the role of JAG1 in neurogenic differentiation, a small interfering RNA (siRNA) of JAG1 was designed, synthesized, and verified (**Figure 2E**). Then, miR-128-3p mimics, inhibitor, and siRNA-JAG1 were separately added to the induced AECs, and flow cytometry was used to analyze the relative expression of β III-tubulin and GFAP. miR-128-3p and siRNA-JAG1 efficiently prevented β III-tubulin expression, the miR-128-3p inhibitor increased expression, while GFAP had the opposite effect of β III-tubulin (**Figures 2F,G**).

Notch intracellular domain and HES5 were analyzed using immunofluorescence to test for activation of the Notch pathway after ATRA treatment in AECs. NICD and HES5 levels significantly increased in induced AECs, but the opposite data were observed after overexpressed miR-128 in induced AECs (**Figures 3A,B**). Avagacestat (BMS-708163) is a potent inhibitor of γ-secretase and NICD and exhibits potency for Notch processing inhibition, so the effect of BMS-708163 and JAG1 was determined by separately adding them to induced AECs. Flow cytometry showed that JAG1 increased the amount of β III-tubulin, while BMS-708163 reduced its expression (**Figure 3C**). To determine the influence of BMS-708163 or JAG1 on NICD and HES5 in the nucleus, we extracted nuclear protein to test expression. NICD and HES5 expression dramatically increased by JAG1 treatment, while the opposite occurred with BMS-708163 treatment. β III-Tubulin expression increases following activation of the Notch pathway (**Figures 3D,E**), suggesting that this plays an important role in the expression of neuron-specific genes in AEC neurogenic differentiation derived from AECs, but the mechanisms by which HES5 regulates the expression of neuron-specific genes to influence cell fate remains poorly understood.

To determine the mechanisms underlying the elevated expression of neuron-specific genes after activation of the Notch pathway, the promoter regions (3 kb upstream) of β III-tubulin, *NSE*, and *PSA-NCAM* were screened

[2]http://www.targetscan.org/vert_72/

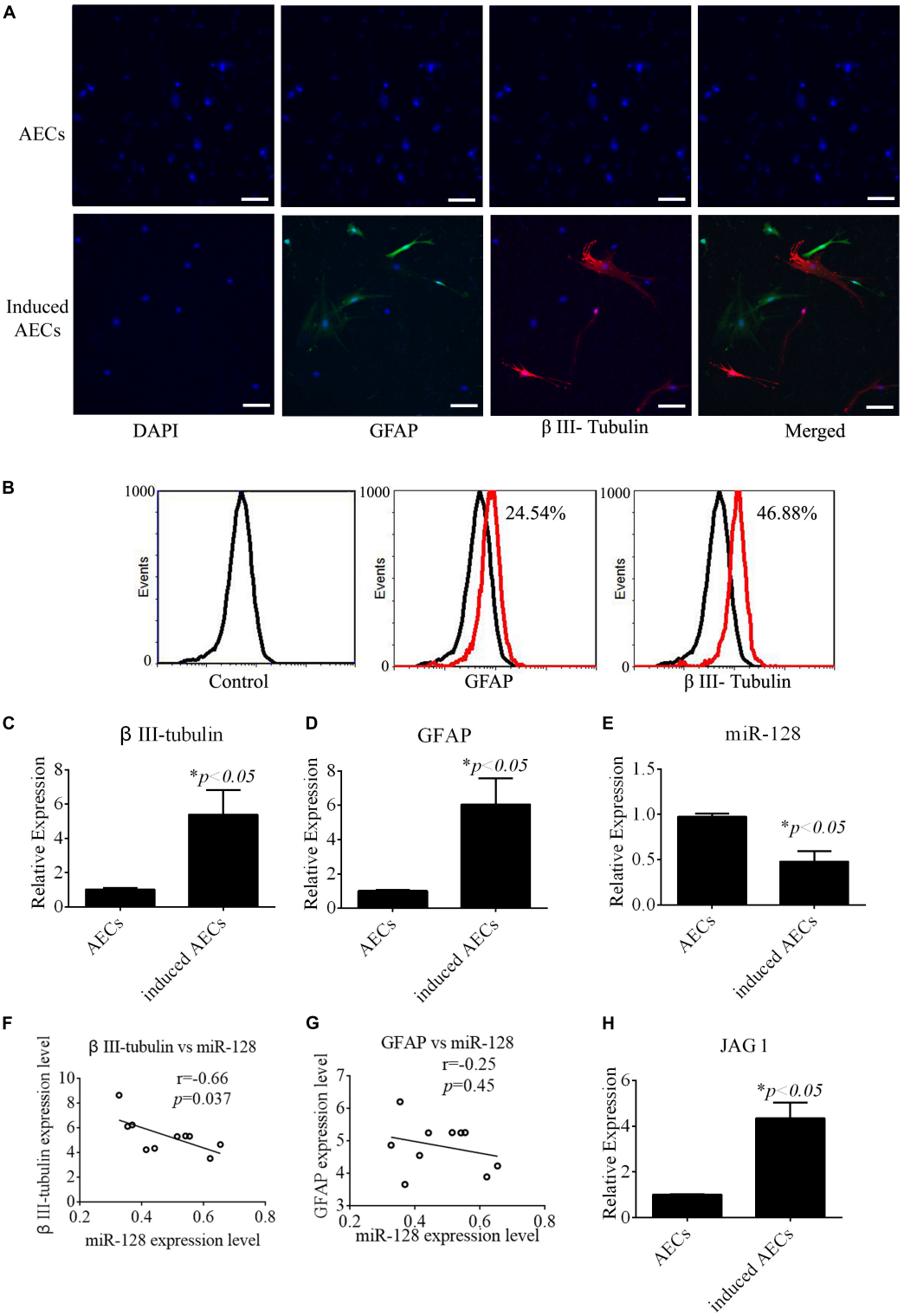

FIGURE 1 | Neurogenic differentiation derived from amniotic epithelial cells (AECs). AECs were induced with all-trans retinoic acid (ATRA) for 18 days. **(A,B)** Neurogenic markers were detected by immunofluorescence staining and flow cytometry. Neuron-specific genes (β III-tubulin) and astrocyte-specific genes (glial fibrillary acidic protein: GFAP) were detected. Scale bar = 100 μm. **(C–E)** RT-qPCR was used to determine the relative expression of β III-tubulin, GFAP, and miR-128-3p in non-induced AECs and induced AECs. **(F,G)** Comparative analysis of miR-128-3p and β III-tubulin or GFAP in neurogenic differentiation. **(H)** The expression of Jagged 1 (JAG1), a putative target for miR-128-3p in neurogenic differentiation, was significantly altered in induced AECs. $^*P < 0.05$.

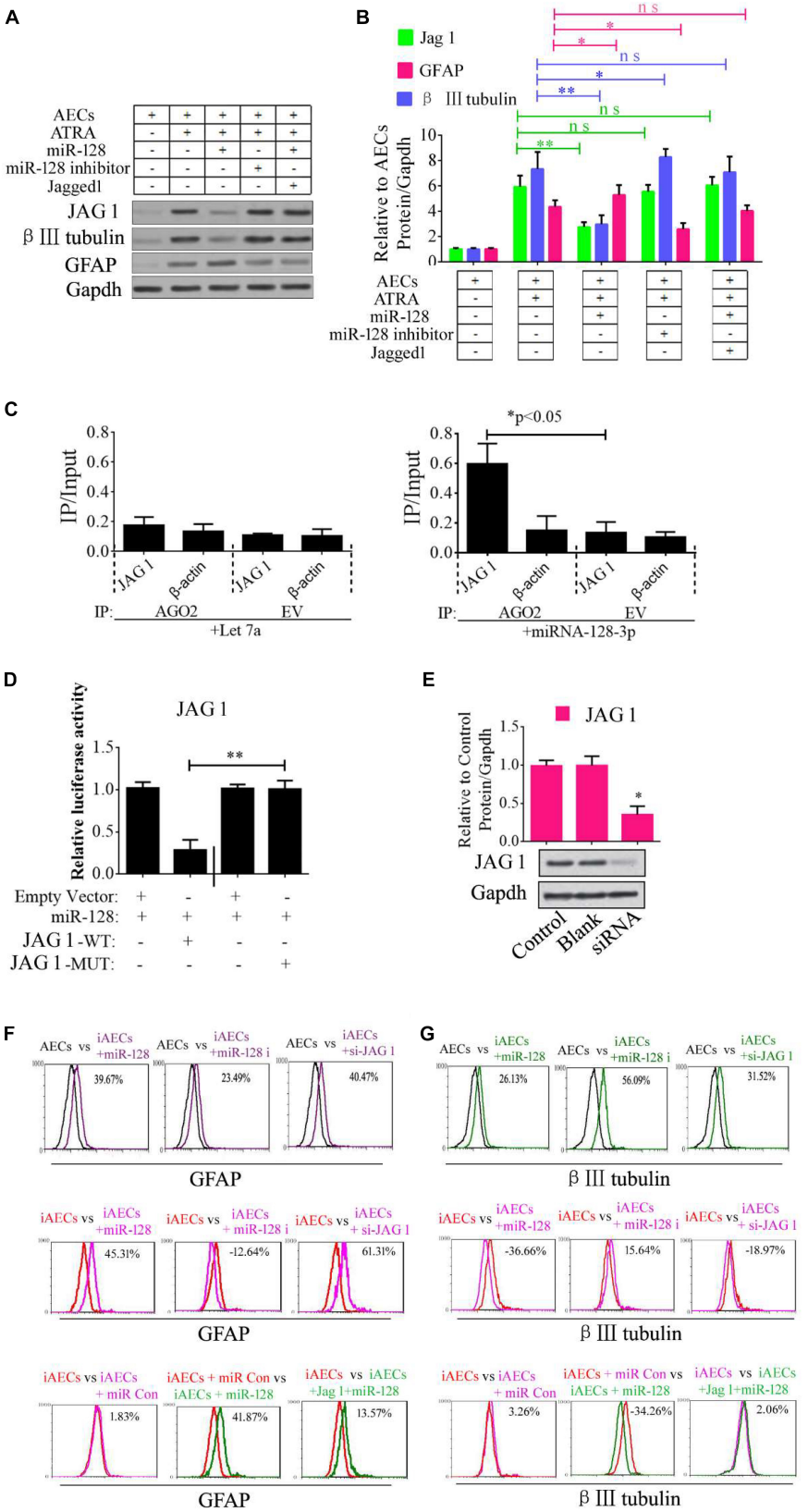

FIGURE 2 | Continued

FIGURE 2 | Role of miR-128-3p in neurogenic differentiation from AECs. **(A,B)** Neurocyte markers were tested using Western blotting after AECs were exposed to miR-128-3p, miR-128-3p inhibitor, and Jagged 1, respectively. Protein abundance was analyzed using ImageJ tools. The data revealed that Jagged1 could rescue the β III-tubulin expression after overexpressed miR-128 in AECs. $^{*}P < 0.05$; $^{**}P < 0.01$; ns, non-significant. **(C)** Immunoprecipitation of Myc-tagged Argonaute 2 (AGO2) from AECs co-transfected with Myc-AGO2 and either miR-128-3p or Let-7a (negative control). The empty vector (EV) served as the Myc-AGO2-related negative control. Jag 1 and β-actin mRNA levels were quantified using qPCR, and the relative immunoprecipitate (IP)/input (cell total RNA) values were plotted. $^{*}P < 0.05$. **(D)** The effect of miR-128-3p on JAG1 expression was evaluated using luciferase reporter assays. $^{**}P < 0.01$. **(E)** Western blot analysis of JAG1 expression was performed following siRNA targeting. Protein abundance was analyzed using ImageJ tools. Glyceraldehyde-3-phosphate dehydrogenase (GAPDH) was used as an endogenous control and Scramble was used as a control. Western blot images are representative of at least three independent replicates. $^{*}P < 0.05$. **(F,G)** Neurocyte markers were tested using flow cytometry after induced AECs were exposed to various small RNAs or Jagged 1. iAECs, induced AECs; miR-128 i, miR-128 inhibitor; miR Con, miR-128 mimics control.

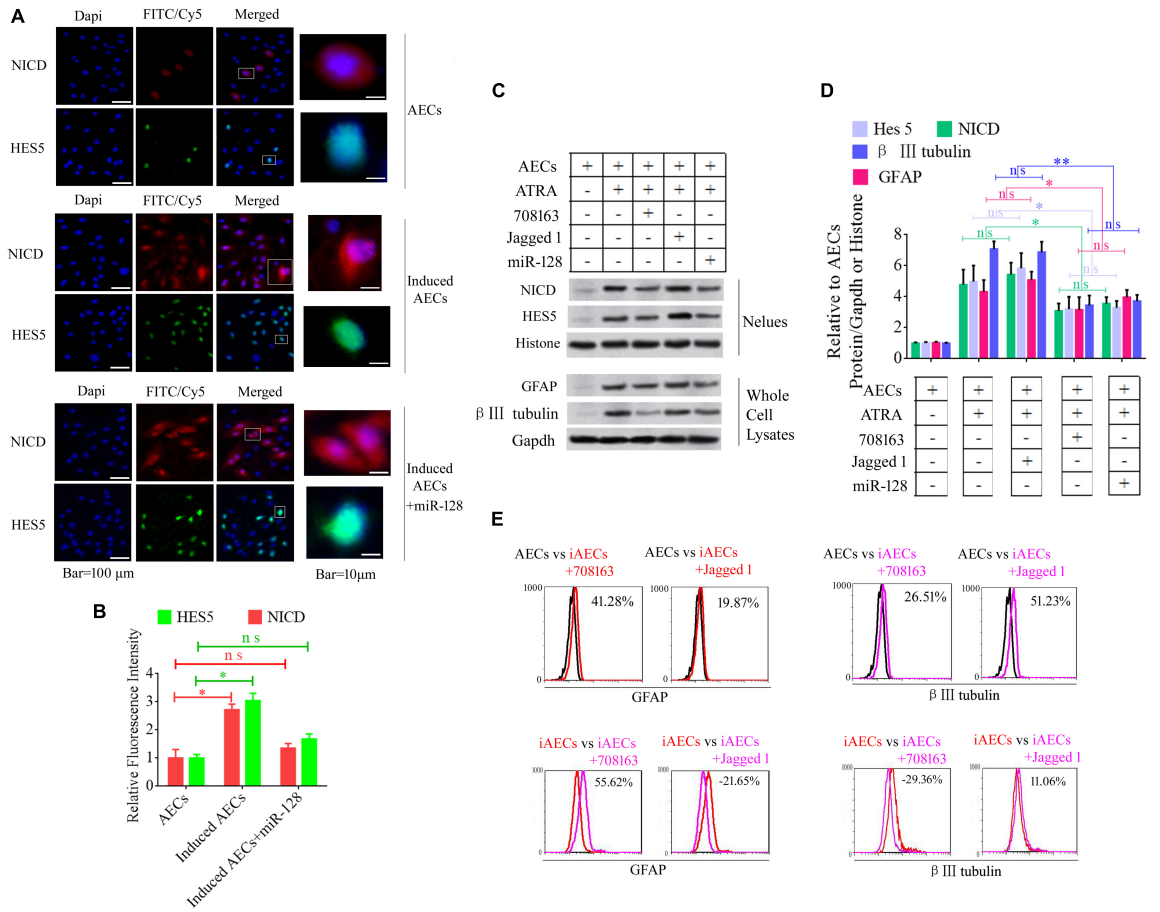

FIGURE 3 | Notch pathway inhibition by miR-128-3p decreases the expression of neurocyte markers in neurogenic differentiation. **(A)** Immunofluorescence staining illustrates activation of the Notch pathway based on the nuclear expression of intercellular activated notch 1 (Notch intracellular domain: NICD) and Hes 5 after ATRA induction and miR-128 addition. **(B)** Fluorescence intensity was analyzed using ImageJ tools. **(C,D)** Western blot data of NICD and HES5 expression after JAG1, BMS-708163, or miR-128 overexpression treatment. Protein abundance was analyzed using ImageJ tools. $^{*}P < 0.05$; $^{**}P < 0.01$; ns, non-significant. **(E)** Neurocyte markers were tested using flow cytometry in induced AECs exposed to 708163 (an inhibitor of the Notch pathway) or Jagged 1 (activator for the Notch pathway). iAECs, induced AECs.

using JASPAR tools and multiple HES5-binding sites were found (**Figure 4A**). To test for physical interactions and to accurately compare the amounts of HES5 enriched in these promoter regions, ChIP coupled with qPCR analysis was performed. Non-specific IgG was used as a negative control, and the input sample (whole lysate prior to ChIP being performed) was used as a positive control. As shown in **Figures 4B–D**, the fold change in occupancy was higher in induced AECs than in normal AECs, with observed fold changes of 4.57, 6.15, and 3.31 for β III-tubulin, *NSE*, and *PSA-NCAM*, respectively.

LncRNA MEG3 as a Competing Endogenous RNA to Influence the Expression of miR-128-3p

Competing endogenous RNAs are widely involved in eukaryotic development by regulating other mRNA transcripts by

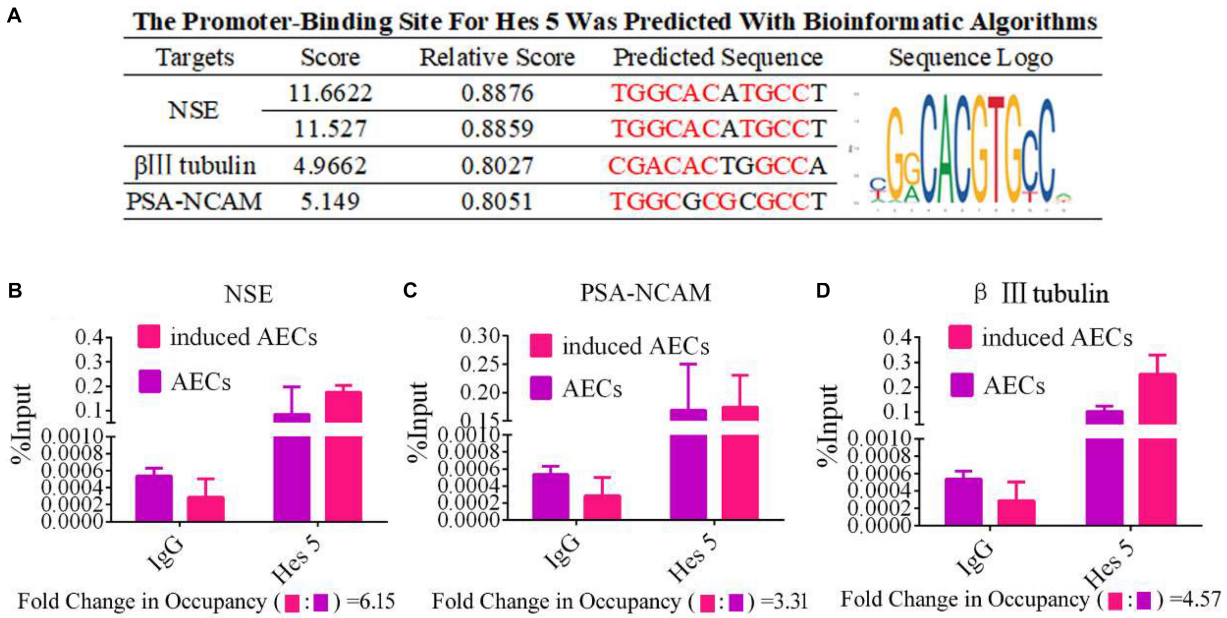

FIGURE 4 | HES5 promotes transcription of the neurocyte marker genes β III-tubulin, *NSE*, and *PSA-NCAM* via physical interactions with their promoters. **(A)** HES5 promoter-binding sites were predicted using bioinformatics algorithms in the promoter region of β III-tubulin, *NSE*, and *PSA-NCAM*. Predicted sequences were calculated according to the relative frequency of promotor sequences, which have the potential to bind Hes 5 but do not completely conform to the sequence logo of Hes 5. Consensus sequences are shown in red. **(B–D)** The amount of HES5 enriched within neurocyte marker gene promoter regions in normal and induced AECs was quantified by ChIP-coupled real-time PCR. The percentage of input was calculated according to threshold cycle values. The negative control for Hes 5 binding sites is shown in the **Supplementary Material**. Data are presented as the mean ± SD (three independent experiments).

competing for shared miRNAs (Das et al., 2019). In this study, we assumed that the down-regulation of miR-128-3p was regulated by lncRNAs or circRNAs. Therefore, we used the StarBase bioinformatics algorithm to screen for interactions between competing endogenous (ce)RNAs and miR-128-3p to investigate the low abundance of miR-128-3p in neurogenic differentiation from AECs. The lncRNAs and circRNAs we found are listed in **Supplementary Tables S2, S3**. Based on this analysis, and combined with data from a previous study (Lan et al., 2018), the lncRNA MEG3 was selected as a candidate target. MEG3 is ∼1.6 kb in humans with a number of splice isoforms and evidence of retained introns creating longer transcripts. It is widely expressed early in the visceral yolk sac, embryonic ectoderm, paraxial mesoderm, epithelial ducts, skeletal muscle, cochlea, brain, and eye. We first detected MEG3 expression levels in normal and induced AECs, and showed them to dramatically increase after ATRA treatment (**Figure 5A**).

The binding sites between MEG3 and miR-128-3p were predicted using StarBase and are shown in **Figure 5B**. To investigate the interaction of miR-128-3p and MEG2 in induced AECs, miR-128-3p binding sites in MEG3 were mutated using PCR methods (**Figure 5B**). Then, full-length MEG3 (MEG3-WT) and MEG3 with mutated sites (MEG3-MUT) were cloned and linked downstream of a luciferase reporter gene. These constructs were co-transfected into HEK293T cells with either pre-miR-128-3p or control. Luciferase activity significantly decreased following MEG3-WT transfection relative to that in cells co-transfected with MEG3-MUT (**Figure 5C**). To determine whether AGO2 serves as a binding platform for MEG3 and miR-128-3p, we performed Myc-AGO2 IP in HEK293T cells containing either an AGO expression vector or an empty vector and transiently co-expressing miR-128-3p or Let-7a (negative control). The binding site of Let-7a was not found in the MEG3 sequence after analysis using bioinformatics algorithms; therefore, Let-7a was used as a negative control in this study. MEG3 levels were analyzed by qPCR of the IP products, and shown to be specifically enriched by more than 8- to 10-fold in the presence of AGO2 in miR-128-3p-transfected cells compared with the control (Let-7a-transfected cells, **Figure 5D**). These data suggest that miR-128-3p interacts with MEG3 in the RISC complex.

CREB Promotes MEG3 Expression to Increase the Expression of Neuron-Specific Genes

To determine the function of MEG3 in the expression of neuron-specific genes from differentiated AECs, siRNA for MEG3 (si-MEG3) was designed and synthesized to depress the expression of MEG3 in induced AECs (**Figure 6A**). si-MEG3 and MEG3 were added to induced AECs, respectively, to assay the percentage of β III-tubulin and GFAP using flow cytometry. si-MEG3 dramatically increased the amount of GFAP, and inhibited the expression of β III-tubulin, while the opposite was observed after overexpressing MEG3 in induced AECs (**Figure 6G**). MEG3 can modulate neurogenic differentiation from AECs under ATRA treatment, but the mechanisms underlying this are unclear.

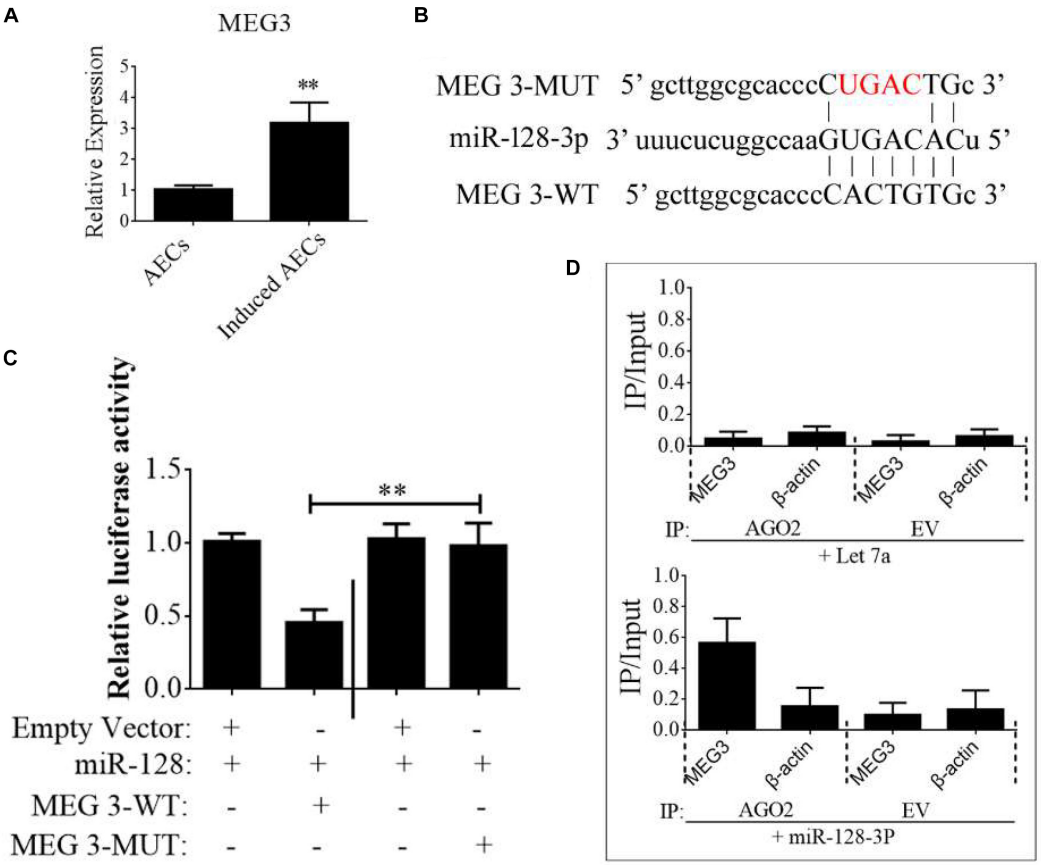

FIGURE 5 | lncRNA MEG3 targets miR-128-3p in neurogenic differentiation from AECs. **(A)** The expression of MEG3 was analyzed in normal and induced AECs using RT-qPCR. **(B)** The binding site between MEG3 and miR-128-3p was predicted using bioinformatics algorithms and subsequently mutated to verify interactions. **(C)** Full-length MEG3 (WT) and sequences containing different mutated variants of the miR-128-3p binding site (MUT) were tested to determine the effect on miR-15/16 expression. The pRL-40 vector alone was used as an internal control. Results are expressed as relative luciferase activity and represent the mean ± SD of at least three replicates. **(D)** Immunoprecipitation of Myc-tagged Argonaute 2 (AGO2) from AECs co-transfected with Myc-AGO2 and either miR-128-3p or Let-7a (negative control). Empty vector (EV) served as the Myc-AGO2-related negative control. MEG3 and β-actin mRNA levels were quantified using qPCR, and relative immunoprecipitate (IP)/input (cell total RNA) values were plotted. $^{*}P < 0.05$; $^{**}P < 0.01$.

Previous work (Zhao et al., 2006; Zhu et al., 2019) described how elevated cAMP levels enhanced endogenous MEG3 expression through cAMP-response element (CRE) directly binding the MEG3 promoter region. We detected the concentration of cAMP after ATRA treatment in AECs using a cAMP assay kit (competitive ELISA, Fluorometric) and combined this with our previous data (Zhao et al., 2004). We detected a marked increase in intracellular cAMP levels in induced AECs (**Figure 6B**). The CRE-binding protein CREB was previously shown to enter the nucleus and to combine with CRE to enhance MEG3 transcription, after elevating the concentration of cAMP (Zhao et al., 2006; Zhu et al., 2019). Here, we detected the expression of phosphorylated CREB and total CREB in whole cell lysates using Western blot and immunofluorescence. Both phosphorylated CREB and total CREB dramatically increased after ATRA treatment (**Figures 6C,E**). Use of the CREB inhibitor (666-15), which reduces CREB phosphorylation to inhibit its transcriptional activity independently of direct CREB or CREB-binding protein interactions (Zhang et al., 2019), significantly decreased phosphorylated CREB and total CREB in induced AECs (**Figures 6E,F**). 666-15 was also added to test the effect of CREB in the regulation of MEG3 transcription and was found to effectively depress MEG3 expression in induced AECs (**Figure 6D**). Its effects on inhibiting β III-tubulin and increasing GFAP were in line with the si-MEG3 experiment (**Figures 6E–G**). JAG1 was shown to block the function of si-MEG3 in neurogenic differentiation from AECs, implying that *MEG3* is an upstream regulatory gene for miR-128-3p influencing neurogenic differentiation.

Taking these findings together, the flow cytometry data show that miR-128-3p alone decreases the expression of neuron-specific genes compared with the anti-miR-128-3p group in neurogenic differentiation from AECs ($P < 0.05$). si-JAG1, JAG1, and the Notch pathway inhibitor BMS-708163 all affect neurogenic differentiation, and activation of the Notch pathway significantly increases levels of β III-tubulin ($P < 0.05$). MEG3 plays an important role in the expression of neuron-specific genes by targeting miR-128-3p to activate the Notch pathway during

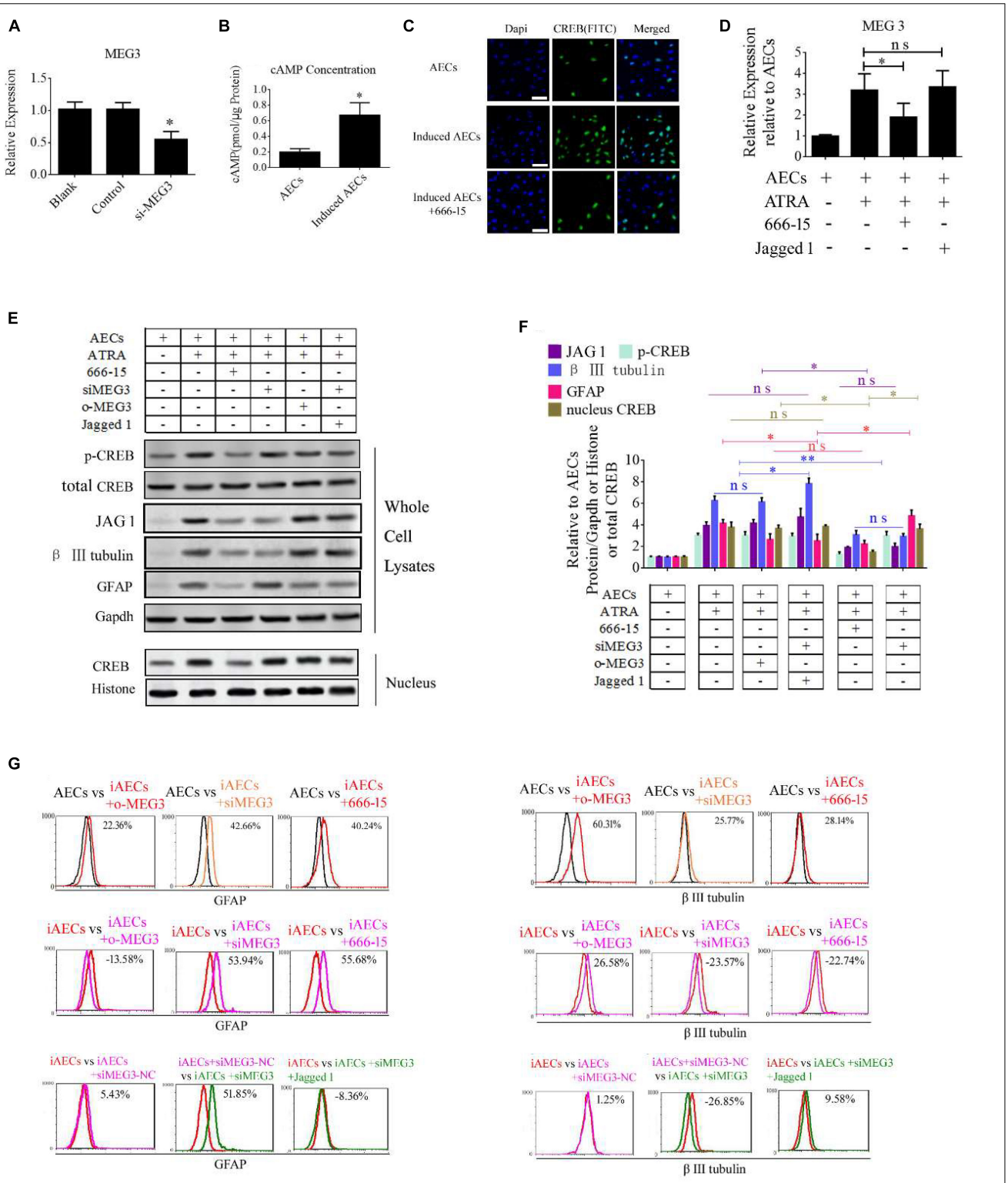

FIGURE 6 | ATRA increases the expression of MEG3 through the cAMP/CREB pathway to modulate neurogenic differentiation. **(A)** A siRNA for MEG3 (si-MEG3) effectively depressed the expression of MEG3 in induced AECs ($P < 0.05$). **(B)** The concentration of cAMP was detected between normal significantly increased in induced compared with normal AECs ($P < 0.05$). **(C)** Expression of cAMP response element-binding protein (CREB) was detected under ATRA or 666-15 (a CREB inhibitor) treatment using immunofluorescence staining. **(D)** MEG3 expression was analyzed under 666-15 or Jagged 1 treatment by RT-qPCR. **(E,F)** Expression of β III-tubulin and GFAP were as assessed using Western blotting. **(G)** β III-tubulin and GFAP expression was analyzed following single or assorted overexpression of MEG3 (o-MEG3), si-MEG3 or 666-15 treatment in induced AECs. iAECs, induced AECs; siMEG3-NC, siMEG3 negative control. *$P < 0.05$; **$P < 0.01$; ns, non-significant.

neurogenic differentiation. β III-tubulin levels dramatically decrease when its expression is knocked down or its transcription is inhibited ($P < 0.05$, **Figures 7**, **8**).

DISCUSSION

Amniotic epithelial cells have important properties that contribute to promising potential usage in nerve regeneration. These include differentiation into all three germ layers, anti-inflammatory properties, and low immunogenicity (Bai et al., 2019). In our previous research (Gao et al., 2016), AECs demonstrated the ability to differentiate into neural cells with characteristics of functional neurons under treatment of ATRA combined with other factors. However, the underlying molecular mechanisms of ATRA were unclear, which carries potential risks for clinical applications.

The RA cell-signaling pathway plays an important role in nervous regeneration and is essential in neuronal differentiation. RA signaling has been demonstrated to promote neural differentiation in the developing embryo of zebrafish, chicken, and mice (Samarut et al., 2015; Xavier-Neto et al., 2015). In adults, this pathway's functions are confined to a few brain regions and are involved in the maintenance of adult neurogenesis and the differentiated state of neurons. The RA pathway generates a series of physiological effects by causing a regulated cascade of gene transcription after it is activated in cells.

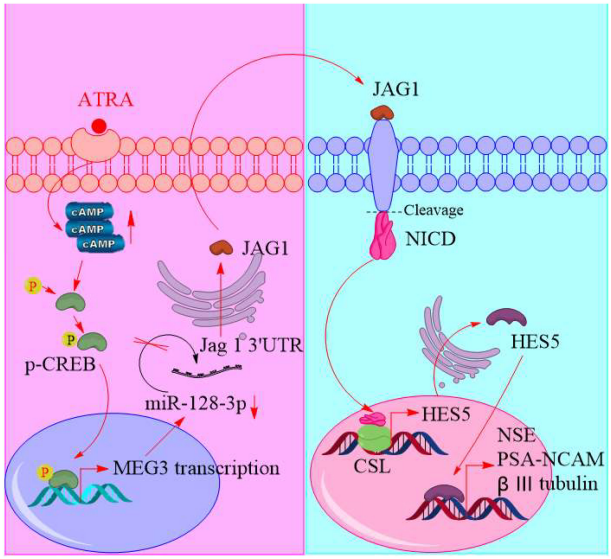

FIGURE 8 | Schematic of promoting neurogenic differentiation from human amniotic epithelial cells.

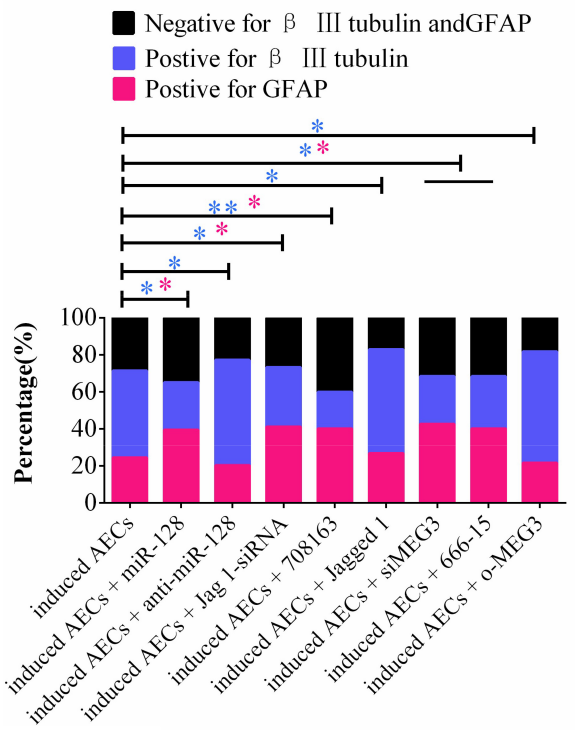

FIGURE 7 | Statistical analysis of FCM data in miR-128-3p and its upstream or downstream genes affecting neurogenic differentiation. miR-128-3p reduces the amount of neurons and increases the amount of gliocytes by targeting JAG1 to prevent Notch pathway activation, which may enhance the transcription of neuron-specific markers. MEG3 increases the amount of neurons and reduces the amount of gliocytes via targeting miR-128-3p to activate the Notch pathway (*$P < 0.05$; **$P < 0.01$; blue asterisk: neurons; pink asterisk: gliocyte).

In our research, the Notch pathway was activated after RA treatment during neurogenic differentiation. The Notch pathway plays a critical role in many developmental processes, including proliferation, differentiation, and apoptosis. It has four classic transmembrane receptors (notch 1, notch 2, notch 3, and notch 4) that interact with specific ligands (Jagged 1 and Jagged 2) to influence cell fate. Intercellular notch receptors are cleaved by the γ-secretase complex when these ligands have interacted with a notch receptor. The NICD is cleaved several times and then trafficked into the nucleus where it interacts with special transcription factors (HES, HEY, and HERP) to increase the expression of downstream target genes. The Notch pathway is activated after RA treatment during stem cell differentiation (Osathanon et al., 2017; Kong et al., 2018), and our data reveal dramatically increased NICD and HES5 expression levels after ATRA treatment, which promote the expression of neuron-specific genes in neurogenic differentiation from AECs.

miR-128 is a brain-enriched miRNA that has been reported to participate in the regulation of neural cell differentiation and to protect neurons after FTY720 treatment. In our research in induced AECs, we found that the overexpression of miR-128 reduced neuron differentiation and increased the number of gliocytes. Gliocytes have the capacity to nourish and protect neurons *in vitro* and *in vivo*; therefore, miR-128-3p protects neurons under drug treatment by increasing the number of gliocytes. However, the molecular mechanisms involved in the low expression of miR-128-3p in our neurogenic differentiation experiments remain unclear.

Competing endogenous RNAs regulate other RNA transcripts by competing for shared miRNAs (Das et al., 2019), and lncRNAs have various biological functions including the silencing of miRNAs (Ji et al., 2018). The lncRNA MEG3 is important for growth and development and is a tumor suppressor with roles that activate p53 and prevent cell proliferation. Previous studies have found that MEG3 promoter activity is mainly attributable to a CRE site and demonstrated that proteins from the CREB family directly bind to this site. Additionally, elevated cAMP levels were reported to stimulate transcription from the MEG3 promoter and enhance MEG3 expression (Zhao et al., 2006; Zhu et al., 2019). Another study found that ATRA enhanced intracellular cAMP accumulation and CREB phosphorylation (Suwa et al., 2016). In the present study, we showed that as the concentration of intracellular cAMP accumulates, and nuclear CREB concentrations also increase after ATRA treatment in AECs. These data imply that the molecular pathway of elevated MEG3 expression involves an ATRA/cAMP/CREB/MEG3 axis. We also demonstrated the interaction between MEG3 and miR-128-3p, which is largely in agreement with other previously reported work (Lan et al., 2018). Thus, MEG3 appears to modulate the percentage of neurons versus gliocytes in neurogenic differentiation from AECs through activation of the Notch pathway to increase the expression of neuron-specific genes.

Figure 8 shows a schematic of our predicted model of this process, in which intracellular concentrations of cAMP are dramatically elevated after ATRA treatment, causing CREB phosphorylation. Phosphorylated CREB enters the nucleus to enhance lncRNA MEG3 transcription, which, as a ceRNA, interacts with miR-128-3p. JAG1 is the canonical ligand to activate the Notch pathway and is inhibited by miR-128-3p binding its 3′-UTR. JAG1 translation is therefore increased after ATRA treatment through MEG3 competitively interacting with miR-128-3p. The NICD is cleaved from the cytomembrane, translocates into the nucleus, and associates with the CSL to activate HES members, which enhances neuronal gene transcription.

CONCLUSION

In this study, we elucidated the molecular pathway involved in ATRA-induced neurogenic differentiation from AECs. ATRA induction enhances the transcription of β III-tubulin, NSE, and PSA-NCAM neuron-specific genes via activation of the Notch signaling pathway. Additionally, the lncRNA MEG3, a key negative regulator of miR-128-3p, is up-regulated intracellularly by the cAMP/CREB pathway. In turn, this process directly down-regulates miR-128-3p through ceRNAs, which up-regulates JAG1 expression, the target of miR-128-3p, and activates the Notch signaling pathway. Our study, which particularly focuses on the involvement of miR-128-3p in neuron differentiation from AECs, may assist in the future development of effective cell transplant therapies for the treatment of neurodegenerative disease.

DATA AVAILABILITY STATEMENT

The raw data supporting the conclusions of this article will be made available by the authors, without undue reservation, to any qualified researcher.

ETHICS STATEMENT

The animal study was reviewed and approved by the Ethics Committee of Jining Medical University (2017-JZ-003).

AUTHOR CONTRIBUTIONS

YG performed the cell differentiation, Western blotting, and FCM, and drafted the manuscript. SD, XZ, and RZ cultured the cells. CB performed the RNAi, cultured the cells, and reviewed the manuscript. XL analyzed the data and reviewed the manuscript. WY and GW participated in its design and coordination.

FUNDING

This research was supported by the National Natural Science Foundation of China (Grant No. 81801463 to YG, Grant Nos. 31972755 and 81700685 to CB, and Grant No. 31672404 to XL), the Shandong Provincial Natural Science Foundation, China (ZR2017BH105 to YG and ZR2017BH002 to CB), the Project of Shandong Province Higher Educational Science and Technology Program (J17KA229 to YG), the Project of Shandong Province Higher Educational Youth Innovation Science and Technology Program (2019KJK010), the Supporting Fund for Teachers' Research of Jining Medical University (JY2017KJ027), and the Faculty Start-up Funds of Jining Medical University (to CB and YG).

SUPPLEMENTARY MATERIAL

The Supplementary Material for this article can be found online at: https://www.frontiersin.org/articles/10.3389/fcell.2019.00342/full#supplementary-material

REFERENCES

Bai, C., Zhang, H., Zhang, X., Yang, W., Li, X., and Gao, Y. (2019). MiR-15/16 mediate crosstalk between the MAPK and Wnt/beta-catenin pathways during hepatocyte differentiation from amniotic epithelial cells. *Biochim. Biophys. Acta Gene Regul. Mech.* 1862, 567–581. doi: 10.1016/j.bbagrm.2019.02.003

Bofill-De Ros, X., Yang, A., and Gu, S. (2019). IsomiRs: expanding the miRNA repression toolbox beyond the seed. *Biochim. Biophys. Acta Gene Regul. Mech.* doi: 10.1016/j.bbagrm.2019.03.005 [Epub ahead of print].

Das, A., Das, A., Das, D., Abdelmohsen, K., and Panda, A. C. (2019). Circular RNAs in myogenesis. *Biochim. Biophys. Acta Gene Regul. Mech.* doi: 10.1016/j.bbagrm.2019.02.011 [Epub ahead of print].

Davenport, C., Diekmann, U., Budde, I., Detering, N., and Naujok, O. (2016). Anterior-Posterior patterning of definitive endoderm generated from human embryonic stem cells depends on the differential signaling of retinoic acid. Wnt-, and BMP-Signaling. *Stem Cells* 34, 2635–2647. doi: 10.1002/stem.2428

Gao, Y., Bai, C., Zheng, D., Li, C., Zhang, W., Li, M., et al. (2016). Combination of melatonin and Wnt-4 promotes neural cell differentiation in bovine amniotic epithelial cells and recovery from spinal cord injury. *J. Pineal Res.* 60, 303–312. doi: 10.1111/jpi.12311

Ji, E., Kim, C., Kim, W., and Lee, E. K. (2018). Role of long non-coding RNAs in metabolic control. *Biochim. Biophys. Acta Gene Regul. Mech.* doi: 10.1016/j.bbagrm.2018.12.006 [Epub ahead of print].

Khan, A., Fornes, O., Stigliani, A., Gheorghe, M., Castro-Mondragon, J. A., Van Der Lee, R., et al. (2018). JASPAR 2018: update of the open-access database of transcription factor binding profiles and its web framework. *Nucleic Acids Res.* 46, D260–D266.

Kong, H. J., Ryu, J. H., Kim, J., Kim, J. W., Seong, B., Whang, I., et al. (2018). Generation of motor neurons requires spatiotemporal coordination between retinoic acid and Mib-mediated Notch signaling. *Anim. Cells Syst.* 22, 76–81. doi: 10.1080/19768354.2018.1443494

Lan, Y., Li, Y. J., Li, D. J., Li, P., Wang, J. Y., Diao, Y. P., et al. (2018). Long non-coding RNA MEG3 prevents vascular endothelial cell senescence by impairing miR-128-dependent Girdin down-regulation. *Am. J. Physiol. Cell Physiol.* 316, C830–C843.

Mark, M., Teletin, M., Vernet, N., and Ghyselinck, N. B. (2015). Role of retinoic acid receptor (RAR) signaling in post-natal male germ cell differentiation. *Biochim. Biophys. Acta* 1849, 84–93. doi: 10.1016/j.bbagrm.2014.05.019

Osathanon, T., Manokawinchoke, J., Egusa, H., and Pavasant, P. (2017). Notch signaling partly regulates the osteogenic differentiation of retinoic acid-treated murine induced pluripotent stem cells. *J. Oral Sci.* 59, 405–413. doi: 10.2334/josnusd.16-0552

Samarut, E., Fraher, D., Laudet, V., and Gibert, Y. (2015). ZebRA: an overview of retinoic acid signaling during zebrafish development. *Biochim. Biophys. Acta* 1849, 73–83. doi: 10.1016/j.bbagrm.2014.05.030

Suwa, H., Kishi, H., Imai, F., Nakao, K., Hirakawa, T., and Minegishi, T. (2016). Retinoic acid enhances progesterone production via the cAMP/PKA signaling pathway in immature rat granulosa cells. *Biochem. Biophys. Rep.* 8, 62–67. doi: 10.1016/j.bbrep.2016.08.013

Vargas-Medrano, J., Yang, B., Garza, N. T., Segura-Ulate, I., and Perez, R. G. (2019). Up-regulation of protective neuronal MicroRNAs by FTY720 and novel FTY720-derivatives. *Neurosci. Lett.* 690, 178–180. doi: 10.1016/j.neulet.2018.10.040

Volvert, M. L., Rogister, F., Moonen, G., Malgrange, B., and Nguyen, L. (2012). MicroRNAs tune cerebral cortical neurogenesis. *Cell Death Differ.* 19, 1573–1581. doi: 10.1038/cdd.2012.96

Xavier-Neto, J., Sousa Costa, A. M., Figueira, A. C., Caiaffa, C. D., Amaral, F. N., Peres, L. M., et al. (2015). Signaling through retinoic acid receptors in cardiac development: doing the right things at the right times. *Biochim. Biophys. Acta* 1849, 94–111. doi: 10.1016/j.bbagrm.2014.08.003

Yi, D. Y., Su, Q., Zhang, F. C., Fu, P., Zhang, Q., Cen, Y. C., et al. (2018). Effect of microRNA-128 on cisplatin resistance of glioma SHG-44 cells by targeting JAG1. *J. Cell. Biochem.* 119, 3162–3173. doi: 10.1002/jcb.26469

Zhang, B., Zhang, P., Tan, Y., Feng, P., Zhang, Z., Liang, H., et al. (2019). C1q-TNF-related protein-3 attenuates pressure overload-induced cardiac hypertrophy by suppressing the p38/CREB pathway and p38-induced ER stress. *Cell Death Dis.* 10:520. doi: 10.1038/s41419-019-1749-0

Zhang, W., Kim, P. J., Chen, Z., Lokman, H., Qiu, L., Zhang, K., et al. (2016). MiRNA-128 regulates the proliferation and neurogenesis of neural precursors by targeting PCM1 in the developing cortex. *eLife* 5:e11324. doi: 10.7554/eLife.11324

Zhang, W., Thevapriya, S., Kim, P. J., Yu, W. P., Je, H. S., Tan, E. K., et al. (2014). Amyloid precursor protein regulates neurogenesis by antagonizing miR-574-5p in the developing cerebral cortex. *Nat. Commun.* 5:3330. doi: 10.1038/ncomms4330

Zhao, J., Zhang, X., Zhou, Y., Ansell, P. J., and Klibanski, A. (2006). Cyclic AMP stimulates MEG3 gene expression in cells through a cAMP-response element (CRE) in the MEG3 proximal promoter region. *Int. J. Biochem. Cell Biol.* 38, 1808–1820. doi: 10.1016/j.biocel.2006.05.004

Zhao, Q., Tao, J., Zhu, Q., Jia, P. M., Dou, A. X., Li, X., et al. (2004). Rapid induction of cAMP/PKA pathway during retinoic acid-induced acute promyelocytic leukemia cell differentiation. *Leukemia* 18, 285–292. doi: 10.1038/sj.leu.2403226

Zhu, X., Li, H., Wu, Y., Zhou, J., Yang, G., Wang, W., et al. (2019). CREB-upregulated lncRNA MEG3 promotes hepatic gluconeogenesis by regulating miR-302a-3p-CRTC2 axis. *J. Cell. Biochem.* 120, 4192–4202. doi: 10.1002/jcb.27706

Conflict of Interest: The authors declare that the research was conducted in the absence of any commercial or financial relationships that could be construed as a potential conflict of interest.

frontiers in Genetics

ORIGINAL RESEARCH
published: 10 January 2020
doi: 10.3389/fgene.2019.01320

SHU00238 Promotes Colorectal Cancer Cell Apoptosis Through miR-4701-3p and miR-4793-3p

Haoyu Wang[1,2†], *Yurui Ma*[2†], *Yifan Lin*[1], *Rui Chen*[2], *Bin Xu*[1,3] *and Jiali Deng*[2*]

[1] Department of Chemistry, Qianweichang College, Shanghai University, Shanghai, China, [2] School of Life Science, Shanghai University, Shanghai, China, [3] Innovative Drug Research Center, Shanghai University, Shanghai, China

Colorectal cancer is one of the most leading causes of death. Searching for new therapeutic targets for colorectal cancer is urgently needed. SHU00238, an isoxazole derivative, was reported to suppress colorectal tumor growth through microRNAs. But the underlying mechanisms still remain unknown. Here, we explored the mechanism of SHU00238 on colorectal cancer by RT-PCR, CCK-8, flow cytometry, mirTarBase, and GO enrichment analysis. We screened partial microRNAs regulated by SHU00238 in colorectal cancer cells. Furthermore, we identified that miR-4701-3p and miR-4793-3p can reverse the acceleration of SHU00238 on colorectal cancer cell apoptosis in HCT116 Cells. Finally, we found that SMARCA5, MBD3, VPS53, EHD4 are estimated to mediate the regulation of miR-4701-3p and miR-4793-3p on colorectal cancer cell apoptosis, which targets ATP-dependent chromatin remodeling pathway and endocytic recycling pathway. Taken together, our study reveals that SHU00238 promotes colorectal cancer cell apoptosis through miR-4701-3p and miR-4793-3p, which provide a potential drug target and therapeutic strategy for colorectal cancer.

Keywords: SHU00238, colorectal cancer, miR-4701-3p, miR-4793-3p, target

OPEN ACCESS

Edited by:
Dragos Cretoiu, Carol Davila University of Medicine and Pharmacy, Romania

Reviewed by:
Daniel Pereira Bezerra, Oswaldo Cruz Foundation (Fiocruz), Brazil
Fei Wang, Tongji University, China
Xiaoming Hu, Shanghai Institutes for Biological Sciences (CAS), China

***Correspondence:**
Jiali Deng
dengjiali@shu.edu.cn

[†]*These authors have contributed equally to this work*

Specialty section:
This article was submitted to RNA, a section of the journal Frontiers in Genetics

Received: *15 October 2019*
Accepted: *04 December 2019*
Published: *10 January 2020*

Citation:
Wang H, Ma Y, Lin Y, Chen R, Xu B and Deng J (2020) SHU00238 Promotes Colorectal Cancer Cell Apoptosis Through miR-4701-3p and miR-4793-3p. Front. Genet. 10:1320. doi: 10.3389/fgene.2019.01320

INTRODUCTION

Colorectal cancer (CRC) is one of the most common malignant tumors that endanger human health. According to the latest statistics, the incidence of CRC ranks third among malignant tumors worldwide and the mortality rate ranks second. It is estimated to be more than 1.8 million new cases and 881,000 deaths in 2018 (Saus et al., 2016; Bray et al., 2018). However, the pathogenesis of CRC is not clear and the prognosis is poor. At present, the treatment of CRC mainly uses surgery, radiotherapy, chemotherapy, exercises, and chemical synthetic antineoplastic drugs (Nilsson et al., 2013; Kuipers et al., 2015; Mach and Fuster-Botella, 2017; Batacan et al., 2018). However, most of the patients had been diagnosed in the middle and late stages and were insensitive to radiotherapy (Hosseinimehr et al., 2019), and new antineoplastic drugs are expensive and have some side effects (Baker et al., 2000). Therefore, searching for highly effective and low toxic antineoplastic drugs is the focus of current treatment for CRC.

SHU00238 is an isoxazole derivative, which was reported to suppress colorectal tumor growth through microRNAs (Wang et al., 2019). But the underlying mechanisms still remain unknown. MicroRNAs are noncoding single strand RNAs (Zhou et al., 2019), encoded by endogenous genes

with a length of about 18–25 nucleotides (Wang et al., 2018), which play a vital role in the inhibition of posttranscriptional translation of mRNAs (Ambros, 2004; Bartel, 2004). Two microRNAs from the opposite side of the pre-microRNA name -3p or -5p (Voinnet, 2009). In recent years, studies have discovered that microRNAs play an essential role in the pathogenesis of CRC. Dysregulated patterns of expression of microRNAs such as miR-320a and miR-21 are associated with CRC cell proliferation and migration (Sun et al., 2012; Xiong et al., 2013), while miR-34a and miR-365 are implicated in the control of CRC cell apoptosis (Yamakuchi et al., 2008; Nie et al., 2012; Liu et al., 2019). These microRNAs have been reported to regulate target genes and contribute to CRC.

In this present study, we first screened partial microRNAs regulated by SHU00238 in CRC cells. Furthermore, we identified that miR-4701-3p and miR-4793-3p can reverse the acceleration of SHU00238 on CRC cell apoptosis in HCT116 Cells by CCK-8 and flow cytometry. Finally, we used miRNA target prediction algorithms and GO enrichment analysis and revealed that SMARCA5, MBD3, VPS53, and EHD4 are estimated to mediate the regulation of miR-4701-3p and miR-4793-3p on CRC cell apoptosis, which targets ATP-dependent chromatin remodeling pathway and endocytic recycling pathway. Taken together, our study reveals that SHU00238 promotes CRC cell apoptosis through miR-4701-3p and miR-4793-3p, which provide a potential drug target and therapeutic strategy for CRC.

MATERIALS AND METHODS

Cell Culture

Human CRC cell HCT116 was purchased from Chinese Academy of Sciences (CAS) Cell Bank (Shanghai, China). Cells were cultured in Dulbecco's modified Eagle medium (DMEM, Corning, NY, USA) supplemented with 10% fetal bovine serum (FBS, CellMax, Shanghai, China) and 1% penicillin-streptomycin (PS, Thermo Scientific, MA, USA) at 37°C in a 5% CO2 atmosphere.

Transfection and Treatment

HCT116 cells were transfected with microRNAs mimics (50 nM; RiboBio, Guangzhou, China), inhibitors (75 nM; RiboBio, Guangzhou, China), or negative control for 8 h using Lipofectamine 2000 (Invitrogen, CA, USA) as manufacturer's instructions, followed by SHU00238 (0.3 μM) or DMSO treatment for 48 h. The microRNAs mimics, inhibitors and negative control were purchased from RiboBio (Guangzhou, China).

Cell Viability Assay

Cell viability was detected with cell counting kit-8 (CCK-8, Bioworld, Shanghai, China). HCT116 cells were seeded in 96-well culture plate at 2 × 104 cells/well and treated as indicated. Cells were incubated with CCK-8 at 37°C for 1 h. The optical density was measured at 450 nm by microplate reader (Bio-Rad, CA, USA).

Cell Apoptosis Assay

Annexin V-FITC Apoptosis Detection Kit (Beyotime, Shanghai, China) was used to measure the apoptosis level of HCT116 cells treated as indicated. Cells were stained with Annexin V and PI according to the instructions and then analyzed by flow cytometry (Beckman, CA, USA).

Real-Time PCR

RNA isolation and relative quantification RT-PCR were performed as described previously (Xiao et al., 2017; Deng et al., 2019). The microRNAs primers were purchased from RiboBio (Guangzhou, China).

Analysis of miRNA Target Genes and Possible Downstream Signaling Pathway

The downstream target genes of a miRNA were screened using the miRTarBase website (http://mirtarbase.mbc.nctu.edu.tw/php/index.php), and the common downstream target genes of miRNAs were obtained by comparison. DAVID website (https://david.ncifcrf.gov/home.jsp) was used for GO ONTOLOGY and PATHWAY analysis to screen metabolic pathways and gene products significant affected by common target genes.

Statistical Analysis

All data were presented as mean ± SEM from three independent experiments. All statistical analyses were performed through IBM SPSS Statistics 20 (Armonk, NY, USA). Comparison of quantitative data was performed using an independent-samples t-test or one-way ANOVA test followed by Bonferroni's *post hoc* test. P Values < 0.05 were considered statistically significant.

RESULTS

SHU00238 Regulates Partial miRNAs in CRC Cells

Preliminary data showed that SHU00238 could regulate a set of miRNAs (Wang et al., 2019). Here, we examined the mRNA level of these miRNAs in HCT116 cells treated with SHU00238 or DMSO. As shown in **Figure 1**, miR-181d-5p, miR-9-3p, miR-30e-3p, mir-550a-3p, and miR-1304-5p are upregulated, while miR-4701-3p and miR-4793-3p are downregulated by SHU00238.

MiR-4701-3p and MiR-4793-3p Reverse the Acceleration of SHU00238 on CRC Cell Apoptosis in HCT116 Cells

To investigate the downstream of SHU00238 on CRC cell apoptosis, we examined the reverse ability of miR-181d-5p, miR-9-3p, miR-30e-3p, mir-550a-3p, miR-1304-5p, miR-4701-3p, and miR-4793-3p in HCT116 cells treated with SHU00238 with CCK-8 assay. The results showed that miR-181d-5p, miR-9-3p, miR-30e-3p, mir-550a-3p, and miR-1304-5p cannot reverse the inhibition of SHU00238 on HCT116 cell viability (**Figure 2A**), while miR-4701-3p and miR-4793-3p reverse the inhibition of SHU00238 on HCT116 cell viability (**Figure 2B**).

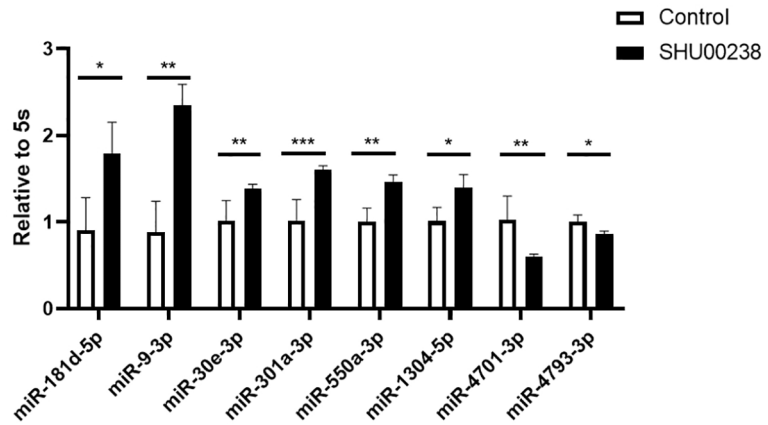

FIGURE 1 | SHU00238 regulates partial miRNAs in colorectal cancer cells. All values were the average of at least three biological replicates, and the data shown are mean ± SEM. *P < 0.05, **P < 0.01, ***P < 0.001.

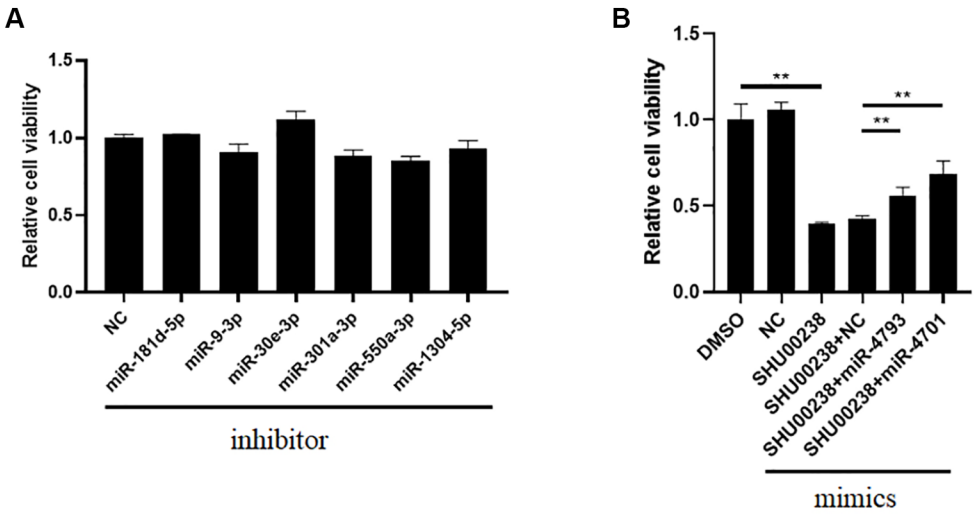

FIGURE 2 | MiR-4701-3p and miR-4793-3p reverse the inhibition of SHU00238 on HCT116 cell viability. **(A)** Cell viability analysis of HT116 cells transfected with miR-181d-5p, miR-9-3p, miR-30e-3p, mir-550a-3p, miR-1304-5p inhibitors or NC, followed by SHU00238 treatment, was analyzed by CCK-8 kit. **(B)** Cell viability analysis of HT116 cells transfected with miR-4701-3p and miR-4793-3p mimics or NC, followed by SHU00238 treatment, was analyzed by CCK-8 assay. All values were the average of at least three biological replicates, and the data shown are mean ± SEM. **P < 0.01 relative to the control.

Furthermore, we detected the cell apoptosis and necrosis by Annexin V and PI staining, we found that miR-4701-3p and miR-4793-3p` reverse the acceleration of SHU00238 on CRC cell apoptosis in HCT116 Cells (**Figure 3**).

SMARCA5, MBD3, VPS53, EHD4 Are Estimated to Mediate the Regulation of miR-4701-3p and miR-4793-3p on CRC Cell Apoptosis

To investigate the underlying mechanism of miR-4701-3p and miR-4793-3p on CRC cell apoptosis, we screened 62 common targets of miR-4701-3p and miR-4793-3p through mirTarBase including SMARCA5, MBD3, VPS53, EHD4, and so on. GO enrichment analysis revealed that ATP-dependent chromatin remodeling pathway and endocytic recycling pathway were significantly changed by the targets of miR-4701-3p or miR-4793-3p. SMARCA5 and MBD3 are associated with ATP-dependent chromatin remodeling (Aydin et al., 2014; Biswas et al., 2019), VPS53 and EHD4 are related to endocytic recycling (George et al., 2011; Feinstein et al., 2014) (**Figure 4**). Overall, our study demonstrates that SHU00238 promotes CRC cell apoptosis through miR-4701-3p and miR-4793-3p.

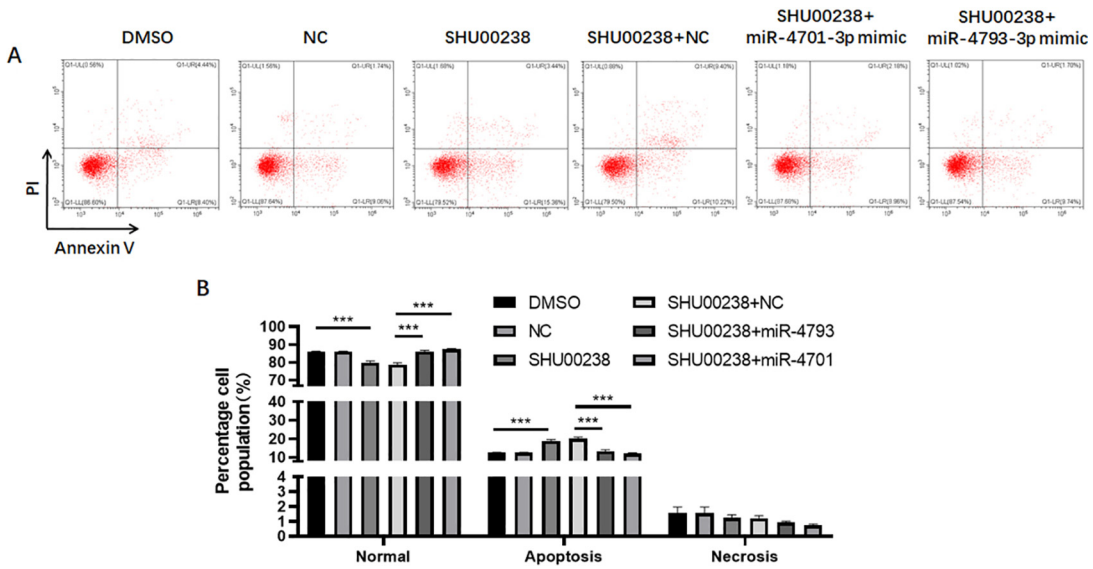

FIGURE 3 | MiR-4701-3p and miR-4793-3p reverse the acceleration of SHU00238 on colorectal cancer cell apoptosis in HCT116 Cells. **(A)** Apoptosis level of HCT116 cells transfected with miR-4701-3p and miR-4793-3p mimics or NC, followed by SHU00238 treatment, was measured by Annexin V-FITC Apoptosis Detection Kit. **(B)** The Statistical results of apoptosis and necrosis analysis of HCT116 cells transfected with miR-4701-3p and miR-4793-3p mimics or NC, followed by SHU00238 treatment. All values were the average of at least three biological replicates, and the data shown are mean ± SEM. ***P < 0.001 relative to the control.

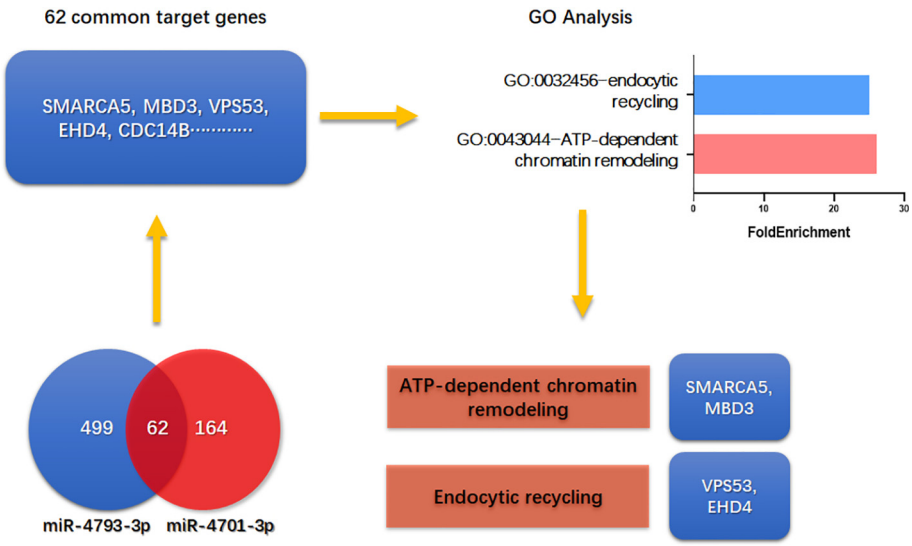

FIGURE 4 | SMARCA5, MBD3, VPS53, and EHD4 are estimated to mediate the regulation of miR-4701-3p and miR-4793-3p on colorectal cancer cell apoptosis.

DISCUSSION

Isoxazole derivatives play important roles in antitumor (Jensen et al., 2008; Zhu et al., 2018). Our previous data showed SHU00238, an isoxazole derivative, suppresses colorectal tumor growth through microRNAs (Wang et al., 2019). In this study, we screened partial microRNAs regulated by SHU00238 in CRC cells. Further analysis showed that miR-4701-3p and miR-4793-3p can reverse the acceleration of SHU00238 on CRC cell apoptosis in HCT116 Cells.

Taken together, our study reveals that SHU00238 promotes CRC cell apoptosis through miR-4701-3p and miR-4793-3p, which provide a potential drug target and therapeutic strategy for CRC. However, extensive studies are needed to explore the participation of miR-4701-3p and miR-4793-3p in the regulation of SHU00238 on CRC tumor in animals and human (Liang et al., 2017).

MiR-4701-3p, derived from exosomes, was shown to influence clopidogrel-induced liver injury, platelet reactivity, and drug-induced toxicity (Freitas et al., 2016; de Freitas et al., 2017). MiR-4701-3p was downregulated in patients with high risk of cadiovascular disease. BTNL3 and CFD mRNAs are regulated by miR-4701-3p. BTNL3 is involved in proliferation, development, inflammation, and immune response. CFD has a role in coronary heart disease. (Freitas et al., 2016). But miR-4701-3p has not been identified in cancer especially in CRC. The research showed that miR-4793-3p might be associated with angiogenesis, arginine metabolism, cell adhesion and chemotaxis, extracellular matrix remodeling, hypoxia/oxidative stress, inflammation, and muscle contraction (Ng et al., 2015). MiR-4793-3p is significantly increased in small bowel tissues of necrotizing enterocolitis compared with control tissues. TLR4 is a target of miR-4793-3p. Recent study identified miR-4793-3p was differently express in hepatocellular carcinoma (Pascut et al., 2019). More and more research showed that abundant microRNAs play a vital role in CRC. For example, miR-375 inhibits CRC cell proliferation mainly through targeting both JAK2/STAT3 and MAP3K8/ERK signaling pathways (Wei et al., 2017), miR-30a regulates cell proliferation and tumor growth of CRC by targeting CD73 (Xie et al., 2017), miR-374b regulates CRC cell apoptosis (Gong et al., 2017). But the role of miR-4701-3p and miR-4793-3p which we identified in this study in CRC cell proliferation and apoptosis remains unknown.

In addition, miRNA target prediction algorithms and GO enrichment analysis revealed that SMARCA5, MBD3, VPS53, and EHD4 may mediate the regulation of miR-4701-3p and miR-4793-3p on CRC cell apoptosis, which targets ATP-dependent chromatin remodeling pathway and endocytic recycling pathway. Gut-specific conditional deletion of mbd3 mice showed a large increase in proliferating cells in the colon after DSS treatment compared to control animals, markedly increased susceptibility to colitis-induced tumorigenesis *via* c-Jun-MBD5/NuRD-AP-1 signaling. Recent study showed that MBD3 is a target of miR-8073, which is reported to be a colorectal tumor suppressor (Mizoguchi et al., 2018). There are no report about the role of SMARCA5, VPS53, and EHD4 in CRC. Further studies are needed to explore whether SMARCA5, MBD3, VPS53, EHD4 mediate miR-4701-3p, and miR-4793-3p's function *in vivo* and *in vitro* (Jiao et al., 2017).

Chromatin remodeling means position or composition of a nucleosome is altered in the chromatin, including ATP-dependent and ATP-independent pathway. ATP-dependent chromatin remodeling pathway constitutes the majority of the remodeling activity (Mayes et al., 2014). The important member of ATP-dependent chromatin remodeling pathway is SWI/SNF, which contains a Swi2/Snf2 ATPase subunit (Osley et al., 2007). ATP-dependent chromatin remodeling pathway participates in DNA damage repair (van Attikum and Gasser, 2005), coronary development (Huang et al., 2008), pancreatic neuroendocrine tumors (Clynes et al., 2013), epithelioid sarcomas (Kohashi and Oda, 2017). But the participation of ATP-dependent chromatin remodeling pathway in CRC remains unknown. Cells transport extracellular materials into cells by endocytosis. The endocytic recycling pathway returns most of the protein and lipids to the plasma membrane. The balance between endocytosis and recycling controls the composition of plasma membrane and participates in many processes (Grant and Donaldson, 2009). These recycling pathways are essential for maintaining the proper composition of various organelles and for returning essential molecules that carry out specific functions to the appropriate compartments (Maxfield and McGraw, 2004). Endocytic recycling pathway plays roles in cell adhesion, morphogenesis, cell fusion, learning, and memory (Grant and Donaldson, 2009), autophagy (Nixon, 2013), nutrient absorption, immune response (Lin and Shi, 2019), CRC metastasis (Huang et al., 2019). Further studies are needed to explore whether endocytic recycling pathway mediate CRC cell proliferation and apoptosis.

In summary, we identified miR-4701-3p and miR-4793-3p mediate SHU00238's effect on CRC cell apoptosis, which open a new approach for CRC.

DATA AVAILABILITY STATEMENT

The data for this study are available by contacting the corresponding author.

AUTHOR CONTRIBUTIONS

HW and YM carried out the experiments. YL, RC, and BX contributed to the helpful discussion. JD directed the project, wrote and edited the manuscript. All authors read and approved the manuscript.

FUNDING

This work was supported by the National Natural Science Foundation of China [81700761 to JD], China Postdoctoral Science Foundation [2016M601664 to JD], and Innovation Program of Shanghai Municipal Education Commission (No. 2019-01-07-00-09-E00008 to BX).

REFERENCES

Ambros, V. (2004). The functions of animal microRNAs. *Nature* 431 (7006), 350–355. doi: 10.1038/nature02871

Aydin, O. Z., Marteijn, J. A., Ribeiro-Silva, C., Rodriguez Lopez, A., Wijgers, N., Smeenk, G., et al. (2014). Human ISWI complexes are targeted by SMARCA5 ATPase and SLIDE domains to help resolve lesion-stalled transcription. *Nucleic Acids Res.* 42 (13), 8473–8485. doi: 10.1093/nar/gku565

Baker, S. D., Diasio, R. B., O'Reilly, S., Lucas, V. S., Khor, S. P., Sartorius, S. E., et al. (2000). Phase I and pharmacologic study of oral fluorouracil on a chronic daily schedule in combination with the dihydropyrimidine dehydrogenase inactivator eniluracil. *J. Clin. Oncol.* 18 (4), 915–926. doi: 10.1200/JCO.2000.18.4.915

Bartel, D. P. (2004). MicroRNAs: genomics, biogenesis, mechanism, and function. *Cell* 116 (2), 281–297. doi: 10.1016/s0092-8674(04)00045-5

Batacan, R. B.Jr., Duncan, M. J., Dalbo, V. J., Buitrago, G. L., and Fenning, A. S. (2018). Effect of different intensities of physical activity on cardiometabolic

markers and vascular and cardiac function in adult rats fed with a high-fat high-carbohydrate diet. *J. Sport Health Sci.* 7 (1), 109–119. doi: 10.1016/j.jshs.2016.08.001

Biswas, M., Chatterjee, S. S., Boila, L. D., Chakraborty, S., Banerjee, D., and Sengupta, A. (2019). MBD3/NuRD loss participates with KDM6A program to promote DOCK5/8 expression and Rac GTPase activation in human acute myeloid leukemia. *FASEB J.* 33 (4), 5268–5286. doi: 10.1096/fj.201801035R

Bray, F., Ferlay, J., Soerjomataram, I., Siegel, R. L., Torre, L. A., and Jemal, A. (2018). Global cancer statistics 2018: GLOBOCAN estimates of incidence and mortality worldwide for 36 cancers in 185 countries. *CA Cancer J. Clin.* 68 (6), 394–424. doi: 10.3322/caac.21492

Clynes, D., Higgs, D. R., and Gibbons, R. J. (2013). The chromatin remodeller ATRX: a repeat offender in human disease. *Trends Biochem. Sci.* 38 (9), 461–466. doi: 10.1016/j.tibs.2013.06.011

de Freitas, R. C. C., Bortolin, R. H., Lopes, M. B., Tamborlin, L., Meneguello, L., Silbiger, V. N., et al. (2017). Modulation of miR-26a-5p and miR-15b-5p exosomal expression associated with clopidogrel-induced hepatotoxicity in HepG2 cells. *Front. Pharmacol.* 8, 906. doi: 10.3389/fphar.2017.00906

Deng, J., Guo, Y., Yuan, F., Chen, S., Yin, H., Jiang, X., et al. (2019). Autophagy inhibition prevents glucocorticoid-increased adiposity *via* suppressing BAT whitening. *Autophagy*, 1–15. doi: 10.1080/15548627.2019.1628537

Feinstein, M., Flusser, H., Lerman-Sagie, T., Ben-Zeev, B., Lev, D., Agamy, O., et al. (2014). VPS53 mutations cause progressive cerebello-cerebral atrophy type 2 (PCCA2). *J. Med. Genet.* 51 (5), 303–308. doi: 10.1136/jmedgenet-2013-101823

Freitas, R. C. C., Bortolin, R. H., Lopes, M. B., Hirata, M. H., Hirata, R. D. C., Silbiger, V. N., et al. (2016). Integrated analysis of miRNA and mRNA gene expression microarrays: Influence on platelet reactivity, clopidogrel response and drug-induced toxicity. *Gene* 593 (1), 172–178. doi: 10.1016/j.gene.2016.08.028

George, M., Rainey, M. A., Naramura, M., Foster, K. W., Holzapfel, M. S., Willoughby, L. L., et al. (2011). Renal thrombotic microangiopathy in mice with combined deletion of endocytic recycling regulators EHD3 and EHD4. *PloS One* 6 (3), e17838. doi: 10.1371/journal.pone.0017838

Gong, H., Cao, Y., Han, G., Zhang, Y., You, Q., Wang, Y., et al. (2017). p53/microRNA-374b/AKT1 regulates colorectal cancer cell apoptosis in response to DNA damage. *Int. J. Oncol.* 50 (5), 1785–1791. doi: 10.3892/ijo.2017.3922

Grant, B. D., and Donaldson, J. G. (2009). Pathways and mechanisms of endocytic recycling. *Nat. Rev. Mol. Cell Biol.* 10 (9), 597–608. doi: 10.1038/nrm2755

Hosseinimehr, S. J., Safavi, Z., Kangarani Farahani, S., Noaparst, Z., Ghasemi, A., and Asgarian-Omran, H. (2019). The synergistic effect of mefenamic acid with ionizing radiation in colon cancer. *J. Bioenerg Biomembr* 51 (3), 249–257. doi: 10.1007/s10863-019-09792-w

Huang, X., Gao, X., Diaz-Trelles, R., Ruiz-Lozano, P., and Wang, Z. (2008). Coronary development is regulated by ATP-dependent SWI/SNF chromatin remodeling component BAF180. *Dev. Biol.* 319 (2), 258–266. doi: 10.1016/j.ydbio.2008.04.020

Huang, X., Ye, Q., Chen, M., Li, A., Mi, W., Fang, Y., et al. (2019). N-glycosylation-defective splice variants of neuropilin-1 promote metastasis by activating endosomal signals. *Nat. Commun.* 10 (1), 3708. doi: 10.1038/s41467-019-11580-4

Jensen, M. R., Schoepfer, J., Radimerski, T., Massey, A., Guy, C. T., Brueggen, J., et al. (2008). NVP-AUY922: a small molecule HSP90 inhibitor with potent antitumor activity in preclinical breast cancer models. *Breast Cancer Res.* 10 (2), R33. doi: 10.1186/bcr1996

Jiao, G., Huang, Q., Hu, M., Liang, X., Li, F., Lan, C., et al. (2017). Therapeutic Suppression of miR-4261 Attenuates Colorectal Cancer by Targeting MCC. *Mol. Ther. Nucleic Acids* 8, 36–45. doi: 10.1016/j.omtn.2017.05.010

Kohashi, K., and Oda, Y. (2017). Oncogenic roles of SMARCB1/INI1 and its deficient tumors. *Cancer Sci.* 108 (4), 547–552. doi: 10.1111/cas.13173

Kuipers, E. J., Grady, W. M., Lieberman, D., Seufferlein, T., Sung, J. J., Boelens, P. G., et al. (2015). Colorectal cancer. *Nat. Rev. Dis. Primers* 1, 15065. doi: 10.1038/nrdp.2015.65

Liang, X., Lan, C., Jiao, G., Fu, W., Long, X., An, Y., et al. (2017). Therapeutic inhibition of SGK1 suppresses colorectal cancer. *Exp. Mol. Med.* 49 (11), e399. doi: 10.1038/emm.2017.184

Lin, L., and Shi, A. B. (2019). [Endocytic recycling pathways and the regulatory mechanisms]. *Yi Chuan* 41 (6), 451–468. doi: 10.16288/j.yczz.19-124

Liu, Y., Liu, Z., Xie, Y., Zhao, C., and Xu, J. (2019). Serum Extracellular Vesicles Retard H9C2 Cell Senescence by Suppressing miR-34a Expression. *J. Cardiovasc. Transl. Res.* 12 (1), 45–50. doi: 10.1007/s12265-018-9847-4

Mach, N., and Fuster-Botella, D. (2017). Endurance exercise and gut microbiota: A review. *J. Sport Health Sci.* 6 (2), 179–197. doi: 10.1016/j.jshs.2016.05.001

Maxfield, F. R., and McGraw, T. E. (2004). Endocytic recycling. *Nat. Rev. Mol. Cell Biol.* 5 (2), 121–132. doi: 10.1038/nrm1315

Mayes, K., Qiu, Z., Alhazmi, A., and Landry, J. W. (2014). ATP-dependent chromatin remodeling complexes as novel targets for cancer therapy. *Adv. Cancer Res.* 121, 183–233. doi: 10.1016/B978-0-12-800249-0.00005-6

Mizoguchi, A., Takayama, A., Arai, T., Kawauchi, J., and Sudo, H. (2018). MicroRNA-8073: Tumor suppressor and potential therapeutic treatment. *PloS One* 13 (12), e0209750. doi: 10.1371/journal.pone.0209750

Ng, P. C., Chan, K. Y., Leung, K. T., Tam, Y. H., Ma, T. P., Lam, H. S., et al. (2015). Comparative MiRNA expressional profiles and molecular networks in human small bowel tissues of necrotizing enterocolitis and spontaneous intestinal perforation. *PloS One* 10 (8), e0135737. doi: 10.1371/journal.pone.0135737

Nie, J., Liu, L., Zheng, W., Chen, L., Wu, X., Xu, Y., et al. (2012). microRNA-365, down-regulated in colon cancer, inhibits cell cycle progression and promotes apoptosis of colon cancer cells by probably targeting Cyclin D1 and Bcl-2. *Carcinogenesis* 33 (1), 220–225. doi: 10.1093/carcin/bgr245

Nilsson, P. J., van Etten, B., Hospers, G. A., Pahlman, L., van de Velde, C. J., Beets-Tan, R. G., et al. (2013). Short-course radiotherapy followed by neo-adjuvant chemotherapy in locally advanced rectal cancer–the RAPIDO trial. *BMC Cancer* 13, 279. doi: 10.1186/1471-2407-13-279

Nixon, R. A. (2013). The role of autophagy in neurodegenerative disease. *Nat. Med.* 19 (8), 983–997. doi: 10.1038/nm.3232

Osley, M. A., Tsukuda, T., and Nickoloff, J. A. (2007). ATP-dependent chromatin remodeling factors and DNA damage repair. *Mutat. Res.* 618 (1-2), 65–80. doi: 10.1016/j.mrfmmm.2006.07.011

Pascut, D., Cavalletto, L., Pratama, M. Y., Bresolin, S., Trentin, L., Basso, G., et al. (2019). Serum miRNA Are Promising Biomarkers for the Detection of Early Hepatocellular Carcinoma after Treatment with Direct-Acting Antivirals. *Cancers (Basel)* 11 (11), 1–16. doi: 10.3390/cancers11111773

Saus, E., Brunet-Vega, A., Iraola-Guzman, S., Pegueroles, C., Gabaldon, T., and Pericay, C. (2016). Long non-coding RNAs as potential novel prognostic biomarkers in colorectal cancer. *Front. Genet.* 7, 54. doi: 10.3389/fgene.2016.00054

Sun, J. Y., Huang, Y., Li, J. P., Zhang, X., Wang, L., Meng, Y. L., et al. (2012). MicroRNA-320a suppresses human colon cancer cell proliferation by directly targeting beta-catenin. *Biochem. Biophys. Res. Commun.* 420 (4), 787–792. doi: 10.1016/j.bbrc.2012.03.075

van Attikum, H., and Gasser, S. M. (2005). ATP-dependent chromatin remodeling and DNA double-strand break repair. *Cell Cycle* 4 (8), 1011–1014. doi: 10.4161/cc.4.8.1887

Voinnet, O. (2009). Origin, biogenesis, and activity of plant microRNAs. *Cell* 136 (4), 669–687. doi: 10.1016/j.cell.2009.01.046

Wang, L., Lv, Y., Li, G., and Xiao, J. (2018). MicroRNAs in heart and circulation during physical exercise. *J. Sport Health Sci.* 7 (4), 433–441. doi: 10.1016/j.jshs.2018.09.008

Wang, H., Ma, Y., Lin, Y., Liu, J., Chen, R., Xu, B., et al. (2019). An Isoxazole Derivative SHU00238 Suppresses Colorectal Cancer Growth through miRNAs Regulation. *Molecules* 24 (12), 1–10. doi: 10.3390/molecules24122335

Wei, R., Yang, Q., Han, B., Li, Y., Yao, K., Yang, X., et al. (2017). microRNA-375 inhibits colorectal cancer cells proliferation by downregulating JAK2/STAT3 and MAP3K8/ERK signaling pathways. *Oncotarget* 8 (10), 16633–16641. doi: 10.18632/oncotarget.15114

Xiao, J., Lv, D., Zhou, J., Bei, Y., Chen, T., Hu, M., et al. (2017). Therapeutic Inhibition of miR-4260 Suppresses Colorectal Cancer *via* Targeting MCC and SMAD4. *Theranostics* 7 (7), 1901–1913. doi: 10.7150/thno.19168

Xie, M., Qin, H., Luo, Q., Huang, Q., He, X., Yang, Z., et al. (2017). MicroRNA-30a regulates cell proliferation and tumor growth of colorectal cancer by targeting CD73. *BMC Cancer* 17 (1), 305. doi: 10.1186/s12885-017-3291-8

Xiong, B., Cheng, Y., Ma, L., and Zhang, C. (2013). MiR-21 regulates biological behavior through the PTEN/PI-3 K/Akt signaling pathway in human colorectal cancer cells. *Int. J. Oncol.* 42 (1), 219–228. doi: 10.3892/ijo.2012.1707

Yamakuchi, M., Ferlito, M., and Lowenstein, C. J. (2008). miR-34a repression of SIRT1 regulates apoptosis. *Proc. Natl. Acad. Sci. U. S. A.* 105 (36), 13421–13426. doi: 10.1073/pnas.0801613105

Zhou, S., Lei, D., Bu, F., Han, H., Zhao, S., and Wang, Y. (2019). MicroRNA-29b-3p Targets SPARC Gene to Protect Cardiocytes against Autophagy and Apoptosis in Hypoxic-Induced H9c2 Cells. *J. Cardiovasc. Transl. Res.* 12 (4), 358–365. doi: 10.1007/s12265-018-9858-1

Zhu, J., Mo, J., Lin, H. Z., Chen, Y., and Sun, H. P. (2018). The recent progress of isoxazole in medicinal chemistry. *Bioorg Med. Chem.* 26 (12), 3065–3075. doi: 10.1016/j.bmc.2018.05.013

Conflict of Interest: The authors declare that the research was conducted in the absence of any commercial or financial relationships that could be construed as a potential conflict of interest.

frontiers in Cell and Developmental Biology

ORIGINAL RESEARCH
published: 30 January 2020
doi: 10.3389/fcell.2020.00015

Agrin Influences Botulinum Neurotoxin A-Induced Nerve Sprouting via miR-144-agrin-MuSK Signaling

*Lin Ma[1,2], Lizhen Pan[2,3], Wuchao Liu[2,3], Ying Liu[3], Xuerui Xiang[3], Yougui Pan[3], Xiaolong Zhang[3] and Lingjing Jin[2,3]**

[1] Department of Interventional Radiology, Shanghai Tongji Hospital, Tongji University School of Medicine, Shanghai, China, [2] Neurotoxin Research Center, Tongji University School of Medicine, Key Laboratory of Spine and Spinal Cord Injury Repair and Regeneration, Ministry of Education of the People's Republic of China, Shanghai, China, [3] Department of Neurology, Shanghai Tongji Hospital, Tongji University School of Medicine, Shanghai, China

Botulinum neurotoxin (BoNT) has become a powerful therapeutic tool, and is extensively used in aesthetic medicine and in the treatment of neurological disorders. However, its duration of effect is limited, mainly owing to nerve sprouting. Inhibition of nerve sprouting to prolong the effective duration of BoNT is therefore of great clinical interest. However, appropriate interventional strategies to accomplish this are currently unavailable. In this study, we determined the role of the neurogenic regulator agrin in BoNT type A (BoNT/A)-induced nerve sprouting in a rat model. We then determined whether agrin could be used as an interventional target for prolonging the duration of effect of BoNT/A, and made a preliminary study of the upstream and downstream regulatory mechanisms by which agrin could influence the effective duration of BoNT/A. Our results showed that agrin was involved in the regulation of BoNT/A-induced nerve sprouting, and blocking of agrin function with anti-agrin antibody temporarily could delay muscle strength recovery and prolong the duration of BoNT/A effect. Moreover, agrin influenced the duration of BoNT/A effect by regulating downstream myogenic muscle-specific receptor tyrosine kinase (MuSK), and was simultaneously regulated by upstream miR-144. In conclusion, agrin could regulate BoNT/A-induced nerve sprouting through miR-144-agrin-MuSK signaling; it influences the effective duration of BoNT/A, and could find clinical application as an interventional target for prolonging the effect of BoNT/A.

Keywords: botulinum neurotoxin, nerve sprouting, agrin, muscle-specific receptor tyrosine kinase, microRNA

OPEN ACCESS

Edited by:
Junjie Xiao,
Shanghai University, China

Reviewed by:
Yu-Qiang Ding,
Fudan University Shanghai, China
Dongsheng Wang,
Lanzhou University, China

****Correspondence:***
Lingjing Jin
lingjingjin@hotmail.com

Specialty section:
This article was submitted to Signaling, a section of the journal Frontiers in Cell and Developmental Biology

Received: *03 November 2019*
Accepted: *10 January 2020*
Published: *30 January 2020*

Citation:
Ma L, Pan L, Liu W, Liu Y, Xiang X, Pan Y, Zhang X and Jin L (2020) Agrin Influences Botulinum Neurotoxin A-Induced Nerve Sprouting via miR-144-agrin-MuSK Signaling. Front. Cell Dev. Biol. 8:15. doi: 10.3389/fcell.2020.00015

INTRODUCTION

The highly toxic botulinum neurotoxin (BoNT) is produced by neurotoxic anaerobic and spore-forming strains of bacteria of the genus *Clostridium*. BoNT is extensively used in aesthetic medicine and treatment of conditions such as cervical dystonia, spasticity, cerebral palsy, chronic migraine, and Raynaud's syndrome (Krishnan, 2005; Chinnapongse et al., 2010; Foley et al., 2013; Grazzi and Usai, 2014; Zhang et al., 2015). Seven immunologically distinct BoNT serotypes (type A-G) have been reported, of which type A (BoNT/A) is the most widely used in clinical therapeutics.

BoNT/A selectively blocks the release of chemical transmitters at neuromuscular junctions (NMJs). However the blocking effect of BoNT/A gradually fades 3–4 months after application (Dolly and Aoki, 2006). Repeated injections are therefore usually required to maintain the therapeutic effect of BoNT/A. However, repetitive injection could cause immune responses and toxin resistance (Pellizzari et al., 1999). Thus, novel methods to prolong the duration of BoNT/A effect are of great clinical interest.

Nerve terminal sprouting triggered by BoNT/A is the main factor that limits the effective duration time of BoNT/A. Nerve sprouts continue chemical transmission and restore muscle contraction, and also restore original motor endplates by accelerating synaptic vesicle recycling (Juzans et al., 1996; Santafe et al., 2000). Therefore, inhibition of nerve sprouting could vastly improve the successful application of BoNT/A; however, it is also challenging—there are few effective interventional targets for prolonging the effect time of BoNT/A.

Agrin, a neuronal aggregating factor, is a 400–600 KD heparin sulfate glycoprotein molecule and a vital regulator of synaptic differentiation and maturation (Bezakova et al., 2001; Sanes and Lichtman, 2001; Ngo et al., 2007). Agrin is mainly synthesized by motor neurons and transported to nerve endings for release. Motor-neuron-derived agrin can activate MuSK by binding to the lipoprotein receptor related protein 4 (Lrp4), and induce the aggregation of acetylcholine receptors (AChRs) (Reist et al., 1992; Kim et al., 2008; Zong and Jin, 2013; Tezuka et al., 2014). However, there has been no research to determine whether agrin is involved in regulating BoNT/A-induced nerve sprouting. In the current study, we aimed to determine the effect of agrin on nerve sprouting induced by BoNT/A, and the interventional potential of agrin for prolonging the effect time of BoNT/A in decreasing muscle strength. Furthermore, we explored the mechanisms underlying the effects of agrin on the duration of BoNT/A effect.

MATERIALS AND METHODS

Animals and Injections

The animals used in this study were maintained in accordance with the Guide for the Care and Use of Laboratory Animals published by the US National Institution of Health (NIH Publication No 85-23, revised 1996) and the Policy of Animal Care and Use Committee of Tongji University. Male Sprague-Dawley rats (200–220 g) and rats at the 1st, 4th, and 8th week after birth were obtained from B&K Universal Group Limited (Shanghai, China). Adult rats were fed with chow and water *ad libitum* at the Animal Center of Tongji Hospital, and maintained under controlled temperature (20–22°C) and a 12 h light/dark cycle.

Adult rats were randomly divided into three groups: control group (n = 21), BoNT/A group (n = 21), and agrin-Ab groups. BoNT/A (BOTOX®, Allergan, Co. Mayo, Ireland) was reconstituted in saline (NS) to a final concentration of 2 U/100 μL. Animals of the BoNT/A and agrin-Ab groups were injected unilaterally with 100 μL BoNT/A in the right gastrocnemius muscle under anesthesia with an intraperitoneal injection of pentobarbital (30 mg/kg). On the 3rd day after BoNT/A injection, the each subgroups of agrin-Ab were injected with 100 μL agrin-Ab (R&D Systems, Minnesota, CA, United States) at a dosage of 0.6, 2, 6, 20, or 60 μg respectively at once. Controls received an equivalent volume of NS injections in the right gastrocnemius muscle.

Muscle Strength Determination

A survey system (CN102599921A) composed of a fixing device, sensing means, and data handling equipment was used to evaluate the muscle strength of the right hind limb of rat (Feng et al., 2017). Rats were lightly anesthetized with an intraperitoneal injection of pentobarbital (30 mg/kg) and secured on a special adjustable operating table invented by us (CN202036227U) on days 0 and 3, and after 1, 2, 4, 8, 10, and 12 weeks after BoNT/A injection. Stimulation (28 V over 0.4 ms) of the sciatic nerve led to contraction of the gastrocnemius and plantar flexion and rotation of a footboard, which was converted to electrical signals by a muscular tension energy transducer and recorded by the computer.

Western Blot Assay

Tissue from the right gastrocnemius muscles of rats of each group at each time point after injection, and the spinal cords of rats 1, 4, and 8 weeks after birth were collected and homogenized in cold radioimmunoprecipitation assay lysis buffer (Beyotime, China) with 1:100 volume PMSF. After centrifugation at 1000 × g for 5 min at 4°C, proteins were extracted and the concentrations were assayed in duplicate by using the BCA protein assay kit (Pierce, United States). Protein samples (20 μg/lane) were separated by SDS-PAGE and transferred onto Hybond-P polyvinylidene difluoride (PVDF) membranes (Millipore, United States). After blocking in 5% (w/v) BSA (Sigma, United States) and washing with tris-buffered saline with Tween-20 (TBST), the membranes were then incubated with antibodies against agrin (R&D Systems, Minnesota, CA, United States), anti-MuSK (Abcam, United States), and anti-GAPDH (Abcam, United States) at 4°C overnight. After incubating with IRDye800-conjugated secondary antibody (Rockland, Philadelphia, PA, United States) for 1 h at room temperature and washing with TBST, images were acquired and band density was analyzed using Odyssey Infrared Imaging System (LI-COR Biosciences, United States). GAPDH was used as a loading control.

RNA Isolation and Real-Time qRCR

Total RNA was extracted from the right gastrocnemius muscles of each group of rats at each time point after injection and spinal cords of rats 1, 4, and 8 weeks after birth by using Trizol reagent (Invitrogen, Carlsbad, CA, United States). The reaction mixture containing 1 μg RNA was reverse transcribed into cDNA by using the PrimeScript™RT reagent Kit (TaKaRa, Dalian, China). For miRNA expression analysis, the total RNA (1 μg) was polyadenylated with ATP and poly A polymerase (PAP) at 37°C for 1 h in a 20-μl reaction mixture following the manufacturer's protocol (Poly A Tailing Kit, Ambion, United States). After phenol-chloroform extraction and ethanol precipitation, the RNAs were reverse-transcribed using specific RT primers and PrimerScript Reverse Transcriptase (TaKaRa, Dalian, China).

Quantitative real-time PCR was performed using SYBR Premix Ex Taq^{TM} (TaKaRa, Dalian, China), with primers specific for AGRIN, MuSK, and miRNA-144 according to the manufacturer's protocol. Gene expression levels were calculated based on the comparative quantitative method ($\Delta\Delta C_T$ method) with GAPDH and 5S ribosome RNA as internal reference RNA. The primer sequences used were:

AGRIN: forward 5′-GGGAATGTTATGTGGCTTTGGTG-3′ reverse 5′-CATGAGGCAGTCTGTCCGTCAG-3′;

MuSK: forward 5′-GACACCCGCTACAGCATCCG-3′ reverse 5′-CACCGCTCCTCCCACTCCAT-3′;

GAPDH: forward 5′-GACAACTTTGGCATCGTGGA-3′ reverse 5′-ATGCAGGGATGATGTTCTGG-3′;

Rno-miR-144: forward 5′-TACAGTATAGATGATGTACTA-3′ reverse 5′ -GCTGTCAACGATACGCTACGTAACG-3′;

Rno-miR-27a: forward 5′-TTCACAGTGGCTAAGTTCCG C-3′ reverse 5′-GCTGTCAACGATACGCTACGTAACG-3′;

Rno-miR-29a: forward 5′-TAGCACCATCTGAAATCGGT TA-3′ reverse 5′-GCTGTCAACGATACGCTACGTAACG-3′;

5S ribosome RNA: forward 5′-GTCTACGGCCATACCCTGA AC-3′ reverse 5′-GCTGTCAACGATACGCTACGTAACG-3′.

Luciferase Assay

The 3′-UTR and mutant fragment of agrin and were subcloned into the Xbal restriction site downstream of the firefly luciferase gene of the pGL3-Basic Vector (Promega, United States) as pGL3-3′-UTR. The pRL-TK vector (Promega, United States) containing *Renilla* luciferase gene was used as an internal control reporter vector. The DNA sequences of pre-miR-144, pre-miR-27a, and pre-miR-29a were amplified by PCR and subcloned into pSuper-EGFP1 vector as pSuper-144, pSuper-27a, and pSuper-29a. At 24 h post-transfection of pSuper-miRNAs vector, the constructed luciferase reporter plasmids and the pRL-TK vectors were co-transfected into HEK293T cells at a ratio of 50:1. Luciferase activity was measured 24 h after transfection by using the dual luciferase reporter assay system (Promega, United States) according to the manufacturer's protocol. Firefly luciferase activity was normalized to *Renilla* luciferase activity.

α-Bungarotoxin Staining

Gastrocnemius muscle samples were harvested and fixed with 4% paraformaldehyde. Cross-sections from the fixed samples were rehydrated in PBS for 5 min at room temperature. The sections of 10 μm were blocked in immunofluorescence blocking buffer (Beyotime, China) for 30 min at room temperature and incubated with staining solution containing 1 μg/mL of α-bungarotoxin conjugated with tetramethylrhodamine (Biotium Inc., Fremont, CA, United States) in immunofluorescence blocking buffer at 4°C overnight. After rinsing three times, nuclei were counterstained with 4′,6-diamidino-2-phenylindole (DAPI). Nikon instruments were used to capture fluorescence pictures.

Statistical Analysis

All data were expressed as the mean ± standard deviation (SD). A one-way analysis of variance (ANOVA) was conducted to evaluate the data. Statistical significance was determined by Student's *t*-test. $P < 0.05$ was considered statistically significant.

RESULTS

Agrin Participates in Regulating BoNT/A-Induced Nerve Sprouting

To determine whether agrin is involved in regulating nerve sprouting induced by BoNT/A, we first studied agrin expression at NMJs 3 days and 1, 2, 4, 8, and 12 weeks after BoNT/A application. Results showed that compared with the control group, the expression of agrin in the BoNT/A group began to increase on day 3, increased to the highest level at 1 week, and gradually returned to normal (control) level, suggesting that agrin might participate in the regulation of nerve sprouting after BoNT/A application (**Figures 1A,B**).

To confirm that agrin participates in regulating nerve sprouting, anti-agrin antibody (agrin-Ab; 20 μg) was injected into the rats' gastrocnemius muscle after BoNT/A injection to antagonize agrin. α-bungarotoxin staining was performed to observe nerve sprouting and NMJs. We found that the number of AChRs increased significantly after BoNT/A injection in the 1st week ($P = 0.007$), and was significantly lower in the agrin-Ab group than in the BoNT/A group ($P = 0.029$; **Figures 1C,D**). These results indicated that agrin participated in regulating BoNT/A-induced nerve sprouting.

Agrin Could Serve as an Interventional Target for Prolonging the Effective Duration of BoNT/A

After concluding that agrin is involved in the regulation of BoNT/A-induced nerve sprouting, we confirmed that agrin influences the duration of BoNT/A effect by regulating nerve sprouting, and hypothesized that agrin could be used as an interventional target for prolonging the duration effect of BoNT/A. To verify our hypothesis, the function of agrin was inhibited using agrin-Ab. Various doses of recombinant agrin-Ab (0.6, 2, 6, 20, or 60 μg) were intramuscularly injected into the gastrocnemius muscle on day 3 after BoNT/A injection. As indicated in **Figure 2A**, muscle strength in the control group gradually increased with an increase in weight. Compared with the control group, muscle strength in the BoNT/A group were significantly lower at 3 days and weeks 1, 2, 4, and 8 after BoNT/A injection. Muscle strength in the BoNT/A group returned to the control level at week 10. However, compared with the BoNT/A group, muscle strength in the agrin-Ab groups decreased further at weeks 2, 4, 8, and 10. Moreover, muscle strength in the agrin-Ab groups reverted to the level of the control group at week 12, which was two weeks longer than that in the BoNT/A group ($P = 0.002$), suggesting that agrin-Ab can prolong the duration of effect of BoNT/A in decreasing muscle strength. Agrin-Ab showed a dose-dependent effect in maintaining the decreased muscle strength caused by BoNT/A, and there was no difference in effect between the 20 and 60 μg dosage subgroups (**Figure 2B**). 20 μg is therefore likely the threshold dose, and was selected for subsequent experiments (**Figure 2C**). These findings revealed that agrin could be used as an interventional target for prolonging the duration of effect of BoNT/A in decreasing muscle strength.

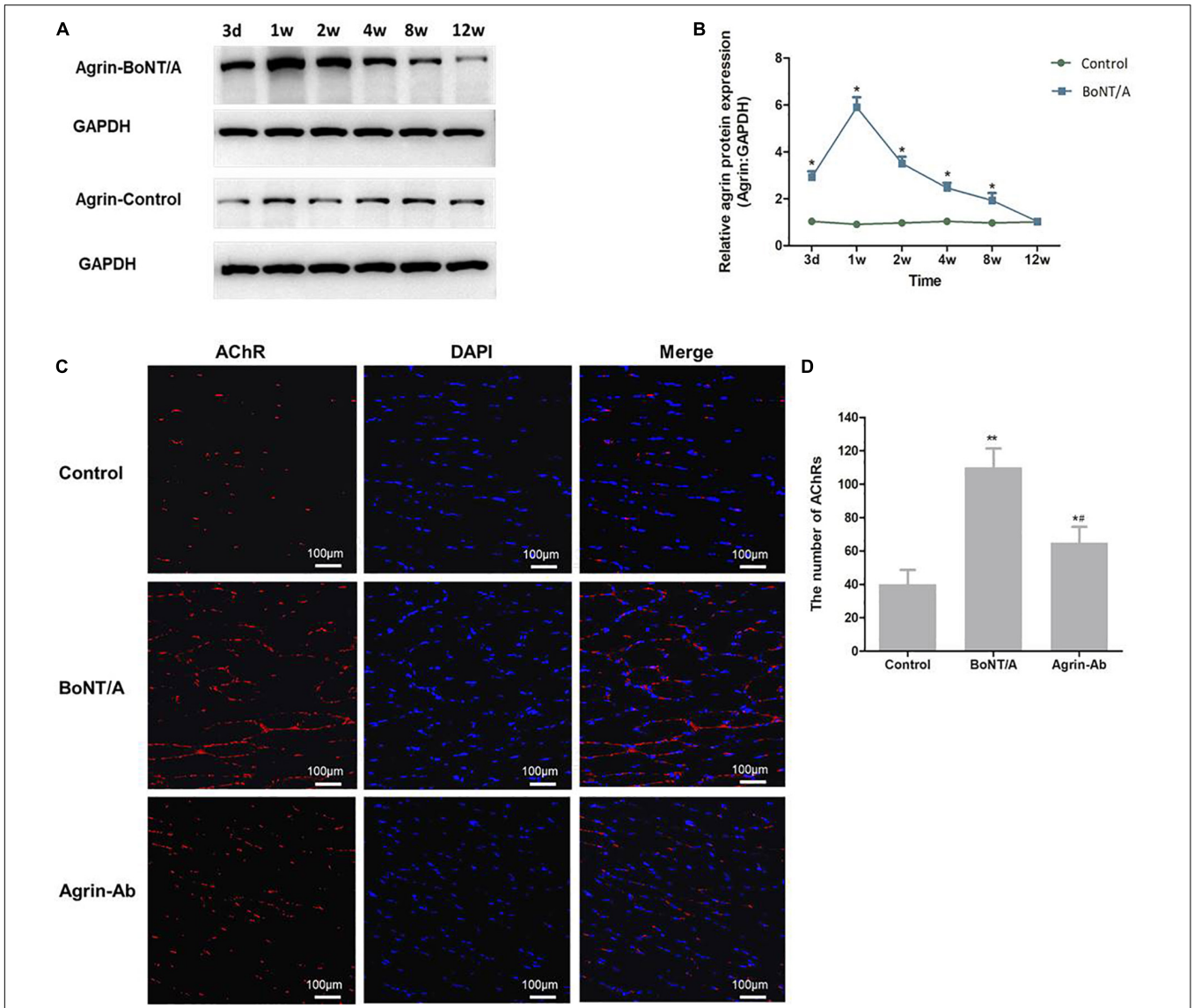

FIGURE 1 | Agrin participates in regulating nerve sprouting after BoNT/A application. **(A)** Western blot analysis of agrin at NMJs after BoNT/A injection. GAPDH was used as internal control. **(B)** Quantitation of agrin protein was performed using GeneTools from SynGene software and normalized to GAPDH. $^{*}P < 0.05$ versus control. **(C)** α-Bungarotoxin staining analysis of the number of AChRs after BoNT/A and agrin-Ab injection at week 1. Nuclei were counterstained with DAPI (4′-6-diamidino-2-phenylindole; blue). Images were merged as indicated. Scale bar, 100 μm. **(D)** Number of AChRs; bars represent mean ± SD of three different experiments. $^{*}P < 0.05$, $^{**}P < 0.01$ compared to the control group. $\#P < 0.05$ compared to the BoNT/A group.

Agrin Influences the Duration of BoNT/A Effect by Regulating Downstream MuSK

The trends observed in agrin expression after BoNT/A injection were similar to those of MuSK, which we previously reported (Jin et al., 2013), suggesting that agrin might regulate MuSK expression. Therefore, we speculated that agrin influences nerve sprouting via agrin-MuSK signaling and thereby influences the effective duration time of BoNT/A. After agrin-Ab (Ab 20 μg) injection, MuSK mRNA and protein levels at different times after BoNT/A injection were analyzed by qPCR and western blot. MuSK expression increased in the 1st week, and reached its peak in the 2nd week in the agrin-Ab group, which was later than that in the BoNT/A group (**Figures 3A–C**). These findings, combined with our previous findings (Jin et al., 2013; Guo et al., 2015), indicated that agrin influences the effective duration time of BoNT/A by regulating downstream MuSK.

Agrin Expression Is Regulated by Upstream miR-144

To elucidate the regulatory microRNAs (miRNAs) of agrin, we searched for putative miRNAs by using prediction algorithms (miRDB, miRanda and TargetScan). Three miRNAs with high scores, miR-144, miR-27a, and miR-29a, were selected as candidates (**Figure 4A**). Luciferase assay results showed that

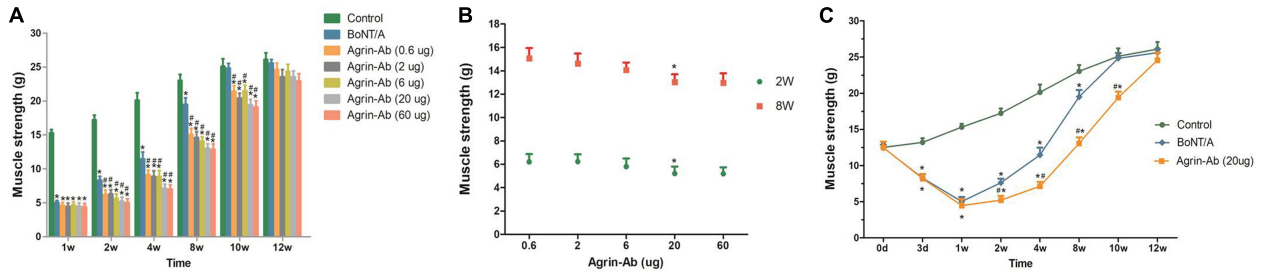

FIGURE 2 | Agrin-Ab prevents the recovery of muscle strength and prolongs the duration of BoNT/A effect in a dose-dependent manner. **(A)** Muscle strength was determined by a survey system for rat lower limb nerve and muscle function at different times after injection of BoNT/A and agrin-Ab at different doses. $^{*}P < 0.05$ versus the control group; $\#P < 0.05$ versus the BoNT/A group. **(B)** Dose-dependent effect of agrin-Ab in maintaining the decreased muscle strength caused by BoNT/A at week 2 and week 8. Muscle strength was determined by a survey system for rat lower limb nerve and muscle function. $^{*}P < 0.05$ versus the 6 μg group. **(C)** The paralytic effect of BoNT/A lasted longer after injection of 20 μg agrin-Ab. $^{*}P < 0.05$, compared to the control group. $\#P < 0.05$, compared to the BoNT/A group.

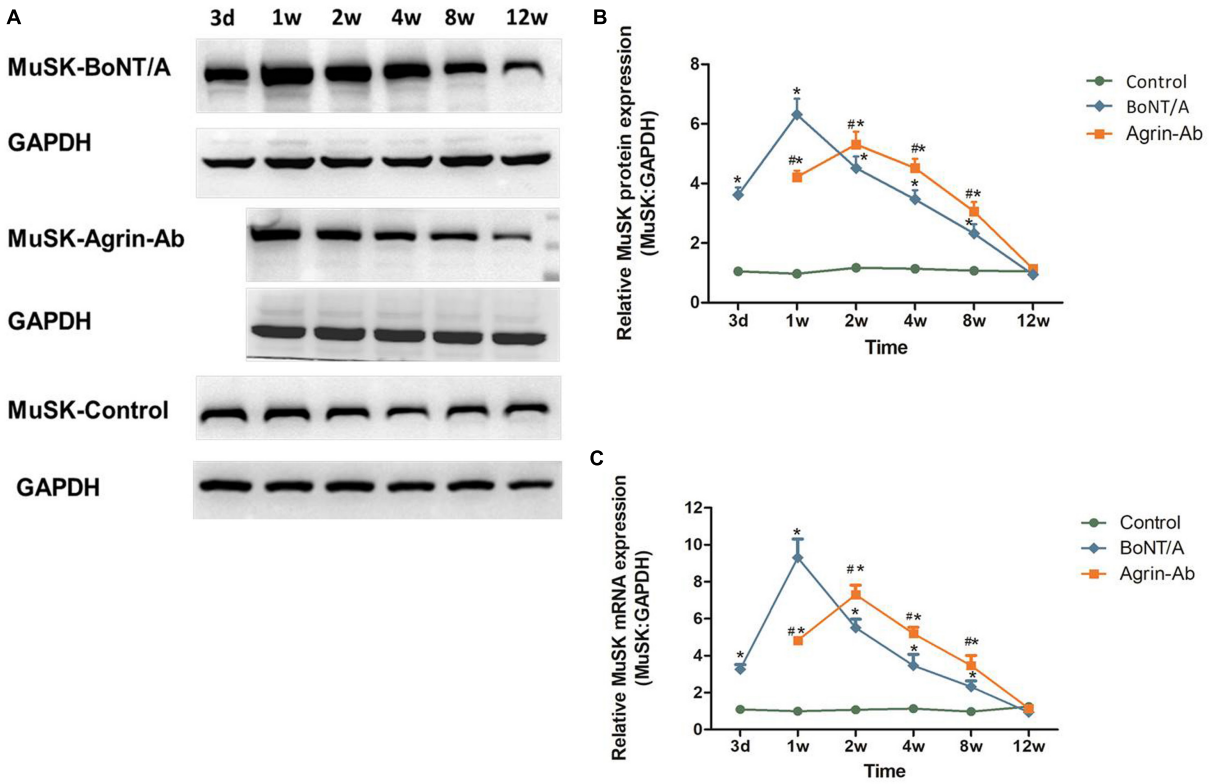

FIGURE 3 | Agrin-Ab delays the increase of MuSK expression. **(A)** Protein levels of MuSK were assayed by western blot after BoNT/A and agrin-Ab injection. GAPDH was used as an internal control. **(B)** Protein quantification was normalized to GAPDH and data are presented as mean ± SD of three different experiments. $^{*}P < 0.05$ compared to the control group. $\#P < 0.05$ compared to the BoNT/A group. **(C)** mRNA levels of MuSK were assayed by qPCR after BoNT/A and agrin-Ab injection. GAPDH was used as an internal control. Data represent the mean ± SD of three different experiments. $^{*}P < 0.05$ compared to the control group. $\#P < 0.05$ compared to the BoNT/A group.

luciferase activity was reduced by 40% in HEK 293T cells transfected with pSuper-144 compared with the control pSuper-EGFP1, pSuper-27a, and pSuper-29a, suggesting that miR-144 could suppress gene expression by binding sequences at the 3′ UTR of agrin ($P = 0.006$; **Figure 4B**). To determine whether agrin is a direct target of miR-144, we mutated the seed sequence of miR-144 in the agrin 3′ UTR shown in **Figure 4A**. Co-transfection of pSuper-144 with the firefly luciferase reporter gene linked to the wild-type segment of the agrin 3′ UTR strongly repressed luciferase activity, and the luciferase activity in the group with the mutant-type (MUT) segment of the agrin 3′ UTR was rescued (**Figure 4C**). These results showed that miR-144 could directly target the 3′ UTR of agrin mRNA.

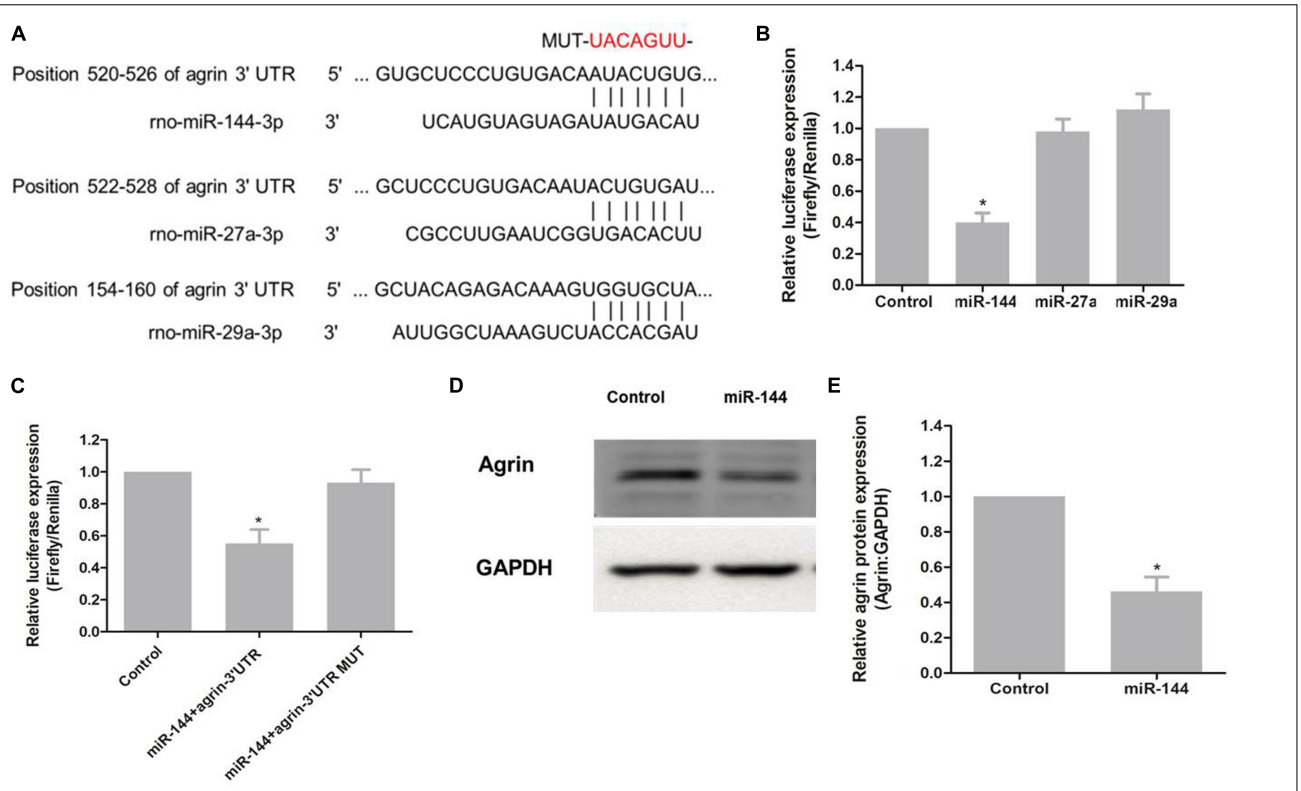

FIGURE 4 | miR-144 regulates agrin expression by directly targeting the 3′ UTR of agrin mRNA. **(A)** Schematic representation of three putative miRNA-binding sites on the agrin 3′ UTR sequence. **(B)** The 3′ UTR fragment of agrin was cloned into the Xbal restriction site downstream of the firefly luciferase gene of the pGL3-Basic vector. Luciferase activity of each sample was measured 48h after transfection and normalized to *Renilla* luciferase activity. pGL3-Basic vector was used as control. Graph error bars indicate SD calculated from at least three independent experiments. *$P < 0.05$, compared with the control. **(C)** Co-transfection of pSuper-144 with the firefly luciferase reporter gene linked to the wild-type and mutant-type sequence of miR-144 binding site within the agrin 3′ UTR. Luciferase activity was measured and normalized to phRL-TK activity. Three independent experiments were performed and data are presented as mean ± SD. *$P < 0.05$, compared with the control. **(D)** Protein level of agrin was assayed by western blotting. GAPDH was used as an internal control. **(E)** Protein expression was normalized to GAPDH. *$P < 0.05$, compared to the control group.

To determine whether miR-144 regulates agrin expression, pSuper-144 was transfected into primary neural progenitor cells according to a previously reported protocol (Zhang et al., 2013), and the expression of agrin was examined. Agrin protein levels notably decreased after pSuper-144 over-expression compared with the control group ($P = 0.006$; **Figures 4D,E**). These results suggested that miR-144 regulates agrin expression by targeting the 3′ UTR of agrin mRNA.

The Regulatory Effect of Agrin on Nerve Sprouting Is Regulated by Upstream miR-144

To determine whether the regulatory effect of agrin on nerve sprouting after BoNT/A injection is regulated by upstream miR-144, we examined the expression of miR-144 in the rats' spinal cord anterior horn. Compared to miR-144 expression in the control group, miR-144 expression in the BoNT/A group began to decrease on day 3, decreased to the lowest level at 1 week, and gradually returned to normal (control) level. This was opposite to the trend observed in agrin protein expression (**Figures 5A,B**), indicating that the regulatory effect of agrin on nerve sprouting is regulated by upstream miR-144.

To confirm that miR-144-agrin signaling is involved in regulating the development of original motor endplates, the expression of miR-144 in spinal cord anterior horn and the expression of agrin in the gastrocnemius muscle from the rats were examined 1, 4, and 8 weeks after birth. As shown in **Figures 5C,D**, the expression of agrin protein gradually increased after birth, increased to the highest level at the 4th week, and then decreased to the normal level (8w), which corresponds to the development of original motor endplates (Grinnell, 1995). Further, miR-144 expression showed a contrasting trend to that of agrin expression (**Figures 5E,F**). These results suggested that miR-144-agrin signaling participates in regulating NMJ formation in nerve sprouting and the development of original motor endplates.

DISCUSSION

In this study, we revealed that agrin plays a role in regulating BoNT/A-induced nerve sprouting via miR-144-agrin-MuSK

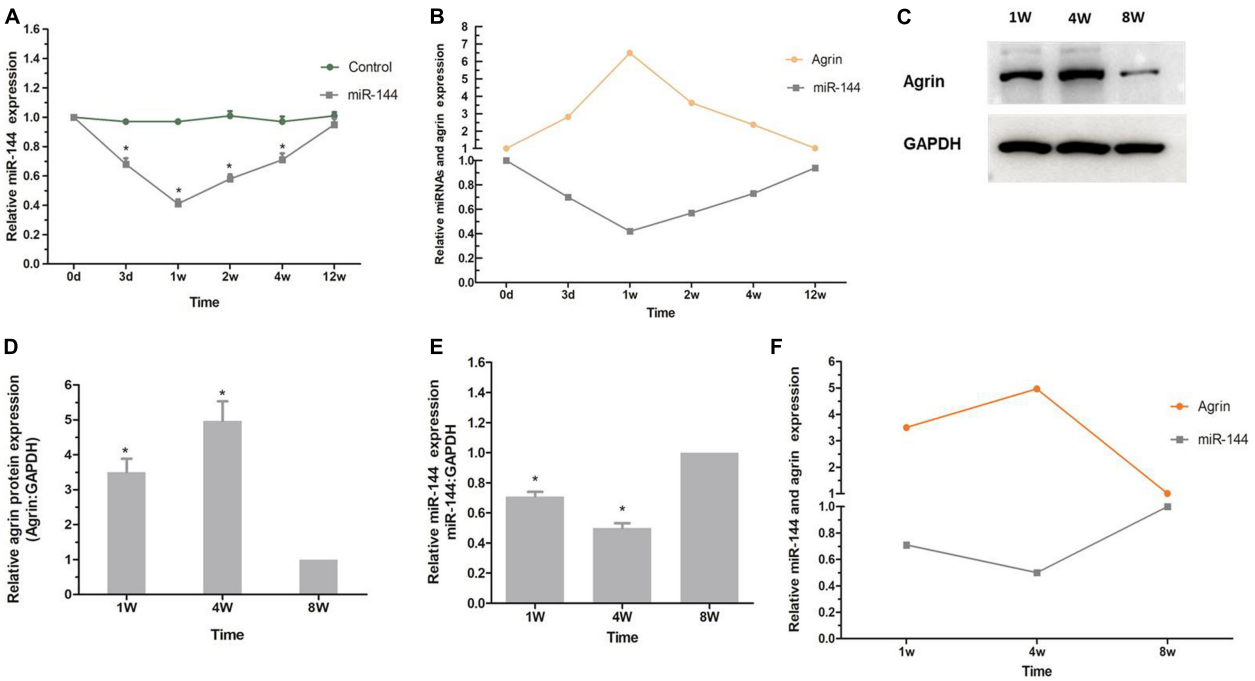

FIGURE 5 | miR-144-agrin signaling participates in regulating NMJ formation. **(A)** Real time RT-PCR analysis of miR-144 expression after BoNT/A injection. *$P < 0.05$, compared with the control group. Data represent mean ± SD of three different experiments. **(B)** The relative trends of miR-144 and agrin expression (BoNT/A group/Control group). **(C)** The relative expression level of agrin from rats 1, 4, and 8 weeks after birth analyzed by western blot. GAPDH was used as an internal control. **(D)** Protein levels were normalized to those of GAPDH. *$P < 0.05$, compared to the control (8W) group. **(E)** The relative expression level of miR-144 from rats 1, 4, and 8 weeks after birth analyzed by real time RT-PCR assay. GAPDH was used as an internal control. *$P < 0.05$, compared to the control (8W) group. **(F)** The relative trends of miR-144 and agrin expression (BoNT/A group/Control group).

signaling, which influences the effective duration time of BoNT/A. Blocking agrin function with agrin-Ab temporarily could delay muscle strength recovery and prolong the duration of effect of BoNT/A. Agrin therefore shows potential as an interventional target for prolonging the effect time of BoNT/A in decreasing muscle strength. Our work revealed the role and the underlying mechanism of agrin in the process of nerve sprouting after BoNT/A application, and simultaneously explored a novel interventional target for prolonging the effect of BoNT/A.

Effective duration time is a vital factor that limits the clinical applications of BoNT/A. There have been several attempts to prolong the duration of BoNT/A effect, including usage of higher dosages, high-volume preparation, and electrical stimulation post-injection (Dressler, 2004; Rha et al., 2008; Boyle et al., 2009; Hu et al., 2009). However, the results of these approaches were unsatisfactory. Novel methods to prolong the effect of BoNT/A remain elusive. BoNT/A-induced nerve sprouting is the main factor that reduces the effect time of BoNT/A; inhibiting nerve sprouting could potentially prolong the effect of BoNT/A. The extent and length of nerve sprouting triggered by BoNT/A could be reduced by treatment with antibodies to insulin-like growth factor 1 (IGF-1) or neural cell adhesion molecule (NCAM) (Booth et al., 1990; Schafer and Wernig, 1998; Rind and von Bartheld, 2002; Apel et al., 2010). Our group verified that the duration of BoNT/A effect could be prolonged by inhibition of IGF-1 or NCAM function with IGF-1 or NCAM antibodies (Jin et al., 2013; Guo et al., 2015). These findings provide a basis to develop novel approaches to prolong the effect of BoNT/A.

Although agrin has been proved to have a vital role in the development of original motor endplates, there are no reports on the involvement of agrin in nerve sprouting. In this study, we found that the expression of agrin in the BoNT/A group began to increase on day 3, increased to the highest level at 1 week, and gradually returned to the normal level. The trends of agrin expression after BoNT/A application were similar to those in MuSK, which we reported previously (Jin et al., 2013; Guo et al., 2015). Moreover, the increase in nerve sprouting was significantly lower in the agrin-Ab group than in the BoNT/A group ($P = 0.029$). These results indicate the regulatory role of agrin in BoNT/A-induced nerve sprouting.

Some studies have shown that agrin-Ab can block aggregation of AChRs at original motor endplates on muscle surface (Reist et al., 1992; Gautam et al., 1996), however there have been no studies on whether agrin-Ab could prevent the recovery of NMJs and prolong the effect of BoNT/A. In this study, agrin-Ab was used to antagonize agrin after BoNT/A injection, and muscle strength was detected at different times. Compared with the BoNT/A group, muscle strength in the agrin-Ab groups declined more at weeks 2, 4, 8, and 10, and took two weeks longer to recover to normal levels. Although the effect of exogenous IgG protein did not exclude in this study, we did a dose effect curve for the agrin-Ab, and the results displayed that agrin-Ab

showed a dose-dependent effect in maintaining the decreased muscle strength caused by BoNT/A (**Figures 2A,B**). The results still provide us the important message that agrin-Ab could prevent the recovery of muscle strength and prolong the effect of BoNT/A. Even so, exogenous IgG protein is still a factor that has to be eliminated in the future. Our results confirmed the interventional potential of agrin in prolonging the effect of BoNT/A in decreasing muscle strength, and revealed a novel potential interventional target for extending BoNT/A effects.

The trends of agrin expression after BoNT/A application were similar to those of MuSK. Therefore, we speculated that agrin participates in regulating nerve sprouting via agrin-MuSK signaling. Then we conducted further experiments that shows inhibition of agrin with agrin-Ab delays upregulation of MuSK, and thereby suppresses BoNT/A-induced nerve sprouting. Previous studies have shown that agrin binds to the first β-propeller domain of Lrp4, which evidently induces a conformational change in Lrp4 and enhances the interaction between Lrp4 and MuSK (Zhang W. et al., 2011; Zong et al., 2012; Hubbard and Gnanasambandan, 2013). Therefore, based on previous research findings, our research results could reflect the regulatory role of agrin-Lrp4-MuSK signaling in BoNT/A-induced nerve sprouting and the function recovery of NMJs after injection of BoNT/A.

Currently, there is no report on the upstream regulatory signaling of agrin. miRNAs, a vital class of upstream regulatory factors of gene expression, negatively regulate gene expression at the post-transcriptional level by binding to the 3′ UTR of target mRNAs. miRNAs are broadly involved in various biological processes including development, cell differentiation, and apoptosis *in vivo* and *in vitro* (Bartel, 2004; Ouellet et al., 2006; Wang et al., 2018). However, the regulatory miRNA of agrin has not been reported. In this study, we searched for putative miRNAs by using common prediction algorithms (miRDB, miRanda, and TargetScan) and selected three miRNAs with high scores in at least 2 algorithms simultaneously, as reported previously (Gong et al., 2015; Jiang et al., 2019). Subsequent studies indicated that only miR-144 could regulate the expression of agrin, and miR-144/agrin/MuSK axis might regulate NMJ formation in nerve sprouting and the development of original motor endplates. Zhang H.Y. et al. (2011) reported that miR-144 was down-regulated following sciatic nerve transection. Rau et al. (2010) also found that miR-144 was down-regulated after sciatic nerve denervation. We speculated that the secretion of agrin was blocked after sciatic nerve denervation, which activated the upstream signals and caused downregulation of miR-144. These findings therefore indirectly support our results. The current study showed, for the first time, that agrin could be targeted by miR-144 in neurons. Future *in vivo* and *in vitro* studies are required to elucidate the regulatory role of miR-144/agrin/MuSK signaling in the development of NMJs.

CONCLUSION

Agrin is a crucial neurogenic regulator in the development of original motor endplates; however, its role in nerve sprouting remains unclear. In this study, we demonstrated that agrin participates in regulating BoNT/A-induced nerve sprouting, which limits BoNT/A efficacy, and revealed a novel mechanism of nerve sprouting. In addition, we confirmed that agrin-Ab could prevent the recovery of muscle strength and prolong the duration of effect of BoNT/A, indicating that agrin could be used as an interventional target for prolonging the duration of effect of BoNT/A in decreasing muscle strength.

DATA AVAILABILITY STATEMENT

All datasets generated for this study are included in the article/supplementary material.

ETHICS STATEMENT

The animal study was reviewed and approved by the Committee of Tongji University.

AUTHOR CONTRIBUTIONS

LM and LJ conceived and designed the experiments. WL, YL, and XX performed the experiments. YP and XZ performed informatics analysis. LM, LP, and LJ wrote the manuscript. All authors read and approved the final manuscript.

FUNDING

This work was supported by grants from the National Key R&D Program of China (No. 2018YFC1314700), National Natural Science Foundation of China (No. 81600980), Fundamental Research Funds for the Central Universities (No. 22120180111), Priority of Shanghai Key Discipline of Medicine (No. 2017ZZ02020), Shanghai "Rising Stars of Medical Talent" Youth Development Program (No. [2019] 72), and Shanghai Science and Technology Commission Medical Guidance Project (No. 16411970000).

REFERENCES

Apel, P. J., Ma, J., Callahan, M., Northam, C. N., Alton, T. B., Sonntag, W. E., et al. (2010). Effect of locally delivered IGF-1 on nerve regeneration during aging: an experimental study in rats. *Muscle Nerve* 41, 335–341. doi: 10.1002/mus.21485

Bartel, D. P. (2004). MicroRNAs: genomics, biogenesis, mechanism, and function. *Cell* 116, 281–297.

Bezakova, G., Rabben, I., Sefland, I., Fumagalli, G., and Lomo, T. (2001). Neural agrin controls acetylcholine receptor stability in skeletal muscle fibers. *Proc Natl Acad Sci U S A* 98, 9924–9929. doi: 10.1073/pnas.171539698

Booth, C. M., Kemplay, S. K., and Brown, M. C. (1990). An antibody to neural cell adhesion molecule impairs motor nerve terminal sprouting in a mouse muscle locally paralysed with botulinum toxin. *Neuroscience* 35, 85–91. doi: 10.1016/0306-4522(90)90123-l

Boyle, M. H., McGwin, G. Jr., Flanagan, C. E., Vicinanzo, M. G., and Long, J. A. (2009). High versus low concentration botulinum toxin A for benign essential blepharospasm: does dilution make a difference? *Ophthalmic Plast Reconstr Surg* 25, 81–84. doi: 10.1097/IOP.0b013e31819946c4

Chinnapongse, R., Pappert, E. J., Evatt, M., Freeman, A., and Birmingham, W. (2010). An open-label, sequential dose-escalation, safety, and tolerability study of rimabotulinumtoxinb in subjects with cervical dystonia. *Int J Neurosci* 120, 703–710. doi: 10.3109/00207454.2010.515047

Dolly, J. O., and Aoki, K. R. (2006). The structure and mode of action of different botulinum toxins. *Eur J Neurol* 13(Suppl. 4), 1–9. doi: 10.1111/j.1468-1331.2006.01648.x

Dressler, D. (2004). Clinical presentation and management of antibody-induced failure of botulinum toxin therapy. *Mov Disord* 19(Suppl. 8), S92–S100. doi: 10.1002/mds.20022

Feng, Y., Liu, W., Pan, L., Jiang, C., Zhang, C., Lu, Y., et al. (2017). Comparison of neurotoxic potency between a novel chinbotulinumtoxinA with onabotulinumtoxinA, incobotulinumtoxinA and lanbotulinumtoxinA in rats. *Drug Des Devel Ther* 11, 1927–1939. doi: 10.2147/DDDT.S138489

Foley, N., Pereira, S., Salter, K., Fernandez, M. M., Speechley, M., Sequeira, K., et al. (2013). Treatment with botulinum toxin improves upper-extremity function post stroke: a systematic review and meta-analysis. *Arch Phys Med Rehabil* 94, 977–989. doi: 10.1016/j.apmr.2012.12.006

Gautam, M., Noakes, P. G., Moscoso, L., Rupp, F., Scheller, R. H., Merlie, J. P., et al. (1996). Defective neuromuscular synaptogenesis in agrin-deficient mutant mice. *Cell* 85, 525–535. doi: 10.1016/s0092-8674(00)81253-2

Gong, X., Wang, Y., Zeng, J., Li, S., and Luo, Y. (2015). Computational identification and experimental validation of microRNAs binding to the fragile X syndrome gene Fmr1. *Neurochem Res* 40, 109–117. doi: 10.1007/s11064-014-1471-3

Grazzi, L., and Usai, S. (2014). Botulinum toxin A: a new option for treatment of chronic migraine with medication overuse. *Neurol Sci* 35(Suppl. 1), 37–39. doi: 10.1007/s10072-014-1739-z

Grinnell, A. D. (1995). Dynamics of nerve-muscle interaction in developing and mature neuromuscular junctions. *Physiol Rev* 75, 789–834. doi: 10.1152/physrev.1995.75.4.789

Guo, Y., Pan, L., Liu, W., Pan, Y., Nie, Z., and Jin, L. (2015). Polyclonal neural cell adhesion molecule antibody prolongs the effective duration time of botulinum toxin in decreasing muscle strength. *Neurol Sci* 36, 2019–2025. doi: 10.1007/s10072-015-2291-1

Hu, G. C., Chuang, Y. C., Liu, J. P., Chien, K. L., Chen, Y. M., and Chen, Y. F. (2009). Botulinum toxin (Dysport) treatment of the spastic gastrocnemius muscle in children with cerebral palsy: a randomized trial comparing two injection volumes. *Clin Rehabil* 23, 64–71. doi: 10.1177/0269215508097861

Hubbard, S. R., and Gnanasambandan, K. (2013). Structure and activation of MuSK, a receptor tyrosine kinase central to neuromuscular junction formation. *Biochim Biophys Acta* 1834, 2166–2169. doi: 10.1016/j.bbapap.2013.02.034

Jiang, S., Guo, S., Li, H., Ni, Y., Ma, W., and Zhao, R. (2019). Identification and Functional Verification of MicroRNA-16 Family Targeting Intestinal Divalent Metal Transporter 1 (DMT1) in vitro and in vivo. *Front Physiol* 10:819. doi: 10.3389/fphys.2019.00819

Jin, L., Pan, L., Liu, W., Guo, Y., Zheng, Y., Guan, Q., et al. (2013). IGF-1 antibody prolongs the effective duration time of botulinum toxin in decreasing muscle strength. *Int J Mol Sci* 14, 9051–9061. doi: 10.3390/ijms14059051

Juzans, P., Comella, J. X., Molgo, J., Faille, L., and Angaut-Petit, D. (1996). Nerve terminal sprouting in botulinum type-A treated mouse levator auris longus muscle. *Neuromuscul Disord* 6, 177–185. doi: 10.1016/0960-8966(96)00041-7

Kim, N., Stiegler, A. L., Cameron, T. O., Hallock, P. T., Gomez, A. M., Huang, J. H., et al. (2008). Lrp4 is a receptor for Agrin and forms a complex with MuSK. *Cell* 135, 334–342. doi: 10.1016/j.cell.2008.10.002

Krishnan, R. V. (2005). Botulinum toxin: from spasticity reliever to a neuromotor re-learning tool. *Int J Neurosci* 115, 1451–1467. doi: 10.1080/00207450590956576

Ngo, S. T., Noakes, P. G., and Phillips, W. D. (2007). Neural agrin: a synaptic stabiliser. *Int J Biochem Cell Biol* 39, 863–867. doi: 10.1016/j.biocel.2006.10.012

Ouellet, D. L., Perron, M. P., Gobeil, L. A., Plante, P., and Provost, P. (2006). MicroRNAs in gene regulation: when the smallest governs it all. *J Biomed Biotechnol* 2006, 69616. doi: 10.1155/JBB/2006/69616

Pellizzari, R., Rossetto, O., Schiavo, G., and Montecucco, C. (1999). Tetanus and botulinum neurotoxins: mechanism of action and therapeutic uses. *Philos Trans R Soc Lond B Biol Sci* 354, 259–268. doi: 10.1098/rstb.1999.0377

Rau, C. S., Jeng, J. C., Jeng, S. F., Lu, T. H., Chen, Y. C., Liliang, P. C., et al. (2010). Entrapment neuropathy results in different microRNA expression patterns from denervation injury in rats. *BMC Musculoskelet Disord* 11:181. doi: 10.1186/1471-2474-11-181

Reist, N. E., Werle, M. J., and McMahan, U. J. (1992). Agrin released by motor neurons induces the aggregation of acetylcholine receptors at neuromuscular junctions. *Neuron* 8, 865–868. doi: 10.1016/0896-6273(92)90200-w

Rha, D. W., Yang, E. J., Chung, H. I., Kim, H. B., Park, C. I., and Park, E. S. (2008). Is electrical stimulation beneficial for improving the paralytic effect of botulinum toxin type A in children with spastic diplegic cerebral palsy? *Yonsei Med J* 49, 545–552. doi: 10.3349/ymj.2008.49.4.545

Rind, H. B., and von Bartheld, C. S. (2002). Target-derived cardiotrophin-1 and insulin-like growth factor-I promote neurite growth and survival of developing oculomotor neurons. *Mol Cell Neurosci* 19, 58–71. doi: 10.1006/mcne.2001.1069

Sanes, J. R., and Lichtman, J. W. (2001). Induction, assembly, maturation and maintenance of a postsynaptic apparatus. *Nat Rev Neurosci* 2, 791–805. doi: 10.1038/35097557

Santafe, M. M., Urbano, F. J., Lanuza, M. A., and Uchitel, O. D. (2000). Multiple types of calcium channels mediate transmitter release during functional recovery of botulinum toxin type A-poisoned mouse motor nerve terminals. *Neuroscience* 95, 227–234. doi: 10.1016/s0306-4522(99)00382-6

Schafer, R., and Wernig, A. (1998). Polyclonal antibodies against NCAM reduce paralysis-induced axonal sprouting. *J Neurocytol* 27, 615–624.

Tezuka, T., Inoue, A., Hoshi, T., Weatherbee, S. D., Burgess, R. W., Ueta, R., et al. (2014). The MuSK activator agrin has a separate role essential for postnatal maintenance of neuromuscular synapses. *Proc Natl Acad Sci U S A* 111, 16556–16561. doi: 10.1073/pnas.1408409111

Wang, L., Lv, Y., Li, G., and Xiao, J. (2018). MicroRNAs in heart and circulation during physical exercise. *J Sport Health Sci* 7, 433–441. doi: 10.1016/j.jshs.2018.09.008

Zhang, H. Y., Zheng, S. J., Zhao, J. H., Zhao, W., Zheng, L. F., Zhao, D., et al. (2011). MicroRNAs 144, 145, and 214 are down-regulated in primary neurons responding to sciatic nerve transection. *Brain Res* 1383, 62–70. doi: 10.1016/j.brainres.2011.01.067

Zhang, J., Zhang, J., Zhou, Y., Wu, Y. J., Ma, L., Wang, R. J., et al. (2013). Novel cerebellum-enriched miR-592 may play a role in neural progenitor cell differentiation and neuronal maturation through regulating Lrrc4c and Nfasc in rat. *Curr Mol Med* 13, 1432–1445. doi: 10.2174/15665240113139990072

Zhang, W., Coldefy, A. S., Hubbard, S. R., and Burden, S. J. (2011). Agrin binds to the N-terminal region of Lrp4 protein and stimulates association between Lrp4 and the first immunoglobulin-like domain in muscle-specific kinase (MuSK). *J Biol Chem* 286, 40624–40630. doi: 10.1074/jbc.M111.279307

Zhang, X., Hu, Y., Nie, Z., Song, Y., Pan, Y., Liu, Y., et al. (2015). Treatment of Raynaud's phenomenon with botulinum toxin type A. *Neurol Sci* 36, 1225–1231. doi: 10.1007/s10072-015-2084-6

Zong, Y., and Jin, R. (2013). Structural mechanisms of the agrin-LRP4-MuSK signaling pathway in neuromuscular junction differentiation. *Cell Mol Life Sci* 70, 3077–3088. doi: 10.1007/s00018-012-1209-9

Zong, Y., Zhang, B., Gu, S., Lee, K., Zhou, J., Yao, G., et al. (2012). Structural basis of agrin-LRP4-MuSK signaling. *Genes Dev* 26, 247–258. doi: 10.1101/gad.180885.111

Conflict of Interest: The authors declare that the research was conducted in the absence of any commercial or financial relationships that could be construed as a potential conflict of interest.

frontiers in Genetics

ORIGINAL RESEARCH
published: 19 February 2020
doi: 10.3389/fgene.2020.00078

Downregulation of miR-26b-5p, miR-204-5p, and miR-497-3p Expression Facilitates Exercise-Induced Physiological Cardiac Hypertrophy by Augmenting Autophagy in Rats

Jie Qi[1], *Xue Luo*[2], *Zhichao Ma*[3], *Bo Zhang*[1], *Shuyan Li*[4] *and Jun Zhang*[1]*

[1] College of Physical Education, Shanghai Normal University, Shanghai, China, [2] Medical College, Yangzhou Polytechnic College, Yangzhou, China, [3] The School of Physical Education, Wuhan Business University, Wuhan, China, [4] College of Physical Education, Yangzhou University, Yangzhou, China

OPEN ACCESS

Edited by:
Saumya Das,
Harvard Medical School,
United States

Reviewed by:
Chi-Ming Wong,
The University of Hong Kong,
Hong Kong
Harsh Dweep,
Wistar Institute,
United States

***Correspondence:**
Jun Zhang
zhangjyzh@sina.com

Specialty section:
This article was submitted to RNA, a section of the journal Frontiers in Genetics

Received: 10 September 2019
Accepted: 23 January 2020
Published: 19 February 2020

Citation:
Qi J, Luo X, Ma Z, Zhang B, Li S and Zhang J (2020) Downregulation of miR-26b-5p, miR-204-5p, and miR-497-3p Expression Facilitates Exercise-Induced Physiological Cardiac Hypertrophy by Augmenting Autophagy in Rats. Front. Genet. 11:78. doi: 10.3389/fgene.2020.00078

Exercise-induced autophagy is associated with physiological left ventricular hypertrophy (LVH), and a growing body of evidence suggests that microRNAs (miRNAs) can regulate autophagy-related genes. However, the precise role of miRNAs in exercise induced autophagy in physiological LVH has not been fully defined. In this study, we investigated the microRNA–autophagy axis in physiological LVH and deciphered the underlying mechanism using a rat swimming exercise model. Rats were assigned to sedentary control (CON) and swimming exercise (EX) groups; those in the latter group completed a 10-week swimming exercise without any load. For *in vitro* studies, H9C2 cardiomyocyte cell line was stimulated with IGF-1 for hypertrophy. We found a significant increase in autophagy activity in the hearts of rats with exercise-induced physiological hypertrophy, and miRNAs showed a high score in the pathway enriched in autophagy. Moreover, the expression levels of miR-26b-5p, miR-204-5p, and miR-497-3p showed an obvious increase in rat hearts. Adenovirus-mediated overexpression of miR-26b-5p, miR-204-5p, and miR-497-3p markedly attenuated IGF-1-induced hypertrophy in H9C2 cells by suppressing autophagy. Furthermore, miR-26b-5p, miR-204-5p, and miR-497-3p attenuated autophagy in H9C2 cells through targeting ULK1, LC3B, and Beclin 1, respectively. Taken together, our results demonstrate that swimming exercise induced physiological LVH, at least in part, by modulating the microRNA–autophagy axis, and that miR-26b-5p, miR-204-5p, and miR-497-3p may help distinguish physiological and pathological LVH.

Keywords: autophagy, exercise, insulin-like growth factor 1, cardiac hypertrophy, microRNA

INTRODUCTION

The two types of left ventricular hypertrophy (LVH), namely physiological and pathological LVH, differ greatly in the left ventricular phenotype. Both of them have an increased myocyte volume and heart size. The difference is that physiological LVH is induced by aerobic exercise training, postnatal growth, and pregnancy, and characterized by unchanged fetal and apoptosis gene expression and increased cardiac function while pathological LVH is stimulated by pressure or volume overload or cardiomyopathy, and characterized by apoptosis and fibrosis and depressed cardiac function (Bernardo et al., 2010; Nakamura and Sadoshima, 2018; Oldfield et al., 2019). For example, LVH induced by swimming exercise training is an adaption for a chronic increase in hemodynamic overload (Xiao et al., 2014; Bernardo et al., 2018), whereas myocardial infarction induced pathological LVH is associated with increased fibrosis, lowered aerobic capacity, and maladaptive remodeling (McMullen and Izumo, 2006; Dorn, 2007; Schiattarella and Hill, 2015). The physiological LVH exerts cardioprotection in patients with cardiovascular diseases. However, the mechanism of exercise-induced LVH remains unclear.

Physical exercise has been identified as an inducer of autophagy (Halling and Pilegaard, 2017; Martin-Rincon et al., 2018). Exercise was reported to induce autophagy in several organs such as cardiac tissue, skeletal muscle, liver, pancreas, hippocampus, and adipose tissue (Brandt et al., 2018; Li et al., 2018b). Induction of skeletal and cardiac muscle autophagy during endurance training triggers beneficial adaptive changes in mitochondrial metabolism and is associated with enhanced physical fitness (Lira et al., 2013). Autophagy is required for exercise training-induced skeletal muscle adaption and for the improvement of physical performance (Gottlieb and Mentzer, 2013; Fritzen et al., 2016; Sanchez, 2016). However, the mechanism of exercise-induced autophagy remains unknown.

Accumulated evidences showed that microRNA (miRNA, miR) networks changed in response to exercise contributed to physiological cardiac hypertrophy (Carè et al., 2007; Fernandes et al., 2011; Fernandes et al., 2015). However, different types of exercise training have been reported to cause changes in different miRNAs (Martinelli et al., 2014; Melo et al., 2015; Ramasamy et al., 2015). MiRNAs could target autophagy-related genes and negatively regulate their activities (Shen et al., 2016; Aredia and Scovassi, 2017; Chen et al., 2017). MiRNAs modulate autophagy at different stages, such as at autophagic induction, vesicle nucleation, and vesicle elongation and completion stages, by targeting autophagy-related genes or autophagy complexes (Martinelli et al., 2014; Zhang and Chen, 2018). Although a growing body of evidence indicates that miRNAs regulate autophagy-related genes, their precise role in autophagy pathways has not been fully defined in physiological cardiac hypertrophy. Therefore, we established physiological *in vitro* and *in vivo* LVH models to investigate the microRNA–autophagy axis in physiological hypertrophy.

MATERIALS AND METHODS

Animal Care and Exercise Protocols

All care policies and procedures in this study conformed to the Guide for the Care and Use of Laboratory Animals published by the US National Institutes of Health (NIH publication No. 85–23, revised 1996) and were approved by the Ethics Committee for the Use of Experimental Animals at Shanghai Normal University, China. Female Wistar rats (200 ± 20 g, n = 32) were fed a standard diet, exposed to a 12-h light–12-h dark cycle, and maintained in a constant room temperature (22 ± 2°C) and humidity (50 ± 10%) (Fernandes et al., 2011). The rats were randomly assigned to two groups: 1) sedentary control (CON, n = 16) and 2) swimming exercise (EX, n = 16). For 10 weeks, from Monday to Friday, the rats in the EX group completed a 1-h swimming exercise schedule without any load. The exercise training was performed by placing the rats in a swimming pool (150 cm × 60 cm × 70 cm) filled with warm water to a depth of 60 cm. The pool was divided by plastic barriers into eight lanes. The water temperature was maintained at 31 ± 1°C. All the animals were weighed once a week. In contrast, rats in the CON group were exposed to the water twice weekly—they were placed in the swimming pool at these junctures for 10-min sessions. The O_2 uptake for rats swimming individually was about 50–65% of the maximum oxygen uptake. This low-intensity, long-period swimming exercise protocol is effective for promoting cardiovascular adaptations and for increasing muscle oxidative capacity. These protocols were previously reported by Fernandes et al. (2011) and Oliveira et al. (2009).

Measurement of Blood Pressure and Heart Rate

Blood pressure (BP) and heart rate (HR) were measured after 24 h of the last exercise session. The hemodynamic parameters of rats were measured with a blood pressure analyzer (BP-98A; Softron, Tokyo, Japan), after they had been placed undisturbed in a restrainer for a minimum of 5 min, following the tail-cuff method. The recorded data indicated the average of all values of systolic blood pressure (SBP), diastolic blood pressure (DBP), HR, and mean arterial pressure (MBP) over the entire recording time of 20 min.

Measurement of Cardiac Hypertrophy

The rats were euthanized by cervical dislocation under anesthesia induced by intraperitoneal injection of 3% sodium pentobarbital. To measure the cardiac function, the hearts were stopped at diastole by perfusion of 14 mM KCl. After the heart weight (HW) was measured, the left ventricle (LV) was dissected corresponding to the remaining tissue upon the removal of both atria and the free wall of the right ventricle (RV). The interventricular septum remained as part of the LV. Left cardiac hypertrophy was assessed by determining the ratio of LV weight to HW (HW/BW) (Fernandes et al., 2011). Then the LVs were fixed with 10% formalin and embedded in paraffin. Heart sections (5 μm in thickness) were made and stained with hematoxylin and eosin

(HE) for imaging the heart structures. Four random sections from each heart were visualized using light microscopy at 40X magnification. Myocytes with a visible nucleus and intact cellular membrane were chosen for determination of the myocyte diameter. The width of individually isolated cardiomyocytes were displayed on a viewing screen that was manually traced, across the middle of the nuclei, with a digitizing pad and determined using a computer-assisted image analysis system (ScopePhoto 3.0 for Scope Technology). For each group, 20 visual fields were assayed.

Transmission Electron Microscopy

Transmission electron microscopy was performed by the method described by Nadal and Gold (2012). In brief, freshly prepared cardiac tissues were fixed overnight in 2% glutaraldehyde at 4°C. Thereafter, the sections were immersed in 1% buffered osmium tetroxide for 2 h. The specimens were then dehydrated through a graded series of ethanol and embedded in an epoxy resin. The specimens were then sliced into ultrathin sections (80 nm) with 0.1% citrate lead and 10% uranium acetate. The sections were examined under a transmission electron microscope (Hitachi, Tokyo, Japan).

Cell Culture

The rat H9C2 cells were purchased from the cell bank of the Chinese Academy of Sciences (Shanghai, China) and cultured in Dulbecco's modified Eagle's medium (Gibco, USA), supplemented with 100 U/ml penicillin–streptomycin, and 10% fetal bovine serum (BSA) in a 5% CO_2 humidified atmosphere at 37°C. The cells were grown at a density of 4×10^5 cells/ml. For the hypertrophy model, cells were grown with 10 μM insulin-like growth factor (IGF-1, Sigma-Aldrich, MO, USA) for 48 h at 37°C in a 5% CO_2 incubator.

Immunofluorescence Staining

For immunofluorescence analysis, H9C2 cells were fixed with 4% paraformaldehyde for 15 min, permeabilized with 0.1% Triton X-100 in PBS for 10 min, and blocked with 3% BSA solution for 1 h. These cells or paraffin-embedded sections were incubated overnight with a microtubule-associated protein 1 light chain 3B (LC3B) antibody (Cell Signaling Technology; 1:200) at 4°C, washed, and stained with a fluorescent dye (Alexa Fluor 555)-conjugated secondary antibody (Cell Signaling Technology; 1:200). The tissue sections or cells were subsequently mounted with a fluorescent mounting medium (Beyotime Biotechnology, Shanghai, China) and coverslips were placed over them. Immunofluorescence was analyzed with a fluorescence microscope (Carl Zeiss, Germany), and the number of LC3 puncta was determined using Image-Pro Plus 6.0 software.

Ribonucleic Acid Extraction and Microribonucleic Acid Microarray

Total RNA and miRNAs were extracted using TRIzol (Invitrogen, Waltham, MA) and miRNeasy mini kit (QIAGEN, Germany), respectively, according to the manufacturer's instructions. After quantitating the RNA with NanoDrop 1000 spectrophotometer (NanoDrop Technologies, USA) and standard denaturing agarose gel electrophoresis, samples from two animals in each group were pooled and labeled using the miRCURY™ Hy3™/Hy5™ Power Labeling Kit (Exiqon, Vedbaek, Denmark). They were then hybridized on the miRCURY™ LNA Array (v.16.0) (Exiqon, Vedbaek, Denmark). Next, the slides were scanned using the Axon GenePix 4000B Microarray Scanner (Axon Instruments, Foster City, CA). The scanned images were then imported into GenePix Pro 6.0 software (Axon) for grid alignment and data extraction. Replicated miRNAs were averaged and miRNAs that intensities ≥ 30 in all samples were chosen for calculating normalization factor. Expressed data were normalized using the Median normalization. After normalization, significant differentially expressed miRNAs between two groups were identified through Fold change (≥1.5) and P-value ($P \leq 0.05$). An electronic link to the miRNA microarray platform is available at http://www.ncbi.nlm.nih.gov/geo/query/acc.cgi?acc=GPL11434.

Bioinformatics

After microarray analyze, predicted target genes of candidate miRNAs were determined using three bioinformatics prediction tools: miRBase (http://www.mirbase.org/), TargetScan (http://www.targetscan.org, Jacobsen et al., 2013), and miRDB (http://www.mirdb.org/miRDB/, Liu and Wang, 2019). MiRBase was used to define the miRNA sequences, and TargetScan and miRDB were used to predict the target genes of miRNAs. The predicted miRNA target genes were then subjected to Gene Ontology (GO) and Kyoto Encyclopedia of Genes and Genomes (KEGG) analyses using DAVID (http://david.abcc.ncifcrf.gov/) online (Han et al., 2012). Eighty-three pathways were enriched with the miRNA target genes and the autophagy pathway was the second pathway of the top 10. The autophagy pathway included 16 miRNAs. Among them, one most upregulated (fold change >2.5) and four most downregulated (fold change <0.25) miRNA were selected and homology was analyzed. Again, TargetScan and miRDB were used to predict the target genes of the selected miRNAs, and the information from the two databases were integratively considered.

Quantitative Real-Time Polymerase Chain Reaction Analysis of Messenger Ribonucleic Acid and Microribonucleic Acid Expression

For reverse transcription, total RNA was prepared from cells using the TRIzol reagent according to the manufacturer's instructions (Invitrogen). Total RNA (2 μg) was reverse transcribed using the PrimeScript™ RT Master Mix Kit (Takara, Kusatsu, Japan) and Mir-X™ miRNA First-Strand Synthesis Kit (Clontech, USA) for SYBR Green PCR, respectively. Quantitative real-time PCR (qRT-PCR) was performed in triplicate using the ABI 7500 System (ABI, New York, USA) in a 20-μl reaction volume. The real-time PCR and data collection were subsequently performed, as described previously (Ma et al., 2013). The relative expression levels of the indicated mRNAs normalized against glyceraldehyde 3-phosphate dehydrogenase (GAPDH) mRNA were calculated using the $2^{-\Delta\Delta CT}$ method. The primer sequences used for RT-

qPCR are listed in **Supplementary Table 1**. For microRNAs, the expression level of U6 was used as an internal control.

Protein Extraction and Western Blot Analysis

Western blotting was performed following the standard method. Briefly, the samples were placed in protein extraction solution (RIPA) and ultrasonicated at maximum speed at 4°C for 30 s (Sonics, Newtown, USA). The homogenate was centrifuged at 12,000 × *g* at 4°C for 30 min. After denaturation, the samples were subjected to 10% sodium dodecyl sulfate polyacrylamide gel electrophoresis (SDS-PAGE) and the resolved proteins were transferred onto polyvinylidene fluoride membranes (Millipore, Billerica, USA). The membranes were blocked for 1 h with 5% milk and then probed with anti-LC3B (cat. no. 3868; 1:1,000), anti-Beclin 1 (cat. no. 3495; 1:1,000), anti-unc-51 like autophagy activating kinase 1 (ULK1) (cat. no. 8054; 1:1,000), anti-Atg4B (cat. no. 5299; 1:1,000), anti-Atg5 (cat. no. 12994; 1:1,000), anti-Atg7 (cat. no. 2631; 1:1,000), anti-Atg12 (cat. no. 4180; 1:1,000), anti-ANP (cat. no. 209232, 1:1,000), anti-brain natriuretic peptide (BNP) (cat. no. 19645, 1:1,000), or anti-SQSTM1 (cat. no. 39749; 1:1,000) antibodies, which were all purchased from Cell Signaling Technology, MA, USA, at 4°C overnight. After washing three times with TBST (Thermo Fisher Scientific, Inc., Waltham, MA), the membranes were incubated with the corresponding horseradish peroxidase-conjugated secondary antibodies (goat anti-rabbit; cat. no. ab6721; 1:2,000; Cell Signaling Technology) for 2 h at room temperature. The immunoreactive protein bands were visualized with Pierce ECL Plus Western Blot Substrate (Thermo Fisher Scientific, Rockford, IL, USA). GAPDH was used as an internal loading control. The band intensity was quantified using ImageJ software (NIH) and was defined as fold-change relative to the band intensity in the CON samples after normalization against GAPDH.

Adenovirus-Mediated Microribonucleic Acid Infection

We performed adenovirus-mediated infection of H9C2 cells for overexpression of miR-26b-5p (Ad-26b-5p), miR-204-5p (Ad-204-5p), miR-497-3p (Ad-497-3p), let-7a-5p (Ad-7a-5p), and miR-181a-5p sponges (Ad-181a-5p) (Vigenebio, Shandong, China) at a multiplicity of infection 10, respectively. After 48 h of infection, the cells were collected for RT-qPCR and western blot assays.

Statistical Analysis

Data were presented at mean ± SD. Statistical analysis was performed using Prism Software (GraphPad Prism 5.0). For analysis of two groups, Student's t-test was used; for comparison of three or more groups, one-way ANOVA followed by Bonferroni's post-test was applied. For each analysis, $P < 0.05$ was considered significant.

RESULTS

Ten-Weeks Swimming Exercise Induces Physiological Cardiac Hypertrophy in Rats

To evaluate whether 10-week swimming exercise induced LVH, the systolic, diastolic, and mean blood pressure, and heart rate were measured for rats in the CON (n=16) and EX groups (n=16) (**Figures 1A, B**). There were no differences in the blood pressure between the two groups ($P > 0.05$), but the heart rate in the EX group was significantly lower than in the CON group (304.6 ± 12.1 bpm *vs*. 348.8 ± 11.7 bpm; $P < 0.05$) after 10-week swimming exercise. The LV/BW and HW/BW ratios were used to evaluate LVH. Compared with the CON group, the HW/BW ratio was markedly increased in the EX group (4.73 ± 0.42 *vs*. 2.17 ± 0.14 for EX *vs*. CON; $P < 0.05$, n = 16; **Figure 1C**). The value of LV/BW in the EX group was 1.37-fold (2.97 ± 0.19; $P < 0.01$, **Figure 1D**), which was also higher than in the CON group (2.17 ± 0.14). Moreover, as evident from the HE staining (**Figure 1E**), in the CON group, the myocardial cells were arranged orderly and there was less amount of extracellular matrix, whereas in the EX group, the myocardial fibers were evenly colored, the myocardial cells were arranged more orderly, the number of nuclei was increased, and the structure was normal. Furthermore, when compared with the CON group, a significant increase in the diameter of the LV myocytes was observed in the EX group (14.77 ± 1.64 *vs*. 12.15 ± 1.42 μm for EX *vs*. CON; $P < 0.05$, n = 16; **Figure 1F**).

The indices of pathological cardiac hypertrophy (Lowes et al., 1997; Weinberg et al., 1999), such as the atrial natriuretic polypeptide (ANP), sarco-endoplasmic reticulum Ca^{2+}-ATPase (SERCA-2α), the skeletal muscle α-actin, and the ratio of α/β-myosin heavy chain (α/β-MHC), were not altered in the EX group compared to those in the CON group (**Figures 1G–J**). Diagram depicting the experimental process of this study was shown in **Figure 1K**.

Autophagy Is Markedly Enhanced in Swimming-Induced Physiological Cardiac Hypertrophy in Rats

To detect the activation of autophagy, the expression levels of LC3, Beclin 1, and SQSTM1 mRNAs and proteins were assessed by RT-qPCR and western blot analyses, respectively. The mRNA levels of LC3 II and Beclin 1 in the EX group (n=16) were obviously increased, by 2.53± 0.15- ($P < 0.01$) and 2.09 ± 0.13-fold ($P < 0.01$), respectively, compared to the respective levels in the CON group (n = 16), whereas the level of SQSTM1 mRNA was significantly decreased ($P < 0.01$) (**Figure 2A**). Furthermore, the expression levels of LC3 II and Beclin 1 proteins were upregulated in the EX group (the increase was by 1.93 ± 0.17- and 1.86 ± 0.12-fold compared with the respective levels in the CON group, and in both cases, the increase was significant at $P < 0.01$); the SQSTM1 protein level showed an obvious decrease with respect to its level in the CON group; $P < 0.01$ (**Figures 2B, C**).To further confirm the swimming exercise induced

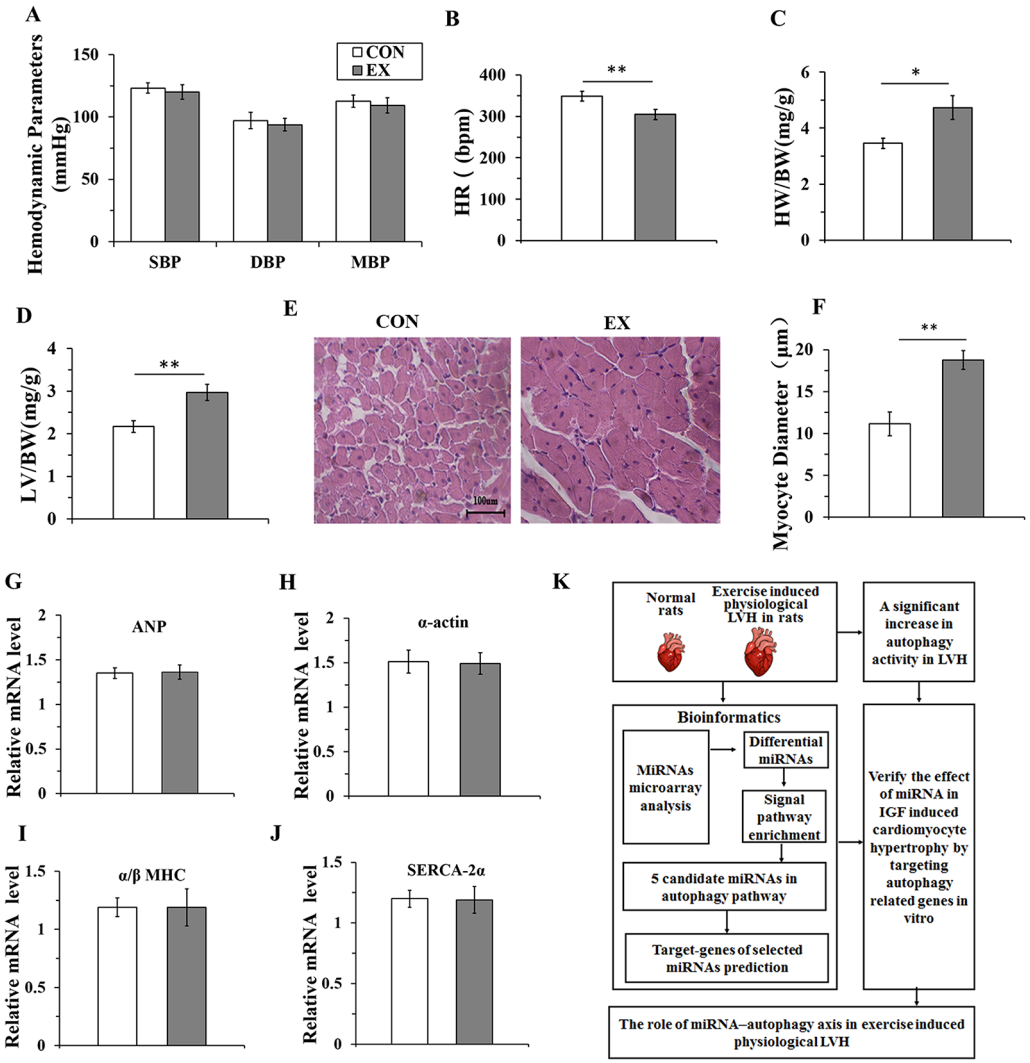

FIGURE 1 | Ten-weeks swimming exercise induces physiological cardiac hypertrophy in rats. **(A)**, The systolic blood pressure (SBP), diastolic blood pressure (DBP), and mean arterial pressure (MBP) in the control (CON) and swimming exercise (EX) groups. **(B)**, The heart rate (HR) in the EX group. **(C**, **D)**, Ten-week swimming exercise increased the HW/BW and LV/BW ratios in the EX group. BW, body weight; LV, left ventricular weight; HW, heart weight. **(E**, **F)**, Hematoxylin staining of LV myocytes in the CON group and EX group. Images were obtained at a magnification of ×400. **(G–J)**, The levels of atrial natriuretic polypeptide (ANP) and the skeletal muscle α-actin (α-actin), and the ratio of α/β-myosin heavy chain (α/β-MHC) and levels of sarco-endoplasmic reticulum Ca^{2+}-ATPase (SERCA-2α) in the CON group and EX group. **(K)**, Diagram depicting the experimental process of this study. * $P < 0.05$, ** $P < 0.01$, EX group (n=16) *vs*. CON group (n=16). Data are presented as mean ± SD. Statistical significance was evaluated with the two-tailed Student's t test.

autophagy, the protein levels of Atg4B, Atg5, Atg7, Atg12, and ULK1 in the LV were determined by western blot analysis. As shown in **Figures 2D, E**, the expression levels of these five proteins were significantly increased by 1.3 ± 0.18- ($P < 0.05$), 1.44 ± 0.12- ($P < 0.01$), 1.52 ± 0.16- ($P < 0.01$), 1.35 ± 0.11- ($P < 0.01$), and 1.21 ± 0.1- ($P < 0.05$) fold, respectively, in the EX group compared to their levels in the CON group. In addition, the ultrastructure of rat hearts were observed by electron microscopy. The double membrane structure of autophagosomes was observed in the EX group, whereas in the CON group, we did not observe the typical structure of autophagosomes (**Figure 2F**).

Microribonucleic Acid Targeting the Autophagy Pathway Are Significantly Downregulated in Physiological Cardiac Hypertrophy

Through miRNA microarray analysis, we found 216 differential miRNA (77 upregulated, 139 downregulated) between normal and exercised heart. GO analyses showed that most of the miRNA

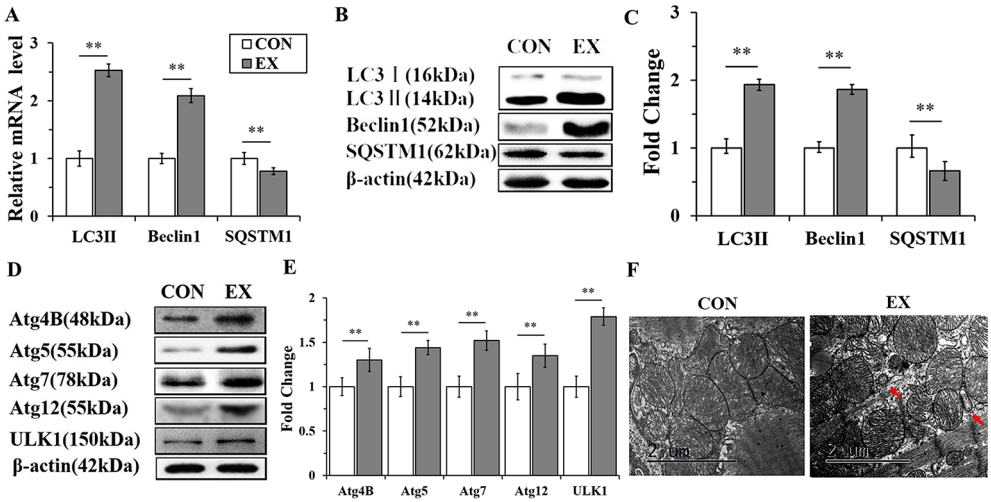

FIGURE 2 | Autophagy is markedly enhanced in swimming-induced physiological cardiac hypertrophy in rats. **(A)**, Real-time quantitative (RT-q)PCR analysis for mRNA expression of LC3B, Beclin 1, and SQSTM1 (relative to β-actin). **(B**, **C)**, Western blot analysis for LC3B, Beclin 1, and SQSTM1 (relative to β-actin). **(D**, **E)**, Western blot analysis of samples from CON and EX group detected Atg4B, Atg5, Atg7, Atg12 and ULK1. **(F)**, Representative transmission electron microscopic images of autophagosomes. Autophagosomes (red arrows). Images were obtained at a magnification ×13,000. Scale bar, 2 μm. ** $P < 0.01$, EX group (n=16) *vs*. CON group (n=16). Data are presented as means ± SD. Statistical significance was evaluated with the two-tailed Student's t test.

target gene was enriched in cell membrane structure (**Figure 3A**). A total of 83 pathways were enriched and we listed the top 10 pathways in the decreasing order of their enrichment scores. The autophagy pathway was the second most enriched pathway (**Figure 3B**, **Supplementary Table 2**). The autophagy pathway included 16 miRNAs (**Figure 3C**). Among them, one most upregulated (fold change >2.5) and four most downregulated (fold change <0.25) miRNA were selected and homology was analyzed. After analyzing the gene homology among rat, rhesus, and human sequences (**Figures 3D–H**) using DNAMAN software, we found that miR-26b-5p, miR-204-5p, miR-497-3p, let-7a-5p, and miR-181a-5p in rat were highly homologous to their human counterparts. We further analyzed these five miRNAs using RT-qPCR and found that miR-26b-5p, let-7a-5p, miR-204-5p, and miR-497-3p were significantly downregulated in the EX group ($P < 0.01$), whereas miR181a-5p was upregulated in the EX group (1.86-fold increase over expression in the CON group; $P < 0.05$) (**Figure 3I**).

Overexpression of miR-26b-5p, miR-204-5p, and miR-497-3p Attenuates IGF-1 Induced Cardiomyocyte Hypertrophy by Suppressing Autophagy

H9C2 cells were incubated with IGF-1 (10 μM) for 48 h to induce cardiomyocyte hypertrophy. As shown in **Figures 4A, B**, the cells stimulated with IGF-1 were markedly hypertrophic. However, IGF-1 upregulated the mRNA level of ANP and BNP ($P < 0.05$), but not α-actin (**Figure 4C**) ($P > 0.05$). Meanwhile, IGF-1 promoted autophagy activity with increased LC3II and Beclin1, and decreased SQSTM1 protein levels ($P < 0.01$, respectively) (**Figures 4D, E**). Then, the IGF-1 treated H9C2 cells were subjected to adenovirus-mediated miRNA infection. The cell surface area showed a significant decrease in the IGF-1+Ad-26b-5p, IGF-1+Ad-204-5p, and IGF-1+Ad-497-3p groups (**Figure 4F, G**) ($P < 0.01$, $P < 0.05$, $P < 0.01$, respectively), but no significant changes were observed in the other groups ($P > 0.05$). In addition, overexpression of miR-26b-5p, miR-204-5p, and miR-497-3p attenuated IGF-1 induced cardiomyocyte hypertrophy by downregulating ANP and BNP in both mRNA (**Figures 4H, I**) and protein levels (**Figures 4K–M**), while leaving α-actin unchanged (**Figures 4J, K, N**). These data indicated that IGF-1 stimulation obviously induced cardiomyocyte hypertrophy and that miR-26b-5p, miR-204-5p, and miR-497-3p could inhibit it.

To gain insights into the effects of miRNAs on IGF-1-induced autophagy, we performed immunofluorescence staining and western blot analysis. As shown in **Figures 5A, B**, Ad-26b-5p, Ad-204-5p, and Ad-497-3p infections significantly decreased the IGF-1 induced expression of LC3 II in cardiomyocyte hypertrophy, as reflected by reduced fluorescence ($P < 0.01$, $P < 0.05$, $P < 0.01$, respectively). The results of the western blot assay were consistent with those of immunofluorescence staining (**Figures 5C, D**). The infection with Ad-26b-5p, Ad-204-5p, and Ad-497-3p significantly decreased the IGF-1-induced expression of LC3 II and Beclin 1 proteins in cardiomyocyte hypertrophy ($P < 0.01$). Moreover, a marked increase in SQSTM1 was also observed ($P < 0.01$). In contrast, the levels of LC3 II, Beclin 1, and SQSTM1 were not changed significantly in cells infected with Ad-7a-5p and Anti-181a-5p ($P > 0.05$).

In addition, to investigate the mechanism of miR-26b-5p, miR-204-2p, and miR-497-3p mediated amelioration of

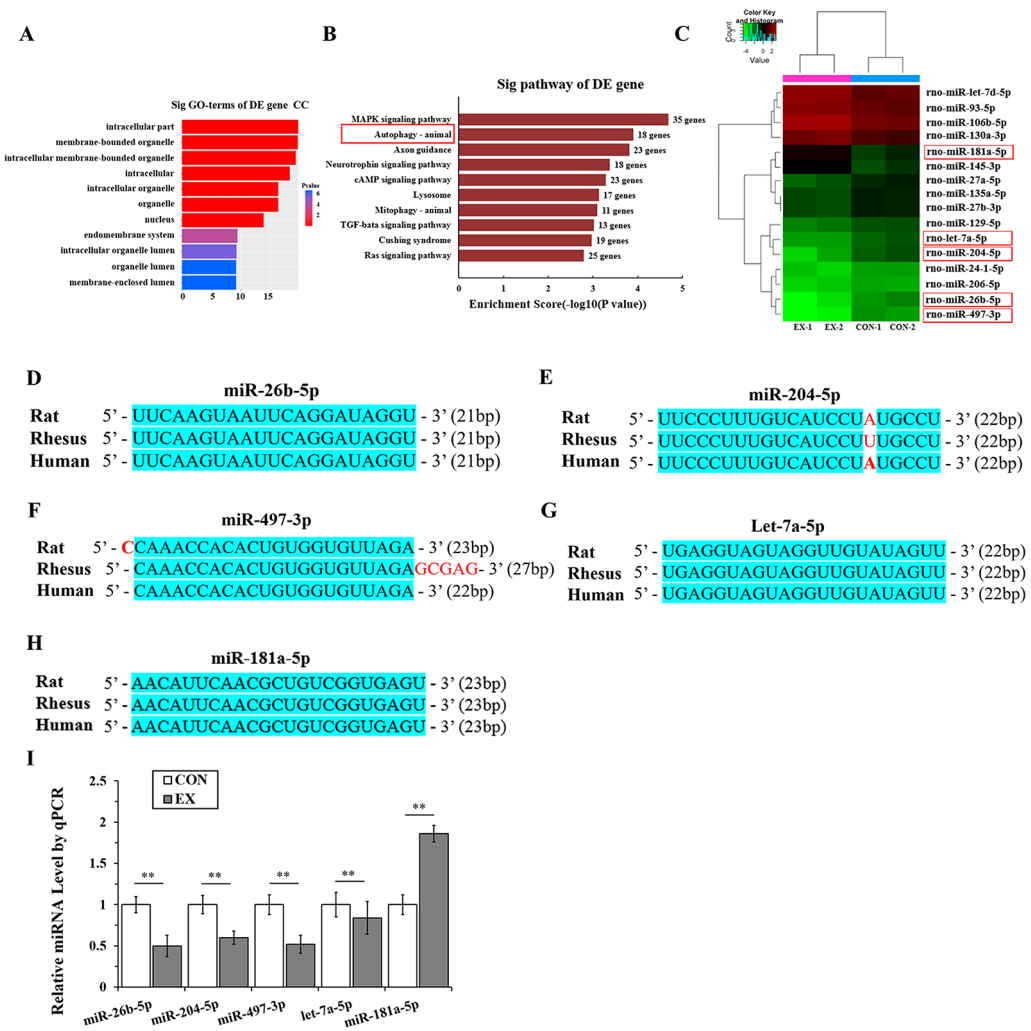

FIGURE 3 | MicroRNAs (miRNAs) targeting the autophagy pathway are significantly downregulated in physiological cardiac hypertrophy. **(A),** Gene ontology (GO) analyses showed that most of the miRNA target genes were enriched in cell membrane structure. **(B)**, Kyoto Encyclopedia of Genes and Genomes (KEGG) analyses. Horizontal axis indicates pathway enrichment score; vertical axis indicates the pathway name. The data label on the right stands for the differentially expressed (DE) gene number associated with the pathway. **(C)**, Heat map for clustering analysis of miRNA expression data in the CON (n = 2) and EX (n = 2) groups; the miRNAs in the red box are those that bind to the autophagy-related genes in LVH. **(D–H)**, The sequence homology among rat, rhesus, and human miRNAs; the blue shading area represents the same sequence. **(I)**, Determination of miRNAs by real-time (RT)-qPCR. Targeted miRNAs were normalized with respect to the U6 levels. ** $P < 0.01$, EX group (n=16) *vs*. CON group (n=16). Data are presented as means ± SD. Statistical significance was evaluated with the two-tailed Student's t test.

cardiomyocyte hypertrophy induced by IGF-1, we predicted that the autophagy-related genes, ULK1, LC3B, and Beclin 1, were the target genes of miR-26b-5p, miR-204-5p, and miR-497-3p, respectively (**Supplementary Table 3**). The predicted binding sites of miR-26b-5p, miR-204-5p, and miR-497-3p in the 3′-UTR of ULK1, LC3B, and Beclin 1, respectively, are listed in **Figure 5E**. The western blot analysis showed that in the cardiomyocytes infected with Ad-26b-5p, Ad-204-5p, and Ad-497-3p, the protein levels of these predicted target genes were markedly decreased ($P < 0.01$) (**Figures 5F–H**). These data indicated that IGF-1 induced cardiomyocyte hypertrophy was significantly suppressed by miR-26b-5p, miR-204-5p, and miR-497-3p through autophagy inhibition.

DISCUSSION

The degree of physiologic hypertrophy is associated with the intensity and duration of the exercise training and is also related to the aerobic or anaerobic metabolism (de Bold et al., 2001). Although cardiac hypertrophy induced by treadmills is widely observed, it has failed to induce cardiac hypertrophy in some

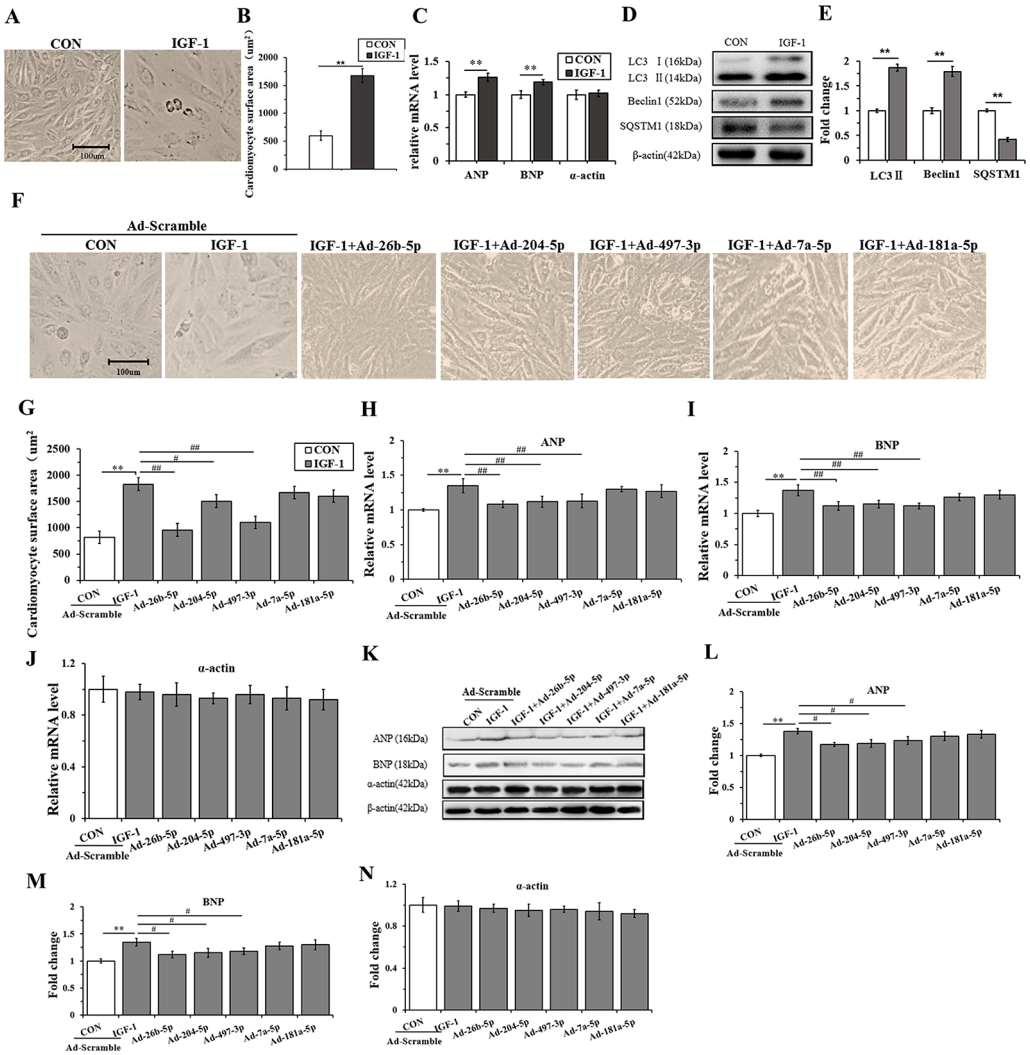

FIGURE 4 | Overexpression of miR-26b-5p, miR-204-5p, and miR-497-3p attenuates IGF-1 induced cardiomyocyte hypertrophy. **(A, B)**, The morphology of H9C2 cells treated with IGF-1 (10 μM)for 48 h. **(C)**, The messenger RNA (mRNA) levels of atrial natriuretic polypeptide (ANP), brain natriuretic peptide (BNP), and α-actin in H9C2 cells treated with IGF-1 (10 μM). **(D, E)**, The protein expression of autophagy maker (LC3B, Beclin1, and SQSTM1) of H9C2 cells treated with IGF-1 (10 μM). **(F, G)**, Cardiomyocyte surface area of H9C2 cells in response to IGF-1 (10 μM) with adenovirus-mediated microRNA (miRNA) infection. **(H–J)** mRNA levels of cardiomyocyte hypertrophy makers of H9C2 cells treated with IGF-1 (10 μM) and adenovirus mediated miRNAs. **(K–N)** Protein levels of cardiomyocyte hypertrophy makers of H9C2 cells treated with IGF-1 (10 μM) and adenovirus mediated miRNAs. ** $P < 0.01$, IGF+scramble (n=6) *vs*. CON+scramble group (n=6). $^{\#}P < 0.05$, $^{\#\#}P < 0.01$, miRNA adenovirus intervention group (n=6) *vs*. IGF-1+scramble group (n=6). Data are presented as means ± SD. Statistical significance was evaluated with the two-tailed Student's t test **(B**, **C**, **E)** and one-way analysis of variance with Bonferroni *post-hoc* analysis **(G–J**, **L–N)**.

cases (Wang et al., 2010). Accumulated evidences demonstrated that swimming training leads to LVH (Geenen et al., 1996; Pelliccia and Maron, 1997; Medeiros et al., 2004) and the degree of the hypertrophy is associated with the endurance (Kaplan et al., 1994; Evangelista and Krieger, 2006). Indeed, some researchers have observed that the swimming training induces robust cardiac hypertrophy when compared to treadmill training in rats and mice (Medeiros et al., 2004; Evangelista and Krieger, 2006; Oliveira et al., 2009; Wang et al., 2010; Soci et al., 2011). Thus, we chose the swimming training to study the mechanisms of physiological LVH. To induce physiological LVH in rats, we referred to the Bedford animal exercise load standard for setting the exercise intensity (Bedford et al., 1979). The 60-min swimming exercise employed in the present study was of moderate intensity for the rats. The 10-week moderate-intensity swimming exercise enlarged and thickened cardiomyocytes. Although an increase in cardiomyocyte volume is also observed in pathological cardiomegaly, increased fetal gene expression such as ANP, BNP, β-MHC were also significantly upregulated in pathological LVH (Swynghedauw, 1986; Dorn et al., 1994; Bernardo et al., 2010; Nakamura and Sadoshima, 2018; Oldfield et al., 2019). In our swimming exercise-induced cardiomyocyte hypertrophy, the

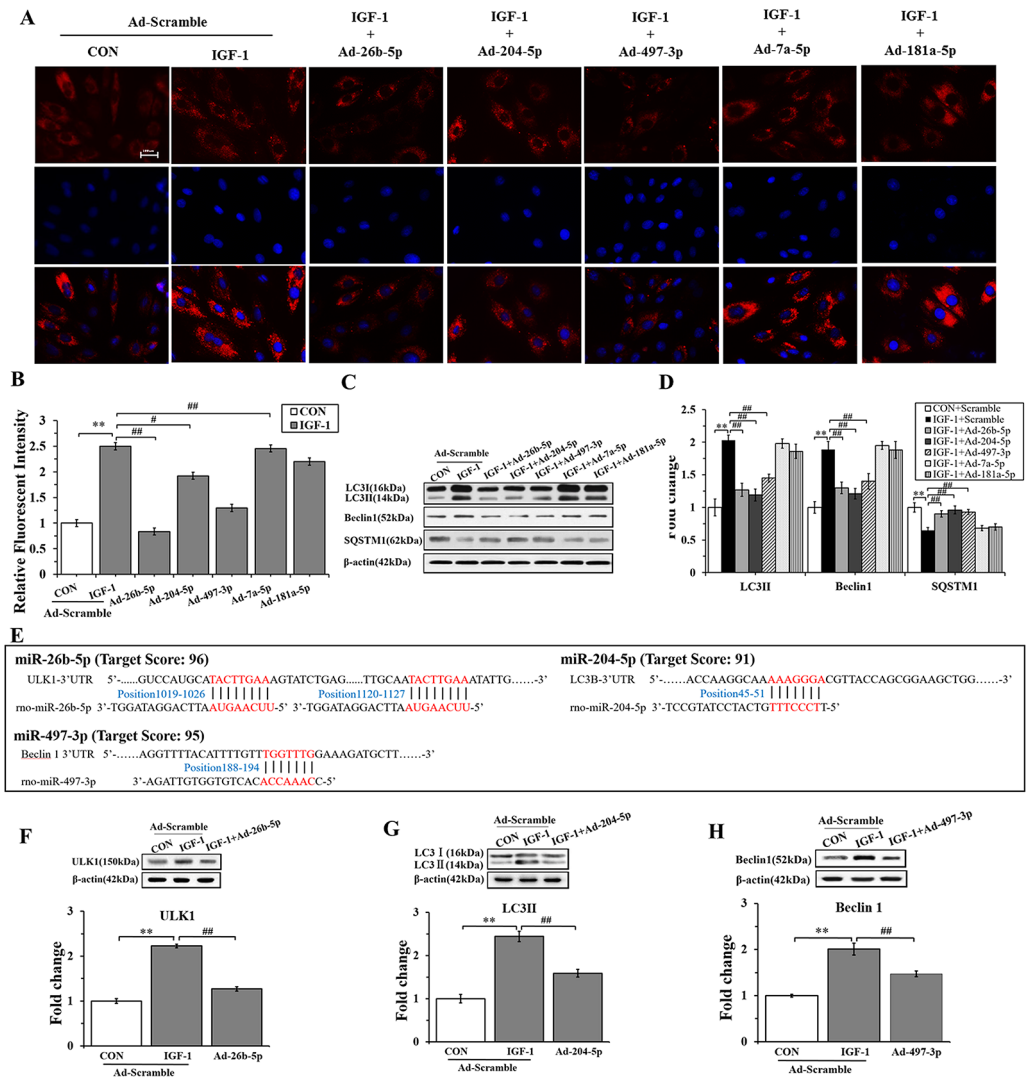

FIGURE 5 | miR-26b-5p, miR-204-5p, and miR-497-3p attenuate IGF-1 induced cardiomyocyte hypertrophy by suppressing autophagy **(A)**, microRNAs (miRNAs) adenovirus intervention in hypertrophic cardiomyocyte, LC3B immunofluorescence staining in various groups. **(B)** The LC3B fluorescent intensity in the various groups. **(C**, **D)**, Western blot analysis showing the expression of the autophagy markers (LC3B, Beclin 1, and SQSTM1). **(E)** The binding sites of miR-26b-5p, miR-204-5p, and miR-497-3p predicted using TargetScan. **(F)** Expression of LC3B protein in H9C2s and H9C2s subjected to adenovirus-mediated miR-204-5p over-expression or the control adenovirus. **(G)** Expression of ULK1 protein in H9C2 cells and in H9C2 cells subjected to adenovirus-mediated miR-26b-5p over-expression or to control adenovirus. **(H)** Expression of Beclin 1 protein in H9C2 cells and in H9C2 cells subjected to adenovirus-mediated miR-497-3p over-expression or control adenovirus. ** $P < 0.01$, IGF+scramble (n=6) *vs*. CON+scramble group (n=6). $^{\#}P < 0.05$, $^{\#\#} P < 0.01$, miRNA adenovirus intervention group (n=6) *vs*. IGF-1+scramble group (n=6). Data are presented as means ± SD. Statistical significance was evaluated with one-way analysis of variance with Bonferroni *post-hoc* analysis.

expression of ANP, α-actin, and the ratio of β-MHC to α-MHC was not significantly changed, indicating a physiological LVH model was successfully induced. Previous studies have shown that physiological cardiac hypertrophy is associated with an exercise-induced increase in the levels of IGF-1 (Neri Serneri et al., 2001). We found that the cardiomyocyte surface area in response to IGF-1 for 48 hours was significantly larger than that of the non-stimulated H9C2 cells, and the levels of hypertrophy markers (ANP and BNP) were also significantly increased in mRNA levels, while leaving α-actin mRNA unchanged, which is considered as a trigger for physiological cardiac hypertrophy (McMullen and Izumo, 2006; Weeks et al., 2017).

Autophagy is a highly conserved and ubiquitous metabolic pathway in living organisms (Sandoval et al., 2008). Previous studies have demonstrated that Beclin 1 is the earliest self-localizing gene in the structure of autophagic precursors and is believed to regulate other autophagic genes (Maejima et al., 2016; Sun et al., 2018), cardiac-specific overexpression of Beclin-1 promoted autophagy, and improved cardiac function. We observed a dramatic increase in LC3II and Beclin 1 in

physiological LVH of rat. In addition, 5 weeks of exercise induced activation of the autophagic pathway including enhanced expression of Atg5 and Atg7 and increased the LC3-II/LC3-I ratio (Willis et al., 2013). Knocking-out of the Atg5 gene or silencing of the Atg7 gene in cardiomyocytes, decreased the autophagic activity (Bernardo et al., 2010). We then measured the expression of Atg5 and Atg7, and found that the two genes were also obviously upregulated in LVH. Moreover, we found that the expression of other key autophagy-related genes such as ULK1, Atg12, and Atg4B, was significantly upregulated at the protein level in the left ventricle of rats with exercise-induced myocardial hypertrophy, whereas SQSTM1 (a marker of reduced autophagy) was downregulated. The findings are in concordance with previous results demonstrating that autophagy is enhanced by exercise training (He et al., 2012; Yan et al., 2017; Li et al., 2019; Moradi et al., 2019), and endurance exercise provided cardioprotective effect by upregulating autophagy (Lee et al., 2017). Consistently, a highly activated autophagy was also observed in IGF-1 induced cardiomyocyte hypertrophy, which was agreed with that IGF-1 inhibition attenuated autophagosome formation (Renna et al., 2013). Taken together, these results suggest that exercise training can increase the autophagy in cardiomyocytes, which plays an important role in physiological cardiac hypertrophy.

Exercise can induce cardiomegaly by upregulating or downregulating certain miRNAs in the myocardium and regulates cardiac hypertrophy and proliferation, cardiovascular regeneration, and myocardial interstitial hypertrophy (Fernandes et al., 2015; Ramasamy et al., 2015). A number of studies have shown that miRNAs play a key role in the regulation of autophagic pathways in different tissues (Frost and Olson, 2011; Lee et al., 2011; Lee et al., 2012; Patnaik et al., 2012; Roggli et al., 2012). Based on bioinformatics analysis, we found the target genes of the differential miRNAs between normal and physiological LVH were enriched in autophagy process. Three highly homologous miRNAs, miR-26b-5p, miR-204-5p, and miR-497-3p, were markedly decreased in rat heart with physiological LVH, which was consistent with the enhanced autophagy observed in physiological LVH. Moreover, overexpression of miR-26b-5p, miR-204-5p, and miR-497-3p attenuated IGF-1 induced cardiomyocyte hypertrophy by downregulating autophagy related genes. In agreement with our results, cardiac and plasma miR-26b expressions were significantly reduced in the transverse aortic constriction (TAC) induced cardiac hypertrophy model of rats (Zhang et al., 2013.). Overexpression of miR-26b reduced TAC- induced cardiac hypertrophy in mice (Han et al., 2012). In ischemia-reperfusion induced cardiomyocytes autophagy, miR-204 targeted LC3-II protein and was significantly down-regulated (Xiao et al., 2011). MiR-497 was also significantly reduced in Ang II-induced cardiomyocytes and TAC mice, overexpression of miR-497 reversed Ang II-induced cardiomyocytes protein synthesis and suppressed cardiac hypertrophy in TAC mice (Xiao et al., 2016). Thus, decreased miR-26b, miR-204 and miR-497 were associated with the increased autophagy and cardiac hypertrophy. Previous studies also demonstrated that ULK1 and LC3B were activated during cardiac hypertrophy, and Beclin1 mediated autophagy was also enhanced during right ventricular remodeling (Huang et al., 2015; Deng et al., 2017; Zhang et al., 2019), supporting our finding that ULK1, LC3B, and Beclin1 were up-regulated in physiological LVH. Given LVH in response to endurance exercise is protective, the miRNA changes in physiological LVH is supposed to be adaptive and to promote moderate autophagy which is essential for physiological LVH. Of note, miR-26b-5p, miR-204-5p, and miR-497-3p had been detected in plasma and were used as a potential diagnostic biomarker for diseases such as lung cancer (Du et al., 2015; Guo et al., 2015; Lu et al., 2018; Nakata et al., 2019). Distinct plasma gradients of miR-204-5p in the pulmonary circulation were observed in patients with different pulmonary hypertension subtypes (Estephan et al., 2019). Thus, the dynamic profile of these miRNA in plasma may help distinguish physiological and pathological LVH.

Taken together, cardiomyocyte autophagy has been considered to play a key role in controlling the hypertrophic response; miR-26b-5p, miR-204-5p, and miR-497-3p were found to play a major role in physiological cardiac hypertrophy by targeting their respective autophagy genes.

CONCLUSIONS

Our results demonstrate that long-term endurance swimming exercise may induce physiological LVH, at least in part, by modulating the microRNA–autophagy axis.

DATA AVAILABILITY STATEMENT

Our microarray data submitted to GEO has been assigned the GEO accession number GSE143935.

ETHICS STATEMENT

All researches involving animals were conducted according to animal ethics guidelines and approved by the Animal Care and Use Committee of Shanghai Normal University (Shanghai, China).

AUTHOR CONTRIBUTIONS

JZ designed the project and JQ contributed to data analysis and wrote the paper. XL developed the experimental design and contributed to data generation. BZ conducted the mRNA analysis from cardiac tissue. ZM and SL analyzed the protein expression in cardiac tissue and contributed to paper writing. JQ, XL, ZM, and BZ contributed to the work equally. All authors read and approved the manuscript.

FUNDING

This study was supported financially by the National Natural Science Foundation of China (Grant no. 31571223).

ACKNOWLEDGMENTS

We thank all the study participants, research staff, and students who assisted in animal sampling and technical support, and we give thanks to the members of Shen's team at Yangzhou University for their help with experimental processing.

SUPPLEMENTARY MATERIAL

The Supplementary Material for this article can be found online at: https://www.frontiersin.org/articles/10.3389/fgene.2020.00078/full#supplementary-material

REFERENCES

Aredia, F., and Scovassi, A. I. (2017). A new function for miRNAs as regulators of autophagy. *Future Med. Chem.* 9 (1), 25–36. doi: 10.4155/fmc-2016-0173

Bedford, T. G., Tipton, C. M., Wilson, N. C., Oppliger, R. A., and Gisolfi, C. V. (1979). Maximum oxygen consumption of rats and its changes with various experimental procedures. *J. Appl. Physiol. Respir. Environ. Exercise Physiol.* 47 (6), 1278–1283. doi: 10.1152/jappl.1979.47.6.1278

Bernardo, B. C., Weeks, K. L., Pretorius, L., and McMullen, J. R. (2010). Molecular distinction between physiological and pathological cardiiac hypertrophy: Experimental findings and therapeutic strategies. *Pharmacol. Ther.* 128 (1), 191–227. doi: 10.1016/j.pharmthera.2010.04.005

Bernardo, B. C., Ooi, J. Y. Y., Weeks, K. L., Patterson, N. L., and McMullen, J. R. (2018). Understanding key mechanisms of exercise-induced cardiac protection to mitigate disease: current knowledge and emerging concepts. *Physiol. Rev.* 98 (1), 419–475. doi: 10.1152/physrev.00043.2016

Brandt, N., Gunnarsson, T. P., Bangsbo, J., and Pilegaard, H. (2018). Exercise and exercise training-induced increase in autophagy markers in human skeletal muscle. *Physiol. Rep.* 6 (7), e13651. doi: 10.14814/phy2.13651

Carè, A., Catalucci, D., Felicetti, F., Bonci, D., Addario, A., Gallo, P., et al. (2007). MicroRNA-133 controls cardiac hypertrophy. *Nat. Med.* 13 (5), 613–618. doi: 10.1038/nm1582

Chen, L., Zhou, Y., Sun, Q., Zhou, J., Pan, H., and Sui, X. (2017). Regulation of Autophagy by MiRNAs and their emerging roles in tumorigenesis and cancer treatment. *Int. Rev. Cell Mol. Biol.* 334, 1–26. doi: 10.1016/bs.ircmb.2017.03.003

de Bold, A. J., Ma, K. K., Zhang, Y., de Bold, M. L., Bensimon, M., and Khoshbaten, A. (2001). The physiological and pathophysiological modulation of the endocrine function of the heart. *Can. J. Physiol. Pharmacol.* 79 (8), 705–714. doi: 10.1139/cjpp-79-8-705

Deng, Y., Wu, W., Guo, S., Chen, Y., Liu, C., Gao, X., et al. (2017). Altered mTOR and Beclin-1 mediated autophagic activation during right ventricular remodeling in monocrotaline-induced pulmonary hypertension. *Respir. Res.* 18 (1), 53. doi: 10.1186/s12931-017-0536-7

Dorn, G. W.2nd, Robbins, J., Ball, N., and Walsh, R. A. (1994). Myosin heavy chain regulation and myocyte contractile depression after LV hypertrophy in aortic-banded mice. *Am. J. Physiol.* 267 (1 Pt 2), H400–H405. doi: 10.1152/ajpheart.1994.267.1.H400

Dorn, G. W.2nd (2007). The fuzzy logic of physiological cardiac hypertrophy. *Hypertension* 49 (5), 962–9705. doi: 10.1161/HYPERTENSIONAHA.106.079426

Du, M. L., Shi, D. N., Yuan, L., Li, P. C., Chu, H. Y., Qin, C., et al. (2015). Circulating miR-497 and miR-663b in plasma are potential novel biomarkers for bladder cancer. *Sci. Rep.* 5, 10437. doi: 10.1038/srep10437

Estephan, L. E., Genuardi, M. V., Kosanovich, C. M., Risbano, M. G., Zhang, Y., Petro, N., et al. (2019). Distinct plasma gradients of microRNA-204 in the pulmonary circulation of patients suffering from WHO Groups I and II pulmonary hypertension. *Pulm. Circ.* 9 (2), 2045894019840646. doi: 10.1177/2045894019840646

Evangelista, F. S., and Krieger, J. E. (2006). Small gene effect and exercise training-induced cardiac hypertrophy in mice: an Ace gene dosage study. *Physiol. Genomics* 27 (3), 231–236. doi: 10.1152/physiolgenomics.00022.2006

Fernandes, T., Hashimoto, N. Y., Magalha˜es, F. C., Fernandes, F. B., Casarini, D. E., Carmona, A. K., et al. (2011). Aerobic exercise training-induced left ventricular hypertrophy involves regulatory microRNAs, decreased angiotensin-converting enzyme-angiotensin II, and synergistic regulation of angiotensin converting enzyme 2-angiotensin (1–7). *Hypertension* 58 (2), 182–1895. doi: 10.1161/HYPERTENSIONAHA.110.168252

Fernandes, T., Baraúna, V. G., Negrão, C. E., Phillips, M. I., and Oliveira, E. M. (2015). Aerobic exercise training promotes physiological cardiac remodeling involving a set of microRNAs. *Am. J. Physiol. Heart Circ. Physiol.* 309 (4), H543–H552. doi: 10.1152/ajpheart.00899.2014

Fritzen, A. M., Madsen, A. B., Kleinert, M., Treebak, J. T., Lundsgaard, A. M., Jensen, T. E., et al. (2016). Regulation of autophagy in human skeletal muscle: effects of exercise, exercise training and insulin stimulation. *J. Physiol.* 594 (3), 745–761. doi: 10.1113/JP271405

Frost, R. J., and Olson, E. N. (2011). Control of glucose homeostasis and insulin sensitivity by the Let-7 family of microRNAs. *Proc. Natl. Acad. Sci. U. S. A.* 108 (52), 21075–21080. doi: 10.1073/pnas.1118922109

Geenen, D. L., Malhotra, A., and Buttrick, P. M. (1996). Angiotensin receptor 1 blockade does not prevent physiological cardiac hypertrophy in the adult rat. *J. Appl. Physiol.* 81 (2), 816–821. doi: 10.1152/jappl.1996.81.2.816

Gottlieb, R. A., and Mentzer, R. M.Jr. (2013). Autophagy: an affair of the heart. *Heart Fail Rev.* 18 (5), 575–584. doi: 10.1007/s10741-012-9367-2

Guo, W., Zhang, Y., Zhang, Y., Shi, Y., Xi, J., Fan, H., et al. (2015). Decreased expression of miR-204 in plasma is associated with a poor prognosis in patients with non-small cell lung cancer. *Int. J. Mol. Med.* 36 (6), 1720–1726. doi: 10.3892/ijmm.2015.2388

Halling, J. F., and Pilegaard, H. (2017). Autophagy-dependent beneficial effects of exercise. *Cold Spring Harb Perspect. Med.* 7 (8), a029777. doi: 10.1101/cshperspect.a029777

Han, M., Yang, Z., Sayed, D., He, M., Gao, S., Lin, L., et al. (2012). GATA4 expression is primarily regulated *via a* miR-26b-dependent post-transcriptional mechanism during cardiac hypertrophy. *Cardiovasc. Res.* 93 (4), 645–654. doi: 10.1093/cvr/cvs001

He, C., Bassik, M. C., Moresi, V., Sun, K., Wei, Y., Zou, Z., et al. (2012). Exercise-induced Bcl_2-regulated autophagy is required for muscle glucose homeostasis. *Nature* 481 (7382), 511–515. doi: 10.1038/nature10758

Huang, J., Pan, W., Ou, D., Dai, W., Lin, Y., Chen, Y., et al. (2015). LC3B, a Protein that serves as an autophagic marker, modulates Angiotensin II-induced Myocardial Hypertrophy. *J. Cardiovasc. Pharmacol.* 66 (6), 576–583. doi: 10.1097/FJC.0000000000000306

Jacobsen, A., Silber, J., Harinath, G., Huse, J. T., and Schultz, C. (2013). Analysis of microRNA-target interactions across diverse cancer types. *Nat. Struct. Mol. Biol.* 20, 1325–1332. doi: 10.1038/nsmb.2678

Kaplan, M. L., Cheslow, Y., Vikstrom, K., Malhotra, A., Geenen, D. L., Nakouzi, A., et al. (1994). Cardiac adaptations to chronic exercise in mice. *Am. J. Physiol.* 267 (3 Pt 2), H1167–H1173. doi: 10.1152/ajpheart.1994.267.3.H1167

Lee, E. K., Lee, M. J., Abdelmohsen, K., Kim, W., Kim, M. M., Srikantan, S., et al. (2011). miR-130 suppresses adipogenesis by inhibiting peroxisome proliferator- activated receptor gamma expression. *Mol. Cell Biol.* 31 (4), 626–638. doi: 10.1128/MCB.00894-10

Lee, S. T., Chu, K., Jung, K. H., Kim, J. H., Huh, J. Y., Yoon, H., et al. (2012). miR-206 regulates brain derived neurotrophic factor in Alzheimer disease model. *Ann. Neurol.* 72 (2), 269–277. doi: 10.1002/ana.23588

Lee, Y., Kwon, I., Jang, Y., Song, W., Cosio-Lima, L. M., and Roltsch, M. H. (2017). Potential signaling pathways of acute endurance exercise-induced cardiac

autophagy and mitophagy and its possible role in cardioprotection. *J. Physiol. Sci.* 67 (6), 639–654. doi: 10.1007/s12576-017-0555-7

Li, Y., Yao, M., Zhou, Q., Cheng, Y., Che, L., Xu, J., et al. (2018b). Dynamic regulation of circulating microRNAs during acute exercise and long-term exercise training in basketball athletes. *Front. Physiol.* 9, 282. doi: 10.3389/fphys.2018.00282

Li, J. Y., Pan, S. S., Wang, J. Y., and Lu, J. (2019). Changes in autophagy levels in rat myocardium during exercise preconditioning-initiated cardioprotective effects. *Int. Heart J.* 60 (2), 419–428. doi: 10.1536/ihj.18-310

Lira, V. A., Okutsu, M., Zhang, M., Greene, N. P., Laker, R. C., Breen, D. S., et al. (2013). Autophagy is required for exercise training-induced skeletal muscle adaption and improvement of physical performance. *FASEB J.* 27 (10), 4184–4193. doi: 10.1096/fj.13-228486

Liu, W., and Wang, X. (2019). Prediction of functional microRNA targets by integrative modeling of microRNA binding and target expression data. *Genome Biol.* 20 (1), 18. doi: 10.1186/s13059-019-1629-z

Lowes, B. D., Minobe, W., Abraham, W. T., Rizeq, M. N., Bohlmeyer, T. J., Quaife, R. A., et al. (1997). Changes in gene expression in the intact human heart. *J. Clin. Invest.* 100 (9), 315–2324. doi: 10.1172/JCI119770

Lu, S., Kong, H., Hou, Y., Ge, D., Huang, W., Ou, J., et al. (2018). Two plasma microRNA panels for diagnosis and subtype discrimination of lung cancer. *Lung Cancer* 123, 44–51. doi: 10.1016/j.lungcan.2018.06.027

Ma, Z. C., Qi, J., Meng, S., Wen, B. J., and Zhang, J. (2013). Swimming exercise training-induced left ventricular hypertrophy involves microRNAs and synergistic regulation of the PI3K/AKT/mTOR signaling pathway. *Eur. J. Appl. Physio.l.* 113 (10), 2473–2486. doi: 10.1007/s00421-013-2685-9

Maejima, Y., Isobe, M., and Sadoshima, J. J. (2016). Regulation of autophagy by Beclin 1 in the heart. *Mol. Cell Cardiol.* 95, 19–25. doi: 10.1016/j.yjmcc.2015.10.032

Martinelli, N. C., Cohen, C. R., Santos, K. G., Castro, M. A., Biolo, A., Frick, L., et al. (2014). An analysis of the global expression of microRNAs in an experimental model of physiological left ventricular hypertrophy. *PloS One* 9 (4), e93271. doi: 10.1371/journal.pone.0093271

Martin-Rincon, M., Morales-Alamo, D., and Calbet, J. A. L. (2018). Exercise-mediated modulation of autophagy in skeletal muscle. *Scand. J. Med. Sci. Sports* 28 (3), 772–781. doi: 10.1111/sms.12945

McMullen, J. R. , and Izumo, S. (2006). Role of the insulin-like growth factor 1 IGF1)/phosphoinositide- 3 - kinase (PI3K) pathway mediating physiological cardiac hypertrophy. *Novartis Found. Symp.* 274, 90–111. discussion 111-117, 152-155, 272-276. doi: 10.1002/0470029331.ch7

Medeiros, A., Oliveira, E. M., Gianolla, R., Casarini, D. E., Negrao, C. E., and Brum, P. C. (2004). Swimming training increases cardiac vagal activity and induces cardiac hypertrophy in rats. *Braz. J. Med. Biol. Res.* 37 (12), 1909–1917. doi: 10.1590/s0100-879x2004001200018

Melo, S. F., Barauna, V. G., Júnior, M. A., Bozi, L. H., Drummond, L. R., Natali, A. J., et al. (2015). Resistance training regulates cardiac function through modulation of miRNA-214. *Int. J. Mol. Sci.* 16 (4), 6855–6867. doi: 10.3390/ijms16046855

Moradi, F., Imani, A. R., and Faghihi, M. (2019). Effects of regular exercise plus food restriction on left ventricular pathological remodeling in heart failure-induced rats. *Bratisl Lek Listy* 120(4), 243–248. doi: 10.4149/BLL_2019_044

Nadal, M., and Gold, S. E. (2012). Assessment of autophagosome formation by transmission electron microcopy. *Methods Mol. Biol.* 835, 481–489. doi: 10.1007/978-1-61779-501-5_29

Nakamura, M., and Sadoshima, J. (2018). Mechanisms of physiological and pathological cardiac hypertrophy. *Nat. Rev. Cardiol.* 15 (7), 387–407. doi: 10.1186/s12917-019-1944-3

Nakata, K., Heishima, K., Sakai, H., Yamato, O., Furusawa, Y., Nishida, H., et al. (2019). Plasma microRNA miR-26b as a potential diagnostic biomarker of degenerative myelopathy in Pembroke welsh corgis. *BMC Vet. Res.* 15 (1), 192. doi: 10.1186/s12917-019-1944-3

Neri Serneri, G. G., Boddi, M., Modesti, P. A., Cecioni, I., Coppo, M., Padeletti, L., et al. (2001). Increased cardiac sympathetic activity and insulin-like growth factor-I formation are associated with physiological hypertrophy in athletes. *Circ. Res.* 89 (11), 977–982. doi: 10.1161/hh2301.100982

Oldfield, C. J., Duhamel, T. A., and Dhalla, N. S. (2019). Mechanisms for the transition from physiological to pathological cardiac hypertrophy. *Can. J. Physiol. Pharmacol.* doi: 10.1139/cjpp-2019-0566

Oliveira, E. M., Sasaki, M. S., Cere^ncio, M., Barau´na, V. G., and Krieger, J. E. (2009). Local reninangiotensin system regulates left ventricular hypertrophy induced by swimming training independent of circulating renin: a pharmacological study. *J. Renin Angiotensin Aldosterone Syst.* 10 (1), 15–23. doi: 10.1177/1470320309102304

Patnaik, S. K., Dahlgaard, J., Mazin, W., Kannisto, E., Jensen, T., Knudsen, S., et al. (2012). Expression of microRNAs in the NCI-60 cancer cell-lines. *PloS One* 7 (11), e49918. doi: 10.1371/journal.pone.0049918

Pelliccia, A., and Maron, B. J. (1997). Outer limits of the athlete's heart, the effect of gender, and relevance to the differential diagnosis with primary cardiac diseases. *Cardiol. Clin.* 15 (3), 381–396. doi: 10.1016/S0733-8651(05)70347-7

Ramasamy, S., Velmurugan, G., Shanmugha Rajan, K., Ramprasath, T., and Kalpana, K. (2015). MiRNAs with apoptosis regulating potential are differentially expressed in chronic exercise-induced physiologically hypertrophied hearts. *PloS One* 10 (13), e0121401. doi: 10.1371/journal.pone.0121401

Renna, M., Bento, C. F., Fleming, A., Menzies, F. M., Siddiqi, F. H., Ravikumar, B., et al. (2013). IGF-1 receptor antagonism inhibits autophagy. *Hum. Mol. Genet.* 22 (22), 4528–4544. doi: 10.1093/hmg/ddt300

Roggli, E., Gattesco, S., Caille, D., Briet, C., Boitard, C., Meda, P., et al. (2012). Changes in microRNA expression contribute to pancreatic beta-cell dysfunction in prediabetic NOD mice. *Diabetes* 61 (7), 1742–1751. doi: 10.2337/db11-1086

Sanchez, A. M. (2016). Autophagy regulation in human skeletal muscle during exercise. *J. Physiol.* 594 (18), 5053–5054. doi: 10.1113/JP272993

Sandoval, H., Thiagarajan, P., Dasgupta, S. K., Schumacher, A., Prchal, J. T., Chen, M., et al. (2008). Essential role for Nix in autophagic maturation of erythroid cells. *Nature* 454 (7201), 232–235. doi: 10.1038/nature07006

Schiattarella, G. G., and Hill, J. A. (2015). Inhibition of hypertrophy is a good therapeutic strategy in ventricular pressure overload. *Circulation* 131 (16), 1435–1447. doi: 10.1161/CIRCULATIONAHA.115.013894

Shen, G., Ren, H., Qiu, T., Liang, D., Xie, B., Zhang, Z., et al. (2016). Implications of the interaction between miRNAs and Autophagy in Osteoporosis. *Calcif. Tissue Int.* 99 (1), 1–12. doi: 10.1007/s00223-016-0122-x

Soci, U. P., Fernandes, T., Hashimoto, N. Y., Mota, G. F., Amadeu, M. A., Rosa, K. T., et al. (2011). MicroRNAs 29 are involved in the improvement of ventricular compliance promoted by aerobic exercise training in rats. *Physiol. Genomics* 43 (11), 665–673. doi: 10.1152/physiolgenomics.00145.2010

Sun, Y., Yao, X., Zhang, Q. J., Zhu, M., Liu, Z. P., Ci, B., et al. (2018). Beclin-1-Dependent Autophagy Protects the Heart During Sepsis. *Circulation* 138 (20), 2247–2262. doi: 10.1161/CIRCULATIONAHA.117.032821

Swynghedauw, B. (1986). Developmental and functional adaptation of contractile proteins in cardiac and skeletal muscles. *Physiol. Rev.* 66 (3), 710–771. doi: 10.1152/physrev.1986.66.3.710

Wang, Y., Wisloff, U., and Kemi, O. J. (2010). Animal models in the study of exercise-induced cardiac hypertrophy. *Physiol. Res.* 59 (5), 633–644. doi: 10.1088/0967-3334/31/1/R01

Weeks, K. L., Bernardo, B. C., Ooi, J. Y. Y., Patterson, N. L., and McMullen, J. R. (2017). The IGF1-PI3K-Akt signaling pathway in mediating exercise-induced cardiac hypertrophy and protection. *Adv. Exp. Med. Biol.* 1000, 187–210. doi: 10.1007/978-981-10-4304-8_12

Weinberg, E. O., Thienelt, C. D., Katz, S. E., Bartunek, J., Tajima, M., Rohrbach, S., et al. (1999). Gender differences in molecular remodeling in pressure overload hypertrophy. *J. Am. Coll. Cardiol.* 34 (1), 264–273. doi: 10.1016/s0735-1097(99)00165-5

Willis, M. S., Min, J. N., Wang, S., McDonough, H., Lockyer, P., Wadosky, K. M., et al. (2013). Carboxyl terminus of Hsp70-interacting protein (CHIP) is required to modulate cardiac hypertrophy and attenuate autophagy during exercise. *Cell Biochem. Funct.* 31 (8), 724–735. doi: 10.1002/cbf.2962

Xiao, J., Zhu, X., He, B., Zhang, Y., Kang, B., Wang, Z., et al. (2011). MiR-204 regulates cardiomyocyte autophagy induced by ischemia-reperfusion through LC3-II. *J. BioMed. Sci.* 18, 35. doi: 10.1186/1423-0127-18-35

Xiao, J. J., Xu, T. Z., Li, J., Lv, D. C., Chen, P., Zhou, Q. L., et al. (2014). Exercise-induced physiological hypertrophy initiates activation of cardiac progenitor cells. *Int. J. Clin. Exp. Pathol.* 7 (2), 663–669.

Xiao, Y., Zhang, X., Fan, S., Cui, G., and Shen, Z. (2016). MicroRNA-497 inhibits cardiac Hypertrophy by targeting Sirt4. *PloS One* 11 (12), e0168078. doi: 10.1371/journal.pone.0168078

Yan, Z., Kronemberger, A., Blomme, J., Call, J. A., Caster, H. M., Pereira, R. O., et al. (2017). Exercise leads to unfavourable cardiac remodelling and enhanced metabolic homeostasis in obese mice with cardiac and skeletal muscle autophagy deficiency. *Sci. Rep.* 7 (1), 7894. doi: 10.1038/s41598-017-08480-2

Zhang, Y., and Chen, N. (2018). Autophagy is a promoter for aerobic exercise performance during high altitude training. *Oxid. Med. Cell Longev.* 2018, 3617508. doi: 10.1155/2018/3617508

Zhang, Z. H., Li, J., Liu, B. R., Luo, C. F., Dong, Q., Zhao, L. N., et al. (2013). MicroRNA-26 was decreased in rat cardiac hypertrophy model and may be a promising therapeutic target. *J. Cardiovasc. Pharmacol.* 62 (3), 312–319. doi: 10.1097/FJC.0b013e31829b82e6

Zhang, A., Wang, M., and Zhuo, P. (2019). Unc-51 like autophagy activating kinase 1 accelerates angiotensin II-induced cardiac hypertrophy through promoting oxidative stress regulated by Nrf-2/HO-1 pathway. *Biochem. Biophys. Res. Commun.* 509 (1), 32–39. doi: 10.1016/j.bbrc.2018.11.190

Conflict of Interest: The authors declare that the research was conducted in the absence of any commercial or financial relationships that could be construed as a potential conflict of interest.

frontiers in Cell and Developmental Biology

REVIEW
published: 28 February 2020
doi: 10.3389/fcell.2020.00071

miRNAs in the Diagnosis and Prognosis of Skin Cancer

Monica Neagu[1,2,3], Carolina Constantin[1,3], Sanda Maria Cretoiu[4] and Sabina Zurac[3,5]*

[1] Immunology Laboratory, "Victor Babeş" National Institute of Pathology, Bucharest, Romania, [2] Doctoral School, Faculty of Biology, University of Bucharest, Bucharest, Romania, [3] Department of Pathology, Colentina Clinical Hospital, Bucharest, Romania, [4] Division of Cell and Molecular Biology and Histology, "Carol Davila" University of Medicine and Pharmacy, Bucharest, Romania, [5] Department of Pathology, Faculty of Dental Medicine, "Carol Davila" University of Medicine and Pharmacy, Bucharest, Romania

Skin cancer is, at present, the most common type of malignancy in the Caucasian population. Its incidence has increased rapidly in the last decade for both melanoma and non-melanoma skin cancer. Differential expression profiles of microRNAs (miRNAs) have been reported for a variety of different cancers, including skin cancers. Since miRNAs' discovery as regulators of gene expression, their importance grew in the field of oncology. miRNAs can post-transcriptionally regulate gene expression, tumor initiation, development progression, and aggressiveness. Nowadays, these short regulatory RNAs are perceived as one of the epigenetic markers for the identification of new diagnostic and/or prognostic molecular markers. Moreover, as miRNAs can drive tumorigenesis, they might eventually represent new therapy targets. Some miRNAs are pleiotropic, such as miR-214, which was found deregulated in several other tumors besides skin cancers. Some others are specific for one or more skin cancer types, like miR-21 and miR-221 for cutaneous melanoma and cutaneous squamous carcinoma or miR-155 for melanoma and cutaneous lymphoma. The goal of this review was to summarize some of the main miRNA detection technologies that are used to evaluate miRNAs in tissues and body fluids. Furthermore, their quantification limits, conformity, and robustness are discussed. Aberrant miRNA expression is analyzed for cutaneous melanoma, cutaneous squamous cell carcinoma (CSCC), skin lymphomas, cutaneous lymphoma, and Merkel cell carcinoma (MCC). In this type of disease, miRNAs are described as potential biomarkers to diagnose early lesion and/or early metastatic disease. In the future, whether in tissue or circulating in body fluids, miRNAs will gain their place in skin cancer diagnosis, prognosis, and future therapeutic targets.

Keywords: miRNA, cutaneous melanoma, cutaneous squamous carcinoma, cutaneous lymphoma, Merkel cell carcinoma

OPEN ACCESS

Edited by:
Saumya Das,
Harvard Medical School,
United States

Reviewed by:
Kamalakannan Rajasekaran,
Genentech, Inc., United States
George Calin,
University of Texas MD Anderson Cancer Center, United States

***Correspondence:**
Carolina Constantin
caroconstantin@gmail.com

Specialty section:
This article was submitted to Signaling, a section of the journal Frontiers in Cell and Developmental Biology

Received: *23 September 2019*
Accepted: *27 January 2020*
Published: *28 February 2020*

Citation:
Neagu M, Constantin C, Cretoiu SM and Zurac S (2020) miRNAs in the Diagnosis and Prognosis of Skin Cancer. Front. Cell Dev. Biol. 8:71. doi: 10.3389/fcell.2020.00071

INTRODUCTION

In the last decade, the dramatic increase of diseases that are linked to changes in RNA modifications has shown that the epitranscriptomic domain will impact health science. Innovative methods used for molecular modification pattern detection will further lead to the expansion of improved diagnosis and new therapeutics will be approved for various human diseases (Jantsch et al., 2018).

MicroRNAs (miRNAs) are a large group of short, non-coding RNA molecules that are approximately 22-nt long and are involved in post-transcriptional control of gene expression (Quinodoz and Guttman, 2014). Their action is completed by base pairing with messenger RNA (mRNA) transcripts that encompass target sequences, resulting in an increase of mRNA decay and/or translational attenuation (Caron et al., 2012). Through this action, miRNAs are involved in many physiological processes, and any deregulations at this level will trigger abnormalities and further human diseases (Cretoiu et al., 2016a,b). The involvement of miRNAs in pathological processes has made them to be recognized as potential therapeutic targets as well as future biomarkers with diagnostic and/or prognostic potential (Horsham et al., 2015; Monroig-Bosque Pdel et al., 2015).

There is also a series of unconventional roles for these molecules. Thus, miRNAs can activate Toll-like receptors displaying a pro-inflammatory/pro-metastatic potential, and hence, specific miRNAs can become future therapy targets. Also, miRNAs can act on protein expression in a cell cycle-dependent manner. For example, miR-369 directs the association of Argonaute (AGO2) protein and fragile X mental retardation-related protein 1 (FXR1) with AU-rich elements (AREs) in tumor necrosis factor alpha (TNF-a) mRNA to activate translation (Vasudevan et al., 2007). Nevertheless, miRNAs associate with non-AGO proteins acting as a decoy for another RNA binding protein interfering with its function. At the mitochondrial level, miRNAs have been shown to inhibit mitochondrially encoded cytochrome c oxidase subunit 1 (MT-COX1) protein expression while increasing MT-COX2 mRNA expression (Das et al., 2012). miRNAs that are localized in the nucleus can inhibit the maturation of other miRNAs *via* direct interaction with the primary transcript, an interaction that can lead to hindering apoptosis. Last, but not least, miRNAs can directly activate transcription. Therefore, miRNAs with AGO1/AGO2 can be imported into the nucleus and bind to the promoter RNA of cyclooxygenase-2 (COX2), leading to COX2 transcription (Matsui et al., 2013). Classic miRNAs functioning along with unconventional pathways prove that miRNAs are involved in complex cellular regulatory functions (Dragomir et al., 2018).

Therefore, miRNAs were brought into the spotlight because they were found to regulate and to be regulated in tumorigenesis seminal processes like tumor development, progression, and metastasis/aggressiveness of all types of cancer (Albulescu et al., 2011; Bobbili et al., 2017). For example, recently, the miR-17-92 cluster was identified as overexpressed in many tumors, promoting uncontrolled cell proliferation (Liu et al., 2017; Zhang et al., 2018). Within this cluster, miR-17-5p is associated with cancer aggressiveness and therapy responsiveness in liver, gastric, or colorectal cancers, where it has an oncogene function. In other cancers, such as breast, prostate, and lung cancers, it can have a tumor-suppressive action (Li et al., 2017; Liu et al., 2017). Moreover, miR-17-5p has also been found elevated in the circulation of patients diagnosed with various cancers (Monroig-Bosque Pdel et al., 2015; Bobbili et al., 2017). Another example is miR-7, a molecule generated from three different genes, regulating major cellular processes, this finding pointing out the complexity of miRNA generation. Besides several other cancers, miR-7 is involved in skin cancer, having the potency to be further developed as a biomarker and future therapy target (Horsham et al., 2015).

Mouse models are used to decipher the dynamics of molecular events. In a skin carcinogenesis mouse model, the miRNA-200 family members were found correlated with staging and progression. miR-205-5p overexpression in spindle cancer cells was shown to decrease tumor cell proliferation and invasiveness (Skourti et al., 2016).

Out of all skin cancers, the most abundant studies regarding miRNA evaluation are developed in cutaneous melanoma.

In this direction, miR-214, a pleiotropic molecule, was found deregulated in melanoma, this RNA molecule coordinating important signaling networks (e.g. PTEN/AKT, β-catenin, and tyrosine kinase receptor pathways), gene expression modulators (e.g. Ezh2, p53, and TFAP2), and even other miRNAs like miR-148b. Through all these functions, it is involved in tumor cell proliferation, in particular tumor cell characteristics like stemness, invasiveness, and other complex processes like angiogenesis and metastasis (Penna et al., 2013). Once more, this shows that this miRNA can be a potential diagnostic/prognostic biomarker in skin cancer, this finding pointing out that there are miRNAs that have a ubiquitous role in tumorigenesis (Penna et al., 2015). Almost concomitantly, another group has shown that skin cancer is associated with the methylation status of miRNA-148a. Using methylation-specific PCR, it was demonstrated that, in tumor tissues, DNA methylation of miR-148a was higher compared to healthy tissues. Moreover, miR-148a methylation status was correlated with various parameters (e.g. age, pathological differentiation, and lymph node metastasis) and with patient's survival; therefore, miR-148a methylation status can be a candidate for a prognostic biomarker in skin cancer (Tian Y. et al., 2015).

In the last decade, several other miRNAs were associated with skin cancers, as further described in the following sections. One important note from the epitranscriptomic domain is that these miRNAs can have dual functions: pro- or anti-tumoral action.

Nowadays, miRNA expression uses microarrays, bioinformatics analysis, and finally validation with qPCR. In the future, complex technologies are to be used to identify miRNA molecules that can identify particular subgroups of patients with worse prognosis.

MAIN TECHNOLOGIES THAT ARE USED FOR miRNA IDENTIFICATION FROM BIOLOGICAL SAMPLES

Aberrant miRNA expression was found in tumors and biological fluids. More and more data show that miRNAs could be excreted into circulation *via* extracellular vesicles or bound to proteins such as AGO or high-density lipoprotein (HDL) (Larrea et al., 2016; Voichitoiu et al., 2019). Thus, circulating miRNAs may serve as a reflection of the underlying disease, but this approach is hampered for the moment by the complicated and lengthy PCR-based procedures used by most laboratories.

MicroRNAs as non-coding RNAs (ncRNAs) are transcribed by RNA polymerases (Pol) II and III and, upon transcription, generate primary transcripts (pri-miRNAs). These pri-miRNAs can comprise one or more miRNAs, and from the structural point, these molecules are 5′-capped and polyadenylated (Hube and Francastel, 2015). Pol III also transcribes a minor group of miRNAs associated with Alu repeats (Lin and Gregory, 2015; Taucher et al., 2016). pri-miRNAs are further processed in the nucleus by a complex composed of two proteins: the double-stranded RNA-specific RNase DROSHA and the RNA-binding protein DGCR8 (DiGeorge Syndrome Critical Region 8). Upon processing, a precursor miRNA (pre-miRNA) is generated, which is afterward cleaved into a mature miRNA by DICER, an RNAse III enzyme (Kozomara and Griffiths-Jones, 2011). From the technological point of view, this transcription molecular flow can be depicted using several high-end approaches. Moreover, these applied methodologies are used to establish whether the studied miRNA(s) have a pro- or anti-oncogenic role in a certain cellular process, in both time and space. When a gene that encodes an oncogenic miRNA is overexpressed, amplified, or its epigenetic silencing is hindered, an anti-oncogenic pathway is deregulated. Dissimilarly, if deletion, mutations, or epigenetic silencing is active on a tumor-suppressive miRNA that would normally regulate oncogenes, this may lead to enhanced oncogenic activity (Markopoulos et al., 2017).

Technologies are diverse and have specific characteristics; thus, if some of them analyze many targets in a few samples (like sequencing and microarrays), others analyze few targets in many samples (like quantitative reverse transcription PCR, qRT-PCR).

Quantitative PCR Methods

The quantitative PCR (qPCR) technique struggles between perception and reality. While it is perceived as a precise and quantitative data reflecting the tested experimental parameters, without strict guidelines, validation, and data analysis procedures, the obtained results can be frequently false and opposed to the actual process developed in the experiment (Sanders et al., 2018). The reality is that the planning process is fundamental for the correctness of the results, and protocols [sample handling, harvesting, nucleic acid extraction, reverse transcription (RT), and qPCR] should be carefully designed to obtain the correct results.

Along with microarray platforms, quantitative real-time PCR (RT-qPCR) technology is used for investigating tissues or circulating miRNAs, especially in the cancer diagnosis biomarker field. The two most powerful methods used in this endeavor are relative quantification PCR and absolute qPCR. The major difference between these two is related to the suitable internal/external controls in PCR reaction. qPCR overpasses this issue, but has other technical difficulties related to the standard curve needed for specific miRNAs. This issue claims a series of standards, making the method laborious and expensive (Wang and Chen, 2014). The RT-PCR methodology is developed in several versions such as TaqMan, two-tailed RT-qPCR miRNA, miRCURY LNA qPCR assay, and so on, depending on the actual manufacturing company (Androvic et al., 2017; Leti and DiStefano, 2018).

The RT-PCR principle comprises the first step of complementary DNA (cDNA) synthesis, followed by the detection of amplified products checked by a conventional PCR version. The RT-PCR method detects short-length miRNA targets; hence, the miRNA primers for both cDNA synthesis and detection must be carefully designed to assure the RT-qPCR's specificity and sensitivity. This step is followed by the absolute quantification of small miRNA panels. Although it is easy to be included into routine measurement workflow with robust automation, RT-PCR cannot be enrolled for new miRNA species detection; moreover, the reaction conditions may differ according to each miRNA due to sequence-specific differences in primer annealing (Dave et al., 2019). Specific miRNAs are altered in solid tumors, including melanoma, and hence, RT-PCR is very useful in detecting such modified expressions.

Normalization strategy is a critical point in this technology and accounts for the variability of results. Classically, "housekeeping" genes are used for the normalization of qPCR data and are actually endogenous controls subjected to the same experimental workflow as the target genes. While quantifying miRNAs, the references used are stable small RNA controls, typically small non-coding RNAs, small nuclear RNAs, and small nucleolar RNAs (e.g. SNORD44, SNORD48, and RNU6-1). When quantifying circulating miRNAs, normalization cannot be done with the above-mentioned small RNAs because they are variable (Reid et al., 2011; Benz et al., 2013). In this case, an exogenous synthetic RNA spike-in control for normalization could be used, for example, *Caenorhabditis elegans* cel-miR-39 or *Arabidopsis thaliana* ath-miR-159a. This external reference, although subjected to the same workflow, will not overcome the sources of variability, like total circulating miRNA concentration that is inter-individually and/or is disease-associated (Marabita et al., 2016).

Quantitative RT PCR analysis was used by Wang and Zhang (2015) to characterize the expression levels of miR-203 in 148 cases of melanoma tissues and adjacent non-cancerous tissues. They demonstrated that miR-203 expression was significantly decreased in melanoma tissues, and its downregulation was significantly associated with tumor thickness and tumor stage.

In a recent study, miR-29a's role in repressing melanoma was highlighted. Thus, RT-PCR was used in a complex molecular approach for demonstrating the downregulation of miR-29 in an A375 melanoma cell line; miR-29a could potentially suppress melanoma by negatively regulating apoptosis-related protein Bmi1 (Xiong et al., 2018). The intra-tumor expression of miRNA could be a biomarker for predicting melanoma patients' survival. Thus, in a recent study using RT by means of the TaqMan version for miRNA RT on over 130 primary and metastatic tumors, several miRNA expressions were shown. Especially for primary melanomas, this approach showed the downregulation of intra-tumor expression for several miRNA species, such as miR-125b, miR-182, miR-200c, and miR-205, which could promote tumor dissemination. The TaqMan method could label miRNA-125b, miRNA-200c, and miRNA-205 as useful prognostic biomarkers correlated with shorter survival and, thus, able to select high-risk patients (Sanchez-Sendra et al., 2018). A notable version of the TaqMan method for miRNA detection is *SplintR-qPCR*, the major

difference between the SplintR-qPCR and TaqMan being related to the tactics used for cDNA synthesis. While the SplintR involves a ligation step of complementary oligonucleotides followed by qPCR to generate a DNA copy of the miRNA, the TaqMan relies on a miRNA-specific DNA hairpin as a primer for newly created cDNAs (Jin et al., 2016). Regardless of the technique version enrolled, RT-PCR remains, for the moment, the gold standard for cancer research and for diagnostic purposes (Hunt et al., 2015).

Microarray Platforms

The microarray principle relies on target hybridization with a specific probe usually bound on a solid surface to measure the miRNA/DNA abundance based on the fluorescence detection method (Wang and Xi, 2013). This technology is usually applied in characterizing previously identified miRNA species. The main advantages of the microarray assay rely on approaching hundreds of miRNA expression targets, high throughput, and speed of detection, providing mostly a relative quantification of miRNA. In cutaneous melanoma, these types of microarray platforms are mainly used to identify circulating miRNAs as diagnostic markers. One of the first attempts in this line was completed by Leidinger et al. (2010) by detecting a panel of 16 species of miRNAs isolated from a patient's blood. These miRNAs can discriminate with high sensitivity and specificity between melanoma metastatic cases (stages III and IV) and healthy subjects. Later on, Komina et al. (2016), using a microarray and, subsequently, validation by RT-PCR, demonstrated that the expression of over 1,100 miRNAs was altered in melanoma samples compared to melanocytic nevi. Moreover, they showed that miR-4286 mediates the proliferation and apoptosis in melanoma cells, having a pleiotropic effect by triggering several pathways (Komina et al., 2016).

A more recent study by Van Laar et al.'s (2018) group performed microarray profiling on the plasma of patients with stages I–IV melanoma and compared the profiles with those obtained in healthy subjects. The study discovered a 38-miRNA panel able to differentiate between melanoma and normal controls with high sensitivity and specificity (Mumford et al., 2018).

However, apart from the sensitivity and specificity of the detection, the necessary microarray equipment is fairly expensive as well as the required personnel expertise, and therefore, microarray platforms are rather suitable for miRNA expression surveys concerning a certain disease (Krepelkova et al., 2019; Ouyang et al., 2019).

miRNA Sequencing

Technologies like qPCR and microarrays are viewed as traditional techniques for miRNA expression because qPCR is a sensitive technique, can evaluate a dynamic molecule range, and its workflow can be accessible for any lab. However, this technology has its intrinsic limitations, as described in the section "Quantitative PCR Methods."

Next-generation sequencing (NGS) for miRNAs (miRNA-seq) comes with a series of key advantages (Ozsolak and Milos, 2011). Therefore, the sequence of a certain miRNA can be unknown, so the technology can be used in the discovery phase. It has an improved specificity for members of the same miRNA family, where the technique can distinguish molecules only one to two bases different. However, the main limitation of this technology is the computational platform that allows data interpretation. Various software programs have been developed, and most recently, a comprehensive pipeline analysis, *miARma-Seq*, was published, identifying mRNAs, miRNAs, and circular RNAs (circRNAs), along with evaluating differential expression, target identification, and functional evaluation (Andres-Leon et al., 2016, 2018). Recent data, as detailed further, have shown that, using this technology for miRNA discovery in melanoma, new miRNA panels were identified associated with clinical patient prognosis (Jayawardana et al., 2016).

miRNA Enzyme Immunoassay

miRNA enzyme immunoassay (miREIA) represents a relatively novel immunoassay technology designated for miRNA measurement in biological samples. Briefly, miRNAs isolated from a biological sample (e.g. blood) are hybridized to a biotinylated oligonucleotide, resulting in DNA/RNA hetero-hybrids that further would be incubated with streptavidin-labeled microparticles. Next, an antibody labeled with acridinium ester would specifically bind to the resulted hybrids quantitatively, proportional to the hetero-hybrid amount and, therefore, to the amount of the specific miRNA from the analyzed sample. The coupling reaction is identified by chemiluminescence-based detection (Kappel et al., 2015). The entire workflow for miREIA is analogous to ELISA, which is suitable for biomedical purposes and is routinely used in clinical laboratories. Therefore, this novel miRNA measurement approach would be soon extended to novel cancer types and new detected miRNA species that will be linked with the tumorigenesis of human cancers, including skin melanoma (Kappel et al., 2015; Thyagarajan et al., 2019). Using this method, it was shown that miR-150-5p is upregulated in patients of all stages of melanoma and that the diagnostic sensitivity and specificity were greatly improved when this miRNA was included along with miR-149-3p and miR-193a-3p (Mumford et al., 2018). Future results will be obtained with the newly available miREIA kit hsa-miR-150-5p.

miRNA Multiplexing Systems

Multiplexed miRNA analysis comprises the use of the flow cytometry principle and PCR. The detection involves a three-dimensional hydrogel particle (Tanase et al., 2011) that can sustain good hybridization properties and large nucleic acid binding capacity. The method can analyze plasma, serum, exosomes, saliva, and urine, but it can also be used on tumor tissue and/or tumor cell suspensions. It can detect a range of 5–400 miRNAs from a single sample. The principle behind this technology is very simple: each particle type has a barcode that is specific for the analyzed miRNA; when the biological sample is in contact with these particles, the target miRNA will bind to its specific particle. This first step is then followed by molecular steps that will lead on each particle to a bound DNA–miRNA–DNA complex. This complex is amplified through PCR using specific oligos and, adding, in the end, a biotin label to the PCR

product. Like in classical flow cytometry, the biotin is labeled with a streptavidin reporter complex that will be read in a cytometer. The fluorescent intensities of each coded particle will indicate the miRNA expression level (Elias et al., 2017; Leng et al., 2018). Multiplexed microarray profiling was used to identify let-7b and miR-199a as the most significant discriminators associated with metastasis in uveal melanoma, and the results were validated by qPCR (Worley et al., 2008).

Another multiplex-based assay is one that uses Firefly technology (FirePlex® miRNA Assay V2 – Assay Protocol, Protocol Booklet version 2.2, February 2019), and this assay is based on FirePlex® particles. These particles are bioinert hydrogels that are coupled with the post-hybridization labeling method. They have a site for a specific miRNA and another one for tagging, so that the actual binding will be detected in this type of multiplexing *via* fluorescence.

This technology was used for detecting miRNAs in brain diseases (Hoss et al., 2015), in brain metastases of breast cancer (Le et al., 2014), or, more recently, in Richter syndrome, the syndrome that shows the switch of chronic lymphocytic leukemia into its aggressive form (Van Roosbroeck et al., 2019). Unfortunately, although this technology has good potential, reports using this assay in skin cancer are not yet published.

There is a large panel of technologies that aid miRNA detection, and one of the main issues is to make the proper selection for the flow of technologies that will be providing high throughput and validation of the searched miRNA molecules. In **Figure 1**, a visual representation of the main types of technologies put in use in miRNA detection in terms of high-throughput detection in multiple samples is presented.

Sampling for miRNA Detection

As presented in the previous section, assays that identify miRNAs in tissue and/or in circulation are very diverse.

Tests that focus on circulating miRNAs can have several advantages in comparison to a tissue biopsy, which is an invasive procedure (Young et al., 2007), Moreover, if the tumor is small, there is an increased failure of the biopsy, this case being frequent in small skin tumors as in other types of cancers (Corcoran et al., 2012). Therefore, in terms of availability and the invasiveness of the procedure, circulating miRNAs are the preferred test. As presented in several sections, circulating miRNA have a superior robustness and stability against tissue miRNAs (Mitchell et al., 2008). For monitoring the therapy and overall clinical outcome of a patient, it is more proper to use miRNAs that circulate in whole blood, plasma, serum, and urine (Lawrie et al., 2008). Important challenges in using miRNAs as biomarkers in oncology still remain. Therefore, there are conflicting results that show a miRNA as an oncomir in one type of cancer while in others the same molecule is a tumor suppressor. Probably all these results come from using different technologies, different methods to enrich and identify a certain miRNA or a panel of miRNAs, and, last but not least, the sample type, tissue, or plasma (Git et al., 2010; de Planell-Saguer and Rodicio, 2011).

Circulating miRNAs are generated from tumor cells, circulating normal/abnormal cells, or even other non-tumor tissues; therefore, the picture of circulating miRNAs has a wholesome characteristic (Philippidou et al., 2010; Greenberg et al., 2011).

In both circulation and tissue, miRNA identification stumbles upon an important issue, namely, having proper control of the miRNA expression (Greenberg et al., 2011). If tissue sampling can partially overcome this issue when compared to normal tissue, in circulation this still remains a point to be argued for.

Some of the advantages and disadvantages of evaluating miRNAs in tissue samples *versus* body fluid samples are resumed in **Table 1**.

miRNAs DETECTED IN CUTANEOUS MELANOMA

The majority of publications regarding miRNA evaluation focus on cutaneous melanoma. The reasons for this concentrated research rely on the highly metastatic potential of this skin cancer, increased recurrence, resistance to standard chemotherapies, and the high genomic heterogeneity. Thus, several areas study miRNAs in melanoma: in the accurate differentiation between other skin cancers, in developing new therapeutic targets, and in evaluating the prognostic and diagnostic potential of these molecules.

Cutaneous melanoma has a particular molecular biology due to the many genetic alterations that have been identified, and this feature has triggered the development of targeted therapies. But not only genetic alterations, which characterize this skin cancer, epigenetic deregulation was also identified concerning melanoma initiation and progression (Luo et al., 2014). Deregulated miRNA expression was identified in miRNAs involved in the tumor cell cycle, proliferation, migration, invasion, apoptosis, and the triggered immune response. Abnormal hypermethylation was identified in over 70 genes that are involved in cutaneous melanoma pathogenesis (de Unamuno et al., 2015), and alterations identified in the miRNA-processing enzyme DICER were reported several years ago. Besides the involvement in seminal melanoma tumorigenesis, miRNAs interact with the main transcription factor of melanocyte, a microphthalmia-associated transcription factor (Leibowitz-Amit et al., 2012). It was reported that over 800 different miRNAs can be found within cells and that their expression will vary during tumorigenesis stages. In melanoma, miR-21, miR-125b, miR-150, miR-155, miR-205, and miR-211 were the molecules that were searched for their prognostic value and for which targeted therapy was developed to obliviate their onco-miRNA action (Latchana et al., 2016). Relating these miRNAs with the main molecular deregulated pathways, e.g. the RAS/MAPK pathway, the MITF pathway, the p16INK4A-CDK4-RB pathway, and the PI3K-AKT pathway, would offer new insights in deciphering the aggressive and metastatic feature of melanoma (Segura et al., 2012; Greenberg et al., 2014).

In 2019, a complex retrospective study based on mRNA-seq, miRNA-seq, and DNA methylation was performed on tissue samples of almost 450 patients. In the group that had the best prognosis, immune-related genes were found upregulated, along with DNA hypomethylation and a high number of mutations.

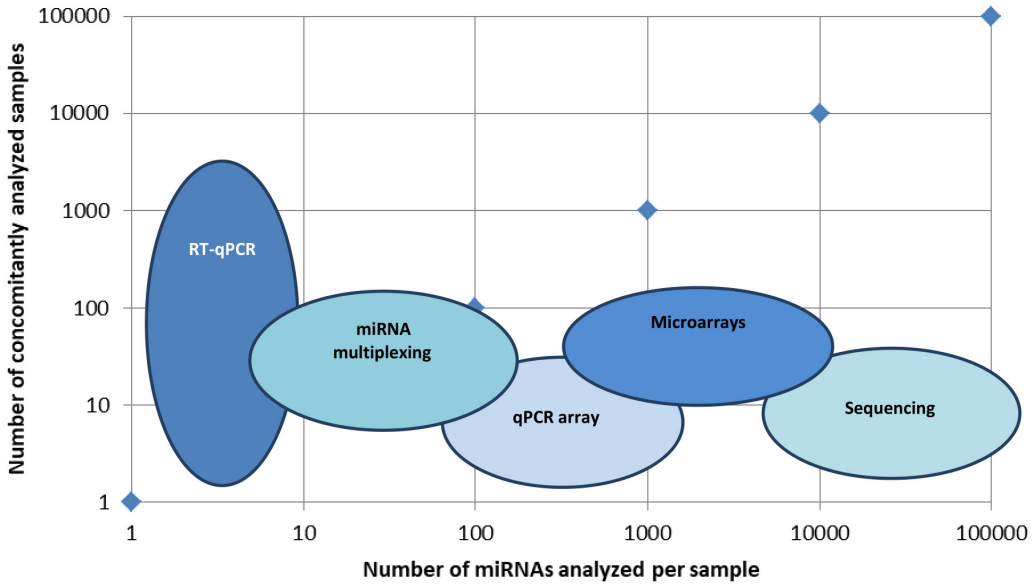

FIGURE 1 | Main technologies used in miRNA identification. Graphical representation of several miRNAs identified per sample *versus* a number of concomitantly analyzed samples. Technologies like RT-qPCR identify a few types of miRNAs, but in a large set of samples, miRNA multiplexing can identify hundreds of miRNAs in hundreds of different samples, while microarrays and sequencing can identify up to hundreds of thousands of miRNAs in hundreds of different samples.

TABLE 1 | Sample type advantages and disadvantages for miRNA identification.

Sample	Advantages	Disadvantages
Serum/plasma/urine	miRNAs are stable and robust. Non-invasive approach, easily repeated. Offers real-time monitoring of the disease, of the therapy, of the clinical outcome of the patient. Can be applied for early detection.	Detection methods are various, usually non-standardized, and with low sensitivity. The selected panel of miRNA can have non-detectable levels. Circulating miRNAs can have various origins besides tumor cells *per se*: immune cells, platelets, and so on, thus an increased variability.
Tissue	Methods are usually standardized having high sensitivity. miRNAs are disease-related.	Invasive, difficult to repeat. Does not detect the initiation of metastasis at distant organs. It is not proper for therapy monitoring.

The mutational signature in the better prognosis group was associated with ultraviolet light exposure. This integrated study highlighted once more the molecular heterogeneity of cutaneous melanoma (Li and Cai, 2019).

Several years ago, when evaluating stage III melanoma patients, it was shown that the standard clinical/pathological information needs to be combined with information developed by various omics platforms (Jayawardana et al., 2015). It becomes more and more obvious that information coming from the proteomic domain must collide with the information from the genomic, transcriptomic, and metabolomic domains (Neagu et al., 2019b) to provide an individualized treatment approach for the patient.

miRNAs as Diagnostic and Prognostic Markers in Cutaneous Melanoma

In the search for their diagnostic and prognostic potential, extensive work was done in evaluating miRNA expression in tumor tissue, isolated tumor cells, tumor microenvironment, and body fluids like serum/plasma. In comparison to tissue-related studies, reports regarding the circulating level of miRNAs in melanoma patients are scarce.

Circulating miRNAs in Cutaneous Melanoma

MicroRNAs can circulate in the blood completely free or complexed with proteins, or in vesicles, like exosomes and microvesicles. As already mentioned, these circulating forms are stable, but a disadvantage in terms of specificity is that they can have different origins. They can originate from the primary tumor, but also from a tumor metastasis, being the result of cancer cells or even of other cells from the tumor microenvironment. Then, circulating mRNAs can originate from inflammatory circulating cells, immune cells, and any cells that are involved in an anti- or pro-tumor response (Taylor and Gercel-Taylor, 2013; Ma et al., 2014). Taking into account these bottlenecks (see also **Table 2**), studies regarding the identification of circulating mRNAs in melanoma patients started >10 years ago.

Thus, work done almost a decade ago has shown that miR-221, which is aberrantly expressed in melanoma cells, can also be found in the sera of patients diagnosed with cutaneous

TABLE 2 | Overview of the main miRNAs found in melanoma tissue or/and in circulation in patients diagnosed with cutaneous melanoma.

miRNAs	Sample		Observation	References
	Serum/plasma	Tissue		
miR-214		X	Regulates PTEN/AKT, β-catenin, tyrosine kinase receptor pathways, genes *Ezh2*, *p53*, *TFAP2*, and other miRNAs like miR-148b	Penna et al., 2015
miR-148a		X	Downregulated; is regulated by DNA methylation; an independent indicator of prognosis	Tian Y. et al., 2015
miR-221	X	X	Downmodulates p27Kip1/CDKN1B and c-KIT receptor; favors tumorigenesis	Kanemaru et al., 2011; Friedman et al., 2012
miR-16	X		Correlates with tumor thickness, ulceration, stage, and tissue Ki-67 expression	Guo et al., 2016
miR-29c		X	Downregulated and correlates with stage, overall survival; regulates cell surface glycoprotein B7-H3	Nguyen et al., 2011; Wang et al., 2013
miR-146a-5p		X	Regulates Toll-like receptor, NF-κB, ErB, and measles signaling pathways; regulates 38 target genes; most important NRAS gene	Aksenenko et al., 2019
miR-205		X	Low expression correlates with shorter survival	Hanna et al., 2012
Pattern miR-142-5p, miR-150-5p, miR-342-3p, miR-155-5p, miR-146b-5p		X	Associated with patient clinical prognosis	Jayawardana et al., 2016
miR-10b		X	Increased expression in primary melanomas and further increased in metastases	Saldanha et al., 2016
miR-203		X	Decreased expression in tissues compared to healthy tissue; associated with tumor thickness and stage	Wang and Zhang, 2015
let-7a and let-7b, miR-148, miR-155, miR-182, miR-200c, miR-211, miR-214, miR-221, miRNA-222	X	X	Linked to NRAS, microphthalmia-associated transcription factor, receptor tyrosine kinase c-KIT, and AP-2 transcription factor	Mirzaei et al., 2016
miR-106b		X	High expression correlated with Breslow index, ulceration, and clinical stage	Lin et al., 2015
7 miRNAs (MELmiR-7)	X	X	MELmiR-7′ correlates with overall survival	Stark et al., 2015

melanoma. This miR-221 downmodulates p27Kip1/CDKN1B and the c-KIT receptor in melanocytes and, hence, favors tumorigenesis. Using quantitative real-time polymerase chain reaction, circulating miR-221 was quantified in a patient's serum and was found significantly higher compared to controls. Moreover, the serum level correlated with stage, the tumor thickness, and recurrence. It is one of the first published reports that show a circulating miRNA that has good potential as a prognosticator in melanoma (Kanemaru et al., 2011). Later on, serum miR-221 was investigated by another group as well using RT-qPCR. Circulating miR-221 was also found significantly increased in patients' sera and identified as an independent prognosticator of worse outcome, reinforcing the previously published data (Li et al., 2014).

Another group has investigated 355 miRNAs in the sera of melanoma patients using qRT-PCR technology. Out of all these screened circulating miRNAs, a pattern of three miRNAs could classify high- *versus* low-recurrence-risk patient groups and was associated with tumor burden. This was one of the first studies to identify circulating miRNAs in melanoma, and this finding would indicate the prognostic value of circulating miR-199a-5p, miR-33a, and miR-424 (Friedman et al., 2012).

While some of the circulating miRNAs are found elevated, there are also studies showing decreased miRNA circulating levels. Thus, in a patient's serum, a significant reduction of the circulating miR-16 level was reported when compared to controls. Serum miR-16 correlated with tumor thickness, ulceration, stage, and tissue Ki-67 expression. This miRNA also has prognostic value as it independently predicted patients' survival outcome (Guo et al., 2016). miR-16 was previously included in the miRNA panel reported by another group (Stark et al., 2015).

Using RT-qPCR, circulating miR-206 was detected in low concentrations compared to controls. Moreover, low serum miR-206 indicated patients with melanoma metastasis and a significantly shorter overall survival. This finding indicated circulating miR-206 as a possible prognostic biomarker (Tian R. et al., 2015).

Blood-based molecules with a biomarker role can improve early detection of metastasis, therapy initiation, and, hence, patient prognosis. In this picture, the recently developed "liquid biopsy" using blood samples gains more and more utility in melanoma disease monitoring. From blood samples, circulating tumor cells (CTCs) can be detected along with cell-free circulating tumor DNA (ctDNA) and circulating miRNAs (cmiRNA). These tests performed some years ago on stages III and IV melanoma patients have shown that these molecular combined analyses (CTC, ctDNA, and cmiRNA) can lead to individualized therapy. In this light, technologies like massive parallel sequencing (MPS) can aid the classical molecular assays to enlarge the panel of powerful biomarkers (Huang and Hoon, 2016).

Circulating free miRNAs populate the serum because they are released into the interstitial fluid and, further, in the main circulation. They are stable even outside the cell(s), can be tissue-specific, can vary with cancer dynamics, and change according to disease progression or therapeutic response. All these characteristics make them good blood-based biomarkers. The downfall of these molecular biomarkers consists in the analytical methods, in the normalization strategies that need standardization before entering clinical tests (Polini et al., 2019).

Panels of circulating miRNAs were also studied. Aberrant genes associated with melanoma (e.g. NRAS, microphthalmia-associated transcription factor, receptor tyrosine kinase c-KIT, and AP-2 transcription factor) were found linked to the aberrant activation of sets of circulating miRNAs (e.g. let-7a and b, miR-148, miR-155, miR-182, miR-200c, miR-211, miR-214, miR-221, and miR-222) and can aid the large set of potential biomarkers and/or therapeutic targets in melanoma (Mirzaei et al., 2016).

In a combined serum and tissue analysis, it was reported that the expression of a set of 17 miRNAs (MELmiR-17) can select some good prognosticators. In serum, a seven-miRNA set (MELmiR-7) characterized the overall survival of patients even better than did the classical serum markers lactate dehydrogenase (LDH) and S100B. This MELmiR-7 could indicate melanoma progression, recurrence, and survival to detect any very early relapse. MELmiR-7 consists of miR-16, miR-211-5p, miR-4487, miR-4706, miR-4731, and miR-509-5p (Stark et al., 2015).

Tumor Tissue miRNA Expression in Cutaneous Melanoma

Tissue analysis of miRNA expression goes back more than 10 years ago when tissue miR-221 and miR-222 were reported as abnormally expressed. These miRNAs were found downregulating c-KIT receptor and p27Kip. This finding highlighted that a new therapeutic pathway can be opened using the regulatory potential of miRNAs (Felicetti et al., 2008). It is to be noted that miR-221 was also later found in circulation in melanoma patients (Kanemaru et al., 2011).

Using quantitative *in situ* hybridization (qISH) on over 100 primary melanomas, a test that was further validated on over 200 additional samples, low levels of miR-205 were shown to be correlated with lower survival in patients. Moreover, these low levels were independent of stage, age, gender, and Breslow index. Thus, miR-205 was reported as a tumor suppressor miRNA in melanoma (Hanna et al., 2012).

Using RT-qPCR, several isoforms of miR-29 were studied. Out of all the studied isoforms, reduced expression of miR-29c was correlated with late stages of melanoma. Moreover, the hypermethylation status of the promoter region of tumor-related genes (TRGs) and non-coding MINT loci is in opposite correlation with miR-29c expression. MiR-29 downregulates DNMT3A and DNMT3B (DNA methyltransferases) that methylate TRGs. DNMT3B expression and miR-29c were found significantly correlated with the overall survival of patients. These molecular traits can be epigenetic biomarkers in melanoma prognosis (Nguyen et al., 2011). MiR-29c regulates a cell surface glycoprotein, B7-H3, namely its down-expression. Using RT and RT-PCR, it was shown that B7-H3 is overexpressed and, furthermore, that it is correlated with the migration and invasion of melanoma cells (Wang et al., 2013).

Using RT-qPCR, miR-10b was shown increased in primary melanoma tissues, and further, its levels were found increased in melanoma metastasis. The combination of miR-10b and miR-200b showed that their expressions have independent prognostic value. Using identification of these miRNAs on aggressive thick melanomas (Saldanha et al., 2016), miR-203 expression was found to be significantly decreased in melanoma tissues, while its downregulation was found to be associated with tumor thickness, stage, and reduced overall survival rate (Wang and Zhang, 2015).

As previously established, an inverse correlation between tyrosinase-related protein 1 (TYRP1) mRNA expression in metastatic tissues and survival was reported. An additional study of miR-155 involvement was reported several years ago. TYRP1 mRNA has two miR-155-5p binding sites. In melanoma cell lines, it was demonstrated that miR-155 induced TYRP1 mRNA decay and, in metastatic tissues, TYRP1 mRNA inversely correlated with miR-155 expression. This mechanistic study proved that polymorphisms in the 3′-UTR of TYRP1 mRNA affect the regulation performed by miR-155 and, further, its translation into the protein. Therefore, there are subgroups of melanoma patients that display this polymorphism, hindering miR-155 regulation and proving its prognostic power (El Hajj et al., 2015). An additional study published in 2019 has shown that miR-155 has a new target, namely, protein kinase WEE1. In an experimental mouse model, it was shown that miR-155 increased the expression and silenced WEE1, leading to decreased metastases. In the late stages of melanoma, during the metastasis process, decreased miR-155 and increased expression of WEE1 significantly contributed to the metastatic potential of melanoma cells (DiSano et al., 2019).

Another miRNA that was studied in melanoma tissues and in tumor cell lines is miR-675, whose expression was found downregulated. Using functional assays, it was demonstrated that in upregulating miR-675, hindrance of tumor cell proliferation and invasion was obtained. In the search for its target and using an array of technologies (e.g. bioinformatics analysis, luciferase reporter assay, RT quantitative polymerase chain reaction, and Western blot analysis), it was demonstrated that metatherian (MTDH) is the direct target of miR-675; therefore, miR-675 can be further developed as a potential therapeutic target (Liu et al., 2018). Recently, in melanoma cell lines and further in tissues, miR-135b expression was studied and found overexpressed. Using luciferase reporter assay and Western blot analysis, the target gene for this miRNA was found to be the large tumor suppressor kinase 2 (LATS2). In melanoma cell lines, if this miRNA was found to be overexpressed, cell proliferation and migration was enhanced; conversely, its low expression suppressed growth/metastasis and increased tumor cell apoptosis. This molecular tandem miR-135 and LATS2 can decipher new oncogenic mechanisms in melanoma (Hu et al., 2019). Another recent finding showed miR-204 as a complex regulator in melanoma. Using a large panel of methods [e.g. Western blotting, qRT-PCR, and chromatin immunoprecipitation (ChIP) assay], it was demonstrated that Semaphorin-5A (Sema5A) regulates cell migration and invasion.

Sema5A expression was controlled by the transcription factor c-Myb, and if miR-204 overexpression was induced in melanoma cell lines, a concomitant decrease of Sema5A, Bcl-2, and c-Myb protein expression was observed (D'Aguanno et al., 2018).

Panels of tissue miRNAs were also the focus of recent studies. In tumor tissue, the downregulation of miR-125b, miR-182, miR-200c, and miR-205 expressions was reported from primary melanomas to metastatic samples. The combination of miR-125b, miR-200c, and miR-205 was found to be correlated with shorter survival. The authors highlight that the downregulation of miR-205 alters the melanoma cells' interaction with the extracellular matrix favoring metastasis. The panel of miR-125b, miR-200c, and miR-205 can be developed in a prognostic biomarker panel and for selecting high-risk-recurrence patients (Sanchez-Sendra et al., 2018).

Earlier studies have shown that global miRNA expression profiles are differentially expressed in correlation with *BRAF* mutation. Therefore, when *BRAF* mutation appears, several miRNAs were found underexpressed, namely, miR-193a, miR-338, and miR-565. The association of low miR-191 expression with high miR-193b expression is associated with poor survival. Authors pointed out that a miRNA classifier is needed to validate prognostic miRNA biomarkers (Caramuta et al., 2010). In the same year (2010), using miRNA arrays, 18 miRNAs were identified as associated with survival. Out of this set, a six-miRNA signature could prognosticate stage III patients' clinical evolution. This panel of miRNAs comprised the following molecules: miR-150, miR-342-3p, miR-455-3p, miR-145, miR-155, and miR-497 (Segura et al., 2010).

Evaluating in a meta-analysis a large set of 16 studies that identified 25 miRNA expressions in over 2,600 melanoma patients, the association between survival outcome and miRNA expression was analyzed. A subgroup emerged where miR-10b, miR-16, and miR-21 were associated with poor prognosis. This study, published in 2018, showed the need to largely analyze the prognostic power of miRNAs (Sabarimurugan et al., 2018).

Tumor Microenvironment miRNA Expression in Cutaneous Melanoma

Like in other solid tumors, the melanoma tumor microenvironment has an important role in the tumorigenesis dynamics (Neagu et al., 2019a). The tumor microenvironment consists of cancer-associated fibroblasts (CAFs), tumor-associated macrophages (TAMs), endothelial cells, immune cells, and a myriad of molecules with different origins. From this amazing concert of molecules in the tumor microenvironment, miRNAs have a paracrine function. Melanoma tissue and the peritumoral region were subjected to microarray analysis using Gene Atlas Microarray System, further validated by RT-PCR. This study, published in 2019, has revealed over 140 different miRNAs expressed in tumor compared to adjacent tissues, out of which hsa-miR-146a-5p was the most prominent overexpressed molecule in tumor cells. MiR-146a-5p regulates several important cellular pathways like Toll-like receptor, NF-κB, and ErB. Actually, miRNA-146a-5p targets almost 40 genes, one of them being the well-known *NRAS* gene (Aksenenko et al., 2019). Prognostic miRNA tissue signatures that match the recent ones were reported several years ago. Twelve-miRNA and 15-miRNA signatures were associated with stage III patients' extended survival. Cross-validation between these two datasets revealed five miRNAs (miR-142-5p, miR-150-5p, miR-342-3p, miR-155-5p, and miR-146b-5p) that were highly and reproducibly associated with clinical patient prognosis (Jayawardana et al., 2016).

Discriminating Melanoma From Other Skin Cancers Through miRNAs

Discriminating between benign and malign proliferation of melanocytes and discriminating between different skin cancers are any pathologist's goals. As skin cancer has the highest frequency in humans, discriminating between non-melanoma skin cancers and melanoma is extremely important. A gene-specific intron retention signature was developed to differentiate melanoma from other skin cancers. Using RT-qPCR technology, total RNA was isolated from all types of skin cancer samples. Complex bioinformatics was performed, and the *c-MYC*, *SRPX2*, and *Sestrin-1* genes were demonstrated to undergo intron retention just in melanoma. miRNAs were generated for these genes, and thus this pattern could molecularly differentiate other skin cancers from melanoma (Giannopoulou et al., 2019).

Using RT-PCR, the miRNA expression profile was studied in melanocytic lesions, namely, benign nevi, cutaneous melanoma, and borderline melanocytic tumors. The authors show that, in melanomas, there are increased expressions for miR-21 and miR-155 compared to benign nevi. In borderline lesions, miR-21 and miR-155 were significantly overexpressed and associated with mitotic activity and thickness. miRNA expression can characterize atypical melanocytic proliferation (Grignol et al., 2011). One year later, using TaqMan® RT-PCR assay, miR-21 was also studied by another group investigating dysplastic nevi and primary melanomas. MiR-21 was found increased in a continuous level from dysplastic nevi to melanomas and once more elevated in melanoma metastases. The expression level of miR-21 was found correlated with Breslow index, clinical stage, and shorter overall survival. Experimental *in vitro* antisense-mediated miR-21 inhibition reduced the tumor growth and induced apoptosis and therapy sensitivity through an increased Bax/Bcl-2 ratio (Jiang et al., 2012).

An earlier study comparing melanocytic nevi, melanoma tissue, and melanoma cell lines has shown that, in melanomas, miR-15b and miR-210 were significantly upregulated, while miR-34a was found significantly downregulated. In a clinical follow-up, only a high expression of miR-15b was associated with worse overall survival. It is one of the first studies that highlighted miRNA expression being different in malignant *versus* benign melanocytes (Satzger et al., 2010).

Using microarray analysis validated by qRT-PCR, improved molecular tissue markers were reported when three miRNAs (namely, miR-200c, miR-205, and miR-211) were found differentially expressed in primary compared to metastatic melanomas, these miRNAs acting like tumor suppressors (Xu et al., 2012). Using qRT-PCR for analyzing dysplastic nevi, in comparison to primary and metastatic melanomas, miR-106b

expression was investigated. A high miR-106b expression was found correlated with Breslow index, tumor ulceration, clinical stage, and overall patient survival, pointing out that these miRNAs are independent prognostic factors for overall survival and patients' risk stratification (Lin et al., 2015).

An outline of the main findings regarding miRNA expression in melanoma tissues and/or in the circulating form is presented in **Table 2**.

In cutaneous melanoma, besides the clear histopathological and clinical criteria stated by the American Joint Committee on Cancer (AJCC), such as tumor thickness, ulceration, mitoses, and lymph node and distant organ spread, new prognostic markers should be entered into this panel. Particular determinants like genetic mutation(s), particular epigenetic features, and the host's immune response are important criteria for predicting patient outcomes (Neagu et al., 2013). Future validation studies for new epigenetic prognostic biomarkers should be expanded (Weiss et al., 2015).

miRNA Involvement in Therapy Resistance in Cutaneous Melanoma

With the advent of targeted therapy in melanoma, namely, BRAF kinase inhibitors for *BRAF* mutant tumors, epigenetic studies emerged focusing on the processes that underlie therapy resistance. miRNomes and transcriptomes were studied in *in vitro* melanoma cellular models. The study revealed that particular miRNAs and genes are differently expressed in drug-resistant *versus* drug-sensitive cell lines (e.g. miR-92a-1-5p, miR-708-5p, and *DOK5* and *PCSK2* genes). In drug-resistant cell lines, it was shown that a low MITF/AXL ratio is regulated by miRNAs. Thus, the drug resistance process in melanoma therapy has particular sets of miRNAs that regulate particular genes that would lead to resistance (Kozar et al., 2017).

In combined therapies with BRAF and MEK inhibitors, therapy resistance occurs quite rapidly during therapy initiation. A low expression of miR-579-3p was found correlated with poor survival and with staging. Moreover, in melanoma cell lines that are resistant to BRAF/MEK inhibitors, this miRNA expression was reported as low. MiR-579-3p targets the 3′-UTR region of oncoproteins BRAF and E3 ubiquitin-protein ligase, MDM2. In tumor samples harvested before and after therapy resistance occurrence, miR-579-3p is strongly downregulated upon resistance installment (Fattore et al., 2016).

Recent reports have studied the involvement of miRNAs in the chemoresistance of melanoma cells, as it is known that this type of tumor lacks sensitivity to cytostatics. Using qRT-PCR and mouse xenograft assay, it was shown that miR-211 was found decreased. Bisulfite sequencing PCR technology indicated that DNA hypermethylation induced the downregulation of miR-211 in tumor tissues. Reversing the process, namely, the epigenetic modification that downregulates miR-211, chemosensitivity of melanoma cells can be achieved (Li et al., 2019). Resistance to MAK inhibitors was shown to be associated with another miRNA, namely, miR-214. Using RNA-seq analysis, it was demonstrated that melanoma cells frequently express β-catenin mRNA isoforms and lack a miR-214 target site. Therefore, using tandem miRNA and mRNA-seq analysis, new targets were identified for miR-214 action. The novel miR-214 targets were ankyrin repeat domain 6 (ANKRD6) and C-terminal-binding protein 1 (CTBP1), these being involved in the negative regulation of Wnt signaling. Mechanistically, the overexpression of miR-214/knockdown of ANKRD6 or CTBP1 increases the melanoma cell's pro-tumorigenic characteristics, proliferation, and migration and decreases its sensitivity to MAPK inhibitors (Prabhakar et al., 2019).

miRNAs as Therapy Efficacy Markers

When following therapy efficacy in melanoma, in addition to the classical circulating markers as LDH, S100 calcium-binding protein B (S100B), melanoma inhibitory activity (MIA) (Neagu et al., 2009), and, lately, ctDNA (Seremet et al., 2019), circulating miRNAs gained interest. As circulating miRNAs have structural stability, they can become robust non-invasive biomarkers when several technicalities can be standardized, such as the sample type (plasma *versus* serum) and pre-analytical and analytical workflows (Mumford et al., 2018).

With the advent of clinical approval of immunotherapy in melanoma (Ancuceanu and Neagu, 2016), finding miRNA efficacy markers is an important goal. In melanoma patients, the accumulation of myeloid-derived suppressor cells with the phenotype $CD14^{+}HLA\text{-}DR^{-}$ (myeloid-derived suppressor cells, MDSCs) stands for the cells that can hinder immunotherapy efficacy. In a recent study, it was shown that a panel of miRNAs (e.g. miR-146a, miR-155, miR-125b, miR-100, let-7e, miR-125a, miR-146b, and miR-99b) is related to MDSCs and immune checkpoint inhibitor resistance. Actually, these miRNAs were found involved in the transformation of monocytes in MDSCs and in melanoma patients. These miRNAs were found increased in blood $CD14^{+}$ cells, were identified circulating in plasma, and, in tumor tissues, were correlated with MDSC infiltrates. Various methods were implied by the group; thus, after RNA extraction from circulating monocytes, from extracellular vesicles, from melanoma cells, and from melanoma specimens using mirVana miRNA isolation kit, qPCR analysis was performed to evaluate the gene and miRNA expression levels.

Before immunotherapy installment (whether CTLA-4 or PD-1 blockade), the miRNA levels in patients' plasma could indicate the future clinical efficacy of the immunotherapy. Thus, miRNAs that append to the circulating MDSCs can be validated further in blood markers for therapy efficacy (Huber et al., 2018).

Studies regarding responders *versus* non-responders to therapy in melanoma do not abound. Nevertheless, a study published in 2019 focusing on BRAF and MEK inhibitors has evaluated the miRNA profiling of melanoma patients at baseline and during resistance acquirement to therapy. The authors point out that restoring miR-126-3p expression in dabrafenib-resistant melanomas could increase the drug sensitivity of non-responders (Caporali et al., 2019).

It is highly probable that, in terms of finding new therapy efficacy markers and stratifying patients that would best benefit from a certain therapy, circulating miRNAs would gain future clinical importance.

lncRNA – Regulators of miRNAs in Melanoma

Long ncRNAs (lncRNAs) have recently been recognized as important regulators of transcriptional, post-transcriptional, and translational processes. lncRNAs are non-coding RNAs (200 nt and 100 kb) with multiple functions as chromatin regulators, ribonucleoprotein scaffolds, regulators of transcription factors, and matrix for other post-transcriptional molecules such as miRNAs (Dinescu et al., 2019).

In melanoma, lncRNA ILF3-AS1 was found upregulated in both melanoma tumors and melanoma cell lines. The expression of this lncRNA was correlated with worse prognosis for melanoma patients. Experimental findings showed that ILF3-AS1 interacts with EZH2, promoting the link of EZH2 to the miR-200b/a/429 promoter, and, hence, represses miR-200b/a/429 expression. This negative correlation between ILF3-AS1 and miR-200b/a/429 was verified in melanoma tumor tissues. Functional tests have shown that, when lncRNA ILF3-AS1 is upregulated, several pro-tumorigenesis functions are increased – cell proliferation, migration, and invasion – processes that repress miR-200b/a/429. The authors point out that this tandem could become a new therapy focus in melanoma (Chen et al., 2017). Interestingly, another lncRNA was reported as having similar activity to ILF3-AS1. lncRNA-HEIH is also highly expressed in melanoma tissues, promotes tumor proliferation, migration, and invasion, and it binds to the miR-200b/a/429 promoter, repressing its transcription. Therefore, lncRNA-HEIH is another player in the miR-200b/a/429 expression involved in melanoma tumorigenesis and a prognostic epigenetic biomarker (Zhao et al., 2017).

A study published in 2019 showed an integrative analysis of a large group of epigenetic-related molecules, namely, lncRNA, miRNA, and mRNA, to design a competing endogenous RNA (ceRNA) network in melanoma. After complex analysis using data from The Cancer Genome Atlas (TCGA), the Gene Ontology (GO) database, and the Kyoto Encyclopedia of Genes and Genomes (KEGG), some epigenetic traits were found for metastatic melanoma. Overall survival was correlated with differentially expressed mRNAs, miRNAs (e.g. miR-29c, miR-100, miR-142-3p, miR-150, and miR-516a-2), and lncRNAs (e.g. AC068594.1, C7orf71, FAM41C, GPC5-AS1, MUC19, and LINC00402). It is remarked that the ceRNA network should be further developed to identify the best epigenetic pattern that can predict prognosis in melanoma patients (Wang et al., 2019).

As miRNAs regulate over 60% of human genes and since cutaneous melanoma has a high genetic heterogeneity, miRNA alterations, stable and detectable in tissue/body fluids, make them robust candidate biomarkers in melanoma (Varamo et al., 2017). Melanoma incidence is steadily rising in the last decades (Aftab et al., 2014); thus, melanoma molecular biology features should be thoroughly studied. miRNAs are probably key players in melanogenesis as inducers and blockers. Already, miRNA expression profiling with a focus on some sets was identified as linked to tumor proliferation, migration, and invasion, but is also correlated to apoptosis induction and generation of an anti-tumoral immune response (Ross et al., 2018).

miRNAs IN NON-MELANOMA SKIN CANCERS

Cutaneous Squamous Cell Carcinoma

In non-melanoma skin cancers, the majority of published work regarding miRNA involvement in the diagnosis/prognosis focuses on cutaneous squamous cell carcinoma (CSCC). CSCC has a rising tendency and is the second most frequent cancer in humans. In mouse cancer cell lines, miRNAs were identified, and in these studies, the same miRNA panel was searched for in human tumors. MiR-205 and miR-203 were selected and matched the CSCC clinical prognosis. Thus, miR-205 was associated with desmoplasia, perineural invasion, and infiltrative pattern, all these features being known to be associated with poor prognosis. MiR-205 was associated clinically with local recurrence and poor prognosis. In contrast, miR-203 was expressed in tumors that displayed tissue characteristics associated with favorable prognosis. Therefore, the authors point out that, in CSCC, miR-205 and miR-203 expressions are mutually exclusive, pinpointing that these molecules can have prognostic potential (Canueto et al., 2017). Another miRNA recently found overexpressed in CSCC samples is miR-221. Functional tests have shown that *PTEN* is the direct target gene for miR-221. Thus, in CSCC, miR-221 has an oncogenic function by interacting with *PTEN*. Moreover, future anti-miR-221 can be developed for CSCC diagnosis and treatment (Gong et al., 2019).

An earlier study focused on miR-20a as a prognostic biomarker in CSCC. Using qRT-PCR applied to over 150 CSCC tissues and compared to healthy adjacent normal tissues, it was shown that miR-20a expression was lower in CSCC tissues compared to normal tissues, and this expression was correlated with the TNM stage. Moreover, these findings showed that patients had a significantly worse overall survival when miR-20a expression was found upregulated in comparison to patients with high tissue expression. This tissue molecule can become an independent prognostic biomarker of CSCC and, in the future, can even enter the treatment armamentarium (Zhang et al., 2015).

An extensive review published in 2019 has shown that, in CSCC, there is an array of miRNAs with oncogenic functions while other miRNAs are tumor suppressors. Therefore, families of tumor inductors that were reported in CSCCs comprise a large set of miRNAs (e.g. miR-21, miR-205 miR-365, miR-31, miR-186, miR-142, and miR-135b) that act generally on *PTEN*, *PDCD4*, *GRHL3 HOXA9*, and *RhoBTB*, these genes being involved in seminal pro-tumorigenic processes like tumor growth, invasion, migration, maintenance of stem cell properties, and hindrance of apoptosis. From the tumor suppressor family of miRNAs (e.g. miR-34a, miR-125b, miR-181a, miR-148a, miR-20a, miRNA-203, miR-204, miR-199a, miR-124, and miR-214), there are members that regulate genes like HMGB1, SIRT6, MMPs, MAP kinases, KRAS, LIMK1, c-MYC, SHP2, CD44, BCAM, FZD6, DDR1 and ERKs. Their action is to regulate processes like cell cycle, epithelial–mesenchymal transition, and stemness while promoting cellular apoptosis and senescence (Garcia-Sancha et al., 2019).

Cutaneous Lymphoma

Cutaneous lymphoma, a non-Hodgkin's lymphoma subtype, is triggered by abnormal B or T cells. Cutaneous T cell lymphoma (CTCL) and cutaneous B cell lymphoma (CBCL) induce alterations in the skin and several other sites (e.g. lymph nodes, peripheral blood, and internal organs). CTCL is the most common type, covering up to 80% of all cases of cutaneous lymphomas (Willemze et al., 2005). Recently, CTCL was entered into miRNA guided therapy because CTCL progression is characterized by aberrant miRNAs (Kohnken and Mishra, 2019). Mycosis fungoides (MF), the most common form of CTCL, has around 30% of patients diagnosed with an aggressive form (Willemze et al., 2005).

DICER, the ribonuclease III-like enzyme that processes miRNA, was investigated in various CTCL forms. Out of all the types, DICER was proven by immunohistochemical analysis to be a negative predictive factor in MF patients with no correlation with gender, histological subtype, primary localization, age, and recurrence. The note that the authors pointed out in this study published in 2011 was that "miRNA(s) might be of clinical relevance in CTCL" (Valencak et al., 2011). Just 1 year after this publication, another group showed in MF biopsies harvested from early and advanced stages that the assertion regarding miRNAs is correct. The group of Maj has identified, after isolation, reverse transcriptase reactions, and cDNA amplification, a panel of miRNAs: miR-15a, miR-16, miR-155, let-7a, let-7d, and let-7f. MF was characterized by a miR-155 overexpression, and metastatic MF was found with lower concentrations of let-7a, let-7d, and let-7f. Moreover, the level of let-7a expression proved to be an independent prognostic indicator (Maj et al., 2012).

In 2019, evaluating miRNA machinery genes (e.g. Dicer and Drosha) in MF patients, interesting new data were obtained. Low Drosha expression seems to be an independent predictor biomarker for advanced stages. Moreover, this expression was associated with lymphoma-specific death, the authors pointing out the tumor suppressor gene function of Drosha (Gambichler et al., 2019).

In 2018, utilizing a RT-qPCR platform, the miRNA expressions in tumor samples harvested from over 150 patients with early-stage MF were analyzed. A three-miRNA classifier

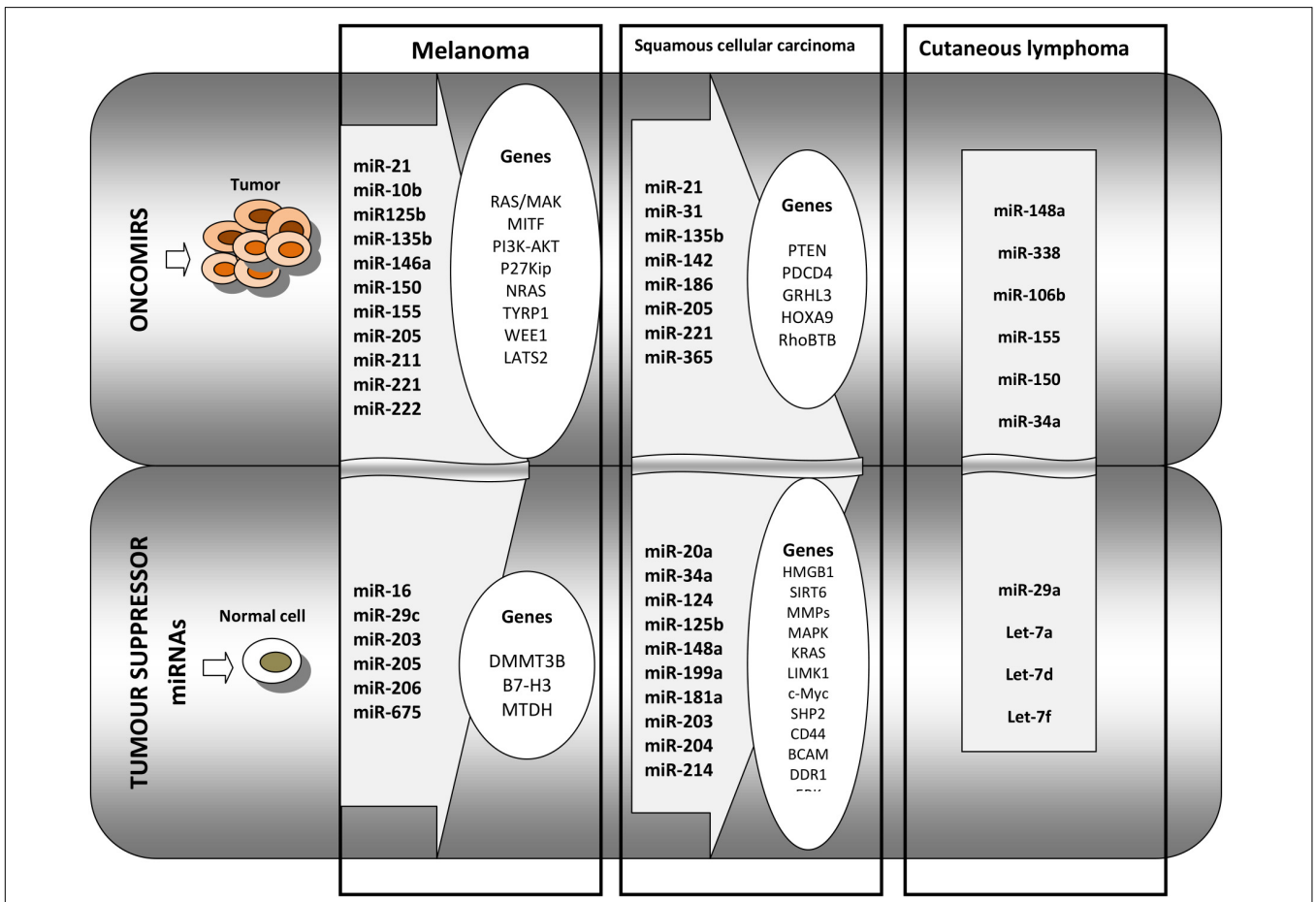

FIGURE 2 | Overview of the main miRNAs and the regulated genes that are identified in melanoma, in squamous cell carcinoma, and in cutaneous lymphoma. The **first panel** of oncomirs represents the miRNAs that regulate pro-tumoral genes in melanoma, squamous cell carcinoma, and in cutaneous lymphoma. The **second panel** represents tumor suppressor miRNAs regulating genes that are involved in anti-tumoral processes in squamous cell carcinoma and in cutaneous lymphoma.

was developed comprising miR-106b-5p, miR-148a-3p, and miR-338-3p, which correlated with clinical progression. Furthermore, this panel could stratify patients into high- and low-risk groups. This miRNA-based classifier has a good prognostic value and can further be used to orient patients' therapy (Lindahl et al., 2018).

Cutaneous B cell lymphoma, although rarer, has a high relapse rate, up to 40%; thus, identification of patient groups most likely to relapse is of utmost importance. Using RT-PCR, 11 miRNAs were identified as being associated with the differentiation stage of B cells. From this set, miR-150 was found overexpressed in CBCL-type primary cutaneous marginal zone B cell lymphomas compared to the other CBCL type, centrofollicular lymphoma. Low levels of miR-155 and miR-150 were found associated with shorter progression-free survival in primary cutaneous marginal zone B cell lymphomas type. Thus, miRNA tumor analysis can aid in the diagnosis and prognosis of CBCL (Monsalvez et al., 2013). An overview of miRNAs functioning as tumor activating or tumor suppressors in melanoma, squamous cell carcinoma and cutaneous lymphoma is presented in **Figure 2**.

Merkel Cell Carcinoma

Merkel cell carcinoma (MCC) is a rare tumor that develops in the skin. Development in elderly Caucasian males is frequent, in mostly immunocompromised individuals, where it has an aggressive evolution with >30% of deaths. Merkel cells that reside in the basal epithelial layer are subjected to malignant transformation, probably induced by Merkel cell polyomavirus infection. Discovered in 2008, Merkel cell polyomavirus was shown to be expressed in over 90% of MCC (Feng et al., 2008). MCC therapy comprises excision, chemo-, and radiotherapy, and, more recently, some Merkel cell polyomavirus vaccination (Zeng et al., 2012). However, local recurrence and early metastasis are registered in spite of the installed therapies. Novel therapies using antisense oligonucleotides or miRNAs that can regulate Atonal homolog 1 (*ATOH1*) expression, a tumor suppressor gene, could bring new clinical approaches in this disease (Krejci et al., 2010). Indeed, in 2019, new data emerged; thus, *ATOH1* was proven to bind and further activate miR-375, the highest abundant miRNA in MCC. In experimental models, it was shown that *ATOH1* knockdown in cell lines drastically reduced miR-375 expression. *ATOH1* overexpression induced a more metastasizing pattern in cell lines and an increased miR-375 expression. Testing Merkel cell polyomavirus infection in this model, it was demonstrated that the infection induces carcinogenesis *via* the induction of *ATOH1*. This approach can be developed further in a therapy target for MCC (Fan et al., 2019).

CONCLUSION

Skin cancers, with their steadily increasing incidence, and with melanoma being one of the deadliest forms of cancer, need constant attention regarding the discovery of molecular mechanisms that govern tumorigenesis, metastasis, therapy resistance, and, last but not least, the development of new therapeutic strategies.

In the molecular events that characterize these complex processes, miRNAs, small non-coding RNAs that control gene expression at the post-transcriptional level, are recently gaining increased importance. Moreover, miRNA expression can constitute an important diagnosis/prognosis and therapy monitoring markers. As miRNAs have high stability and can be identified in circulation as well, their expression profiles in body fluids can reflect the progression status, and therefore their quantification can be developed in biomarkers with prognostic value. Using circulating miRNAs should overcome some issues regarding sensitivity and specificity, and probably in the future, additional epigenomic platforms could overcome these bottlenecks.

However, the involvement of miRNAs in non-melanoma skin cancer is less characterized concerning tumor initiation, metastasis, and progression stages; hence, a miRNA signature should also be further developed in diagnostic and prognostic biomarkers.

As miRNAs have gained a role in the substantial armamentarium of biomolecules regarded as disease markers, the need for implementing a reliable technology for assessing miRNAs, especially in clinic workflow, is mandatory. Current technologies comprise qPCR or microarray platforms, but these are still challenging due to high costs and the personnel expertise required. New hopes come from classic concepts transposed into a new perspective technology, such as miREIA which has the potential to be clinic-friendly besides its high sensitivity and specificity of detection.

In the epitranscriptomic domain, the research done recently has shown that miRNAs can have dual functions: pro- or anti-tumoral activity; therefore, their thorough evaluation is more so important for establishing accurate diagnostic and/or prognostic molecular markers in skin cancers.

AUTHOR CONTRIBUTIONS

MN conceived and designed the manuscript and wrote the sections "Main Technologies That Are Used for miRNAs Identification From Biological Samples" and "miRNAs Detected in Cutaneous Melanoma" of the manuscript. SC collected the data and wrote the abstract and the section "Introduction" of the manuscript. CC conceived the manuscript and was in charge of the overall direction and planning, and wrote the section "miRNAs Detected in Cutaneous Melanoma" of the manuscript. SZ wrote the sections "miRNAs in Non-melanoma Skin Cancer" and "Conclusion" of the manuscript. MN and SC organized the sections of the manuscript and revised the final form of the manuscript.

FUNDING

This study was supported by grants PN 19.29.01.01, PN-III-P1-1.2-PCCDI-2017-0341/2018, COST CA16120-European Epitranscriptomics Network (EPITRAN), and COST CA18127-International Nucleom Consortium (INC).

REFERENCES

Aftab, M. N., Dinger, M. E., and Perera, R. J. (2014). The role of microRNAs and long non-coding RNAs in the pathology, diagnosis, and management of melanoma. *Arch. Biochem. Biophys.* 563, 60–70. doi: 10.1016/j.abb.2014.07.022

Aksenenko, M., Palkina, N., Komina, A., Tashireva, L., and Ruksha, T. (2019). Differences in microRNA expression between melanoma and healthy adjacent skin. *BMC Dermatol.* 19:1. doi: 10.1186/s12895-018-0081-1

Albulescu, R., Neagu, M., Albulescu, L., and Tanase, C. (2011). Tissular and soluble miRNAs for diagnostic and therapy improvement in digestive tract cancers. *Expert Rev. Mol. Diagn.* 11, 101–120. doi: 10.1586/erm.10.106

Ancuceanu, R., and Neagu, M. (2016). Immune based therapy for melanoma. *Indian J. Med. Res.* 143, 135–144. doi: 10.4103/0971-5916.180197

Andres-Leon, E., Nunez-Torres, R., and Rojas, A. M. (2016). miARma-Seq: a comprehensive tool for miRNA, mRNA and circRNA analysis. *Sci. Rep.* 6:25749. doi: 10.1038/srep25749

Andres-Leon, E., Nunez-Torres, R., and Rojas, A. M. (2018). Corrigendum: miARma-Seq: a comprehensive tool for miRNA, mRNA and circRNA analysis. *Sci. Rep.* 8:46928. doi: 10.1038/srep46928

Androvic, P., Valihrach, L., Elling, J., Sjoback, R., and Kubista, M. (2017). Two-tailed RT-qPCR: a novel method for highly accurate miRNA quantification. *Nucleic Acids Res.* 45:e144. doi: 10.1093/nar/gkx588

Benz, F., Roderburg, C., Vargas Cardenas, D., Vucur, M., Gautheron, J., Koch, A., et al. (2013). U6 is unsuitable for normalization of serum miRNA levels in patients with sepsis or liver fibrosis. *Exp. Mol. Med.* 45:e42. doi: 10.1038/emm.2013.81

Bobbili, M. R., Mader, R. M., Grillari, J., and Dellago, H. (2017). OncomiR-17-5p: alarm signal in cancer? *Oncotarget* 8, 71206–71222. doi: 10.18632/oncotarget.19331

Canueto, J., Cardenoso-Alvarez, E., Garcia-Hernandez, J. L., Galindo-Villardon, P., Vicente-Galindo, P., Vicente-Villardon, J. L., et al. (2017). MicroRNA (miR)-203 and miR-205 expression patterns identify subgroups of prognosis in cutaneous squamous cell carcinoma. *Br. J. Dermatol.* 177, 168–178. doi: 10.1111/bjd.15236

Caporali, S., Amaro, A., Levati, L., Alvino, E., Lacal, P. M., Mastroeni, S., et al. (2019). miR-126-3p down-regulation contributes to dabrafenib acquired resistance in melanoma by up-regulating ADAM9 and VEGF-A. *J. Exp. Clin. Cancer Res.* 38:272. doi: 10.1186/s13046-019-1238-4

Caramuta, S., Egyhazi, S., Rodolfo, M., Witten, D., Hansson, J., Larsson, C., et al. (2010). MicroRNA expression profiles associated with mutational status and survival in malignant melanoma. *J. Invest. Dermatol.* 130, 2062–2070. doi: 10.1038/jid.2010.63

Caron, M. P., Bastet, L., Lussier, A., Simoneau-Roy, M., Masse, E., and Lafontaine, D. A. (2012). Dual-acting riboswitch control of translation initiation and mRNA decay. *Proc. Natl. Acad. Sci. U.S.A.* 109, E3444–E3453. doi: 10.1073/pnas.1214024109

Chen, X., Liu, S., Zhao, X., Ma, X., Gao, G., Yu, L., et al. (2017). Long noncoding RNA ILF3-AS1 promotes cell proliferation, migration, and invasion via negatively regulating miR-200b/a/429 in melanoma. *Biosci. Rep.* 37:BSR20171031. doi: 10.1042/BSR20171031

Corcoran, N. M., Hovens, C. M., Hong, M. K., Pedersen, J., Casey, R. G., Connolly, S., et al. (2012). Underestimation of Gleason score at prostate biopsy reflects sampling error in lower volume tumours. *BJU Int.* 109, 660–664. doi: 10.1111/j.1464-410X.2011.10543.x

Cretoiu, D., Xu, J., Xiao, J., and Cretoiu, S. M. (2016a). Telocytes and their extracellular vesicles-evidence and hypotheses. *Int. J. Mol. Sci.* 17:1322. doi: 10.3390/ijms17081322

Cretoiu, D., Xu, J., Xiao, J., Suciu, N., and Cretoiu, S. M. (2016b). Circulating MicroRNAs as potential molecular biomarkers in pathophysiological evolution of pregnancy. *Dis. Markers* 2016:3851054. doi: 10.1155/2016/3851054

D'Aguanno, S., Valentini, E., Tupone, M. G., Desideri, M., Di Martile, M., Spagnuolo, M., et al. (2018). Semaphorin 5A drives melanoma progression: role of Bcl-2, miR-204 and c-Myb. *J. Exp. Clin. Cancer Res.* 37:278. doi: 10.1186/s13046-018-0933-x

Das, S., Ferlito, M., Kent, O. A., Fox-Talbot, K., Wang, R., Liu, D., et al. (2012). Nuclear miRNA regulates the mitochondrial genome in the heart. *Circ. Res.* 110, 1596–1603. doi: 10.1161/CIRCRESAHA.112.267732

Dave, V. P., Ngo, T. A., Pernestig, A. K., Tilevik, D., Kant, K., Nguyen, T., et al. (2019). MicroRNA amplification and detection technologies: opportunities and challenges for point of care diagnostics. *Lab. Invest.* 99, 452–469. doi: 10.1038/s41374-018-0143-3

de Planell-Saguer, M., and Rodicio, M. C. (2011). Analytical aspects of microRNA in diagnostics: a review. *Anal. Chim. Acta* 699, 134–152. doi: 10.1016/j.aca.2011.05.025

de Unamuno, B., Palanca, S., and Botella, R. (2015). Update on melanoma epigenetics. *Curr. Opin. Oncol.* 27, 420–426. doi: 10.1097/CCO.0000000000000217

Dinescu, S., Ignat, S., Lazar, A. D., Constantin, C., Neagu, M., and Costache, M. (2019). Epitranscriptomic signatures in lncRNAs and their possible roles in cancer. *Genes* 10:E52. doi: 10.3390/genes10010052

DiSano, J. A., Huffnagle, I., Gowda, R., Spiegelman, V. S., Robertson, G. P., and Pameijer, C. R. (2019). Loss of miR-155 upregulates WEE1 in metastatic melanoma. *Melanoma Res.* 29, 216–219. doi: 10.1097/CMR.0000000000000545

Dragomir, M. P., Knutsen, E., and Calin, G. A. (2018). SnapShot: unconventional miRNA functions. *Cell* 174:e1031. doi: 10.1016/j.cell.2018.07.040

El Hajj, P., Gilot, D., Migault, M., Theunis, A., Van Kempen, L. C., Sales, F., et al. (2015). SNPs at miR-155 binding sites of TYRP1 explain discrepancy between mRNA and protein and refine TYRP1 prognostic value in melanoma. *Br. J. Cancer* 113, 91–98. doi: 10.1038/bjc.2015.194

Elias, K. M., Fendler, W., Stawiski, K., Fiascone, S. J., Vitonis, A. F., Berkowitz, R. S., et al. (2017). Diagnostic potential for a serum miRNA neural network for detection of ovarian cancer. *eLife* 6:e28932. doi: 10.7554/eLife.28932

Fan, K., Gravemeyer, J., Ritter, C., Rasheed, K., Gambichler, T., Moens, U., et al. (2019). MCPyV Large T antigen induced atonal homolog 1 (ATOH1) is a lineage-dependency oncogene in Merkel cell carcinoma. *J. Invest. Dermatol.* 140, 56–65.e3. doi: 10.1016/j.jid.2019.06.135

Fattore, L., Mancini, R., Acunzo, M., Romano, G., Lagana, A., Pisanu, M. E., et al. (2016). miR-579-3p controls melanoma progression and resistance to target therapy. *Proc. Natl. Acad. Sci. U.S.A.* 113, E5005–E5013. doi: 10.1073/pnas.1607753113

Felicetti, F., Errico, M. C., Segnalini, P., Mattia, G., and Care, A. (2008). MicroRNA-221 and -222 pathway controls melanoma progression. *Expert Rev. Anticancer Ther.* 8, 1759–1765. doi: 10.1586/14737140.8.11.1759

Feng, H., Shuda, M., Chang, Y., and Moore, P. S. (2008). Clonal integration of a polyomavirus in human Merkel cell carcinoma. *Science* 319, 1096–1100. doi: 10.1126/science.1152586

Friedman, E. B., Shang, S., De Miera, E. V., Fog, J. U., Teilum, M. W., Ma, M. W., et al. (2012). Serum microRNAs as biomarkers for recurrence in melanoma. *J. Transl. Med.* 10:155. doi: 10.1186/1479-5876-10-155

Gambichler, T., Salveridou, K., Schmitz, L., Kafferlein, H. U., Bruning, T., Stockfleth, E., et al. (2019). Low Drosha protein expression in cutaneous T-cell lymphoma is associated with worse disease outcome. *J. Eur. Acad. Dermatol. Venereol.* 33, 1695–1699. doi: 10.1111/jdv.15652

Garcia-Sancha, N., Corchado-Cobos, R., Perez-Losada, J., and Canueto, J. (2019). MicroRNA dysregulation in cutaneous squamous cell carcinoma. *Int. J. Mol. Sci.* 20:E2181. doi: 10.3390/ijms20092181

Giannopoulou, A. F., Konstantakou, E. G., Velentzas, A. D., Avgeris, S. N., Avgeris, M., Papandreou, N. C., et al. (2019). Gene-specific Intron retention serves as molecular signature that distinguishes melanoma from non-melanoma cancer cells in Greek patients. *Int. J. Mol. Sci.* 20:E937. doi: 10.3390/ijms20040937

Git, A., Dvinge, H., Salmon-Divon, M., Osborne, M., Kutter, C., Hadfield, J., et al. (2010). Systematic comparison of microarray profiling, real-time PCR, and next-generation sequencing technologies for measuring differential microRNA expression. *RNA* 16, 991–1006. doi: 10.1261/rna.1947110

Gong, Z. H., Zhou, F., Shi, C., Xiang, T., Zhou, C. K., Wang, Q. Q., et al. (2019). miRNA-221 promotes cutaneous squamous cell carcinoma progression by targeting PTEN. *Cell. Mol. Biol. Lett.* 24:9. doi: 10.1186/s11658-018-0131-z

Greenberg, E., Hershkovitz, L., Itzhaki, O., Hajdu, S., Nemlich, Y., Ortenberg, R., et al. (2011). Regulation of cancer aggressive features in melanoma cells by microRNAs. *PLoS One* 6:e18936. doi: 10.1371/journal.pone.0018936

Greenberg, E., Nemlich, Y., and Markel, G. (2014). MicroRNAs in cancer: lessons from melanoma. *Curr. Pharm. Des.* 20, 5246–5259. doi: 10.2174/1381612820666140128210105

Grignol, V., Fairchild, E. T., Zimmerer, J. M., Lesinski, G. B., Walker, M. J., Magro, C. M., et al. (2011). miR-21 and miR-155 are associated with mitotic activity and lesion depth of borderline melanocytic lesions. *Br. J. Cancer* 105, 1023–1029. doi: 10.1038/bjc.2011.288

Guo, S., Guo, W., Li, S., Dai, W., Zhang, N., Zhao, T., et al. (2016). Serum miR-16: a potential biomarker for predicting melanoma prognosis. *J. Invest. Dermatol.* 136, 985–993. doi: 10.1016/j.jid.2015.12.041

Hanna, J. A., Hahn, L., Agarwal, S., and Rimm, D. L. (2012). In situ measurement of miR-205 in malignant melanoma tissue supports its role as a tumor suppressor microRNA. *Lab. Invest.* 92, 1390–1397. doi: 10.1038/labinvest.2012.119

Horsham, J. L., Ganda, C., Kalinowski, F. C., Brown, R. A., Epis, M. R., and Leedman, P. J. (2015). MicroRNA-7: a miRNA with expanding roles in development and disease. *Int. J. Biochem. Cell Biol.* 69, 215–224. doi: 10.1016/j.biocel.2015.11.001

Hoss, A. G., Labadorf, A., Latourelle, J. C., Kartha, V. K., Hadzi, T. C., Gusella, J. F., et al. (2015). miR-10b-5p expression in Huntington's disease brain relates to age of onset and the extent of striatal involvement. *BMC Med. Genomics* 8:10. doi: 10.1186/s12920-015-0083-3

Hu, Y., Wang, Q., and Zhu, X. H. (2019). MiR-135b is a novel oncogenic factor in cutaneous melanoma by targeting LATS2. *Melanoma Res.* 29, 119–125. doi: 10.1097/CMR.0000000000000524

Huang, S. K., and Hoon, D. S. (2016). Liquid biopsy utility for the surveillance of cutaneous malignant melanoma patients. *Mol. Oncol.* 10, 450–463. doi: 10.1016/j.molonc.2015.12.008

Hube, F., and Francastel, C. (2015). Mammalian introns: when the junk generates molecular diversity. *Int. J. Mol. Sci.* 16, 4429–4452. doi: 10.3390/ijms16034429

Huber, V., Vallacchi, V., Fleming, V., Hu, X., Cova, A., Dugo, M., et al. (2018). Tumor-derived microRNAs induce myeloid suppressor cells and predict immunotherapy resistance in melanoma. *J. Clin. Invest.* 128, 5505–5516. doi: 10.1172/JCI98060

Hunt, E. A., Broyles, D., Head, T., and Deo, S. K. (2015). MicroRNA detection: current technology and research strategies. *Annu. Rev. Anal. Chem.* 8, 217–237. doi: 10.1146/annurev-anchem-071114-040343

Jantsch, M. F., Quattrone, A., O'connell, M., Helm, M., Frye, M., Macias-Gonzales, M., et al. (2018). Positioning Europe for the EPITRANSCRIPTOMICS challenge. *RNA Biol.* 15, 829–831. doi: 10.1080/15476286.2018.1460996

Jayawardana, K., Schramm, S. J., Haydu, L., Thompson, J. F., Scolyer, R. A., Mann, G. J., et al. (2015). Determination of prognosis in metastatic melanoma through integration of clinico-pathologic, mutation, mRNA, microRNA, and protein information. *Int. J. Cancer* 136, 863–874. doi: 10.1002/ijc.29047

Jayawardana, K., Schramm, S. J., Tembe, V., Mueller, S., Thompson, J. F., Scolyer, R. A., et al. (2016). Identification, review, and systematic cross-validation of microRNA prognostic signatures in metastatic melanoma. *J. Invest. Dermatol.* 136, 245–254. doi: 10.1038/JID.2015.355

Jiang, L., Lv, X., Li, J., Li, J., Li, X., Li, W., et al. (2012). The status of microRNA-21 expression and its clinical significance in human cutaneous malignant melanoma. *Acta Histochem.* 114, 582–588. doi: 10.1016/j.acthis.2011.11.001

Jin, J., Vaud, S., Zhelkovsky, A. M., Posfai, J., and Mcreynolds, L. A. (2016). Sensitive and specific miRNA detection method using SplintR Ligase. *Nucleic Acids Res.* 44:e116. doi: 10.1093/nar/gkw399

Kanemaru, H., Fukushima, S., Yamashita, J., Honda, N., Oyama, R., Kakimoto, A., et al. (2011). The circulating microRNA-221 level in patients with malignant melanoma as a new tumor marker. *J. Dermatol. Sci.* 61, 187–193. doi: 10.1016/j.jdermsci.2010.12.010

Kappel, A., Backes, C., Huang, Y., Zafari, S., Leidinger, P., Meder, B., et al. (2015). MicroRNA *in vitro* diagnostics using immunoassay analyzers. *Clin. Chem.* 61, 600–607. doi: 10.1373/clinchem.2014.232165

Kohnken, R., and Mishra, A. (2019). MicroRNAs in cutaneous T-cell lymphoma: the future of therapy. *J. Invest. Dermatol.* 139, 528–534. doi: 10.1016/j.jid.2018.10.035

Komina, A., Palkina, N., Aksenenko, M., Tsyrenzhapova, S., and Ruksha, T. (2016). Antiproliferative and pro-apoptotic effects of MiR-4286 inhibition in melanoma cells. *PLoS One* 11:e0168229. doi: 10.1371/journal.pone.0168229

Kozar, I., Cesi, G., Margue, C., Philippidou, D., and Kreis, S. (2017). Impact of BRAF kinase inhibitors on the miRNomes and transcriptomes of melanoma cells. *Biochim. Biophys. Acta* 1861, 2980–2992. doi: 10.1016/j.bbagen.2017.04.005

Kozomara, A., and Griffiths-Jones, S. (2011). miRBase: integrating microRNA annotation and deep-sequencing data. *Nucleic Acids Res.* 39, D152–D157. doi: 10.1093/nar/gkq1027

Krejci, K., Zadrazil, J., Tichy, T., Horak, P., Ciferska, H., Hodulova, M., et al. (2010). [Merkel cell skin carcinoma]. *Klin. Onkol.* 23, 210–217.

Krepelkova, I., Mrackova, T., Izakova, J., Dvorakova, B., Chalupova, L., Mikulik, R., et al. (2019). Evaluation of miRNA detection methods for the analytical characteristic necessary for clinical utilization. *Biotechniques* 66, 277–284. doi: 10.2144/btn-2019-0021

Larrea, E., Sole, C., Manterola, L., Goicoechea, I., Armesto, M., Arestin, M., et al. (2016). New concepts in cancer biomarkers: circulating miRNAs in liquid biopsies. *Int. J. Mol. Sci.* 17:E627. doi: 10.3390/ijms17050627

Latchana, N., Ganju, A., Howard, J. H., and Carson, W. E. III (2016). MicroRNA dysregulation in melanoma. *Surg. Oncol.* 25, 184–189. doi: 10.1016/j.suronc.2016.05.017

Lawrie, C. H., Gal, S., Dunlop, H. M., Pushkaran, B., Liggins, A. P., Pulford, K., et al. (2008). Detection of elevated levels of tumour-associated microRNAs in serum of patients with diffuse large B-cell lymphoma. *Br. J. Haematol.* 141, 672–675. doi: 10.1111/j.1365-2141.2008.07077.x

Le, M. T., Hamar, P., Guo, C., Basar, E., Perdigao-Henriques, R., Balaj, L., et al. (2014). miR-200-containing extracellular vesicles promote breast cancer cell metastasis. *J. Clin. Invest.* 124, 5109–5128. doi: 10.1172/JCI75695

Leibowitz-Amit, R., Sidi, Y., and Avni, D. (2012). Aberrations in the microRNA biogenesis machinery and the emerging roles of micro-RNAs in the pathogenesis of cutaneous malignant melanoma. *Pigment Cell Melanoma Res.* 25, 740–757. doi: 10.1111/pcmr.12018

Leidinger, P., Keller, A., Borries, A., Reichrath, J., Rass, K., Jager, S. U., et al. (2010). High-throughput miRNA profiling of human melanoma blood samples. *BMC Cancer* 10:262. doi: 10.1186/1471-2407-10-262

Leng, Q., Wang, Y., and Jiang, F. (2018). A direct plasma miRNA assay for early detection and histological classification of lung cancer. *Transl. Oncol.* 11, 883–889. doi: 10.1016/j.tranon.2018.05.001

Leti, F., and DiStefano, J. K. (2018). miRNA quantification method using quantitative polymerase chain reaction in conjunction with C q method. *Methods Mol. Biol.* 1706, 257–265. doi: 10.1007/978-1-4939-7471-9_14

Li, J., Lai, Y., Ma, J., Liu, Y., Bi, J., Zhang, L., et al. (2017). miR-17-5p suppresses cell proliferation and invasion by targeting ETV1 in triple-negative breast cancer. *BMC Cancer* 17:745. doi: 10.1186/s12885-017-3674-x

Li, N., Liu, Y., Pang, H., Lee, D., Zhou, Y., and Xiao, Z. (2019). Methylation-mediated silencing of microRNA-211 decreases the sensitivity of melanoma cells to cisplatin. *Med. Sci. Monit.* 25, 1590–1599. doi: 10.12659/MSM.911862

Li, P., He, Q. Y., Luo, C. Q., and Qian, L. Y. (2014). Circulating miR-221 expression level and prognosis of cutaneous malignant melanoma. *Med. Sci. Monit.* 20, 2472–2477. doi: 10.12659/MSM.891327

Li, X., and Cai, Y. (2019). Better prognostic determination and feature characterization of cutaneous melanoma through integrative genomic analysis. *Aging* 11, 5081–5107. doi: 10.18632/aging.102099

Lin, N., Zhou, Y., Lian, X., and Tu, Y. (2015). Expression of microRNA-106b and its clinical significance in cutaneous melanoma. *Genet. Mol. Res.* 14, 16379–16385. doi: 10.4238/2015.December.9.6

Lin, S., and Gregory, R. I. (2015). MicroRNA biogenesis pathways in cancer. *Nat. Rev. Cancer* 15, 321–333. doi: 10.1038/nrc3932

Lindahl, L. M., Besenbacher, S., Rittig, A. H., Celis, P., Willerslev-Olsen, A., Gjerdrum, L. M. R., et al. (2018). Prognostic miRNA classifier in early-stage mycosis fungoides: development and validation in a Danish nationwide study. *Blood* 131, 759–770. doi: 10.1182/blood-2017-06-788950

Liu, F., Zhang, F., Li, X., Liu, Q., Liu, W., Song, P., et al. (2017). Prognostic role of miR-17-92 family in human cancers: evaluation of multiple prognostic outcomes. *Oncotarget* 8, 69125–69138. doi: 10.18632/oncotarget.19096

Liu, K., Jin, J., Rong, K., Zhuo, L., and Li, P. (2018). MicroRNA675 inhibits cell proliferation and invasion in melanoma by directly targeting metadherin. *Mol. Med. Rep.* 17, 3372–3379. doi: 10.3892/mmr.2017.8264

Luo, C., Weber, C. E., Osen, W., Bosserhoff, A. K., and Eichmuller, S. B. (2014). The role of microRNAs in melanoma. *Eur. J. Cell Biol.* 93, 11–22.

Ma, H., Liang, C., Wang, G., Jia, S., Zhao, Q., Xiang, Z., et al. (2014). MicroRNA-mediated cancer metastasis regulation via heterotypic signals in the microenvironment. *Curr. Pharm. Biotechnol.* 15, 455–458. doi: 10.2174/1389201015666140516112042

Maj, J., Jankowska-Konsur, A., Sadakierska-Chudy, A., Noga, L., and Reich, A. (2012). Altered microRNA expression in mycosis fungoides. *Br. J. Dermatol.* 166, 331–336. doi: 10.1111/j.1365-2133.2011.10669.x

Marabita, F., De Candia, P., Torri, A., Tegner, J., Abrignani, S., and Rossi, R. L. (2016). Normalization of circulating microRNA expression data obtained by quantitative real-time RT-PCR. *Brief. Bioinform.* 17, 204–212. doi: 10.1093/bib/bbv056

Markopoulos, G. S., Roupakia, E., Tokamani, M., Chavdoula, E., Hatziapostolou, M., Polytarchou, C., et al. (2017). A step-by-step microRNA guide to cancer development and metastasis. *Cell. Oncol.* 40, 303–339. doi: 10.1007/s13402-017-0341-9

Matsui, M., Chu, Y., Zhang, H., Gagnon, K. T., Shaikh, S., Kuchimanchi, S., et al. (2013). Promoter RNA links transcriptional regulation of inflammatory pathway genes. *Nucleic Acids Res.* 41, 10086–10109. doi: 10.1093/nar/gkt777

Mirzaei, H., Gholamin, S., Shahidsales, S., Sahebkar, A., Jaafari, M. R., Mirzaei, H. R., et al. (2016). MicroRNAs as potential diagnostic and prognostic biomarkers in melanoma. *Eur. J. Cancer* 53, 25–32.

Mitchell, P. S., Parkin, R. K., Kroh, E. M., Fritz, B. R., Wyman, S. K., Pogosova-Agadjanyan, E. L., et al. (2008). Circulating microRNAs as stable blood-based markers for cancer detection. *Proc. Natl. Acad. Sci. U.S.A.* 105, 10513–10518. doi: 10.1073/pnas.0804549105

Monroig-Bosque Pdel, C., Rivera, C. A., and Calin, G. A. (2015). MicroRNAs in cancer therapeutics: "from the bench to the bedside". *Expert Opin. Biol. Ther.* 15, 1381–1385. doi: 10.1517/14712598.2015.1074999

Monsalvez, V., Montes-Moreno, S., Artiga, M. J., Rodriguez, M. E., Espiridion, B. S., Lozano, M., et al. (2013). MicroRNAs as prognostic markers in indolent primary cutaneous B-cell lymphoma. *Mod. Pathol.* 26:617. doi: 10.1038/modpathol.2012.209

Mumford, S. L., Towler, B. P., Pashler, A. L., Gilleard, O., Martin, Y., and Newbury, S. F. (2018). Circulating microRNA biomarkers in melanoma: tools and challenges in personalised medicine. *Biomolecules* 8:E21. doi: 10.3390/biom8020021

Neagu, M., Constantin, C., Bostan, M., Caruntu, C., Ignat, S. R., Dinescu, S., et al. (2019a). Proteomics technologies "lens" for epithelial–mesenchymal transition process identification in oncology. *Anal. Cell. Pathol.* 2019:3565970.

Neagu, M., Constantin, C., Manda, G., and Margaritescu, I. (2009). Biomarkers of metastatic melanoma. *Biomark. Med.* 3, 71–89. doi: 10.2217/17520363.3.1.71

Neagu, M., Constantin, C., Popescu, I. D., Zipeto, D., Tzanakakis, G., Nikitovic, D., et al. (2019b). Inflammation and metabolism in cancer cell-mitochondria key player. *Front. Oncol.* 9:348. doi: 10.3389/fonc.2019.00348

Neagu, M., Constantin, C., and Zurac, S. (2013). Immune parameters in the prognosis and therapy monitoring of cutaneous melanoma patients: experience, role, and limitations. *Biomed. Res. Int.* 2013:107940. doi: 10.1155/2013/107940

Nguyen, T., Kuo, C., Nicholl, M. B., Sim, M. S., Turner, R. R., Morton, D. L., et al. (2011). Downregulation of microRNA-29c is associated with hypermethylation of tumor-related genes and disease outcome in cutaneous melanoma. *Epigenetics* 6, 388–394. doi: 10.4161/epi.6.3.14056

Ouyang, T., Liu, Z., Han, Z., and Ge, Q. (2019). MicroRNA detection specificity: recent advances and future perspective. *Anal. Chem.* 91, 3179–3186. doi: 10.1021/acs.analchem.8b05909

Ozsolak, F., and Milos, P. M. (2011). RNA sequencing: advances, challenges and opportunities. *Nat. Rev. Genet.* 12, 87–98. doi: 10.1038/nrg2934

Penna, E., Orso, F., Cimino, D., Vercellino, I., Grassi, E., Quaglino, E., et al. (2013). miR-214 coordinates melanoma progression by upregulating ALCAM through TFAP2 and miR-148b downmodulation. *Cancer Res.* 73, 4098–4111. doi: 10.1158/0008-5472.CAN-12-3686

Penna, E., Orso, F., and Taverna, D. (2015). miR-214 as a key hub that controls cancer networks: small player, multiple functions. *J. Invest. Dermatol.* 135, 960–969. doi: 10.1038/jid.2014.479

Philippidou, D., Schmitt, M., Moser, D., Margue, C., Nazarov, P. V., Muller, A., et al. (2010). Signatures of microRNAs and selected microRNA target genes in human melanoma. *Cancer Res.* 70, 4163–4173. doi: 10.1158/0008-5472.CAN-09-4512

Polini, B., Carpi, S., Romanini, A., Breschi, M. C., Nieri, P., and Podesta, A. (2019). Circulating cell-free microRNAs in cutaneous melanoma staging and recurrence or survival prognosis. *Pigment Cell Melanoma Res.* 32, 486–499. doi: 10.1111/pcmr.12755

Prabhakar, K., Rodriotaguez, C. I., Jayanthy, A. S., Mikheil, D. M., Bhasker, A. I., Perera, R. J., et al. (2019). Role of miR-214 in regulation of beta-catenin and the malignant phenotype of melanoma. *Mol. Carcinog.* 58, 1974–1984. doi: 10.1002/mc.23089

Quinodoz, S., and Guttman, M. (2014). Long noncoding RNAs: an emerging link between gene regulation and nuclear organization. *Trends Cell Biol.* 24, 651–663. doi: 10.1016/j.tcb.2014.08.009

Reid, G., Kirschner, M. B., and Van Zandwijk, N. (2011). Circulating microRNAs: association with disease and potential use as biomarkers. *Crit. Rev. Oncol. Hematol.* 80, 193–208. doi: 10.1016/j.critrevonc.2010.11.004

Ross, C. L., Kaushik, S., Valdes-Rodriguez, R., and Anvekar, R. (2018). MicroRNAs in cutaneous melanoma: role as diagnostic and prognostic biomarkers. *J. Cell. Physiol.* 233, 5133–5141. doi: 10.1002/jcp.26395

Sabarimurugan, S., Madurantakam Royam, M., Das, A., Das, S., K M, G., and Jayaraj, R. (2018). Systematic review and meta-analysis of the prognostic significance of miRNAs in melanoma patients. *Mol. Diagn. Ther.* 22, 653–669. doi: 10.1007/s40291-018-0357-5

Saldanha, G., Elshaw, S., Sachs, P., Alharbi, H., Shah, P., Jothi, A., et al. (2016). microRNA-10b is a prognostic biomarker for melanoma. *Mod. Pathol.* 29, 112–121. doi: 10.1038/modpathol.2015.149

Sanchez-Sendra, B., Martinez-Ciarpaglini, C., Gonzalez-Munoz, J. F., Murgui, A., Terradez, L., and Monteagudo, C. (2018). Downregulation of intratumoral expression of miR-205, miR-200c and miR-125b in primary human cutaneous melanomas predicts shorter survival. *Sci. Rep.* 8:17076. doi: 10.1038/s41598-018-35317-3

Sanders, R., Bustin, S., Huggett, J., and Mason, D. (2018). Improving the standardization of mRNA measurement by RT-qPCR. *Biomol. Detect. Quantif.* 15, 13–17. doi: 10.1016/j.bdq.2018.03.001

Satzger, I., Mattern, A., Kuettler, U., Weinspach, D., Voelker, B., Kapp, A., et al. (2010). MicroRNA-15b represents an independent prognostic parameter and is correlated with tumor cell proliferation and apoptosis in malignant melanoma. *Int. J. Cancer* 126, 2553–2562. doi: 10.1002/ijc.24960

Segura, M. F., Belitskaya-Levy, I., Rose, A. E., Zakrzewski, J., Gaziel, A., Hanniford, D., et al. (2010). Melanoma MicroRNA signature predicts post-recurrence survival. *Clin. Cancer Res.* 16, 1577–1586. doi: 10.1158/1078-0432.CCR-09-2721

Segura, M. F., Greenwald, H. S., Hanniford, D., Osman, I., and Hernando, E. (2012). MicroRNA and cutaneous melanoma: from discovery to prognosis and therapy. *Carcinogenesis* 33, 1823–1832. doi: 10.1093/carcin/bgs205

Seremet, T., Jansen, Y., Planken, S., Njimi, H., Delaunoy, M., El Housni, H., et al. (2019). Undetectable circulating tumor DNA (ctDNA) levels correlate with favorable outcome in metastatic melanoma patients treated with anti-PD1 therapy. *J. Transl. Med.* 17:303. doi: 10.1186/s12967-019-2051-8

Skourti, E., Logotheti, S., Kontos, C. K., Pavlopoulou, A., Dimoragka, P. T., Trougakos, I. P., et al. (2016). Progression of mouse skin carcinogenesis is associated with the orchestrated deregulation of mir-200 family members, mir-205 and their common targets. *Mol. Carcinog.* 55, 1229–1242. doi: 10.1002/mc.22365

Stark, M. S., Klein, K., Weide, B., Haydu, L. E., Pflugfelder, A., Tang, Y. H., et al. (2015). The prognostic and predictive value of melanoma-related microRNAs using tissue and serum: a microRNA expression analysis. *EBioMedicine* 2, 671–680. doi: 10.1016/j.ebiom.2015.05.011

Tanase, C. P., Albulescu, R., and Neagu, M. (2011). Application of 3D hydrogel microarrays in molecular diagnostics: advantages and limitations. *Expert Rev. Mol. Diagn.* 11, 461–464. doi: 10.1586/erm.11.30

Taucher, V., Mangge, H., and Haybaeck, J. (2016). Non-coding RNAs in pancreatic cancer: challenges and opportunities for clinical application. *Cell. Oncol.* 39, 295–318. doi: 10.1007/s13402-016-0275-7

Taylor, D. D., and Gercel-Taylor, C. (2013). The origin, function, and diagnostic potential of RNA within extracellular vesicles present in human biological fluids. *Front. Genet.* 4:142. doi: 10.3389/fgene.2013.00142

Thyagarajan, A., Tsai, K. Y., and Sahu, R. P. (2019). MicroRNA heterogeneity in melanoma progression. *Semin. Cancer Biol.* 59, 208–220. doi: 10.1016/j.semcancer.2019.05.021

Tian, R., Liu, T., Qiao, L., Gao, M., and Li, J. (2015). Decreased serum microRNA-206 level predicts unfavorable prognosis in patients with melanoma. *Int. J. Clin. Exp. Pathol.* 8, 3097–3103.

Tian, Y., Wei, W., Li, L., and Yang, R. (2015). Down-regulation of miR-148a promotes metastasis by DNA methylation and is associated with prognosis of skin cancer by targeting TGIF2. *Med. Sci. Monit.* 21, 3798–3805. doi: 10.12659/msm.894826

Valencak, J., Schmid, K., Trautinger, F., Wallnofer, W., Muellauer, L., Soleiman, A., et al. (2011). High expression of Dicer reveals a negative prognostic influence in certain subtypes of primary cutaneous T cell lymphomas. *J. Dermatol. Sci.* 64, 185–190. doi: 10.1016/j.jdermsci.2011.08.011

Van Laar, R., Lincoln, M., and Van Laar, B. (2018). Development and validation of a plasma-based melanoma biomarker suitable for clinical use. *Br. J. Cancer* 118, 857–866. doi: 10.1038/bjc.2017.477

Van Roosbroeck, K., Bayraktar, R., Calin, S., Bloehdorn, J., Dragomir, M. P., Okubo, K., et al. (2019). The involvement of microRNA in the pathogenesis of Richter syndrome. *Haematologica* 104, 1004–1015. doi: 10.3324/haematol.2018.203828

Varamo, C., Occelli, M., Vivenza, D., Merlano, M., and Lo Nigro, C. (2017). MicroRNAs role as potential biomarkers and key regulators in melanoma. *Genes Chromosomes Cancer* 56, 3–10. doi: 10.1002/gcc.22402

Vasudevan, S., Tong, Y., and Steitz, J. A. (2007). Switching from repression to activation: microRNAs can up-regulate translation. *Science* 318, 1931–1934. doi: 10.1126/science.1149460

Voichitoiu, A. D., Radu, B. M., Pavelescu, L., Cretoiu, D., Deftu, A. T., Suciu, N., et al. (2019). "Extracellular vesicles in cancer," in *Extracellular Vesicles*, ed. A. Gil De Bona, (London: InTech Open).

Wang, B., and Xi, Y. (2013). Challenges for microRNA microarray data analysis. *Microarrays* 2, 34–50. doi: 10.3390/microarrays2020034

Wang, J., Chong, K. K., Nakamura, Y., Nguyen, L., Huang, S. K., Kuo, C., et al. (2013). B7-H3 associated with tumor progression and epigenetic regulatory activity in cutaneous melanoma. *J. Invest. Dermatol.* 133, 2050–2058. doi: 10.1038/jid.2013.114

Wang, K., and Zhang, Z. W. (2015). Expression of miR-203 is decreased and associated with the prognosis of melanoma patients. *Int. J. Clin. Exp. Pathol.* 8, 13249–13254.

Wang, L. X., Wan, C., Dong, Z. B., Wang, B. H., Liu, H. Y., and Li, Y. (2019). Integrative analysis of long noncoding RNA (lncRNA), microRNA (miRNA) and mRNA expression and construction of a competing endogenous RNA (ceRNA) network in metastatic melanoma. *Med. Sci. Monit.* 25, 2896–2907. doi: 10.12659/MSM.913881

Wang, W. T., and Chen, Y. Q. (2014). Circulating miRNAs in cancer: from detection to therapy. *J. Hematol. Oncol.* 7:86.

Weiss, S. A., Hanniford, D., Hernando, E., and Osman, I. (2015). Revisiting determinants of prognosis in cutaneous melanoma. *Cancer* 121, 4108–4123. doi: 10.1002/cncr.29634

Willemze, R., Jaffe, E. S., Burg, G., Cerroni, L., Berti, E., Swerdlow, S. H., et al. (2005). WHO-EORTC classification for cutaneous lymphomas. *Blood* 105, 3768–3785. doi: 10.1182/blood-2004-09-3502

Worley, L. A., Long, M. D., Onken, M. D., and Harbour, J. W. (2008). Micro-RNAs associated with metastasis in uveal melanoma identified by multiplexed microarray profiling. *Melanoma Res.* 18, 184–190. doi: 10.1097/CMR.0b013e3282feeac6

Xiong, Y., Liu, L., Qiu, Y., and Liu, L. (2018). MicroRNA-29a inhibits growth, migration and invasion of melanoma A375 cells *in vitro* by directly targeting BMI1. *Cell. Physiol. Biochem.* 50, 385–397. doi: 10.1159/000494015

Xu, Y., Brenn, T., Brown, E. R., Doherty, V., and Melton, D. W. (2012). Differential expression of microRNAs during melanoma progression: miR-200c, miR-205 and miR-211 are downregulated in melanoma and act as tumour suppressors. *Br. J. Cancer* 106, 553–561. doi: 10.1038/bjc.2011.568

Young, A. L., Malik, H. Z., Abu-Hilal, M., Guthrie, J. A., Wyatt, J., Prasad, K. R., et al. (2007). Large hepatocellular carcinoma: time to stop preoperative biopsy. *J. Am. Coll. Surg.* 205, 453–462. doi: 10.1016/j.jamcollsurg.2007.04.033

Zeng, Q., Gomez, B. P., Viscidi, R. P., Peng, S., He, L., Ma, B., et al. (2012). Development of a DNA vaccine targeting Merkel cell polyomavirus. *Vaccine* 30, 1322–1329. doi: 10.1016/j.vaccine.2011.12.072

Zhang, L., Xiang, P., Han, X., Wu, L., Li, X., and Xiong, Z. (2015). Decreased expression of microRNA-20a promotes tumor progression and predicts poor prognosis of cutaneous squamous cell carcinoma. *Int. J. Clin. Exp. Pathol.* 8, 11446–11451.

Zhang, X., Li, Y., Qi, P., and Ma, Z. (2018). Biology of MiR-17-92 cluster and its progress in lung cancer. *Int. J. Med. Sci.* 15, 1443–1448. doi: 10.7150/ijms.27341

Zhao, H., Xing, G., Wang, Y., Luo, Z., Liu, G., and Meng, H. (2017). Long noncoding RNA HEIH promotes melanoma cell proliferation, migration and invasion via inhibition of miR-200b/a/429. *Biosci. Rep.* 37:BSR20170682. doi: 10.1042/BSR20170682

Conflict of Interest: The authors declare that the research was conducted in the absence of any commercial or financial relationships that could be construed as a potential conflict of interest.

frontiers in Genetics

ORIGINAL RESEARCH
published: 03 March 2020
doi: 10.3389/fgene.2020.00180

LINC00319-Mediated miR-3127 Repression Enhances Bladder Cancer Progression Through Upregulation of RAP2A

Xiaoqing Wang[1], Ran Meng[2] and Qing-Mei Hu[1]*

[1] Department of Operation Room, Shangqiu First People's Hospital of Henan, Shangqiu, China, [2] Department of Urology, Shangqiu First People's Hospital of Henan, Shangqiu, China

Recent studies suggested that microRNA-3127 (miR-3127) was dysregulated in multiple tumor types and has important roles in tumorigenesis and cancer progression. However, its biological roles and the mechanisms that regulate its expression in bladder cancer (BCA) remain to be determined. The expression level of miR-3127 was measured in BCA tissues and its cellular functions were examined using both *in vitro* and *in vivo* experiments. The interaction between miR-3127 and long non-coding RNA (lncRNA) LINC00319 was explored using RNA immunoprecipitation assay and luciferase reporter assays. We showed that miR-3127 expression was significantly downregulated in human BCA tissues and BCA cell lines. Lower miR-3127 levels were associated with worse survival in BCA patients. The overexpression of miR-3127 impaired BCA cell proliferation and invasion, and the knockdown of miR-3127 enhanced BCA cell proliferation and invasion *in vitro.* Importantly, miR-3127 was able to suppress cell growth *in vivo*. We demonstrated that miR-3127 repressed the proliferation and invasion of BCA cells though directly targeted the 3′-UTR of *RAP2A*, which served as a novel oncogene in BCA cells. The suppression of cell proliferation and invasion caused by miR-3127 overexpression could be partially abrogated by ectopic expression of RAP2A. Furthermore, high expression of LINC00319 was correlated with adverse survival in BCA patients. LINC00319 could bind directly with miR-3127 and inhibited its expression, and the tumor-promoting effects of LINC00319 could be reversed by re-expression of miR-3127 in BCA cells. Our findings indicated that lncRNA LINC00319-mediated miR-3127 repression promotes BCA progression through the upregulation of RAP2A. The re-introduction of miR-3127 or inhibition of LINC00319 might represent a promising therapeutic strategy for BCA treatment.

Keywords: miR-3127, RAP2A, LINC00319, bladder cancer, lncRNA

OPEN ACCESS

Edited by:
Dragos Cretoiu,
Carol Davila University of Medicine and Pharmacy, Romania

Reviewed by:
Guoping Li,
Harvard Medical School, United States
Stéphane Chabaud,
Laval University, Canada

****Correspondence:***
Xiaoqing Wang
xiaoqingwang0706@yahoo.co.jp

Specialty section:
This article was submitted to RNA, a section of the journal Frontiers in Genetics

Received: *06 July 2019*
Accepted: *14 February 2020*
Published: *03 March 2020*

Citation:
Wang X, Meng R and Hu Q-M (2020) LINC00319-Mediated miR-3127 Repression Enhances Bladder Cancer Progression Through Upregulation of RAP2A. Front. Genet. 11:180. doi: 10.3389/fgene.2020.00180

INTRODUCTION

Bladder cancer (BCA) is the 9th most common cancer worldwide (Antoni et al., 2017). The American Cancer Society estimates that in 2018 there will be 81,190 new cases of BCA and 17,240 deaths in the United States (Siegel et al., 2018). During the past few years, the incidence and mortality rates of BCA have increased gradually in China (Pang et al., 2016). Approximately

15–30% of patients are diagnosed with muscle-invasive BCA, and many patients with muscle-invasive BCA develop a metastatic disease (Antoni et al., 2017). These patients with metastatic BCA often faced meager treatment options and a worse prognosis (Fletcher et al., 2011). Thus, a better understanding of the molecular basis of BCA is needed so that novel therapeutic approaches can be designed.

Both genetic and epigenetic alterations have been demonstrated to play important roles during bladder tumorigenesis and metastasis (Mitra et al., 2006). BCAs are generally characterized by alterations in the p53, PI3K/AKT and retinoblastoma pathways, and tumor angiogenesis further contributes to the neoplastic growth (Mitra et al., 2006). In particular, activation of the PI3K/AKT pathway appears to play a central role in the development of BCA (Mitra et al., 2006). RAP2A (a member of the small GTPase superfamily) mediates a variety of cellular processes such as proliferation, differentiation, cell adhesion, and cell cycle control (Bos, 2005). RAP2A has a key role in enhancing migration, invasion and metastasis by upregulating the phosphorylation level of AKT (Wu et al., 2015). RAP2A expression was dramatically increased in renal cell carcinoma tissues compared with normal renal tissues, and the ectopic expression of RAP2A enhanced the migration and invasive ability of cancer cells through an AKT-dependent mechanism (Wu et al., 2017). However, the expression and function of RAP2A has not been fully elucidated in the development of human BCA.

Epigenetic alterations, including DNA methylation, histone modification and non-coding RNAs play pivotal roles in the development of BCA (Porten, 2018). Long non-coding RNAs (lncRNAs) are a cluster of non-coding RNAs longer than 200 nucleotides, with little or no protein-coding potential (Xia et al., 2018). Many lncRNAs are reported to influence gene expression by working as guides, dynamic scaffolds and molecular decoys (Balas and Johnson, 2018; Dong et al., 2019). In human tumors, aberrant expression of lncRNAs is associated with tumorigenesis, metastasis and chemotherapy resistance (Balas and Johnson, 2018; Dong et al., 2019). In addition, microRNAs (miRNAs) are small endogenous non-coding RNAs composed of approximately 19–24 nucleotides that regulate target genes post-transcriptionally (Dong et al., 2017), and miRNAs play key roles in the modulation of tumor growth and metastasis (Dong et al., 2017, 2018b). It has been reported that miR-3127 acts as either a tumor suppressor or an oncogene in cancers, such as glioma (Pan et al., 2019), lung cancer (Sun et al., 2014; Yang et al., 2018) and hepatocellular carcinoma (Jiang et al., 2015). Downregulation of miR-3127-5p promotes epithelial-mesenchymal transition through activating the Wnt/FZD4/β-catenin pathway in non-small-cell lung cancer (Yang et al., 2018). However, miR-3127 promotes the proliferation and tumorigenesis in hepatocellular carcinoma by inducing the AKT/FOXO1 signaling (Jiang et al., 2015). Recent investigation has shown that several lncRNAs (including GACAT3, FOXD2-AS1, and LINC00319) modulate the malignant properties of tumor cells through sponging miR-3127 (Pan et al., 2019; Yang et al., 2020; Zhang and Chen, 2020). Thus, miR-3127 appears to be a central regulator connecting cancer progression with a wide range of cancer-related lncRNAs. Currently, the role of miR-3127 in BCA progression and the mechanisms that regulate miR-3127 expression were unclear.

In this study, we discovered that the expression of miR-3127 was reduced in BCA tissues and BCA cell lines. Enforced expression of miR-3127 impaired BCA cell proliferation and invasion, and repressed tumor growth *in vivo*. We have identified oncogene *RAP2A*, which was directly repressed by miR-3127 in BCA cells. Furthermore, we showed that lncRNA LINC00319 sponged miR-3127 and inhibited the levels of miR-3127, thereby promoting the proliferation and invasion of BCA cells. Lower levels of miR-3127 or higher expression of LINC00319 were correlated with adverse survival in BCA patients. Taken together, our results support the tumor-suppressive roles of miR-3127 in BCA cells, and gave a potential explanation for decreased miR-3127 expression in BCA.

MATERIALS AND METHODS

Patients and Tissue Specimens

A total of 50 paired BCA tissue and adjacent normal tissues were included in this study. This study was approved by the Clinical Research Ethics Committee of Shangqiu First People's Hospital of Henan, and written consent was obtained from each patient before sample collection. Fresh tissues were stored at −80°C before use.

Cell Culture and Transfection

Human BCA cell lines (a grade 1 cancer cell line SW780 and a grade 3 cancer cell line T24) and human normal urothelial cell line SV-HUC-1 were obtained from Shanghai Institute of Cell Biology (Shanghai, China). T24 and SW780 cells were cultured in RPMI-1640 medium (Gibco, Waltham, MA, United States) supplemented with 10% fetal bovine serum (FBS). SV-HUC-1 cells were propagated in DMEM/F12 medium (Invitrogen, Carlsbad, CA, United States) supplemented with 10% FBS. We purchased the RAP2A or LINC00319 overexpression plasmids or the control plasmid from GenePharma (Shanghai, China). The siRNAs targeting LINC00319 or RAP2A, control siRNA, miR-3127 mimic, control mimic, miR-3127 inhibitor and control inhibitor were obtained from IGEbio (Guangzhou, China). Lipofectamine 3000 (Invitrogen, Waltham, MA, United States) was used according to the manufacturer's protocol.

RNA Extraction and Quantitative RT-PCR (qRT-PCR) Analysis

Total RNA was extracted from tissues or cells using TRIzol reagent (Invitrogen, Carlsbad, CA, United States), and cDNA was synthesized from 1 μg of RNA with an M-MLV Reverse Transcriptase Kit (Invitrogen, Carlsbad, CA, United States). The qRT-PCR analysis was performed using the SYBR Green quantitative real-time PCR Master Mix kit (Toyobo, Osaka, Japan) on an ABI-7500 RT-PCR system (Applied Biosystems). The primers for LINC00319, *RAP2A* and *GAPDH* were obtained from GenePharma (Shanghai, China). For the measurement of miR-3127 expression, we used the mirVanaTM qRT-PCR

microRNA Detection Kit (Ambion, Austin, TX, United States) according to the manufacturer's instructions. The relative expression of miR-3127 was normalized against that of the U6 endogenous control.

Cell Proliferation Assay

Cell proliferation assay was performed using Cell Counting Kit-8 (CCK-8) assay (Dojindo, Japan) according to the manufacturer's instructions. 5000 BCA cells were seeded into a 96-well plate and cultured with 100 μl of 10% FBS in the culture medium, and 10 μl of CCK-8 reagent was added into each well and incubated at the scheduled time points. The absorbance was measured at 450 nm by a microplate reader (Bio-Rad, Hercules, CA, United States). Each experiment was performed in triplicate.

Matrigel Cell Invasion Assay

Transwell invasion assay was performed as described previously (Dong et al., 2018a). 2×10^4 BCA cells in serum-free medium were seeded in the upper wells of Matrigel-coated Transwell plates (Corning Costar Co., Lowell, CA, United States). The medium containing 10% FBS was added to the lower chamber. After culturing for 24 h, the membranes were treated with 10% formaldehyde for 3 min, and stained with 2% crystal violet for 15 min at room temperature. Cells that invaded across the transwell membrane were counted using a light microscope in 10 randomly selected high-power fields.

Western Blotting Analysis

Bladder cancer cells were lysed with cell lysis buffer (Beyotime, Guangzhou, China) supplemented with a protease inhibitor cocktail (Merck, Darmstadt, Germany). Protein concentrations of the total protein extracts were measured using a Bicinchoninic Acid Assay kit (Pierce, Rockford, IL, United States). 20 μg proteins were applied to 15% SDS-PAGE gel and transferred to a PVDF membrane (Millipore, Bedford, MA, United States). The membranes were then probed with primary antibody for RAP2A

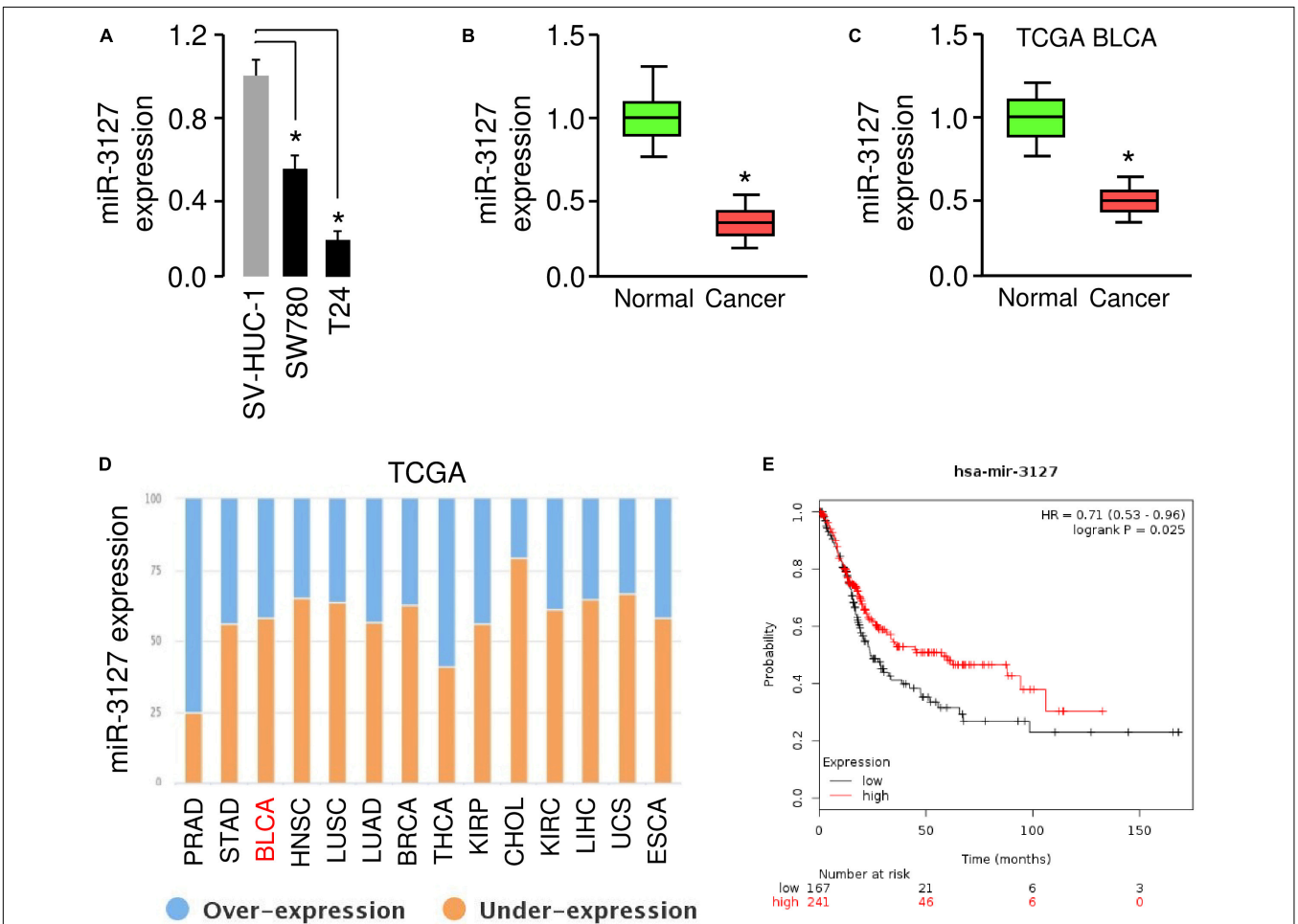

FIGURE 1 | MiR-3127 is downregulated in human BCA **(A)**. Examination of miR-3127 expression in a normal urothelial epithelial cell line SV-HUC-1 and two BCA cell lines using qRT-PCR assays **(B)**. Expression of miR-3127 in human BCA tissues compared with matched adjacent normal tissues using qRT-PCR analysis **(C)**. Analysis of miR-3127 expression profiles in BCA samples and normal samples using the TCGA data retrieved in the MethHC database **(D)**. The expression trend for miR-3127 was analyzed in different cancer types using the BioXpress database **(E)**. The probability of overall survival in BCA patients expressing high or low miR-3127 levels assessed using the KMplotter database. *$P < 0.05$.

(1:2000, Santa Cruz, CA, United States) and GAPDH (1:5000, Santa Cruz, CA, United States) at 4°C overnight, incubated with horseradish peroxidase (HRP)-conjugated secondary antibody (in 5% fat-free milk) for 2 h, and finally visualized using the ECL reagent (Amersham Biosciences, Buckinghamshire, United Kingdom). GAPDH served as the loading control.

Luciferase Reporter Assay

The luciferase reporter vectors containing wild-type LINC00319 (LINC00319-WT) and mutant LINC00319 (LINC00319-MUT), or wild-type *RAP2A* 3′-UTR (RAP2A-WT) and mutant *RAP2A* 3′-UTR (RAP2A-MUT), were constructed by GenePharma (Shanghai, China). BCA cells were co-transfected with 100 ng reporter plasmid containing LINC00319 (WT or MUT) or *RAP2A* 3′-UTR (WT or MUT) and 30 nM miR-3127 mimic or miR-3127 inhibitor using Lipofectamine 3000 reagent (Invitrogen, Waltham, MA, United States). Forty-eight hours later, the relative luciferase activity was measured with the Dual-Luciferase Reporter Assay System (Promega, Madison, WI, United States). Mutated LINC00319 or mutated *RAP2A* 3′-UTR was constructed by GenePharma (Shanghai, China) using the QuikChange Lightning Site-Directed Mutagenesis kit (Agilent Technologies, Santa Clara, CA, United States).

RNA Immunoprecipitation Assay

RNA Immunoprecipitation (RIP) assays were performed to investigate whether LINC00319 could bind with miR-3127 using the Magna RIP RNA-Binding Protein Immunoprecipitation Kit (Millipore, Bedford, MA, United States) according to the manufacturer's instructions. Briefly, cells were lysed in RIP lysis buffer, and the extracts were incubated with magnetic beads conjugated to human anti-Argonaute2 (Millipore, Bedford, MA, United States) or normal mouse IgG (Millipore, Bedford, MA, United States). The beads were incubated with Proteinase K to remove proteins. Finally, the purified RNAs were subjected to qRT-PCR analysis to detect the expression of LINC00319.

Lentiviral Transfection

MiR-3127-overexpression lentiviral vector and control lentiviral vector, as well as miR-3127-sponge lentiviral vector and control lentiviral vector, were purchased from GenePharma (Shanghai, China). Lentivirus preparation and *in vitro* infection were

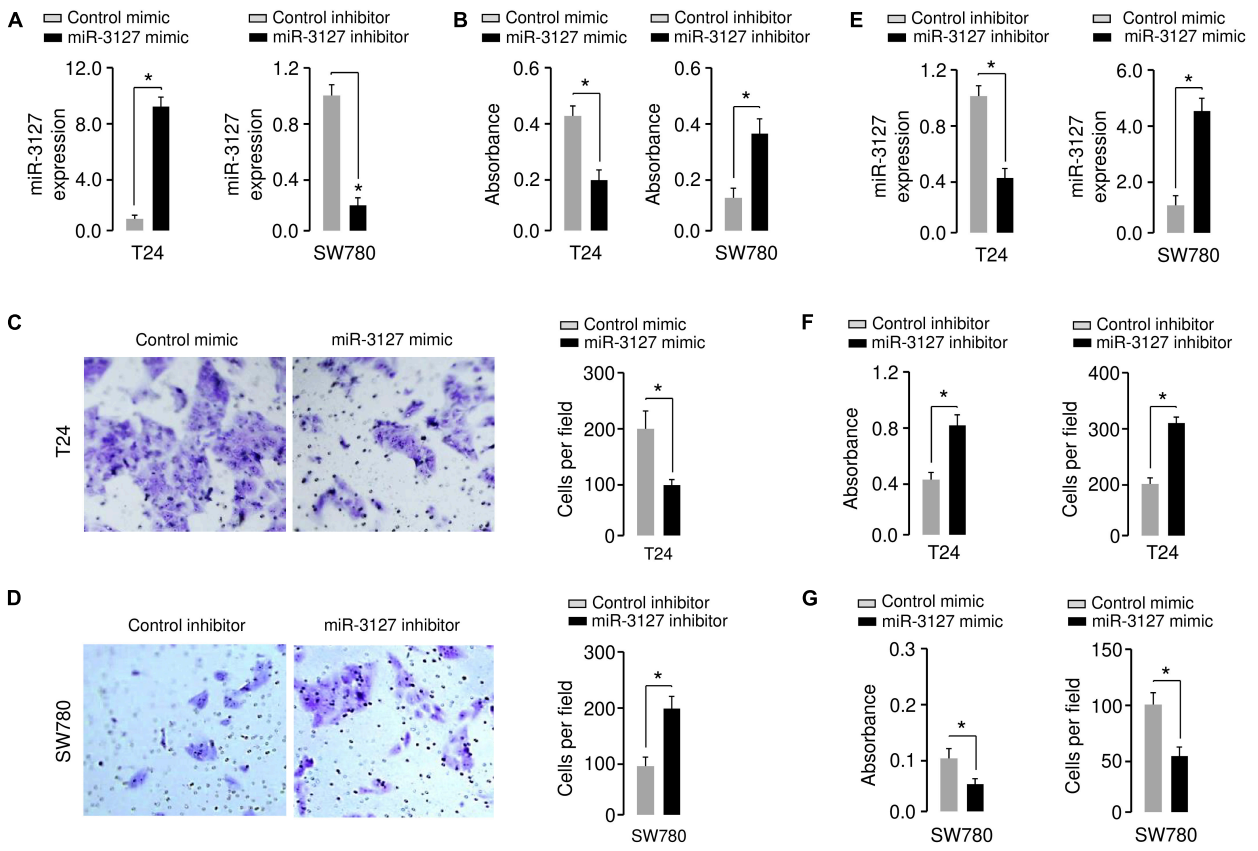

FIGURE 2 | Overexpression of miR-3127 decreases cellular invasion and proliferation of BCA cells. **(A)** MiR-3127 levels in T24 cells transfected with miR-3127 mimic (or control mimic) and in SW780 cells transfected with miR-3127 inhibitor (or control inhibitor). **(B)** Proliferation assays in BCA cells after overexpression or knockdown of miR-3127. **(C,D)** Cell invasion assays in T24 cells transfected with miR-3127 mimic or control mimic **(C)**, and in SW780 cells transfected with miR-3127 inhibitor or control inhibitor **(D)**. **(E)** MiR-3127 levels in SW780 cells transfected with miR-3127 mimic (or control mimic) and in T24 cells transfected with miR-3127 inhibitor (or control inhibitor). **(F)** Proliferation and invasion assays in T24 cells after knockdown of miR-3127. **(G)** Proliferation and invasion assays in SW780 cells after overexpression of miR-3127. $^*P < 0.05$.

performed as previously reported (Peng et al., 2019). In brief, T24 cells were infected by miR-3127-overexpression lentiviral vector or control vector, and SW780 cells were infected by miR-3127-sponge lentiviral vector or control vector. The stable cell lines were selected with 2 μg/ml puromycin (Sigma-Aldrich, Shanghai, China) for 14 days.

Tumor Xenograft Experiments

The study was approved by the Institutional Animal Care and Use Committee of Shangqiu First People's Hospital of Henan. BALB/c nude mice (4 weeks old) were purchased from Beijing HFK Bioscience (Beijing, China) and maintained under pathogen-free conditions. BCA cells (2×10^6) with miR-3127 overexpression or inhibition were implanted subcutaneously into the right flank of the nude mice. Tumor growth was monitored using calipers and tumor volume measurement was performed every 3 days, using the following formula: volume = length (mm) × width^2 (mm^2)/2. After three weeks, the mice were sacrificed and the tumors were collected for immunohistochemical assay. The paraffin sections were refrigerated with anti-Ki-67 antibody the rabbit (1:1000, Abcam, Cambridge, United Kingdom) at 4°C overnight. After incubated with HRP-conjugated streptavidin, the sections were stained using 3, 3′-diaminobenzidine (ZLI9018, ZSGBBIO, China).

Statistical Analysis

Statistical analysis was performed using SPSS 17.0 statistical software (SPSS, Chicago, United States). Statistical differences were determined using the Student's *t*-test, one-way ANOVA test, or Wilcoxon signed-rank test. Values were expressed as the mean ± standard deviation of at least three independent experiments. *P*-values of less than 0.05 were considered statistically significant.

RESULTS

MiR-3127 Expression Is Downregulated in Human BCA Tissues and BCA Cells

To investigate the role of the miR-3127 in BCA, we first used one normal urothelial epithelial cell line SV-HUC-1 and two BCA cell lines (SW780 and T24) to analyze miR-3127 expression in normal cells and BCA cells. The results of qRT-PCR analysis showed that miR-3127 levels were markedly decreased in BCA cells in comparison with SV-HUC-1 cells (**Figure 1A**). Consistent with the above findings, the expression of miR-3127 was downregulated in human BCA tissues compared with matched adjacent normal tissues, as examined by qRT-PCR assays (**Figure 1B**). In addition, we searched the MethHC database for miR-3127 expression in BCA tissues and normal tissues from the TCGA BCA datasets (Huang et al., 2015). We found that the levels of miR-3127 in BCA samples were significantly lower than those in the normal samples (**Figure 1C**). We also analyzed RNA-sequencing gene expression data of BCA samples and normal samples, which are available in the BioXpress database (Wan et al., 2015). The results suggested that miR-3127 expression was reduced in multiple cancer types including BCA (**Figure 1D**). To investigate the prognostic role of miR-3127 expression in BCA patients, we used an online database KMPlotter (Győrffy et al., 2010). We used the median value to separate high and low groups for the survival analysis. The results showed that low expression of miR-3127 was significantly associated with poor overall survival in BCA patients (**Figure 1E**).

MiR-3127 Inhibits the Proliferation and Invasion of BCA Cells

Using qRT-PCR assays, we confirmed the upregulation of miR-3127 in T24 cells that were transfected with miR-3127 mimic, and the downregulation of miR-3127 in SW780 cells that were transfected with miR-3127 inhibitor (**Figure 2A**). We tried to explore the functions of miR-3127 in regulating the growth and invasiveness of BCA cells using CCK-8 assays and Matrigel invasion assays. The overexpression of miR-3127 significantly decreased the proliferation and invasion of T24 cells, while the downregulation of miR-3127 largely increased the abilities of SW780 cells to proliferate and invade (**Figures 2B–D**). To further validate these results, we transfected SW780 cells with miR-3127 mimic, and transfected T24 cells with miR-3127 inhibitor (**Figure 2E**). Then, we performed CCK-8 assays and Matrigel invasion assays and found that overexpression of miR-3127 in SW780 cells decreased cell proliferation and invasion, and knockdown of miR-3127 in T24 cells enhanced cell proliferation and invasion (**Figures 2F,G**). Taken together, our data supports an important role for miR-3127 in inhibiting the growth and invasiveness of BCA cells *in vitro*.

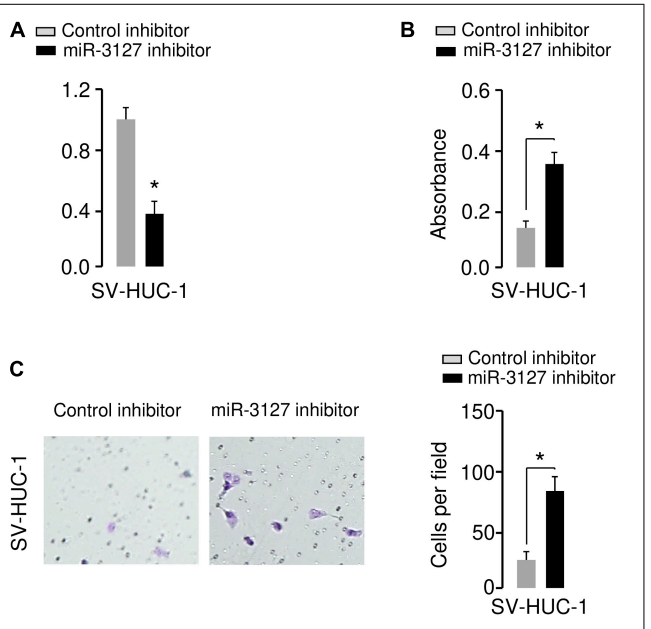

FIGURE 3 | Downregulation of miR-3127 promotes cellular proliferation and invasion of SV-HUC-1 cells. **(A)** MiR-3127 expression in SV-HUC-1 cells transfected with miR-3127 inhibitor or control inhibitor. **(B,C)** Proliferation **(B)** and invasion **(C)** assays in SV-HUC-1 cells after knockdown of miR-3127. *$P < 0.05$.

We further investigated the functional role of miR-3127 in the human normal urothelial cell line SV-HUC-1. The inhibition of miR-3127 by using miR-3127 inhibitor dramatically decreased miR-3127 levels (**Figure 3A**), and significantly increased the growth and invasion of SV-HUC-1 cells (**Figures 3B,C**). These results indicate that downregulation of miR-3127 could increase cell proliferation and invasion of SV-HUC-1 cells.

MiR-3127 Represses the Proliferation of BCA Cells *in vivo*

To examine whether miR-3127 could influence the growth of BCA cells *in vivo*, we transfected T24 cells with miR-3127-overexpression lentiviral vector or control lentiviral vector, and also transfected SW780 cells with miR-3127-silenced lentiviral vector or control lentiviral vector. The efficiency of stable miR-3127 overexpression or knockdown was verified by qRT-PCR analysis (**Figure 4A**). The stably transfected cells were then introduced into a nude mouse xenograft model, respectively. Three weeks post-injection of the BCA cells, the volume of tumors in mice injected with T24 cells transfected with miR-3127-overexpression lentiviral vector were significantly smaller than those in the control group (**Figure 4B**). Conversely, the lentivirus-mediated miR-3127 suppression significantly enhanced the proliferation of SW780 cells *in vivo* (**Figure 4C**). Immunohistochemistry-based studies revealed lower Ki-67 expression levels in the tumors from T24 cells overexpressing miR-3127 compared with those in the

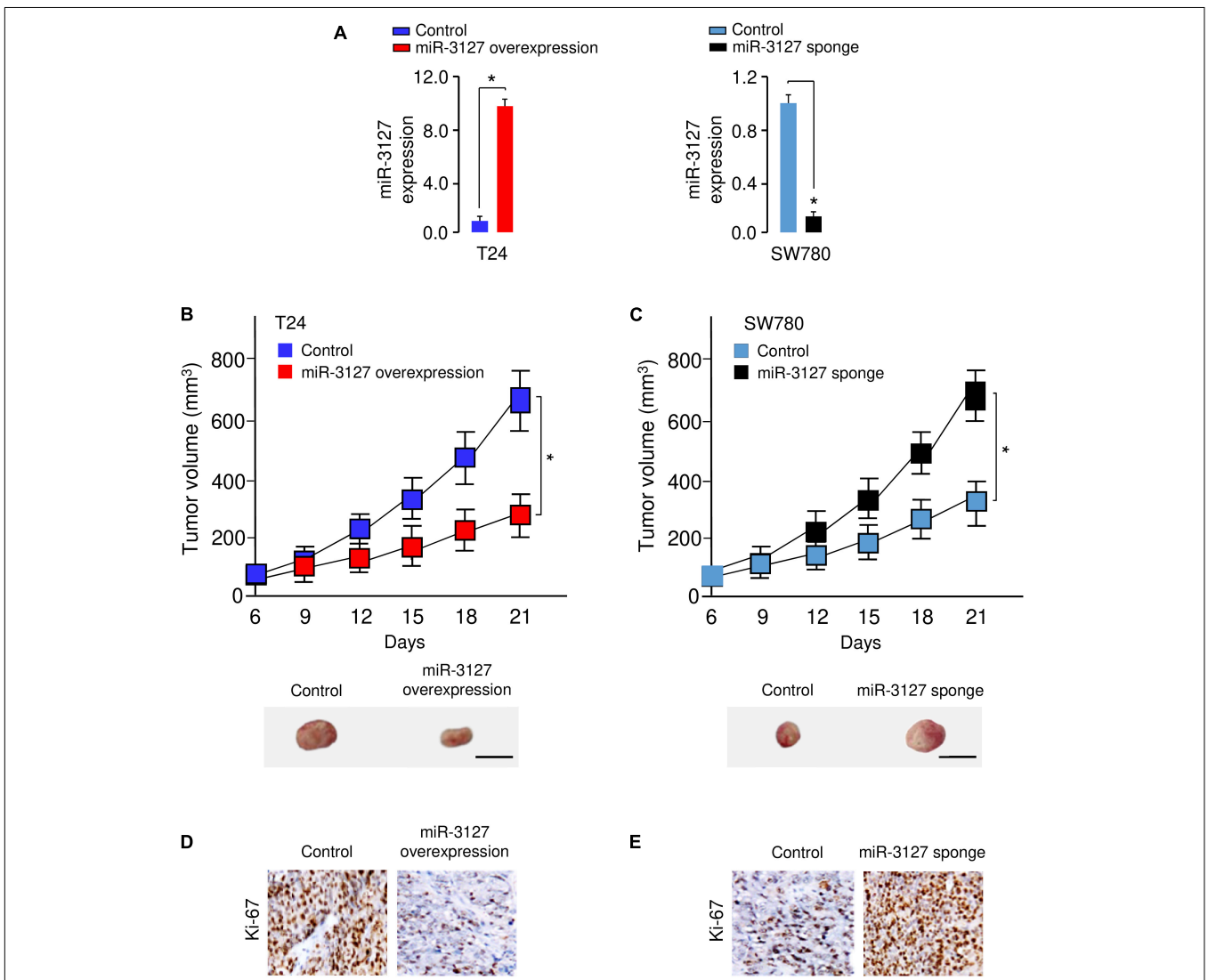

FIGURE 4 | MiR-3127 overexpression impairs tumor growth *in vivo*. **(A)** MiR-3127-overexpression lentiviral vector or control lentiviral vector (control) was stably transfected into T24 cells, and miR-3127-silenced lentiviral vector or control lentiviral vector (control) was stably transfected into SW780 cells. The efficiency of miR-3127 overexpression and knockdown was verified using qRT-PCR analysis. **(B,C)** The stably transfected T24 **(B)** cells or SW780 **(C)** cells were subcutaneously injected into nude mice. The tumor growth curves were presented. Scale bar, 1 cm. **(D,E)** Immunohistochemical analysis of Ki-67 expression in tumors dissected from mice shown in panels **(B)** and **(C)**. *$P < 0.05$.

tumors from the control group, and higher Ki-67 expression in the tumors from SW780 cells transfected with miR-3127-silenced lentiviral vector (**Figures 4D,E**), indicating that miR-3127 reduces BCA cell growth *in vivo*.

MiR-3127 Directly Targets and Suppresses the Expression of RAP2A

The possible target genes of miR-3127 were predicted using the target prediction database TargetScan. Among various candidates, *RAP2A* showed complementary sequences with miR-3127 (**Figure 5A**). RAP2A was believed to be a crucial upstream activator of the PI3K/AKT pathway in cancer cells (Wu et al., 2015, 2017). Thus, we analyzed the expression of RAP2A in tumor and normal tissue samples using the BioXpress database, and found that RAP2A was overexpressed in several tumor types including BCA (**Figure 5B**). The presence of mutation, copy number alteration and expression of RAP2A in BCA samples were recognized using the cBioPortal database (Gao et al., 2013). The alterations of RAP2A (including mutation, copy number amplification and mRNA overexpression) were found in 10% of all cases (**Figure 5C**). The alterations of RAP2A were significantly associated with worse overall survival of BCA patients (**Figure 5C**). Additionally, the expression level of RAP2A was found to be significantly higher in BCA cells when compared with normal cells (**Figure 5D**), suggesting a negative correlation between miR-3127 and RAP2A expression in BCA cells.

To validate the possible interaction between miR-3127 and RAP2A, we conducted luciferase reporter assays with WT *RAP2A* 3′-UTR or MUT *RAP2A* 3′-UTR reporter plasmids. We found that the overexpression of miR-3127 significantly reduced the luciferase activities of WT *RAP2A* 3′-UTR in T24 cells, and the

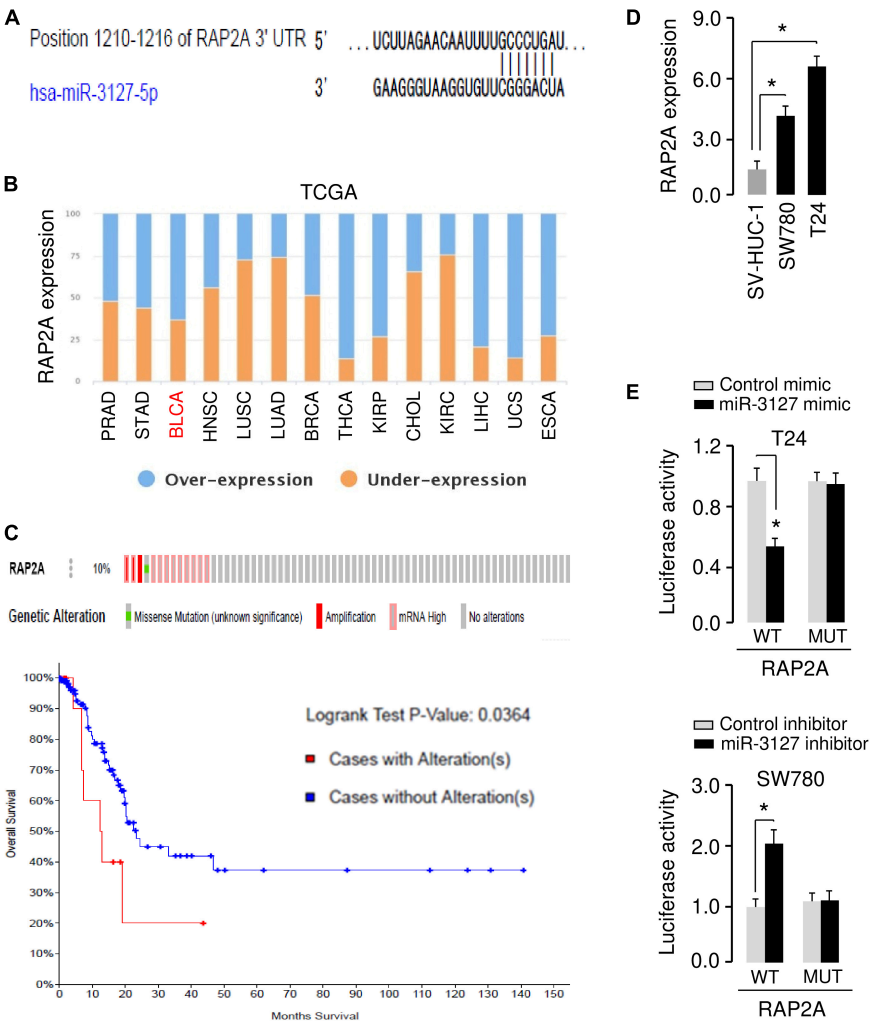

FIGURE 5 | MiR-3127 directly targets and suppresses the expression of RAP2A. **(A)** Illustration of the predicted miR-3127 binding site in the *RAP2A* 3′-UTR. **(B)** The expression trend for RAP2A was analyzed in different cancer types using the BioXpress database. **(C)** Analysis of RAP2A alterations in BCA using the cBioPortal database (upper panel). Survival curves of patients without alterations in *RAP2A* (blue) compared to patients with genetic alterations in *RAP2A* (red) (bottom panel). **(D)** Examination of RAP2A expression in a normal urothelial epithelial cell line SV-HUC-1 and two BCA cell lines using qRT-PCR assays. **(E)** Luciferase reporter assays in BCA cells transfected with the wild type or mutant *RAP2A* 3′-UTR, along with miR-3127 mimic or miR-3127 inhibitor, respectively. *$P < 0.05$.

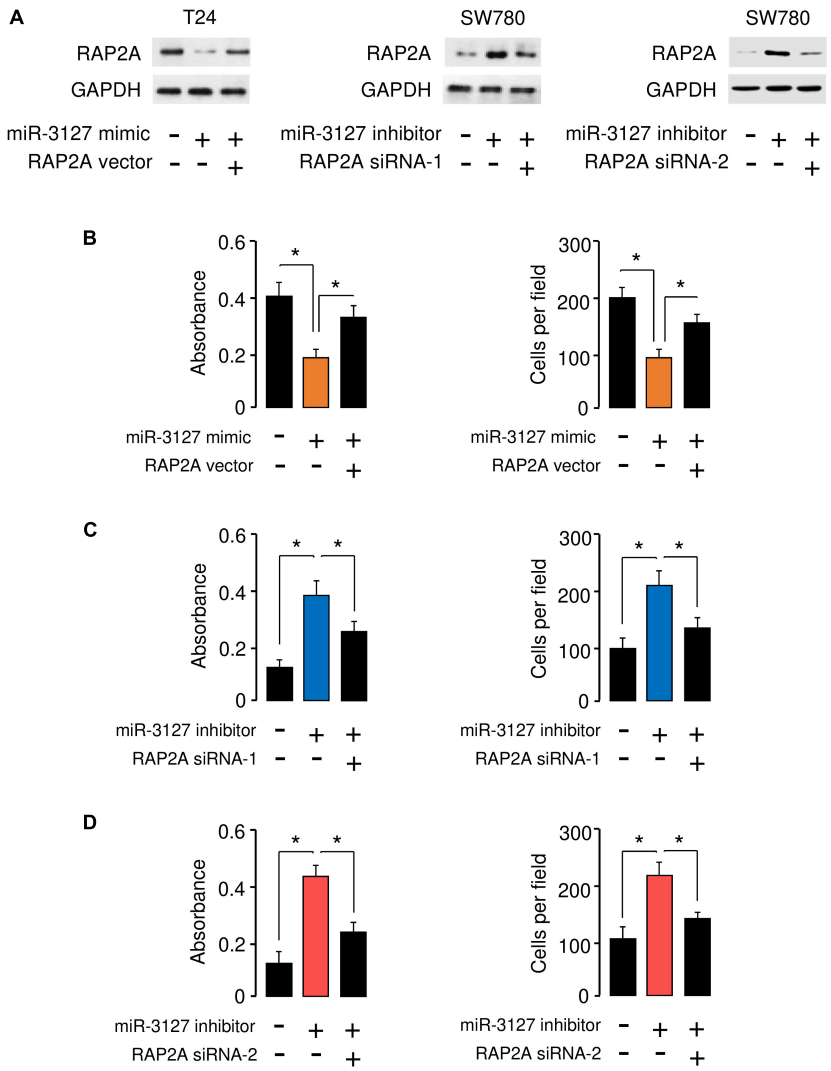

FIGURE 6 | RAP2A overexpression reverses the inhibitory effects of miR-3127 on BCA cell proliferation and invasion. **(A)** The protein expression of RAP2A was examined in T24 cells transfected with control mimic or miR-3127 mimic, together with control vector or RAP2A vector (left panel), as well as in SW780 cells transfected with control inhibitor or miR-3127 inhibitor, together with control siRNA or RAP2A siRNA-1 (middle panel), or together with control siRNA or RAP2A siRNA-2 (right panel). **(B)** Proliferation and invasion assays in T24 cells transfected with control mimic or miR-3127 mimic, along with control vector or RAP2A expression vector. **(C,D)** Proliferation and invasion assays in SW780 cells transfected with control inhibitor or miR-3127 inhibitor, along with control siRNA or RAP2A siRNA-1 **(C)**, or along with control siRNA or siRNA 2 **(D)**. The minus sign indicated control mimic, control vector, control inhibitor, or control siRNA.*$P < 0.05$.

downregulation of miR-3127 increased the luciferase activities of WT *RAP2A* 3′-UTR in SW780 cells (**Figure 5E**). The transfection with miR-3127 mimic or miR-3127 inhibitor in BCA cells had no significant effects on the luciferase activities of MUT *RAP2A* 3′-UTR (**Figure 5E**). These data suggest that RAP2A is a direct target of miR-3127 in BCA cells.

RAP2A Overexpression Reverses the Inhibitory Effects of miR-3127 on BCA Cell Proliferation and Invasion

To determine whether miR-3127 repressed the proliferation and invasion of BCA cells by targeting RAP2A, we transfected RAP2A expression vector together with miR-3127 mimic into T24 cells, and transfected siRNAs that target RAP2A together with miR-3127 inhibitor into SW780 cells. Western blotting analysis suggested overexpression of miR-3127 decreased the protein expression of RAP2A in T24 cells transfected with miR-3127 mimic, while downregulation of miR-3127 increased the protein levels of RAP2A in SW780 cells (**Figure 6A**). The results form cell proliferation and invasion assays demonstrated that miR-3127 over-expression inhibited the proliferation and invasion of T24 cells, while the restoration of RAP2A expression significantly rescued the proliferation and invasion of T24 cells that were suppressed by miR-3127 overexpression (**Figure 6B**). We also found that the downregulation of miR-3127 elevated the proliferation and invasion of SW780 cells, and the knockdown of RAP2A significantly reversed these effects of miR-3127 silencing

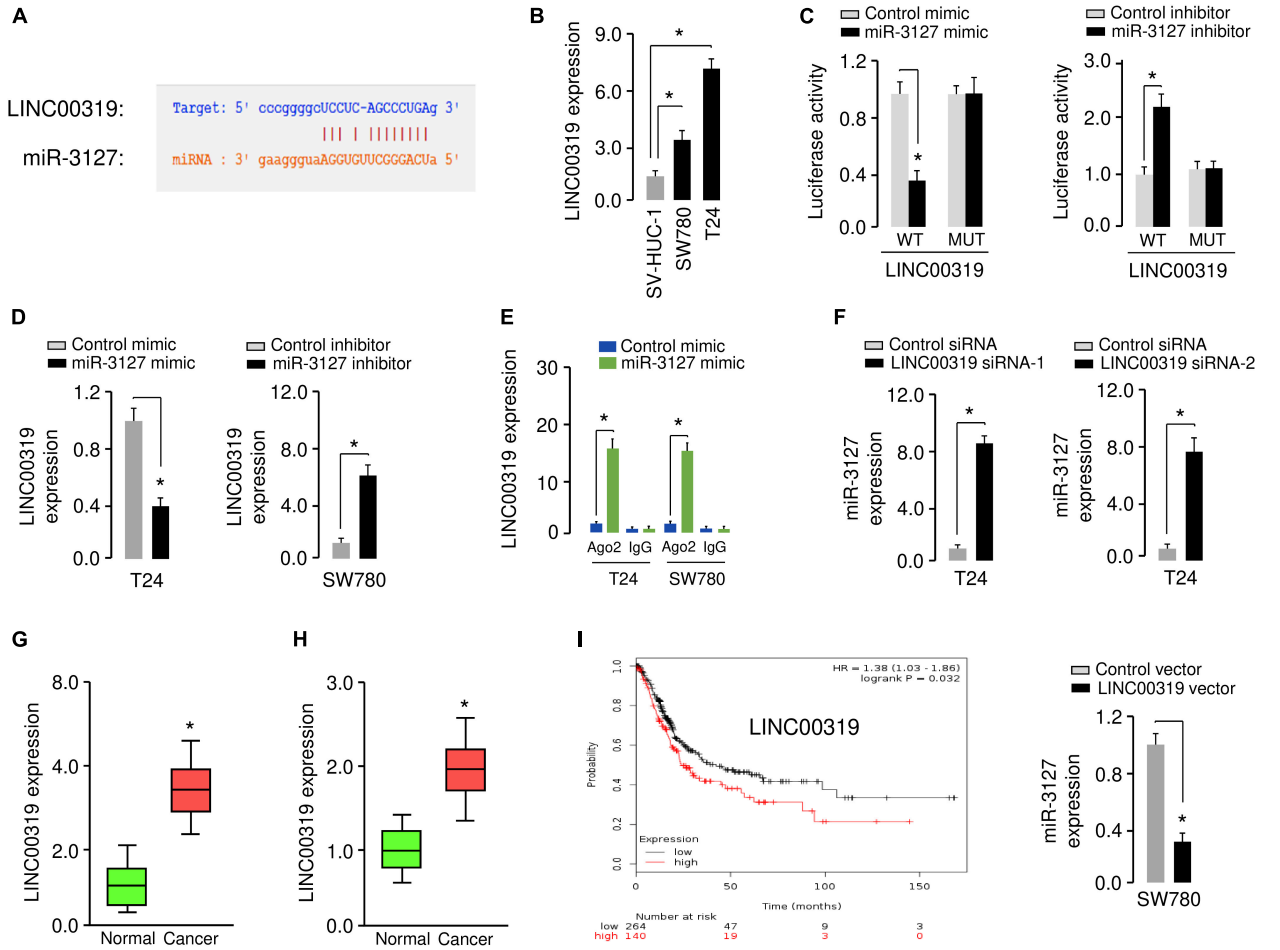

FIGURE 7 | LINC00319 sponges miR-3127 to inhibit its levels in BCA cells. **(A)** The putative binding site for miR-3127 in the LINC00319 sequence. **(B)** Expression of LINC00319 in normal urothelial epithelial cells and BCA cell lines using qRT-PCR assays. **(C)** Luciferase reporter assays in BCA cells transfected with the wild type or mutant LINC00319, along with miR-3127 mimic or miR-3127 inhibitor, respectively. **(D)** Examination of LINC00319 expression in BCA cells following overexpression or knockdown of miR-3127. **(E)** RIP assays were done to verify the association between miR-3127 and LINC00319. **(F)** Expression of miR-3127 in BCA cells transfected with siRNAs targeting LINC00319 or LINC00319 expression vector. **(G)** Analysis of LINC00319 expression in human BCA tissues compared with matched adjacent normal tissues using qRT-PCR assays. **(H)** Analysis of LINC00319 expression in BCA samples and normal samples using the MethHC database. **(I)** The probability of overall survival in BCA patients expressing high or low LINC00319 levels assessed using the KMplotter database. $^*P < 0.05$.

(**Figures 6C,D**). These results suggest that RAP2A is a functional target of miR-3127 in BCA cells.

LINC00319 Sponges miR-3127 to Promote BCA Cell Proliferation and Invasion

Increasing evidence has shown that lncRNAs could act as a sponge for miRNAs and inhibit their expression (Xiao et al., 2015). To test whether the expression of miR-3127 can be regulated by lncRNAs, we predicted the interactions between miR-3127 and lncRNAs using the starBase v2.0 database (Li et al., 2014), and observed the miR-3127-binding site in lncRNA LINC00319 (**Figure 7A**). Our qRT-PCR assays showed that LINC00319 levels were higher in BCA cells compared with normal cells (**Figure 7B**), indicating that the expression level of miR-3127 was negatively correlated with that of LINC00319. To further explore the association between miR-317 and LINC00319, the dual-luciferase reporter assay was performed. The transfection with miR-3127 mimics reduced the luciferase activity of WT LINC00319 reporter vector, but not that of MUT LINC00319 reporter vector (**Figure 7C**). On the other hand, the transfection with miR-3127 inhibitor induced the luciferase activity of the WT LINC00319 reporter vector, but did not affect the MUT LINC00319 reporter vector (**Figure 7C**). Our qRT-PCR results suggested that overexpression of miR-3127 reduced, whereas knockdown of miR-3127 increased the levels of LINC00319 in BCA cells (**Figure 7D**). Then, RIP assays were used to determine whether LINC00319 and miR-3127 exist in the same RNA-induced silencing complex. Compared with the control group transfected with control mimic, the endogenous LINC00319 was specifically enriched in the cells of miR-3127 mimic-transfected group (**Figure 7E**). Consistent with these data, qRT-PCR assays indicated that knockdown of LINC00319 could

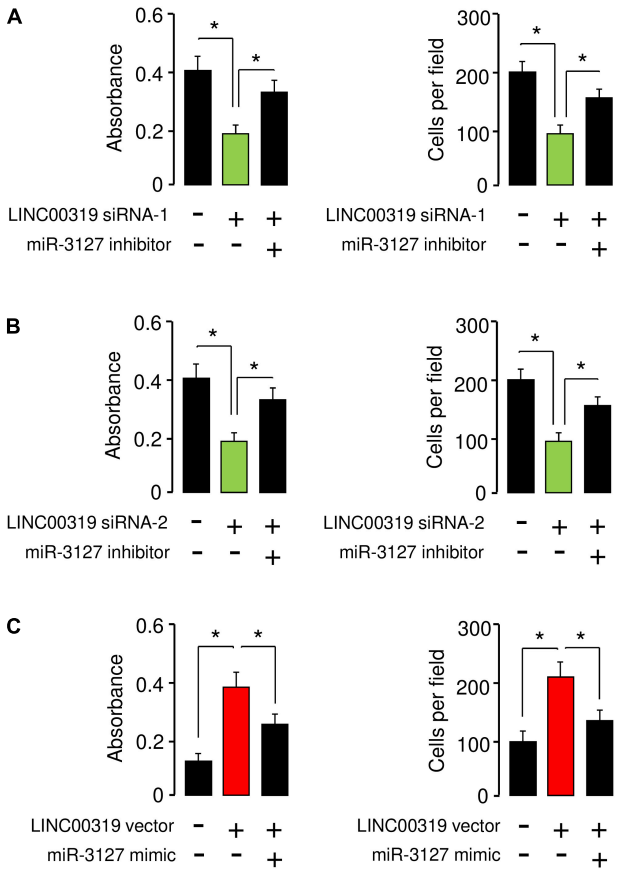

FIGURE 8 | LINC00319 promotes the proliferation and invasion of BCA cells by inhibiting miR-3127 expression. **(A,B)** Cell proliferation and invasion assays in T24 cells transfected with control siRNA or LINC00319 siRNA-1, along with control inhibitor or miR-3127 inhibitor **(A)**, and in T24 cells transfected with control siRNA or LINC00319 siRNA-2, along with control inhibitor or miR-3127 inhibitor **(B)**. **(C)** Cell proliferation and invasion assays in SW780 cells transfected with control vector or LINC00319 expression vector, along with control mimic or miR-3127 mimic. The minus sign indicated control siRNA, control inhibitor, control vector, or control mimic. $^*P < 0.05$.

increase the expression of miR-3127 in T24 cells, and ectopic expression of LINC00319 in SW780 cells reduced the levels of miR-3127 (**Figure 7F**), indicating a reciprocal repression between miR-3127 and LINC00319 in BCA cells.

We analyzed the expression of LINC0319 in 50 paired BCA samples and normal samples using qRT-PCR assays. We found that LINC0039 was significantly upregulated in BCA tissues compared with adjacent normal tissues (**Figure 7G**). We also determined the levels of LINC00319 in BCA tissues and normal tissues using the TCGA data downloaded from the MethHC database. As expected, the expression of LINC00319 was increased in BCA samples compared with normal samples (**Figure 7H**). Finally, we assessed the association between LINC00319 expression and survival of BCA patients using the KMPlotter database. Patients with high LINC00319 expression levels had poorer overall survival (**Figure 7I**). Together, these results suggest that lncRNA LINC00319 may play an important role in the pathogenesis and prognosis of BCA.

LINC00319 Promotes the Proliferation and Invasion of BCA Cells by Inhibiting miR-3127 Expression

We performed rescue assays to determine whether LINC00319 mediates the growth and invasion of BCA cells via inhibiting the expression of miR-3127. T24 cells were co-transfected with LINC00319 siRNAs and miR-3127 inhibitor, and SW780 cells were co-transfected with the LINC00319 expression vector and miR-3127 mimic. Our cell proliferation and invasion assays indicated that LINC00319 siRNAs-mediated suppression of cell proliferation and invasion was increased by the introduction of miR-3127 inhibitor in T24 cells (**Figures 8A,B**). In SW780 cells, overexpression of LINC00319 induced cell proliferation and invasion, which was suppressed by the transfection with miR-3127 mimic (**Figure 8C**). These data show that LINC00319 promotes BCA cell proliferation and invasion, at least in part through the downregulation of miR-3127.

DISCUSSION

There is a large unmet medical need for exploring the mechanism of BCA metastasis and developing new treatments for BCA patients with progressive disease (Bukhari et al., 2018). In this study, we identified the loss of miR-3127 expression in BCA samples using qRT-PCR assays and the TCGA RNA-sequencing data of human BCA. Concordantly, those patients harboring BCAs with lower levels of miR-3127 exhibited decreased overall survival. Then, our subsequent studies revealed that restoration of miR-3127 attenuated cell proliferation and invasion, partly through suppressing the expression of oncogene *RAP2A*. Further *in vivo* studies showed that overexpression of miR-3127 delayed tumor growth in a mouse model of BCA. Our results suggest that miR-3127 plays a tumor-suppressing role in BCA and thus could be a target for preventing BCA progression.

The functions of miRNAs depend on their target genes. For example, it has been reported that miR-3127 directly targets FZD4, thereby activating the Wnt/β-catenin signaling pathway in non-small-cell lung cancer (Yang et al., 2018). In another study, miR-3127 was shown to repress NSCLC cell proliferation and invasion via the direct regulation of oncogene *ABL1*, leading to the inhibition of the RAS/ERK pathway (Sun et al., 2014). However, there were still conflicting reports that miR-3127 actually acted as an oncogene in hepatocellular carcinoma by activating AKT/FOXO1 signaling, via directly targeting the 3′-UTR of *PHLPP1/2* (Jiang et al., 2015). The precise mechanisms of action and target genes of miR-3127 in BCA are not clear. RAP2A expression is increased in renal cell carcinoma tissues compared with normal renal tissues, and ectopic expression of RAP2A enhanced the migration and invasive ability of renal cell carcinoma cells at least by promoting the phosphorylation level of AKT (Wu et al., 2017). The results of the present study confirmed that RAP2A was a functional downstream effector of miR-3127 in BCA cells, and plays an important role in regulating the

growth and invasiveness of BCA cells. Additional studies should be performed to determine the genes that were targeted by miR-3127.

Previous studies have shown that aberrant expression of lncRNAs affects the levels of miRNAs, thereby modulating the malignant phenotypes of tumor cells (Balas and Johnson, 2018; Dong et al., 2019). To date, the underlying mechanisms involved in the downregulation of miR-3127 in BCA remain unclear. Here, we have identified a novel lncRNA LINC00319 as a key regulator of miR-3127, and showed that LINC00319 can downregulate the expression of miR-3127 in BCA cells by functioning as a miRNA sponge. LINC00319 was highly expressed in many human tumors and associated with poorer survival of patients (Zhou et al., 2017; Li et al., 2018; Zhang et al., 2018, 2019; Song and Yin, 2019). LINC00319 was shown to promote the proliferative, migratory and invasive capabilities of tumor cells by stabilizing SIRT6 (Zhang et al., 2019) or by interacting with miR-1207 (Song and Yin, 2019), miR-450 (Zhang et al., 2018) and miR-32 (Zhou et al., 2017). Interestingly, a recent study revealed a direct interaction between lncRNA LINC00319 and miR-3127 in cervical cancer cells, and demonstrated that LINC00319 promotes migration, invasion and epithelial-mesenchymal transition process via regulating miR-3127 (Yang et al., 2020). Consistent with this finding, our data confirmed that LINC00319 directly bound to and reduced the expression of miR-3127 in BCA cells, indicating that LINC00319 and miR-3127 seem to be therapeutic targets in BCA treatment.

In summary, we found that LINC00319-mediated miR-3127 repression promotes BCA cell growth and invasion through upregulation of RAP2A. Therefore, enhancing the expression of miR-3127 or inhibition of LINC00319 expression might represent a promising therapeutic strategy for BCA treatment.

DATA AVAILABILITY STATEMENT

All datasets generated for this study has been included in the article.

ETHICS STATEMENT

This study was approved by the Clinical Research Ethics Committee of Shangqiu First People's Hospital of Henan. The patients/participants provided their written informed consent to participate in this study. The study was approved by the Institutional Animal Care and Use Committee of Shangqiu First People's Hospital of Henan.

AUTHOR CONTRIBUTIONS

XW designed the experiments. All authors performed the experiments, analyzed the data, wrote the manuscript, and read and approved the final manuscript.

FUNDING

This work was supported by a grant from Shangqiu First People's Hospital of Henan, China.

REFERENCES

Antoni, S., Ferlay, J., Soerjomataram, I., Znaor, A., Jemal, A., and Bray, F. (2017). Bladder cancer incidence and mortality: a global overview and recent trends. *Eur. Urol.* 71, 96–108. doi: 10.1016/j.eururo.2016.06.010

Balas, M. M., and Johnson, A. M. (2018). Exploring the mechanisms behind long noncoding RNAs and cancer. *Noncoding RNA Res.* 3, 108–117. doi: 10.1016/j.ncrna.2018.03.001

Bos, J. L. (2005). Linking Rap to cell adhesion. *Curr. Opin. Cell Biol.* 17, 123–128. doi: 10.1016/j.ceb.2005.02.009

Bukhari, N., Al-Shamsi, H. O., and Azam, F. (2018). Update on the treatment of metastatic urothelial carcinoma. *Sci. World J.* 2018:5682078. doi: 10.1155/2018/5682078

Dong, F., Xu, T., Shen, Y., Zhong, S., Chen, S., Ding, Q., et al. (2017). Dysregulation of miRNAs in bladder cancer: altered expression with aberrant biogenesis procedure. *Oncotarget* 8, 27547–27568. doi: 10.18632/oncotarget

Dong, P., Xiong, Y., Yu, J., Chen, L., Tao, T., Yi, S., et al. (2018a). Control of PD-L1 expression by miR-140/142/340/383 and oncogenic activation of the OCT4-miR-18a pathway in cervical cancer. *Oncogene* 37, 5257–5268. doi: 10.1038/s41388-018-0347-4

Dong, P., Xiong, Y., Yue, J., Hanley, J. B. S., Kobayashi, N., Todo, Y., et al. (2019). Exploring lncRNA-mediated regulatory networks in endometrial cancer cells and the tumor microenvironment. *Adv. Challeng. Cancers* 11:E234. doi: 10.3390/cancers11020234

Dong, P., Xiong, Y., Yue, J., Hanley, S. J. B., and Watari, H. (2018b). miR-34a, miR-424 and miR-513 inhibit MMSET expression to repress endometrial cancer cell invasion and sphere formation. *Oncotarget.* 9, 23253–23263. doi: 10.18632/oncotarget.25298

Fletcher, A., Choudhury, A., and Alam, N. (2011). Metastatic bladder cancer: a review of current management. *ISRN Urol.* 2011:545241. doi: 10.5402/2011/545241

Gao, J., Aksoy, B. A., Dogrusoz, U., Dresdner, G., Gross, B., Sumer, S. O., et al. (2013). Integrative analysis of complex cancer genomics and clinical profiles using the cBioPortal. *Sci. Signal.* 6:l1. doi: 10.1126/scisignal.2004088

Győrffy, B., Lanczky, A., Eklund, A. C., Denkert, C., Budczies, J., Li, Q., et al. (2010). An online survival analysis tool to rapidly assess the effect of 22,277 genes on breast cancer prognosis using microarray data of 1,809 patients. *Breast Cancer Res. Treat.* 123, 725–731. doi: 10.1007/s10549-009-0674-9

Huang, W. Y., Hsu, S. D., Huang, H. Y., Sun, Y. M., Chou, C. H., Weng, S. L., et al. (2015). MethHC: a database of DNA methylation and gene expression in human cancer. *Nucleic Acids Res.* 43, D856–D861. doi: 10.1093/nar/gku1151

Jiang, J., Zhang, Y., Guo, Y., Yu, C., Chen, M., Li, Z., et al. (2015). MicroRNA-3127 promotes cell proliferation and tumorigenicity in hepatocellular carcinoma by disrupting of PI3K/AKT negative regulation. *Oncotarget* 6, 6359–6372. doi: 10.18632/oncotarget.3438

Li, F., Liao, J., Duan, X., He, Y., and Liao, Y. (2018). Upregulation of LINC00319 indicates a poor prognosis and promotes cell proliferation and invasion in cutaneous squamous cell carcinoma. *J. Cell Biochem.* 119, 10393–10405. doi: 10.1002/jcb.27388

Li, J. H., Liu, S., Zhou, H., Qu, L. H., and Yang, J. H. (2014). starBase v2.0: decoding miRNA-ceRNA, miRNA-ncRNA and protein-RNA interaction networks from large-scale CLIP-Seq data. *Nucleic Acids Res.* 42, D92–D97. doi: 10.1093/nar/gkt1248

Mitra, A. P., Datar, R. H., and Cote, R. J. (2006). Molecular pathways in invasive bladder cancer: new insights into mechanisms, progression, and target identification. *J. Clin. Oncol.* 24, 5552–5564. doi: 10.1200/jco.2006.08.2073

Pan, B., Zhao, M., and Xu, L. (2019). Long noncoding RNA gastric cancer-associated transcript 3 plays oncogenic roles in glioma through sponging miR-3127-5p. *J. Cell Physiol.* 234, 8825–8833. doi: 10.1002/jcp.27542

Pang, C., Guan, Y., Li, H., Chen, W., and Zhu, G. (2016). Urologic cancer in China. *Jpn. J. Clin. Oncol.* 46, 497–501. doi: 10.1093/jjco/hyw034

Peng, C. W., Yue, L. X., Zhou, Y. Q., Tang, S., Kan, C., Xia, L. M., et al. (2019). miR-100-3p inhibits cell proliferation and induces apoptosis in human gastric cancer through targeting to BMPR2. *Cancer Cell Int.* 19, 354. doi: 10.1186/s12935-019-1060-2

Porten, S. P. (2018). Epigenetic alterations in bladder cancer. *Curr. Urol. Rep.* 19:102. doi: 10.1007/s11934-018-0861-5

Siegel, R. L., Miller, K. D., and Jemal, A. (2018). Cancer statistics. *CA Cancer J. Clin.* 68, 7–30. doi: 10.3322/caac.21442

Song, P., and Yin, S. C. (2019). Long non-coding RNA 319 facilitates nasopharyngeal carcinoma carcinogenesis through regulation of miR-1207-5p/KLF12 axis. *Gene* 680, 51–58. doi: 10.1016/j.gene.2018.09.032

Sun, Y., Chen, C., Zhang, P., Xie, H., Hou, L., Hui, Z., et al. (2014). Reduced miR-3127-5p expression promotes NSCLC proliferation/invasion and contributes to dasatinib sensitivity via the c-Abl/Ras/ERK pathway. *Sci. Rep.* 4:6527. doi: 10.1038/srep06527

Wan, Q., Dingerdissen, H., Fan, Y., Gulzar, N., Pan, Y., Wu, T. J., et al. (2015). BioXpress: an integrated RNA-seq-derived gene expression database for pan-cancer analysis. *Database* 2015:bav019. doi: 10.1093/database/bav019

Wu, J. X., Du, W. Q., Wang, X. C., Wei, L. L., Huo, F. C., Pan, Y. J., et al. (2017). Rap2a serves as a potential prognostic indicator of renal cell carcinoma and promotes its migration and invasion through up-regulating p-Akt. *Sci. Rep.* 7:6623. doi: 10.1038/s41598-017-06162-7

Wu, J. X., Zhang, D. G., Zheng, J. N., and Pei, D. S. (2015). Rap2a is a novel target gene of p53 and regulates cancer cell migration and invasion. *Cell Signal.* 27, 1198–1207. doi: 10.1016/j.cellsig.2015.02.026

Xia, Y., Liu, Z., Yu, W., Zhou, S., Shao, L., Song, W., et al. (2018). The prognostic significance of long noncoding RNAs in bladder cancer: a meta-analysis. *PLoS One* 13:e0198602. doi: 10.1371/journal.pone.0198602

Xiao, H., Tang, K., Liu, P., Chen, K., Hu, J., Zeng, J., et al. (2015). LncRNA MALAT1 functions as a competing endogenous RNA to regulate ZEB2 expression by sponging miR-200s in clear cell kidney carcinoma. *Oncotarget* 6, 38005–38015. doi: 10.18632/oncotarget.5357

Yang, J., Hou, S., and Liang, B. (2020). LINC00319 promotes migration, invasion and epithelial-mesenchymal transition process in cervical cancer by regulating miR-3127-5p/RPP25 axis. *In Vitro Cell Dev. Biol. Anim.* doi: 10.1007/s11626-019-00425-5 [Epub ahead of print].

Yang, Y., Sun, Y., Wu, Y., Tang, D., Ding, X., Xu, W., et al. (2018). Downregulation of miR-3127-5p promotes epithelial-mesenchymal transition via FZD4 regulation of Wnt/β-catenin signaling in non-small-cell lung cancer. *Mol. Carcinog.* 57, 842–853. doi: 10.1002/mc.22805

Zhang, Y., and Chen, X. (2020). lncRNA FOXD2-AS1 affects trophoblast cell proliferation, invasion and migration through targeting miRNA. *Zygote* doi: 10.1017/S0967199419000807 [Epub ahead of print].

Zhang, Y., Huang, Z., Sheng, F., and Yin, Z. (2019). MYC upregulated LINC00319 promotes human acute myeloid leukemia (AML) cells growth through stabilizing SIRT6. *Biochem. Biophys. Res. Commun.* 509, 314–321. doi: 10.1016/j.bbrc.2018.12.133

Zhang, Z. W., Chen, J. J., Xia, S. H., Zhao, H., Yang, J. B., Zhang, H., et al. (2018). Long intergenic non-protein coding RNA 319 aggravates lung adenocarcinoma carcinogenesis by modulating miR-450b-5p/EZH2. *Gene* 650, 60–67. doi: 10.1016/j.gene.2018.01.096

Zhou, B., Yuan, W., and Li, X. (2017). Long intergenic noncoding RNA 319 (linc00319) promotes cell proliferation and invasion in lung cancer cells by directly downregulating the tumor suppressor MiR-32. *Oncol. Res.* doi: 10.3727/096504017X15016337254650 [Epub ahead of print].

Conflict of Interest: The authors declare that the research was conducted in the absence of any commercial or financial relationships that could be construed as a potential conflict of interest.

frontiers in Genetics

ORIGINAL RESEARCH
published: 05 March 2020
doi: 10.3389/fgene.2020.00167

Circulating MicroRNAs in Plasma Decrease in Response to Sarcopenia in the Elderly

*Nana He[1,2], Yue Lin Zhang[3], Yue Zhang[3], Beili Feng[3], Zaixing Zheng[3], Dongjuan Wang[3], Shun Zhang[1,2], Qi Guo[4] and Honghua Ye[3]**

[1] Department of Experimental Medical Science, HwaMei Hospital, University of Chinese Academy of Sciences, Ningbo, China, [2] Key Laboratory of Diagnosis and Treatment of Digestive System Tumors of Zhejiang Province, Ningbo, China, [3] Department of Cardiology, HwaMei Hospital, University of Chinese Academy of Sciences, Ningbo, China, [4] Shanghai University of Medicine and Health Sciences Affiliated Zhoupu Hospital, Shanghai, China

sarcopenia has been defined as the aging-related disease with the declined mass, strength, and function of skeletal muscle, which is a major cause of morbidity and mortality in elders. Current diagnostic criteria of sarcopenia have not been agreed internationally, and the clinical diagnostic biomarkers for sarcopenia have not been identified. Circulating miRNAs (miRNAs, miRs) have recently been characterized as novel biomarkers for sarcopenia. However, the change of circulating miRNAs in response to sarcopenia are still not fully understood. Here, we enrolled a total of 93 elderly patients clinically diagnosed with sarcopenia and matching 93 non-sarcopenia elderly in this study. Specifically, levels of candidate circulating miRNAs which were involved in angiogenesis, inflammation and enriched in muscle and/or cardiac tissues were detected in these two groups. In small-sample screening experiments, plasma miR-155, miR-208b, miR-222, miR-210, miR-328, and miR-499 levels were significantly down-regulated in sarcopenia compared to those who non-sarcopenia. In contrast, miR-1, mir-133a, miR-133b, miR-21, miR-146a, miR-126, miR-221, and miR-20a were not changed significantly. Subsequently, we expanded the sample size to further detection and verification, and found that plasma miR-155, miR-208b, miR-222, miR-210, miR-328, and miR-499 levels in the sarcopenia group were significantly reduced compared to the non-sarcoma group, which is consistent with the results of the small-sample screening experiment. In addition, we showed that ASM/Height2, handgrip strength, knee extension and 4-meter velocity in sarcopenia group were significantly lower than those in non-sarcopenia group. Here we correlated the decrease of miR-208b, miR-499, miR-155, miR-222, miR-328, and miR-210 in sarcopenia group and non-sarcopenia group with diagnostic indexes of sarcopenia (ASM/Height2, Handgrip strength and 4-meter velocity) after adjusting sex. The results showed that miR-208b and miR-155 changes were significantly correlated with handgrip strength in woman, miR-208b, miR-499, and miR-222 changes were significantly correlated with ASM/Height2 in man, while other miRNAs changes did not show a strong correlation with these diagnostic indexes. In conclusion, plasma miR-208b, miR-499, miR-155, miR-222, miR-328, and miR-210

OPEN ACCESS

Edited by:
Junjie Xiao,
Shanghai University, China

Reviewed by:
Yunpeng Shang,
Affiliated Hospital of Jiangsu University, China
Yabin Wang,
Chinese PLA General Hospital, China

****Correspondence:***
Honghua Ye
lindayenbzjch@163.com

Specialty section:
This article was submitted to RNA, a section of the journal Frontiers in Genetics

Received: *11 December 2019*
Accepted: *12 February 2020*
Published: *05 March 2020*

Citation:
He N, Zhang YL, Zhang Y, Feng B, Zheng Z, Wang D, Zhang S, Guo Q and Ye H (2020) Circulating MicroRNAs in Plasma Decrease in Response to Sarcopenia in the Elderly. Front. Genet. 11:167. doi: 10.3389/fgene.2020.00167

decrease in response to sarcopenia in the elderly. Although further studies are needed to clarify the potential use of circulating miRNAs as biomarkers of sarcopenia, present findings set the stage for defining circulating miRNAs as biomarkers and suggesting their physiological roles in elderly with sarcopenia.

Keywords: circulating microRNAs, sarcopenia, biomarker, plasma, elderly

INTRODUCTION

With the increasing pressure of global aging population, diseases related to the elderly are of great concern. As a major cause of death and disability in the elderly, sarcopenia has been widely recognized and concerned. Sarcopenia is a syndrome characterized by the decline of skeletal muscle mass, a progressive loss of muscle strength and function with age (Chen et al., 2014; Landi et al., 2018; Sanchez-Rodriguez et al., 2019). The occurrence of sarcopenia is a complex process, which is controlled by both extrinsic and intrinsic factors, including the decrease of exercise volume, the change of hormone level, the degeneration of motor neurons and the metabolic disorder of nutritional factors (Cruz-Jentoft et al., 2019). Recently, there have been more and more studies on sarcopenia, but most of them are still in the exploratory stage, and the pathogenesis and diagnostic criteria are still unclear.

Due to the increase of age, the body's metabolic capacity is gradually decreasing, and the incidence of sarcopenia has also increased (Cruz-Jentoft et al., 2014). It is easy to trigger a series of health problems. Sarcopenia is associated with increased adverse outcomes including falls, functional decline, frailty, and mortality (Bjorkman et al., 2019; Yang et al., 2019). Sarcopenia also reduces the amount of metabolically active tissue; thus, it increases the risk for metabolic diseases, including cardiovascular disease, diabetes, hypertension and hyperlipidemia and other elderly diseases (Biolo et al., 2014; Wang et al., 2018; Yilmaz and Bahat, 2019). This will bring heavy economic burden to the family of the elderly, society and medical service system. However, the harm caused by sarcopenia has not yet attracted enough attention from clinicians and society.

MicroRNA (miRNA, miR) is regarded as the most promising small molecule RNA for targeted diagnosis and treatment in the 21st century, which plays a key role in a wide range of physiological and pathological processes (Brown and Goljanek-Whysall, 2015). MiRNAs are a class of non-coding regulatory RNA molecules with a length of about 20–30 nucleotides that regulate gene expression at the post-transcriptional level. Some miRNAs are ubiquitously expressed in tissue, while others are tissue-specific or tissue-enriched (e.g., skeletal muscle). MiRNAs can be released by cells and are found in various body fluid, including serum and plasma (Gautam et al., 2016). Therefore, detecting changes in miRNA levels in the circulation can provide information about the original tissue or cell. At present, people are mainly concerned about the function of miRNA in tissues and cells. Increasing evidence has reported that circulating miRNAs are present in serum or plasma, and circulating miRNAs are remarkably stable, easily detectable, and sensitive to changes in health status (Kroh et al., 2010; Jung and Suh, 2014; Troiano et al., 2016). Therefore, miRNAs in serum or plasma can be used as potential biomarkers for the diagnosis and treatment of diseases. To date, a growing number of evidence suggests that circulating miRNAs as potential therapeutic biomarkers for sarcopenia, and a number of circulating miRNAs are found to be associated with age-related muscle missing in elderly (McGregor et al., 2014; Siracusa et al., 2018). Recently, several works have demonstrated that various circulating miRNAs are differentially expressed during aging. However, the response of circulating miRNAs to sarcopenia in elderly is undetermined.

Here, we investigate how specific circulating miRNAs with well-established roles is linked to sarcopenia in elderly. Specifically, we determined the change of circulating miRNA levels in elderly with sarcopenia and non- sarcopenia. We fund that plasma miR-208b, miR-499, miR-155, miR-222, miR-328, and miR-210 levels were significantly down-regulated in response to sarcopenia in elderly, while miR-1, mir-133a, miR-133b, miR-21, miR-146a, miR-126, miR-221, and miR-20a were not changed significantly. Moreover, we correlated the circulating miRNA changes with diagnostic indicators of sarcopenia (ASM/Height2, Handgrip strength and 4-meter velocity), showing the potential of circulating miRNA as biomarkers of sarcopenia in elderly.

MATERIALS AND METHODS

Participants

All subjects in this study were from Ximen Community of Ningbo, China. A total of 1047 older individuals (age $\geq$65 years) were enrolled our examination program and finished a comprehensive geriatric assessment from November 2016 to March 2017. Inclusion criteria of this trial: (1) older individuals (age $\geq$65 years); and (2) People who can independently detect walking speed, grip strength and muscle mass. Exclusion criteria of this trial: (1) People who refused to participate in the study; (2) People who cannot complete the required inspection items independently; and (3) older individuals (age $\leq$65 years). According to the AWGs criteria for the diagnosis of sarcopenia, the subjects were further divided into sarcopenia group (n = 93) and non-sarcopenia group (n = 93). The matching factors were gender and age. We adhered to the principles of the Declaration of Helsinki, and the study protocol was approved by the Ethics Committee of Ningbo No. 2 Hospital. All participants gave informed written consent.

Plasma Sampling

Venous blood was collected in silicone-coated serum tubes with increased silica act clot activator, followed by processing within

1 h after collection. At 4°C, blood samples were centrifuged at 3,000 rpm for 15 min, and plasma and erythrocytes were separated. Aliquots of plasma were collected into RNase/DNase-free tubes and immediately aliquoted and frozen at −80°C until the assays were performed.

RNA Isolation

The total RNA extraction was performed using a mirVana PARIS isolation kit (Ambion, Austin, Texas) according to the manufacturer's instructions. To avoid variability of results, repeated freeze-thaw cycles of serum samples were minimized and all samples were extracted and analyzed in a single batch. Briefly, 400 μl of plasma was used to extract the total RNA. After equal volume of denaturing solution was added, 50 pmol/L Caenorhabditis elegans miR-39 (cel-miR-39) was added to normalize the miRNA serum levels.

Quantification of Circulating MiRNA Levels

For quantitative miRNA analysis, Bulge-LoopTM miRNA qPCR Primer Sets (RiboBio) were used to detect selected miRNAs expressions by quantitative reverse transcription polymerase chain reactions (qRT-PCRs) with iTaqTM Universal SYBR Green Supermix (BIO-RAD) in the 7900HT Fast Real-Time PCR System as previously reported. All qRT-PCR reactions were performed in triplicate, and the signal was collected at the end of every cycle. As there is no consensus on endogenous stable miRNAs in the circulation to act as house-keepers, the expression level of miRNAs in serum were normalized using spike-in cel-miR-39, which lacks sequence homology to human miRNAs.

Assessment of Muscle Strength and Physical Performance

Body composition features were measured by a direct segmental multifrequency bioelectrical impedance analysis; Appendicular skeletal muscle mass (ASM) was calculated as the sum of skeletal muscle in the arms and legs; Relative skeletal muscle mass index (ASM/Ht2) was defined as ASM divided by body height in meters squared; We collected muscle strength to the nearest 0.1 kg with a accurate handgrip dynamometer; The 4-meter walking speed test was carried out on a straight corridor with a 6-meter mark on the ground.

Other Measurement

Each participant's age, gender, occupation, medical history, intake of medications, and smoking and drinking habits were asked by an experienced staff through a standardized questionnaire. They measured body height and waist circumference to the nearest 0.5 cm. Body mass index was weight in kilograms divided by the height in meters squared.

Office blood pressure was measured by means of the Omron HEM-1300 monitor (Omron Healthcare, Inc., Kyoto, Japan). After participants had rested in the sitting position for at least 5 min 3 consecutive blood pressure readings were obtained according to the recommendations of the European Society of Hypertension. For analysis, the three readings were averaged. Office hypertension was a blood pressure of at least 140 mmHg systolic or 90 mmHg diastolic.

Venous blood samples, obtained after overnight fasting, were analyzed by automated enzymatic methods for serum total and high-density lipoprotein cholesterol, serum creatinine and uric acid, and plasma glucose. Hypertension was a former diagnosis or use of antihypertensive drugs. Diabetes mellitus was a glycosylated hemoglobin level of 7.0% or higher or use of anti-diabetic drugs, or prior diagnosis. Dyslipidaemia was a total cholesterol concentration above 5.0 mmol/L, a high-density-lipoprotein cholesterol level lower than 1.2 mmol/L in women or below 1.0 mmol/L in men, or use of lipid-lowering drugs.

Statistical Analysis

Subject characteristics, biochemical measurements and general echocardiographic indexes are presented as means ± standard error of the mean (SEM). For the analysis of qRT-PCR data, the relative expression level for each miRNA was calculated using the $2^{-\Delta\Delta Ct}$ method and the data were expressed as the mean ± SE. Paired-samples were compared by *t*-test as appropriate for analyzing the changes of miRNAs. Correlation analyses between changes of circulating miRNAs and diagnostic indexes of sarcopenia (ASM/Height2, Handgrip strength and 4-meter velocity) were performed using the Pearson's method as appropriate for data distribution. Statistical significance is defined as *P*-values <0.05.

RESULTS

Subject Characteristics

The cohort used in this study is the same as previously reported (Zhang et al., 2019). The clinical characteristics for these subjects were shown in **Table 1**. The height of the non-sarcopenia group is higher than that of the sarcopenia group (159.73 ± 0.78 vs. 156.03 ± 0.74, $p < 0.05$); Body mass in non-sarcopenia group is greater than that in sarcopenia group (64.72 ± 1.19 vs. 52.97 ± 0.80, $p < 0.05$); BMI in non-sarcopenia group is greater than that in sarcopenia group (25.32 ± 0.41 vs. 21.75 ± 0.29, $p < 0.05$). There was no significant difference in age, systolic blood pressure and diastolic blood pressure between the two groups. **Table 2** lists the detailed anthropometric indexes of participants. ASM/Height2, handgrip strength, knee extension and 4-meter velocity in sarcopenia group were significantly lower than those in non-sarcopenia group ($p < 0.05$). There was no significant difference of body muscle mass (%) and body fat mass (%) between the two groups. We analyzed the biochemical measurements of participants in non-sarcopenia and sarcopenia group (**Table 3**). The results showed that there were no significant changes of blood lipids (Total cholesterol, LDL cholesterol, Triglyceride), renal function (serum creatinine), arterial stiffness (BaPWV) and plasma glucose (HbA1c) between non-sarcopenia and sarcopenia group, while blood lipids marker HDL cholesterol of sarcopenia group was significantly higher than that of non-sarcopenia group.

TABLE 1 | Clinical characteristic of participants.

Clinical parameters	Mean ± SEM		*P*
	Non-sarcopenia group (*n* = 93)	sarcopenia group (*n* = 93)	
Age(years)	76.19 ± 0.58	76.15 ± 0.58	>0.05
Height(cm)	159.73 ± 0.78	156.03 ± 0.74	<0.05
Body mass(kg)	64.72 ± 1.19	52.97 ± 0.80	<0.05
BMI(kg/m^2)	25.32 ± 0.41	21.75 ± 0.29	<0.05
Systolic blood pressure (mmHg)	140.11 ± 1.80	137.35 ± 2.44	>0.05
Diastolic blood pressure (mmHg)	72.18 ± 1.09	72.36 ± 1.30	>0.05
Pressure (mmHg)			

TABLE 2 | Anthropometric indexes of participants.

Anthropometric indexes	Mean ± SEM		*p*
	Non-sarcopenia group	sarcopenia group	
ASM/Height^2(kg/m^2)	6.71 ± 0.10	5.63 ± 0.07	<0.05
Body muscle mass(%)	62.64 ± 0.67	64.23 ± 0.71	>0.05
Body fat mass(%)	33.55 ± 0.72	31.71 ± 0.75	>0.05
Handgrip strength(kg)	24.18 ± 0.94	17.33 ± 0.55	<0.05
Knee extension(kg)	19.93 ± 0.81	14.76 ± 0.59	<0.05
4-meter velocity(m/s)	1.12 ± 0.02	1.00 ± 0.03	<0.05

TABLE 3 | Physiological functions of participants.

Physiological functions	Mean ± SEM		*p*
	Non-sarcopenia group	sarcopenia group	
Blood lipids			
Total cholesterol(mmol/L)	4.42 ± 0.11	4.69 ± 0.11	>0.05
HDL cholesterol(mmol/L)	1.48 ± 0.04	1.69 ± 0.05	<0.05
LDL cholesterol(mmol/L)	2.84 ± 0.10	3.04 ± 0.10	>0.05
Triglyceride(mmol/L)	1.69 ± 0.10	1.44 ± 0.07	>0.05
Renal function			
Serum creatinine(μmol/L)	75.01 ± 2.31	74.42 ± 2.98	>0.05
Arterial stiffness			
BaPWV(cm/s)	1883.14 ± 41.45	1999.18 ± 50.76	>0.05
Plasma glucose			
HbA1c(%)	6.22 ± 0.09	6.17 ± 0.10	>0.05

Circulating MiR-155, MiR-208b, MiR-222, MiR-210, MiR-328, and MiR-499 Decrease in Response to Sarcopenia in the Elderly

We determined the expression of angiogenesis-related miRNAs (miR-20a, miR-126, miR-210, miR-221, miR-222, and miR-328) (Dews et al., 2006; Poliseno et al., 2006; Kuehbacher et al., 2007; Fasanaro et al., 2008; Soeki et al., 2016), inflammation-related miRNAs (miR-21, miR-146a, and miR-155) (Taganov et al., 2006; Urbich et al., 2008; Wang et al., 2017) and cardiac or muscle-specific/enriched miRNAs (miR-1, miR-133a, miR-133b, miR-208b, miR-486, and miR-499) (Chen et al., 2006; Alexander et al., 2014; Soci et al., 2016). Firstly, the results of small-sample screening experiment showed that plasma miR-208b, miR-499, miR-155, miR-222, miR-328, and miR-210 levels were significantly down-regulated in sarcopenia group compared to those who non-sarcopenia. In contrast, miR-1, mir-133a, miR-133b, miR-21, miR-146a, miR-126, miR-221, and miR-20a were not changed significantly **(Figure 1)**. Then, we further expanded the experimental sample size to verify the expression trend of these differentially expressed miRNAs. The results also showed that miR-208b, miR-499, miR-155, miR-222, miR-328, and miR-210 levels were significantly down-regulated in sarcopenia group compared to those who non-sarcopenia (**Figure 2**).

Correlation Analysis Between Changes of MiR-208b, MiR-499, MiR-155, MiR-222, MiR-328 and MiR-210 and ASM/Height2, Handgrip Strength or 4-Meter Velocity

According to AWGs standard, sarcopenia was diagnosed as low muscle mass, low muscle strength and/or low physical strength. ASM/height^2, handgrip strength and 4- meter velocity were used for detection respectively. The levels of ASM/height^2, handgrip strength and knee extension were significantly decreased in the elderly with sarcopenia (**Table 2**). Here we correlated the decrease of miR-208b, miR-499, miR-155, miR-222, miR-328, and miR-210 in sarcopenia group and non-sarcopenia group with diagnostic indicators of sarcopenia (ASM/Height^2, Handgrip strength and 4-meter velocity) after adjusting sex. The results showed that miR-208b and miR-155 changes were significantly correlated with handgrip strength in woman **(Figure 3)**, miR-208b, miR-499, and miR-222 changes were significantly correlated with ASM/Height2 in man **(Figure 4)**, while other miRNAs changes did not show a strong correlation with these diagnostic indexes.

DISCUSSION

Sarcopenia is a progressive decline in skeletal muscle mass, strength, and quality during aging. Although the molecular mechanisms involved in sarcopenia development are not entirely understood, it is well-documented that transcriptomic, proteomic and epigenetic changes during the progression of aging are the main causative factors for sarcopenia. This study was designed to explore how specific circulating miRNAs are changed in response to sarcopenia in the elderly. Here we reported that plasma miR-208b, miR-499, miR-155, miR-222, miR-328, and miR-210 levels were significantly down-regulated in sarcopenia compared to those who non-sarcopenia. We also showed that the levels of ASM/height2, handgrip strength, knee extension and 4-meter velocity were significantly decreased in elderly with sarcopenia. Here we correlated the decrease of miR-208b, miR-499, miR-155, miR-222, miR-328, and miR-210 with predictor of sarcopenia (ASM/Height2, Handgrip strength and 4-meter velocity) after adjusting sex.

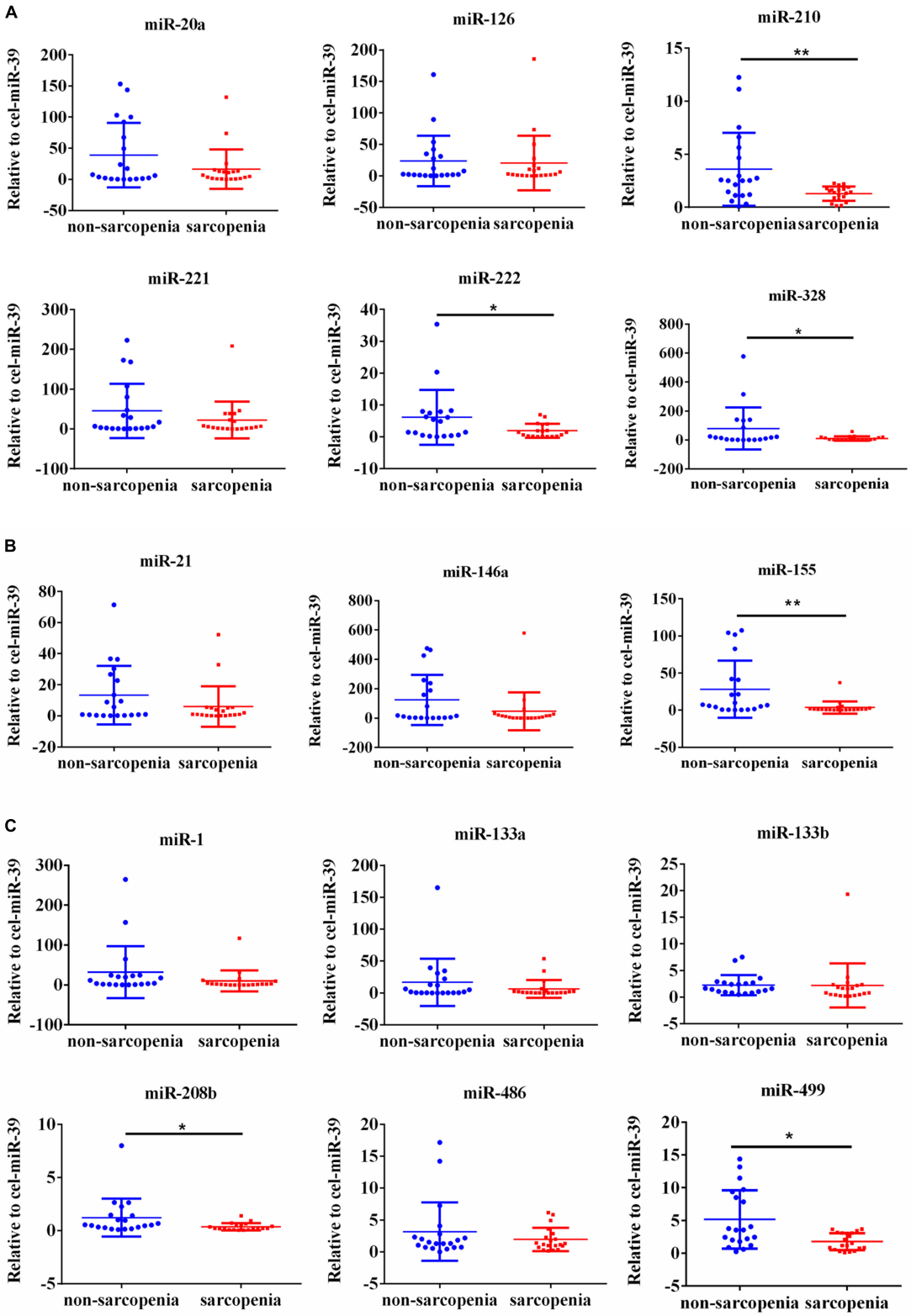

FIGURE 1 | Changes in circulating microRNAs in response to sarcopenia in the elderly. **(A)** Changes of angiogenesis-related miRNAs when normalized to cel-miR-39 in small-sample screening experiment; *compared to non-sarcopenia of the elderly, $P < 0.05$; **compared to non-sarcopenia of the elderly, $P < 0.01$. **(B)** Changes of inflammation-related miRNAs when normalized to cel-miR-39 in small-sample screening experiment; *compared to non-sarcopenia of the elderly, $P < 0.05$; **compared to non-sarcopenia of the elderly, $P < 0.01$. **(C)** Changes of cardiac or muscle-specific/enriched miRNAs when normalized to cel-miR-39 in small-sample screening experiment; *compared to non-sarcopenia of the elderly, $P < 0.05$; **compared to non-sarcopenia of the elderly, $P < 0.01$.

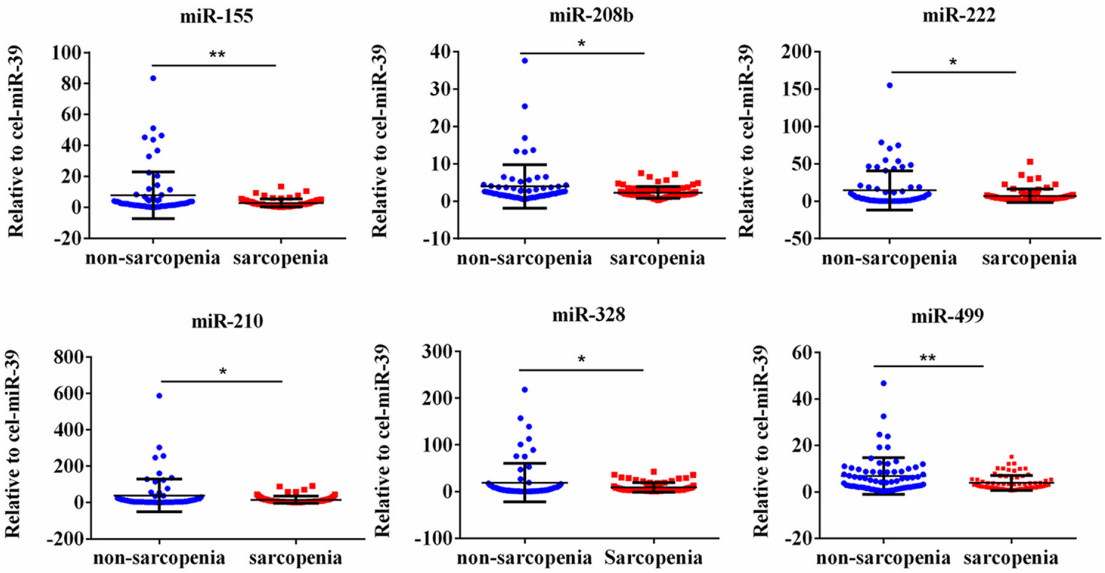

FIGURE 2 | CirculatingmiR-155, miR-208b, miR-222, miR-210, miR-328 and miR-499 decrease in response to age-associated loss of muscle in elderly patients; *compared to non-sarcopenia of the elderly, $P < 0.05$; **compared to non-sarcopenia of the elderly, $P < 0.01$.

The results showed that miR-208b and miR-155 changes were significantly correlated with handgrip strength in woman, miR-208b, miR-499, and miR-222 changes were significantly correlated with ASM/Height2 in man, while other miRNAs changes did not show a strong correlation with these diagnostic indexes. Given that miRNA changes were correlated with diagnostic indicators of sarcopenia, the present study also provides potential biomarkers for sarcopenia in the elderly. Moreover, the potential biological function of these dysregulated miRNAs responsible for beneficial effects of sarcopenia in elderly warrants further studied.

Several circulating miRNAs have been identified as closely related to sarcopenia in the elderly. Increasing evidence has shown that miRNAs are differentially expressed in skeletal muscle with age. Specifically, miR-1, miR-21, mir-133a, miR-133b, miR-206, miR-146a, and miR-155 were up-regulated while miR-20a, miR-208b, miR-210, miR-221, miR-222, and miR-499 were down-regulated in aged muscle compared to young muscle (Kim et al., 2014; Margolis and Rivas, 2018; Jung et al., 2019). However, all these studies were conducted in aged muscle. To the best of our knowledge, the present study is the first to identify plasma miRNAs that change in response to sarcopenia in the elderly. The differentially expressed miRNAs in earlier studies appeared consistently in the plasma of sarcopenia in the elderly from our study. For example, the expression pattern of miR-208b, miR-499, miR-222, and miR-210 are similar to previous studies. Here we reported that plasma miR-208b, miR-499, miR-222, and miR-210 were significantly down-regulated in plasma in the elderly with sarcopenia while other miRNAs determined in this study were not changed, indicating that individual differences of participants might affect levels of circulating miRNAs. Considering most of the previous studies focused on miRNA expression changes in aged muscles, our results of circulating miRNA expression in plasma provide new insights for the diagnosis and treatment of sarcopenia.

Sarcopenia is a kind of senile syndrome, and its pathogenesis is very complex. Many diseases can cause muscle changes, resulting in decreased muscle mass and strength, so there is a close relationship between sarcopenia and various diseases. According to statistics from the literature, the incidence of sarcopenia in patients with liver cirrhosis is 40 to 70%, which is much higher than the incidence of sarcopenia in patients without liver disease (Dasarathy, 2012; Sinclair et al., 2016). At the same time, sarcopenia is one of the most common complications in patients with cirrhosis, and there are few effective treatments for it. Studies have shown that sarcopenia is one of the risk factors for chronic cardiovascular disease. Patients with heart failure (HF) often suffer from sarcopenia at the same time, and improving muscle loss in HF patients is an effective treatment strategy (Chin et al., 2013; Loncar et al., 2013; Cipryan, 2018). It was reported that the muscle mass, strength and function of the leg muscles of diabetic patients are rapidly decreasing compared with those with normal blood glucose, and it has been proposed that the development of personalized functional exercises for the elderly with diabetes is of great significance in preventing and treating sarcopenia (Leenders et al., 2013; Wang et al., 2018). The miRNAs selected in this study have potential biological relevance in sarcopenia-related diseases, including diabetes, cardiovascular disease, and inflammation. Among the miRNAs analyzed here are angiogenesis-related miRNAs (miR-20a, miR-126, miR-210, miR-221, miR-222, and miR-328), inflammation-related miRNAs (miR-21, miR-146a, and miR-155) and cardiac or muscle-specific/enriched miRNAs (miR-1, miR-133a, miR-133b, miR-208b, miR-486, and miR-499). Among them, miR-208b, miR-499, miR-155, miR-222, and miR-210 were significantly down-regulated in the plasma of

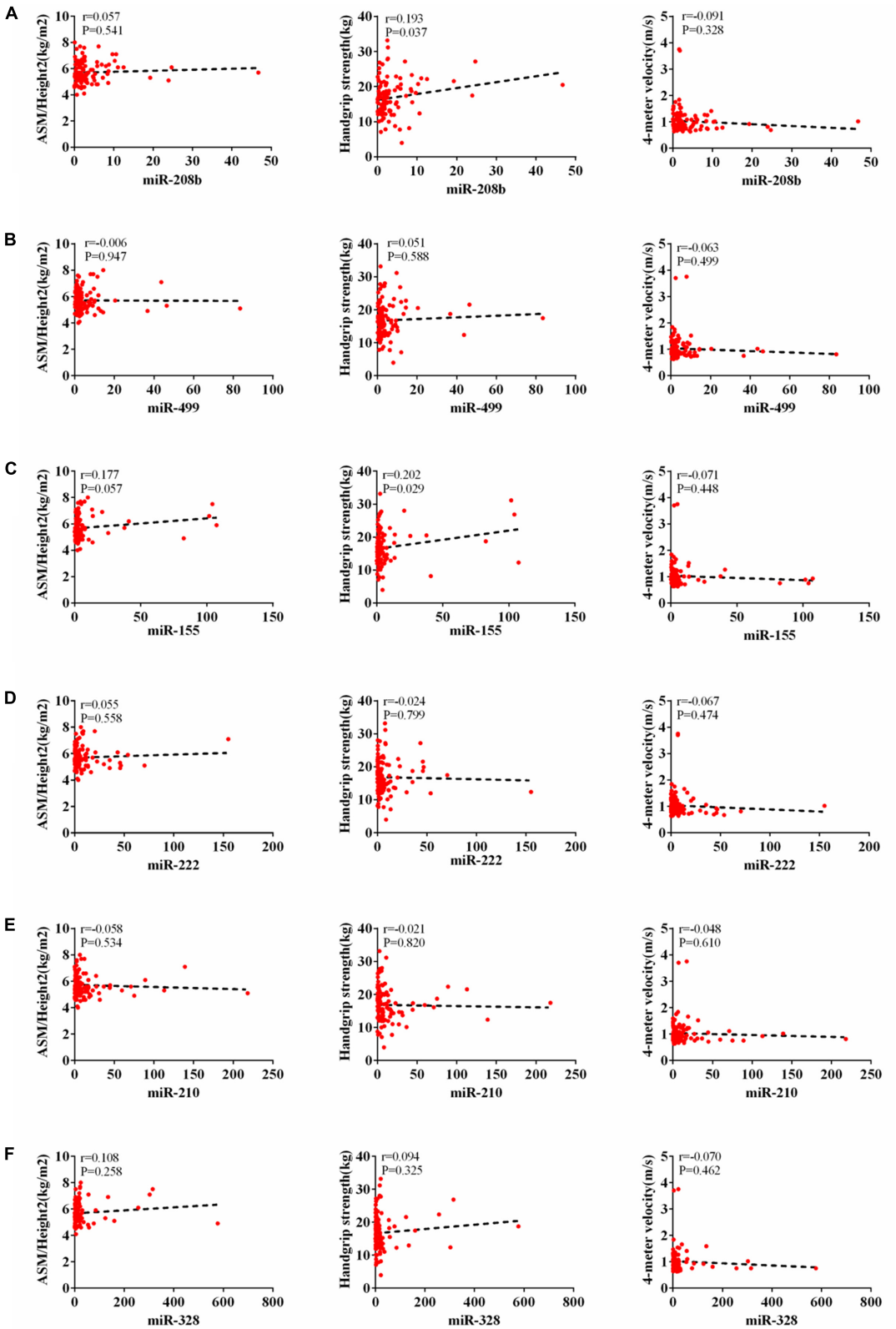

FIGURE 3 | Correlation analysis between the changes of miR-208b **(A)**, miR-499 **(B)**, miR-155 **(C)**, miR-222 **(D)**, miR-210 **(E)** and miR-328 **(F)** and ASM/Height2(kg/m2), Handgrip strength(kg) and 4-meter velocity(m/s) in woman, $P < 0.05$.

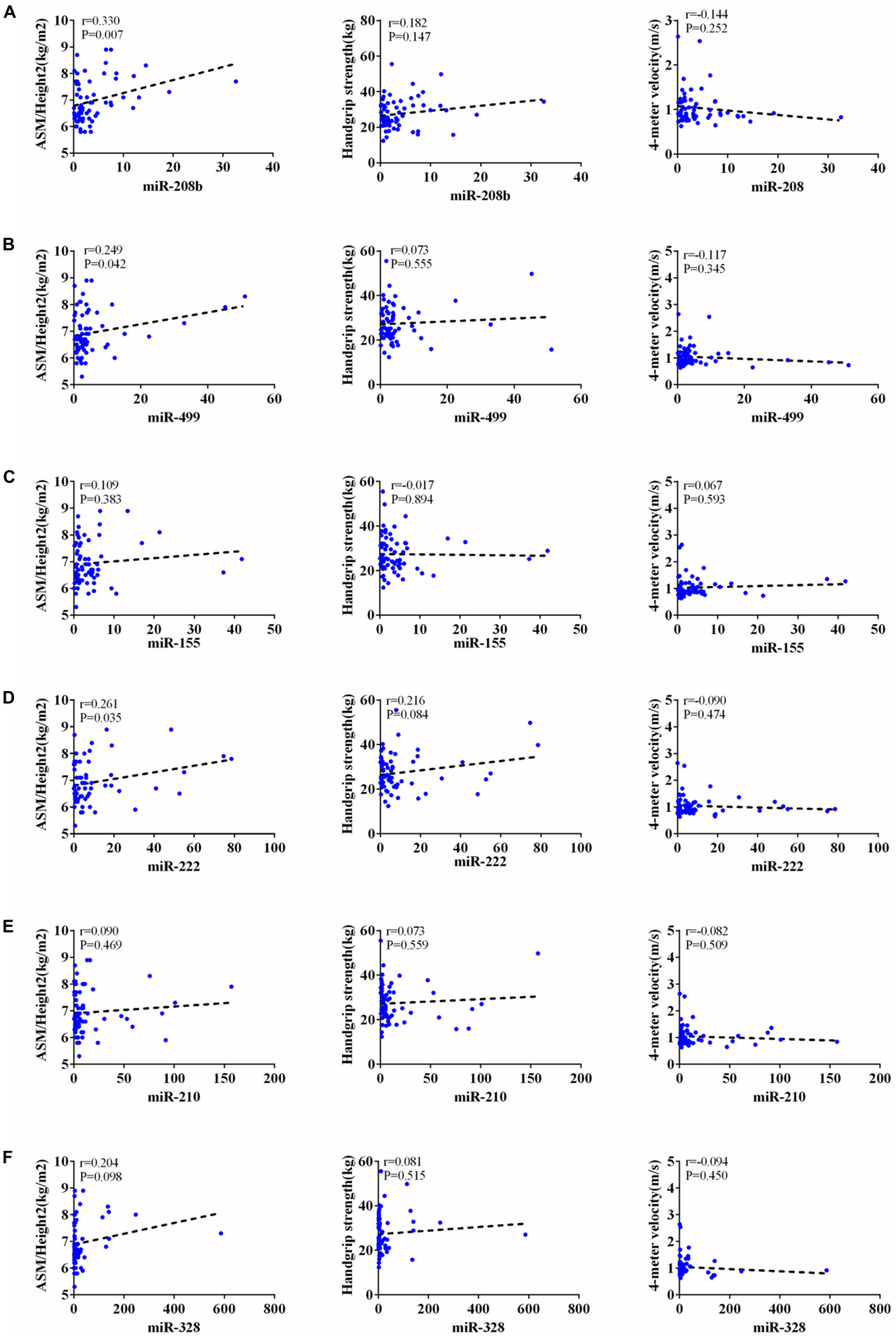

FIGURE 4 | Correlation analysis between the changes of miR-208b **(A)**, miR-499 **(B)**, miR-155 **(C)**, miR-222 **(D)**, miR-210 **(E)** and miR-328 **(F)** and ASM/Height2(kg/m2), Handgrip strength(kg) and 4-meter velocity(m/s) in man, $P < 0.05$.

sarcopenia in the elderly. Here, our results indicate that these miRNAs may be promising biomarkers for sarcopenia, and have important significance for the screening of early sarcopenia and improvement of sarcopenia-related diseases.

Because the current diagnostic criteria for sarcopenia use ASM/Height2, Handgrip strength and 4-meter velocity, these diagnostic indicators can indicate the severity of sarcopenia (Chen et al., 2014). According to the consensus report of the Asian Working Group on sarcopenia (AWGS) in 2014, we found that the diagnostic criteria for sarcopenia are different between men and women: muscle mass assessment using ASM/Height2, ASM/Height2 $\leq$ 7.0 kg/m2 (male), ASM/Height2 $\leq$ 5.7 kg/m2 (female); the handgrip strength was used for the measurement of muscle strength. The cut point of muscle strength was less than 26 kg for men and less than 18 kg for women; 4-meter velocity is selected for muscle function measurement, if 4-meter velocity $\leq$0.8 m/s, indicates a decline in motor ability. In this study, we correlated the decrease of miR-208b, miR-499, miR-155, miR-222, miR-328, and miR-210 with diagnostic indexes of sarcopenia (ASM/Height2, Handgrip strength and 4-meter velocity) after adjusting sex.

The results showed that miR-208b and miR-155 changes were significantly correlated with handgrip strength in woman, miR-208b, miR-499, and miR-222 changes were significantly correlated with ASM/Height2 in man, while other miRNAs changes did not show a strong correlation with these diagnostic indexes. The results of this study suggest that with the decrease of ASM/hight2, handgrip strength and 4-meter velocity in patients with sarcopenia, the level of miRNA in plasma is gradually reduced. The detection of the level of miRNAs in plasma is helpful for the diagnosis of sarcopenia, indicating that circulating miRNAs can be used as a potential biomarkers of sarcopenia.

As an initial study, several limitations of this study were still existent. On the one hand, the sample size is limited, and the sample source is regional in this study, It is still necessary to increase the sample size, expand the sample coverage area and include more analysis indicators to confirm the application of plasma miRNAs in the diagnosis of sarcopenia. On the other hand, the underlying molecular mechanism between circulating miRNA and sarcopenia is unclear. As more and more miRNAs have been found, their roles in biology have been paid more and more attention. The regulatory network of miRNAs mainly involves post-transcriptional regulation (Kong et al., 2008). However, miRNAs, mRNA and their specific molecular mechanism of disease are still unclear. The regulatory role of miRNAs is very complicated. One miRNA can have hundreds of target genes, and one mRNA may be regulated by multiple miRNAs (Dalmay, 2013). The regulatory mechanism of miRNAs on sarcopenia may be through the regulation of multiple target gene expressions, multiple signal pathways, and they cross each other and interact. In our next study, the molecular mechanisms underlying circulating miRNAs which were related with sarcopenia should be further elucidated.

CONCLUSION

In conclusion, plasma miR-208b, miR-499, miR-155, miR-222, miR-328, and miR-210 decrease in response to sarcopenia in the elderly. Future studies aim at providing an opportunity to develop circulating miRNAs as potential and useful biomarkers of sarcopenia and to elucidate the molecular mechanisms underlying muscle dysfunction with age.

DATA AVAILABILITY STATEMENT

The datasets generated for this study are available on request to the corresponding author.

ETHICS STATEMENT

Ethical approval for this study was obtained from the Ethics Community of Ningbo No. 2 Hospital. All subjects gave written informed consent in accordance with the Declaration of Helsinki.

AUTHOR CONTRIBUTIONS

HY and NH conceived and designed this study. NH performed the experiments. NH, YLZ, and YZ collected and analyzed the data. NH, BF, ZZ, DW, SZ, and QG contributed reagents, materials, and analysis tools used in this study. NH wrote the manuscript. HY revised the manuscript.

FUNDING

This study was funded by the Ningbo Health Branding Subject Fund (PPXK2018-01), Ningbo Medical Science and Technology Project (2016Z01), Zhejiang Provincial Public Service and Application Research Foundation, China (LGF20H250001), and Ningbo HwaMei Research Fund (2019HMZD09).

REFERENCES

Alexander, M. S., Casar, J. C., Motohashi, N., Vieira, N. M., Eisenberg, I., Marshall, J. L., et al. (2014). MicroRNA-486-dependent modulation of DOCK3/PTEN/AKT signaling pathways improves muscular dystrophy-associated symptoms. *J. Clin. Invest.* 124, 2651–2667. doi: 10.1172/jci73579

Biolo, G., Cederholm, T., and Muscaritoli, M. (2014). Muscle contractile and metabolic dysfunction is a common feature of sarcopenia of aging and chronic diseases: from sarcopenic obesity to cachexia. *Clin. Nutr.* 33, 737–748. doi: 10.1016/j.clnu.2014.03.007

Bjorkman, M., Jyvakorpi, S. K., Strandberg, T. E., Pitkala, K. H., and Tilvis, R. S. (2019). Sarcopenia indicators as predictors of functional decline and need for care among older people. *J. Nutr. Health Aging.* 23, 916–922. doi: 10.1007/s12603-019-1280-0

Brown, D. M., and Goljanek-Whysall, K. (2015). microRNAs: modulators of the underlying pathophysiology of sarcopenia? *Ageing Res. Rev.* 24(Pt B), 263–273. doi: 10.1016/j.arr.2015.08.007

Chen, J. F., Mandel, E. M., Thomson, J. M., Wu, Q., Callis, T. E., Hammond, S. M., et al. (2006). The role of microRNA-1 and microRNA-133 in skeletal muscle proliferation and differentiation. *Nat. Genet.* 38, 228–233. doi: 10.1038/ng1725

Chen, L. K., Liu, L. K., Woo, J., Assantachai, P., Auyeung, T. W., Bahyah, K. S., et al. (2014). Sarcopenia in Asia: consensus report of the Asian Working Group for Sarcopenia. *J. Am. Med. Dir. Assoc.* 15, 95–101. doi: 10.1016/j.jamda.2013.11.025

Chin, S. O., Rhee, S. Y., Chon, S., Hwang, Y. C., Jeong, I. K., Oh, S., et al. (2013). Sarcopenia is independently associated with cardiovascular disease in older Korean adults: the Korea National health and nutrition examination survey (KNHANES) from 2009. *PLoS One* 8:e60119. doi: 10.1371/journal.pone.0060119

Cipryan, L. (2018). The effect of fitness level on cardiac autonomic regulation, IL-6, total antioxidant capacity, and muscle damage responses to a single bout of high-intensity interval training. *J. Sport Health Sci.* 7, 363–371. doi: 10.1016/j.jshs.2016.11.001

Cruz-Jentoft, A. J., Bahat, G., Bauer, J., Boirie, Y., Bruyere, O., Cederholm, T., et al. (2019). Sarcopenia: revised European consensus on definition and diagnosis. *Age Ageing* 48, 16–31. doi: 10.1093/ageing/afy169

Cruz-Jentoft, A. J., Landi, F., Schneider, S. M., Zuniga, C., Arai, H., Boirie, Y., et al. (2014). Prevalence of and interventions for sarcopenia in ageing adults: a systematic review. Report of the International Sarcopenia Initiative (EWGSOP and IWGS). *Age Ageing* 43, 748–759. doi: 10.1093/ageing/afu115

Dalmay, T. (2013). Mechanism of miRNA-mediated repression of mRNA translation. *Essays Biochem.* 54, 29–38. doi: 10.1042/bse0540029

Dasarathy, S. (2012). Consilience in sarcopenia of cirrhosis. *J. Cachexia Sarcopenia Muscle* 3, 225–237. doi: 10.1007/s13539-012-0069-3

Dews, M., Homayouni, A., Yu, D., Murphy, D., Sevignani, C., Wentzel, E., et al. (2006). Augmentation of tumor angiogenesis by a Myc-activated microRNA cluster. *Nat. Genet.* 38, 1060–1065. doi: 10.1038/ng1855

Fasanaro, P., D'Alessandra, Y., Di Stefano, V., Melchionna, R., Romani, S., Pompilio, G., et al. (2008). MicroRNA-210 modulates endothelial cell response to hypoxia and inhibits the receptor tyrosine kinase ligand Ephrin-A3. *J. Biol. Chem.* 283, 15878–15883. doi: 10.1074/jbc.M800731200

Gautam, A., Kumar, R., Dimitrov, G., Hoke, A., Hammamieh, R., and Jett, M. (2016). Identification of extracellular miRNA in archived serum samples by next-generation sequencing from RNA extracted using multiple methods. *Mol. Biol. Rep.* 43, 1165–1178. doi: 10.1007/s11033-016-4043-6

Jung, H. J., Lee, K. P., Kwon, K. S., and Suh, Y. (2019). MicroRNAs in skeletal muscle aging: current issues and perspectives. *J. Gerontol. A Biol. Sci. Med. Sci.* 74, 1008–1014. doi: 10.1093/gerona/gly207

Jung, H. J., and Suh, Y. (2014). Circulating miRNAs in ageing and ageing-related diseases. *J. Genet. Genomics* 41, 465–472. doi: 10.1016/j.jgg.2014.07.003

Kim, J. Y., Park, Y.-K., Lee, K.-P., Lee, S.-M., Kang, T.-W., Kim, H.-J., et al. (2014). Genome-wide profiling of the microRNA-mRNA regulatory network in skeletal muscle with aging. *Aging* 6, 524–544. doi: 10.18632/aging.100677

Kong, Y. W., Cannell, I. G., de Moor, C. H., Hill, K., Garside, P. G., Hamilton, T. L., et al. (2008). The mechanism of micro-RNA-mediated translation repression is determined by the promoter of the target gene. *Proc. Natl. Acad. Sci. U.S.A.* 105, 8866–8871. doi: 10.1073/pnas.0800650105

Kroh, E. M., Parkin, R. K., Mitchell, P. S., and Tewari, M. (2010). Analysis of circulating microRNA biomarkers in plasma and serum using quantitative reverse transcription-PCR (qRT-PCR). *Methods* 50, 298–301. doi: 10.1016/j.ymeth.2010.01.032

Kuehbacher, A., Urbich, C., Zeiher, A. M., and Dimmeler, S. (2007). Role of Dicer and Drosha for endothelial microRNA expression and angiogenesis. *Circ. Res.* 101, 59–68. doi: 10.1161/circresaha.107.153916

Landi, F., Calvani, R., Cesari, M., Tosato, M., Martone, A. M., Ortolani, E., et al. (2018). Sarcopenia: an overview on current definitions, diagnosis and treatment. *Curr. Protein Pept. Sci.* 19, 633–638. doi: 10.2174/1389203718666170607113459

Leenders, M., Verdijk, L. B., van der Hoeven, L., Adam, J. J., van Kranenburg, J., Nilwik, R., et al. (2013). Patients with type 2 diabetes show a greater decline in muscle mass, muscle strength, and functional capacity with aging. *J. Am. Med. Dir. Assoc.* 14, 585–592. doi: 10.1016/j.jamda.2013.02.006

Loncar, G., Fulster, S., von Haehling, S., and Popovic, V. (2013). Metabolism and the heart: an overview of muscle, fat, and bone metabolism in heart failure. *Int. J. Cardiol.* 162, 77–85. doi: 10.1016/j.ijcard.2011.09.079

Margolis, L. M., and Rivas, D. A. (2018). Potential role of MicroRNA in the anabolic capacity of skeletal muscle with aging. *Exerc. Sport Sci. Rev.* 46, 86–91. doi: 10.1249/jes.0000000000000147

McGregor, R. A., Poppitt, S. D., and Cameron-Smith, D. (2014). Role of microRNAs in the age-related changes in skeletal muscle and diet or exercise interventions to promote healthy aging in humans. *Ageing Res. Rev.* 17, 25–33. doi: 10.1016/j.arr.2014.05.001

Poliseno, L., Tuccoli, A., Mariani, L., Evangelista, M., Citti, L., Woods, K., et al. (2006). MicroRNAs modulate the angiogenic properties of HUVECs. *Blood* 108, 3068–3071. doi: 10.1182/blood-2006-01-012369

Sanchez-Rodriguez, D., Marco, E., and Cruz-Jentoft, A. J. (2019). Defining sarcopenia: some caveats and challenges. *Curr. Opin. Clin. Nutr. Metab. Care* 23, 127–132. doi: 10.1097/mco.0000000000000621

Sinclair, M., Gow, P. J., Grossmann, M., and Angus, P. W. (2016). Review article: sarcopenia in cirrhosis-aetiology, implications and potential therapeutic interventions. *Aliment Pharmacol. Ther.* 43, 765–777. doi: 10.1111/apt.13549

Siracusa, J., Koulmann, N., and Banzet, S. (2018). Circulating myomiRs: a new class of biomarkers to monitor skeletal muscle in physiology and medicine. *J. Cachexia Sarcopenia Muscle* 9, 20–27. doi: 10.1002/jcsm.12227

Soci, U. P. R., Fernandes, T., Barauna, V. G., Hashimoto, N. Y., de Fatima Alves Mota, G., Rosa, K. T., et al. (2016). Epigenetic control of exercise training-induced cardiac hypertrophy by miR-208. *Clin. Sci.* 130, 2005–2015. doi: 10.1042/cs20160480

Soeki, T., Matsuura, T., Bando, S., Tobiume, T., Uematsu, E., Ise, T., et al. (2016). Relationship between local production of microRNA-328 and atrial substrate remodeling in atrial fibrillation. *J. Cardiol.* 68, 472–477. doi: 10.1016/j.jjcc.2015.12.007

Taganov, K. D., Boldin, M. P., Chang, K.-J., and Baltimore, D. (2006). NF-κB-dependent induction of microRNA miR-146, an inhibitor targeted to signaling proteins of innate immune responses. *Proc. Natl. Acad. Sci. U.S.A.* 103, 12481–12486. doi: 10.1073/pnas.0605298103

Troiano, G., Boldrup, L., Ardito, F., Gu, X., Lo Muzio, L., and Nylander, K. (2016). Circulating miRNAs from blood, plasma or serum as promising clinical biomarkers in oral squamous cell carcinoma: a systematic review of current findings. *Oral Oncol.* 63, 30–37. doi: 10.1016/j.oraloncology.2016.11.001

Urbich, C., Kuehbacher, A., and Dimmeler, S. (2008). Role of microRNAs in vascular diseases, inflammation, and angiogenesis. *Cardiovasc. Res.* 79, 581–588. doi: 10.1093/cvr/cvn156

Wang, C., Zhang, C., Liu, L., A, X., Chen, B., Li, Y., et al. (2017). Macrophage-derived mir-155-containing exosomes suppress fibroblast proliferation and promote fibroblast inflammation during cardiac injury. *Mol. Ther.* 25, 192–204. doi: 10.1016/j.ymthe.2016.09.001

Wang, L., Lv, Y., Li, G., and Xiao, J. (2018). MicroRNAs in heart and circulation during physical exercise. *J. Sport Health Sci.* 7, 433–441. doi: 10.1016/j.jshs.2018.09.008

Yang, M., Liu, Y., Zuo, Y., and Tang, H. (2019). Sarcopenia for predicting falls and hospitalization in community-dwelling older adults: EWGSOP versus EWGSOP2. *Sci. Rep.* 9:17636. doi: 10.1038/s41598-019-53522-6

Yilmaz, O., and Bahat, G. (2019). Muscle mass adjustment method affects association of sarcopenia and sarcopenic obesity with metabolic syndrome. *Geriatr. Gerontol. Int.* 19:272. doi: 10.1111/ggi.13609

Zhang, L., Guo, Q., Feng, B.-L., Wang, C.-Y., Han, P.-P., Hu, J., et al. (2019). A cross-sectional study of the association between arterial stiffness and Sarcopenia in chinese community-dwelling elderly using the asian working group for Sarcopenia criteria. *J. Nutr. Health Aging* 23, 195–201. doi: 10.1007/s12603-018-1147-9

Conflict of Interest: The authors declare that the research was conducted in the absence of any commercial or financial relationships that could be construed as a potential conflict of interest.

frontiers in Cell and Developmental Biology

REVIEW
published: 10 March 2020
doi: 10.3389/fcell.2020.00143

MicroRNA Involvement in Signaling Pathways During Viral Infection

Madalina Gabriela Barbu[1†], Carmen Elena Condrat[1†], Dana Claudia Thompson[1], Oana Larisa Bugnar[1], Dragos Cretoiu[1,2], Oana Daniela Toader[3,4], Nicolae Suciu[1,3,4] and Silviu Cristian Voinea[5]*

[1] Alessandrescu-Rusescu National Institute for Mother and Child Health, Fetal Medicine Excellence Research Center, Bucharest, Romania, [2] Department of Cell and Molecular Biology and Histology, Carol Davila University of Medicine and Pharmacy, Bucharest, Romania, [3] Division of Obstetrics, Gynecology and Neonatology, Carol Davila University of Medicine and Pharmacy, Bucharest, Romania, [4] Department of Obstetrics and Gynecology, Alessandrescu-Rusescu National Institute for Mother and Child Health, Polizu Clinical Hospital, Bucharest, Romania, [5] Department of Surgical Oncology, Institute of Oncology Prof. Dr. Alexandru Trestioreanu, Carol Davila University of Medicine and Pharmacy, Bucharest, Romania

OPEN ACCESS

Edited by:
Dale Frank,
Technion - Israel Institute of Technology, Israel

Reviewed by:
Ole-Morten Seternes,
Arctic University of Norway, Norway
Francisco Iñesta-Vaquera,
University of Dundee, United Kingdom

***Correspondence:**
Dana Claudia Thompson
dana.lunganu@gmail.com

† These authors have contributed equally to this work

Specialty section:
This article was submitted to Signaling, a section of the journal Frontiers in Cell and Developmental Biology

Received: *10 December 2019*
Accepted: *20 February 2020*
Published: *10 March 2020*

Citation:
Barbu MG, Condrat CE, Thompson DC, Bugnar OL, Cretoiu D, Toader OD, Suciu N and Voinea SC (2020) MicroRNA Involvement in Signaling Pathways During Viral Infection. Front. Cell Dev. Biol. 8:143. doi: 10.3389/fcell.2020.00143

The study of miRNAs started in 1993, when Lee et al. observed their involvement in the downregulation of a crucial protein known as LIN-14 in the nematode *Caenorhabditis elegans.* Since then, great progress has been made regarding research on microRNAs, which are now known to be involved in the regulation of various physiological and pathological processes in both animals and humans. One such example is represented by their interaction with various signaling pathways during viral infections. It has been observed that these pathogens can induce the up-/downregulation of various host miRNAs in order to elude the host's immune system. In contrast, some miRNAs studied could have an antiviral effect, enabling the defense mechanisms to fight the infection or, at the very least, they could induce the pathogen to enter a latent state. At the same time, some viruses encode their own miRNAs, which could further modulate the host's signaling pathways, thus favoring the survival and replication of the virus. The goal of this extensive literature review was to present how miRNAs are involved in the regulation of various signaling pathways in some of the most important and well-studied human viral infections. Further on, knowing which miRNAs are involved in various viral infections and what role they play could aid in the development of antiviral therapeutic agents for certain diseases that do not have a definitive cure in the present. The clinical applications of miRNAs are extremely important, as miRNAs targeted inhibition may have substantial therapeutic impact. Inhibition of miRNAs can be achieved through many different methods, but chemically modified antisense oligonucleotides have shown the most prominent effects. Though scientists are far from completely understanding all the molecular mechanisms behind the complex cross-talks between miRNA pathways and viral infections, the general knowledge is increasing on the different roles played by miRNAs during viral infections.

Keywords: microRNA, signaling, viral, HPV, HIV, hepatitis, herpes

INTRODUCTION

MicroRNAs are small molecules of non-coding RNAs, which contain from 17 to 25 nucleotides (Wang et al., 2016) and exert their functions by modulating gene expression (Macfarlane and Murphy, 2010; Wahid et al., 2010). They were first described in 1993 by Lee et al., who observed that microRNAs downregulated a crucial protein known as LIN-14, involved in the progression of the nematode *Caenorhabditis elegans* from L1 to L2 larval stage (Lee et al., 1993; Bhaskaran and Mohan, 2014). Since then, great progress has been made regarding research on microRNAs, which are now known to be involved in the regulation of various physiological and pathological processes in both animals and humans.

The biogenesis of microRNAs is a dynamic process, involving a multitude of mechanisms that will finally result in the formation of mature miRNAs (Ketting, 2010). Any disrupting event that appears on this pathway could lead to an increased or decreased production of miRNAs in the targeted tissue, leading to various diseases such as neoplasia, ischemic heart disease, hematological diseases, muscular dystrophies, neurodegenerative diseases, psychiatric disorders, brain tumors, kidney disease, etc., according to the physiological functions regulated by the impaired miRNA (Sayed and Abdellatif, 2011; Garofalo et al., 2014; Trionfini et al., 2015; Barwari et al., 2016; Luoni and Riva, 2016).

The process of miRNA formation begins in the nucleus, with the transcription of the miRNA genes, by RNA polymerase II (Pol II), resulting in a "hairpin" structured primary transcript encoding miRNA sequences (Ha and Kim, 2014). This step is positively or negatively regulated by RNA Pol II-associated transcription factors like p53, ZEB1 and ZEB2, MYC and also by epigenetic modulators such as the methylation of DNA and histone modification (Lee et al., 2004; Davis-Dusenbery and Hata, 2010; Krol et al., 2010; Ha and Kim, 2014). Further on, the primary miRNA (pri-miRNA) goes through a series of maturation processes, the first one taking place in the nucleus. At this point, RNase III Drosha along with the co-factor DGCR8 forms the Microprocessor complex, which crops the loop end of pri-miRNA, forming precursor miRNA which also has a "hairpin"-like structure (pre-miRNA) (Denli et al., 2004; Gregory et al., 2004; Han et al., 2004).

The resulting product is exported by Exportin-5 into the cytoplasm to undergo the following steps for maturation (Ha and Kim, 2014). There, the pre-miRNA is once again cropped near the loop end by another RNase named Dicer, resulting in a small RNA duplex (Ketting et al., 2001; Knight and Bass, 2001; Hutvagner et al., 2001). Further on, the generated product forms, with an argonaute (AGO) protein, the RNA-induced silencing complex (RISC) (Hammond et al., 2001).

The most important roles that miRNAs have are gene regulation and intercellular signaling (O'Brien et al., 2018). For the first one, the miRISC can work through two mechanisms known as canonical, or most frequently used, the non-canonical mechanism (Bartel, 2009; Helwak et al., 2013; Chevillet et al., 2014; Eichhorn et al., 2014; Kai et al., 2018). The canonical mode of action involves the binding of miRISC to the 3′-untranslated region (3′-UTR) of the targeted mRNA, leading to a cessation of translation when the two strains are almost completely complementary, or to a decrease in translation when the complementarity is limited (Reinhart et al., 2000; Dalmay, 2008; Sand, 2014). The non-canonical pathway does not require such high complementarity (Helwak et al., 2013). Early studies determined that within the seed region, only 6-nt matches were required in order to obtain a functional miRNA - targeted mRNA interaction (Bartel, 2009). As a result, the canonical sites were defined as it follows: 3 possible canonical sites for 6-mers matches to positions 1-6, 2-7, and 3-8, 2 possible canonical sites for 7-mers matches to positions 2-8 and 1-7, and one possible canonical site for 8-mer match, to position 1-8 (Lee et al., 1993; Wightman et al., 1993; Poy et al., 2004).

In contrast, it has been found that miRISC complexes, targeting sites different from the seed region, with a diminished complementarity, do exert some modest regulatory functions (Helwak et al., 2013). Examples of non-canonical sites are "nucleation bulges," formed from 5 consecutive nucleotides, located on positions 2-6, which following the "pivot pairing rule" proposed by Chi et al. in 2012, pair themselves in position 6 of the miRNA, known as "pivot" (Chi et al., 2012; Seok et al., 2016). It is apparent that many miRNAs studied have a pivot nucleotide able to bind a nucleation bulge. For example, miR-124 has a C nucleotide in position 6 that would bind a complementary G-bulge, let-7 has a U pivot nucleotide and miR-708 contains a G pivot nucleotide (Chi et al., 2012). "Seed-like motifs" are also non-canonical binding sites found on targeted mRNA (Seok et al., 2016). These sites seem to have certain mismatches or deletions that demand additional 3′ interactions in order to make the association functional (Seok et al., 2016). However, the non-canonical pathways have not been thoroughly researched and their exact functions are still to be determined.

MiRNAs have also been shown to have a role in viral infections. As we already know, viruses are intracellular organisms that solely rely on the host environment to multiply (Girardi et al., 2018). It has been observed that these pathogens can induce the up-/downregulation of various host miRNAs in order to elude the host's immune system (Scheel et al., 2016; Girardi et al., 2018; Shimakami et al., 2012; Trobaugh et al., 2014). In contrast, some miRNAs studied could have an antiviral effect, enabling the defense mechanisms to fight the infection or, at the very least, they could induce the pathogen to enter a latent state (Guo et al., 2013; O'Connor et al., 2014; Pan et al., 2014; Girardi et al., 2018). Knowing which miRNAs are involved in various viral infections and what role they play could aid in the development of antiviral therapeutic agents for certain diseases that do not have a definitive cure in the present.

CLASSIFICATION OF MicroRNAs INVOLVED IN VIRAL INFECTIONS

Although we only presented host miRNAs so far, we have to acknowledge that some viruses can also synthesize their own miRNAs (Pfeffer et al., 2004). As a result, in the beginning of

our classification we could divide them into host miRNAs and viral miRNAs, according to their source (**Table 1**). Similar to host miRNAs, the viral ones participate in the life cycle of the virus and could induce certain modifications in the host cells (Guo et al., 2015; Bruscella et al., 2017). Likewise, they are also processed by the previously mentioned RNases Drosha and Dicer, although some viral miRNAs have been described to skip the first step and pass directly to Dicer processing (Bogerd et al., 2010; Diebel et al., 2010; Tycowski et al., 2015).

Regarding the role they play, host miRNAs could be classified as proviral or antiviral according to their actions once a certain virus has entered the host cell. Through the interaction between viral and host miRNAs, the latter could enable the viral replication and infection, thus exerting a proviral function (Masaki et al., 2015; Scheel et al., 2016; Bruscella et al., 2017). Furthermore, proviral miRNAs can promote viral infection by suppressing antiviral factors, such as interferon (IFN), allowing the virus to escape the immune response of the host (Sharma et al., 2015; Bruscella et al., 2017). In contrast, various host miRNAs can act have antiviral functions by influencing the production of viral RNA, blocking the viral replication, suppressing proviral proteins or by inducing the virus to enter a latent phase (Zheng et al., 2013; Wu et al., 2014; Slonchak et al., 2015; Ho et al., 2016).

A more general classification, valid for all miRNAs, not only for those involved in viral infection, would be based on the state in which they can be found in body fluids. Their presence has been detected in all biological fluids, among them being blood, tears, urine, amniotic fluid, breast milk, semen and saliva (Turchinovich et al., 2012). Thus, approximately 90% of the extracellular or circulating miRNAs can be found associated with AGO proteins and the other 10% is transported in microvesicles like exosomes and apoptotic bodies (Turchinovich et al., 2013). Both proteins and microvesicles protect the miRNAs they carry from the degradation of RNases and confer them a high stability in an unfavorable extracellular environment (Turchinovich et al., 2013). A comprehensive list of the functions and pathways targeted by each miRNA described in this manuscript can be found in **Table 2**.

IDENTIFYING TECHNIQUES FOR MicroRNAs

Developing an efficient, inexpensive method for the detection of miRNAs involved in a way or another in viral infections would be beneficial not only for the diagnostic process of the more serious infectious diseases, but also for discovering new miRNAs previously unknown to be involved in this pathology. However, there are many challenges to finding such a detection method, partially because miRNAs represent a fairly new field of research and as a result many of their characteristics, such as detection levels, concentration in the biological samples, up-/downregulation in healthy and pathological samples yet remain unknown (Gillespie et al., 2018).

TABLE 1 | Classification of microRNAs based on their source and roles.

Classification criteria	
Source	Host microRNAs
	Viral microRNAs
Roles	*Host microRNAs:*
	Proviral microRNAs
	Antiviral microRNAs

By far, the preferred method for the identification of miRNAs is quantitative reverse transcriptase Polymerase Chain Reaction - PCR (RT-qPCR) (Chen et al., 2018; Gillespie et al., 2018; Yuan et al., 2018). The most frequently used PCR quantitation technique is stem-loop reverse transcription (RT)-based TaqMan MicroRNA assay, which provides high sensitivity and specificity (Chen C. et al., 2011). Schematically, this technique requires two steps, the first one being stem-loop reverse transcription, in which the primers bind the 3′ end of miRNA molecules that will further on be reverse transcribed, and a second step for the quantification of microRNAs using real-time PCR (Chen et al., 2005). Other PCR methods available are poly (A) tailing-based and direct RT-based SYBR miRNA assays (Chen Y. et al., 2011). However, the RT-qPCR method is not lacking in disadvantages either, since it presents a high risk of contamination during the amplification steps, as well as of sensing errors for the samples (Gillespie et al., 2018).

Another popular quantitative method for the detection of miRNAs is Northern blot hybridization, which requires the total RNA to be separated on polyacrylamide gel with denaturation proprieties, after which it is transferred to a nylon membrane, UV-cross-linked and finally hybridized with the help of a probe labeled with a radioactive substance (Kruszka et al., 2014; Barciszewska-Pacak et al., 2015; Pacak et al., 2016; Smoczynska et al., 2019). Still, it is a laborious, time-consuming technique which requires high amounts of RNA and can sometimes miss the identification of rare miRNAs (Smoczynska et al., 2019). Recently, new protocols have been developed in order to enhance the technique, leading to the use of lower levels of RNA and to a shortening of the time needed to execute the procedure (Varallyay et al., 2007; Pall and Hamilton, 2008; Wang X. et al., 2010).

In situ hybridization (ISH) and next-generation sequencing (NGS) could also be used for the identification of miRNAs. ISH allows the visualization of RNA in fixed tissue samples and the comparison of miRNA expression levels in different cell types using fluorescent, dioxygenin or radioactive probes to bind the targeted RNA (Javelle and Timmermans, 2012). However, this is also a time-consuming, laborious technique, prone to error at each step of the process (Javelle and Timmermans, 2012). NGS is actually a second-generation method of sequencing, following the well-known Sanger technique (Hu et al., 2017). There are various NGS platforms available that also provide kits for miRNAs quantification. The general principle on which they all function is based on the amplification and sequencing of DNA fragments, with additional steps for miRNA sequencing, starting with miRNA extraction after which the miRNAs are reverse transcribed into cDNA (Bar et al., 2008; Creighton et al., 2009; Hu et al., 2017). NGS is able to identify single miRNA with the high resolution of one nucleotide, yet the

TABLE 2 | Classification, functions and targeted signaling pathways by miRNA.

miRNA	Source	Characteristics	Pathway(s) targeted	References
miR-34 family	Host	– Repressor of Wnt pathway – Antiviral functions – especially on flaviviruses	Wnt signaling pathway	Kim et al., 2011; Cha et al., 2012; Smith et al., 2017
miR-155	Host	– Stimulator of Type I Interferon signaling pathway – Increases the innate and adaptive immune response – Antiviral functions – Inhibitor of the HBV replication – Higher levels in HIV infected cells – Inhibition of NF-κB signaling pathway – promotion of viral latency – Higher levels in HCV infection → increase the activity of	Type I Interferon signaling pathway NF-κB signaling pathway Wnt/β-catenin signaling	Jiang et al., 2010; Wang P. et al., 2010; Yao et al., 2012; Zhang et al., 2012; Li et al., 2013; Ruelas et al., 2015
miR-19a	Host	– Stimulator of Type I Interferon signaling pathway – Increases the innate and adaptive immune response – Antiviral functions	Type I Interferon signaling pathway	Pichiorri et al., 2008; Jiang et al., 2010; Wang P. et al., 2010; Su et al., 2011; Yao et al., 2012; Li et al., 2013
miR-122	Host	– Stimulator of Type I Interferon signaling pathway – Increases the innate and adaptive immune response – Antiviral functions – Liver-specific – Antiviral functions in HBV infection – Inhibition of HBV replication – Diminished levels — promotion of viral persistence and oncogenesis – Antitumorigenic effects by regulation of Wnt/β-catenin pathway – Impairment of RhoA/Rock pathway	Type I Interferon signaling pathway Wnt/β-catenin pathway RhoA/Rock pathway	Pichiorri et al., 2008; Kalluri and Weinberg, 2009; Jiang et al., 2010; Wang P. et al., 2010; Chen Y. et al., 2011; Su et al., 2011; Jopling, 2012; Wang et al., 2012; Xu et al., 2012; Yao et al., 2012; Li et al., 2013
let-7 family	Host	– Decreased expression in Kaposi sarcoma associated to herpesvirus and HIV infections – Their low levels increase the expression of the NF-κB signaling pathway → increased inflammation – Increasing the level of let-7a → decreased STAT3 supplies	NF-κB signaling pathway STAT3 signaling pathway	Androulidaki et al., 2009; Shishodia et al., 2014
miR-233	Host	– Decreased expression in Kaposi sarcoma associated to herpesvirus and HIV infections – Their low levels increase the expression of the NF-κB signaling pathway → increased inflammation	NF-κB signaling pathway	Androulidaki et al., 2009
miR-146	Host	– Increased in HIV and HCV infections – Decreased activity of the NF-κB signaling pathway – Proviral functions	NF-κB signaling pathway	Bhaumik et al., 2008; Houzet et al., 2008
miR-21	Host	– Increased in HIV and HCV infections – Decreased activity of the NF-κB signaling pathway – Proviral functions in HIV and HCV infection – Antiviral functions in Coxsackievirus B3 infection – Decreasing its level in HPV infections → downregulation of STAT3	NF-κB signaling pathway MAP2K3/p38 MAPK pathway STAT3 signaling pathway	Bhaumik et al., 2008; Houzet et al., 2008; Shishodia et al., 2014; He et al., 2019
miR-218-5p	Host	– Down-regulation of NF-κB signaling pathway in HPV induced cervical cancer	NF-κB signaling pathway	Xu et al., 2018
hsa-miR-483-3p	Host	– Up-regulated by HCV – Increase the activity of PI3K/Akt signaling pathway, prolonging cell survival – Proviral functions	PI3K/Akt signaling pathway	Shwetha et al., 2013
hsa-miR-320c	Host	– Up-regulated by HCV – Increase the activity of PI3K/Akt signaling pathway, prolonging cell survival – Proviral functions	PI3K/Akt signaling pathway	Shwetha et al., 2013
miR-199a-5p	Host	– Proviral functions – Its downregulation blocks the PI3K/Akt signaling pathway in HCV infection – Low levels lead to a decrease of viral replication in HCV infection	PI3K/Akt signaling pathway	Wang et al., 2015

(Continued)

TABLE 2 | Continued

miRNA	Source	Characteristics	Pathway(s) targeted	References
miR-125b	Host	– Suppressor of PI3K/Akt signaling pathway – Downregulated in HPV infection → limited cancer cell growth and increased apoptosis – Higher levels → apoptosis inhibition	PI3K/Akt signaling pathway	Cui et al., 2012; Wang et al., 2013; Banzhaf-Strathmann and Edbauer, 2014; Ribeiro and Sousa, 2014
miR-H4b	Viral– produced by HSV	– inhibition of PI3K/Akt signaling pathway and mTOR signaling pathways → better adaptation for viral replication and latency	PI3K/Akt signaling pathway mTOR signaling pathways	Gottwein and Cullen, 2008; Zhao et al., 2015
miR-744	Host	– Antiviral functions against RSV and influenza viruses	MAPK signaling pathway	McCaskill et al., 2017
miR-24	Host	– Antiviral functions against RSV and influenza viruses	MAPK signaling pathway	McCaskill et al., 2017
miR-124	Host	– Antiviral functions against RSV and influenza viruses	MAPK signaling pathway	McCaskill et al., 2017
miR-499a	Host	– Proviral functions in HCV infection	Notch signaling pathway	Sarma et al., 2012
miR-BART7-3p	Viral — produced by EBV	–Regulatory functions for the PI3K/Akt/GSK-3β pathway – Aberant regulation of Wnt pathway → excessive cellular proliferation	PI3K/ Akt/GSK-3β pathway Wnt signaling pathway	Cai L.M. et al., 2015; Wang et al., 2017
miR-BART1	Viral — produced by EBV	– Activation of PI3K/Akt/GSK-3β pathway	PI3K/Akt/GSK-3β pathway	Cai L.M. et al., 2015
miR-BART16	Viral — produced by EBV	– Inhibition of IFN signaling pathway – Proviral function → increased replication	IFN signaling pathway	Hooykaas et al., 2017
miR-BART19-3p, miR-BART17-5p, miR-BART14, miR-BART18-5p	Viral — produced by EBV	– Inhibition of Wnt pathway inhibitory genes	Wnt signaling pathway	Wong et al., 2012
miR-718	Host	– Upregulated in patients with both HIV and Kaposi sarcoma – Inhibition of PTEN/AKT/mTOR pathway → inhibition of the tumor suppressor action of PTEN	PTEN/AKT/mTOR pathway	Xue et al., 2014
miR-942 miR-711	Host	– Upregulated in patients with both HIV and Kaposi sarcoma – Activation of NF-κB signaling pathway inhibition of the KSHV lytic replication	NF-κB signaling pathway	Yan et al., 2018
miR-146a/b	Host	– Increased during viral infections – Downregulation of NF-κB signaling pathway – Proviral activity — increased inflammatory state, HIV persistence	NF-κB signaling pathway	Taganov et al., 2006; Huang et al., 2018
hiv1-miR-88 hiv1-miR-99	Viral — produced by HIV	– Activation of TLR8 signaling pathway – Chronic inflammation which favors the progression to AIDS	TLR8 signaling pathway	Silvestri and Feinberg, 2003; Bernard et al., 2014
miR-tar-3p miR-tar-5p	Viral: HIV-1-derived TAR miRNAs	– Regulation of host gene expression – Upregulation of pro-apoptotic proteins – Activation of Fas signaling pathway → complete apoptosis – In early stages of the infection → delay of the viral induced apoptosis	Fas signaling pathway	Bartz and Emerman, 1999; Ouellet et al., 2013
miR-132	Host	– Downregulated in HBV infection → enhanced carcinogenic feature of HBV – Normal levels → inhibition of HCC cell proliferation	Akt-signaling pathway	Wei et al., 2013; Liu et al., 2015; Chen et al., 2019
miR-372 miR-373	Host	– Upregulated in HBV infection – Levels correlated with the number of HBV DNA copies – Proviral functions → increased viral expression and replication during HBV infection	NFIB-dependent pathway	Guo et al., 2011; Langroudi et al., 2015; Wei et al., 2015; Ghasemi et al., 2018; Ullmann et al., 2018

high cost of this method, compared to the others, limits its accessibility (Smoczynska et al., 2019). However, this technique has numerous other crucial attributes that should be taken into consideration when choosing a quantification method, such as its high throughout, meaning that the samples one researcher sends would be sequenced in the same time with many other samples (Hu et al., 2017). In addition, NGS offers the possibility of discovering new miRNAs, an advantage that is not provided by a hybridization technique, as well as a high accuracy (Hu et al., 2017).

MicroRNA SIGNALING IN VIRAL INFECTION

Viruses represent microorganisms that are entirely dependent on a host cell in order to survive, proliferate and perform all the other functions necessary for their life cycle. To achieve this goal, they have evolved a number of mechanisms aimed to elude the immune system of the host.

The first step in every infection, regardless of the type of virus involved, is the entrance of the microorganism into a susceptible host cell, through the binding between the viral proteins found in the virion and the surface molecules of the host cell, which can also influence the tropism of the infection (Marsh and Helenius, 2006; Greber and Puntener, 2009). Upon attaching to the surface of the cell, the virus needs to pass through the membrane into the cytoplasm. This can be achieved through numerous mechanisms, such as the fusion between the host and virus membranes (Sodeik et al., 1997; Maurer et al., 2008), clathrin-dependent pathways or endocytosis (Marsh and Helenius, 2006; Greber and Puntener, 2009). The following steps are now influenced by the type of virus attempting to infect the organism. For example, in the case of DNA viruses, the genome found in the nucleocapsid has to pass through the cytoplasm and to reach the nucleus, where the transcription of the viral genes takes place. However, the maximum size of the free molecules allowed in the cytoplasm is restricted to approximately 500 kDa (Sodeik, 2000, 2002), therefore oversized viruses make use of the motor proteins and cytoskeleton to achieve this desiderate. The replication of the majority of RNA viruses, on the other hand, takes place solely in the cytoplasm (Greber and Way, 2006), with the exception of retroviruses, which, in the nucleus of the host cell, create a DNA provirus using reverse transcription that is ultimately incorporated into the genome of the host, thus leading to a resistant and prolonged infection (Cullen, 2001).

MicroRNAs play a very important role in the modulation systems of the host, therefore inevitably interacting with a variety of viruses (Umbach and Cullen, 2009). There are a number of potential interactions described in literature between the two entities. First of all, the host miRNA could regulate different phases of the viral life cycle, such as translation, by attaching itself to the viral RNA or mRNA. Also, the virus could exert an effect upon the host miRNA, thus leading to an altered expression of the latter's targets. Moreover, the microorganism could produce its own miRNAs, which would further regulate the viral or host RNA targets (Roberts et al., 2011).

However, indirect roles played by the miRNAs in viral infections have also been described. One such example is the involvement of miRNAs in the modulation of various signaling pathways (Bruscella et al., 2017).

Signaling Pathways Involved in Viral Infections and the Mechanisms Through Which miRNAs Influence Them

Wnt Signaling Pathway

Wnt represents in fact a group of pathways, through which the signal is carried from the extracellular environment into the cytosol and that is evolutionarily preserved in vertebrates. Its name has its origins in a combination between the name of the segment polarity gene of Drosophila ("Wingless") and the name of its analog found in vertebrates ("Integrated") (Wodarz and Nusse, 1998). When the Wnt signal reaches the intracellular medium, it triggers several cascades, which are divided as it follows: the canonical pathway or β-catenin dependent and the non-canonical one or β-catenin-independent. The last one can also be subdivided into the Wnt/Ca2 + cascade and the Planar Cell Polarity cascade (Habas and Dawid, 2005). Wnt signaling pathway plays a critical role in cellular growth, polarity, motility and development (Komiya and Habas, 2008).

One of the miRNA members that has been shown to have an effect on this pathway is the miR-34 family (Kim et al., 2011; Cha et al., 2012; Smith et al., 2017). Previous studies have demonstrated the effect of this miRNA on various flaviviruses subtypes (but not limited to them) and the highly potent inhibition role it plays (Smith et al., 2017). At the same time, it was pointed out that a possible relationship could exists between the Wnt pathway and the innate cellular immune mechanisms (Yang et al., 2010; Zhu et al., 2011; Hack et al., 2012; Baril et al., 2013; Hillesheim et al., 2014; Khan et al., 2015). Because of this discovery and also because of previous observations that miR-34 represses Wnt signaling, theories have emerged stating that type I Interferon (IFN) signaling in viral infections could be enhanced as a result (Smith et al., 2017; **Figure 1**).

Type I Interferon Signaling Pathway

Type I IFN is a very well-known molecule, which has strong antiviral effects. This is achieved by regulating numerous IFN stimulated genes (ISGs), which in turn encode proteins responsible for creating an antiviral state inside the cell (Sen, 2001). The ISG transcription is induced through the activation of Jak/STAT pathway (Darnell et al., 1994). All type I IFNs attach to the same receptor found on the surface of the cell (Interferon alpha/beta receptor - IFNAR), resulting in the activation of the tyrosine kinases Janus kinase 1 (Jak1) and Tyrosine kinase 2 (Tyk2) associated with the receptor. Following the phosphorylation of the kinases, Signal transducers and activators of transcription 1 and 2 (STAT1 and STAT2) are being activated, and then transported to the nucleus, where they attach to various DNA subunits, thus acting as ISGs promoters. The most important role of ISGs is antiviral, but they can also play a part in apoptosis, inflammation, lipid metabolism and protein degradation (de Veer et al., 2001).

Numerous miRNAs have been shown to interfere in this pathway, more precisely by targeting the receptor IFNAR1. For example, they can indirectly regulate the signal delivery by interacting with Suppressor of cytokine signaling 1 (SOCS1), which decreases the activity of JAK-STAT cascade through binding to the TYK2 part of the receptor complex (Piganis et al., 2011). Some of the miRNAs that have been demonstrated to act in this manner are miR-155, miR-19a and miR-122, leading to an increase in type I IFN signaling and consequentially to an enhancement of the innate and adaptive immune reactions (Pichiorri et al., 2008; Jiang et al., 2010; Wang P. et al., 2010; Yao et al., 2012; Li et al., 2013). Also, in the case of miR-155,

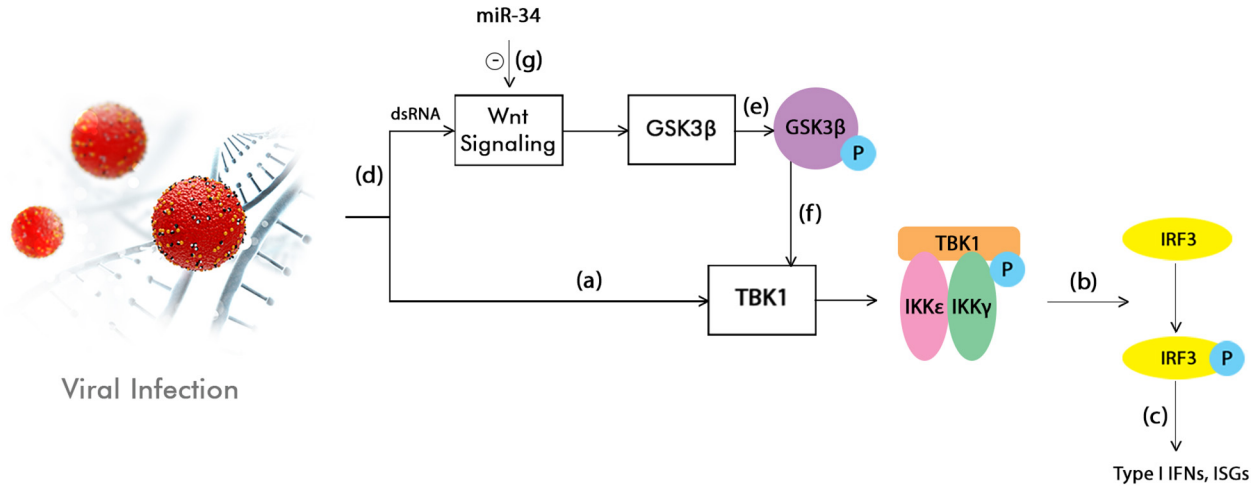

FIGURE 1 | Interferon (IFN) signaling enhancement by the inhibition of the Wnt pathway through miR-34. TANK-binding kinase 1 (TBK1) phosphorylation is firstly induced by the activation of the innate immunity in response to a viral infection **(a)**. This is followed by the phosphorylation or homodimerization of the interferon regulatory factor 3 (IRF3) **(b)**, which is subsequently translocated into the nucleus. Here, it stimulates the production of type I IFNs and interferon stimulated genes (ISGs) **(c)**. At the same time, the viral infection or dsRNA treatments also activate the Wnt signaling pathway **(d)**, which in turn leads to the inhibition of the Glycogen synthase kinase 3 beta (GS3Kβ) phosphorylation **(e)**. This event suppresses the IFN pathway by interacting with TBK1 **(f)**. This model shows that the Wnt signaling pathway has the ability to modulate the innate inflammatory response. By acting as an inhibitor of the Wnt pathway, miR-34 could enhance type I IFN signaling, therefore leading to a cellular antiviral status (**g**; Smith et al., 2017).

it has been shown that this type of interaction results in an increased activation of the anti-viral genes, therefore inhibiting the Hepatitis B virus (HBV) replication (Su et al., 2011).

NF-κB Signaling Pathway

Nuclear factor κB (NF-κB) signaling pathway is responsible for regulating a number of genes that are essential for the innate and adaptive immunity. Its activation depends on the recognition of pathogen associated molecular patterns (PAMPs) by the pattern recognition receptors (PRRs) encoded by the germ line (Janeway, 1989). NF-κB consists of reticuloendotheliosis protein dimers (Rel) which attach to a DNA sequence called the κB site. There are two types of Rels, divided according to the state that they can be found: mature or immature. The immature ones include NF-κB1 (p105) and NF-κB2 (p100), which turn into p50 and p52, and the mature ones are represented by RelA (p65), RelB and c-Rel. The most abundant form in the majority of dormant cells is the p50-RelA dimer (Ryseck et al., 1995).

The NF-κB signaling pathway can be activated in two different ways (Karin et al., 2002; Karin, 2006). The canonical pathway includes the dimers that contain RelA, p50 or c-Rel, all of which are held in the cytoplasm by κB proteins inhibitors, such as IκBα, IκBβ, IκBγ, IκBε, IκBζ, IκBNS, and Bcl-3. This first pathway is triggered by members of the proinflammatory cytokines, such as Tumor necrosis factor alpha (TNF-α) and, through the toll-like receptor (TLR), targets the β-subunit of the IκB kinase (IKKβ) complex. The non-canonical pathway is activated by TNF cytokines (Lymphotoxin beta - LTβ), whose target is the α-subunit of IKK (IKKα), using the TNF receptor (Ma et al., 2011).

According to previous studies, the expression of the miRNAs implicated in the modulation of NF-κB can be altered by viral infections and also, through targeting the NF-κB pathway, the viral miRNAs could be responsible for the variations of the immune response (Ma et al., 2011). One of the ways miRNAs use to regulate the NF-κB pathway is by controlling the expression of PRRs. For example, it has been shown that Kaposi sarcoma associated herpesvirus (KSHV) and Human immunodeficiency virus (HIV) infections lead to a decrease in the expression of miR-233 and Let-7 family, therefore upregulating the expression of TLR3 and TLR4 and, as a result, increasing the levels of tissue damage and inflammation (Androulidaki et al., 2009). Also, evidence suggest that the expression of miR-146 and miR-21 is increased in HIV and Hepatitis C virus (HCV) infections, leading to a decrease in the expression of Tumor necrosis factor receptor associated factor 6 (TRAF6) and Interleukin 1 Receptor Associated Kinase 1 (IRAK1), thus reducing the NF-κB activity (Bhaumik et al., 2008; Houzet et al., 2008).

PI3K/Akt Signaling Pathway

Phosphoinositide 3-kinase/Protein kinase B (PI3K/Akt) Signaling Pathway represents an important option for viruses to influence a variety of cellular functions. One of the most significant ways in which microorganisms can alter the normal life cycle of the cell is slowing down apoptosis, therefore increasing the time for the virus to replicate. As a result, viruses could also facilitate the induction of carcinogenesis. Recently, other roles played by this pathway in the interaction between the virus and the host have been proposed, such as regulation of the cell metabolism, morphology or immune response (Ji and Liu, 2008). Amongst the viruses that have been reported to activate the PI3K/Akt signaling pathway are hepatitis B virus (HBV), human cytomegalovirus (HCMV), human immunodeficiency virus (HIV), human papilloma virus type 16 (HPV16) and

hepatitis C virus (HCV) (Deregibus et al., 2002; Kim et al., 2006; Shen et al., 2006; Guo et al., 2007; Alisi et al., 2008; Chugh et al., 2008).

MicroRNAs are influenced by the virus-host interaction, in the sense of promoting the survival of the virus. For example, studies have demonstrated that HCV upregulates hsa-miR-483-3p and hsa-miR-320c, which in turn target the PI3K/Akt pathway and enhance the cell survival (Shwetha et al., 2013). Also, the downregulation of miR-199a-5p is responsible for blocking PI3K/Akt signaling in HCV infection, thus inhibiting the replication of the virus (Wang et al., 2015). Even though the exact mechanism is not yet fully understood, prior studies have shown an important reduction in the phosphorylated Akt (p-Akt) levels, leading to the conclusion that PI3K/Akt pro-survival pathway is significantly blocked by knocking down miR-199a-5p (Wang et al., 2015; **Figure 2**).

MAPK Signaling Pathway

MAPK or mitogen activated protein kinase signaling pathway is responsible for converting a variety of extracellular signals into intracellular actions, such as immune response, differentiation, proliferation and apoptosis (Pearson et al., 2001; Dong et al., 2002). In mammals, it can be divided into 3 main pathways: p38 MAPK, SAPK/HNK and MAPK/ERK. The MAPKK is responsible for regulating the activities of these 4 enzymes. For example, MKK3/6 and MKK4/7 are involved in the activation of p38 and JNK (responsible for the expression of cytokines and apoptosis) (Ludwig et al., 2001), while MEK5 activates the enzyme ERK5 (Ludwig et al., 2006). This signaling pathway has been shown to play an important role in viral infections, such as HCV (which increases the activity of p38 MAPK pathway), HIV (which upregulates the ERK activation) (Gaur et al., 2011) or cytomegalovirus (which, by increasing the activity of MAP2K3, maintains p38 active for viral replication) (Johnson et al., 2000).

MiRNAs have also been found to participate in this cascade during viral infections. For instance, miR-21 could act as a protective factor during Coxsackievirus B3 (CVB3) infection, by targeting the MAP2K3/p38 MAPK pathway. In this process, miR-21 has been shown to inhibit the expression of MAP2K3, leading to a reduced phosphorylation of the p38 MAPK, thus resulting in a significant decrease in the release of viral progeny (**Figure 3**; He et al., 2019). Also acting upon the same pathway are miR-744, miR-24 and miR-124, which are considered potential antiviral agents for RSV virus and influenza. In this case, the mechanism seems to be similar to the one described in the case of miR-21 and CVB3, with decreased levels of phosphorylated p38 showing a reduced activation of this component. Furthermore, a significant reduction in the expression of p38 MAPK has also been demonstrated through decreased levels of proteins (McCaskill et al., 2017).

Notch Signaling Pathway

The Notch pathway is responsible for the cellular differentiation, proliferation and apoptosis. Notch actually represents a receptor

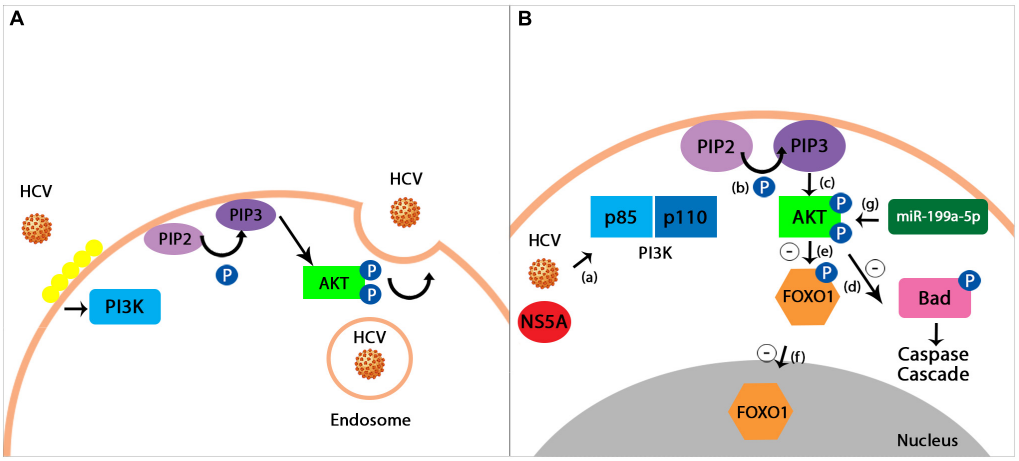

FIGURE 2 | (A) HCV entrance into the host cell using PI3K/Akt pathway. Hepatitis C virus uses a pH-dependent way in order to enter the intracellular environment of the host. The virus causes the lipids on the cellular surface to cluster (depicted in the figure through a yellow lining of the membrane), thus triggering the process of endocytosis mediated by the PI3K/Akt signaling pathway (Diehl and Schaal, 2013). **(B)** miR-199a-5p proposed effect on PI3K/Akt pathway during HCV infection. HCV infection activates the PI3K member of the signaling pathway with the help of a viral protein known as Non-structural protein 5A (NS5A) **(a)**. PI3K is a heterodimer formed by the two subunits, p85 and p110. The first one to be phosphorylated is the p85 subunit, followed by p110. This process represents the catalyst of the conversion between phosphatidylinositol 4,5 -bisphosphate (PIP2) and phosphatidylinositol 3,4,5 -trisphosphate (PIP3) **(b)**. PIP3 then activates Protein kinase B (Akt) through phosphorylation **(c)**. Signals produced by the virus in order to survive determine an inhibitory phosphorylation, mediated by the Akt, of the intracellular agents causing apoptosis, such as BCL2 associated agonist of cell death (BAD), which in turn leads to the suppression of the Caspase Cascade **(d)**. Furthermore, the phosphorylation of Forkhead box protein O1 (FOXO1), an important transcription factor **(e)**, stops it from translocating into the nucleus, therefore leading to an inhibition upon the pro-apoptotic genes expression **(f)**. Prior studies have demonstrated the fact that the overexpression of miR-199a-5p plays an important role in enhancing the pro-survival PI3K/Akt pathway. Their results have shown that by decreasing the miR-199a-5p levels, the phosphorylated Akt (p-Akt) levels are also significantly diminished, therefore leading to the proposed mechanism through which miR-199a-5p exerts its actions by promoting Akt phosphorylation (**g**; Diehl and Schaal, 2013; Wang et al., 2015; Adimonye et al., 2018).

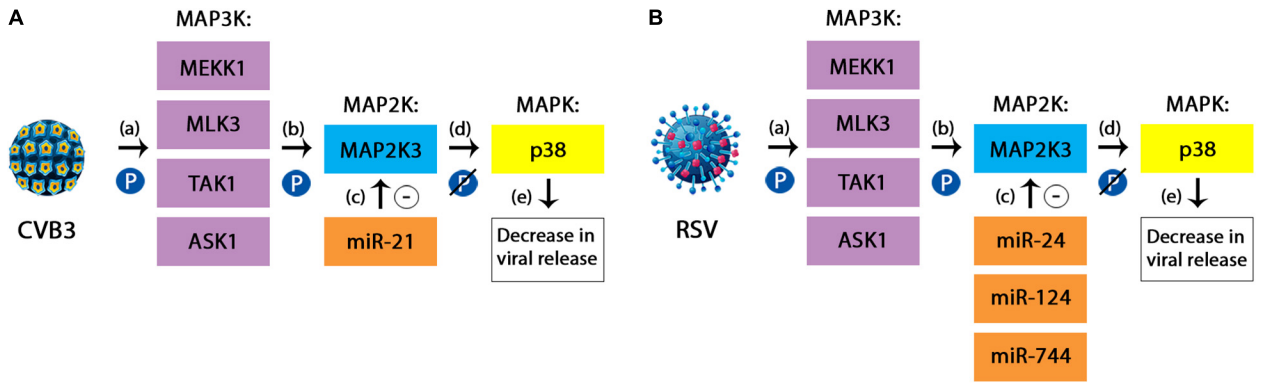

FIGURE 3 | (A) The protective mechanism of miR-21 against Coxsackievirus B3 (CVB3). CVB3 is responsible for activating the p38 component of the MAPK signaling pathway during the course of infection. The simplified mechanism relies on three subsequent phosphorylations, targeting the MAP3K members **(a)**, the MAP2K (which in the case of CVB3 is represented by MAP2K3 or MKK3) **(b)** and finally the MAPK, represented here by the p38 kinase. This cascade leads to an increased viral replication in the infected cells. miR-21 has been shown to inhibit the expression of MAP2K3 **(c)**, therefore leading to a reduced phosphorylation of p38 **(d)** and consequently, a decrease in the viral release **(e)**. **(B)** The protective mechanism of miR-24, miR-124, and miR-744 against Respiratory Syncytial Virus. RSV infection follows the same steps in order to activate the p38 MAPK pathway. In this case, the miRNAs involved are miR-24, miR-124, and miR-744. However, besides the decrease in the activation of p38 component due to a lack of phosphorylation, there has also been demonstrated a reduction in the overall levels of the same member (McCaskill et al., 2017; He et al., 2019).

found on the surface of the cell that intercepts nearby signals through its interactions with the transmembrane ligands of neighboring cells, such as Jagged and Delta-like. The Notch intracellular domain (NICD) is then cleaved and released in the intracellular environment, traveling through the Golgi apparatus to the nucleus, where it modulates the transcription of complexes that contain the protein CSL, with the ability to bind DNA (Kopan, 2012).

In viral infections, the ability of this pathway to regulate the differentiation and proliferation of the cell makes it an appealing target for viruses that depend on cellular differentiation, such as HCV, HPV, KSHV, EBV and adenovirus. While HPV enhances the already activated Notch pathway, KSHV and EBV can imitate this type of signaling. However, all of these viruses also have the potential to interfere in the control of the cellular cycle, thus leading to a dysregulated growth (Hayward, 2004). One of the miRNAs that was shown to have an effect on the Notch pathway is miR-449a. *In vitro* studies have demonstrated that in HCV infected patients, miR-449a targets Notch1, which in turn regulates the expression of Chitinase-3-like protein 1 (YKL40). The latter is thought to play an important role in the development of hepatic fibrosis and the control of inflammatory responses (Sarma et al., 2012).

MicroRNA Signaling in HPV Infection

Human papillomavirus (HPV) is a small virus containing 8kb of double stranded DNA in its genome (Bouvard et al., 2009). Over 150 different HPVs are known so far, out of which 12 are indisputably linked to cancer by the World Health Organization. Probably the most studied are Human papillomavirus 16 (HPV16) and Human papillomavirus 18 (HPV18), mainly because of their frequent association with cancer. Both of them contain two types of genes called "early" (E1, E2, E4, E5, E6 and E7) and "late" (L1 and L2) genes. Even though E1, E2, L1 and L2 are always encountered in all HPVs, the other genes may vary (Stubenrauch et al., 2007; Nobre et al., 2009). The major oncogenes are considered to be E5, E6 and E7, which are also known for altering a variety of signaling pathways, such as Wnt, Notch, PI3K/Akt, MAPK, IFN and NF-κB and others (Gupta et al., 2018; Xu et al., 2018; Wang and Chen, 2019). However, studies have demonstrated that the HPV infection could alter the interaction between miRNAs and some of these pathways.

MicroRNA Modulation of PI3K/Akt Signaling in HPV Infection

PI3K/Akt pathway plays an essential role in numerous human cancers associated with HPV. Both E6 and E7 oncogenes activate PI3K/Akt signaling pathway by influencing a number of events, therefore leading to carcinogenesis. In HPV positive laryngeal papilloma, the activity of PI3K/Akt is significantly upregulated, causing the stimulation of the Epidermal Growth Factor Receptor (EGFR) and consequently, the activation of MAPK/ERK cascade (Rodon et al., 2013). Furthermore, the E7 oncogene and its ability to increase the activity of this pathway, has been linked to the inactivation of Retinoblastoma (Rb) protein, leading to high-grade cervical neoplasia (Menges et al., 2006).

One of the miRNAs that affects this pathway due to the HPV infection is miR-125b. Some studies have shown that E6 oncogene downregulates the levels of miR-125b (Ribeiro and Sousa, 2014), which is responsible for the suppression of the PI3K/Akt signaling pathway, therefore limiting the growth of cancerous cells and promoting apoptosis (Cui et al., 2012). However, a more recent study discovered increased levels of miR-125b induced by the overexpression of octamer-binding transcription factor 4 (OCT4) gene, which, in turn, reduced the expression of Bcl-2 homologous antagonist/killer (BAK1) protein, therefore decreasing the apoptosis of cervical cancer cells (Wang et al., 2013). The different findings were explained by

the fact that miR-125b has a variety of targets, its roles being influenced by the various levels of expression of their genes (Banzhaf-Strathmann and Edbauer, 2014).

MicroRNA Modulation of MAPK/ERK Signaling in HPV Infection

In HPV infection, the MAPK/ERK signaling pathway is activated by the E5 oncogene (Fanger, 1999). Mitogen activated protein kinase (MAPK) signaling pathway is essential for the regulation of cancerous cell invasion and metastasis, primarily because of the role it plays in cellular differentiation, proliferation and apoptosis. Some of the miRNAs that could influence this pathway in the HPV infected organisms are miR-23b, miR329-3p and miR200c. MiR-23b acts as an inhibitor of metastasis in cervical cancer (Li et al., 2018), while miR-329-3p (Li et al., 2017) and miR-200c (Mei et al., 2018) are known for suppressing the migration of the cells and further invasion by targeting MAPK1 and MAPK4.

miR-23b exerts its tumor suppressor function by downregulating the MAPK1 expression, through direct binding to the 3′UTR end of MAPK1. Furthermore, MAPK1 is responsible for mediating the expression of the matrix metallopeptidase 9 (MMP-9), a molecule that has been associated with tumor migration (Nelson et al., 2000). miR-329-3p also binds directly to MAPK1 through a target sequence encountered in its 3′UTR end, leading to a subsequent suppression of the invasion, migration and proliferation of cancerous cells (Li et al., 2017). MAPK4 could involve p38, c-Jun N-terminal kinase (JNK) and extracellular signal-regulated kinase (ERK) signaling pathways in order to accomplish its functions in the malignancy (Bouzakri and Zierath, 2007). It is responsible for cellular proliferation, invasion and metastasis, angiogenesis and apoptosis inhibition. miR-200c binds to MAPK4 through the same direct mechanism, via the 3′UTR region (Mei et al., 2018).

MicroRNA Modulation of IFN Signaling in HPV Infection

Signal transducer and activator of transcription (STAT) family is responsible for the survival and progression of HPV associated cervical cancer, in particular STAT3 member, whose aberrant expression has been linked to transforming attributes (Aggarwal et al., 2006). STAT3 carries signals to the target genes via the JAK/STAT signaling pathway. A potential binding site for STAT3 could exist on the Long Control Region (LCR) of HPV16, at the 5′ end, which could regulate the expression of the viral oncogenes (Arany et al., 2002).

Previous studies linked miR-21 and Let-7a with this signaling pathway. Inhibition of STAT3 signaling using pharmacological substances like curcumin resulted in a cellular decrease of miR-21 (Shishodia et al., 2014). Furthermore, the downregulation of miR-21 levels with the help of a miR-21 inhibitor lead to a negative regulation of STAT3 and decreased amounts of active pSTAT3. Apart from this miRNA's action upon STAT3, Let-7a is another member that has been shown to have an effect on this pathway. An increased level of Let-7a, using a chemically produced analog, decreased the STAT3 supplies. In conclusion, the silencing of the HPV E6 oncogene has been linked to an increase in Let-7a and a decrease in miR-21, therefore downregulating the STAT3 signaling pathway (Shishodia et al., 2014). The inhibition of miR-21 results in elevated PTEN levels, which is a well-known tumor suppressor gene. miR-21 targets this gene through a sequence found on the 3′ UTR. PTEN is responsible for the downregulation of STAT3 activity, while its expression is only partially influenced. The mechanism through which Let-7a downregulates STAT3 involves a direct binding site encountered on the 3′UTR of STAT3 for this particular miRNA (Wang Y. et al., 2010). Let-7a has been demonstrated to suppress the growth of cancerous cells, both *in vivo* and *in vitro* (Trang et al., 2010).

MicroRNA Modulation of NF-κB Signaling in HPV Infection

Nuclear Factor κB signaling pathway plays an important role in the progression of HPV induced cervical cancer progression, through its increased DNA binding potential (Prusty and Das, 2005; Branca et al., 2006). In the case of oral cancers caused by HPV16, the excessive expression of E6 and E7 oncogenes and the interaction with the NF-κB pathway lead to a better tumor differentiation, as well as an improved prognosis (Gupta et al., 2018). There were two miRNAs found to interact with this signaling pathway during HPV infection, and more specifically, in cervical cancers: miR-143-3p and miR-218-5p (Xu et al., 2018). Both of them have the mRNA LYN as a target, which was found to be highly expressed in HPV induced cervical cancers, thus increasing the activity of NF-κB pathway. MiR-218-5p acts as a negative regulator of this pathway, by decreasing the expression of LYN (Xu et al., 2018).

MicroRNA Signaling in Herpes Virus Infection

Herpesviridae is a vast family of enveloped dsDNA viruses that are infectious to both humans and animals (Grey, 2015). Although to date over 130 viruses have been recognized (Brown and Newcomb, 2011), the ones that infect humans are comprised of three subgroups, namely α-herpesviruses, which include herpes simplex virus (HSV) types 1 and 2 and the varicella-zoster virus (VZV), β-herpesviruses which encompass the cytomegalovirus (CMV) and human herpesviruses 6 and 7 (HHV), as well as the γ-herpesviruses, involving the Epstein-Barr virus and Human Herpesvirus-8 (HHV8) (Wagner and Bloom, 1997; Carter, 2007).

MicroRNA Signaling in Herpes Simplex Virus Infection

HSV-1 and HSV-2 are most common herpes viruses, infecting individuals mainly through oral and/or genital contact, at the hand of shed viral particles. The virus drifts from the mucosa until it reaches the neighboring autonomic neurons, where it sets up a latent infection (Du et al., 2015). It has long been shown that during latent infection, viral gene expression is limited to the latency-associated transcript (LAT) (Wagner et al., 1988). While this non-coding viral ARN is not fundamental in the latency of infection (Randall et al., 2000), it does play a role in latency-associated processes such as establishment,

maintenance and reactivation, arguably by means of LAT-encoded miRNAs (Perng et al., 1994; Umbach et al., 2009; Nicoll et al., 2012).

HSV-1 and -2 encode 18 precursor miRNAs that are responsible for ultimately producing 27 and 24 mature miRNAs, respectively (Kozomara et al., 2018). Despite efforts to attribute exact functions to these miRNAs (Tang et al., 2009; Duan et al., 2012), they still remain largely unexplained, with most studies suggesting their involvement in latency regulation (Piedade and Azevedo-Pereira, 2016). To this extent, HSV miR-H3 and miR-H4 are two miRNAs that have been shown to decrease the expression of the infected cell polypeptide 34.5 (ICP34.5), a protein that promotes viral replication and reactivation in neurons (Tang et al., 2008; Tang et al., 2009). Moreover, when targeting the p16 protein, miR-H4b inhibits the PI3K/Akt and mTOR signaling pathways, therefore modifying the cellular environment in order to better adapt it for viral replication and latency (Gottwein and Cullen, 2008; Zhao et al., 2015). Along the same lines, miR-H6 has also been shown to promote the maintenance of a latent state of HSV-1 by targeting the Infected-cell polypeptide 4 (ICP4), which normally pushes the virus toward entering the lytic cycle (Tang et al., 2009; Duan et al., 2012). Infected-cell polypeptide 0 (ICP0) is another protein that stimulates the reactivation of HSV-1, as well as viral replication (Everett, 2000), and it has been shown that its activity is hindered by miR-H2 (Umbach et al., 2008). Recently identified miR-H28 and miR-H29, expressed late during reactivation, also tend to reduce excessive viral replication (Han et al., 2016). It was later demonstrated by Huang et al. that only miR-H28 induces IFNγ in human cell lines in order to limit the viral spread to uninfected neighboring cells. They showed that both miR-H28 overexpression and IFNγ induction happen at the same time, at the end of the reproductive cycle. Their study found increased levels of IFNγ at 7 h and, most notably, at 18 h after transfection with miR-H28 (Huang et al., 2019). Han et al. had previously suggested that IFN could be activated at the hand of the stimulator of interferon genes (STING) member of the signaling pathways, which is exported through exosomes from infected cells to healthy ones (Han et al., 2016). It is hypothesized that HSV tends to decrease its replication in order to avoid its spread to the central nervous system, which would in all likelihood kill the host (Han et al., 2016). On the other hand, several viral miRNAs have been shown to accumulate during viral replication and reactivation, such as miR-H8-5p, -H15, -H17, -H18, -H26, and -H27, leading to speculation regarding their involvement in promoting these processes (Du et al., 2015).

MicroRNA Signaling in Cytomegalovirus Infection

Cytomegalovirus is also characterized by the establishing of life-long latency following infection resolution, and poses great risks for immunocompromised patients (Varani and Landini, 2011). To date, the miRBase database reports the identification of 26 mature human CMV miRNAs originating from 15 precursor miRNAs (miRBase, 2018). Their main functions are thought to be immune system evasion, cell cycle regulation and vesicular transport (Hook et al., 2014).

Hook et al. have shown that HCMV miRNAs UL112-1, US5-1, and US5-2 target different components of the secretory pathway, among which are the Ras-related protein Rab-11A (RAB11A), the vesicle-associated membrane protein 3 (VAMP3) and the synaptosome-associated protein of 23 kDa (SNAP23) (Hook et al., 2014). Under normal conditions, these endocytic proteins facilitate the release of Interleukin-6 (IL-6) and Tumor necrosis factor alpha (TNF-α), whose suppression permits a bypass of the innate immune response (Gealy et al., 2005; Jarvis et al., 2006). Moreover, miR-UL112 has also been shown to decrease the natural killer (NK) cell recognizing of the virus-infected cells by targeting the major histocompatibility complex class-I related chain B (MICB) (Stern-Ginossar et al., 2007). A thought-provoking observation was developed by Nachmani et al., when they found that this viral miRNA acted in synergy with a host miRNA, hsa-miR-376a, thus decreasing NK-mediated virally infected cell killing (Nachmani et al., 2010). A diminishing in the recognition by the NK cells has also been observed to be determined by miR-US25-2-3p, a viral miRNA that also targets the tissue inhibitors of metalloproteinase 3 (TIMP3), leading to an increase in the shedding of MICA/B (Esteso et al., 2014). Furthermore, two fairly newly discovered HCMV miRNAs, miR-US5-1 and miR-UL112-3p, have recently been shown to target members of the IκB kinase (IKK) complex, IKKα and IKKβ, therefore reducing NF-κB signaling during late infection (Hancock et al., 2017) and, consequently, the expression of proinflammatory genes encoding cytokines and chemokines (Liu et al., 2017). The secretion of cytokines and chemokines including IL-6 is further inhibited by miR-UL148D, viral miRNA that has been shown to be predominantly expressed during latency (Lau et al., 2016; Goodwin et al., 2018).

MicroRNA Signaling in Epstein Barr Virus Infection

Much the same as other herpesviruses, EBV also causes latent life-long infection by means of episomes maintained within memory B-lymphocytes (Babcock et al., 1998; Thorley-Lawson et al., 2013), its persistence having been associated with lymphoproliferative disorders such as Burkitt's lymphoma, Hodgkin's lymphoma, and diffuse large B cell lymphoma (Shannon-Lowe et al., 2017).

EBV miRNAs play a number of roles in its pathogenesis, including apoptosis inhibition - BART miRNAs (Marquitz et al., 2011), immune evasion - BHRF1-3 (Xia et al., 2008), BART2-5p (Nachmani et al., 2009), BART15 (Haneklaus et al., 2012) and, perhaps the most crucial in tumorigenesis, cellular proliferation and transformation (Wong et al., 2012; Lei et al., 2013), mainly by modulating the expression of tumor suppressor genes. On this note, miR-BART3 has been shown to inhibit the activity of deleted in cancer 1 (DICE1) protein, therefore counteracting its tumor suppressive activity (Lei et al., 2013). Moreover, EBV miR-BART7-3p has been found to regulate the PI3K/Akt/GSK-3β pathway by targeting the phosphatase and tensin homolog (PTEN) tumor suppressor gene. This leads to an accumulation of Snail and β-catenin proteins, whose degradation is further inhibited by the suppression of the beta-transducin repeat containing E3 ubiquitin protein ligase gene (BTRC) mediated by miR-BART10, thus favoring epithelial mesenchymal transition

(EMT) and metastasis in nasopharyngeal carcinoma (Cai L.M. et al., 2015). A similar mechanism of action involving the decrease of PTEN activity followed by the activation of PI3K-Akt, FAK-p130^{Cas} and Shc-MAPK/ERK1/2 signaling pathways has been attributed to miR-BART1 in nasopharyngeal cancer cells (Cai L. et al., 2015). Moreover, miR-BART16 has been shown to target the CREB-binding protein (CBP), a key factor of the IFN signaling pathway (Hooykaas et al., 2017). By impairing the IFN pathway, EBV not only ensures its own replication, but it also damages the anti-tumor effects of IFN (Budhwani et al., 2018). On the other hand, inhibitory genes of the Wnt signaling pathway can be inhibited by EBV miRNAs such as miR-BART-19-3p (targets WNT Inhibitory Factor 1, WIF1), miR-BART7, 17-5p, and 19-3p (targets the adenomatous polyposis coli gene, APC) and miR-BART14, 18-5p, 19-3p (targets nemo-like kinase, Nlk) (Wong et al., 2012). Similar to the impairing of PI3K/Akt/GSK-3β pathway by miR-BART7-3p, an aberrant regulation of the Wnt pathway causes a shift of cytoplasmic β-catenin into the nucleus, which ultimately leads to excessive cellular proliferation (Wang et al., 2017).

MicroRNA Signaling in HIV Infection

The human immunodeficiency viruses (HIV) are RNA viruses belonging to the Retroviridae family and consist of two genetically distinct types: HIV-1, the more common and more virulent one, and HIV-2, which is mainly limited to the West African territory and is associated with lower transmission rates and forms of disease (Gilbert et al., 2003). HIV-1 infection gradually leads to a decrease in T-cell CD4$^+$ cells, therefore weakening the patient's immune defense, making them susceptible to many infections. The means by which HIV manages to evade the host's immune strategies involves the reshaping of the host cells with the aid of viral accessory proteins and RNA (Fruci et al., 2017). However, while host miRNAs can play either positive or negative roles in viral replication and disease evolution (Balasubramaniam et al., 2018), the existence of viral miRNAs has only relatively recently been demonstrated and their role in pathogenesis is still disputed (Omoto et al., 2004).

Cellular MicroRNAs Involved in Cell Signaling Pathways During HIV Infection

A crucial step in HIV infection is the maintenance of latency, which is facilitated by transcription, a process which involves various cellular and viral factors, perhaps the most important of which is the viral transcriptional activator Tat (Asamitsu et al., 2018). A recent study pointed out that hsa-miR-21 and -222 upregulation mediated by Tat may offer protection against apoptosis while also leading to anergy in infected CD4$^+$ T cells. This is made possible due to the impairment of the PTEN-AKT-FOXO3a pathway in infected cells, which leads to the inhibition of PTEN-mediated apoptosis (Sanchez-Del Cojo et al., 2017). Furthermore, Sardo et al. have shown that, when binding to certain Dicer proteins, Tat downregulates particular cellular miRNAs, specifically miR-539, -135a, -129, -499, -523, -524, 181a, and let-7. This, in turn, interferes with the Wnt/β-catenin pathway, with Tat lysine motifs at positions 41 and 51 playing crucial yet still poorly understood roles in inducing the suppression of the β-catenin activity. The developing of HIV-associated neurocognitive disorders is consequently promoted, the Wnt/β-catenin pathway being just one of the pathways involved in their pathogenesis (Sardo et al., 2016). An important defense mechanism employed by eukaryotic cells is the RNAi pathway, which has been shown to play an important role in HIV infection (Scarborough and Gatignol, 2017). Nef is an accessory protein that plays a key role in both viral replication and downregulation of CD4$^+$ T cells (Lundquist et al., 2002), and Omoto et al. were the first to demonstrate that Nef-shRNA decreased the transcription of HIV-1, thus implying that Nef-miRNAs produced by infected cells have a blocking action on Nef activity through the RNAi pathway (Omoto et al., 2004).

An interesting finding was further highlighted by Xue et al. when looking at HIV-associated Kaposi sarcoma: they found that the HIV-1 Nef and KSHV K1 oncoprotein acted in synergy and upregulated miR-718. Using a dual-luciferase reporter assay system, they managed to show that, of the nine tested miRNAs which were positively expressed when transduced with K1 and/or Nef, only miR-718 directly targeted PTEN. By attaching to a specific binding site on PTEN 3′UTR luciferase reporter, miR-718 decreased PTEN's tumor suppressor activity in a dose-dependent manner, thus activating the AKT/mTOR signaling pathway and therefore promoting cell proliferation and angiogenesis (Xue et al., 2014). On the same note, Yan et al. have found that, in patients infected with both HIV-1 and KSHV, miR-942 and -711 were upregulated, both leading to an activation of the NF-κB signaling pathway, which, in turn, inhibited KSHV lytic replication (Yan et al., 2018). The NF-κB signaling network has previously been shown to be consistently activated during viral infections, promoting an inflammatory state as well as HIV persistence due to its ability to activate the viral transcription (Hiscott et al., 2001). During HIV infection, it has been shown to be influenced by both cellular and viral miRNAs (Gao et al., 2014). miR-146a/b, which is increased during viral infections in general (Taganov et al., 2006), and HIV in particular (Huang et al., 2018), has been shown to downregulate the NF-κB pathway by targeting the TNF receptor-associated factor 6 (TRAF6) (Paik et al., 2011). Furthermore, higher levels of miR-155 have also been found in infected cells. By targeting the tripartite motif containing 32 (TRIM32) it has been found to block the ubiquitination of IκBα, thus inhibiting the NF-κB pathway and, as a result, promoting viral latency reestablishment (Ruelas et al., 2015).

Viral MicroRNAs Involved in Cell Signaling Pathways During HIV Infection

On the other hand, viral miRNAs are also important players in persistent inflammation and disease progression. Hiv1-miR-88 and hiv1-miR-99 have been shown to activate the TLR8 signaling pathway resulting in a steady release of macrophage TNFα (Bernard et al., 2014), which ensures a chronic state of inflammation that ultimately favors progression to AIDS (Silvestri and Feinberg, 2003). Furthermore, HIV-1-derived TAR miRNAs, miR-tar-3p and miR-tar-5p, have been proposed to regulate host gene expression. Ouellet et al. elicited the assumption that TAR miRNAs, by acting on mRNA, regulate

apoptosis-related genes, thus impacting HIV-induced cell death (Ouellet et al., 2013). To this extent, an upregulation of pro-apoptotic proteins as a result of these viral miRNAs has been observed, which ultimately activate the Fas signaling pathway, leading to complete apoptosis (Bartz and Emerman, 1999). On the other hand, during the early stages of infection, TAR miRNAs could also delay the viral induced apoptosis in order to gain time for viral replication and assembly (Ouellet et al., 2013).

MicroRNA Signaling in HBV and HCV Infection

Viral hepatitis is an important public health concern that is mainly caused by the hepatitis B (HBV) and C (HCV) viruses. Chronic infection leads to persistent liver inflammation and damage, which may ultimately end up in hepatocellular carcinoma (HCC) due to the development of oncogenic changes (Shih et al., 2016). To date, there is mounting evidence attesting to the importance of aberrant miRNA expression in the pathogenesis of viral hepatitis.

MicroRNA Signaling in HBV Infection

Hepatitis B virus is a DNA virus belonging to the Hepadnaviridae family that causes acute hepatitis which, in around 5% of cases, proceeds to chronic disease (Mui et al., 2017). In some cases, patients suffering from HBV may in time develop hepatocellular carcinoma (HCC) due to the chronic inflammatory state that it ensures and the pro-tumorigenic pathways that it activates (Levrero and Zucman-Rossi, 2016).

While the presence and function of HBV-miRNAs has only been speculated on, multiple studies have highlighted the importance of the impaired expression of cellular miRNAs during HBV infection and oncogenesis. MiR-122 is a liver specific miRNA that plays an important role in cholesterol metabolism, tumor suppression and the maintaining of an overall healthy liver (Jopling, 2012). Wang et al. have shown that HBV replication is negatively influenced by miRNA-122, which increases p53 activity through the downregulation of cyclin G1. Therefore, loss of miR-122 expression has been shown to promote viral persistence as well as oncogenesis (Chen Y. et al., 2011; Wang et al., 2012). Furthermore, Xu et al. have demonstrated that miR-122 has a pronounced antitumor effect by regulating the Wnt/β-catenin pathway. Their experiment indicated that miR-122, by binding to 3′-UTR Wnt1 which included the target sequence, managed to inhibit its activity by almost 50%, this suppressive effect being absent when a miR-122 inhibitor was used. This blocking activity subsequently led to hindering of HCC cell proliferation and promotion of cell apoptosis (Xu et al., 2012). Furthermore, it has been suggested that miR-122 can actively prevent the epithelial-mesenchymal transition while blocking HCC cell motility due to its ability to impair the RhoA/Rock pathway, which is deeply involved in cytoskeletal events such as fiber bundles formation (Kalluri and Weinberg, 2009; Wang et al., 2014). To this extent, Wang et al. tested this hypothesis by using dual luciferase reporter plasmids (RhoA and Rac1) containing the binding sites for miR-122. Their experiment showed that miR-122 significantly diminished the number of total and active forms of RhoA and Rac1 (Wang et al., 2014). Moreover, an inhibition of HBV replication is possible through the regulation of IFN signaling pathway: Gao et al. have shown that the IFN circuitry can be hindered by the overexpression of the suppressor of cytokine signaling 3 (SOCS3), which happens as a result of a down-regulated miR-122 (Gao et al., 2015).

miR-132 has been shown to associate tumor suppressive properties in various types of cancer (Liu et al., 2015; Chen et al., 2019). However, during HBV infection, the hepatitis B virus x (HBx) protein downregulates its expression, thus enhancing HBV's carcinogenic feature. Wei et al. have demonstrated that HCC cell proliferation was markedly inhibited by miR-132, which interfered with the Akt-signaling pathway. After transfection of tumor cells with miR-132, they found that p-Akt, cyclin D1, p-GSK3β and β-catenin were substantially under-expressed, this outcome indicating the involvement of the Akt signaling cascade and miR-132 in HCC tumorigenesis (Wei et al., 2013).

The miR-371-373 cluster can act either as tumor-suppressors (Langroudi et al., 2015; Ullmann et al., 2018) or potential oncogenes (Wei et al., 2015; Ghasemi et al., 2018) in various human malignancies. In HBV infection, the upregulation of miRs-372-373 has been shown to positively correlate with the number of HBV DNA copies. Guo et al. have highlighted that, by targeting an NFIB-dependent pathway, miR-372-373 promote HBV expression and replication, thus favoring viral progression (Guo et al., 2011).

MicroRNA Signaling in HCV Infection

Hepatitis C virus (HCV) is an RNA virus belonging to the Flaviviridae family, which, as opposed to HBV, causes chronic viral hepatitis in around 60-80% of infected individuals (Rehermann and Nascimbeni, 2005). Around 5 to 20% of chronic hepatitis C patients proceed to develop cirrhosis or HCC (Chen and Morgan, 2006). The RNA-dependent RNA polymerase (RdRp) of HCV operates in an error-prone manner which results in a highly diverse population of viral quasispecies (Gomez et al., 1999). The ensuing heterogeneity of HCV poses great challenge not only in developing new treatments and effective vaccines, but also in diagnosis (Li and Lo, 2015).

While miRNAs impaired by HBV are mainly involved in DNA damage and repair, transcription and apoptosis, those suppressed by HCV have been shown to have an impact mainly on antigen presentation, immune regulation and cell-division cycle. Moreover, it would seem that in HCV infection there are more down-regulated miRNAs than in HBV infection (Ura et al., 2009), with Jopling et al. suggesting that some cellular miRNAs may be depleted during the defense against RNA viruses (Jopling et al., 2005). For instance, Huang et al. have shown that Wnt1 acts as a target gene, holding two binding sites for miR-152, situated at the 3′-UTR region of Wnt, namely at 262–268 bp and 688–694 bp, respectively. They indicated that the expression of miR-152, which normally has an inhibitory effect over Wnt1, was notably downregulated in HCV infection, attributing it to the overexpression of HCV core protein. The ensuing increased activity of the Wnt/β-catenin pathway promotes excessive cell proliferation (Huang et al., 2014). Wnt/β-catenin signaling has also been shown to be

increased by the overly expressed miR-155 that is seen in HCV infection, as suggested by Zhang et al. (Zhang et al., 2012). In Wnt signaling, the glycogen synthase kinase 3 beta (GSK3b) enzyme, along with the adenomatous polyposis coli (APC) and Axin proteins assemble a multimeric structure meant to abolish Wnt signaling by phosphorylating β-catenin at its N-terminal end which leads to its degradation through the ubiquitin proteasome system (Verheyen and Gottardi, 2010). In their experiment, miR-155 significantly decreased APC levels, thus leading to the activation of the Wnt/β-catenin signaling cascade (Zhang et al., 2012).

However, HCV infection also results in the upregulation of certain miRNAs, and such is the case of miR-21, which is upregulated by HCV. MiR-21 acts by targeting elements of the toll-like receptor (TLR) signaling pathway, like interleukin-1 receptor-associated kinases (IRAK) 1 and 4, tumor necrosis factor receptor-associated factor 6 (TRAF6) and myeloid differentiation primary response (MyD88) 88 protein, ultimately leading to IFN type I suppression in order to evade the immune response (Chen et al., 2013). Liver-specific miRNA, miR-122, can also be up-regulated during HCV infection, predicting a poorer response to IFN therapy (Khan et al., 2015). Enhanced miR-122 tends to promote the expression of the suppressor of cytokine signaling 3 (SOCS3) and therefore reduce STAT3 activation, thus reducing the induction of antiviral genes through the interferon-stimulated gene factor 3 (ISGF3) (Zhu et al., 2011). IFN resistance is further aided by miR-373, which targets IFN-regulatory factor 9 (IRF9) and JAK1, therefore impairing the JAK/STAT signaling pathway (Mukherjee et al., 2015).

CLINICAL APPLICATION OF MIRNAS IN VIRAL INFECTION AND THERAPY

In the past years, using miRNA as a tool in order to modify gene expression became one of the most important and new frontier in modern medicine (Chakraborty et al., 2017). Recently, an increased significance has been granted to the field of infectious diseases. MiRNAs are interesting molecules with reference to antiviral therapy because of their low immunogenicity and their capability of being tests in various animal models in preclinical studies (Girardi et al., 2018). Even if there are many ways to inhibit (Li and Rana, 2014) or to overexpress a given miRNA (Yang, 2015) *in vivo*, the delivery process still remains challenging for miRNA-based therapy in clinical applications (Girardi et al., 2018).

An interesting example of miRNA-based treatment for antiviral therapy is Miravirsen, an LNA-modified anti-miR-122 which can combat hepatitis C virus infection (Janssen et al., 2013). LNA is a 15-nucleotide locked nucleic acid oligonucleotide which suffered phosphonothioate modifications and was named SPC3649 or Miravirsen. It was shown that the systematic delivery of LNA, complementary to the 5′ end of miR-122, results in sequestration of miRNA in non-human primates with no associated toxicity (Elmen et al., 2008). Also, in chimpanzees with chronic HCV infection the silencing of miR-122 by the antisense oligonucleotide Miravirsen was also achieved, and long lasting viral suppression was observed (Lanford et al., 2010). 3 years later, Janssen et al. carried out a second phase of the study in chronic HCV infected patients who received 5-weekly injections of Miravirsen, and they observed that the treatment resulted in a prolonged and dose-dependent reduction in HCV RNA levels (Janssen et al., 2013; van der Ree et al., 2014; Kreth et al., 2018). More recently, the evaluation of miR-122 plasma levels in chronic HCV infected patients during Miravirsen treatment demonstrated a specific, significant and prolonged decrease in miR-122 expression, very close to detection limits in some cases. Despite this fact, a substantial decrease in viral load was not observed (van der Ree et al., 2016). The reduction in the viral load was obtained later, in another experiment conducted by van der Ree et al., when RG-101, an N-acetylgalactosamine conjugated antisense oligonucleotide for miR-122 was elaborated in order to increase miR-122 sequestration. Viral load reduction was observed in all treated patients within 4 weeks (van der Ree et al., 2017).

In another study performed on mice, it was demonstrated that the administration of five chemically modified miRNA mimics via intranasal pathway was able to target the viral RNA, suppressing H1N1 replication and protecting the mice from viral infection. The miRNA mimics corresponded to highly expressed miRNAs in respiratory epithelial cells (Peng et al., 2018).

Furthermore, the neurotropic virus JEV is able to induce miR-301 expression in neuronal infected cells, which affects the antiviral host response. *In vivo*, inhibition of miR-301 by intracranial injection with modified miR-301a phosphorodiamidate morpholine oligomer restores the IFN response and improves the survival of JEV infected mice by enabling IFNβ production and restricting viral propagation (Hazra and Kumawat, 2017). Even if miRNAs are a very promising source for the treatment of neurotropic viral infection, the main difficulty for small RNA-based approaches in lies in the crossing of the blood-brain barrier.

One of the most successful interventions nowadays available are live attenuated vaccines against human viral pathogens. Vaccines not only function well for acute diseases, but also for chronic infections such as HIV, even if these are more challenging for reasons of safety and efficacy (Minor, 2015). MiRNAs have a natural capacity to inhibit viruses through direct targeting of viral RNAs, capacity which can be used to generate new attenuated vaccines in specific tissue manner by incorporating cell-specific miRNA target sequences into their genomes. For example, the insertion of complementary sequences for the neural-specific miR-124 into the poliovirus genome restricts its tissue tropism in mice while also preventing pathogenicity of the attenuated viral strain (Barnes et al., 2008).

Another interesting approach refers to the modification of viral tropism in order to develop safer replication-competent oncolytic viruses (Kaufman et al., 2015). It is known that oncolytic viruses replicate in cancer cells and, in turn, trigger the activation of immune response against the tumor, but they can also induce toxicity in normal tissues. To impair this issue, an alternative way is to integrate target sequences complementary to a specific miRNA into the viral genome. The replication in normal cells is reduced while the oncolytic potential is

maintained in tumor cells. The oncolytic picornavirus Coxsackie A21, the cause for lethal myositis in tumor-bearing mice, is such an example. The myotoxicity was reduced and the oncolytic properties were maintained when binding sites for the muscle-specific miR-206 and miR-133 were added (Kelly et al., 2008).

CONCLUSION

MiRNAs are evolutionarily conserved non-coding RNAs that play crucial roles in regulating gene expression in both animals and humans. In this review, we have extensively covered various aspects involving miRNAs interactions with various signaling pathways during viral infections. It is important to keep in mind that some viruses encode their own miRNAs, which complicates the regulation mediated by the virus.

The importance of these viral small molecules during infection comes from their ability to modify the cell environment in a non-immunogenic way once they are selected by the virus. The overexpression of miRNA triggered by pathogens is not always correlated with their survival or pathogenesis, and sometimes it can be cell- or tissue-specific. The exact mechanisms of modulation of host cellular miRNA by viruses and specific virulence factors are still unclear. However, miRNAs can play important roles in clinical applications in diagnostic and therapy against viral infections.

MiRNAs are essential mediators of host response to different pathogens. Knowing the roles of miRNAs in host response to various viral infections provides an interesting tool for identifying key genes and pathways that must be activated, enhanced, silenced or repressed in order to impel an effective immune response. The clinical applications of miRNAs are extremely important, as miRNAs targeted inhibition may have substantial therapeutic impact. Inhibition of miRNAs can be achieved through many different methods, but chemically modified antisense oligonucleotides have shown the most prominent effects. Though we are far from completely understanding all the molecular mechanisms behind the complex cross-talks between miRNA pathways and viral infections, the general knowledge is increasing on the different roles played by miRNAs during viral infections.

AUTHOR CONTRIBUTIONS

MB, CC, and DT contributed to the conceptualization. DC and OT performed the methodology. OB investigated the data. NS carried out the resources. MB, CC, DT, and OB wrote the original draft of the manuscript. DC contributed to writing, reviewing, and editing and supervised the manuscript. OT visualized the data. DT carried out the project administration. NS and SV performed the funding acquisition.

FUNDING

This work and the APC were supported by grants of the Romanian Ministry of Research and Innovation, CCCDI – UEFISCDI, projects number PN-III-P1-1.2-PCCDI-2017-0833/68/2018 within PNCDI III.

REFERENCES

Adimonye, A., Stankiewicz, E., Kudahetti, S., Trevisan, G., Tinwell, B., Corbishley, C., et al. (2018). Analysis of the PI3K-AKT-mTOR pathway in penile cancer: evaluation of a therapeutically targetable pathway. *Oncotarget* 9, 16074–16086.

Aggarwal, B. B., Sethi, G., Ahn, K. S., Sandur, S. K., Pandey, M. K., Kunnumakkara, A. B., et al. (2006). Targeting signal-transducer-and-activator-of-transcription-3 for prevention and therapy of cancer: modern target but ancient solution. *Ann. N. Y. Acad. Sci.* 1091, 151–169.

Alisi, A., Giannini, C., Spaziani, A., Caini, P., Zignego, A. L., and Balsano, C. (2008). Involvement of PI3K in HCV-related lymphoproliferative disorders. *J. Cell Physiol.* 214, 396–404. doi: 10.1002/jcp.21211

Androulidaki, A., Iliopoulos, D., Arranz, A., Doxaki, C., Schworer, S., Zacharioudaki, V., et al. (2009). The kinase Akt1 controls macrophage response to lipopolysaccharide by regulating microRNAs. *Immunity* 31, 220–231. doi: 10.1016/j.immuni.2009.06.024

Arany, I., Grattendick, K. G., and Tyring, S. K. (2002). Interleukin-10 induces transcription of the early promoter of human papillomavirus type 16 (HPV16) through the 5′-segment of the upstream regulatory region (URR). *Antivir. Res.* 55, 331–339. doi: 10.1016/s0166-3542(02)00070-0

Asamitsu, K., Fujinaga, K., and Okamoto, T. (2018). HIV Tat/P-TEFb interaction: a potential target for novel anti-HIV therapies. *Molecules* 23:933. doi: 10.3390/molecules23040933

Babcock, G. J., Decker, L. L., Volk, M., and Thorley-Lawson, D. A. (1998). EBV persistence in memory B cells in vivo. *Immunity* 9, 395–404. doi: 10.1016/s1074-7613(00)80622-6

Balasubramaniam, M., Pandhare, J., and Dash, C. (2018). Are microRNAs important players in HIV-1 Infection? An Update. *Viruses* 10:110. doi: 10.3390/v10030110

Banzhaf-Strathmann, J., and Edbauer, D. (2014). Good guy or bad guy: the opposing roles of microRNA 125b in cancer. *Cell Commun. Signal.* 12:30. doi: 10.1186/1478-811x-12-30

Bar, M., Wyman, S. K., Fritz, B. R., Qi, J., Garg, K. S., Parkin, R. K., et al. (2008). MicroRNA discovery and profiling in human embryonic stem cells by deep sequencing of small RNA libraries. *Stem Cells* 26, 2496–2505. doi: 10.1634/stemcells.2008-0356

Barciszewska-Pacak, M., Milanowska, K., Knop, K., Bielewicz, D., Nuc, P., Plewka, P., et al. (2015). Arabidopsis microRNA expression regulation in a wide range of abiotic stress responses. *Front. Plant Sci.* 6:410. doi: 10.3389/fpls.2015.00410

Baril, M., Es-Saad, S., Chatel-Chaix, L., Fink, K., Pham, T., Raymond, V. A., et al. (2013). Genome-wide RNAi screen reveals a new role of a WNT/CTNNB1 signaling pathway as negative regulator of virus-induced innate immune responses. *PLoS Pathog.* 9:e1003416. doi: 10.1371/journal.ppat.1003416

Barnes, D., Kunitomi, M., Vignuzzi, M., Saksela, K., and Andino, R. (2008). Harnessing endogenous miRNAs to control virus tissue tropism as a strategy for developing attenuated virus vaccines. *Cell Host Microb.* 4, 239–248. doi: 10.1016/j.chom.2008.08.003

Bartel, D. P. (2009). MicroRNAs: target recognition and regulatory functions. *Cell* 136, 215–233. doi: 10.1016/j.cell.2009.01.002

Bartz, S. R., and Emerman, M. (1999). Human immunodeficiency virus type 1 Tat induces apoptosis and increases sensitivity to apoptotic signals by up-regulating FLICE/caspase-8. *J. Virol.* 73, 1956–1963. doi: 10.1128/jvi.73.3.1956-1963.1999

Barwari, T., Joshi, A., and Mayr, M. (2016). MicroRNAs in cardiovascular disease. *J. Am. Coll. Cardiol.* 68, 2577–2584.

Bernard, M. A., Zhao, H., Yue, S. C., Anandaiah, A., Koziel, H., and Tachado, S. D. (2014). Novel HIV-1 miRNAs stimulate TNFα release in human macrophages via TLR8 signaling pathway. *PLoS One* 9:e106006. doi: 10.1371/journal.pone.0106006

Bhaskaran, M., and Mohan, M. (2014). MicroRNAs: history, biogenesis, and their evolving role in animal development and disease. *Vet. Pathol.* 51, 759–774. doi: 10.1177/0300985813502820

Bhaumik, D., Scott, G. K., Schokrpur, S., Patil, C. K., Campisi, J., and Benz, C. C. (2008). Expression of microRNA-146 suppresses NF-kappaB activity with reduction of metastatic potential in breast cancer cells. *Oncogene* 27, 5643–5647. doi: 10.1038/onc.2008.171

Bogerd, H. P., Karnowski, H. W., Cai, X., Shin, J., Pohlers, M., and Cullen, B. R. (2010). A mammalian herpesvirus uses noncanonical expression and processing mechanisms to generate viral MicroRNAs. *Mol. Cell* 37, 135–142. doi: 10.1016/j.molcel.2009.12.016

Bouvard, V., Baan, R., Straif, K., Grosse, Y., Secretan, B., El Ghissassi, F., et al. (2009). A review of human carcinogens–Part B: biological agents. *Lancet Oncol.* 10, 321–322. doi: 10.1016/s1470-2045(09)70096-8

Bouzakri, K., and Zierath, J. (2007). MAP4K4 gene silencing in human skeletal muscle prevents tumor necrosis factor- -induced insulin resistance. *J. Biol. Chem.* 282, 7783–7789. doi: 10.1074/jbc.m608602200

Branca, M., Giorgi, C., Ciotti, M., Santini, D., Di Bonito, L., Costa, S., et al. (2006). Upregulation of nuclear factor-κB (NF-κB) is related to the grade of cervical intraepithelial neoplasia, but is not an independent predictor of high-risk human papillomavirus or disease outcome in cervical cancer. *Diagn. Cytopathol.* 34, 555–563. doi: 10.1002/dc.20514

Brown, J. C., and Newcomb, W. W. (2011). Herpesvirus capsid assembly: insights from structural analysis. *Curr. Opin. Virol.* 1, 142–149. doi: 10.1016/j.coviro.2011.06.003

Bruscella, P., Bottini, S., Baudesson, C., Pawlotsky, J. M., Feray, C., and Trabucchi, M. (2017). Viruses and miRNAs: more friends than foes. *Front. Microbiol.* 8:824. doi: 10.3389/fmicb.2017.00824

Budhwani, M., Mazzieri, R., and Dolcetti, R. (2018). Plasticity of Type I interferon-mediated responses in cancer therapy: from anti-tumor immunity to resistance. *Front. Oncol.* 8:322. doi: 10.3389/fonc.2018.00322

Cai, L., Ye, Y., Jiang, Q., Chen, Y., Lyu, X., Li, J., et al. (2015). Epstein-Barr virus-encoded microRNA BART1 induces tumour metastasis by regulating PTEN-dependent pathways in nasopharyngeal carcinoma. *Nat. Commun.* 6:7353.

Cai, L. M., Lyu, X. M., Luo, W. R., Cui, X. F., Ye, Y. F., Yuan, C. C., et al. (2015). EBV-miR-BART7-3p promotes the EMT and metastasis of nasopharyngeal carcinoma cells by suppressing the tumor suppressor PTEN. *Oncogene* 34, 2156–2166. doi: 10.1038/onc.2014.341

Carter, J. (2007). *Virology: Principles and Applications*. 1st Edn, Hoboken, NJ: Wiley.

Cha, Y. H., Kim, N. H., Park, C., Lee, I., Kim, H. S., and Yook, J. I. (2012). MiRNA-34 intrinsically links p53 tumor suppressor and Wnt signaling. *Cell Cycle* 11, 1273–1281. doi: 10.4161/cc.19618

Chakraborty, C., Sharma, A. R., Sharma, G., Doss, C. G. P., and Lee, S.-S. (2017). Therapeutic miRNA and siRNA: moving from bench to clinic as next generation medicine. *Mol. Ther. Nucleic Acids* 8, 132–143. doi: 10.1016/j.omtn.2017.06.005

Chen, C., Ridzon, D. A., Broomer, A. J., Zhou, Z., Lee, D. H., Nguyen, J. T., et al. (2005). Real-time quantification of microRNAs by stem-loop RT-PCR. *Nucleic Acids Res.* 33:e179. doi: 10.1093/nar/gni178

Chen, C., Tan, R., Wong, L., Fekete, R., and Halsey, J. (2011). Quantitation of microRNAs by real-time RT-qPCR. *Methods Mol. Biol.* 687, 113–134. doi: 10.1007/978-1-60761-944-4_8

Chen, S. L., and Morgan, T. R. (2006). The natural history of hepatitis C virus (HCV) infection. *Int. J. Med. Sci.* 3, 47–52. doi: 10.7150/ijms.3.47

Chen, X., Li, M., Zhou, H., and Zhang, L. (2019). miR-132 Targets FOXA1 and exerts tumor-suppressing functions in thyroid cancer. *Oncol. Res.* 27, 431–437. doi: 10.3727/096504018x15201058168730

Chen, Y., Chen, J., Wang, H., Shi, J., Wu, K., Liu, S., et al. (2013). HCV-induced miR-21 contributes to evasion of host immune system by targeting MyD88 and IRAK1. *PLoS Pathog.* 9:e1003248. doi: 10.1371/journal.ppat.1003248

Chen, Y., Shen, A., Rider, P. J., Yu, Y., Wu, K., Mu, Y., et al. (2011). A liver-specific microRNA binds to a highly conserved RNA sequence of hepatitis B virus and negatively regulates viral gene expression and replication. *FASEB J.* 25, 4511–4521. doi: 10.1096/fj.11-187781

Chen, Y. X., Huang, K. J., and Niu, K. X. (2018). Recent advances in signal amplification strategy based on oligonucleotide and nanomaterials for microRNA detection-a review. *Biosens. Bioelectron.* 99, 612–624. doi: 10.1016/j.bios.2017.08.036

Chevillet, J. R., Lee, I., Briggs, H. A., He, Y., and Wang, K. (2014). Issues and prospects of microRNA-based biomarkers in blood and other body fluids. *Molecules* 19, 6080–6105. doi: 10.3390/molecules19056080

Chi, S. W., Hannon, G. J., and Darnell, R. B. (2012). An alternative mode of microRNA target recognition. *Nat. Struct. Mol. Biol.* 19, 321–327. doi: 10.1038/nsmb.2230

Chugh, P., Bradel-Tretheway, B., Monteiro-Filho, C. M., Planelles, V., Maggirwar, S. B., Dewhurst, S., et al. (2008). Akt inhibitors as an HIV-1 infected macrophage-specific anti-viral therapy. *Retrovirology* 5:11. doi: 10.1186/1742-4690-5-11

Creighton, C. J., Reid, J. G., and Gunaratne, P. H. (2009). Expression profiling of microRNAs by deep sequencing. *Brief Bioinform.* 10, 490–497. doi: 10.1093/bib/bbp019

Cui, F., Li, X., Zhu, X., Huang, L., Huang, Y., Mao, C., et al. (2012). MiR-125b inhibits tumor growth and promotes apoptosis of cervical cancer cells by targeting phosphoinositide 3-kinase catalytic subunit delta. *Cell Physiol. Biochem.* 30, 1310–1318. doi: 10.1159/000343320

Cullen, B. R. (2001). Journey to the center of the cell. *Cell* 105, 697–700. doi: 10.1016/s0092-8674(01)00392-0

Dalmay, T. (2008). Identification of genes targeted by microRNAs. *Biochem. Soc. Trans.* 36(Pt 6), 1194–1196. doi: 10.1042/bst0361194

Darnell, J. E. Jr., Kerr, I. M., and Stark, G. R. (1994). Jak-STAT pathways and transcriptional activation in response to IFNs and other extracellular signaling proteins. *Science* 264, 1415–1421. doi: 10.1126/science.8197455

Davis-Dusenbery, B. N., and Hata, A. (2010). Mechanisms of control of microRNA biogenesis. *J. Biochem.* 148, 381–392.

de Veer, M. J., Holko, M., Frevel, M., Walker, E., Der, S., Paranjape, J. M., et al. (2001). Functional classification of interferon-stimulated genes identified using microarrays. *J. Leukoc. Biol.* 69, 912–920.

Denli, A. M., Tops, B. B., Plasterk, R. H., Ketting, R. F., and Hannon, G. J. (2004). Processing of primary microRNAs by the microprocessor complex. *Nature* 432, 231–235. doi: 10.1038/nature03049

Deregibus, M. C., Cantaluppi, V., Doublier, S., Brizzi, M. F., Deambrosis, I., Albini, A., et al. (2002). HIV-1-Tat protein activates phosphatidylinositol 3-kinase/AKT-dependent survival pathways in Kaposi's sarcoma cells. *J. Biol. Chem.* 277, 25195–25202. doi: 10.1074/jbc.m200921200

Diebel, K. W., Smith, A. L., and van Dyk, L. F. (2010). Mature and functional viral miRNAs transcribed from novel RNA polymerase III promoters. *RNA* 16, 170–185. doi: 10.1261/rna.1873910

Diehl, N., and Schaal, H. (2013). Make yourself at home: viral hijacking of the PI3K/Akt signaling pathway. *Viruses* 5, 3192–3212. doi: 10.3390/v5123192

Dong, C., Davis, R. J., and Flavell, R. A. (2002). MAP kinases in the immune response. *Annu. Rev. Immunol.* 20, 55–72. doi: 10.1146/annurev.immunol.20.091301.131133

Du, T., Han, Z., Zhou, G., and Roizman, B. (2015). Patterns of accumulation of miRNAs encoded by herpes simplex virus during productive infection, latency, and on reactivation. *Proc. Natl. Acad. Sci. U.S.A.* 112, E49–E55.

Duan, F., Liao, J., Huang, Q., Nie, Y., and Wu, K. (2012). HSV-1 miR-H6 inhibits HSV-1 replication and IL-6 expression in human corneal epithelial cells in vitro. *Clin. Dev. Immunol.* 2012:192791.

Eichhorn, S. W., Guo, H., McGeary, S. E., Rodriguez-Mias, R. A., Shin, C., Baek, D., et al. (2014). mRNA destabilization is the dominant effect of mammalian microRNAs by the time substantial repression ensues. *Mol. Cell* 56, 104–115. doi: 10.1016/j.molcel.2014.08.028

Elmen, J., Lindow, M., Schutz, S., Lawrence, M., Petri, A., Obad, S., et al. (2008). LNA-mediated microRNA silencing in non-human primates. *Nature* 452, 896–899. doi: 10.1038/nature06783

Esteso, G., Luzon, E., Sarmiento, E., Gomez-Caro, R., Steinle, A., Murphy, G., et al. (2014). Altered microRNA expression after infection with human cytomegalovirus leads to TIMP3 downregulation and increased shedding of metalloprotease substrates, including MICA. *J. Immunol.* 193, 1344–1352. doi: 10.4049/jimmunol.1303441

Everett, R. D. (2000). ICP0, a regulator of herpes simplex virus during lytic and latent infection. *Bioessays* 22, 761–770. doi: 10.1002/1521-1878(200008)22:8<761::aid-bies10>3.0.co;2-a

Fanger, G. R. (1999). Regulation of the MAPK family members: role of subcellular localization and architectural organization. *Histol. Histopathol.* 14, 887–894.

Fruci, D., Rota, R., and Gallo, A. (2017). The role of HCMV and HIV-1 MicroRNAs: processing, and mechanisms of action during viral infection. *Front. Microbiol.* 8:689. doi: 10.3389/fmicb.2017.00689

Gao, D., Zhai, A., Qian, J., Li, A., Li, Y., Song, W., et al. (2015). Down-regulation of suppressor of cytokine signaling 3 by miR-122 enhances interferon-mediated suppression of hepatitis B virus. *Antivir. Res.* 118, 20–28. doi: 10.1016/j.antiviral.2015.03.001

Gao, Z., Dou, Y., Chen, Y., and Zheng, Y. (2014). MicroRNA roles in the NF- κB signaling pathway during viral infections. *Biomed. Res. Int.* 2014:436097.

Garofalo, M., Leva, G. D., and Croce, C. M. (2014). MicroRNAs as anti-cancer therapy. *Curr. Pharm. Des.* 20, 5328–5335. doi: 10.2174/1381612820666140128211346

Gaur, P., Munjhal, A., and Lal, S. K. (2011). Influenza virus and cell signaling pathways. *Med. Sci. Monit.* 17, RA148–RA154.

Gealy, C., Denson, M., Humphreys, C., McSharry, B., Wilkinson, G., and Caswell, R. (2005). Posttranscriptional suppression of interleukin-6 production by human cytomegalovirus. *J. Virol.* 79, 472–485. doi: 10.1128/jvi.79.1.472-485.2005

Ghasemi, M., Samaei, N. M., Mowla, S. J., Shafiee, M., Vasei, M., and Ghasemian, N. (2018). Upregulation of miR-371-373 cluster, a human embryonic stem cell specific microRNA cluster, in esophageal squamous cell carcinoma. *J. Cancer Res. Therap.* 14(Suppl.), S132–S137.

Gilbert, P. B., McKeague, I. W., Eisen, G., Mullins, C., Gueye, N. A., Mboup, S., et al. (2003). Comparison of HIV-1 and HIV-2 infectivity from a prospective cohort study in Senegal. *Statist. Med.* 22, 573–593. doi: 10.1002/sim.1342

Gillespie, P., Ladame, S., and O'Hare, D. (2018). Molecular methods in electrochemical microRNA detection. *Analyst* 144, 114–129. doi: 10.1039/c8an01572d

Girardi, E., Lopez, P., and Pfeffer, S. (2018). On the importance of host MicroRNAs during viral infection. *Front. Genet.* 9:439. doi: 10.3389/fgene.2018.00439

Gomez, J., Martell, M., Quer, J., Cabot, B., and Esteban, J. I. (1999). Hepatitis C viral quasispecies. *J. Viral Hepatit.* 6, 3–16. doi: 10.1046/j.1365-2893.1999.t01-1-6120131.x

Goodwin, C. M., Ciesla, J. H., and Munger, J. (2018). Who's driving? Human Cytomegalovirus, Interferon, and NFκB signaling. *Viruses* 10:447. doi: 10.3390/v10090447

Gottwein, E., and Cullen, B. R. (2008). Viral and cellular microRNAs as determinants of viral pathogenesis and immunity. *Cell Host Microb.* 3, 375–387. doi: 10.1016/j.chom.2008.05.002

Greber, U. F., and Puntener, D. (2009). DNA-tumor virus entry–from plasma membrane to the nucleus. *Semin. Cell Dev. Biol.* 20, 631–642. doi: 10.1016/j.semcdb.2009.03.014

Greber, U. F., and Way, M. (2006). A superhighway to virus infection. *Cell* 124, 741–754. doi: 10.1016/j.cell.2006.02.018

Gregory, R. I., Yan, K. P., Amuthan, G., Chendrimada, T., Doratotaj, B., Cooch, N., et al. (2004). The Microprocessor complex mediates the genesis of microRNAs. *Nature* 432, 235–240. doi: 10.1038/nature03120

Grey, F. (2015). Role of microRNAs in herpesvirus latency and persistence. *J. Gen. Virol.* 96(Pt 4), 739–751. doi: 10.1099/vir.0.070862-0

Guo, H., Liu, H., Mitchelson, K., Rao, H., Luo, M., Xie, L., et al. (2011). MicroRNAs-372/373 promote the expression of hepatitis B virus through the targeting of nuclear factor I/B. *Hepatology* 54, 808–819. doi: 10.1002/hep.24441

Guo, H., Zhou, T., Jiang, D., Cuconati, A., Xiao, G. H., Block, T. M., et al. (2007). Regulation of hepatitis B virus replication by the phosphatidylinositol 3-kinase-akt signal transduction pathway. *J. Virol.* 81, 10072–10080. doi: 10.1128/jvi.00541-07

Guo, X. K., Zhang, Q., Gao, L., Li, N., Chen, X. X., and Feng, W. H. (2013). Increasing expression of microRNA 181 inhibits porcine reproductive and respiratory syndrome virus replication and has implications for controlling virus infection. *J. Virol.* 87, 1159–1171. doi: 10.1128/jvi.02386-12

Guo, Y. E., Oei, T., and Steitz, J. A. (2015). *Herpesvirus saimiri* MicroRNAs preferentially target host cell cycle regulators. *J. Virol.* 89, 10901–10911. doi: 10.1128/jvi.01884-15

Gupta, S., Kumar, P., and Das, B. C. (2018). HPV: molecular pathways and targets. *Curr. Probl. Cancer* 42, 161–174. doi: 10.1016/j.currproblcancer.2018.03.003

Ha, M., and Kim, V. N. (2014). Regulation of microRNA biogenesis. *Nat. Rev. Mol. Cell Biol.* 15, 509–524.

Habas, R., and Dawid, I. B. (2005). Dishevelled and Wnt signaling: is the nucleus the final frontier? *J. Biol.* 4:2.

Hack, K., Reilly, L., Proby, C., Fleming, C., Leigh, I., and Foerster, J. (2012). Wnt5a inhibits the CpG oligodeoxynucleotide-triggered activation of human plasmacytoid dendritic cells. *Clin. Exp. Dermatol.* 37, 557–561. doi: 10.1111/j.1365-2230.2012.04362.x

Hammond, S. M., Boettcher, S., Caudy, A. A., Kobayashi, R., and Hannon, G. J. (2001). Argonaute2, a link between genetic and biochemical analyses of RNAi. *Science* 293, 1146–1150. doi: 10.1126/science.1064023

Han, J., Lee, Y., Yeom, K. H., Kim, Y. K., Jin, H., and Kim, V. N. (2004). The drosha-DGCR8 complex in primary microRNA processing. *Genes Dev.* 18, 3016–3027. doi: 10.1101/gad.1262504

Han, Z., Liu, X., Chen, X., Zhou, X., Du, T., Roizman, B., et al. (2016). miR-H28 and miR-H29 expressed late in productive infection are exported and restrict HSV-1 replication and spread in recipient cells. *Proc. Natl. Acad. Sci.U.S.A.* 113, E894–E901.

Hancock, M. H., Hook, L. M., Mitchell, J., and Nelson, J. A. (2017). Human cytomegalovirus MicroRNAs miR-US5-1 and miR-UL112-3p block proinflammatory cytokine production in response to NF-κB-activating factors through direct downregulation of IKKα and IKKβ. *mBio* 8:e0109-17.

Haneklaus, M., Gerlic, M., Kurowska-Stolarska, M., Rainey, A. A., Pich, D., McInnes, I. B., et al. (2012). Cutting edge: miR-223 and EBV miR-BART15 regulate the NLRP3 inflammasome and IL-1beta production. *J. Immunol.* 189, 3795–3799. doi: 10.4049/jimmunol.1200312

Hayward, S. D. (2004). Viral interactions with the notch pathway. *Semin. Cancer Biol.* 14, 387–396. doi: 10.1016/j.semcancer.2004.04.018

Hazra, B., and Kumawat, K. L. (2017). The host microRNA miR-301a blocks the IRF1-mediated neuronal innate immune response to Japanese encephalitis virus infection. *Sci. Signal.* 10:eaaf5185. doi: 10.1126/scisignal.aaf5185

He, F., Xiao, Z., Yao, H., Li, S., Feng, M., Wang, W., et al. (2019). The protective role of microRNA-21 against coxsackievirus B3 infection through targeting the MAP2K3/P38 MAPK signaling pathway. *J. Transl. Med.* 17:335.

Helwak, A., Kudla, G., Dudnakova, T., and Tollervey, D. (2013). Mapping the human miRNA interactome by CLASH reveals frequent noncanonical binding. *Cell* 153, 654–665. doi: 10.1016/j.cell.2013.03.043

Hillesheim, A., Nordhoff, C., Boergeling, Y., Ludwig, S., and Wixler, V. (2014). beta-catenin promotes the type I IFN synthesis and the IFN-dependent signaling response but is suppressed by influenza A virus-induced RIG-I/NF-kappaB signaling. *Cell Commun. Signal.* 12:29. doi: 10.1186/1478-811x-12-29

Hiscott, J., Kwon, H., and Génin, P. (2001). Hostile takeovers: viral appropriation of the NF-kappaB pathway. *J. Clin. Invest.* 107, 143–151. doi: 10.1172/jci11918

Ho, B. C., Yang, P. C., and Yu, S. L. (2016). MicroRNA and pathogenesis of *Enterovirus* infection. *Viruses* 8:11. doi: 10.3390/v8010011

Hook, L. M., Grey, F., Grabski, R., Tirabassi, R., Doyle, T., Hancock, M., et al. (2014). Cytomegalovirus miRNAs target secretory pathway genes to facilitate formation of the virion assembly compartment and reduce cytokine secretion. *Cell Host Microb.* 15, 363–373. doi: 10.1016/j.chom.2014.02.004

Hooykaas, M. J. G., van Gent, M., Soppe, J. A., Kruse, E., Boer, I. G. J., van Leenen, D., et al. (2017). EBV MicroRNA BART16 Suppresses Type I IFN Signaling. *J. Immunol.* 198, 4062–4073. doi: 10.4049/jimmunol.1501605

Houzet, L., Yeung, M. L., de Lame, V., Desai, D., Smith, S. M., and Jeang, K. T. (2008). MicroRNA profile changes in human immunodeficiency virus type 1 (HIV-1) seropositive individuals. *Retrovirology* 5:118. doi: 10.1186/1742-4690-5-118

Hu, Y., Lan, W., and Miller, D. (2017). Next-generation sequencing for MicroRNA expression profile. *Methods Mol. Biol.* 1617, 169–177. doi: 10.1007/978-1-4939-7046-9_12

Huang, Q., Chen, L., Luo, M., Lv, H., Luo, D., Li, T., et al. (2018). HIV-1-Induced miR-146a attenuates monocyte migration by targeting CCL5 in human primary macrophages. *AIDS Rese. Hum. Retrovir.* 34, 580–589. doi: 10.1089/aid.2017.0217

Huang, R., Wu, J., Zhou, X., Jiang, H., Guoying Zhou, G., and Roizman, B. (2019). Herpes simplex virus 1 MicroRNA miR-H28 exported to uninfected cells

in exosomes restricts cell-to-cell virus spread by inducing gamma interferon mRNA. *J. Virol.* 93:e01005-19.

Huang, S., Xie, Y., Yang, P., Chen, P., and Zhang, L. (2014). HCV core protein-induced down-regulation of microRNA-152 promoted aberrant proliferation by regulating Wnt1 in HepG2 cells. *PLoS One* 9:81730. doi: 10.1371/journal.pone.0081730

Hutvagner, G., McLachlan, J., Pasquinelli, A. E., Balint, E., Tuschl, T., and Zamore, P. D. (2001). A cellular function for the RNA-interference enzyme Dicer in the maturation of the let-7 small temporal RNA. *Science* 293, 834–838. doi: 10.1126/science.1062961

Janeway, C. A. Jr. (1989). Approaching the asymptote? Evolution and revolution in immunology. *Cold Spring Harb. Symp. Quant. Biol.* 54(Pt 1), 1–13. doi: 10.1101/sqb.1989.054.01.003

Janssen, H. L., Reesink, H. W., Lawitz, E. J., Zeuzem, S., Rodriguez-Torres, M., Patel, K., et al. (2013). Treatment of HCV infection by targeting microRNA. *New Engl. J. Med.* 368, 1685–1694.

Jarvis, M. A., Borton, J. A., Keech, A. M., Wong, J., Britt, W. J., Magun, B. E., et al. (2006). Human cytomegalovirus attenuates interleukin-1beta and tumor necrosis factor alpha proinflammatory signaling by inhibition of NF-kappaB activation. *J. Virol.* 80, 5588–5598. doi: 10.1128/jvi.00060-06

Javelle, M., and Timmermans, M. C. (2012). In situ localization of small RNAs in plants by using LNA probes. *Nat. Protoc.* 7, 533–541. doi: 10.1038/nprot.2012.006

Ji, W. T., and Liu, H. J. (2008). PI3K-Akt signaling and viral infection. *Recent Biotechnol.* 2, 218–226. doi: 10.2174/187220808786241042

Jiang, S., Zhang, H. W., Lu, M. H., He, X. H., Li, Y., Gu, H., et al. (2010). MicroRNA-155 functions as an OncomiR in breast cancer by targeting the suppressor of cytokine signaling 1 gene. *Cancer Res.* 70, 3119–3127. doi: 10.1158/0008-5472.can-09-4250

Johnson, R. A., Huong, S. M., and Huang, E. S. (2000). Activation of the mitogen-activated protein kinase p38 by human cytomegalovirus infection through two distinct pathways: a novel mechanism for activation of p38. *J. Virol.* 74, 1158–1167. doi: 10.1128/jvi.74.3.1158-1167.2000

Jopling, C. (2012). Liver-specific microRNA-122: biogenesis and function. *RNA Biol.* 9, 137–142. doi: 10.4161/rna.18827

Jopling, C. L., Yi, M., Lancaster, A. M., Lemon, S. M., and Sarnow, P. (2005). Modulation of hepatitis C virus RNA abundance by a liver-specific MicroRNA. *Science* 309, 1577–1581. doi: 10.1126/science.1113329

Kai, K., Dittmar, R. L., and Sen, S. (2018). Secretory microRNAs as biomarkers of cancer. *Semin. Cell Dev. Biol.* 78, 22–36. doi: 10.1016/j.semcdb.2017.12.011

Kalluri, R., and Weinberg, R. A. (2009). The basics of epithelial-mesenchymal transition. *J. Clin. Invest.* 119, 1420–1428. doi: 10.1172/jci39104

Karin, M. (2006). Nuclear factor-kappaB in cancer development and progression. *Nature* 441, 431–436. doi: 10.1038/nature04870

Karin, M., Cao, Y., Greten, F. R., and Li, Z. W. (2002). NF-kappaB in cancer: from innocent bystander to major culprit. *Nat. Rev. Cancer.* 2, 301–310. doi: 10.1038/nrc780

Kaufman, H. L., Kohlhapp, F. J., and Zloza, A. (2015). Oncolytic viruses: a new class of immunotherapy drugs. *Nat. Rev. Drug Discov.* 14, 642–662. doi: 10.1038/nrd4663

Kelly, E. J., Hadac, E. M., Greiner, S., and Russell, S. J. (2008). Engineering microRNA responsiveness to decrease virus pathogenicity. *Nat. Med.* 14, 1278–1283. doi: 10.1038/nm.1776

Ketting, R. F. (2010). MicroRNA biogenesis and function. An overview. *Adv. Exp. Med. Biol.* 700, 1–14. doi: 10.1007/978-1-4419-7823-3_1

Ketting, R. F., Fischer, S. E., Bernstein, E., Sijen, T., Hannon, G. J., and Plasterk, R. H. (2001). Dicer functions in RNA interference and in synthesis of small RNA involved in developmental timing in C. *elegans*. *Genes Dev.* 15, 2654–2659. doi: 10.1101/gad.927801

Khan, K. A., Dô, F., Marineau, A., Doyon, P., Clément, J.-F., Woodgett, J. R., et al. (2015). Fine-tuning of the RIG-I-Like receptor/interferon regulatory factor 3-dependent antiviral innate immune response by the glycogen synthase kinase 3/β-catenin pathway. *Mol. Cell. Biol.* 35, 3029–3043. doi: 10.1128/mcb.00344-15

Kim, N. H., Kim, H. S., Kim, N.-G., Lee, I., Choi, H.-S., Li, X.-Y., et al. (2011). p53 and MicroRNA-34 are suppressors of canonical Wnt signaling. *Sci. Signal.* 4:ra71. doi: 10.1126/scisignal.2001744

Kim, S. H., Juhnn, Y. S., Kang, S., Park, S. W., Sung, M. W., Bang, Y. J., et al. (2006). Human papillomavirus 16 E5 up-regulates the expression of vascular endothelial growth factor through the activation of epidermal growth factor receptor. MEK/ ERK1,2 and PI3K/Akt. *Cell Mol. Life Sci.* 63, 930–938. doi: 10.1007/s00018-005-5561-x

Knight, S. W., and Bass, B. L. (2001). A role for the RNase III enzyme DCR-1 in RNA interference and germ line development in *Caenorhabditis elegans*. *Science* 293, 2269–2271. doi: 10.1126/science.1062039

Komiya, Y., and Habas, R. (2008). Wnt signal transduction pathways. *Organogenesis* 4, 68–75. doi: 10.4161/org.4.2.5851

Kopan, R. (2012). Notch signaling. *Cold Spring Harb. Perspect. Biol.* 4:a011213.

Kozomara, A., Birgaoanu, M., and Griffiths-Jones, S. (2018). miRBase: from microRNA sequences to function. *Nucleic Acids Res.* 47, D155–D162.

Kreth, S., Hübner, M., and Hinske, L. C. (2018). MicroRNAs as clinical biomarkers and therapeutic tools in perioperative medicine. *A. Analgesia* 126, 670–681. doi: 10.1213/ane.0000000000002444

Krol, J., Loedige, I., and Filipowicz, W. (2010). The widespread regulation of microRNA biogenesis, function and decay. *Nat. Rev. Genet.* 11, 597–610. doi: 10.1038/nrg2843

Kruszka, K., Pacak, A., Swida-Barteczka, A., Nuc, P., Alaba, S., Wroblewska, Z., et al. (2014). Transcriptionally and post-transcriptionally regulated microRNAs in heat stress response in barley. *J. Exp. Bot.* 65, 6123–6135. doi: 10.1093/jxb/eru353

Lanford, R. E., Hildebrandt-Eriksen, E. S., Petri, A., Persson, R., Lindow, M., Munk, M. E., et al. (2010). Therapeutic silencing of microRNA-122 in primates with chronic hepatitis C virus infection. *Science* 327, 198–201. doi: 10.1126/science.1178178

Langroudi, L., Jamshidi-Adegani, F., Shafiee, A., Hosseini Rad, S. M. A., Keramati, F., Azadmanesh, K., et al. (2015). MiR-371-373 cluster acts as a tumor-suppressor-miR and promotes cell cycle arrest in unrestricted somatic stem cells. *Tumour Biol.* 36, 7765–7774. doi: 10.1007/s13277-015-3519-7

Lau, B., Poole, E., Krishna, B., Sellart, I., Wills, M. R., Murphy, E., et al. (2016). The Expression of human cytomegalovirus MicroRNA MiR-UL148D during latent infection in primary myeloid cells inhibits activin A-triggered secretion of IL-6. *Sci. Rep.* 6:31205.

Lee, R. C., Feinbaum, R. L., and Ambros, V. (1993). elegans heterochronic gene lin-4 encodes small RNAs with antisense complementarity to lin-14. *Cell* 75, 843–854. doi: 10.1016/0092-8674(93)90529-y

Lee, Y., Kim, M., Han, J., Yeom, K. H., Lee, S., Baek, S. H., et al. (2004). MicroRNA genes are transcribed by RNA polymerase II. *EMBO J.* 23, 4051–4060. doi: 10.1038/sj.emboj.7600385

Lei, T., Yuen, K. S., Xu, R., Tsao, S. W., Chen, H., Li, M., et al. (2013). Targeting of DICE1 tumor suppressor by epstein-barr virus-encoded miR-BART3* microRNA in nasopharyngeal carcinoma. *Int. J. Cancer* 133, 79–87. doi: 10.1002/ijc.28007

Levrero, M., and Zucman-Rossi, J. (2016). Mechanisms of HBV-induced hepatocellular carcinoma. *J. Hepatol.* 64 1(Suppl.), S84–S101.

Li, A., Song, W., Qian, J., Li, Y., He, J., Zhang, Q., et al. (2013). MiR-122 modulates type I interferon expression through blocking suppressor of cytokine signaling 1. *Int. J. Biochem. Cell Biol.* 45, 858–865. doi: 10.1016/j.biocel.2013.01.008

Li, H.-C., and Lo, S.-Y. (2015). Hepatitis C virus: virology, diagnosis and treatment. *World J. Hepatol.* 7, 1377–1389.

Li, Q., Feng, Y., Chao, X., Shi, S., Liang, M., Qiao, Y., et al. (2018). HOTAIR contributes to cell proliferation and metastasis of cervical cancer via targetting miR-23b/MAPK1 axis. *Biosci. Rep.* 38:BSR20171563.

Li, W., Liang, J., Zhang, Z., Lou, H., Zhao, L., Xu, Y., et al. (2017). MicroRNA-329-3p targets MAPK1 to suppress cell proliferation, migration and invasion in cervical cancer. *Oncol. Rep.* 37, 2743–2750. doi: 10.3892/or.2017.5555

Li, Z., and Rana, T. M. (2014). Therapeutic targeting of microRNAs: current status and future challenges. *Nat. Rev. Drug Discov.* 13, 622–638. doi: 10.1038/nrd4359

Liu, K., Li, X., Cao, Y., Ge, Y., Wang, J., and Shi, B. (2015). MiR-132 inhibits cell proliferation, invasion and migration of hepatocellular carcinoma by targeting PIK3R3. *Int. J. Oncol.* 47, 1585–1593. doi: 10.3892/ijo.2015.3112

Liu, T., Zhang, L., Joo, D., and Sun, S.-C. (2017). NF-κB signaling in inflammation. *Signal. Trans. Target. Ther.* 2:17023.

Ludwig, S., Ehrhardt, C., Neumeier, E., Kracht, M., Rapp, U. R., and Pleschka, S. (2001). Influenza virus-induced AP-1-dependent gene expression requires activation of the JNK signaling pathway. *J. Biol. Chem.* 276, 10990–10998. doi: 10.1074/jbc.m009902200

Ludwig, S., Pleschka, S., Planz, O., and Wolff, T. (2006). Ringing the alarm bells: signalling and apoptosis in influenza virus infected cells. *Cell. Microbiol.* 8, 375–386. doi: 10.1111/j.1462-5822.2005.00678.x

Lundquist, C. A., Tobiume, M., Zhou, J., Unutmaz, D., and Aiken, C. (2002). Nef-mediated downregulation of CD4 enhances human immunodeficiency virus type 1 replication in primary T lymphocytes. *J. Virol.* 76, 4625–4633. doi: 10.1128/jvi.76.9.4625-4633.2002

Luoni, A., and Riva, M. A. (2016). MicroRNAs and psychiatric disorders: from aetiology to treatment. *Pharmacol. Ther.* 167, 13–27. doi: 10.1016/j.pharmthera.2016.07.006

Ma, X., Becker Buscaglia, L. E., Barker, J. R., and Li, Y. (2011). MicroRNAs in NF-kappaB signaling. *J. Mol. Cell Biol.* 3, 159–166.

Macfarlane, L. A., and Murphy, P. R. (2010). MicroRNA: biogenesis. Function and role in cancer. *Curr. Genom.* 11, 537–561. doi: 10.2174/138920210793175895

Marquitz, A. R., Mathur, A., Nam, C. S., and Raab-Traub, N. (2011). The epstein-barr virus BART microRNAs target the pro-apoptotic protein Bim. *Virology* 412, 392–400. doi: 10.1016/j.virol.2011.01.028

Marsh, M., and Helenius, A. (2006). Virus entry: open sesame. *Cell* 124, 729–740. doi: 10.1016/j.cell.2006.02.007

Masaki, T., Arend, K. C., Li, Y., Yamane, D., McGivern, D. R., Kato, T., et al. (2015). miR-122 stimulates hepatitis C virus RNA synthesis by altering the balance of viral RNAs engaged in replication versus translation. *Cell Host Microb.* 17, 217–228. doi: 10.1016/j.chom.2014.12.014

Maurer, U. E., Sodeik, B., and Grunewald, K. (2008). Native 3D intermediates of membrane fusion in herpes simplex virus 1 entry. *Proc. Natl. Acad. Sci. U.S.A.* 105, 10559–10564. doi: 10.1073/pnas.0801674105

McCaskill, J., Ressel, S., Alber, A., Redford, J., Power, U., Schwarze, J., et al. (2017). Broad-spectrum inhibition of respiratory virus infection by MicroRNA mimics targeting p38 MAPK signaling. *Mol. Ther. Nucleic Acids* 7, 256–266. doi: 10.1016/j.omtn.2017.03.008

Mei, J., Wang, D. H., Wang, L. L., Chen, Q., Pan, L. L., and Xia, L. (2018). MicroRNA-200c suppressed cervical cancer cell metastasis and growth via targeting MAP4K4. *Eur. Rev. Med. Pharmacol. Sci.* 22, 623–631.

Menges, C. W., Baglia, L. A., Lapoint, R., and McCance, D. J. (2006). Human papillomavirus type 16 E7 up-regulates AKT activity through the retinoblastoma protein. *Cancer Res.* 66, 5555–5559. doi: 10.1158/0008-5472.can-06-0499

Minor, P. D. (2015). Live attenuated vaccines: historical successes and current challenges. *Virology* 47, 379–392. doi: 10.1016/j.virol.2015.03.032

miRBase (2018). *miRBase: The Microrna Database*. Available online at: http://www.mirbase.org/ (accessed November 2019).

Mui, U. N., Haley, C. T., and Tyring, S. K. (2017). Viral oncology: molecular biology and pathogenesis. *J. Clin. Med.* 6:111. doi: 10.3390/jcm6120111

Mukherjee, A., Di Bisceglie, A. M., and Ray, R. B. (2015). Hepatitis C virus-mediated enhancement of microRNA miR-373 impairs the JAK/STAT signaling pathway. *J. Virol.* 89, 3356–3365. doi: 10.1128/jvi.03085-14

Nachmani, D., Lankry, D., Wolf, D. G., and Mandelboim, O. (2010). The human cytomegalovirus microRNA miR-UL112 acts synergistically with a cellular microRNA to escape immune elimination. *Nat. Immunol.* 11, 806–813. doi: 10.1038/ni.1916

Nachmani, D., Stern-Ginossar, N., Sarid, R., and Mandelboim, O. (2009). Diverse herpesvirus microRNAs target the stress-induced immune ligand MICB to escape recognition by natural killer cells. *Cell Host Microb.* 5, 376–385. doi: 10.1016/j.chom.2009.03.003

Nelson, A., Fingleton, B., Rothenberg, M., and Matrisian, L. (2000). Matrix metalloproteinases: biologic activity and clinical implications. *J. Clin. Oncol.* 18:1135. doi: 10.1200/jco.2000.18.5.1135

Nicoll, M. P., Proenca, J. T., Connor, V., and Efstathiou, S. (2012). Influence of herpes simplex virus 1 latency-associated transcripts on the establishment and maintenance of latency in the ROSA26R reporter mouse model. *J. Virol.* 86, 8848–8858. doi: 10.1128/jvi.00652-12

Nobre, R. J., Herraez-Hernandez, E., Fei, J. W., Langbein, L., Kaden, S., Grone, H. J., et al. (2009). E7 oncoprotein of novel human papillomavirus type 108 lacking the E6 gene induces dysplasia in organotypic keratinocyte cultures. *J. Virol.* 83, 2907–2916. doi: 10.1128/jvi.02490-08

O'Brien, J., Hayder, H., Zayed, Y., and Peng, C. (2018). Overview of MicroRNA biogenesis. mechanisms of actions, and circulation. *Front. Endocrinol.* 9:402. doi: 10.3389/fendo.2018.00402

O'Connor, C. M., Vanicek, J., and Murphy, E. A. (2014). Host microRNA regulation of human cytomegalovirus immediate early protein translation promotes viral latency. *J. Virol.* 88, 5524–5532. doi: 10.1128/jvi.00481-14

Omoto, S., Ito, M., Tsutsumi, Y., Ichikawa, Y., Okuyama, H., Brisibe, E. A., et al. (2004). HIV-1 nef suppression by virally encoded microRNA. *Retrovirology* 1:44.

Ouellet, D. L., Vigneault-Edwards, J., Létourneau, K., Gobeil, L.-A., Plante, I., Burnett, J. C., et al. (2013). Regulation of host gene expression by HIV-1 TAR microRNAs. *Retrovirology* 10, 86. doi: 10.1186/1742-4690-10-86

Pacak, A., Barciszewska-Pacak, M., Swida-Barteczka, A., Kruszka, K., Sega, P., Milanowska, K., et al. (2016). Heat stress affects pi-related genes expression and inorganic phosphate deposition/accumulation in barley. *Front. Plant Sci.* 7:926. doi: 10.3389/fpls.2016.00926

Paik, J. H., Jang, J. Y., Jeon, Y. K., Kim, W. Y., Kim, T. M., Heo, D. S., et al. (2011). MicroRNA-146a downregulates NFkappaB activity via targeting TRAF6 and functions as a tumor suppressor having strong prognostic implications in NK/T cell lymphoma. *Clin. Cancer Res.* 17, 4761–4771. doi: 10.1158/1078-0432.ccr-11-0494

Pall, G. S., and Hamilton, A. J. (2008). Improved northern blot method for enhanced detection of small RNA. *Nat. Protoc.* 3, 1077–1084. doi: 10.1038/nprot.2008.67

Pan, D., Flores, O., Umbach, J. L., Pesola, J. M., Bentley, P., Rosato, P. C., et al. (2014). A neuron-specific host microRNA targets herpes simplex virus-1 ICP0 expression and promotes latency. *Cell Host Microb.* 15, 446–456. doi: 10.1016/j.chom.2014.03.004

Pearson, G., Robinson, F., Gibson, T., Xu, B. E., Karandikar, M., Berman, K., et al. (2001). Mitogen-activated protein (MAP) kinase pathways: regulation and physiological functions 1. *Endocr. Rev.* 22, 153–183. doi: 10.1210/er.22.2.153

Peng, S., Wang, J., Wei, S., Li, C., Zhou, K., Hu, J., et al. (2018). Endogenous cellular MicroRNAs mediate antiviral defense against influenza A virus. *Mol. Ther. Nucleic Acids* 10, 361–375. doi: 10.1016/j.omtn.2017.12.016

Perng, G. C., Dunkel, E. C., Geary, P. A., Slanina, S. M., Ghiasi, H., Kaiwar, R., et al. (1994). The latency-associated transcript gene of herpes simplex virus type 1 (HSV-1) is required for efficient in vivo spontaneous reactivation of HSV-1 from latency. *J. Virol.* 68, 8045–8055. doi: 10.1128/jvi.68.12.8045-8055.1994

Pfeffer, S., Zavolan, M., Grasser, F. A., Chien, M., Russo, J. J., Ju, J., et al. (2004). Identification of virus-encoded microRNAs. *Science* 304, 734–736. doi: 10.1126/science.1096781

Pichiorri, F., Suh, S. S., Ladetto, M., Kuehl, M., Palumbo, T., Drandi, D., et al. (2008). MicroRNAs regulate critical genes associated with multiple myeloma pathogenesis. *Proc. Natl. Acad. Sci. U.S.A.* 105, 12885–12890. doi: 10.1073/pnas.0806202105

Piedade, D., and Azevedo-Pereira, J. M. (2016). The Role of microRNAs in the pathogenesis of *Herpesvirus* infection. *Viruses* 8:156. doi: 10.3390/v8060156

Piganis, R. A., De Weerd, N. A., Gould, J. A., Schindler, C. W., Mansell, A., Nicholson, S. E., et al. (2011). Suppressor of cytokine signaling (SOCS) 1 inhibits type I interferon (IFN) signaling via the interferon alpha receptor (IFNAR1)-associated tyrosine kinase Tyk2. *J. Biol. Chem.* 286, 33811–33818. doi: 10.1074/jbc.m111.270207

Poy, M. N., Eliasson, L., Krutzfeldt, J., Kuwajima, S., Ma, X., Macdonald, P. E., et al. (2004). A pancreatic islet-specific microRNA regulates insulin secretion. *Nature* 432, 226–230. doi: 10.1038/nature03076

Prusty, B. K., and Das, B. C. (2005). Constitutive activation of transcription factor AP-1 in cervical cancer and suppression of human papillomavirus (HPV) transcription and AP-1 activity in HeLa cells by curcumin. *Int. J. Cancer.* 113, 951–960. doi: 10.1002/ijc.20668

Randall, G., Lagunoff, M., and Roizman, B. (2000). Herpes simplex virus 1 open reading frames O and P are not necessary for establishment of latent infection in mice. *J. Virol.* 74, 9019–9027. doi: 10.1128/jvi.74.19.9019-9027.2000

Rehermann, B., and Nascimbeni, M. (2005). Immunology of hepatitis B virus and hepatitis C virus infection. *Nat. Rev. Immunol.* 5, 215–229.

Reinhart, B. J., Slack, F. J., Basson, M., Pasquinelli, A. E., Bettinger, J. C., Rougvie, A. E., et al. (2000). The 21-nucleotide let-7 RNA regulates developmental timing in *Caenorhabditis elegans*. *Nature* 403, 901–906. doi: 10.1038/35002607

Ribeiro, J., and Sousa, H. (2014). MicroRNAs as biomarkers of cervical cancer development: a literature review on miR-125b and miR-34a. *Mol. Biol. Rep.* 41, 1525–1531. doi: 10.1007/s11033-013-2998-0

Roberts, A. P., Lewis, A. P., and Jopling, C. L. (2011). The role of microRNAs in viral infection. *Prog. Mol. Biol. Transl. Sci.* 102, 101–139. doi: 10.1016/b978-0-12-415795-8.00002-7

Rodon, J., Dienstmann, R., Serra, V., and Tabernero, J. (2013). Development of PI3K inhibitors: lessons learned from early clinical trials. *Nat. Rev. Clin. Oncol.* 10, 143–153. doi: 10.1038/nrclinonc.2013.10

Ruelas, D. S., Chan, J. K., Oh, E., Heidersbach, A. J., Hebbeler, A. M., Chavez, L., et al. (2015). MicroRNA-155 reinforces HIV latency. *J. Biol. Chem.* 290, 13736–13748. doi: 10.1074/jbc.m115.641837

Ryseck, R. P., Novotny, J., and Bravo, R. (1995). Characterization of elements determining the dimerization properties of RelB and p50. *Mol. Cell Biol.* 15, 3100–3109. doi: 10.1128/mcb.15.6.3100

Sanchez-Del Cojo, M., Lopez-Huertas, M. R., Diez-Fuertes, F., Rodriguez-Mora, S., Bermejo, M., Lopez-Campos, G., et al. (2017). Changes in the cellular microRNA profile by the intracellular expression of HIV-1 Tat regulator: a potential mechanism for resistance to apoptosis and impaired proliferation in HIV-1 infected CD4+ T cells. *PLoS One* 12:e0185677. doi: 10.1371/journal.pone.0185677

Sand, M. (2014). The pathway of miRNA maturation. *Methods Mol. Biol.* 1095, 3–10. doi: 10.1007/978-1-62703-703-7_1

Sardo, L., Vakil, P. R., Elbezanti, W., El-Sayed, A., and Klase, Z. (2016). The inhibition of microRNAs by HIV-1 Tat suppresses beta catenin activity in astrocytes. *Retrovirology* 13:25.

Sarma, N. J., Tiriveedhi, V., Subramanian, V., Shenoy, S., Crippin, J. S., Chapman, W. C., et al. (2012). Hepatitis C virus mediated changes in miRNA-449a modulates inflammatory biomarker YKL40 through components of the NOTCH signaling pathway. *PLoS One* 7:e50826. doi: 10.1371/journal.pone.0050826

Sayed, D., and Abdellatif, M. (2011). MicroRNAs in development and disease. *Physiol .Rev.* 91, 827–887.

Scarborough, R. J., and Gatignol, A. (2017). RNA Interference therapies for an HIV-1 functional cure. *Viruses.* 10:8. doi: 10.3390/v10010008

Scheel, T. K., Luna, J. M., Liniger, M., Nishiuchi, E., Rozen-Gagnon, K., Shlomai, A., et al. (2016). A broad RNA virus survey reveals both miRNA dependence and functional sequestration. *Cell Host Microb.* 19, 409–423. doi: 10.1016/j.chom.2016.02.007

Sen, G. C. (2001). Viruses and interferons. *Annu. Rev. Microbiol.* 55, 255–281. doi: 10.1146/annurev.micro.55.1.255

Seok, H., Ham, J., Jang, E. S., and Chi, S. W. (2016). MicroRNA target recognition: insights from transcriptome-wide non-canonical interactions. *Mol. Cells.* 39, 375–381. doi: 10.14348/molcells.2016.0013

Shannon-Lowe, C., Rickinson, A. B., and Bell, A. I. (2017). Epstein-Barr virus-associated lymphomas. *Philos. Trans. R. Soc. Lond. Ser. B Biol. Sci.* 372:20160271.

Sharma, N., Verma, R., Kumawat, K. L., Basu, A., and Singh, S. K. (2015). miR-146a suppresses cellular immune response during Japanese encephalitis virus JaOArS982 strain infection in human microglial cells. *J. Neuroinflamm.* 12:30. doi: 10.1186/s12974-015-0249-0

Shen, Y. H., Zhang, L., Utama, B., Wang, J., Gan, Y., Wang, X., et al. (2006). Human cytomegalovirus inhibits Akt-mediated eNOS activation through upregulating PTEN (phosphatase and tensin homolog deleted on chromosome 10). *Cardiovasc. Res.* 69, 502–511. doi: 10.1016/j.cardiores.2005.10.007

Shih, C., Chou, S. F., Yang, C. C., Huang, J. Y., Choijilsuren, G., and Jhou, R. S. (2016). Control and Eradication strategies of hepatitis B virus. *Trends Microbiol.* 24, 739–749. doi: 10.1016/j.tim.2016.05.006

Shimakami, T., Yamane, D., Jangra, R. K., Kempf, B. J., Spaniel, C., Barton, D. J., et al. (2012). Stabilization of hepatitis C virus RNA by an Ago2-miR-122 complex. *Proc. Natl. Acad. Sci. U.S.A.* 109, 941–946. doi: 10.1073/pnas.1112263109

Shishodia, G., Verma, G., Srivastava, Y., Mehrotra, R., Das, B. C., and Bharti, A. C. (2014). Deregulation of microRNAs Let-7a and miR-21 mediate aberrant STAT3 signaling during human papillomavirus-induced cervical carcinogenesis: role of E6 oncoprotein. *BMC Cancer* 14:996. doi: 10.1186/1471-2407-14-996

Shwetha, S., Gouthamchandra, K., Chandra, M., Ravishankar, B., Khaja, M. N., and Das, S. (2013). Circulating miRNA profile in HCV infected serum: novel insight into pathogenesis. *Sci. Rep.* 3:1555.

Silvestri, G., and Feinberg, M. B. (2003). Turnover of lymphocytes and conceptual paradigms in HIV infection. *J. Clin. Invest.* 112, 821–824. doi: 10.1172/jci19799

Slonchak, A., Shannon, R. P., Pali, G., and Khromykh, A. A. (2015). Human MicroRNA miR-532-5p exhibits antiviral activity against west nile virus via suppression of host genes SESTD1 and TAB3 required for virus replication. *J. Virol.* 90, 2388–2402. doi: 10.1128/jvi.02608-15

Smith, J. L., Jeng, S., McWeeney, S. K., and Hirsch, A. J. (2017). A MicroRNA screen identifies the wnt signaling pathway as a regulator of the interferon response during *Flavivirus* Infection. *J. Virol.* 91:e2388-16.

Smoczynska, A., Sega, P., Stepien, A., Knop, K., Jarmolowski, A., Pacak, A., et al. (2019). miRNA Detection by Stem-Loop RT-qPCR in Studying microRNA Biogenesis and microRNA Responsiveness to Abiotic Stresses. *Methods Mol. Biol.* 1932, 131–150. doi: 10.1007/978-1-4939-9042-9_10

Sodeik, B. (2000). Mechanisms of viral transport in the cytoplasm. *Trends Microbiol.* 8, 465–472. doi: 10.1016/s0966-842x(00)01824-2

Sodeik, B. (2002). Unchain my heart, baby let me go–the entry and intracellular transport of HIV. *J. Cell Biol.* 159, 393–395. doi: 10.1083/jcb.200210024

Sodeik, B., Ebersold, M. W., and Helenius, A. (1997). Microtubule-mediated transport of incoming herpes simplex virus 1 capsids to the nucleus. *J. Cell Biol.* 136, 1007–1021. doi: 10.1083/jcb.136.5.1007

Stern-Ginossar, N., Elefant, N., Zimmermann, A., Wolf, D. G., Saleh, N., Biton, M., et al. (2007). Host immune system gene targeting by a viral miRNA. *Science* 317, 376–381. doi: 10.1126/science.1140956

Stubenrauch, F., Straub, E., Fertey, J., and Iftner, T. (2007). The E8 repression domain can replace the E2 transactivation domain for growth inhibition of HeLa cells by papillomavirus E2 proteins. *Int. J. Cancer* 121, 2284–2292. doi: 10.1002/ijc.22907

Su, C., Hou, Z., Zhang, C., Tian, Z., and Zhang, J. (2011). Ectopic expression of microRNA-155 enhances innate antiviral immunity against HBV infection in human hepatoma cells. *Virol. J.* 8:354. doi: 10.1186/1743-422x-8-354

Taganov, K. D., Boldin, M. P., Chang, K.-J., and Baltimore, D. (2006). NF-kappaB-dependent induction of microRNA miR-146, an inhibitor targeted to signaling proteins of innate immune responses. *Proc. Nat. Acad. Sci. U.S.A.* 103, 12481–12486. doi: 10.1073/pnas.0605298103

Tang, S., Bertke, A. S., Patel, A., Wang, K., Cohen, J. I., and Krause, P. R. (2008). An acutely and latently expressed herpes simplex virus 2 viral microRNA inhibits expression of ICP34.5, a viral neurovirulence factor. *Proc. Nat. Acad. Sci. U.S.A.* 105, 10931–10936. doi: 10.1073/pnas.0801845105

Tang, S., Patel, A., and Krause, P. R. (2009). Novel less-abundant viral microRNAs encoded by herpes simplex virus 2 latency-associated transcript and their roles in regulating ICP34.5 and ICP0 mRNAs. *J. Virol.* 83, 1433–1442. doi: 10.1128/jvi.01723-08

Thorley-Lawson, D. A., Hawkins, J. B., Tracy, S. I., and Shapiro, M. (2013). The pathogenesis of Epstein-Barr virus persistent infection. *Curr. Opin. Virol.* 3, 227–232. doi: 10.1016/j.coviro.2013.04.005

Trang, P., Medina, P. P., Wiggins, J. F., Ruffino, L., Kelnar, K., Omotola, M., et al. (2010). Regression of murine lung tumors by the let-7 microRNA. *Oncogene* 29, 1580–1587. doi: 10.1038/onc.2009.445

Trionfini, P., Benigni, A., and Remuzzi, G. (2015). MicroRNAs in kidney physiology and disease. *Nat. Rev. Nephrol.* 11, 23–33. doi: 10.1038/nrneph.2014.202

Trobaugh, D. W., Gardner, C. L., Sun, C., Haddow, A. D., Wang, E., Chapnik, E., et al. (2014). RNA viruses can hijack vertebrate microRNAs to suppress innate immunity. *Nature* 506, 245–248. doi: 10.1038/nature12869

Turchinovich, A., Samatov, T. R., Tonevitsky, A. G., and Burwinkel, B. (2013). Circulating miRNAs: cell-cell communication function? *Front. Genet.* 4:119. doi: 10.3389/fgene.2013.00119

Turchinovich, A., Weiz, L., and Burwinkel, B. (2012). Extracellular miRNAs: the mystery of their origin and function. *Trends Biochem. Sci.* 37, 460–465. doi: 10.1016/j.tibs.2012.08.003

Tycowski, K. T., Guo, Y. E., Lee, N., Moss, W. N., Vallery, T. K., Xie, M., et al. (2015). Viral noncoding RNAs: more surprises. *Genes Dev.* 29, 567–584. doi: 10.1101/gad.259077.115

Ullmann, P., Rodriguez, F., Schmitz, M., Meurer, S. K., Qureshi-Baig, K., Felten, P., et al. (2018). The miR-371 approximately 373 cluster represses colon cancer

initiation and metastatic colonization by inhibiting the TGFBR2/ID1 signaling axis. 78, 3793–3808. doi: 10.1158/0008-5472.can-17-3003

Umbach, J. L., and Cullen, B. R. (2009). The role of RNAi and microRNAs in animal virus replication and antiviral immunity. *Genes Dev.* 23, 1151–1164. doi: 10.1101/gad.1793309

Umbach, J. L., Kramer, M. F., Jurak, I., Karnowski, H. W., Coen, D. M., and Cullen, B. R. (2008). MicroRNAs expressed by herpes simplex virus 1 during latent infection regulate viral mRNAs. *Nature* 454, 780–783. doi: 10.1038/nature07103

Umbach, J. L., Nagel, M. A., Cohrs, R. J., Gilden, D. H., and Cullen, B. R. (2009). Analysis of human alphaherpesvirus microRNA expression in latently infected human trigeminal ganglia. *J. Virol.* 83, 10677–10683. doi: 10.1128/jvi.01185-09

Ura, S., Honda, M., Yamashita, T., Ueda, T., Takatori, H., Nishino, R., et al. (2009). Differential microRNA expression between hepatitis B and hepatitis C leading disease progression to hepatocellular carcinoma. *Hepatology* 49, 1098–1112. doi: 10.1002/hep.22749

van der Ree, M. H., de Vree, J. M., Stelma, F., Willemse, S., van der Valk, M., Rietdijk, S., et al. (2017). Safety, tolerability, and antiviral effect of RG-101 in patients with chronic hepatitis C: a phase 1B, double-blind, randomised controlled trial. *Lancet* 389, 709–717. doi: 10.1016/s0140-6736(16)31715-9

van der Ree, M. H., van der Meer, A. J., de Bruijne, J., Maan, R., van Vliet, A., Welzel, T. M., et al. (2014). Long-term safety and efficacy of microRNA-targeted therapy in chronic hepatitis C patients. *Antivir. Res.* 111, 53–59. doi: 10.1016/j.antiviral.2014.08.015

van der Ree, M. H., van der Meer, A. J., van Nuenen, A. C., de Bruijne, J., Ottosen, S., Janssen, H. L., et al. (2016). Miravirsen dosing in chronic hepatitis C patients results in decreased microRNA-122 levels without affecting other microRNAs in plasma. *Aliment. Pharmacol. Therapeut.* 43, 102–113. doi: 10.1111/apt.13432

Varallyay, E., Burgyan, J., and Havelda, Z. (2007). Detection of microRNAs by Northern blot analyses using LNA probes. *Methods* 43, 140–145. doi: 10.1016/j.ymeth.2007.04.004

Varani, S., and Landini, M. P. (2011). Cytomegalovirus-induced immunopathology and its clinical consequences. *Herpesviridae* 2:6. doi: 10.1186/2042-4280-2-6

Verheyen, E. M., and Gottardi, C. J. (2010). Regulation of Wnt/beta-catenin signaling by protein kinases. *Dev. Dyn.* 239, 34–44.

Wagner, E., and Bloom, D. (1997). Experimental investigation of HSV latency. *Clin. Microbiol. Rev.* 10, 419–443.

Wagner, E. K., Devi-Rao, G., Feldman, L. T., Dobson, A. T., Zhang, Y. F., Flanagan, W. M., et al. (1988). Physical characterization of the herpes simplex virus latency-associated transcript in neurons. *J. Virol.* 62, 1194–1202. doi: 10.1128/jvi.62.4.1194-1202.1988

Wahid, F., Shehzad, A., Khan, T., and Kim, Y. Y. (2010). MicroRNAs: synthesis, mechanism, function, and recent clinical trials. *Biochim. Biophys. Acta.* 1803, 1231–1243. doi: 10.1016/j.bbamcr.2010.06.013

Wang, H., Gao, H., Duan, S., and Song, X. (2015). Inhibition of microRNA-199a-5p reduces the replication of HCV via regulating the pro-survival pathway. *Virus Res.* 208, 7–12. doi: 10.1016/j.virusres.2015.05.002

Wang, J., Chen, J., and Sen, S. (2016). MicroRNA as biomarkers and diagnostics. *J. Cell Physiol.* 231, 25–30. doi: 10.1002/jcp.25056

Wang, J.-Y., and Chen, L.-J. (2019). The role of miRNAs in the invasion and metastasis of cervical cancer. *Biosci. Rep.* 39:BSR20181377.

Wang, P., Hou, J., Lin, L., Wang, C., Liu, X., Li, D., et al. (2010). Inducible microRNA-155 feedback promotes type I IFN signaling in antiviral innate immunity by targeting suppressor of cytokine signaling 1. *J. Immunol.* 185, 6226–6233. doi: 10.4049/jimmunol.1000491

Wang, S., Qiu, L., Yan, X., Jin, W., Wang, Y., Chen, L., et al. (2012). Loss of microRNA 122 expression in patients with hepatitis B enhances hepatitis B virus replication through cyclin G(1) -modulated P53 activity. *Hepatology* 55, 730–741. doi: 10.1002/hep.24809

Wang, S.-C., Lin, X.-L., Li, J., Zhang, T.-T., Wang, H.-Y., Shi, J.-W., et al. (2014). MicroRNA-122 triggers mesenchymal-epithelial transition and suppresses hepatocellular carcinoma cell motility and invasion by targeting RhoA. *PLoS One* 9:e101330. doi: 10.1371/journal.pone.0101330

Wang, X., Tong, Y., and Wang, S. (2010). Rapid and accurate detection of plant miRNAs by liquid northern hybridization. *Int. J. Mol. Sci.* 11, 3138–3148. doi: 10.3390/ijms11093138

Wang, Y., Guo, Z., Shu, Y., Zhou, H., Wang, H., and Zhang, W. (2017). BART miRNAs: an unimaginable force in the development of nasopharyngeal carcinoma. *Eur. J. Cancer Prev.* 26, 144–150. doi: 10.1097/cej.0000000000000221

Wang, Y., Lu, Y., Toh, S. T., Sung, W. K., Tan, P., Chow, P., et al. (2010). Lethal-7 is down-regulated by the hepatitis B virus x protein and targets signal transducer and activator of transcription 3. *J. Hepatol.* 53, 57–66. doi: 10.1016/j.jhep.2009.12.043

Wang, Y. D., Cai, N., Wu, X. L., Cao, H. Z., Xie, L. L., and Zheng, P. S. (2013). OCT4 promotes tumorigenesis and inhibits apoptosis of cervical cancer cells by miR-125b/BAK1 pathway. *Cell Death Dis.* 4:e760. doi: 10.1038/cddis.2013.272

Wei, F., Cao, C., Xu, X., and Wang, J. (2015). Diverse functions of miR-373 in cancer. *J. Transl. Med.* 13:162.

Wei, X., Tan, C., Tang, C., Ren, G., Xiang, T., Qiu, Z., et al. (2013). Epigenetic repression of miR-132 expression by the hepatitis B virus x protein in hepatitis B virus-related hepatocellular carcinoma. *Cell. Signal.* 25, 1037–1043. doi: 10.1016/j.cellsig.2013.01.019

Wightman, B., Ha, I., and Ruvkun, G. (1993). Posttranscriptional regulation of the heterochronic gene lin-14 by lin-4 mediates temporal pattern formation in *C. elegans*. *Cell* 75, 855–862. doi: 10.1016/0092-8674(93)90530-4

Wodarz, A., and Nusse, R. (1998). Mechanisms of Wnt signaling in development. *Annu. Rev. Cell Dev. Biol.* 14, 59–88.

Wong, A. M., Kong, K. L., Tsang, J. W., Kwong, D. L., and Guan, X. Y. (2012). Profiling of epstein-barr virus-encoded microRNAs in nasopharyngeal carcinoma reveals potential biomarkers and oncomirs. *Cancer* 118, 698–710. doi: 10.1002/cncr.26309

Wu, N., Gao, N., Fan, D., Wei, J., Zhang, J., and An, J. (2014). miR-223 inhibits dengue virus replication by negatively regulating the microtubule-destabilizing protein STMN1 in EAhy926 cells. *Microb. Infect.* 16, 911–922. doi: 10.1016/j.micinf.2014.08.011

Xia, T., O'Hara, A., Araujo, I., Barreto, J., Carvalho, E., Sapucaia, J. B., et al. (2008). EBV microRNAs in primary lymphomas and targeting of CXCL-11 by ebv-mir-BHRF1-3. *Cancer Res.* 68, 1436–1442. doi: 10.1158/0008-5472.can-07-5126

Xu, J., Zhu, X., Wu, L., Yang, R., Yang, Z., Wang, Q., et al. (2012). MicroRNA-122 suppresses cell proliferation and induces cell apoptosis in hepatocellular carcinoma by directly targeting Wnt/beta-catenin pathway. *Liver Int.* 32, 752–760. doi: 10.1111/j.1478-3231.2011.02750.x

Xu, Y., He, Q., Lu, Y., Tao, F., Zhao, L., and Ou, R. (2018). MicroRNA-218-5p inhibits cell growth and metastasis in cervical cancer via LYN/NF-κB signaling pathway. *Cancer Cell Int.* 18:198.

Xue, M., Yao, S., Hu, M., Li, W., Hao, T., Zhou, F., et al. (2014). HIV-1 Nef and KSHV oncogene K1 synergistically promote angiogenesis by inducing cellular miR-718 to regulate the PTEN/AKT/mTOR signaling pathway. *Nucleic Acids Res.* 42, 9862–9879. doi: 10.1093/nar/gku583

Yan, Q., Zhao, R., Shen, C., Wang, F., Li, W., Gao, S.-J., et al. (2018). Upregulation of MicroRNA 711 Mediates HIV-1 Vpr promotion of kaposi's sarcoma-associated herpesvirus latency and induction of pro-proliferation and pro-survival cytokines by targeting the notch/NF-κB-signaling axis. *J. Virol.* 92:e0580-18.

Yang, N. (2015). An overview of viral and nonviral delivery systems for microRNA. *Int. J. Pharm. Investig.* 5, 179–181.

Yang, P., An, H., Liu, X., Wen, M., Zheng, Y., Rui, Y., et al. (2010). The cytosolic nucleic acid sensor LRRFIP1 mediates the production of type I interferon via a beta-catenin-dependent pathway. *Nat. Immunol.* 11, 487–494. doi: 10.1038/ni.1876

Yao, R., Ma, Y. L., Liang, W., Li, H. H., Ma, Z. J., Yu, X., et al. (2012). MicroRNA-155 modulates Treg and Th17 cells differentiation and Th17 cell function by targeting SOCS1. *PLoS One* 7:e46082. doi: 10.1371/journal.pone.0046082

Yuan, Y. H., Chi, B. Z., Wen, S. H., Liang, R. P., Li, Z. M., and Qiu, J. D. (2018). Ratiometric electrochemical assay for sensitive detecting microRNA based on dual-amplification mechanism of duplex-specific nuclease and hybridization chain reaction. *Biosens. Bioelectron.* 102, 211–216. doi: 10.1016/j.bios.2017.11.030

Zhang, Y., Wei, W., Cheng, N., Wang, K., Li, B., Jiang, X., et al. (2012). Hepatitis C virus-induced up-regulation of microRNA-155 promotes hepatocarcinogenesis by activating Wnt signaling. *Hepatology* 56, 1631–1640. doi: 10.1002/hep.25849

Zhao, H., Zhang, C., Hou, G., and Song, J. (2015). MicroRNA-H4-5p encoded by HSV-1 latency-associated transcript promotes cell proliferation, invasion and cell cycle progression via p16-mediated PI3K-Akt signaling pathway in SHSY5Y cells. *Int. J. Clin. Exp. Med.* 8, 7526–7534.

Zheng, Z., Ke, X., Wang, M., He, S., Li, Q., Zheng, C., et al. (2013). Human microRNA hsa-miR-296-5p suppresses enterovirus 71 replication by targeting the viral genome. *J. Virol.* 87, 5645–5656. doi: 10.1128/jvi.02655-12

Zhu, J., Coyne, C. B., and Sarkar, S. N. (2011). PKC alpha regulates Sendai virus-mediated interferon induction through HDAC6 and beta-catenin. *EMBO J.* 30, 4838–4849. doi: 10.1038/emboj.2011.351

Conflict of Interest: The authors declare that the research was conducted in the absence of any commercial or financial relationships that could be construed as a potential conflict of interest.

frontiers in Genetics

ORIGINAL RESEARCH
published: 18 March 2020
doi: 10.3389/fgene.2020.00256

Circulating microRNAs in Response to Exercise Training in Healthy Adults

Qiulian Zhou[1,2], Chao Shi[2], Yicheng Lv[2], Chenglin Zhao[2], Zheng Jiao[1] and Tianhui Wang[2]**

[1] Shanghai Applied Radiation Institute, School of Environmental and Chemical Engineering, Shanghai University, Shanghai, China, [2] Cardiac Regeneration and Ageing Lab, Institute of Cardiovascular Sciences, School of Life Sciences, Shanghai University, Shanghai, China

Circulating microRNAs (miRNAs, miRs) have great potential as cardiac biomarkers and they are also being explored for their roles in intercellular communication and gene expression regulation. The analysis of circulating miRNAs in response to exercise would provide a deeper understanding of the molecular response to physical activity and valuable information for clinical practice. Here, eight male college students were recruited to participate in cardiopulmonary exercise testing (CPET) and 1 h acute exercise training (AET). Blood samples were collected and serum miRNAs involved in angiogenesis, inflammation and enriched in muscle and/or cardiac tissues were analyzed before and after cardiopulmonary exercise and acute exercise. The miRNAs we detected were miR-1, miR-20a, miR-21, miR-126, miR-133a, miR-133b, miR-146, miR155, miR-208a, miR-208b, miR-210, miR-221, miR-222, miR-328, miR-378, miR-499, and miR-940. We found that serum miR-20a was decreased significantly after CPET and serum miR-21 was increased after AET. In addition, no robust correlation was identified between the changes of these miRNAs and makers of cardiac function and exercise capacity, which indicates a distinct adaptation of these miRNAs to exercise. Future studies are highly needed to define the potential use of these circulating miRNAs as useful biomarkers of exercise training, and disclose the biological function of circulating miRNAs as physiological mediators of exercise-induced cardiovascular adaptation.

Keywords: circulating miRNAs, cardiovascular adaptation, acute exercise, cardiopulmonary exercise testing, healthy adults

OPEN ACCESS

Edited by:
Dragos Cretoiu, Carol Davila University of Medicine and Pharmacy, Romania

Reviewed by:
Jianhua Yao, Tongji University, China
Chen Liu, The First Affiliated Hospital, Sun Yat-sen University, China

****Correspondence:***
Zheng Jiao
zjiao@shu.edu.cn
Tianhui Wang
wangth@shu.edu.cn

Specialty section:
This article was submitted to RNA, a section of the journal Frontiers in Genetics

Received: *10 January 2020*
Accepted: *03 March 2020*
Published: *18 March 2020*

Citation:
Zhou Q, Shi C, Lv Y, Zhao C, Jiao Z and Wang T (2020) Circulating microRNAs in Response to Exercise Training in Healthy Adults. Front. Genet. 11:256. doi: 10.3389/fgene.2020.00256

INTRODUCTION

Regular physical exercise is a part of healthy lifestyle, which can prevent and reduce the risk of diseases, including metabolic and aging-related diseases and even cancer, and affect mitochondrial metabolism as well as cognitive, cardiovascular and immune functions (Moore et al., 2012; Febbraio, 2017). Furthermore, the specific training protocols have become non-pharmacological remedies to reduce cardiovascular morbidity and mortality due to exercise-induced cardiovascular benefits (Liu et al., 2017; Ribeiro et al., 2017). Exercise training could impact

multiple signaling pathways and thus influence different exercise-associated traits including energy metabolism, angiogenesis, inflammation, muscle recovery, and mitochondrial biogenesis (Horak et al., 2018). However, the precise cellular and molecular mechanism for beneficial effects of exercise remains unclear. Nevertheless, non-coding RNAs, and especially microRNAs (miRNAs, miRNAs), constitute a new regulatory component that may play a role in exercise-induced adaptations (Silva et al., 2017; Wang et al., 2018).

miRNAs are a group of endogenous small non-coding RNAs of 18–25 nucleotides in length. miRNAs regulate gene expression at post-transcriptional levels through messenger RNA degradation or translational inhibition in a sequence-specific manner (Bartel, 2004, 2007). miRNAs play a role in the progresses of early embryogenesis and proliferation, differentiation, survival, proliferation, apoptosis, metabolism and energy balance of cell (He and Hannon, 2004; Esquela-Kerscher and Slack, 2006). The expression of miRNAs frequently dysregulated in various human diseases, such as inflammation, cardiovascular disease, Alzheimer's disease, muscle hypertrophy, lymphomas, leukemias, and cancer (Mohamed et al., 2011; Hruska-Plochan et al., 2015; Grobbelaar and Ford, 2019).

Recently, miRNAs have been found to be present in body fluids such as serum, plasma, urine, saliva and cerebrospinal fluid (Weber et al., 2010). Circulating miRNAs are stable, easily detectable, and may regulate gene expression in target cells and tissues as a novel mode of intercellular communication (Kosaka et al., 2010). At present, increasing evidence has reported circulating miRNAs as potential clinical biomarkers for specific diseases and administration of pharmaceutical agents (Zhang et al., 2017a; Caglar and Cayir, 2019; Kiyosawa et al., 2019; Reddy et al., 2019). The changes of circulating miRNAs induced by exercise have been widely reported in healthy persons and patients, indicating miRNAs may play a role in physiological adaptations to exercise. Profiles of circulating miRNAs are varying under different exercise type, duration and intensity (Xu et al., 2016; de Gonzalo-Calvo et al., 2018; Horak et al., 2018; Li et al., 2018; Ramos et al., 2018; Sapp and Hagberg, 2019). However, less is known about the changes of circulating miRNAs in the adaptation to cardiopulmonary exercise testing (CPET) and acute exercise training (AET).

Here, we inspected how CPET and AET affect specific circulating miRNAs with well-established roles in major adaptive processes in healthy persons. Specially, to further determine the uniqueness of circulating miRNAs changes, we compared the changes of circulating miRNAs to cardiac functional indexes and exercise capacity at baseline. We found that serum miR-20a was decreased significantly after CPET, while serum miR-21 was increased after AET. Moreover, no robust correlation was identified between changes of these miRNAs and makers of cardiac function and exercise capacity, indicating further studies using high-throughput circulating miRNAs screening techniques are highly needed to identify the potential role of circulating miRNAs in exercise adaptation.

MATERIALS AND METHODS

Participants

This study is in line with the recommendations of Ethics Committee. All subjects included in the study are fully aware of the methods and objectives of the study, and signed the informed consent voluntarily according to the Declaration of Helsinki. This study recruited eight male college students from Shanghai University with an average age of 20.75 ± 0.46 as the research subjects. Relevant clinical indicators including aortic root dimension, left ventricular end diastolic diameter and ejection fraction (EF) were tested.

Cardiopulmonary exercise testing and 1 h of AET were received by each subject, and clinical cardiac function indictors were collected when their exercise reached the anaerobic threshold (AT) and peak oxygen uptake. For CPET, using the

TABLE 1 | Clinical characteristic of participants.

Clinical parameters	Mean ± SEM
Age (year)	20.75 ± 0.46
Height (cm)	176.06 ± 1.61
Body mass (kg)	69.31 ± 1.77
BMI (kg/m^2)	22.34 ± 0.38
Heart rate (beats/min)	77.00 ± 2.47
Systolic blood pressure (mmHg)	106.50 ± 5.19
Diastolic blood pressure (mmHg)	72.25 ± 3.21

TABLE 2 | General echocardiographic indexes of participants.

Clinical parameters	Mean ± SEM
Aortic root dimension (mm)	28.75 ± 1.14
Left ventricular end diastolic diameter (mm)	49.88 ± 1.02
Left ventricular end systolic diameter (mm)	32.38 ± 0.92
End-diastolic volume	117.5 ± 6.00
End-systolic volume	41.25 ± 2.60
Left atrial dimension (mm)	30.00 ± 1.05
Interventricular septal thickness (mm)	8.13 ± 0.21
Left ventricular posterior wall thickness (mm)	8.50 ± 0.31
Ejection fraction (EF %)	65.13 ± 1.19
Fractional shortening (FS %)	35.75 ± 0.98

TABLE 3 | Cardiopulmonary function indexes in AT and peak.

Clinical parameters	Mean ± SEM	
	AT	Peak
Heart rate (beats/min)	121 ± 5.24	175.25 ± 3.41
Systolic blood pressure (mmHg)	138 ± 8.54	172.5 ± 8.03
Diastolic blood pressure (mmHg)	73.13 ± 2.92	81 ± 2.10
VO_2 (ml/min/kg)	18.45 ± 1.33	31.06 ± 0.98
Work load (watts)	97.25 ± 10.62	169.75 ± 6.20
METs	5.27 ± 0.38	8.88 ± 0.28
70% VO_2 max (ml/min/kg)	21.74 ± 0.68	
70%VO_2max work load (watts)	105.5 ± 3.55	

MasterScreen-CPX system (Jaeger, Germany), after a rest of 3 min and an unloaded exercise of 3 min, the workload was increased from 0 J/s for 1 min and increased by 2 J/s ever 6s. All participants continued pedaling until they reached the peak oxygen uptake. For acute exercise, these participants were exercised at Sweden Monark bicycle for 60 min at 70% of peak oxygen uptake. The ECG exercise test of all subjects was negative, and their exercise tolerance and ventilation function were normal.

The Extraction of Serum

A total of 5 ml of whole blood was collected before and immediately after cardiopulmonary exercise and acute exercise with procoagulant tubes. After gentle mixing, blood samples were left at room temperature within 1 h to allow coagulation to occur. Centrifuge at 3000 rpm for 15 min at 4°C, the supernatant clear liquid was taken and stored in −80°C refrigerator.

The Extraction of Serum Total RNA

The mirVana^{TM}PARIS^{TM} (Ambion, United States) was used to homogenize the samples through special cell lysis buffer to isolate total RNA from the serum samples. Take 200 μl of each serum sample and add exogenous cel-miR-39 (Ribobio Guangzhou) as a reference to ensure a final concentration of 50 pmol/L. Cel-miR-39 was used as control in the subsequent real-time quantitative PCR.

Determination of Circulating miRNAs Levels

The miRNA primers involved in the experiment are all purchased from Ribobio. The iScript cDNA synthesis kit (Bio-Rad, United States) was used for reverse transcription of miRNAs. The reaction system of cDNA synthesis is 10 μl, and the transcripts were stored at −20°C. SYBR Green (Bio-Rad, United States) fluorescent dye was used for quantitative PCR amplification. The reaction system was 10 μl. The experiment was performed using the Roche LightCycler® 480 Real-Time PCR system. Data analysis was calculated by using the formula $2^{(-\Delta\Delta Ct)}$.

Statistical Analysis

All data were analyzed by using SPSS.20, and each group of data was expressed as mean ± standard error of mean (SEM). The results before and after exercise were compared by paired sample *T*-test. Correlation analyses were analyzed using

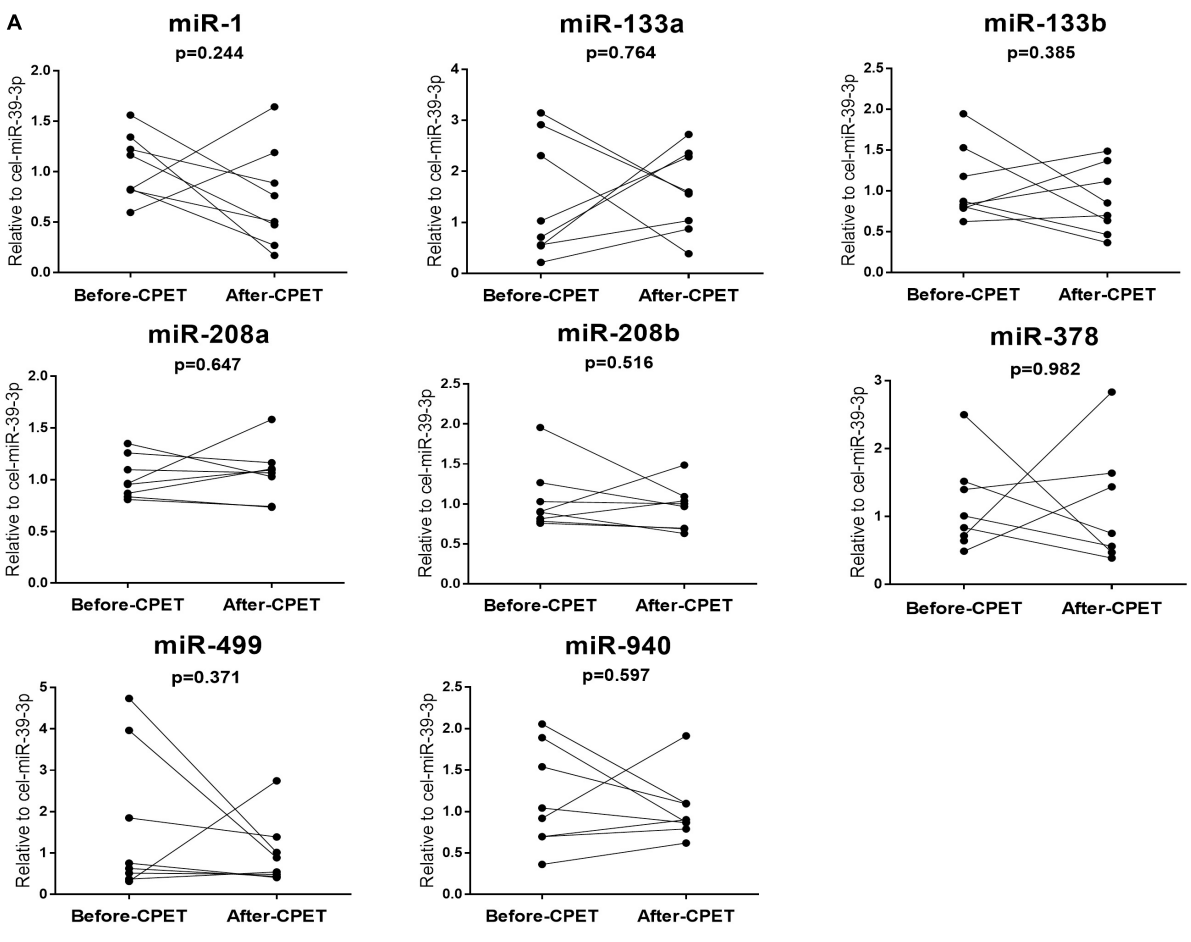

FIGURE 1 | Continued

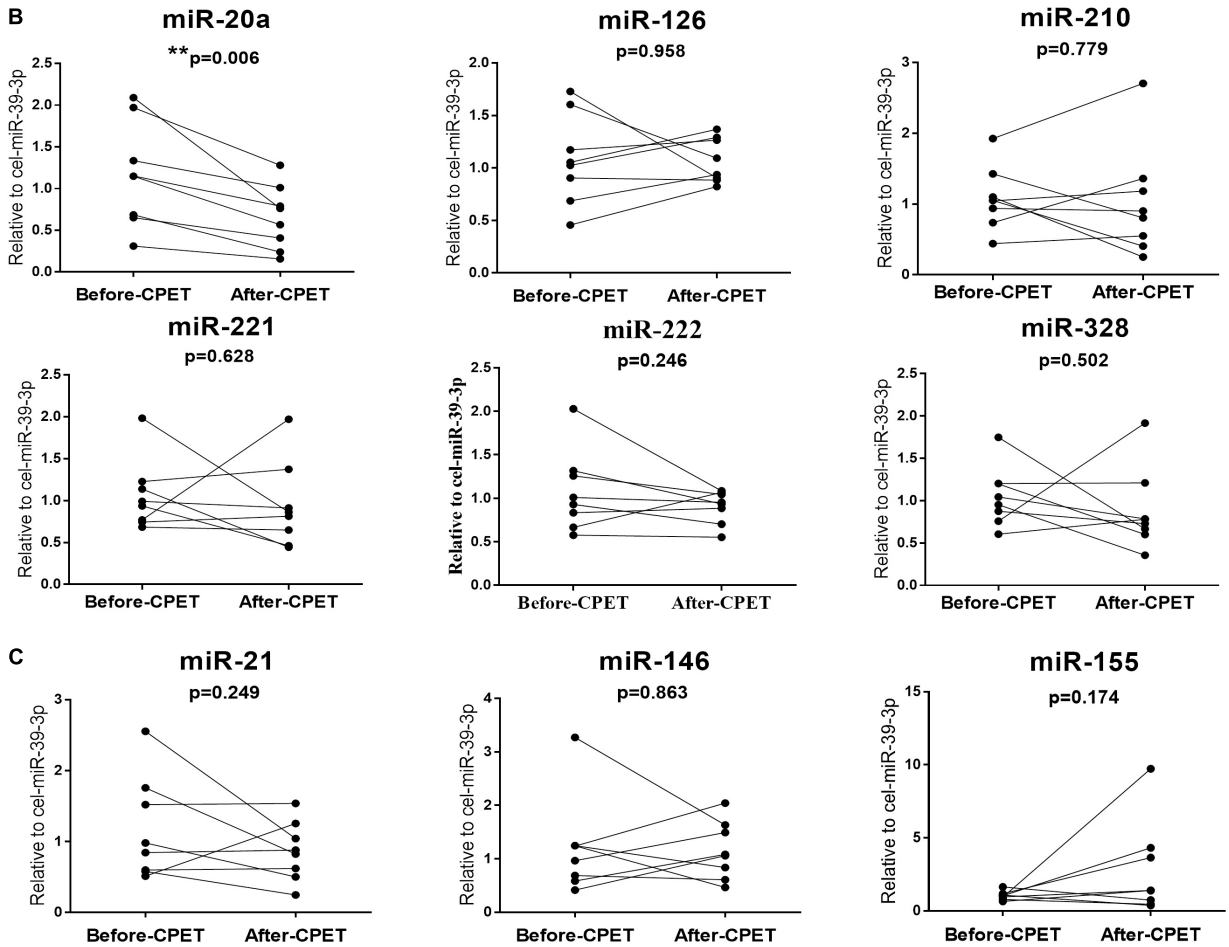

FIGURE 1 | Distinct regulatory profiles of selected circulating miRNAs before and after CPET. **(A)** Serum levels of cardiac or muscle-specific/enriched miRNAs before and after CPET. **(B)** Serum levels of angiogenesis-related miRNAs before and after CPET. **(C)** Serum levels of inflammation-related miRNAs before and after CPET. $^{**}P < 0.01$; $n = 8$.

the Spearman's or Pearson's method as appropriate for data distribution. Statistical significance is defined as P-values < 0.05. Data plots were made by GraphPad Prism.

RESULTS

Subject Characteristics Before and After Acute Exercise Training

Eight male college students with an average age of 20.75 ± 0.46 years were enrolled, and the clinical characteristic for them at the baseline were shown in **Table 1**. Their average height, weight and the BMI are 176.06 ± 1.61 cm, 69.31 ± 1.77 kg, and 22.34 ± 0.38 kg/m^2, respectively. In the basic state, their average heart rate was 77.00 ± 2.47 beats/min, the systolic blood pressure was 106.50 ± 5.19 mmHg, and the diastolic blood pressure was 72.25 ± 3.21 mmHg. **Table 2** lists the detailed general echocardiographic indexes. The average EF was $65.13 \pm 1.19\%$. We analyzed the cardiopulmonary function indexes when their exercise reached the AT and peak oxygen uptake (**Table 3**). The average heart rate was 121 ± 5.24 and 175.25 ± 3.41 beats/min when their exercise reached the AT and peak oxygen uptake (Peak). Cardiopulmonary exercise tests revealed that the AT VO_2 and peak VO_2 were not changed.

Cardiopulmonary Exercise Testing Decreased Circulating miR-20a, While Acute Exercise Training Increased Circulating miR-21

We determined the expression of cardiac or muscle-specific/enriched miRNAs (miR-1, miR-133a, miR-133b, miR-208a, miR-208b, miR-378, miR-499, miR-940), angiogenesis-related miRNAs (miR-20a, miR-126, miR-210, miR-221, miR-222, miR-328), and inflammation-related miRNAs (miR-21, miR-146, miR155). The results showed that serum miR-20a was decreased significantly after CPET (**Figure 1**); while serum miR-21 was increased after AET (**Figure 2**). In contrast, miR-1, miR-133a, miR-133b, miR-208a,

miR-208b, miR-378, miR-499, miR-940, miR-126, miR-210, miR-221, miR-222, miR-328, miR-146, and miR-155 were not changed following CPET or AET.

Correlations Between the Changes of miR-20a Following Cardiopulmonary Exercise Testing and Cardiac Function, Exercise Capacity at Baseline

Here, we correlated the decrease of miR-20a after CPET with the cardiac function and exercise capacity at baseline, however, no robust correlations were found (**Figure 3** and **Table 4**). We also failed to find robust correlations between miR-20a and cardiopulmonary function indexes before and after CPET (**Table 4**).

Correlations Between the Changes of miR-21 Following Acute Exercise Training and Cardiac Function, Exercise Capacity at Baseline

We also correlated the increase of miR-21 after AET with the cardiac function and exercise capacity at baseline, however, no robust correlations were found (**Figure 4** and **Table 5**). We also failed to report robust correlations between miR-21 and cardiopulmonary function indexes before and after AET (**Table 5**).

DISCUSSION

The purpose of this study was to investigate how specific circulating miRNAs were regulated by CPET and AET in healthy adults. Whether there are differences among exercise adaptation in athletes, healthy adults, and the patients of specific diseases have been previously published (Xu et al., 2016; Silva et al., 2017; Li et al., 2018). In previous studies, their participants were either chronic heart failure patients or basketball athletes, which is different from healthy college students in this study. The chronic heart failure patients were subjected to a symptom-limited incremental cardiopulmonary exercise test on a bicycle ergometer using a standardized exercise protocol of revised Ramp10 programs. Basketball athletes were subjected to cardiopulmonary exercise and an amateur basketball season for 3 months. In our cohort, these subjects were subjected to cardiopulmonary exercise and acute exercise for 1h, which is different from those in chronic heart failure

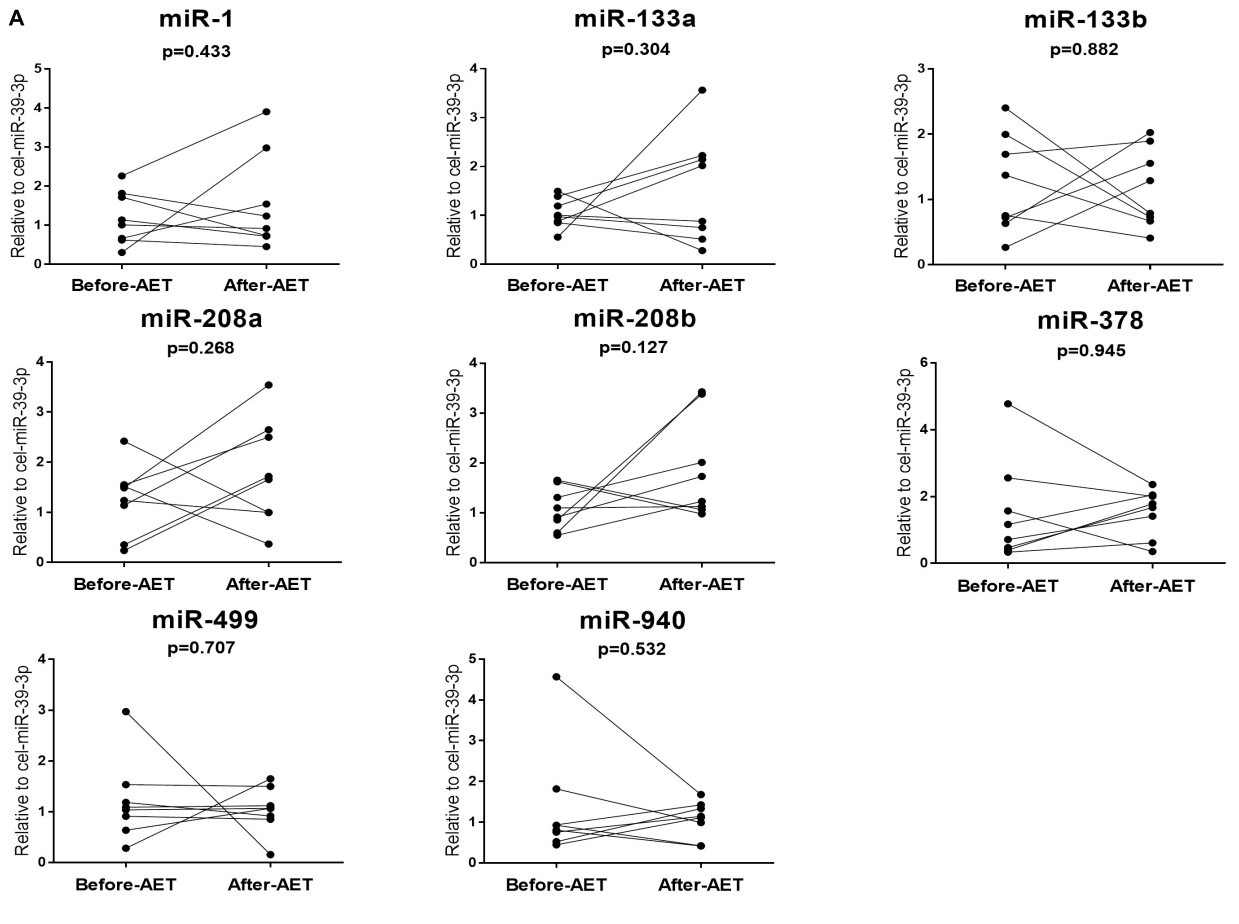

FIGURE 2 | Continued

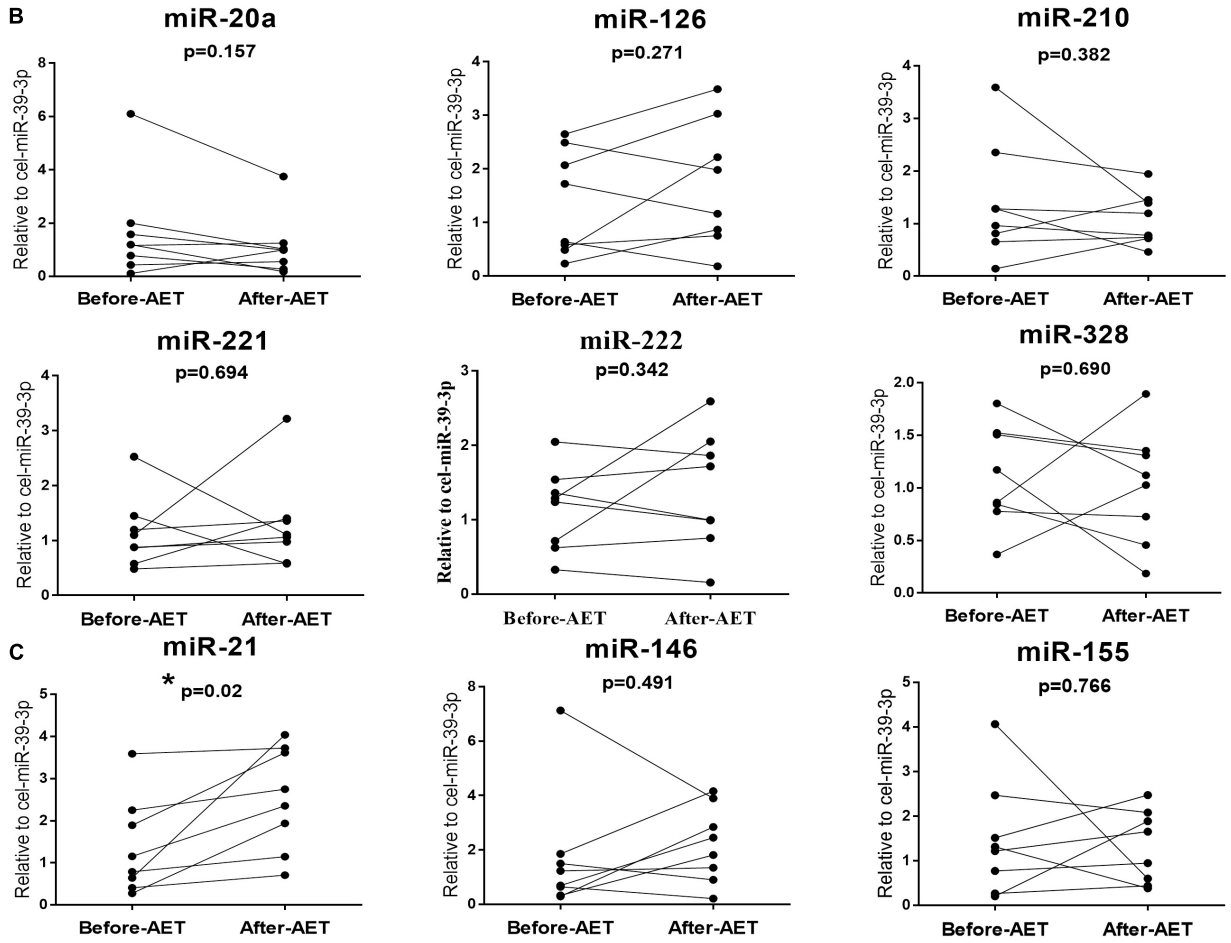

FIGURE 2 | Distinct regulatory profiles of selected circulating miRNAs before and after AET. **(A)** Serum levels of cardiac or muscle-specific/enriched miRNAs before and after AET. **(B)** Serum levels of angiogenesis-related miRNAs before and after AET. **(C)** Serum levels of inflammation-related miRNAs before and after AET. *$P < 0.05$; $n = 8$.

patients or basketball athletes. Here we reported that serum miR-20a decreased in response to CPET, while serum miR-21 increased in response to AET. We also showed that no robust correlations was identified between the changes of miR-21 and miR-20a induced by exercise to makers of cardiac function and exercise capacity, which suggested that these two miRNAs were distinct biomarkers and also further studies using high-throughput circulating miRNAs screening techniques are highly needed.

A few studies have reported changes in circulating miRNAs after acute and chronic exercise in healthy persons or athletes. Specifically, circulating miR-1, miR-133a, miR-133b, miR-139, miR-143, miR-181b, miR-206, miR-208b, miR-214, miR-223, miR-330, miR-338, miR-485, miR-509, miR-517a, miR-518f, miR-520f, miR-522, miR-553, and miR-888 were found increased, while miR-30b, miR-106a, miR-146a, miR-151, miR-221, miR-652 were decreased after an acute exercise (Banzet et al., 2013; Nielsen et al., 2014; Cui et al., 2016; Silva et al., 2017). Circulating miR-20a, miR-103, miR-107, miR-126, miR-376a were increased, whilemiR-16, miR-21, miR-25, miR-27a, miR-28, miR-148a, miR-185, miR-342, and miR-766 were decreased after a chronic exercise (Baggish et al., 2011, 2014; Nielsen et al., 2014; Zhang et al., 2017b). Circulating miR-21, miR-146a, miR-221, miR-222 were increased in response to both acute and chronic exercise (Baggish et al., 2011).Here we reported that serum miR-20a decreased after CPET and serum miR-21 increased after AET, while other miRNAs measured in this study did not change, suggesting that exercise participants, type, duration and intensity might affect levels of circulating miRNAs. Besides, the sample processing, total RNA isolation method, and miRNAs quantification platforms may also affect levels of circulating miRNAs. Interestingly, most of cardiac or muscle-specific/enriched miRNAs have not changed in this study, there must be different mechanisms of circulating miRNAs response to exercise rather than the general response to tissue damage.

The miRNAs measured in this study have potential biological relevance in exercise, including inflammation, angiogenesis and ischemic adaptation. MiR-21 is abundantly expressed in almost all tissues and involved in many cardiovascular

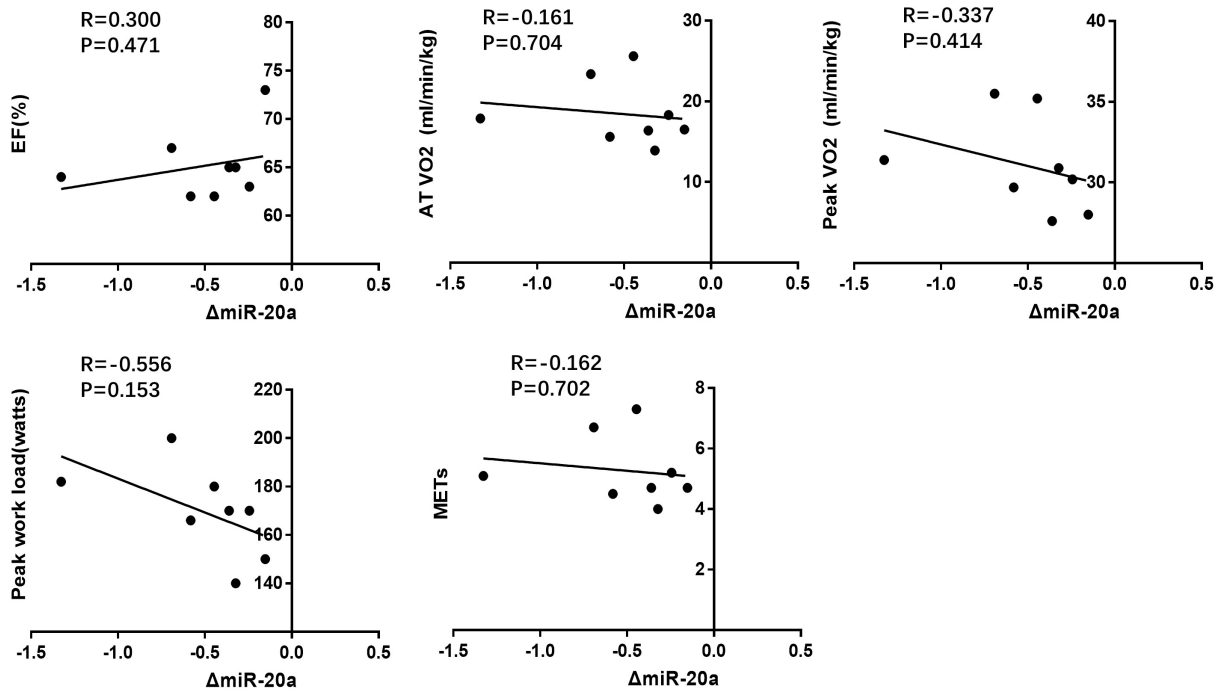

FIGURE 3 | Correlation analysis between the changes of miR-20a following CPET and cardiac function(EF%), exercise capacity (AT VO_2, peak VO_2, peak work load, METs) at baseline.

TABLE 4 | Correlation analysis between miRNA changes following CPET and cardiopulmonary function indexes.

miR-20a	EF		AT VO_2		Peak VO_2		Peak work load		METs	
	R	P	R	P	R	P	R	P	R	P
Before CPET	−0.229	NS	0.062	NS	0.386	NS	0.517	NS	0.07	NS
After CPET	−0.085	NS	−0.053	NS	0.305	NS	0.306	NS	−0.042	NS
Δ	0.3	NS	−0.161	NS	−0.337	NS	−0.556	NS	−0.162	NS

diseases, such as atherosclerosis, pulmonary hypertension, heart failure and myocardial ischemia (Cengiz et al., 2015; Zhao and Zhou, 2017; Pan et al., 2018; Ding et al., 2019; Kan et al., 2019; Sun et al., 2019). MiR-21 plays anti-apoptosis roles in endothelial cells and ischemic cardiomyocytes (Li et al., 2018). The role of miR-21 in response to exercise is to indirectly participate in angiogenesis by inducing the expression of hypoxia inducible factor-1(HIF-1α) and VEGF, regulating apoptosis, increasing the activity of endothelial nitric oxide synthase and mediating anti-inflammatory response in macrophages (Sheedy, 2015; Horak et al., 2018). In this study, we found that serum miR-21 increased in response to AET. We speculated that miR-21 may functions as promoting angiogenesis, anti-inflammatory, and anti-apoptosis effects.

Different from the results of this study, the expression of miR-20a was reported up-regulated in response to sustained aerobic exercise training but no changes to acute exhaustive exercise in athletes (Baggish et al., 2011).Besides, it has also been reported that miR-20a was up-regulated in response to acute resistance exercise in men, which is indicative of a hypertrophic response within skeletal muscle (Margolis et al., 2017). Thus, the adaptive regulation of circulating miRNAs is influenced by exercise type, intensity, duration and human subjects. MiR-20a is able to target the TNFSF15 gene, preventing the latter to function as an inhibitor of angiogenesis. The production of miR-20a is stimulated by the Akt and Erk signals, which is activated by the angiogenic factor VEGF (Wang et al., 2017). In this study, we found that serum miR-20a decreased in response to CPET. We speculated that the decrease of miR-20a was an acute compensatory reaction. As an initial study, several limitations of the present study should be highlighted. Firstly, a major weakness of this study is that the number of enrolled human subjects should be expanded. Secondly, this study was restricted to healthy young persons. Future study is required to determine whether the changes of circulating miRNAs are applicable to the healthy people of different ages and the patients of specific diseases. Thirdly, this study examined circulating miRNAs in response to CPET and acute exhaustive exercise. The dynamic

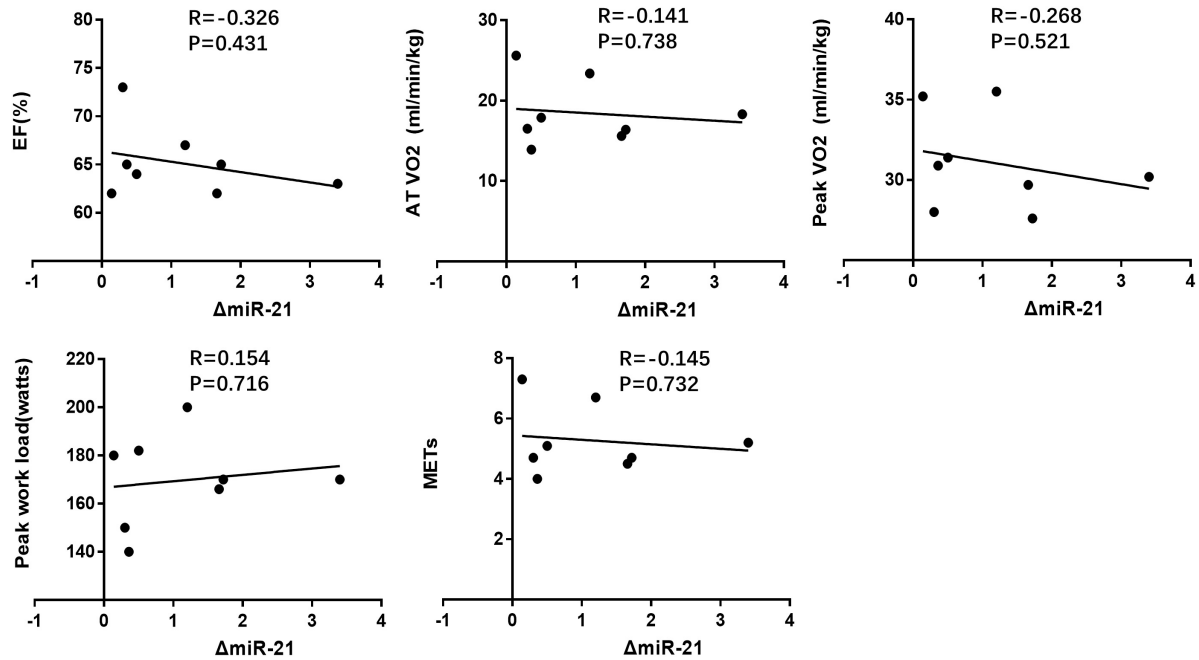

FIGURE 4 | Correlation analysis between the changes of miR-21 following AET and cardiac function (EF%), exercise capacity (AT VO_2, peak VO_2, peak work load, METs) at baseline.

TABLE 5 | Correlation analysis between miRNA changes following AET and cardiopulmonary function indexes.

miR-21	EF		AT VO_2		Peak VO_2		Peak work load		METs	
	R	P	R	P	R	P	R	P	R	P
Before AET	−0.382	NS	0.658	NS	0.506	NS	0.452	NS	0.656	NS
After AET	−0.645	NS	0.482	NS	0.228	NS	0.556	NS	0.477	NS
Δ	−0.326	NS	−0.141	NS	−0.268	NS	0.154	NS	−0.145	NS

regulation of circulating miRNAs after sustained aerobic exercise training need to be further studied. Fourthly, it would be interesting to see what genes are also influenced by the changed circulating miRNAs. Finally, quantitative analysis was limited to a subset of related miRNAs, and high-throughput screening is needed to obtain a more complete profile of circulating miRNAs regulation in adaption to exercise training. Although further studies are needed, present results contribute to the knowledge about effects of CPET and AET on the circulating miRNAs profile.

CONCLUSION

In conclusion, serum miR-20a decreased in response to CPET, while serum miR-21 increased in response to AET. Future studies are highly needed to define the potential use of these circulating miRNAs as useful biomarkers of exercise training, and disclose the direct biological function of circulating miRNAs in adaptation to different modes of exercise training.

DATA AVAILABILITY STATEMENT

The raw data supporting the conclusions of this article will be made available by the authors, without undue reservation, to any qualified researcher.

ETHICS STATEMENT

The studies involving human participants were reviewed and approved by the Shanghai University Ethics Committee. The patients/participants provided their written informed consent to participate in this study.

AUTHOR CONTRIBUTIONS

TW, ZJ, and QZ designed the study, conducted all the experiments, and drafted the manuscript. CS, YL, and CZ conducted the experiments and analyzed the data.

REFERENCES

Baggish, A. L., Hale, A., Weiner, R. B., Lewis, G. D., Systrom, D., Wang, F., et al. (2011). Dynamic regulation of circulating microRNA during acute exhaustive exercise and sustained aerobic exercise training. *J. Physiol.* 589(Pt 16), 3983–3994. doi: 10.1113/jphysiol.2011.213363

Baggish, A. L., Park, J., Min, P. K., Isaacs, S., Parker, B. A., Thompson, P. D., et al. (2014). Rapid upregulation and clearance of distinct circulating microRNAs after prolonged aerobic exercise. *J. Appl. Physiol.* 116, 522–531. doi: 10.1152/japplphysiol.01141.2013

Banzet, S., Chennaoui, M., Girard, O., Racinais, S., Drogou, C., Chalabi, H., et al. (2013). Changes in circulating microRNAs levels with exercise modality. *J. Appl. Physiol.* 115, 1237–1244. doi: 10.1152/japplphysiol.00075.2013

Bartel, D. P. (2004). MicroRNAs: genomics, biogenesis, mechanism, and function. *Cell* 116, 281–297. doi: 10.1016/s0092-8674(04)00045-5

Bartel, D. P. (2007). MicroRNAs: genomics, biogenesis, mechanism, and function (Reprinted from Cell, vol 116, pg 281-297, 2004). *Cell* 131, 11–29. doi: 10.1016/s0092-8674(04)00045-5

Caglar, O., and Cayir, A. (2019). Total circulating cell-free miRNA in plasma as a predictive biomarker of the thyroid diseases. *J. Cell. Biochem.* 120, 9016–9022. doi: 10.1002/jcb.28173

Cengiz, M., Yavuzer, S., Avci, B. K., Yuruyen, M., Yavuzer, H., Dikici, S. A., et al. (2015). Circulating miR-21 and eNOS in subclinical atherosclerosis in patients with hypertension. *Clin. Exp. Hypertens.* 37, 643–649. doi: 10.3109/10641963.2015.1036064

Cui, S. F., Wang, C., Yin, X., Tian, D., Lu, Q. J., Zhang, C. Y., et al. (2016). Similar responses of circulating microRNAs to acute high-intensity interval exercise and vigorous-intensity continuous exercise. *Front. Physiol.* 7:102. doi: 10.3389/fphys.2016.00102

de Gonzalo-Calvo, D., Davalos, A., Fernandez-Sanjurjo, M., Amado-Rodriguez, L., Diaz-Coto, S., Tomas-Zapico, C., et al. (2018). Circulating microRNAs as emerging cardiac biomarkers responsive to acute exercise. *Int. J. Cardiol.* 264, 130–136. doi: 10.1016/j.ijcard.2018.02.092

Ding, F., You, T., Hou, X. D., Yi, K., Liu, X. G., Zhang, P., et al. (2019). MiR-21 regulates pulmonary hypertension in rats via TGF-beta 1/Smad2 signaling pathway. *Eur. Rev. Med. Pharmacol. Sci.* 23, 3984–3992. doi: 10.26355/eurrev_201905_17828

Esquela-Kerscher, A., and Slack, F. J. (2006). Oncomirs – microRNAs with a role in cancer. *Nat. Rev. Cancer* 6, 259–269. doi: 10.1038/nrc1840

Febbraio, M. A. (2017). Exercise metabolism in 2016: health benefits of exercise more than meets the eye! *Nat. Rev. Endocrinol.* 13, 72–74. doi: 10.1038/nrendo.2016.218

Grobbelaar, C., and Ford, A. M. (2019). The role of MicroRNA in paediatric acute lymphoblastic leukaemia: challenges for diagnosis and therapy. *J. Oncol.* 2019:894. doi: 10.1155/2019/8941471

He, L., and Hannon, G. J. (2004). Micrornas: small RNAs with a big role in gene regulation. *Nat. Rev. Genet.* 5, 522–531. doi: 10.1038/nrg1379

Horak, M., Zlamal, F., Iliev, R., Kucera, J., Cacek, J., Svobodova, L., et al. (2018). Exercise-induced circulating microRNA changes in athletes in various training scenarios. *PLoS One* 13:e0191060. doi: 10.1371/journal.pone.0191060

Hruska-Plochan, M., Li, B., Kyburz, D., Kruetzfeldt, J., Landmesser, U., Aguzzi, A., et al. (2015). New and emerging roles of small RNAs in neurodegeneration, muscle, cardiovascular and inflammatory diseases. *Swiss Med. Wkly.* 145:w14192. doi: 10.4414/smw.2015.14192

Kan, C. L., Cao, J. J., Hou, J., Jing, X. Y., Zhu, Y. J., Zhang, J. H., et al. (2019). Correlation of miR-21 and BNP with pregnancy-induced hypertension complicated with heart failure and the diagnostic value. *Exp. Ther. Med.* 17, 3129–3135. doi: 10.3892/etm.2019.7286

Kiyosawa, N., Watanabe, K., Toyama, K., and Ishizuka, H. (2019). Circulating miRNA signature as a potential biomarker for the prediction of analgesic efficacy of hydromorphone. *Int. J. Mol. Sci.* 20:1665. doi: 10.3390/ijms20071665

Kosaka, N., Iguchi, H., Yoshioka, Y., Takeshita, F., Matsuki, Y., and Ochiya, T. (2010). Secretory mechanisms and intercellular transfer of microRNAs in living cells. *J. Biol. Chem.* 285, 17442–17452. doi: 10.1074/jbc.M110.107821

Li, Y., Yao, M., Zhou, Q., Cheng, Y., Che, L., Xu, J., et al. (2018). Dynamic regulation of circulating microRNAs during acute exercise and long-term exercise training in basketball athletes. *Front. Physiol.* 9:282. doi: 10.3389/fphys.2018.00282

Liu, X., Platt, C., and Rosenzweig, A. (2017). The role of microRNAs in the cardiac response to exercise. *Cold Spring Harb. Perspect. Med.* 7:a029850. doi: 10.1101/cshperspect.a029850

Margolis, L. M., Lessard, S. J., Ezzyat, Y., Fielding, R. A., and Rivas, D. A. (2017). Circulating microRNA are predictive of aging and acute adaptive response to resistance exercise in men. *J. Gerontol. A Biol. Sci. Med. Sci.* 72, 1319–1326. doi: 10.1093/gerona/glw243

Mohamed, J. S., Hajira, A., Li, Z., Paulin, D., and Boriek, A. M. (2011). Desmin regulates airway smooth muscle hypertrophy through early growth-responsive Protein-1 and microRNA-26a. *J. Biol. Chem.* 286, 43394–43404. doi: 10.1074/jbc.M111.235127

Moore, S. C., Patel, A. V., Matthews, C. E., de Gonzalez, A. B., Park, Y., Katki, H. A., et al. (2012). Leisure time physical activity of moderate to vigorous intensity and mortality: a large pooled cohort analysis. *PLoS Med.* 9:e1001335. doi: 10.1371/journal.pmed.1001335

Nielsen, S., Akerstrom, T., Rinnov, A., Yfanti, C., Scheele, C., Pedersen, B. K., et al. (2014). The miRNA plasma signature in response to acute aerobic exercise and endurance training. *PLoS One* 9:e87308. doi: 10.1371/journal.pone.0087308

Pan, Y. Q., Li, X. W., Li, Y. C., Li, J. L., and Lin, J. F. (2018). Effect of miR-21/TLR4/NF-kappa B pathway on myocardial apoptosis in rats with myocardial ischemia-reperfusion. *Eur. Rev. Med. Pharmacol. Sci.* 22, 7928–7937. doi: 10.26355/eurrev_201811_16420

Ramos, A. E., Lo, C., Estephan, L. E., Tai, Y.-Y., Tang, Y., Zhao, J., et al. (2018). Specific circulating microRNAs display dose-dependent responses to variable intensity and duration of endurance exercise. *Am. J. Physiol. Heart Circ. Physiol.* 315, H273–H283. doi: 10.1152/ajpheart.00741.2017

Reddy, L. L., Shah, S. A. V., Ponde, C. K., Rajani, R. M., and Ashavaid, T. F. (2019). Circulating miRNA-33: a potential biomarker in patients with coronary artery disease. *Biomarkers* 24, 36–42. doi: 10.1080/1354750x.2018.1501760

Ribeiro, P. A. B., Boidin, M., Juneau, M., Nigam, A., and Gayda, M. (2017). High-intensity interval training in patients with coronary heart disease: prescription models and perspectives. *Ann. Phys. Rehabil. Med.* 60, 50–57. doi: 10.1016/j.rehab.2016.04.004

Sapp, R. M., and Hagberg, J. M. (2019). Circulating microRNAs: advances in exercise physiology. *Curr. Opin. Physiol.* 10, 1–9. doi: 10.1016/j.cophys.2019.03.004

Sheedy, F. J. (2015). Turning 21: induction of miR-21 as a key swith in the inflammatory response. *Front. Immunol.* 6:19. doi: 10.3389/fimmu.2015.00019

Silva, G. J. J., Bye, A., el Azzouzi, H., and Wisloff, U. (2017). MicroRNAs as important regulators of exercise adaptation. *Prog. Cardiovasc. Dis.* 60, 130–151. doi: 10.1016/j.pcad.2017.06.003

Sun, P., Tang, L. N., Li, G. Z., Xu, Z. L., Xu, Q. H., Wang, M., et al. (2019). Effects of MiR-21 on the proliferation and migration of vascular smooth muscle cells in rats with atherosclerosis via the Akt/ERK signaling pathway. *Eur. Rev. Med. Pharmacol. Sci.* 23, 2216–2222. doi: 10.26355/eurrev_201903_17269

Wang, D. W., Wang, Y., Ma, J., Wang, W. P., Sun, B. B., Zheng, T. F., et al. (2017). MicroRNA-20a participates in the aerobic exercise-based prevention of coronary artery disease by targeting PTEN. *Biomed. Pharmacother.* 95, 756–763. doi: 10.1016/j.biopha.2017.08.086

Wang, L. J., Lv, Y. C., Li, G. P., and Xiao, J. J. (2018). MicroRNAs in heart and circulation during physical exercise. *J. Sport Health Sci.* 7, 433–441. doi: 10.1016/j.jshs.2018.09.008

Weber, J. A., Baxter, D. H., Zhang, S., Huang, D. Y., Huang, K. H., Lee, M. J., et al. (2010). The microRNA spectrum in 12 body fluids. *Clin. Chem.* 56, 1733–1741. doi: 10.1373/clinchem.2010.147405

Xu, T., Zhou, Q., Che, L., Das, S., Wang, L., Jiang, J., et al. (2016). Circulating miR-21, miR-378, and miR-940 increase in response to an acute exhaustive exercise in chronic heart failure patients. *Oncotarget* 7, 12414–12425. doi: 10.18632/oncotarget.6966

Zhang, J., Xing, Q., Zhou, X., Li, J., Li, Y., Zhang, L., et al. (2017a). Circulating miRNA-21 is a promising biomarker for heart failure. *Mol. Med. Rep.* 16, 7766–7774. doi: 10.3892/mmr.2017.7575

Zhang, T., Brinkley, T. E., Liu, K. Q., Feng, X., Marsh, A. P., Kritchevsky, S., et al. (2017b). Circulating MiRNAs as biomarkers of gait speed responses to aerobic exercise training in obese older adults. *Aging (Albany N. Y.)* 9, 900–913. doi: 10.18632/aging.101199

Zhao, Z. Y., and Zhou, Y. M. (2017). Circulating miR-21 and miR-423-5p as biomarkers for heart failure in heart valve disease patients. *Int. J. Clin. Exp. Pathol.* 10, 5703–5711.

Conflict of Interest: The authors declare that the research was conducted in the absence of any commercial or financial relationships that could be construed as a potential conflict of interest.

frontiers in Cell and Developmental Biology

REVIEW
published: 20 March 2020
doi: 10.3389/fcell.2020.00182

Exercise Mediates Heart Protection via Non-coding RNAs

*Yuelin Zhang[1,2], Nana He[2,3], Beili Feng[1,2] and Honghua Ye[1,2]**

[1] Department of Cardiology, HwaMei Hospital, University of Chinese Academy of Sciences, Ningbo, China, [2] Ningbo Institute of Life and Health Industry, University of Chinese Academy of Sciences, Ningbo, China, [3] Department of Experimental Medical Science, HwaMei Hospital, University of Chinese Academy of Sciences, Ningbo, China

Cardiovascular diseases (CVDs) have become the central matter of death worldwide and have emerged as a notable concern in the healthcare field. There is accumulating evidence that regular exercise training can be as a reliable and widely favorable approach to prevent the heart from cardiovascular events. Non-coding RNAs (ncRNAs) could act as innovative biomarkers and auspicious therapeutic targets to reduce the incidence of CVDs. In this review, we summarized the regulatory effects of ncRNAs in the cardiac-protection provided by exercise to assess potential therapies for CVDs and disease prevention.

Keywords: non-coding RNA, microRNA, exercise, cardiovascular diseases, oxidative stress

OPEN ACCESS

Edited by:
Junjie Xiao,
Shanghai University, China

Reviewed by:
Meixiang Xiang,
Zhejiang University, China
Reinhard Wetzker,
Friedrich Schiller University Jena, Germany

***Correspondence:**
Honghua Ye
lindayenbzjch@163.com

Specialty section:
This article was submitted to Signaling, a section of the journal Frontiers in Cell and Developmental Biology

Received: *11 December 2019*
Accepted: *04 March 2020*
Published: *20 March 2020*

Citation:
Zhang Y, He N, Feng B and Ye H (2020) Exercise Mediates Heart Protection via Non-coding RNAs. Front. Cell Dev. Biol. 8:182. doi: 10.3389/fcell.2020.00182

INTRODUCTION

Cardiovascular diseases (CVDs) remain the most common cause of morbidity and mortality globally (Li et al., 2019). Hypertension, diabetes, high cholesterol, obesity, and alcohol and tobacco use are all risk factors for cardiac diseases. Despite advancements in therapeutic methods, the burden of CVDs has significantly increased given the high financial burden and associated health care problems they impose; thus, the development of innovative approaches to fight this major health problem is critical (Liu et al., 2017).

Regular exercise training (ET) has been considered to be the most effective intervention in preventing and reducing CVDs (Romeo et al., 2018). Exercise, which is considered the most effective, accessible, and inexpensive therapy a physician can prescribe, aids in blood pressure control, improves blood lipid profiles, and increases insulin sensitivity (Günay et al., 2018).

Numerous recent studies have demonstrated that ET-mediated heart protection involves compound interactions among multiple tissues and plays an intense role in gene expression (Malcolm et al., 2018). Emerging evidence suggests that non-coding RNAs (ncRNAs) set great effect on regulating cardiac-protection. In this review, we summarize the correlations among ET, ncRNAs, and CVDs to obtain a further insight of the molecular mechanisms underlying the physiological and pathological cardiac events with the hope of consequently offering brand-new targets for CVDs' treatment.

THE CLASSIFICATION OF ncRNAs

NcRNAs originate in the genome and are functional molecules that can not be translated to proteins. Based on molecular size, shape and function, they consist of certain different types, such as transfer RNAs (tRNAs), ribosomal RNAs (rRNAs), and short interfering RNAs (siRNAs), circular RNAs (circRNAs), piwi-interacting RNAs (piRNAs), and in much attention microRNAs (miRNAs, miRs) (Gomes et al., 2018; Dong et al., 2019). Notably, these numerous ncRNAs can regulate gene expression from several aspects such as epigenetics, transcription and post-transcriptional

regulation, and thus participate in pathophysiological conditions as well as become central players in the occurrence and development of CVDs (Gomes et al., 2018).

MiRNAs are a class of non-coding RNAs with the length of 17∼22 nucleotides and can be in combination to the target gene's 3′-untranslated region (UTR), thus in degradation of messenger RNA (mRNA) (Margolis and Rivas, 2018) and regulation of gene expression after transcription (Sapp et al., 2017). Each miRNA can bind to various target genes, while one same gene can also be conducted with a few of miRNAs (Zhang and Chen, 2018). It has been reported that miRNAs widely exists in humans, most of which have associations with tumor, inflammation and various diseases of human (Angel et al., 2019). Furthermore, miRNAs have been demonstrated that they can help further our understanding of responses to physical activity (Denham et al., 2018).

LncRNAs, a type of RNAs longer than 200 nt, have recently become a research focus given their functional importance and their ability to attenuate the inhibitory effect of miRNA on target genes and regulate expressions of target genes (Gomes et al., 2018).

CircRNA is defined as a closed cyclic form. Researches are being gradually revealed to analyze circRNA's roles in the adjustment of gene expression (Bei et al., 2018; Zhang et al., 2018). However, the localization, degradation and biological functions of circRNA remain unclear (Bei et al., 2018).

EXERCISE, OXIDATIVE STRESS, AND ncRNAs

Oxidative stress refers to redox balance disturbances when the production of reactive oxygen species (ROS) exceeds the ability of self-clearance, conveying oxidative damage to cells and being the basis for the pathogenesis of numerous diseases. Elevated levels of ROS are not conducive to the utilization of cardiac calcium and related to endothelial dysfunction, acting as signaling molecules in the regulation of angiogenesis, necrosis and apoptosis (Tofas et al., 2019). Exercise as an important mediator of oxidative stress exerts two-sided effect on the regulation of the redox system. ROS generated by short-term physical activities is closely related to the formation of exercise adaptation. On the other hand, prolonged and intense exercise-induced oxidative stress could hinder skeletal muscle contraction and do harm to exercise capacity and body health (Di Meo et al., 2019).

Although there have been a lot of related researches on the relationship of free radicals and exercise adaptation and exercise-induced oxidative injury, the potential mechanisms are complex and insufficient studied. Kelch-like ECH associated protein 1 (*Keap1*)/nuclear transcription factor 2 (Nrf2) is a key signal pathway to resist oxidative damage. Exercise enhanced the expression of antioxidant enzymes and promotes cardiac antioxidant defenses by adjusting the Nrf2/*Keap1* ratio (Alves et al., 2020). Furthermore, during ET removal Nrf2 may activate stress-related kinases in white adipose tissue to impair insulin sensitivity, thereby altering glucose homeostasis (Merry et al., 2020). Moreover, ET could be able to promote sirtuin-1 *(SIRT1)* and better antioxidant activity in heart failure (HF) patients (Corbi et al., 2019). *SIRT1*, involved in the cellular response to exogenous stressors, is considered as sensor of oxidative stress and regulator of cell redox state (Conti et al., 2017).

Oxidative stress can also alter the expression of many ncRNAs. MiRNAs are in the most depth research since they set a huge impact on CVDs by inhibiting protein translation and targeting mRNA degradation. There is accumulating evidence that intracellular ROS can either suppress or induce miRNA expression levels via Nrf2, *SIRT1* and nuclear factor-kappa B (NF-κB) pathways (reviewed in Kura et al., 2020). However, further studies are still required to investigate and understand the underlying mechanism of ROS and ncRNAs during ET.

CARDIAC CHANGES IN RESPONSE TO EXERCISE

Cardiac Hypertrophy and Cardiomyocyte Renewal

Cardiac hypertrophy (CH) is an adaptive compensatory condition to endurance exercise. The significance of exercise on the structure and capacity of the heart has being in topic interest currently (Xu et al., 2017). Thickening of the muscle forces the heart to work harder to circulate blood throughout the body (Samanta et al., 2016). CH can be classified into two forms: physiological hypertrophy and pathological hypertrophy. In contrast to exercise-induced physiological hypertrophy, characterized by changes in cardiomyocytes, thickening myofibrils, an increased number of mitochondria, and expansion of the sarcoplasmic reticulum to increase the cardiac reserve (Bei et al., 2017), pathological hypertrophy is a disease-related condition accompanied by apoptosis, necrosis and fibrosis that contributes to myocardial diastolic insufficiency, which reduces contractility (Gomes et al., 2018).

The pivotal role of miRNAs in cardiac growth has been in exploration in greater depth in recent years. MiR-17-3p was increased in hearts from mice that underwent 21 days of swimming training and was involved in exercise-induced hypertrophy, conceivably contributing to the protective impact of exercise (Shi et al., 2017). A previous study found that miR-17-3p directly and negatively targeted metallopeptidase inhibitor 3 (*TIMP3*) to strengthen cardiomyocyte proliferation and indirectly regulated the phosphatase and tensin homolog (*PTEN*), a natural inhibitor of the phosphoinositide 3-kinase (PI3K) (p110α)-protein kinase B (PKB/Akt) pathway [80], to stimulate physiological hypertrophy (Shi et al., 2017). Additionally, a negative relationship between changes in plasma miR-532 levels and insulin-like growth factor 1 (IGF-1) was observed in a previous study, which activating Akt signaling pathway to promote cell growth and proliferation as well as redox balance, thus promoting the adaptation to resistance exercise (Cui et al., 2017). After eight consecutive weeks of repeated running bouts, miR-1 expression decreased in exercised hearts, while mitochondrial calcium uniporter (*MCU*, a predicted target of the miR-1) protein levels increased (Zaglia et al., 2017).

Therefore, the miR-1/*MCU* axis, controlled by the β-adrenergic receptor system, could affect mitochondrial Ca^{2+} uptake and was a factor in the dynamic adaptation of cardiac cells to hypertrophy (Zaglia et al., 2017). Another study demonstrated that inhibition of miR-222 restrained the homeodomain-interacting protein kinase 1 (*HIPK1*) (Vujic et al., 2018), a direct target of miR-222 with antiproliferative effects in cardiomyocytes (Ding et al., 2017), leading to the regulation of cardiomyocyte generation after exercise (Vujic et al., 2018).

MiR-1 was increased, and NCX1, the essential transport factor of Ca^{2+}, was decreased in pathological hypertrophy in control obese rats (OZRs) (Silveira et al., 2017). Moreover, a decrease in miR-29c in OZRs exerted a positive effect on the cardiac collagen volumetric fraction (CVF) (Silveira et al., 2017). However, cardiac miR-29c and miR-1 levels were standardized through aerobic exercise training and eventually decreased collagen expression (Soci et al., 2011), pathological cardiac alteration and dysfunction, suggesting that AET exert a positive effect against pathological CH.

Angiogenesis

A considerable relationship between endurance exercise and increased neovascularization or angiogenesis has been studied in depth (Liu et al., 2017). MiR-126, known as an endothelial-specific miRNA, targeting sprouty-related protein 1 (*SPRED1*) and phosphatidyl-inositol 3-kinase regulatory subunit 2 (*PIK3R2*), activated ERK and Akt, pathways to enhance the role of vascular endothelial growth factor (VEGF) and thus promote the process of angiogenesis (Fernandes et al., 2017). MiR-210, a hypoxia-specific miRNA, may stimulate neovascularization by downregulation of its target gene, *ephrin A3*, which is an important molecule in VEGF-mediated angiogenesis signaling pathway (Ghorbanzadeh et al., 2017; Naderi et al., 2019). After 8 weeks' voluntary exercise, miR-126, miR-210, Akt, and ERK1/2 in cardiac tissue were upregulated in both the crocin and voluntary exercise groups (Ghorbanzadeh et al., 2017). Another study found that in the diabetic animals there was an decrease of miR-126 and angiogenesis, while the expression level of miR-210 was increased (Naderi et al., 2019). miR-16 decreased, and miR-21 increased after a 5 weeks' high-intensity interval training (HIIT) intervention scenario (Horak et al., 2018). In addition, targeting VEGFR2 and fibroblast growth factor receptor 1 (FGFR1), miR-16 regulated the reduction in proliferation, migration and angiogenic behavior in endothelial cells (ECs) by while its overexpression led to reduced proliferation, migration and cord formation of ECs *in vitro* (Chamorro-Jorganes et al., 2011). miR-21 could be indirectly engaged in angiogenesis by promoting hypoxia inducible factor-1 (HIF-1α) and VEGF expression and thus may be an exceptional biomarker for evaluating the response to physical exercise (Sheedy, 2015).

Anti-inflammation

Overexpression of miR-181b-5p in vascular endothelium has been shown to inhibit NF-κB signaling pathways by directly targeting importin-α3 expression to reduce inflammation/injury, thus serving as a regulator of inflammatory and immune responses (Sun et al., 2012; Cui et al., 2017). As mentioned above, the expression of miR-21 was increased during HIIT (Horak et al., 2018), mediating the anti-inflammatory response in macrophages and making it a novel and elegant target for therapeutic intervention (Sheedy, 2015).

Antifibrosis

Regular exercise training can effectively inhibit oxidative stress, inflammation and apoptosis, thereby preventing the loss of cardiomyocyte and the formation of ventricular fibrosis (Darband et al., 2019). MiR-29a and miR-101a have been reported to increase with the expression of fibrotic proteins and downregulate with controlled intermittent aerobic exercise in infracted hearts, suggesting that miR-29 and miR-101 can be recognized as fibrosis-associated miRNAs (Xiao et al., 2017). By targeting transforming growth factor β 1 (TGFβ-1) or fos, upregulated miR-29a and miR-101a can prohibit myocardial fibrosis modulated by *COL1A1* and *COL3A1*, ultimately protecting myocardial cells from fibrosis and scar tissue formation (Xiao et al., 2017).

Atrial Remodeling

The expression of miR-1 and miR-133a is increased immediately after marathons, and a negative correlation has been observed in the expression levels of miR-1 and miR-133a with left atrial (LA) diameter immediately after and 24 h after marathons in elite runners (ERs) (Clauss et al., 2016). That research implied that endurance exercise would influence energy metabolism (Clauss et al., 2016) and the increase of miRNAs reflect a latent mechanism behind the observation that mitochondrial dysfunction could affect miRNA expression (Baumgart et al., 2015). Circulating miRNAs could be characterized as potential and novel biomarkers for atrial remodeling.

MiRNAs RESPOND TO CARDIAC-PROTECTION BY EXERCISE

The correlation between exercise and CVDs has been in popularity for decades. Several typical signal pathways and molecular mechanisms of miRNAs have been proposed (**Table 1**), which offer an innovative prospect for cure.

Exercise Mediates Protection Against Atherosclerosis and Myocardial Infarction

Atherogenesis (ATH) is a chronic disease of blood vessels and involves various factors, such as inflammation, immune mechanisms and lipid infiltration, leading to many complications, such as myocardial infarction (MI) and stroke (Libby et al., 2011). MI occurs when the coronary artery undergoes acute persistent ischemia and hypoxia, resulting in myocardial necrosis and pathological cardiac remodeling.

Recently, the miRNA expression profile revealed that a series of miRNAs shows great importance in ATH and MI. Epicardial adipose tissue thickness is reported to be one of the major risk factors of coronary artery disease (CAD), and miR-20 is

TABLE 1 | Changes of miRNAs after exercise in CVDs.

Diseases	Exercise types	MiRNAs	Expressions	Targets	Sources
Coronary artery disease	Swimming	miR-20a (Wang et al., 2017)	Increased	*PTEN*	Endothelial cells
Myocardial infarction	Intermittent aerobic exercise	miR-29a and miR-101a (Xiao et al., 2017)	Increased	TGFβ-1 and fos	Heart tissue
Ischemia-reperfusion	Swimming	miR-21 (Zhao and Ma, 2016)	Increased	*PDCD4*	Cardiomyocytes
	Swimming and running	miR-17-3p (Shi et al., 2017)	Increased	*TIMP3*	
Heart failure	Cycling	miR-21,	Increased	*PPAR*?	Serum
		miR-378, and		ATP6?	
		miR-940 (Xu et al., 2016)		Not mentioned	
	Wheel running	miR-222 (Vujic et al., 2018)		*HIPK1*	Cardiomyocyte
Hypertension	Exercise training	miR-34a and miR-181a (Fernandes et al., 2017)	Decreased	*SIRT1*	Heart tissue
	Running	miR-145 (Liao et al., 2018)	Increased	*IRS-1*	Arteries
		miR-214 (Rodrigues et al., 2018)		SERCA2a	Cardiomyocytes
Pulmonary hypertension	Exercise training	miR-22-3p relative to miR-451a (Grunig et al., 2018)	Decreased	Not mentioned	Serum and plasma
Cardiometabolic diseases	Strength training	miR-146a (Morais Junior et al., 2017)	Increased	*TRAF6*	Serum

correlated with adipogenesis (Isabelle et al., 2015). A recent study occurred that miR-20a was enhanced by swimming training in CAD mice. Therefore, A group of associated atherosclerosis genes was regulated, endothelin 1 (*EDN1*), angiotensin II (ANGII), as well as thromboxane A2 (TxA2) downregulated and endothelial nitric oxide synthase (eNOS), prostacyclin (PGI2), and VEGF upregulated (Wang et al., 2017). Increased miR-20a suppressed the expression of *PTEN*, which eventually contributes to increased survival and proliferation of venous ECs through stimulating of PI3K/Akt signaling pathways (Wang et al., 2017). Furthermore, as previously mentioned, after MI, upregulated miR-29a and miR-101a restrained the TGFβ-1/Smad2/3 and fos/TGFβ-1 pathways via aerobic exercise, eventually inhibiting myocardial interstitial fibrosis (Xiao et al., 2017). This finding could lead to a potential therapeutic strategy for cardiac-protection in MI patients. In addition, miR-92a played a pivotal role in angiogenesis and was associated with arterial dysfunction. miR-92a was reported to be downregulated in aging and its outcomes were relevant to increases in major arterial structural proteins, such as type 1 collagen, and proinflammatory receptors, such as tumor necrosis factor receptor 1 (*TNFR1*) (Hazra et al., 2016). Another study demonstrated that miR-92a increased in the process of endothelial injury after acute myocardial infarction (AMI) and inhibited Kruppel-like factor 2 (*KLF2*) and *KLF4* expression (Liu et al., 2016). However, little information is available about the association between exercise and miR-92a. Thus, further studies should be under consideration to assess the miR-92a's functional impacts of exercise.

Exercise Mediates Protection Against Ischemia-Reperfusion Injury (IRI)

Tissue damage induced by ischemia is the leading cause of fatal diseases. In the therapeutic treatment of ischemic diseases, tissue damage is primarily induced by restoration of the recovered blood supply, which contains excessive free radicals, rather than the ischemia itself. Increased ROS can modify cellular signaling proteins and produce functional consequences, thereby mediating the pathological processes involved in the development of IRI.

The heart may undergo an increase in apoptosis during ischemia-reperfusion (I/R) (Duan et al., 2012). Swimming training increased miR-21 levels and decreased programmed cell death protein 4 (*PDCD4*) expression (Zhao and Ma, 2016). miR-21 downregulated *PDCD4* expression, a critical mediator of cancer cell apoptosis, and cardiomyocyte apoptosis induced by I/R was consequently aggravated (Cheng et al., 2010). Although a remarkable correlation between swimming training and the expression of *PDCD4* didn't be observed, that study still indicated that swimming training was beneficial to exercise-mediated cardiac-protection (Zhao and Ma, 2016). As we described above, miR-17-3p was proven to participate in exercise-induced CH. The study also found that the expression of miR-17-3p was efficiently increased in the hearts of both sham and IRI mice, implying that increasing miR-17-3p levels effectively prevent from myocardial IRI (Shi et al., 2017). Compared with the control group, miR-22 is significantly increased in the heart of rats suffered from IRI in reaction to the following oxidative stress (Du et al., 2016). MiR-22 has been proven to potentially regulate *SIRT1* and peroxisome proliferator-activated receptor-coactivator-1α (PGC1α), both of which are proven to improve mitochondrial function and inhibit oxidative stress, thus alleviating MI (Du et al., 2016). However, the role of miR-22 in exercise needs to be further explored.

Exercise Mediates Protection Against HF

HF is a term used to describe a heart that cannot keep up with its workload, resulting in the body not receiving the oxygen it needs. The expression of miRNA species in HF and the accompanying proteomic remodeling has been characterized previously (Pinti et al., 2017). Oxidative stress plays a critical part in the development of HF. Elevated ROS causes systolic failure and

structural damage, leading to myocardial dysfunction (Shirakawa et al., 2019). Exploration of the molecular mechanisms of miRNAs is still in progress.

MiR-21 targeted and suppressed the peroxisome proliferator-activated receptor (*PPAR*) transcript, which regulates plays an important regulatory role in inflammation, ATH, tumors, and fatty acid anabolic, was shown to be increased during HF (Lai et al., 2015; Pinti et al., 2017). Overexpression of miR-378 suppressed ATP synthase F0 subunit 6 (ATP6) and was characterized in the interfibrillar mitochondria amidst diabetes mellitus (Jagannathan et al., 2015; Shepherd et al., 2017; Li et al., 2018). Recent studies showed that cardiopulmonary exercise test was fairly able to elevate the serum levels of miR-21, miR-378, and miR-940 in HF patients (Xu et al., 2016). Although failed to reveal whether the modulation of these miRNAs was associated with acute exhaustive exercise, muscle damage or inflammation, the authors speculated that exercise may release these miRNAs into the circulation by inducing changes in cells nearby or in distant tissues (Xu et al., 2016).

Exercise Mediates Protection Against Hypertension

Hypertension, one of the most common chronic diseases, is the most crucial risk factor for cardiovascular and cerebrovascular diseases. Getting effective command of blood pressure could significantly reduce cardiovascular and cerebrovascular events and enhance quality of patients' lifespan (Improta Caria et al., 2018).

Compared with the sedentary group, the group of rats that underwent ET exhibited a decrease in aortic miR-34a and miR-181a expression, and hypertension was associated with increases in these miRNAs in spontaneously hypertensive rats (SHR) (Fernandes et al., 2017). miR-34a prohibiting *SIRT1* was found to be in the acceleration of endothelial progenitor cell senescence (Zhao et al., 2010). Moreover, low content of NO is associated with endothelial dysfunction and contributes to the maintenance and development of hypertension. Isometric exercise was reported to increase pro-oxidant activity, which resulted in greater NO bioavailability and antioxidant response, thus reducing patients' blood pressure (Olher et al., 2019). The regulation of eNOS/NO system, *SIRT1* activated endothelium-dependent vascular relaxation, thus exhibiting significant protective effects in cellular aging (Ilwola et al., 2007). A previous study showed that miR-34a and miR-181a targeted *SIRT1* in the heart but did not include any discussion about eNOS (Fernandes et al., 2017). The abnormal proliferation of vascular smooth muscle cells (VSMCs, which exert important functions in structural remodeling) are the main pathological basis for hypertensive vascular remodeling and the development of vascular proliferative diseases. MiR-145 abounds in normal arteries, especially in VSMCs. Compared with control groups, miR-145 in spontaneously hypertensive rats was lower and exercise promoted both the levels of miR-145 and Akt phosphorylation (Liao et al., 2018). MiR-145 was also found to target insulin receptor substrate 1 (*IRS1*) and thus regulate the Akt signaling pathway (Liao et al., 2018). Interestingly, another study showed that in hypertensive rats, ET reduced systolic arterial pressure and increased the accessibility of intracellular Ca^{2+} in myocytes of the left ventricle as well as the expression of miR-214 (Rodrigues et al., 2018). However, the results contradicted the author's expectations and data from previous research that revealed decreased miR-214 expression and increased expression of sarcoplasmic reticulum Ca^{2+}-ATPase (SERCA2a), the main facilitator of Ca^{2+} translocation from the cytosol to the sarcoplasmic reticulum (Melo et al., 2015). Thus, further studies are needed to investigate the possible effects of aerobic exercise on hypertensive cardiomyocytes.

Exercise Mediates Protection Against Pulmonary Hypertension

The main feature of pulmonary hypertension (PH) is a progressive increase in pulmonary artery resistance and the right heart, causing pulmonary vascular remodeling and constriction. ET has been a brand new type of therapy to help PH patients improve their mobility and quality of life. ET quite declined expression levels of miR-22-3p relative to those of miR-451a in serum (Grunig et al., 2018). That research highlights that miRNAs were to be future biomarkers, though it did not disclose the molecular mechanisms of miRNAs in response to ET in the pulmonary vasculature (Grunig et al., 2018).

Exercise Mediates Protection Against Cardiometabolic Diseases

The aging process leads to many physiological and pathological changes in the human body, such as dysfunction of organs, loss of muscle mass and imbalance of metabolism (Margolis et al., 2016), thus in danger of cardiometabolic diseases (CMDs). Type 2 diabetes mellitus (T2D) is an eminently predominant metabolic disease that can result in progressive cardiac dysfunction (Hathaway et al., 2018), contributing to an independent risk factor of CVDs (Improta Caria et al., 2018). Aerobic exercise was reported to effectively protect the heart from accumulation of ROS and may have a therapeutic effect on diabetic cardiomyopathy (Wang et al., 2020). MiR-146a was increased after strength training, reducing serum blood glucose levels in patients with diabetes compared with those without (Morais Junior et al., 2017). miR-146a represses TNF receptor associated factor 6 (*TRAF6*), an element of innate and adaptive immunity that serves as an activator in the NF-κB pathway (Morais Junior et al., 2017), to not only dominate the expression levels of inflammatory gene but also limit the shift from "oxidative phosphorylation to glycolytic metabolism during inflammation" (Runtsch et al., 2019).

LncRNAs AND circRNAs RESPOND TO CARDIAC-PROTECTION BY EXERCISE

LncRNA microarray analysis has been in depth use to measure the consequence of exercise in the expression of lncRNA and mRNA. A recent study showed that swimming training might

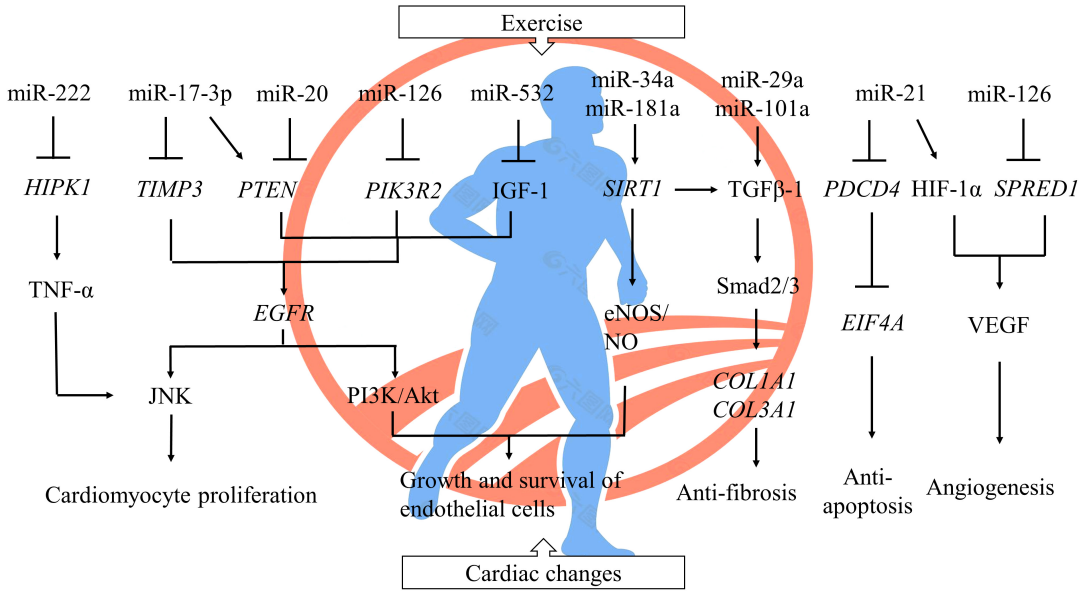

FIGURE 1 | The regulation of miRNAs to cardiac changes after exercise. A single miRNA could have thousands of target genes, and one and the same gene could also be conducted by a host of miRNAs. Exercise-induced cardiac protection involves a series of complex regulation between miRNAs and their signal pathways by inhibiting protein translation and targeting mRNA degradation. ⊥ inhibited; Gene symbols were italicized. *HIPK1,* homeodomain-interacting protein kinase 1; TNF-α, tumor necrosis factor α; *TIMP3*, metallopeptidase inhibitor 3; *PTEN*, phosphatase and tensin homolog; *PIK3R2*, phosphoinositide-3-kinase regulatory subunit 2; IGF-1, insulin-like growth factor 1; *EGFR*, epidermal growth factor receptor; JNK, c-Jun N-terminal kinase; PI3K, phosphoinositide 3-kinase; *SIRT1*, sirtuin-1; NO, nitric oxide; eNOS, endothelial nitric oxide synthase; TGFβ-1, transforming growth factor β 1; *COL1A1*, collagen type I alpha 1 chain; *COL3A1*, collagen type III alpha 1 chain; *PDCD4*, programmed cell death protein 4; *EIF4A*, eukaryotic translation initiation factor 4A; HIF-1α, hypoxia inducible factor-1; *SPRED1,* sprouty-related protein 1; VEGF, vascular endothelial growth factor.

alleviate vascular IRI via FR030200-Col3A1 and FR402720-Rnd1 compared with consumption of a high-fat diet by improving insulin sensitivity (Liu et al., 2018). FR030200-Col3A1, FR402720-Rnd1, and FR030200/FR402720-Rnd3 signaling were identified in the cytoskeletal rearrangement pathway, while E2F1-FR030200/FR402720-Nnat and FR030200/FR402720-Fam46a signaling in the anti-inflammatory process (Liu et al., 2018). A previous study identified the latent correlation between lncRNA-mRNAs and ET as novel biomarker as well as therapeutic strategy for vascular endothelial IRI. Furthermore, lncRNA THRIL, as a transcriptional regulator of TNF-α, was altered after a half marathon race and was speculated beyond of NF-kB signaling pathway (Gary et al., 2019).

Differing from miRNAs and lncRNAs, circRNAs have been studied for only the past several years. A vast majority of complex functions and mechanisms of circRNAs remain unclear, with most research focusing on determining their roles in various diseases (Bei et al., 2018; Zhang et al., 2018). Studies of the connections of circRNAs between exercise and cardiac-protection are still in their infancy.

SUMMARY AND FUTURE PERSPECTIVES

In this review, we have probed into the molecular mechanisms of ncRNAs about exercise-mediated protection of CVDs. MiRNAs, stable in expression, transferred and communicated through extracellular vesicles and released into circulation to accomplish multiple biological functions, have a positive effect on cardiac-protection via targeting related genes in numerous signaling pathways (**Figure 1**), thus becoming the promising biomarkers and targets for diagnosis and treatment of CVDs. LncRNAs regulate expressions of target genes and their signaling pathways in multiple links. However, the roles of circRNAs require further research.

Exercise-derived oxidative stress is one of the most important factors in development of CVDs. There is an interaction between ncRNAs especially miRNAs and ROS, but we still have a finite awareness of the molecular mechanisms of miRNAs regulating CVDs under ROS-related stress conditions. Moreover, it remains challenging to translate the results of recent studies of CVDs to clinical applications. Since this field is only in its early stages, researches on exercise-mediated ncRNAs have been generally based on miRNAs. However, the expression of other ncRNA families in exercise are still in lack of relevant exploration. Above all, these preliminary studies provide an optimistic perspective of ncRNA-based therapeutics for cardiac rehabilitation.

AUTHOR CONTRIBUTIONS

HY designed the theme of the review. YZ wrote the manuscript. NH, BF, and HY reviewed the manuscript. HY approved the final edition.

FUNDING

This work was supported by the Ningbo Medical Science and Technology Project (2016Z01), Ningbo Health Branding Subject Fund (PPXK2018-01), Ningbo HwaMei Research Fund (2017HMKY04), and Zhejiang Provincial Public Service and Application Research Foundation, China (LGF20H250001).

REFERENCES

Alves, R., Suehiro, C. L., Oliveira, F. G., Frantz, E. D. C., Medeiros, R. F., Vieira, R. P., et al. (2020). Aerobic exercise modulates cardiac NAD(P)H oxidase and the NRF2/KEAP1 pathway in a mouse model of chronic fructose consumption. *J. Appl. Physiol. (*1985) 128, 59–69. doi: 10.1152/japplphysiol.00201.2019

Angel, D., Almudena, E., Amelia, A., and Diego, F. (2019). The role of non-coding RNA in congenital heart diseases. *J. Cardiovasc. Dev. Dis.* 6:15. doi: 10.3390/jcdd6020015

Baumgart, B. R., Gray, K. L., Woicke, J., Bunch, R. T., Sanderson, T. P., and Van Vleet, T. R. (2015). MicroRNA as biomarkers of mitochondrial toxicity. *Toxicol. Appl. Pharmacol.* 312, 26–33. doi: 10.1016/j.taap.2015.10.007

Bei, Y., Tao, L., Cretoiu, D., Cretoiu, S. M., and Xiao, J. (2017). MicroRNAs mediate beneficial effects of exercise in heart. *Adv. Exp. Med. Biol.* 1000, 261–280. doi: 10.1007/978-981-10-4304-8_15

Bei, Y., Yang, T., Wang, L., Holvoet, P., Das, S., Sluijter, J. P. G., et al. (2018). Circular RNAs as potential theranostics in the cardiovascular system. *Mol. Ther. Nucleic Acids* 13, 407–418. doi: 10.1016/j.omtn.2018.09.022

Chamorro-Jorganes, A., Araldi, E., Penalva, L. O., Sandhu, D., Fernandez-Hernando, C., and Suarez, Y. (2011). MicroRNA-16 and microRNA-424 regulate cell-autonomous angiogenic functions in endothelial cells via targeting vascular endothelial growth factor receptor-2 and fibroblast growth factor receptor-1. *Arterioscler. Thromb. Vasc. Biol.* 31, 2595–2606. doi: 10.1161/atvbaha.111.236521

Cheng, Y., Zhu, P., Yang, J., Liu, X., Dong, S., Wang, X., et al. (2010). Ischaemic preconditioning-regulated miR-21 protects heart against ischaemia/reperfusion injury via anti-apoptosis through its target PDCD4. *Cardiovasc. Res.* 87, 431–439. doi: 10.1093/cvr/cvq082

Clauss, S., Wakili, R., Hildebrand, B., Kaab, S., Hoster, E., Klier, I., et al. (2016). MicroRNAs as biomarkers for acute atrial remodeling in marathon runners (The miRathon study–a sub-study of the Munich marathon study). *PLoS One* 11:e0148599. doi: 10.1371/journal.pone.0148599

Conti, V., Forte, M., Corbi, G., Russomanno, G., Formisano, L., Landolfi, A., et al. (2017). Sirtuins: possible clinical implications in cardio and cerebrovascular diseases. *Curr. Drug Targets* 18, 473–484. doi: 10.2174/1389450116666151019095903

Corbi, G., Conti, V., Troisi, J., Colucci, A., Manzo, V., Di Pietro, P., et al. (2019). Cardiac rehabilitation increases SIRT1 activity and beta-hydroxybutyrate levels and decreases oxidative stress in patients with HF with preserved ejection fraction. *Oxid. Med. Cell. Longev.* 2019:7049237. doi: 10.1155/2019/7049237

Cui, S., Sun, B., Yin, X., Guo, X., Chao, D., Zhang, C., et al. (2017). Time-course responses of circulating microRNAs to three resistance training protocols in healthy young men. *Sci. Rep.* 7:2203. doi: 10.1038/s41598-017-02294-y

Darband, S. G., Sadighparvar, S., Yousefi, B., Kaviani, M., Mobaraki, K., and Majidinia, M. (2019). Combination of exercise training and L-arginine reverses aging process through suppression of oxidative stress, inflammation, and apoptosis in the rat heart. *Pflugers Arch.* 472, 169–178. doi: 10.1007/s00424-019-02311-1

Denham, J., Gray, A., Scott-Hamilton, J., and Hagstrom, A. D. (2018). Sprint interval training decreases circulating microRNAs important for muscle development. *Int. J. Sports Med.* 39, 67–72. doi: 10.1055/s-0043-120763

Di Meo, S., Napolitano, G., and Venditti, P. (2019). Mediators of physical activity protection against ROS-linked skeletal muscle damage. *Int. J. Mol. Sci.* 20:3024. doi: 10.3390/ijms20123024

Ding, S., Gan, T., Song, M., Dai, Q., Huang, H., Xu, Y., et al. (2017). C/EBPB-CITED4 in exercised heart. *Adv. Exp. Med. Biol.* 1000, 247–259. doi: 10.1007/978-981-10-4304-8_14

Dong, Y., Xu, W., Liu, C., Liu, P., Li, P., and Wang, K. (2019). Reactive oxygen species related noncoding RNAs as regulators of cardiovascular diseases. *Int. J. Biol. Sci.* 15, 680–687. doi: 10.7150/ijbs.30464

Du, J. K., Cong, B. H., Yu, Q., Wang, H., Wang, L., Wang, C. N., et al. (2016). Upregulation of microRNA-22 contributes to myocardial ischemia-reperfusion injury by interfering with the mitochondrial function. *Free Radic. Biol. Med.* 96, 406–417. doi: 10.1016/j.freeradbiomed.2016.05.006

Duan, X., Ji, B., Wang, X., Liu, J., Zheng, Z., Long, C., et al. (2012). Expression of microRNA-1 and microrna-21 in different protocols of ischemic conditioning in an isolated rat heart model. *Cardiology* 122, 36–43. doi: 10.1159/000338149

Fernandes, T., Gomes-Gatto, C. V., Pereira, N. P., Alayafi, Y. R., das Neves, V. J., and Oliveira, E. M. (2017). NO signaling in the cardiovascular system and exercise. *Adv. Exp. Med. Biol.* 1000, 211–245. doi: 10.1007/978-981-10-4304-8_13

Gary, M. A., Tanner, E. A., Davis, A. A., and McFarlin, B. K. (2019). Combined bead-based multiplex detection of RNA and protein biomarkers: implications for understanding the time course of skeletal muscle injury and repair. *Methods* 158, 92–96. doi: 10.1016/j.ymeth.2018.11.012

Ghorbanzadeh, V., Mohammadi, M., Dariushnejad, H., Abhari, A., Chodari, L., and Mohaddes, G. (2017). Cardioprotective effect of crocin combined with voluntary exercise in rat: role of Mir-126 and Mir-210 in heart angiogenesis. *Arq. Bras. Cardiol.* 109, 54–62. doi: 10.5935/abc.20170087

Gomes, C. P. C., de Gonzalo-Calvo, D., Toro, R., Fernandes, T., Theisen, D., Wang, D.-Z., et al. (2018). Non-coding RNAs and exercise: pathophysiological role and clinical application in the cardiovascular system. *Clin. Sci.* 132, 925–942. doi: 10.1042/cs20171463

Grunig, G., Eichstaedt, C. A., Verweyen, J., Durmus, N., Saxer, S., Krafsur, G., et al. (2018). Circulating MicroRNA markers for pulmonary hypertension in supervised exercise intervention and nightly oxygen intervention. *Front. Physiol.* 9:955. doi: 10.3389/fphys.2018.00955

Günay, Y., Emre, B., Ezel, N. K., Dario, N., and Gıyasettin, D. (2018). The association of various social capital indicators and physical activity participation among Turkish adolescents. *J. Sport Health Sci.* 7, 27–33. doi: 10.1016/j.jshs.2017.10.008

Hathaway, Q. A., Pinti, M. V., Durr, A. J., Waris, S., Shepherd, D. L., and Hollander, J. M. (2018). Regulating microRNA expression: at the heart of diabetes mellitus and the mitochondrion. *Am. J. Physiol. Heart Circ. Physiol.* 314, H293–H310. doi: 10.1152/ajpheart.00520.2017

Hazra, S., Henson, G. D., Morgan, R. G., Breevoort, S. R., Ives, S. J., Richardson, R. S., et al. (2016). Experimental reduction of miR-92a mimics arterial aging. *Exp. Gerontol.* 83, 165–170. doi: 10.1016/j.exger.2016.08.007

Horak, M., Zlamal, F., Iliev, R., Kucera, J., Cacek, J., Svobodova, L., et al. (2018). Exercise-induced circulating microRNA changes in athletes in various training scenarios. *PLoS One* 13:e0191060. doi: 10.1371/journal.pone.0191060

Ilwola, M., Cuk-Seong, K., Asma, N., Tohru, Y., Hoffman, T. A., Saet-Byel, J., et al. (2007). SIRT1 promotes endothelium-dependent vascular relaxation by activating endothelial nitric oxide synthase. *Proc. Natl. Acad. Sci. U.S.A.* 104, 14855–14860. doi: 10.1073/pnas.0704329104

Improta Caria, A., Nonaka, C., Pereira, C., Soares, M., Macambira, S., and Souza, B. (2018). Exercise training-induced changes in MicroRNAs: beneficial regulatory effects in hypertension, type 2 diabetes, and obesity. *Int. J. Mol. Sci.* 19:3608. doi: 10.3390/ijms19113608

Isabelle, G., Sarah, M., Tamsyn, C., Vicente, G., Shingo, K., Matthew, W., et al. (2015). Comparative analysis of microRNA expression in mouse and human brown adipose tissue. *BMC Genomics* 16:820. doi: 10.1186/s12864-015-2045-8

Jagannathan, R., Thapa, D., Nichols, C. E., Shepherd, D. L., Stricker, J. C., Croston, T. L., et al. (2015). Translational regulation of the mitochondrial genome following redistribution of mitochondrial MicroRNA in the diabetic heart. *Circ. Cardiovasc. Genet.* 8, 785–802. doi: 10.1161/CIRCGENETICS.115.001067

Kura, B., Szeiffova Bacova, B., Kalocayova, B., Sykora, M., and Slezak, J. (2020). Oxidative stress-responsive MicroRNAs in heart injury. *Int. J. Mol. Sci.* 21:358. doi: 10.3390/ijms21010358

Lai, K.-B., Sanderson, J. E., Izzat, M. B., and Yu, C.-M. (2015). Micro-RNA and mRNA myocardial tissue expression in biopsy specimen from patients with heart failure. *Int. J. Cardiol.* 199, 79–83. doi: 10.1016/j.ijcard.2015.07.043

Li, Y., Huo, C., Pan, T., Li, L., Jin, X., Lin, X., et al. (2019). Systematic review regulatory principles of non-coding RNAs in cardiovascular diseases. *Brief. Bioinform.* 20, 66–76. doi: 10.1093/bib/bbx095

Li, Y., Jiang, J., Liu, W., Wang, H., Zhao, L., Liu, S., et al. (2018). microRNA-378 promotes autophagy and inhibits apoptosis in skeletal muscle. *Proc. Natl. Acad. Sci. U.S.A.* 115, E10849–E10858. doi: 10.1073/pnas.1803377115

Liao, J., Zhang, Y., Wu, Y., Zeng, F., and Shi, L. (2018). Akt modulation by miR-145 during exercise-induced VSMC phenotypic switching in hypertension. *Life Sci.* 199, 71–79. doi: 10.1016/j.lfs.2018.03.011

Libby, P., Ridker, P. M., and Hansson, G. K. (2011). Progress and challenges in translating the biology of atherosclerosis. *Nature* 473, 317–325. doi: 10.1038/nature10146

Liu, H., Li, G., Zhao, W., and Hu, Y. (2016). Inhibition of MiR-92a may protect endothelial cells after acute myocardial infarction in rats: role of KLF2/4. *Med. Sci. Monit.* 22, 2451–2462. doi: 10.12659/msm.897266

Liu, S., Zheng, F., Cai, Y., Zhang, W., and Dun, Y. (2018). Effect of long-term exercise training on lncrnas expression in the vascular injury of insulin resistance. *J. Cardiovasc. Transl. Res.* 11, 459–469. doi: 10.1007/s12265-018-9830-0

Liu, X., Platt, C., and Rosenzweig, A. (2017). The role of MicroRNAs in the cardiac response to exercise. *Cold Spring Harb. Perspect. Med.* 7:a029850. doi: 10.1101/cshperspect.a029850

Malcolm, E., Cesare, G., Julianne, B., Adeel, S., David, B., and Jonathan, P. L. (2018). Impact of a single bout of high-intensity interval exercise and short-term interval training on interleukin-6, FNDC5, and METRNL mRNA expression in human skeletal muscle. *J. Sport Health Sci.* 7, 191–196. doi: 10.1016/j.jshs.2017.01.003

Margolis, L. M., Lessard, S. J., Ezzyat, Y., Fielding, R. A., and Rivas, D. A. (2016). Circulating MicroRNA are predictive of aging and acute adaptive response to resistance exercise in men. *J. Gerontol. A Biol. Sci. Med. Sci.* 72, 1319–1326. doi: 10.1093/gerona/glw243

Margolis, L. M., and Rivas, D. A. (2018). Potential role of MicroRNA in the anabolic capacity of skeletal muscle with aging. *Exerc. Sport Sci. Rev.* 46, 86–91. doi: 10.1249/jes.0000000000000147

Melo, S. F., Barauna, V. G., Neves, V. J., Fernandes, T., Lara Lda, S., Mazzotti, D. R., et al. (2015). Exercise training restores the cardiac microRNA-1 and -214 levels regulating Ca2+ handling after myocardial infarction. *BMC Cardiovasc. Disord.* 15:166. doi: 10.1186/s12872-015-0156-4

Merry, T. L., MacRae, C., Pham, T., Hedges, C. P., and Ristow, M. (2020). Deficiency in ROS-sensing nuclear factor erythroid 2-like 2 causes altered glucose and lipid homeostasis following exercise training. *Am. J. Physiol. Cell Physiol.* 318, C337–C345. doi: 10.1152/ajpcell.00426.2019

Morais Junior, G. S., Souza, V. C., Machado-Silva, W., Henriques, A. D., Melo Alves, A., Barbosa Morais, D., et al. (2017). Acute strength training promotes responses in whole blood circulating levels of miR-146a among older adults with type 2 diabetes mellitus. *Clin. Interv. Aging* 12, 1443–1450. doi: 10.2147/cia.S141716

Naderi, R., Mohaddes, G., Mohammadi, M., Alihemmati, A., Khamaneh, A., Ghyasi, R., et al. (2019). The effect of garlic and voluntary exercise on cardiac angiogenesis in diabetes: the role of MiR-126 and MiR-210. *Arq. Bras. Cardiol.* 112, 154–162. doi: 10.5935/abc.20190002

Olher, R. R., Rosa, T. S., Souza, L. H. R., Oliveira, J. F., Soares, B. R. A., Ribeiro, T. B. A., et al. (2019). Isometric exercise improves redox balance and blood pressure in hypertensive adults. *Med. Sci. Sports Exerc.* doi: doi:10.1249/MSS.0000000000002223 [Epub ahead of print].

Pinti, M. V., Hathaway, Q. A., and Hollander, J. M. (2017). Role of microRNA in metabolic shift during heart failure. *Am. J. Physiol. Heart Circ. Physiol.* 312, H33–H45. doi: 10.1152/ajpheart.00341.2016

Rodrigues, J. A., Prímola-Gomes, T. N., Soares, L. L., Leal, T. F., Nóbrega, C., Pedrosa, D. L., et al. (2018). Physical exercise and regulation of intracellular calcium in cardiomyocytes of hypertensive rats. *Arq. Bras. Cardiol.* 111, 172–179. doi: 10.5935/abc.20180113

Romeo, B. B., Mitch, J. D., Vincent, J. D., Geraldine, L. B., and Andrew, S. F. (2018). Effect of different intensities of physical activity on cardiometabolic markers and vascular and cardiac function in adult rats fed with a high-fat high-carbohydrate diet. *J. Sport Health Sci.* 7, 109–119. doi: 10.1016/j.jshs.2016.08.001

Runtsch, M. C., Nelson, M. C., Lee, S. H., Voth, W., Alexander, M., Hu, R., et al. (2019). Anti-inflammatory microRNA-146a protects mice from diet-induced metabolic disease. *PLoS Genet.* 15:e1007970. doi: 10.1371/journal.pgen.1007970

Samanta, S., Balasubramanian, S., Rajasingh, S., Patel, U., Dhanasekaran, A., Dawn, B., et al. (2016). MicroRNA: a new therapeutic strategy for cardiovascular diseases. *Trends Cardiovasc. Med.* 26, 407–419. doi: 10.1016/j.tcm.2016.02.004

Sapp, R. M., Shill, D. D., Roth, S. M., and Hagberg, J. M. (2017). Circulating microRNAs in acute and chronic exercise: more than mere biomarkers. *J. Appl. Physiol. (*1985) 122, 702–717. doi: 10.1152/japplphysiol.00982.2016

Sheedy, F. J. (2015). Turning 21: induction of miR-21 as a key switch in the inflammatory response. *Front. Immunol.* 6:19. doi: 10.3389/fimmu.2015.00019

Shepherd, D. L., Hathaway, Q. A., Pinti, M. V., Nichols, C. E., Durr, A. J., Sreekumar, S., et al. (2017). Exploring the mitochondrial microRNA import pathway through Polynucleotide Phosphorylase (PNPase). *J. Mol. Cell. Cardiol.* 110, 15–25. doi: 10.1016/j.yjmcc.2017.06.012

Shi, J., Bei, Y., Kong, X., Liu, X., Lei, Z., Xu, T., et al. (2017). miR-17-3p contributes to exercise-induced cardiac growth and protects against myocardial ischemia-reperfusion injury. *Theranostics* 7, 664–676. doi: 10.7150/thno.15162

Shirakawa, R., Yokota, T., Nakajima, T., Takada, S., Yamane, M., Furihata, T., et al. (2019). Mitochondrial reactive oxygen species generation in blood cells is associated with disease severity and exercise intolerance in heart failure patients. *Sci. Rep.* 9:14709. doi: 10.1038/s41598-019-51298-3

Silveira, A. C., Fernandes, T., Soci, U. P. R., Gomes, J. L. P., Barretti, D. L., Mota, G. G. F., et al. (2017). Exercise training restores cardiac MicroRNA-1 and MicroRNA-29c to nonpathological levels in obese rats. *Oxid. Med. Cell. Longev.* 2017:1549014. doi: 10.1155/2017/1549014

Soci, U. P., Fernandes, T., Hashimoto, N. Y., Mota, G. F., Amadeu, M. A., Rosa, K. T., et al. (2011). MicroRNAs 29 are involved in the improvement of ventricular compliance promoted by aerobic exercise training in rats. *Physiol. Genomics* 43, 665–673. doi: 10.1152/physiolgenomics.00145.2010

Sun, X., Icli, B., Wara, A. K., Belkin, N., He, S., Kobzik, L., et al. (2012). MicroRNA-181b regulates NF-kappaB-mediated vascular inflammation. *J. Clin. Invest.* 122, 1973–1990. doi: 10.1172/JCI61495

Tofas, T., Draganidis, D., Deli, C. K., Georgakouli, K., Fatouros, I. G., and Jamurtas, A. Z. (2019). Exercise-induced regulation of redox status in cardiovascular diseases: the role of exercise training and detraining. *Antioxidants* 9:13. doi: 10.3390/antiox9010013

Vujic, A., Lerchenmuller, C., Wu, T. D., Guillermier, C., Rabolli, C. P., Gonzalez, E., et al. (2018). Exercise induces new cardiomyocyte generation in the adult mammalian heart. *Nat. Commun.* 9:1659. doi: 10.1038/s41467-018-04083-1

Wang, D., Wang, Y., Ma, J., Wang, W., Sun, B., Zheng, T., et al. (2017). MicroRNA-20a participates in the aerobic exercise-based prevention of coronary artery disease by targeting PTEN. *Biomed. Pharmacother.* 95, 756–763. doi: 10.1016/j.biopha.2017.08.086

Wang, S. Y., Zhu, S., Wu, J., Zhang, M., Xu, Y., Xu, W., et al. (2020). Exercise enhances cardiac function by improving mitochondrial dysfunction and maintaining energy homoeostasis in the development of diabetic cardiomyopathy. *J. Mol. Med. (Berl.)* 98, 245–261. doi: 10.1007/s00109-019-01861-2

Xiao, L., He, H., Ma, L., Da, M., Cheng, S., Duan, Y., et al. (2017). Effects of miR-29a and miR-101a expression on myocardial interstitial collagen generation after aerobic exercise in myocardial-infarcted rats. *Arch. Med. Res.* 48, 27–34. doi: 10.1016/j.arcmed.2017.01.006

Xu, J., Liu, Y., Xie, Y., Zhao, C., and Wang, H. (2017). Bioinformatics analysis reveals MicroRNAs regulating biological pathways in exercise-induced cardiac physiological hypertrophy. *BioMed Res. Int.* 2017:2850659. doi: 10.1155/2017/2850659

Xu, T., Zhou, Q., Lin, C., Das, S., Wang, L., Jiang, J., et al. (2016). Circulating miR-21, miR-378, and miR-940 increase in response to an acute exhaustive exercise in chronic heart failure patients. *Oncotarget* 7, 12414–12425. doi: 10.18632/oncotarget.6966

Zaglia, T., Ceriotti, P., Campo, A., Borile, G., Armani, A., Carullo, P., et al. (2017). Content of mitochondrial calcium uniporter (MCU) in cardiomyocytes is regulated by microRNA-1 in physiologic and pathologic hypertrophy. *Proc. Natl. Acad. Sci. U.S.A.* 114, E9006–E9015. doi: 10.1073/pnas.1708772114

Zhang, S., and Chen, N. (2018). Regulatory role of MicroRNAs in muscle atrophy during exercise intervention. *Int. J. Mol. Sci.* 19:405. doi: 10.3390/ijms19020405

Zhang, Z., Yang, T., and Xiao, J. (2018). Circular RNAs: promising biomarkers for human diseases. *EBioMedicine* 34, 267–274. doi: 10.1016/j.ebiom.2018.07.036

Zhao, T., Li, J., and Chen, A. F. (2010). MicroRNA-34a induces endothelial progenitor cell senescence and impedes its angiogenesis via suppressing silent information regulator 1. *Am. J. Physiol. Endocrinol. Metab.* 299, E110–E116. doi: 10.1152/ajpendo.00192.2010

Zhao, Y., and Ma, Z. (2016). Swimming training affects apoptosis-related microRNAs and reduces cardiac apoptosis in mice. *Gen. Physiol. Biophys.* 35, 443–450. doi: 10.4149/gpb_2016012

Conflict of Interest: The authors declare that the research was conducted in the absence of any commercial or financial relationships that could be construed as a potential conflict of interest.

frontiers in Genetics

ORIGINAL RESEARCH
published: 31 March 2020
doi: 10.3389/fgene.2020.00299

Functional Characterization and Expression Analyses Show Differential Roles of Maternal and Zygotic Dgcr8 in Early Embryonic Development

Zeyao Zhu[1,2], Yun Liu[3], Wen Xu[2], Taian Liu[4], Yuxin Xie[2], Kathy W. Y. Sham[2], Ou Sha[1] and Christopher H. K. Cheng[2]**

[1] Department of Anatomy, Histology and Developmental Biology, School of Basic Medical Sciences, Shenzhen University, Shenzhen, China, [2] School of Biomedical Sciences, The Chinese University of Hong Kong, Hong Kong, China, [3] State Key Laboratory of Biocontrol, Institute of Aquatic Economic Animals, Sun Yat-sen University, Guangzhou, China, [4] Shenzhen Institutes of Advanced Technology, Chinese Academy of Sciences, Shenzhen, China

OPEN ACCESS

Edited by:
Junjie Xiao, Shanghai University, China

Reviewed by:
Gracjan Michlewski, The University of Edinburgh, United Kingdom
Kan Liu, University of Nebraska-Lincoln, United States

***Correspondence:**
Ou Sha
shaou@szu.edu.cn
Christopher H. K. Cheng
chkcheng@cuhk.edu.hk

Specialty section:
This article was submitted to RNA, a section of the journal Frontiers in Genetics

Received: *24 November 2019*
Accepted: *13 March 2020*
Published: *31 March 2020*

Citation:
Zhu Z, Liu Y, Xu W, Liu T, Xie Y, Sham KWY, Sha O and Cheng CHK (2020) Functional Characterization and Expression Analyses Show Differential Roles of Maternal and Zygotic Dgcr8 in Early Embryonic Development. Front. Genet. 11:299. doi: 10.3389/fgene.2020.00299

Dgcr8 is involved in the biogenesis of canonical miRNAs to process pri-miRNA into pre-miRNA. Previous studies have provided evidence that Dgcr8 plays an essential role in different biological processes. However, the function of maternal and zygotic Dgcr8 in early embryonic development remains largely unknown. Recently, we have reported a novel approach for generating germline-specific deletions in zebrafish. This germline knockout model offers an opportunity to investigate into the differential roles of maternal or zygotic Dgcr8. Although germline specific dgcr8 deletion has no influence on gonad development, maternal or zygotic dgcr8 is essential for embryonic development in the offspring. Both maternal *dgcr8* (M*dgcr8*) and maternal zygotic *dgcr8* (MZ*dgcr8*) mutants display multiple developmental defects and die within 1 week. Moreover, MZ*dcgr8* mutant displays more severe morphogenesis defects. However, when a miR-430 duplex (the most abundantly expressed miRNA in early embryonic stage) is used to rescue the maternal mutant phenotype, the Mdgcr8 embryos could be rescued successfully and grow into adulthood and achieve sexual maturation, whereas the MZ*dgcr8* embryos are only partially rescued and they all die within 1 week. The differential phenotypes between the Mdgcr8 and MZ*dgcr8* embryos provide us with an opportunity to study the roles of individual miRNAs during early development.

Keywords: maternal dgcr8, zygotic dgcr8, microRNAs, zebrafish, embryonic development

INTRODUCTION

The model organism zebrafish (*Danio rerio*) is an excellent system for studying the developmental process of organogenesis. However, its application is limited due to the lack of a conditional knockout (cKO) platform. Recently, we have developed a novel approach for achieving cKO in zebrafish (Liu et al., 2017), making it possible to study the maternal genes in specific tissues or cells. Using this platform, maternal gene knockout zebrafish can be constructed by specifically deleting

maternal genes in the oocytes. Furthermore, maternal mutant models cannot be constructed using the usual knockout methods because of the lethality of maternal homozygous gene knockouts. Therefore, our approach makes it possible to study the function of maternal factors during embryonic development in zebrafish.

Generally, maternal factors are important components in early embryonic development during the cleavage stage to maintain normal meiosis prior to the activation of the embryonic genome (Dosch et al., 2004; Wagner et al., 2004; Harvey et al., 2013). In zebrafish, the first maternal-effect mutant called *janus* was discovered, and this mutant appears to have a phenotype with a partially penetrant axis duplication, but the mechanism of this phenotypic change was not known at that time (Abdelilah et al., 1994). Subsequently, numerous maternal effect genes were discovered in the 1990s (Haffter et al., 1996; Kane et al., 1996; Gritsman et al., 1999; Miller-Bertaglio et al., 1999; Sirotkin et al., 2000). In mammals, thanks to the application of gene knock-out technology in mice, many studies have demonstrated that mammalian embryogenesis also needs maternal regulation, and numerous maternal factors have been identified in mice (Christians et al., 2000; Tong et al., 2000; Payer et al., 2003; Wu et al., 2003; Wagner et al., 2004).

Usually, maternal mutants have no influence on the mother, but normal zygotic development is seriously disrupted even if the mutated allele fails to pass to the offspring (Marlow, 2010). In zebrafish, several maternal genes have been identified by mutagenesis screening (Solnica-Krezel et al., 1996; Dosch et al., 2004; Wagner et al., 2004). Studies of the maternal mutants have revealed that maternal factors not only promote early embryonic cell division but also direct cell fate and organize the embryonic body plan (Tadros and Lipshitz, 2009; Marlow, 2010).

In the present study, we have used a number of approaches to examine the difference in M*dgcr8* and MZ*dgcr8* after rescuing. The absence of maternal Dgcr8 resulted in severe defects, including the disruption of gastrulation or epiboly movement, brain malformation, hematopoiesis defects, heart defects, and body curvature changes. Our findings also demonstrate that most of these defects could be rescued except hematopoiesis and heart defects in MZ*dgcr8*. Further analysis demonstrated that miR-430 partially rescued hematopoiesis and heart function, suggesting that a multitude of miRNAs including miR-430 are the key factors in maintaining development of the heart and hematopoiesis system in early embryonic development.

MATERIALS AND METHODS

Generation of M*dgcr8* and MZ*dgcr8* Zebrafish

We obtained M*dgcr8* and MZ*dgcr8* mutant zebrafish using kop: Cre-UTR-nanos3, *dgcr8* cKO females crossed with wild-type male and kop: Cre-UTR-nanos3, *dgcr8* cKO male, respectively. M*dgcr8* and MZ*dgcr8* embryos were collected from natural spawning in the zebrafish facility system with a 14 h/10 h light/dark cycle, and embryos were collected and kept in 28.5°C incubators with a light/dark cycle. The developmental staging of the embryos was classified according to the universal principle (Kimmel et al., 1995).

RNA Isolation and Real-Time PCR

Total RNA samples were isolated from zebrafish embryos at several developmental stages (shield, 75%-epiboly, prim-6, prim-16) with an RNeasy Mini Kit (Qiagen). The amount and purity of the RNA samples were determined by NanoDrop 2000 spectrophotometry (Thermo Fisher Scientific). The cDNA was synthesized using the PrimeScript RT Reagent Kit (Takara). Real-time PCR was performed on an ABI PRISM 7900 Sequence Detection System (Applied Biosystems) using the SYBR Green I Kit (Applied Biosystem). The primers used in this study are listed in **Supplementary Table S1**. The mRNA transcript levels were normalized against the ef14α transcript level.

Whole-Mount *in situ* Hybridization

Whole mount *in situ* hybridization (ISH) was performed as described (Li et al., 2014). cDNA fragments were amplified by RT-PCR with specific primers (**Supplementary Table S1**), followed by *in vitro* transcription with either T7 RNA polymerase to generate the antisense probe using the DIG RNA Labeling Kit (Roche, United States). Images were captured using a SZX16 stereomicroscope with fluorescence imaging (Olympus, Japan).

Morphological and Histological Analysis

After anesthetization and dissection of adult zebrafish, gonads including testes and ovaries were carefully obtained and then transferred into a culture dish containing 60% L-15 medium for investigation. After fixed in Bouin's fixative buffer (Sigma, United States) or 4% PFA (Sigma, United States) overnight at 4°C, the gonad samples were dehydrated and embedded in paraffin, and then sectioned at 5 μm thickness on a Leica microtome. After drying overnight, the slides were stained with hematoxylin and eosin (H&E) according to the standard protocol (Sabaliauskas et al., 2006). Folliculogenesis (Wang and Ge, 2004) and spermatogenesis (Leal et al., 2009) were staged accordingly.

Mitotic Centrosome Detection

Embryos were fixed with 4% PFA overnight at 4°C and dehydrated in absolute methanol for at least 20 min at −20°C. After washing thrice with 1 × PBST, the embryos were then permeabilized in −20°C acetone for 8 min. After washing, the embryos were blocked with blocking buffer (2% lamb serum, 0.1% dimethyl sulfoxide, 0.1% bovine serum albumin, and 0.2% Triton-X100 in PBS) for 1 h at room temperature. The embryos were treated with anti-γ-tubulin antibody (Sigma) at a dilution of 1:1000 in blocking buffer overnight at 4°C. After washing with PBST for 30 min three to five times at room temperature, the embryos were incubated in fluorescein-conjugated secondary goat antirabbit antibody (Alexa-fluor 555, 1:500, Life Technology, United States) at 1:1000 dilution for 2 h at room temperature. The embryos were then washed eight times in PBST for 5 min each. The whole embryos were mounted in a confocal dish with DAPI Fluoromount-G medium (Southern Biotech) and incubated for 5 min prior to imaging.

Phosphorylation of Histone H3 (PH3) Antibody Staining

Zebrafish embryos were first fixed at 4°C in 4% PFA overnight. After washing three times with PBST (PBS + 0.2% Triton-X100) for 5 min each, the embryos were permeabilized for 8 min in −20°C acetone, washed in PBST three times, blocked for 30 min at room temperature with blocking buffer (2% lamb serum, 0.1% dimethyl sulfoxide, 0.1% bovine serum albumin, and 0.2% Triton-X100 in PBS), and then incubated overnight at 4°C in polyclonal rabbit anti-phospho-histone H3 antibody (Cell Signaling Technology, United States) at a concentration of 1:1000. After washing five times with PBST for 5 min each, the embryos were incubated for 2 h at room temperature in secondary goat antirabbit antibody (Alexa-fluor 555, 1:500, Life Technology, United States). Then, the embryos were washed eight times with PBST for 5 min each and processed for imaging. Changes in the numbers of mitotic cell were quantified by counting the number of phospho-histone 3 (PH3) positive cells in the whole body of the embryo taking the mean of three embryos.

Rescue of M*dgcr8* and MZ*dgcr8* Using miR-430 Duplex

To perform the rescue of the M*dgcr8* and MZ*dgcr8* phenotypes, the miR-430 duplex mimics were synthesized by Shanghai GenePharma Co., Ltd. Working solutions were prepared in RNase free water at 20 μM and stored at −20°C. For the rescue, 1–2 nl of miR-430 duplexes (a mixture of miR-430a, miR-430b, and miR-430c at a ratio of 1:1:1) were injected into one-cell stage M*dgcr8* and MZ*dgcr8* embryos. The phenotypic changes in embryo development were recorded on a stereomicroscope.

Quantifying Heart Rate

From the digital video of 52 h post fertilization (hpf) or 4 dpf embryos, the number of heartbeats were counted for 20 s. Heart rate (beats/min) was calculated by multiplying the number of beats counted by three. Four embryos were counted per group.

Touch Sensitivity Assay

At approximately 48 hpf of development, wild-type, M*dgcr8* and MZ*dgcr8* mutant embryos were touched at the trunk region adjacent to the yolk extension with a glass needle (Giraldez et al., 2005). The response was recorded for three consecutive stimuli and assessed by a touch response behavioral assay (Granato et al., 1996). No response was determined based on the absence of tail movement after touching the embryo three times. A weak response was determined as a wiggle of the tail after stimulation. A strong response was defined as when the fish tail gave a c-bend opposite to the site of the touch. The whole touch procedure was captured on digital video. Different groups of embryos were assessed twice.

O-Dianisidine Staining

O-dianisidine solution was prepared at 0.7 mg/ml in 100% ethanol and protected from exposure to light. The working stain solution was prepared by mixing 1 ml of 0.7 mg/ml O-dianisidine, 1 ml of ddH_2O, 250 μl of 100 mM sodium acetate, and 50 μl of 30% hydrogen peroxide (Giraldez et al., 2005). After anesthetization, the embryos were transferred into a 24-well plate and 0.5 ml of the working solution was added. Embryos were incubated in the dark at room temperature for 20 min, washed three times with PBS, and fixed with 4% PFA overnight. Embryos were placed in 100% glycerol for imaging. The images were acquired on a SZX16 stereomicroscope microscope (Olympus, Japan).

mRNA Sequencing and Small RNAs Sequencing

For mRNA and small RNA sequencing, total RNA was extracted from MZ*dcgr8* and control embryos at 30% epiboly stage of early development representing 4.5 hpf using miRNeasy Mini Kit (Qiagen). RNA integrity was assessed on an Agilent Bioanalyzer 2100 (Agilent). Each group was consisted of 50 embryos. Qualified total RNA was further purified by RNA Clean XP Kit (Beckman) and RNase-Free DNase Set (Qiagen). Library construction and sequencing was performed by Shanghai Biotechnology Corporation. The 30% epiboly stage was chosen because it is a key period in MZT during early vertebrate development. At this stage, the embryo starts to shift from utilization of maternal mRNAs and factors, and initiates zygotic transcription.

Statistical Analysis

In this study, all raw data were analyzed by the GraphPad Instat software (GraphPad Software, United States). Mean values ± SEM. $P < 0.05$ were considered statistically significant using one-way ANOVA. Tukey test was used for multiple comparisons to determine statistical differences. All experiments were performed at least three times to confirm reproducibility.

RESULTS

Germline Specific Dgcr8 Deletion Has No Functional Influence on Gonad Development

As shown in the schematic diagram in **Figure 1A**, we obtained germline specific dgcr8 cKO zebrafish using Tg(BAC-*dgcr8*^{flox}), *dgcr8*$^{-/-}$ male crossed with Tg (kop: cre-UTR-nanos3, CMV: EGFP), *dgcr8*$^{\pm}$ female. To determine the expression levels of *dgcr8* and individual miRNAs in adult ovary of the germline specific *dgcr8* cKO, qRT-PCR was employed, and the results suggested that *dgcr8* was not significantly downregulated, but primary miRNAs were upregulated significantly due to the absence of dgcr8 processing in the adult ovary (**Figure 1B**), and mature miRNAs were downregulated sharply because of disruption of the miRNA biogenesis pathway (**Figure 1C**). The majority of the germline markers were upregulated in the ovary of *dgcr8* cKO except vasa and dnmt1 (**Figure 1D**). The *dgcr8* cKO ovary morphology was also validated by histology, with all the ovarian follicle stages found in the *dgcr8* cKO ovary with no obvious difference compared with the wild-type ovarian follicles (**Figure 1E**).

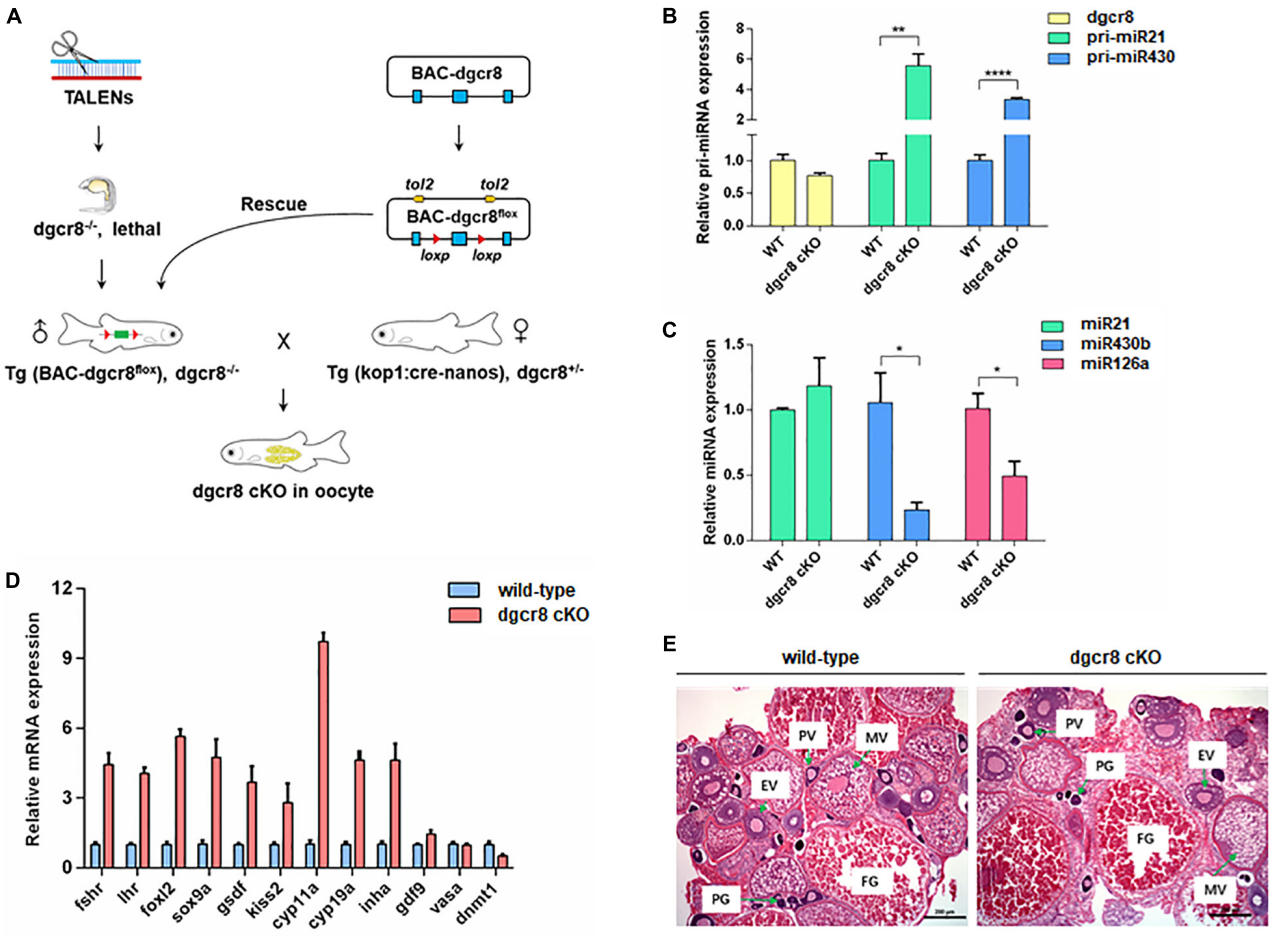

FIGURE 1 | Germline specific dgcr8 deletion has no functional influence on gonad development. **(A)** A basic schematic diagram of generating *dgcr8* germline conditional knockout zebrafish. **(B)** Real-time analysis of the expression of *dgcr8* mRNA and primary miRNAs in ovary of *dgcr8 kop*-cKO fish. **(C)** Real-time PCR analysis of the expression of mature miRNAs in ovary of *dgcr8 kop*-cKO fish. **(D)** Expression of germline markers in the ovary of *dgcr8 kop*-cKO. **(E)** Histology of ovaries in the wild-type and *dgcr8 kop*-cKO female zebrafish. $^{*}p < 0.05$, $^{**}p < 0.01$, and $^{****}p < 0.0001$.

MZdcgr8 Embryos Display More Severe Morphogenesis Defects Than Mdcgr8

To further determine the necessity of maternal Dgcr8 in the early developmental process, we obtained a fish line with maternal Dgcr8 deletion (M*dgcr8* and MZ*dgcr8*) by crossing *dgcr8* cKO female fish with wild-type male fish (**Figure 2A**) and *dgcr8* cKO male fish (**Figure 2B**). M*dgcr8* could provide direct evidence for the role of maternal factors because of the presence of zygotic Dgcr8 of paternal origin in the early developmental stage. The ISH signal of *dgcr8* transcripts decreased from 2.5 to 6 hpf in the wild-type embryos (**Figure 2C**), but the signal in the M*dgcr8* embryos increased due to the presence of zygotic *dgcr8* (**Figure 2C**). Real time-PCR analysis showed that dgcr8 transcripts were decreased during the developmental process from the 256-cell stage to the 75% epiboly stage in the MZ*dgcr8* embryos (**Supplementary Figure S1**).

From the shield stage onward, M*dgcr8* and MZ*dgcr8* mutant embryos exhibited development delay and developed more slowly than the wild-type embryos by approximately 3–4 h at 25 hpf (**Figure 2D**). Their epiboly movements were disrupted with a longer animal-vegetal axis but a shorter dorsal-ventral axis, and the epiboly level was decreased significantly compared to the wild-type embryos at 12 hpf (**Figure 2D**). Intriguingly, the part of the yolk was excised to induce the next developmental stage in MZ*dgcr8* mutants. The accumulation of cells in the region of the anterior axial mesendoderm showed a reduced extent at 13 hpf, but yolk excision did not happen in the M*dgcr8* mutant (**Figure 2E**), suggesting that zygotic *dgcr8* might partially make up for the epiboly defects. From 25 hpf, MZ*dgcr8* and M*dgcr8* mutant embryos exhibited tail curvature until death on 6–10 dpf (**Figure 2D**).

miR-430 Duplex Successfully Rescues M*dgcr8* but Not MZ*dgcr8*

In zebrafish, the miR-430 family is the most abundant miRNA family during early embryogenesis (Chen et al., 2005). During the maternal to zygotic transition (MZT), miR-430 is responsible for targeting and clearing more than 200

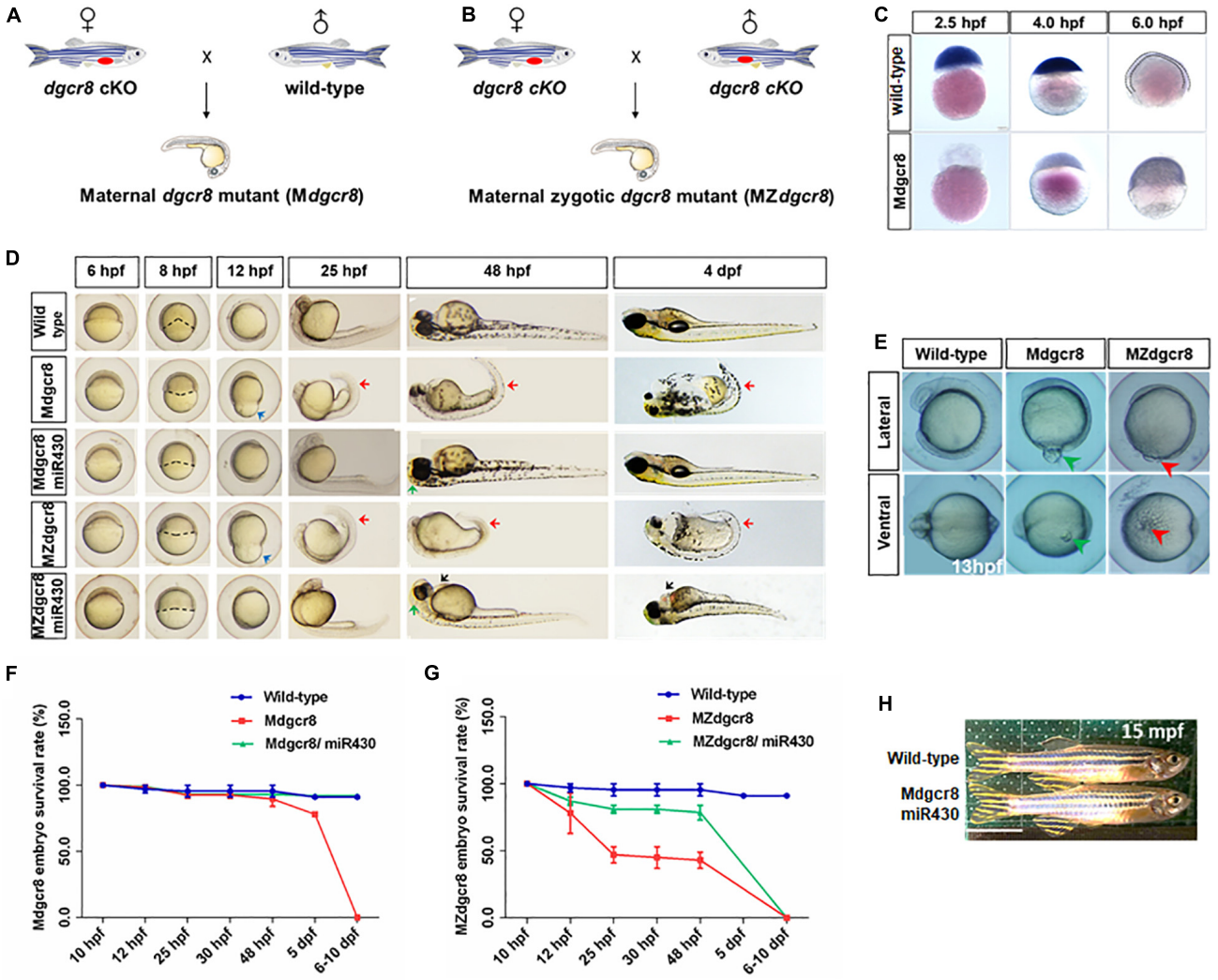

FIGURE 2 | Rescue of M*dgcr8* and MZ*dgcr8* using *miR-430* duplex. **(A)** A schematic diagram of generating M*dgcr8* mutant zebrafish by out-crossing with wild-type male. **(B)** A schematic diagram of generating MZ*dgcr8* mutant zebrafish by in-crossing. **(C)** The expression of *dgcr8* was analyzed by *in situ* hybridization in early embryonic stage. **(D)** M*dgcr8* and MZ*dgcr8* exhibit gastrulation defect, brain malformations, body curvature, and heart developmental defects compared with wild-type. *miR-430* duplex was used to rescue the defects. **(E)** Epiboly defects in M*dgcr8* and MZ*dgcr8*. At 14 hpf, the phenotype of yolk excision could be observed in MZ*dgcr8* mutant (5 X), but not in M*dgcr8*. **(F)** M*dgcr8* embryonic survival rate become normal after rescue. **(G)** MZ*dgcr8* mutant embryos only survived up to 6–10 dpf after rescue. **(H)** M*dgcr8* mutant embryos after rescue could develop to adults and exhibit proper sex ratio. Scale bar 1 cm.

mRNAs in zebrafish embryos (Giraldez et al., 2006). In this study, we found that the M*dcgr8* mutant could be saved and they could even survive to adulthood after rescue, but MZ*dgcr8* could only be partially rescued and they died on 6–10 dpf (**Figure 2D**). At 8 hpf, the epiboly level of M*dgcr8* and MZ*dgcr8* decreased compared with the wild-type, but significantly improved after rescue (**Figure 2D**). In particular, the epiboly defects showing a longer animal-vegetal axis and a shorter dorsal-ventral axis (**Figure 2D**, blue arrows) were rescued completely by miR-430 duplex at 12 hpf. Furthermore, the body curvature (**Figure 2D**, red arrows) was rescued successfully in M*dgcr8* and MZ*dgcr8* at 25 and 48 hpf. However, miR-430 could rescue M*dgcr8* heart defects but failed to do so in the MZ*dgcr8* embryos and hydropericardium (hp) was observed clearly in the MZ*dgcr8*/miR-430 group at 48 hpf (**Figure 2D**, black arrows). Moreover, the brain malformation was rescued successfully in Mdgcr8 and MZdgcr8 embryos at 48 hpf (**Figure 2D**).

After rescue, the M*dgcr8* embryonic survival rate became normal compared to the wild-type (**Figure 2F**), but no MZ*dgcr8*/miR-430 embryo survived beyond 10 dpf (**Figure 2G**), indicating that *dgcr8* or miRNAs other than miR-430 were necessary for the later developmental processes. At 15 months post fertilization (mpf), the morphology of the M*dgcr8*/miR-430 mutants were normal and exhibited a proper sex ratio (male: female = 12:6) (**Figure 2H**), and they could also produce offspring normally by in-cross. Taken together, the miR-430 duplex could rescue M*dgcr8* embryos completely but not MZ*dgcr8*.

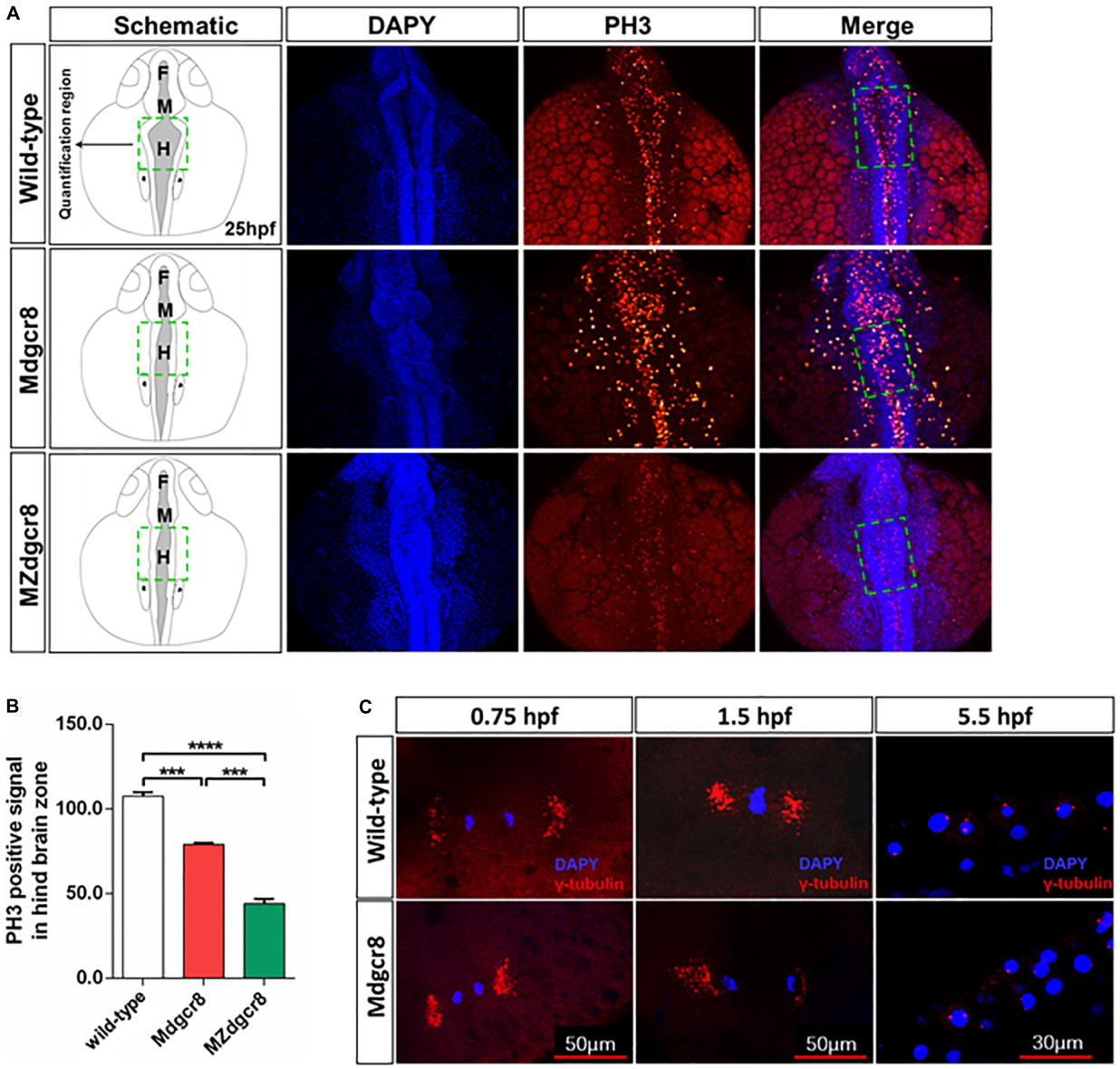

FIGURE 3 | Maternal Dgcr8 regulates mitosis during early embryonic development in M*dgcr8* and MZ*dgcr8*. **(A)** Representative images of 25 hpf WT, M*dgcr8* and MZ*dgcr8* embryos showing the distribution of PH3 immunolabeling cells **(B)** and quantification of positive cells in the hindbrain before the otic vesicle in the dashed box region ($N = 3$). **(C)** Mitotic centrosomes were detected using γ-tubulin immunostaining. ***$p < 0.001$ and ****$p < 0.0001$.

Maternal Dgcr8 Regulates Mitosis During Early Embryonic Development

To investigate the developmental delay in M*dgcr8* mutant embryos, proliferation was assayed by a PH3 immunolabeling G2/M phase mitosis marker. At 25 hpf, the hindbrain zone of the M*dgcr8* embryos showed significant decreases in the PH3 immunolabeling of the positive cells compared to wild-type embryos, and MZ*dgcr8* exhibited a significant decrease in comparison with M*dgcr8* (**Figures 3A,B**). Moreover, the body of M*dgcr8* and MZ*dgcr8* were smaller than the wild-type embryos (**Figure 3A**). To further examine the organization of maternal mutant mitotic centrosomes, γ-tubulin immunostaining was used. Compared with wild-type, M*dgcr8* centrosomes appeared normal at 0.75, 1.5, and 5.5 hpf during early developmental stage (**Figure 3C**). These results suggested that maternal Dgcr8 might regulate cell proliferation through spindle organization other than centrosome organization.

Loss of Maternal or Zygotic *Dgcr8* Causes Cardiac Defects

In zebrafish, the cardiac progenitor cells are localized in the anterior lateral plate mesoderm as two parts on both sides of the embryo at the 5-somite stage (∼12 hpf). Then the two parts of the cardiac progenitor cells migrate toward the middle-line

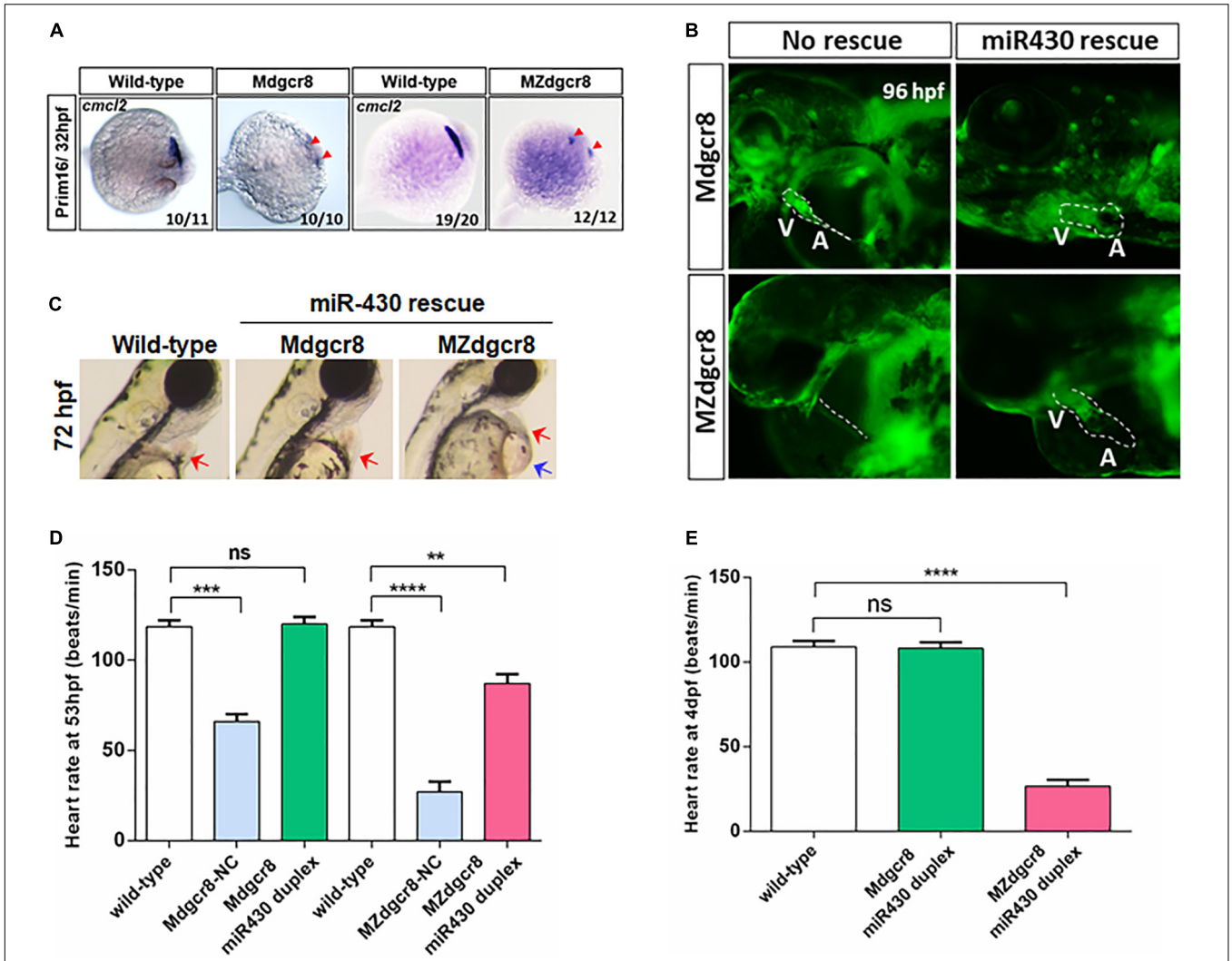

FIGURE 4 | Heart defects was successfully rescued in M*dgcr8*, but not in MZ*dgcr8*. **(A)** The cardiac progenitor cells failed to migrate to the middle-line at prim-16 stage (32 hpf) in M*dgcr8* and MZ*dgcr8* (red arrows). **(B)** After miR430 rescue, cardiogenesis appeared normal including structure of atrium and ventricle. **(C)** MZ*dgcr8* failed to be rescued by mir430, exhibiting hydropericardium phenotype. **(D,E)** Heart-rate results indicated that the heart defects were completely rescued in M*dgcr8*, but only partially in MZ*dgcr8*, and MZ*dgcr8* heart rate gradually decreased at 4 days. $^{**}p < 0.01$, $^{***}p < 0.001$, and $^{****}p < 0.0001$.

and combine together at the 18-somite stage (∼18 hpf). Next they reorganize to constitute a primitive heart tube that starts peristaltic contraction at the 26-somite stage (∼22 hpf), and finally develop into two cardiac chambers, namely, the atrium and ventricle, which become more organized at the long-pec stage (∼48 hpf) (Huang et al., 2009).

To investigate the process of cardiac development, we used ISH to detect the cardiac progenitor cells and found that these cells (marked by *cmcl2*) were specified but failed to migrate toward the middle-line at the Prim-16 stage (32 hpf) in the M*dgcr8* and MZ *dgcr8* mutant, but wild-type embryos formed a complete heart tube (**Figure 4A**). In terms of morphology, the rescued M*dgcr8* exhibited a normal cardiac structure compared to the wild-type (**Figures 4B,C**), but the rescued MZ*dgcr8* only had a thinner cardiac tube and developed a hp syndrome (blue arrow) at 72 hpf (**Figures 4B,C**).

To determine whether maternal Dgcr8 participates in heart development or cardiac function, we investigated the heart rate of the embryos. M*dgcr8* and MZ*dgcr8* had significantly decreased heart rates compared to the wild-type, but no significant changes were observed in the rescued M*dgcr8*, suggesting that miR-430 duplex successfully rescued the heart defects (**Figure 4D**). The mean heart rate in MZ*dgcr8* embryos was only 26 beats/min and this could reach up to 87 beats/min after rescue, which was still much lower than the wild-type (118 beats/min), indicating that the heart defects could be rescued partially by miR-430 in MZ*dgcr8* (**Figure 4D**). At 4 dpf, the heart rate of the rescued M*dgcr8* was normal, but the heart rate of the rescued MZ*dgcr8* decreased gradually because of body malformations (**Figure 4E**). It could thus be concluded that both maternal and zygotic *dgcr8* are essential for heart development and cardiac function.

Loss of Maternal or Zygotic *Dgcr8* Leads to Hematopoietic Defects

In zebrafish, hematopoietic development is divided into two waves. The first wave, named the primitive wave, mainly encompasses induction of erythrocytes and myeloid cells. Primitive blood cells begin to circulate throughout the body of the embryo at 24 hpf (Orkin and Zon, 2008; Paik and Zon, 2010). The second wave is the definitive wave, which occurs in later development and mainly produces the hematopoietic stem and progenitor cells (HSPCs) and multipotent progenitors. Subsequently, HSPCs differentiate into all of the mature blood cells to maintain the embryos throughout life (Ellett and Lieschke, 2010).

To analyze functional hemoglobin in mature primitive erythrocytes in rescued embryos, we employed O-dianisidine staining and found that no O-dianisidine-positive erythroid cells were observed in the yolk sac, but staining accumulation was observed in the tail caudal vein of the maternal mutants at 50 hpf (**Figures 5A–B',B"D',D"**, red arrows). These phenotypes were consistent with qualitative visual observation of a slower circulation and decreased heart rate in Dgcr8 maternal mutant embryos. *Dgcr8* maternal mutants displayed a developmental delay that became more severe as the embryos grew older, and O-dianisidine staining was observed at 74 hpf but with no improvement in hemoglobin function (**Figure 5B**). Moreover, the level of O-dianisidine staining in the 74 hpf mutant embryos was still lower than that of the wild-type at 48 hpf, indicating that the decrease in O-dianisidine staining was unlikely due to the developmental delay alone. After rescuing by the miR-430 duplex, M*dgcr8* could be rescued completely but was only partially rescued in MZ*dgcr8* (**Figures 5A–C',C",E',E"**), indicating that the hematopoiesis defects were successfully rescued in M*dgcr8* but not in MZ*dgcr8*.

Touch-Induced Response Decreases in M*dgcr8* and MZ*dgcr8*

At approximately 2 dpf, the wild-type larvae hatch and start swimming under external stimulation. Swimming occurs by increasing the fin beat amplitude and rhythmic left-right axial cycle response of the tail (Granato et al., 1996). To investigate the role of Dgcr8 in neuronal development, a touch sensitivity assay was employed to determine the level of the escape response. At approximately 60 hpf, wild-type embryos responded to mechanosensory stimulation with a contralateral movement of the tail against where the stimulus was applied, and the tail then exhibited a characteristic c-bend (Granato et al., 1996). The touch response was then categorized as strong, weak, or no response. Analysis of the video frames showed that embryos were almost motionless and failed to respond to touch in M*dgcr8* (no response, 37.65%, $n = 15$) and MZ*dgcr8* (no response, 100%, $n = 23$); or generated a little twitch of the tail in M*dgcr8* (weak, 61%, $n = 25$) and MZ*dgcr8* (weak, 0%) (**Figures 5C,D**). Only 0.9% of the M*dgcr8* embryos displayed a strong response of the tail upon stimulation, and no MZ*dgcr8* embryos showed a strong movement (**Figures 5C,D**). After rescuing by the miR-430 duplex, the level of touch response improved significantly in both M*dgcr8* (strong, 89%, $n = 14$) and MZ*dgcr8* (strong, 77%, $n = 15$) embryos (**Figures 5C,D**). Moreover, the hatching rate of embryos is related to the level of spontaneous coiling movement inside the chorion in addition to the secreted proteolytic enzymes required for chorion-softening. M*dgcr8* and MZ*dgcr8* failed to hatch from the chorion naturally and no coiling movements were observed. Interestingly, the hatch rate of M*dgcr8* could be rescued completely but not the hatch rate of MZ*dgcr8* (**Figure 5E**). These results revealed essential roles of Dgcr8 during zebrafish neurogenesis.

Expression Changes of Downstream Genes in miRNA Biogenesis Pathway

In M*dgcr8* mutant embryos, maternal *dgcr8* mRNA could not be detected in early developmental stage (**Supplementary Figure S1**), the expression of other genes downstream of the canonical miRNA biogenesis pathway (*drosha*, *dicer*1, *xpo5*, and *ago2*) was significantly upregulated at the 256-cell and sphere stage (**Supplementary Figure S1**). This might be the cumulative outcome of ablation of pre-miRNAs due to the lack of maternal Dgcr8. Surprisingly, such a cumulative phenotype was not found in the MZ*dgcr8* mutant (**Supplementary Figure S1**). The expression level of pri-miR-430 was nearly sixfold that of the wild-type at the sphere stage (**Supplementary Figure S1**). Pri-miR-430 in M*dgcr8* embryos was also accumulated abundantly due to the lack of Dgcr8 processing.

Similarly, *dgcr8* mRNA was also not detected in the MZ*dgcr8* mutant embryos (**Supplementary Figure S2**), but the expression level of other genes downstream of the canonical miRNA biogenesis pathway was normal (**Supplementary Figure S2**). These results indicated that all of the miRNA biogenesis transcripts were of maternal origin and were decreased during the developmental process. However, the primary miRNAs were not of maternal origin, and they might begin to be transcribed during the MZT period. Pri-miR-430 was only detected in the sphere stage (**Supplementary Figure S2**), while expression of pri-miR-21 peaked in the shield stage (**Supplementary Figure S2**). Both pri-miR-430 and pri-miR-21 in MZ*dgcr8* embryos accumulated abundantly due to the lack of Dgcr8 processing compared to the wild-type embryos (**Supplementary Figure S2**). In conclusion, these results showed that the canonical miRNA biogenesis pathway was disrupted because of Dgcr8 ablation in MZ*dgcr8* mutant embryos.

Small RNA-Seq Analysis

We have also analyzed the early embryonic transcriptomes and small RNA at the 30% epiboly stage (4.5 hpf) using small RNA-seq MZ*dgcr8* embryos. A total of 13,846,020 raw reads and 12,087,801 raw reads were obtained for the wild-type and MZ*dgcr8* embryos, respectively. We finally obtained 13,759,185 clean effective reads in wild-type and 12,011,626 in MZ*dgcr8* after removal of the reads of the adaptor sequence and low-quality sequences, including those smaller than 18 nt in length and smaller than 10 D in base molecular weight. By blasting with the *Danio* miRbase library, 5830 annotated counts were obtained in the wild-type embryos, but only 591 counts

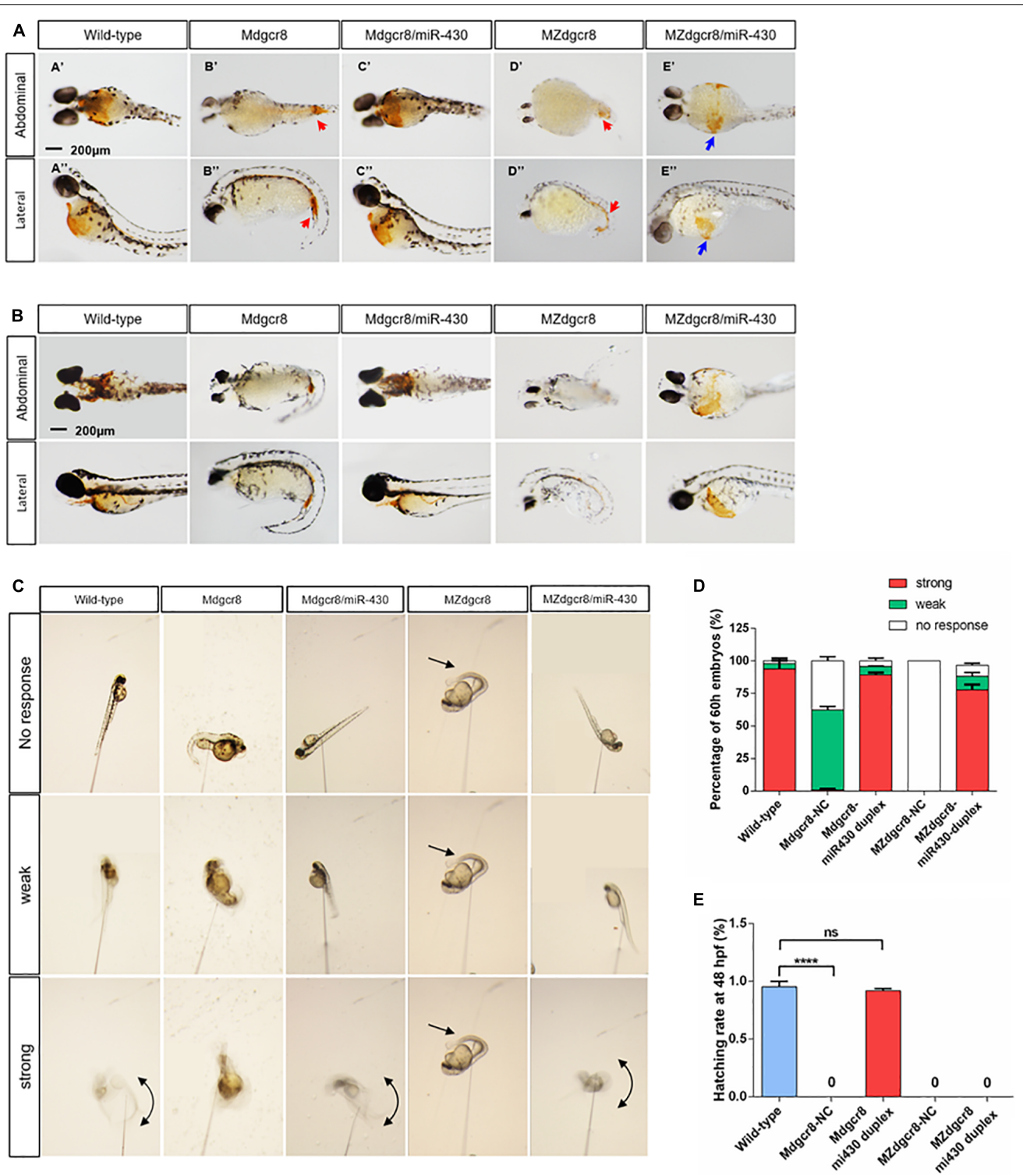

FIGURE 5 | Maternal mutants exhibit reduced erythropoiesis and could be rescued in M*dgcr8*, but not in MZ*dgcr8*. Whole embryo O-dianisidine staining assay was used for assessing functional hemoglobin in mature primitive erythrocytes in wild-type, M*dgcr8*, MZ*dgcr8*, and *miR-430* rescued groups at 50 **(A)** and 74 hpf **(B)**. Hemoglobinized cells accumulate in the yolk sac in wild-type but mainly accumulate in the caudal vein (red arrows) in MZ*dgcr8* and MZ*dgcr8* mutants. 10–15 embryos per groups. Scale bar: 200 μm. **(C)** The touch response was categorized as strong, weak, and no response based on the analysis of the video frames. **(D)** At 60 hpf, the rescue rate was determined in wild-type and maternal mutant embryos. **(E)** At 48 hpf, the hatching rate was detected in wild-type and maternal mutant embryos. $^{****}p < 0.0001$.

were annotated in MZ*dgcr8* (**Supplementary Figures S3A,B**). In the wild-type embryos, small RNAs with lengths of 23 nt were detected in the largest ratio, followed by 21 and 22 nt (**Supplementary Figure S3C**), and this is consistent with the 21–23 nt range of mature miRNAs. However, small RNAs with 21–23 nt in length failed to be detected in MZ*dgcr8* embryos (**Supplementary Figure S3C**). From the sum value reads, we also know that small nucleolar RNA (snoRNA) was downregulated significantly (**Supplementary Figure S3D**), and this is consistent with a previous report that DGCR8 regulated snoRNA biogenesis (Macias et al., 2012). These data revealed that almost all the miRNAs failed to express due to the ablation of maternal and zygotic Dgcr8 in early embryos.

To investigate the expression level or variation of specific miRNAs in early embryonic development, miRNAs with expression values higher than 30 (reads count) were chosen for further analysis. We obtained 80 miRNAs in the wild-type embryos and only 16 miRNAs in MZ*dgcr8* for values greater than 30 (**Figures 6A,B**). In wild-type embryos, the miR-430b is the most abundant miRNA (reads = 240,430) (**Figure 6A**) and in MZ*dgcr8* embryos, the most abundant miRNA is *miR-192* (reads = 277) (**Figure 6B**). Although most of the abundant miRNAs were depleted, several miRNAs still displayed a high residual expression level in MZ*dgcr8* embryos, such as *miR-192* (reads = 277), *miR-21* (reads = 270), and *miR-10a-5p* (reads = 164) (**Figure 6C**). The residual expression of *miR-21* was also validated using real-time PCR in this study (**Figure 1C**) although pri-miR21 was up-regulated about fivefold (**Figure 1B**). The residual expression of *miR-21* was reported in the previous study in *dgcr8* knockout mice (Yi et al., 2009). These results also revealed that there might be an alternative processing pathway independent of Dgcr8 for these miRNAs.

The miR-430 family, the most abundant miRNAs family during early stages, accounted for 99.45% of all the annotated miRNA reads in wild-type embryos (**Figures 6D,E**). However, the miR-430 family was severely depleted in MZ*dgcr8* embryos (**Figures 6D,F**). These RNA-seq data suggested that the miR-430 family is the most important member in embryonic development. We have also validated the results of some individual mature miRNAs using real-time PCR (**Figure 6G**).

mRNA-Seq Analysis

In addition to miRNAs, we also analyzed the mRNAs using RNA sequencing. We found that 2185 genes were upregulated, and 1728 genes were downregulated during the 30% epiboly stage (**Figures 7A,B**). According to the fold change, the top 30 of the upregulated or downregulated genes were further analyzed. The nucleoid binding protein *hnrnpa0a* decreased more than 30-fold (**Figure 7A**), while *seph,* an essential gene regulating organ development in zebrafish, was absent in the MZ*dgcr8* embryo (**Figure 7A**). For the upregulated genes, the targets of miR-430 (*cd82b* and *gstm*) were significantly upregulated in MZ*dgcr8*, and this was verified using real-time PCR as described in our previous study (Liu et al., 2017). The *opa1* required for proper mitochondrial metabolism in early development was also upregulated. During the 30% epiboly stage, the Dgcr8 mRNA could be detected in MZ*dgcr8* embryos after deleting Exon 3 and Exon 4 of the *dgcr8* gene. The expression of other miRNA biogenesis genes including *xpo5*, *dicer*1, and *ago2* was also increased (**Figure 7C**).

To assess whether maternal Dgcr8 was directly related to different biological processes or some cellular components, Kyoto Encyclopedia of Genes and Genomes (KEGG) gene enrichment analysis was performed based on annotations of the zebrafish genes (GRCz10, ENSEMBL). Through KEGG pathway analysis, the scatter plot results displayed highly significant enrichment of genes belonging to "the protein processing in endoplasmic reticulum" (**Supplementary Figure S4**), with a *P*-value of 0.00075. The protein processing pathway was activated due to the upregulation of related genes, and this might be induced by the accumulation of mRNAs owing to the deficiency of Dgcr8 or miRNAs.

DISCUSSION

M*dgcr8* and MZ*dgcr8* mutants were generated using a BACK approach by germline specific deletion of Dgcr8 in zebrafish. Both M*dgcr8* and MZ*dgcr8* were malformed and finally causing embryo lethality. These observations indicate the essentiality of maternal Dgcr8 in early embryonic development. Previous studies observed that MZ*dicer* zebrafish exhibit developmental defects in gastrulation, brain development, and heart development (Giraldez et al., 2005). Compared with other miRNA biogenesis enzymes, Dgcr8 is the only member that specifically processes miRNAs because Dicer is also responsible for processing other small endogenous RNAs. Our data suggest that the canonical miRNAs and other small RNAs processed by Dicer play important roles in early development.

We found that most gene expression patterns were similar in M*dgcr8* and MZ*dgcr8* embryos. Compared with MZ*dcgr8*, the erythroid progenitors (marked by *gata1*) in M*dgcr8* were not severely affected at the 6-somite stage (12 hpf). Consistently, the erythroid cells were accumulated in the tail caudal vein of the M*dgcr8* embryos, but few erythroid cells were observed in MZ*dcgr8*. These results suggest that the specification of erythroid progenitors is regulated by zygotic Dgcr8 in addition to maternal Dgcr8.

The miR-430 family is the most abundant miRNA expressed during early embryonic development, accounting for 99.45% of all the annotated miRNA reads at the 30% epiboly stage using miRNA sequencing. Therefore, we have employed a miR-430 mimic to rescue the M*dgcr8* and MZ*dgcr8* mutants and found that M*dgcr8* mutants could be completely rescued by miR-430, but MZ*dgcr8* could only be partially rescued. A previous study observed that the developmental defects in MZ*dicer* mutants could be partially rescued by miR-430 (Giraldez et al., 2005), suggesting that miR-430 plays an important role in early development. However, rescue of the MZ*dgcr8* mutants by miR-430 is not sufficient for the MZ*dgcr8* mutant to survive to adulthood, indicating that other miRNAs processed by zygotic Dgcr8 are required for the later biological processes.

We further investigated the processes of neurogenesis, cardiogenesis, and hematopoiesis in the M*dgcr8* and MZ*dgcr8*

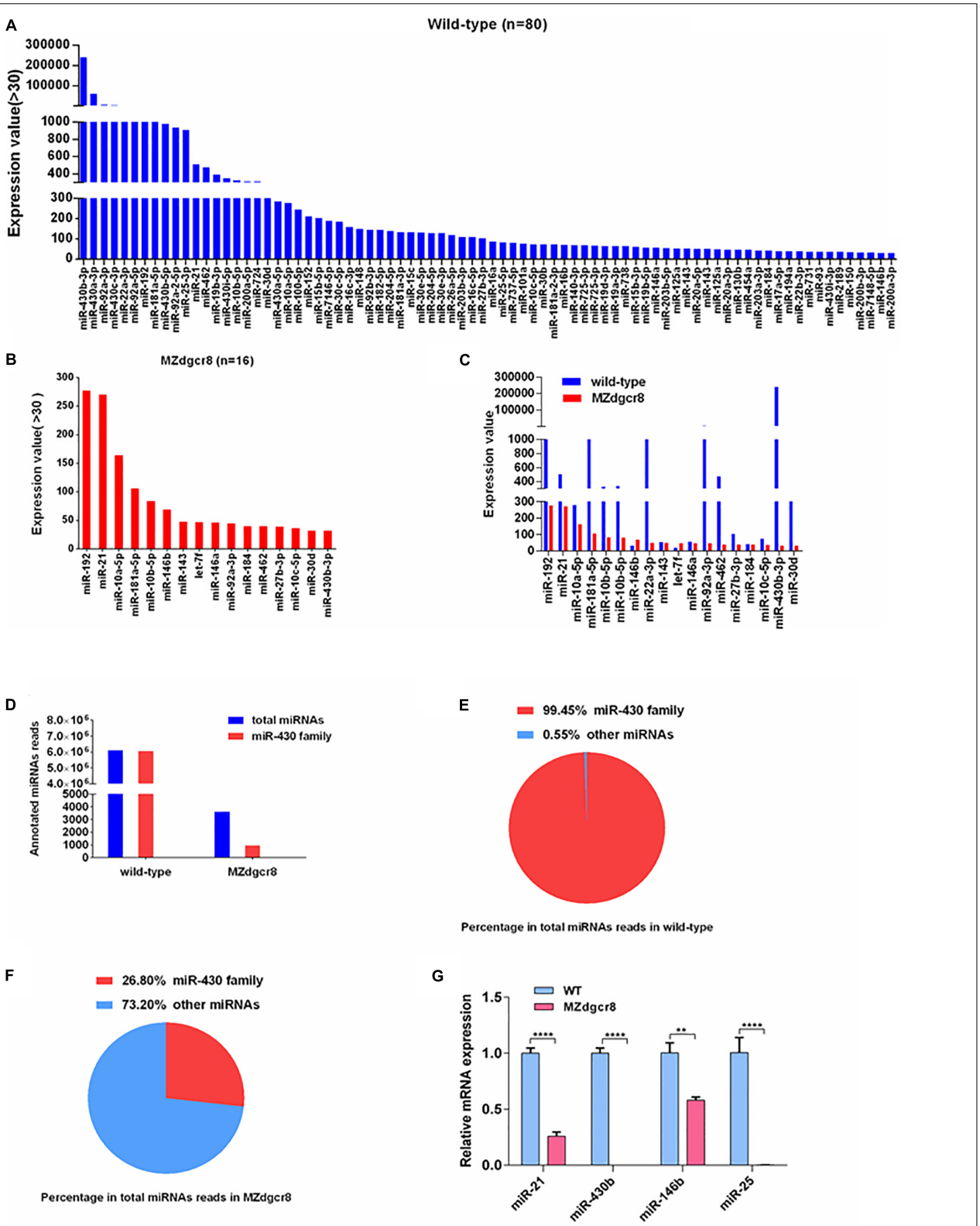

FIGURE 6 | Expression value of miRNAs in wild-type and MZ*dgcr8* embryos and qPCR validations. **(A)** 80 miRNAs for values greater than 30 were obtained in wild-type embryos. **(B)** 16 miRNAs for values greater than 30 were obtained in MZ*dgcr8* embryos. **(C)** miRNAs with higher values in wild-type and MZ*dgcr8*. **(D)** Total miRNAs read count and *miR-430* family read count in wild-type and MZ*dgcr8*. **(E)** Percentage of *miR-430* family in total miRNAs read count in wild-type. **(F)** Percentage of *miR-430* family in total miRNAs read count in MZ*dgcr8*. **(G)** Validation of some mature miRNAs by real-time PCR. $^{**}p < 0.01$ and $^{****}p < 0.0001$.

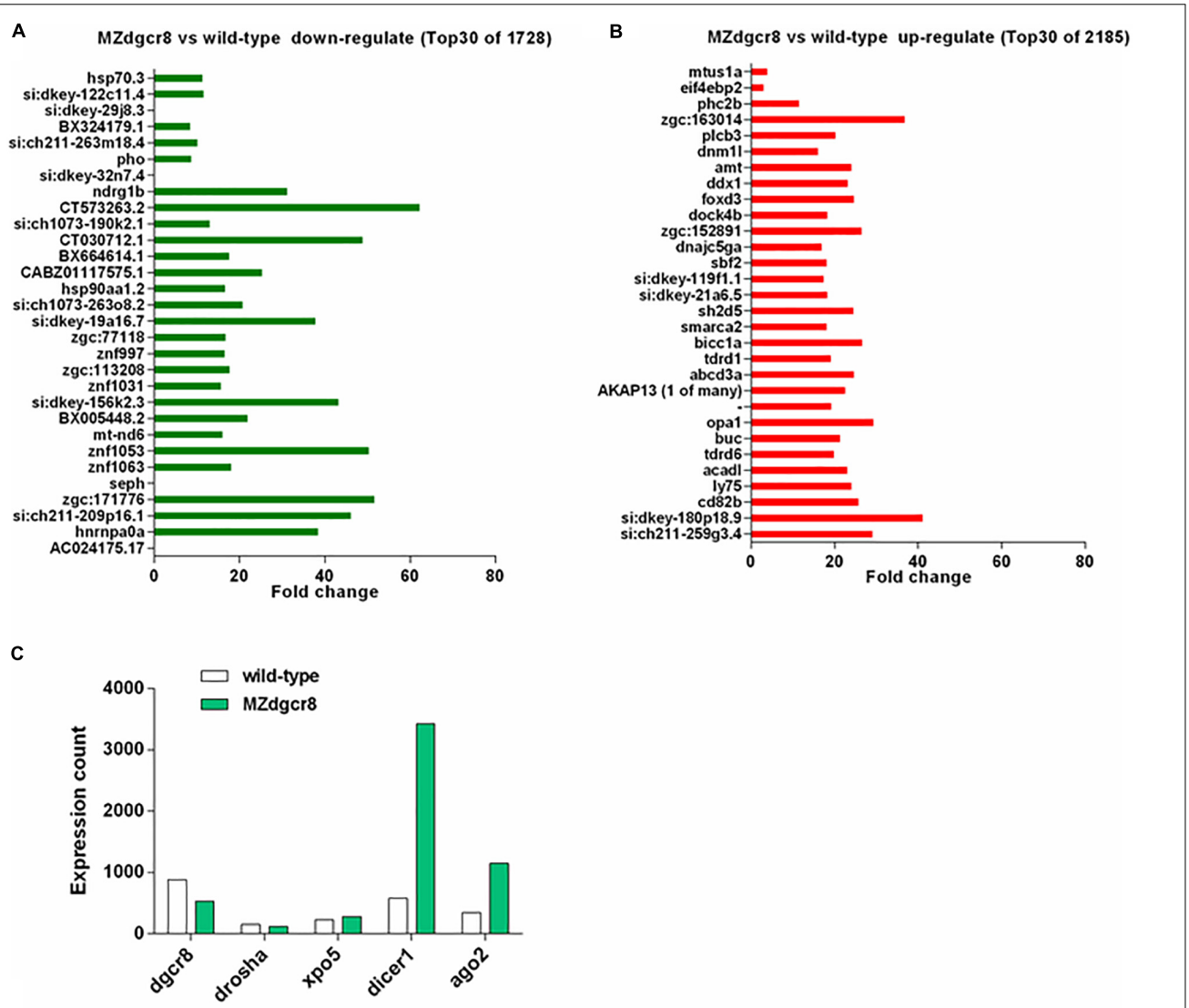

FIGURE 7 | mRNA expression variation in wild-type and MZ*dgcr8* embryos during 30% epiboly stage. **(A)** Top 30 downregulated genes from RNA-seq data. **(B)** Top 30 upregulated genes from RNA-seq data. **(C)** Expression count of miRNAs biogenesis related genes.

mutants after miR-430 rescue. These results suggest that neurogenesis was completely rescued in both M*dgcr8* and MZ*dgcr8* mutants. Remarkably, brain morphogenesis was normal, and the touch response rate was not significantly changed in M*dgcr8* and MZ*dgcr8* mutants after rescue. It has been demonstrated that miR-430 could rescue brain morphogenesis successfully in MZ*dicer* mutants (Giraldez et al., 2005). These observations indicate that miR-430 is both necessary and sufficient for neurogenesis. In contrast, the defects in the development of the heart and hematopoiesis were not rescued by miR-430 in MZ*dgcr8*, consistent with previous study (Giraldez et al., 2005). It has been reported that miR-23 is essential for excessive endocardial cushion cell differentiation in zebrafish embryonic hearts (Lagendijk et al., 2011), and miR-218 mediates the formation of the linear heart tube in zebrafish during heart field migration (Fish et al., 2011). Studies have also demonstrated that miR-451 plays a crucial role in promoting erythroid maturation via its target transcript *gata2* in hematopoiesis (Pase et al., 2009; Cifuentes et al., 2010). These observations show that other individual miRNAs besides miR-430 participate in the process of cardiogenesis and hematopoiesis in early development.

To investigate the role of Dgcr8 in miRNA processing, we sequenced the small RNAs at the 30% epiboly stage in MZ*dgcr8* mutant embryos. Comparing mature miRNA reads between wild-type and MZ*dgcr8* mutants revealed a large decrease (by 90%) of miRNA reads in the MZ*dgcr8* mutants. Interestingly, although most of the microRNAs were depleted in the early embryonic stage, three miRNAs still displayed a high residual expression level in MZ*dgcr8* embryos, including miR-192, miR-21, and miR-10a-5p. These results revealed that these miRNAs might have

alternative miRNA processing pathways independent of Dgcr8. A similar conclusion was reached in another study, suggesting that residual expression of miR-21 was detected in *Dgcr8* knockout mice (Yi et al., 2009).

CONCLUSION

In summary, we have demonstrated that Dgcr8 or global miRNAs are essential for embryonic development. And miR-430 was sufficient to rescue the M*dgcr8* mutant but only partially rescued the MZ*dgcr8*. The MZ*dgcr8* rescue experiments provide us a platform for identifying the novel miRNA candidates in organogenesis, especially cardiogenesis and hematopoiesis.

DATA AVAILABILITY STATEMENT

GEO reference number: GSE146606 is the reference Series for our publication: https://www.ncbi.nlm.nih.gov/geo/query/acc.cgi?acc = GSE146606.

ETHICS STATEMENT

All animal procedures were approved by the Animal Experimentation Ethics Committee of the Chinese University of Hong Kong and were performed according to the animal license issued and endorsed by Department of Health, the Government of the Hong Kong Special Administrative Region.

AUTHOR CONTRIBUTIONS

CC, ZZ, and YL conceived and designed the research. ZZ, YL, WX, TL, and YX developed the methods and performed the experiments. KS prepared the reagents. ZZ analyzed the data and wrote the manuscript. CC and OS edited the manuscript.

FUNDING

This work was supported by the National Natural Science Foundation of China (Grant No: 81773939) and Shenzhen Knowledge Innovation Program-Basic Research Project (Grant No: JCYJ20170818141120342). This work was funded by the General Research Fund (CUHK 14113119) of the Hong Kong Research Grants Council.

ACKNOWLEDGMENTS

We are grateful to Dr. Sun Yonghua for providing Tg(kop: Cre-UTR-nanos3, CMV:EGFP) fishline in the China Zebrafish Resource Center at the Chinese Academy of Sciences. We also thank the Core Laboratories in the School of Biomedical Sciences in the Chinese University of Hong Kong for the provision of equipment and technical support.

SUPPLEMENTARY MATERIAL

The Supplementary Material for this article can be found online at: https://www.frontiersin.org/articles/10.3389/fgene.2020.00299/full#supplementary-material

REFERENCES

Abdelilah, S., Solnica-Krezel, L., Stainier, D. Y., and Driever, W. (1994). Implications for dorsoventral axis determination from the zebrafish mutation janus. *Nature* 370, 468–471.

Chen, P. Y., Manninga, H., Slanchev, K., Chien, M., Russo, J. J., Ju, J., et al. (2005). The developmental miRNA profiles of zebrafish as determined by small RNA cloning. *Genes Dev.* 19, 1288–1293.

Christians, E., Davis, A. A., Thomas, S. D., and Benjamin, I. J. (2000). Embryonic development - Maternal effect of Hsf1 on reproductive success. *Nature* 407, 693–694.

Cifuentes, D., Xue, H., Taylor, D. W., Patnode, H., Mishima, Y., Cheloufi, S., et al. (2010). A novel miRNA processing pathway independent of Dicer requires Argonaute2 catalytic activity. *Science* 328, 1694–1698. doi: 10.1126/science.1190809

Dosch, R., Wagner, D. S., Mintzer, K. A., Runke, G., Wiemelt, A. P., and Mullins, M. C. (2004). Maternal control of vertebrate development before the midblastula transition: mutants from the zebrafish I. *Dev. Cell* 6, 771–780.

Ellett, F., and Lieschke, G. J. (2010). Zebrafish as a model for vertebrate hematopoiesis. *Curr. Opin.Pharmacol.* 10, 563–570. doi: 10.1016/j.coph.2010.05.004

Fish, J. E., Wythe, J. D., Xiao, T., Bruneau, B. G., Stainier, D. Y. R., Srivastava, D., et al. (2011). A Slit/miR-218/Robo regulatory loop is required during heart tube formation in zebrafish. *Development* 138, 1409–1419. doi: 10.1242/dev.060046

Giraldez, A. J., Cinalli, R. M., Glasner, M. E., Enright, A. J., Thomson, J. M., Baskerville, S., et al. (2005). MicroRNAs regulate brain morphogenesis in zebrafish. *Science* 308, 833–838.

Giraldez, A. J., Mishima, Y., Rihel, J., Grocock, R. J., Van Dongen, S., Inoue, K., et al. (2006). Zebrafish MiR-430 promotes deadenylation and clearance of maternal mRNAs. *Science* 312, 75–79.

Granato, M., Van Eeden, F. J., Schach, U., Trowe, T., Brand, M., Furutani-Seiki, M., et al. (1996). Genes controlling and mediating locomotion behavior of the zebrafish embryo and larva. *Development* 123, 399–413.

Gritsman, K., Zhang, J. J., Cheng, S., Heckscher, E., Talbot, W. S., and Schier, A. F. (1999). The EGF-CFC protein one-eyed pinhead is essential for nodal signaling. *Cell* 97, 121–132.

Haffter, P., Granato, M., Brand, M., Mullins, M. C., Hammerschmidt, M., Kane, D. A., et al. (1996). The identification of genes with unique and essential functions in the development of the zebrafish, Danio rerio. *Development* 123, 1–36.

Harvey, S. A., Sealy, I., Kettleborough, R., Fenyes, F., White, R., Stemple, D., et al. (2013). Identification of the zebrafish maternal and paternal transcriptomes. *Development* 140, 2703–2710. doi: 10.1242/dev.095091

Huang, W., Zhang, R., and Xu, X. (2009). Myofibrillogenesis in the developing zebrafish heart: a functional study of tnnt2. *Dev. Biol.* 331, 237–249. doi: 10.1016/j.ydbio.2009.04.039

Kane, D. A., Hammerschmidt, M., Mullins, M. C., Maischein, H. M., Brand, M., Vaneeden, F. J. M., et al. (1996). The zebrafish epiboly mutants. *Development* 123, 47–55.

Kimmel, C. B., Ballard, W. W., Kimmel, S. R., Ullmann, B., and Schilling, T. F. (1995). Stages of embryonic development of the zebrafish. *Dev. Dyn.* 203, 253–310.

Lagendijk, A. K., Goumans, M. J., Burkhard, S. B., and Bakkers, J. (2011). MicroRNA-23 restricts cardiac valve formation by inhibiting Has2 and extracellular hyaluronic acid production. *Circ. Res.* 109, 649–657. doi: 10.1161/CIRCRESAHA.111.247635

Leal, M. C., Cardoso, E. R., Nobrega, R. H., Batlouni, S. R., Bogerd, J., Franca, L. R., et al. (2009). Histological and stereological evaluation of zebrafish (Danio rerio) spermatogenesis with an emphasis on spermatogonial generations. *Biol. Reprod.* 81, 177–187. doi: 10.1095/biolreprod.109.076299

Li, J., Wu, P., Liu, Y., Wang, D., and Cheng, C. H. (2014). Temporal and spatial expression of the four Igf ligands and two Igf type 1 receptors in zebrafish during early embryonic development. *Gene Expr. Patterns* 15, 104–111. doi: 10.1016/j.gep.2014.05.006

Liu, Y., Zhu, Z., Ho, I. H. T., Shi, Y., Xie, Y., Li, J., et al. (2017). Germline-specific dgcr8 knockout in zebrafish using a BACK approach. *Cell Mol. Life Sci.* 74, 2503–2511. doi: 10.1007/s00018-017-2471-7

Macias, S., Plass, M., Stajuda, A., Michlewski, G., Eyras, E., and Caceres, J. F. (2012). DGCR8 HITS-CLIP reveals novel functions for the Microprocessor. *Nat. Struct. Mol. Biol.* 19, 760–766. doi: 10.1038/nsmb.2344

Marlow, F. L. (2010). *Maternal Control of Development in Vertebrates: My Mother Made Me Do It!*. Fort Wayne, IN: Biota Publishing.

Miller-Bertaglio, V., Carmany-Rampey, A., Furthauer, M., Gonzalez, E. M., Thisse, C., Thisse, B., et al. (1999). Maternal and zygotic activity of the zebrafish ogon locus antagonizes BMP signaling. *Dev. Biol.* 214, 72–86.

Orkin, S. H., and Zon, L. I. (2008). Hematopoiesis: an evolving paradigm for stem cell biology. *Cell* 132, 631–644. doi: 10.1016/j.cell.2008.01.025

Paik, E. J., and Zon, L. I. (2010). Hematopoietic development in the zebrafish. *Int. J. Dev. Biol.* 54, 1127–1137.

Pase, L., Layton, J. E., Kloosterman, W. P., Carradice, D., Waterhouse, P. M., and Lieschke, G. J. (2009). miR-451 regulates zebrafish erythroid maturation in vivo via its target gata2. *Blood* 113, 1794–1804. doi: 10.1182/blood-2008-05-155812

Payer, B., Saitou, M., Barton, S. C., Thresher, R., Dixon, J. P. C., Zahn, D., et al. (2003). stella is a maternal effect gene required for normal early development in mice. *Curr. Biol.* 13, 2110–2117.

Sabaliauskas, N. A., Foutz, C. A., Mest, J. R., Budgeon, L. R., Sidor, A. T., Gershenson, J. A., et al. (2006). High-throughput zebrafish histology. *Methods* 39, 246–254.

Sirotkin, H. I., Gates, M. A., Kelly, P. D., Schier, A. F., and Talbot, W. S. (2000). fast1 is required for the development of dorsal axial structures in zebrafish. *Curr. Biol.* 10, 1051–1054.

Solnica-Krezel, L., Stemple, D. L., Mountcastle-Shah, E., Rangini, Z., Neuhauss, S. C., Malicki, J., et al. (1996). Mutations affecting cell fates and cellular rearrangements during gastrulation in zebrafish. *Development* 123, 67–80.

Tadros, W., and Lipshitz, H. D. (2009). The maternal-to-zygotic transition: a play in two acts. *Development* 136, 3033–3042. doi: 10.1242/dev.033183

Tong, Z. B., Gold, L., Pfeifer, K. E., Dorward, H., Lee, E., Bondy, C. A., et al. (2000). Mater, a maternal effect gene required for early embryonic development in mice. *Nat. Genet.* 26, 267–268.

Wagner, D. S., Dosch, R., Mintzer, K. A., Wiemelt, A. P., and Mullins, M. C. (2004). Maternal control of development at the midblastula transition and beyond: mutants from the zebrafish II. *Dev. Cell* 6, 781–790.

Wang, Y., and Ge, W. (2004). Developmental profiles of activin betaA, betaB, and follistatin expression in the zebrafish ovary: evidence for their differential roles during sexual maturation and ovulatory cycle. *Biol. Reprod.* 71, 2056–2064.

Wu, X. M., Viveiros, M. M., Eppig, J. J., Bai, Y. C., Fitzpatrick, S. L., and Matzuk, M. M. (2003). Zygote arrest 1 (Zar1) is a novel maternal-effect gene critical for the oocyte-to-embryo transition. *Nat. Genet.*33, 187–191.

Yi, R., Pasolli, H. A., Landthaler, M., Hafner, M., Ojo, T., Sheridan, R., et al. (2009). DGCR8-dependent microRNA biogenesis is essential for skin development. *Proc. Natl. Acad. Sci. U.S.A.* 106, 498–502. doi: 10.1073/pnas.0810766105

Conflict of Interest: The authors declare that the research was conducted in the absence of any commercial or financial relationships that could be construed as a potential conflict of interest.

frontiers in Cell and Developmental Biology

ORIGINAL RESEARCH
published: 31 March 2020
doi: 10.3389/fcell.2020.00202

Extracellular Vesicles Derived Human-miRNAs Modulate the Immune System in Type 1 Diabetes

*Tine Tesovnik[1,2,3], Jernej Kovač[2], Katka Pohar[4], Samo Hudoklin[5], Klemen Dovč[1], Nataša Bratina[1,3], Katarina Trebušak Podkrajšek[2,6], Maruša Debeljak[2,5], Peter Veranič[5], Emanuele Bosi[7,8], Lorenzo Piemonti[7,8], Alojz Ihan[4] and Tadej Battelino[1,3]**

[1] Department of Pediatric Endocrinology, Diabetes and Metabolic Diseases, University Children's Hospital, University Medical Centre Ljubljana, Ljubljana, Slovenia, [2] Clinical Institute of Special Laboratory Diagnostics, University Medical Centre Ljubljana, University Children's Hospital, Ljubljana, Slovenia, [3] Faculty of Medicine, University of Ljubljana, Chair of Paediatrics, Ljubljana, Slovenia, [4] Faculty of Medicine, Institute of Microbiology and Immunology, University of Ljubljana, Ljubljana, Slovenia, [5] Faculty of Medicine, Institute of Cell Biology, University of Ljubljana, Ljubljana, Slovenia, [6] Faculty of Medicine, Institute of Biochemistry, University of Ljubljana, Ljubljana, Slovenia, [7] IRCCS Ospedale San Raffaele, San Raffaele Diabetes Research Institute, Milan, Italy, [8] Vita-Salute San Raffaele University, Milan, Italy

OPEN ACCESS

Edited by:
Junjie Xiao, Shanghai University, China

Reviewed by:
Carla Perego, University of Milan, Italy
Carolin Daniel, Helmholtz Zentrum München, Germany

***Correspondence:**
Tadej Battelino
tadej.battelino@mf.uni-lj.si

Specialty section:
This article was submitted to Signaling, a section of the journal Frontiers in Cell and Developmental Biology

Received: *22 November 2019*
Accepted: *09 March 2020*
Published: *31 March 2020*

Citation:
Tesovnik T, Kovač J, Pohar K, Hudoklin S, Dovč K, Bratina N, Trebušak Podkrajšek K, Debeljak M, Veranič P, Bosi E, Piemonti L, Ihan A and Battelino T (2020) Extracellular Vesicles Derived Human-miRNAs Modulate the Immune System in Type 1 Diabetes. Front. Cell Dev. Biol. 8:202. doi: 10.3389/fcell.2020.00202

Extracellular vesicles with their molecular cargo can modulate target cell response and may affect the pathogenesis of diseases. The extracellular vesicles containing microRNAs (miRNAs), which are often studied as disease biomarkers, but rarely as mediators of the disease development. The role of extracellular vesicles derived miRNAs in type 1 diabetes is currently not well established. We observed a fraction of blood plasma extracellular vesicles positive for membrane proteins potentially associated with insulin-producing beta-cells and identified differentially expressed extracellular vesicles derived miRNAs in individuals with type 1 diabetes. These differentially expressed extracellular vesicles derived human miRNAs in participants with type 1 diabetes and participants with Langerhans islets beta-cells destruction showed the ability to activate TLR7/8 signaling cascade and increase activation as well as cytotoxicity of the effector blood immune cells with cytokine and chemokine release. Our results illustrate extracellular vesicles derived human miRNAs as modulators of the immune system in type 1 diabetes autoimmunity, providing potentially new insight into the pathogenesis of the disease, and novel molecular targets for intervention and type 1 diabetes prevention.

Keywords: type 1 diabetes, extracellular vesicles, miRNA, immune modulating activity, autoimmune disease, TLR7/8

INTRODUCTION

Type 1 diabetes (T1D) incidence is increasing worldwide (Katsarou et al., 2017), affecting both pediatric (Patterson et al., 2019) and adult populations (Salam et al., 2018; Thomas et al., 2018). T1D is an autoimmune disease involving environmental and genetic factors triggering selective destruction of insulin-producing pancreatic beta-cells (Katsarou et al., 2017). The etiology of the disease remains unknown, nonetheless, the most widely accepted theory attributes the T1D onset to the environmental stress-factors affecting the presentation of self-antigens leading to overt autoimmunity (Christoffersson et al., 2016; Paschou et al., 2017). The disease demands lifelong

applications of exogenous insulin (Battelino et al., 2017; Katsarou et al., 2017) or treatment with Langerhans islet transplantation (Piemonti and Pileggi, 2000). The individuals with T1D are at risk of acute hyper/hypoglycemic periods and persistent glucose variability (Ceriello and Kilpatrick, 2013), that reduce the quality of life and lead to the development of diabetes complications, accelerated cell senescence (Tesovnik et al., 2018), and early mortality (Katsarou et al., 2017). The direct insight into cell pathogenesis is impeded due to the inaccessibility of the Langerhans islets. The increasing disease prevalence, associated healthcare costs and cumulative negative impact on the quality of life for individuals with T1D and their families clearly demonstrate the need to improve the disease management at earliest stages of its development, with the ultimate goal of preventing or even reversing the disease before the critical level of beta-cell destruction. Analysis of extracellular vesicles obtained from body fluids allows us to probe physiological conditions in distant organs, disease monitoring, and define novel biomarkers (Armstrong and Wildman, 2018), which could also provide a better insight into the pathogenesis of T1D.

Extracellular vesicles (EVs) are small spherical structures encased with the cell membrane, released from cells into extracellular space, carrying parental-cell-specific molecules. There are three main types of EVs; exosomes, microvesicles and apoptotic bodies, which differ by cell-release mechanism, their origin and dimensions (Yáñez-Mó et al., 2015; van Niel et al., 2018). However, it is difficult to differentiate between different types of EVs. Using parental cell-specific molecules, such as proteins, lipids, glycosides, and nucleic acids, EVs are able to transfer the information of parental cells' to the neighboring cells (Yáñez-Mó et al., 2015) or even to cells in other organs of the organism, where a target cell response can be triggered (Hoshino et al., 2015). With cell-to-cell communication, EVs are involved in physiological as well as potential pathologically cellular processes (Yuana et al., 2013; Hoshino et al., 2015; Tan et al., 2016). While the immunomodulatory role of EVs has been characterized in cancer (Becker et al., 2016; Kamerkar et al., 2017), a few studies also indicate the EVs role in autoimmunity (Tan et al., 2016; Turpin et al., 2016; Salvi et al., 2018; Pluta et al., 2019). Although initial studies on animal models and cell cultures suggest the potential involvement of beta-cell stress released EVs in the disruption of the immune system (Cianciaruso et al., 2017; Freeman et al., 2018), the role of beta-cells' EVs RNA in autoimmune diabetes has not been defined.

We aimed to determine the presence of insulin-producing beta-cell derived EVs in human blood plasma and demonstrate their potential as a proxy for immune system modulation. Using deep next-generation sequencing, we analyzed human blood plasma EVs' small RNAs, with the focus on micro RNAs (miRNAs), differentially expressed in children with new-onset T1D, and identified miRNAs potentially involved in the autoimmune pathogenesis of T1D. Furthermore, we demonstrated that differentially expressed miRNAs packed in vesicles could be internalized by immune system cells, preferentially monocytes and granulocytes, via the endolysosomal pathway, consequently activating TLR7/8 response of innate immunity and upregulating activation, transition, and cytotoxicity of the adaptive immune system. To the best of our knowledge, this is the first study investigating human-EVs-derived differentially expressed miRNAs as the potential pathogenic modulators of beta-cell-specific autoimmunity in T1D. Our results demonstrated the potential pathologic immunomodulatory effect of human miRNAs in T1D etiology and a novel potential molecular target for disease treatment and prevention.

MATERIALS AND METHODS

The study was designed in three steps: (1) isolating plasma and Langerhans islet medium EVs fraction and TEM EVs imaging (2) comparative EVs plasma miRNA Next-generation sequencing of T1D participants, transplantation individuals and healthy control samples and (3) *in vitro* differentially expressed vesicle miRNA effect study on the human whole blood immune cells. The workflow of our study is presented in **Supplementary Figure S1**.

Participants With T1D Onset; T1D 10-Years Duration; Healthy Controls; Langerhans Islet Transplantation Patients

Three blood plasma samples of healthy individuals were collected for EVs miRNA profile characterization and comparison to total plasma and depleted EVs plasma profile.

Ten T1D onset, ten T1D 10-years duration and ten healthy controls blood samples were collected to evaluate EVs miRNA in T1D. Blood plasma of ten new-onset T1D participants (nT1D) was collected at the time of the first hospital visit after the disease onset, typically on day 5 or 6. All newly diagnosed children with T1D were positive for at least one of T1D related antibodies (GAD65, ZnT8, or IA-2), participants were in a pre-pubertal state with no other diagnosed autoimmune diseases or other disorders at the T1D onset (T1D age onset: 6.49 $\pm$ 2.57 years, 5 females). Participants with 10-year T1D duration (10yT1D) were examined at regular follow-up medical examinations; participants were not diagnosed for other autoimmune disorders nor diabetic complications (age: 17.76 $\pm$ 2.35 years, duration of the disease: 13.03 $\pm$ 1.95 years, 5 females). Ten healthy 5-years-old control (HC) individuals' blood samples were collected during the national systematic check-up examination (age: 5.33 $\pm$ 0.33 years, 4 females). Healthy controls did not have T1D or type 2 diabetes family history and were not diagnosed with T1D at the time of this study, nor did they have detectable T1D related antibodies. The characteristics of the participants are listed in **Table 1**. For characterization of the EVs small non-coding RNA profile, participants' blood was collected into 10 mL K-EDTA tubes, blood plasma was isolated with 3,000$\times g$ for 10 min centrifugation and stored at -80°C before further processing, no longer than 6 months. T1D and 10yT1D were clinically characterized by University Children's Hospital, Department of Pediatric Endocrinology, Diabetes and Metabolic Diseases.

To specify small non-coding RNA EVs profile and signals during active beta-cells destruction in Langerhans

TABLE 1 | Characteristics of cohorts included in EVs small RNA sequencing.

Group	Individual	T1D age onset [years]	Age at the examination [years]	T1D duration [years]	BMI [kg/m^2]	BMI Z-score	T1D antibodies	0' C-peptide [nmol/L]	6' C-peptide [nmol/L]	Delta C-peptide [nmol/L]
nT1D	nT1D_1	6–10	6–10	0	18.9	0.99	GAD65, IA2, ZnT8	0.13	0.61	0.48
	nT1D_2	6–10	6–10	0	13.5	−2.45	ZnT8	0.03	0.07	0.04
	nT1D_3	1–5	6–10	0	15.6	−0.46	GAD65, ZnT8	0	0.05	0.05
	nT1D_4	1–5	1–5	0	13.1	−2.84	GAD65, IA2, ZnT8	0.07	0.16	0.08
	nT1D_5	1–5	6–10	0	12.9	−3.43	GAD65	0	0.16	0.16
	nT1D_6	6–10	6–10	0	13.6	−1.73	GAD65, IA2, ZnT8	0.04	0.07	0.03
	nT1D_7	11–15	6–10	0	16.5	−0.5	GAD65, IA2, ZnT8	0.04	0.11	0.07
	nT1D_8	6–10	6–10	0	13.3	−1.93	GAD65, IA2, ZnT8	0.1	0.2	0.1
	nT1D_9	1–5	1–5	0	17.3	1.24	GAD65	0.1	0.2	0.1
	nT1D_10	6–10	6–10	0	17.6	1.13	GAD65, IA2, ZnT8	0.2	0.4	0.2
10yT1D	10yT1D_1	1–5	16–20	11–15	25.7	1.3	–	–	–	–
	10yT1D_2	1–5	16–20	16–20	20.8	−0.64	–	–	–	–
	10yT1D_3	1–5	16–20	16–20	20.1	−0.42	–	–	–	–
	10yT1D_4	1–5	11–15	11–15	25.1	1.16	–	–	–	–
	10yT1D_5	1–5	16–20	11–15	22.0	0.43	–	–	–	–
	10yT1D_6	1–5	16–20	11–15	18.4	−1.09	–	–	–	–
	10yT1D_7	6–10	16–20	11–15	26.0	0.99	–	–	–	–
	10yT1D_8	11–15	21–25	11–15	24.7	–	–	–	–	–
	10yT1D_9	1–5	16–20	11–15	20.4	0.16	–	–	–	–
	10yT1D_10	11–15	21–25	6–10	22.1	–	–	–	–	–
HC	HC_1	/	1–5	/	17.5	1.22	–	–	–	–
	HC_2	/	1–5	/	15.5	−0.94	–	–	–	–
	HC_3	/	1–5	/	15.7	0.13	–	–	–	–
	HC_4	/	1–5	/	15.1	−0.26	–	–	–	–
	HC_5	/	1–5	/	15.0	−0.8	–	–	–	–
	HC_6	/	1–5	/	16.7	−0.3	–	–	–	–
	HC_7	/	1–5	/	14.1	−1.23	–	–	–	–
	HC_8	/	1–5	/	17.4	1.22	–	–	–	–
	HC_9	/	1–5	/	15.7	0.22	–	–	–	–
	HC_10	/	1–5	/	14.4	−1.86	–	–	–	–

Characteristics of nT1D, 10yT1D, and HC participants: for every participant are reported the age as a range at T1D onset, age as a range at the examination when sample for EVs isolation was obtained, T1D duration and Z-score and BMI (BMI only for participants older than 21 years). nT1D participants were at the onset of the disease positive at least for one of T1D associated antibodies (GAD65, Glutamic Acid Decarboxylase; IA-2, Insulinoma Antigen 2; ZnT8, Zinc Transporter 8) [nT1D, new-onset T1D, n = 10; 10yT1D, 10 years duration T1D, n = 10; HC, healthy controls, n = 10; – : data below the limit of detection; /: no data].

islet transplantation stress *in vivo*, where some beta-cells are damaged, miRNA profiles of human Langerhans islet transplantation patients' (TX) EVs plasma fraction were assessed. Blood samples were obtained prior and after the transplantation procedure from two adult Langerhans islet transplantation recipients (55–50 and 55–60 years old males), both with long-standing T1D. Blood samples were obtained in K-EDTA tubes before the transplantation and after 1, 6, and 24 h. Blood plasma was isolated with 3,000×*g* for 10 min centrifugation and stored at −80°C before further processing, not longer than 4 months. The transplantation plasma samples were provided by the San Raffaele Diabetes Research Institute, IRCCS Ospedale San Raffaele, Milan, Italy. Signed written informed consent was obtained before the study.

Langerhans Islets' EVs

Transmission electron microscopy (TEM) was used to assess the beta-cells EVs in plasma samples, and plasma EVs were compared to Langerhans islets medium EVs, which were used as a beta-cells' EVs positive control. The Langerhans medium samples of 3 adult donors (51–55 year-old female; 41–45 year-old male; 46–50 year-old male) were provided by the San Raffaele Diabetes

Research Institute, IRCCS Ospedale San Raffaele, Milan, Italy. The medium where Langerhans islets were cultured at sufficient purity for transplantation (Layer I; >80% purity) was used for TEM characterization. Raw culture medium consisted of CMRL medium without phenol red and with HAS, Hepes, Di-pep-Gln (CORNING, 99-784-CM), to which Nicotinamide (0.01 M), Glutamine (2 mM), and Penicillin/Streptomycin (100U/L) were added. After the Langerhans islets medium collection, the medium was centrifuged 10 min at 3,000×*g* to remove cell debris and stored at −80°C before further EVs characterization.

Plasma EVs and Langerhans Medium EVs Isolation

Blood plasma and Langerhans medium were thawed and centrifuged for 30 min at 10,000×*g* to remove cell debris. EVs were isolated by the modified protocol based on previously published PEG isolation procedures (Rider et al., 2016; Ludwig et al., 2018). 1 mL of pre-centrifuged plasma was resuspended with 400 μL of PEG-8000 (0.4 g PEG/1mL 1x PBS) (Sigma Aldrich, 81268 and 806544) and incubated for 30 min at 4°C. EVs fraction was collected after 10 min centrifugation at 10,000×*g*.

For isolation Langerhans medium EVs, the medium was centrifuged 30 min at 10,000×*g* to remove cell debris and a higher concentration of precipitation reagent PBS-PEG 8000 was used (500 μL medium, 1 mL 0.5 g PEG/1mL 1x PBS) (isolation based on: Rider et al., 2016) to precipitate EVs. Langerhans islet EVs precipitate fraction was isolated with 10 min centrifugation at 10,000×*g*, after 30 min pre-incubation of PEG-Langerhans medium at 4°C.

Isolated EVs fractions were further used for TEM imaging or miRNA isolation.

TEM Imaging

Pellets of PEG isolated EVs from plasma samples or Langerhans medium were prepared for immuno-electron microscopy following the modified Tokuyasu technique (Hudoklin et al., 2011, 2012). Briefly, samples were fixed with 4% formaldehyde in 0.1 M phosphate buffer, pH 7.2, for 2.5 h at room temperature and washed with PBS 3 × 5 min and with 0.15% glycine/PBS 2x5min. Pellets were embedded in 12% gelatine, cut into 0.5 × 0.5 × 0.5 mm blocks, cryoprotected with 2.3 M sucrose for 24 h at 4°C. The blocks were then mounted on specimen holders and frozen in liquid nitrogen. Ultrathin cryosections were cut with EM-FCS UCT (Leica) at −120°C, thickness 60 nm, and retrieved with 1:1 mixture of 2.3 M sucrose and 2% methylcellulose on Au grids.

For immunolabeling, sections were incubated on 2% gelatine, washed with 0.15% glycine/PBS 5 × 2 min and blocked with 1% BSA-c (Aurion; 900.022).

Primarily antibodies for Langerhans cells' specific EVs markers were selected based on The Human Protein Atlas database ([1]Protein Atlas version 16) with characterized high expression in endocrine pancreas and negligible expression in other tissues. We used validated Human protein atlas antibodies against anti-human-GAD-2 (GAD-65 | Sigma Aldrich, AMAb91048-100UL, HP044637-100UL), anti-human-DGCR-2 (Sigma Aldrich, HPA000873-100UL) and anti-human-PTPRN (IA-2 | Sigma Aldrich, APA007179-100UL). Intra-vesicular EVs INS detection was performed on the plasma samples treated with proteinase K 30min 37°C to degrade plasma free INS. The samples were labeled with anti-human-INS (Abbexa, abx019113) antibody in the combination with selected human protein atlas antibodies (DGCR2, GAD2, PTPRN). Incubation with primary antibodies was performed overnight at 4°C and was followed by incubation with the secondary goat-anti-mouse or goat-anti-rabbit polyclonal antibodies conjugated with 6 and 18 nm colloidal gold (Jackson ImmunoResearch, goat anti rabbit 6 nm 111-195-144, goat anti-rabbit 18 nm 111-215-144, goat anti-mouse 6 nm 115-195-146, and goat anti-mouse 18 nm 115-215-146). Negative controls were done by omitting the primary antibodies, by incubation in rabbit serum, or by using inadequate primary antibodies. After secondary gold-labeled antibody conjugation, sections were stained with methylcellulose/uranyl acetate (Sigma-Aldrich, M-6385; Polysciences 21447), dried, and examined with CM100 transmission electron microscope (Philips) running at 80 kV.

Extracellular Vesicles' miRNA Profile Specification

Plasma EVs PEG enriched precipitate of three adult participants were suspended in 200 μL PBS and resuspended in 1mL of Qiazol reagent (Qiagen). Plasma RNA and EVs depleted plasma (PEG-EVs depleted plasma) RNA samples were isolated from 1 mL of blood plasma and 1.3 mL depleted EVs plasma with the addition of the prescribed volume of Qiazol, following the manufacturer's protocol. RNA was further isolated using RNeasy columns (Qiagen), RWT and RPE buffers (Qiagen) and eluted in nuclease-free water. The RNA profiles were assessed using RNA Pico 6000 kit on Bioanalyzer 2100 (Agilent, 5067-1514) and samples were prepared for sequencing. EVs, blood plasma and EVs depleted blood plasma small RNA libraries were prepared for NGS sequencing using NEBNext Small RNA Library Prep Set for Illumina (New England Biolabs, E7300S) without the size selection step. NGS libraries were checked for QC using DNA 1000 kit on Bioanalyzer 2100 (Agilent, 5067-1505) and quantified using NEBNext Library Quant Kit for Illumina (New England Biolabs, E7630) before being sequenced on MiSeq Illumina sequencer with at least 5M reads per sample. The sample type miRNA profiles specificity was evaluated using bioinformatics analysis.

T1D Extracellular Vesicles' RNA Characterization

Type 1 diabetes, 10yT1D, and HC as well as TX plasma enriched EVs precipitated fractions were resuspended in 200 μL PBS and dissolved in 1 mL Qiazol (Qiagen, 79306). After chloroform-Qiazol centrifugation and aqueous layer phase separation, RNA was isolated following a manufacture's procedure using RNeasy Mini Spin Columns (Qiagen), cleaned with RWT, RPE buffers (Qiagen) and eluted in nuclease free water. Isolated RNA

[1]https://atlasantibodies.com/

size distribution profile and concentration was assessed on Bioanalyzer 2100 using Bioanalyzer 6000 Pico kit (Agilent, 5067–1514) and stored at −80°C before further processing. Small non-coding RNA EVs libraries were prepared using NEBNext Multiplex Small RNA Library Prep Set for Illumina (New England Biolabs, E7300S) following standard protocol without size selection step. NGS libraries were checked for QC using DNA 1000 kit on Bioanalyzer 2100 (Agilent, 5067-1505) and quantified using NEBNext Library Quant Kit for Illumina (New England Biolabs, E7630). Small RNA libraries were pooled in equimolar ratio. EVs plasma miRNA samples were sequenced with 150 M raw sequencing reads for nT1D, 10yT1D, HC, and TX samples on Illumina Hiseq.

miRNAs Bioinformatics Analysis

Raw sequences data were trimmed for the adapter sequence using Cutadapt 1.14 (Martin, 2011) (trimming parameters: $Q \geq 20$, minimal sequence length 15 nucleotides) and further analyzed using sRNAtoolbox (Rueda et al., 2015), a collection of tools for small RNA analysis. sRNAbench module with genome mapping mode was used for alignment and annotation on hg38 human genome reference and sRNAde integrated tool was implemented for differential expression analysis.

For EVs plasma samples miRNA characterization, EVs miRNA profiles were compared to total plasma and EVs depleted plasma. miRNAs of which all the samples of at least one group exceeded 10 miRNAs read counts were compared using the differential expression analysis.

Low sequenced reads per miRNA species were excluded from the differential expression comparison analysis. In the same way miRNA of nT1D, 10yT1D, and HC individuals with a minimum of 10 read counts were compared with the differential expression analysis. Similarly, TX participants' miRNAs profiles after 1, 6, and 24 h after the transplantation were compared to the samples obtained before the transplantation procedure, where miRNAs in at least one group exceeded 100 miRNAs read counts. edgeR results with FDR < 0.05 were considered as statistically significant.

On the basis of differential expression analysis, eight significantly differentially expressed miRNA with FDR < 0.05 were selected for *in vitro* testing. hsa-miR-122-5p, hsa-miR-192-5p, hsa-miR-193b-5p, hsa-miR-185-5p, hsa-miR-195-3p, and hsa-miR-455-5p were selected based on the results of nT1D-HC, 10yT1D-HC and 10yT1D-nT1D differential expression analysis, while hsa-miR-375-3p and hsa-miR-129-5p were the most significantly overexpressed miRNAs in Langerhans islets transplantation patients.

miRNA *in vitro* Whole Blood Early and Transient Activation and Degranulation

The immunomodulatory effect of selected differentially expressed EVs miRNAs was assessed on whole blood samples of ten healthy participants and ten newly diagnosed children with T1D (participants' characteristics in **Table 2**). Whole blood samples of participants were collected into 10 mL Na-heparin tubes. For miRNAs vesicle derived stimulation, the blood of participants was diluted by RPMI in 1:1 ratio and aliquoted to 0.5 mL in sterile round-bottom polystyrene tubes. HPLC purified miRNAs (IDT) hsa-miR-122-5p, hsa-miR-192-5p, hsa-miR-193b-5p, hsa-miR-185-5p, hsa-miR-195-3p, hsa-miR-455-5p, hsa-miR-375-3p, and hsa-miR-129-5p mixture with DOTAP (N-[1- (2,3-Dioleoyloxy)propyl]-N,N,N-trimethylammonium methyl-sulfate; Sigma Aldrich, 11202375001) reagent were used to generate EVs like vesicular species that were added to whole blood samples to be internalized via endolysosomal pathway.

TABLE 2 | Characteristics of new-onset T1D (nT1D) participants and healthy controls (HC) included in DOTAP-miRNA stimulation test.

nT1D	Age [years]	T1D antibodies	HC	Age [years]	T1D antibodies
P1	1–5	GAD65, IA2	N1	6–10	–
P2	11–15	GAD65, IA2, ZnT8	N2	11–15	–
P3	11–15	GAD65	N3	11–15	–
P4	11–15	GAD65, ZnT8	N4	6–10	–
P5	11–15	GAD65, IA2, ZnT8	N5	6–10	–
P6	6–10	GAD65, IA2, ZnT8	N7	6–10	–
P7	6–10	GAD65, IA2, ZnT8	N8	6–10	–
P8	6–10	IA2, ZnT8	N9	6–10	–
P9	6–10	GAD65	N10	11–15	–
P10	6–10	GAD65, IA2, ZnT8	N11	6–10	–

For every nT1D and HC participant are reported the age as a range and the presence of T1D related antibodies (–: below the limit of detection). The cohorts did not statistically differ in age (Wilcoxon parametric t-test: p = 0.8256) and sex (Chi-square test: p = 0.6531).

DOTAP/miRNAs complex was prepared by combining 7.5 μL DOTAP /mL with miRNAs final reaction concentration 0.5 μM. The optimal miRNA concentration was determined from the results of the titration DOTAP/miRNAs complex (**Supplementary Figure S2**). 0.5 μM ssRNA40/LyoVec (Inviogen, tlrl-lrna40), 10 μg/mL Poly (I:C) HWC (Invivogen, tlrl-pic), 2.5 μg/mL PHA with 200 IU/mL IL2 (PHA: Sigma Aldrich, L9017-1MG; IL2: ROCHE, 11011456001) were used as positive controls. Blood alone, 0.5 μM RNA41 (Beignon et al., 2005, 1) (HPLC purified, IDT) with 7.5 μL DOTAP/mL and DOTAP (7.5 μL DOTAP/mL) alone were used as negative controls. To specify the effect of extracellularly delivered miRNAs in non-vesicular form, miRNAs were also added to the cell suspension without DOTAP. Altogether 24 conditions were tested. The stimulation response was monitored after 21 h overnight incubation at 37°C, 5% CO_2. After 20 min labeling using mouse-anti-human antibodies for early and transient activation (CD69) on CD4+ and CD8+ T-cells (BD Biosciencesanti-human-CD69 FITC, 347823; BD Pharmigen: anti-human-CD3 PE, 555340; BD Biosciences: anti-human-CD8 PerCP-Cy 5.5, 341050; BD Pharmigen: anti-human-CD4 APC, 555349), and cytotoxicity/degranulation (CD107a) of CD56+ NK cells and CD8+ T-cells (BD Biosciences: anti-human-CD3 FITC 345762; BD Pharmigen:anti-human-CD107a PE, 555801; BD Biosciences: anti-human-CD8 PerCP-Cy 5.5, 341050; BD Pharmigen:anti-human-CD56 APC, 555518), erythrocytes were lysed using BD FACS Lysing Solution (BD Biosciences; 349202),

and lymphocytes quantified by BD FACSCanto II System (BD Biosciences). The flow cytometry results were analyzed using BD FACSDiva^{TM} Software (BD Biosciences).

Extracellular Vesicle Clearance and Accumulation in Immune Cells

Next, the importance of vesicle delivery and miRNA intracellular accumulation in the cells of the immune system was investigated. miRNA DOTAP vesicle complex internalization and accumulation in the immune cells were assessed on three *in vitro* adult whole blood samples (blood collected in heparinized tubes). Samples were diluted by RPMI in 1:1 ratio transfected *in vitro* with 0.5 μM fluorescent-labeled hsa-miR-375-3p-FAM alone (HPLC purified hsa-miR-375-3p-FAM, IDT), DOTAP/hsa-miR-375-3p-FAM complex, and DOTAP alone.

After 2 h of stimulation, the initial wash step with Phagotest Reagent A (Phagotest; Glycotope Biotechnology, 341060) was used to remove the surplus of miRNA in cell medium, and CD14+ monocytes were labeled for 20 min with anti-human-CD14 PerCP-Cy 5.5 antibody (BD Bioscience; ref: 550787). The fluorescence of potentially attached miRNAs on the cytoplasmic membrane was quenched with the Phagotest Reagent B and after the wash steps, erythrocytes were lysed using Phagotest reagent C. After the wash, cells populations were analyzed using BD FACSCanto II System (BD Biosciences). FSC, SSC, and anti-CD14 parameters were used to specify the lymphocytes, monocytes and granulocytes populations. hsa-miR-375-3p-FAM (FITC absorbance/emission spectrum) signal was used to evaluate miRNA internalization and the quantitative determination of the up-taken vesicles. hsa-miR-375-3p-FAM and DOTAP/hsa-miR-375-3p-FAM were compared to cells-autofluorescence as a result of the stimulation with DOTAP alone. Additionally, internalized and accumulated vesicle DOTAP/miRNA-FAM in the whole blood cells were analyzed after 5 and 30 min, 1, 2, 4, and 6 h from the beginning of the transfection. The results were compared to the sample with the unlabeled hsa-miR-375-3p with DOTAP (DOTAP/miRNA). For every sample at the investigated time of the experiment, the vesicle clearance and accumulation were calculated with the relative median fluorescence intensity ratio of DOTAP delivered hsa-miR-375-3p-FAM vs. DOTAP delivered hsa-miR-375-3p.

Micro-RNAs delivered with DOTAP vesicles' intracellular accumulation as well as intracellular compartmentalization was characterized using fluorescent microscopy. Whole blood samples from adult healthy individuals were obtained and erythrocytes were lysed with RBC Lysis Buffer (Cell Signaling technology, 46232) and after wash step, leukocytes were resuspended in RPMI-1640 Medium (Sigma Aldrich, R8758). The cells were transfected with DOTAP/hsa-miR-375-3p-FAM (0.5 μM miRNA), where DOTAP vesicles were stained using CellBrite Orange Cytoplasmic Membrane Dye (Biotium, 30022) before the transfection. After 2 h of incubation at 37°C 5% CO2, cells were washed with PBS and stained with Lysosomal Staining Reagent (Abcam, ab176828). The samples were fixated using 4% formaldehyde (Sigma Aldrich, F8775), and cytoplasmic membrane was stained using CellBrite Blue Cytoplasmic Membrane Dye (Biotium, 30024). The cells were imaged using Olympus fluorescence microscopy system (Olympus Life Science BX61). Pictures were processed using ImageJ software (Schneider et al., 2012).

Vesicle-miRNAs TLR7/8 Activation, Transfection Reagent Specificity, and miRNAs Structure Dependent Activation

To confirm the vesicle derived miRNAs induction of TLR7/8 signaling the Chloroquine (CQ) (Invivogen, tlrl-chq) was used. The stimulation DOTAP/miRNA effect was inhibited with the increasing concentrations of CQ, after ssRNA40/LyoVec and hsa-miR-455-5p DOTAP stimulation. After the CQ titration, the 20 μM CQ inhibitory concentration was identified as optimal (**Supplementary Figure S3**) and used to inhibit DOTAP hsa-miR-122-5p, hsa-miR-455-5p, hsa-miR-375-3p, hsa-miR-129-5p TLR7/8 activation effect. miRNA TLR7/8 inhibition was assessed on six whole blood adult healthy controls collected in Na-heparin tubes by the aforementioned procedure (labeling protocol: miRNA *in vitro* whole blood early and transient activation and degranulation) with the addition of 20 μM CQ to the reaction tubes before 21h overnight incubation.

Furthermore, the DOTAP transfection reagent specificity was characterized and compared to RNAiMAX Lipofectamine transfection reagent. The parallel sample transfection experiments were performed on three adult donors on the whole blood samples. Transfection reagent specificity was evaluated with transfection of hsa-miR-122-5p, hsa-miR-129-5p, hsa-miR-375-3p, hsa-miR-455-5p, and hsa-miR-193b-5p, including reactions with CQ inhibitor. RNAiMAX Lipofectamine transfection was performed in 0.5 mL 1:1 RPMI diluted whole blood cells following the manufacturer's protocol with the final 0.5 μM miRNA concentration and 3.5 μL RNAiMAX Lipofectamine/mL. The 20 μM CQ concentration was used in inhibition reactions. For both transfection reagents, DOTAP and RNAiMAX Lipofectamine alone were used as negative controls and ssRNA-40/LyoVec as a positive immune activation control.

The immunomodulatory effect was assessed using flow cytometry for assessing early activation marker CD69 on CD4+ and CD8+ T-cells and expression of CD107a+ cytotoxicity marker on CD8+ T-cells and CD56+ NK-cells (described in the "Mirna *in vitro* Whole Blood Early and Transient Activation and Degranulation" section).

Due to different stimulation responses of studied miRNAs in our "miRNA *in vitro* whole blood early and transient activation and degranulation" results, the miRNAs structures were correlated to the immune-stimulation effect. To predict studied miRNAs secondary structure miRNAs sequences were analyzed with RNAfold web server (Lorenz et al., 2011).

Cytokine/Chemokine Profile Detection

DOTAP/miRNA immune system activation was additionally evaluated by assessing cytokine and chemokine inflammatory profiles. The whole blood samples of three healthy adult donors were used for DOTAP-miRNA stimulation reactions (hsa-miR-122-5p, hsa-miR-129-5p, hsa-miR-375-3p, hsa-miR-455-5p, and

hsa-miR-193b-5p), DOTAP alone as a negative control and ssRNA-40/LyoVec as a positive immune activation control. Samples were incubated 21 h overnight (37°C, 5% CO_2). After 5 min centrifugation at 3000×*g*, samples' supernatants were transferred to cryotubes and stored at −80°C. Supernatants were diluted 25-times and the cytokine/chemokine profile was detected using LEGENDplex Human Inflammation Panel multi-analyte flow assay kit (BioLegend, 740118) using BD FACSCanto II System (BD Biosciences) and data were analyzed using LEGENDplex v8.0 software.

Statistics

Multiple comparisons for different miRNAs stimulation experiments were calculated following the rules of estimation statistics to better represent the effect size of the comparison, its distribution, and to compensate for the flaws of the null-hypothesis significance testing (Cumming, 2014; Claridge-Chang and Assam, 2016). The differences in selected parameters between control and stimulation experiments were calculated using paired and unpaired estimation test implemented in Python DABEST package (Ho et al., 2019). Cytokine and chemokine release was evaluated with Kruskal-Wallis one-way ANOVA test. The results (corresponding *p*-Values) of multiple comparisons were corrected for the false discovery rate (FDR) using two-stage Benjamini, Krieger, and Yekutieli (TSBKY) procedure implemented in Python module StatsModels 0.9.0 (Benjamini et al., 2006). Stimulation DOTAP/miRNA flow cytometry results and cytokine release results were considered significant when FDR *q*-Value was lower than 0.05 for paired mean difference analysis and 0.1 for nT1D-HC group unpaired difference analysis.

Titration curve figures and boxplots of DOTAP/miRNAs, QC titration as well as QC inhibitory response were created in R using ggplot2 (Wickham, 2016).

RESULTS

Beta-Cells From Langerhans Islets Release Extracellular Vesicles to Blood Plasma

Due to a low amount of pancreatic beta-cells (Weir and Bonner-Weir, 2013) in proportion to the whole human body, the presence of pancreatic insulin-producing Langerhans islets beta-cells' EVs was investigated in blood plasma. PEG-based EVs precipitation was used to isolate EVs fraction in blood plasma, and TEM was used to morphologically identify and characterize EVs in the isolated fractions. TEM immunogold labeling on cryo-ultrathin sections confirmed the presence of EVs positive endocrine-pancreatic-cell-membrane-specific proteins GAD2 (GAD65), PTPRN (IA-2) and DGCR2 with a diameter of isolated EVs up to 500 nm (**Supplementary Figure S4**). EVs isolated from human Langerhans islet medium, collected during pre-transplantation storage and maintenance of Langerhans islets, were used as a positive control in the immunogold labeling experiment.

The majority of EVs in *ex vivo* cultured Langerhans islets' medium was positive for the expression of DGCR2 (**Figure 1G**), estimated to be 10/100 EVs. Conversely, immunogenic T1D associated proteins GAD2 and PTPRN were detected (**Figures 1E,F**) in a smaller proportion (estimated at 1/100 EVs). EVs in blood plasma were also positive for endocrine-pancreatic cell-membrane specific proteins DGCR2 (estimated at 1/10.000 EVs), GAD2 and PTPRN (**Figures 1A–C**) (estimated at 1/100.000 EVs), confirming the existence of EVs originating from Langerhans islets in the circulating blood. Furthermore, we also detected DGCR2 positive EVs for intra-vesicular insulin (INS) (**Figures 1D,H**).

TEM imaging confirmed our hypothesis of beta-cell-released EVs in the blood plasma and potential beta-cells' communication with other tissues. This led us to further investigate the role of EVs and their RNA cargo in the new-onset T1D plasma EVs.

Extracellular Vesicle, Blood Plasma, EVs Depleted Plasma miRNA Profiles

EVs, the whole blood plasma, and EVs depleted plasma miRNA profiles (**Supplementary Figure S5**) were compared using NGS differential expression analysis (**Supplementary Figure S6**). The analysis revealed different miRNA profiles among EVs, plasma and EVs depleted plasma samples, where the type source of samples (EVs, the whole blood plasma, and EVs depleted plasma) showed greater similarity compared to the samples of the investigated individuals. The sample type clustering is shown in **Supplementary Figure S6**. The results provided evidence of EVs miRNA profile specificity, which allowed our further EVs miRNA analysis of T1D individuals.

Extracellular Vesicles' miRNAs in Type 1 Diabetes and During Intensive Beta-Cell Destruction

The isolated EVs fractions from pediatric pre-pubertal individuals' plasma samples with nT1D were analyzed using next-generation sequencing, which allows profiling whole EVs small-RNA transcriptome. All nT1D individuals were positive for T1D related autoantibodies and had a negative family history for other autoimmune diseases. To specify small RNAs associated with T1D pathogenesis nT1D EVs miRNA profile was compared to the profiles of the cohort with 10yT1D and negative T1D autoantibodies, and to a cohort of HC (Characteristics of participants: **Table 1**).

A higher expression of hsa-miR-122-5p and hsa-miR-192-5p were identified in nT1D cohort when compared to HC (**Figure 2A**). Differential expression analysis of nT1D versus 10yT1D showed ten potentially differentially expressed miRNAs, most of them with higher expression in nT1D: hsa-miR-193b-5p, hsa-miR-122-5p, and hsa-miR-445-5p showing the most significant difference between compared groups (**Figure 2B**). Furthermore, hsa-miR-195-3p and hsa-miR-455-5p expression were lower, and hsa-miR-185-5p expression was higher in the 10yT1D-cohort, compared to HC (**Figure 2C**). Detailed results of differential expression analysis of plasma EVs miRNAs are presented in **Table 3**.

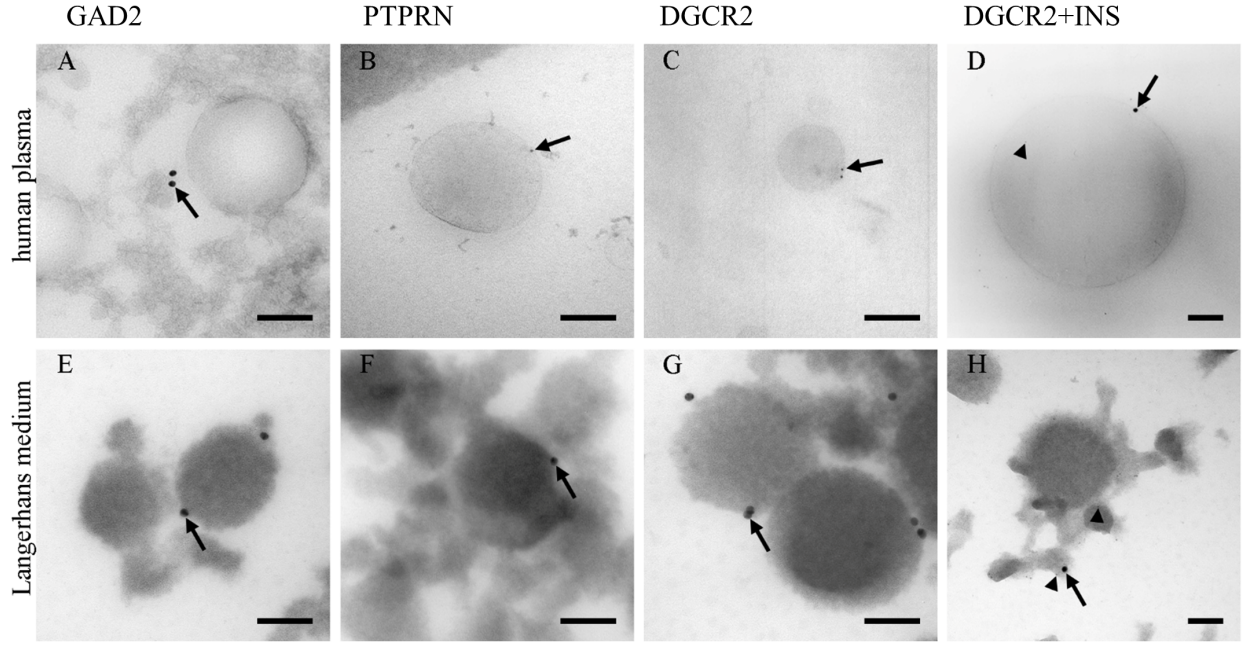

FIGURE 1 | Immunolabeling of EVs. Immunolabeling of EVs isolated from human blood plasma **(A–D)** and the medium of cultured human Langerhans islets **(E–H)**. Antibodies against GAD2 **(A,E)**, PTPRN **(B,F),** and PTPRN **(C,G)** proteins labeled limiting EVs (arrows). Antibodies against insulin were also presented in the lumen of vesicles (arrow-head; **D,H**). INS, insulin; GAD2, Glutamate decarboxylase 2 (GAD65); DGCR2, DiGeorge Syndrome Critical Region Gene 2; PTPRN, Protein tyrosine phosphatase receptor type N. Bars: 100 nm.

The EVs signals from insulin-producing beta-cells affected by autoimmunity might not be successfully assessed in a cohort of nT1D individuals, because of variably in the preserved beta-cells mass. To evaluate and specify the EVs related to beta-cell destruction (transplantation procedure exposes beta-cells in Langerhans islets to elevated stress characterized by a stress-signature released miRNA), two TX recipients' blood plasma samples were taken before and one, six and 24 h after the transplantation. EVs from these plasma samples were sequenced (average 125M+ reads/sample), and miRNAs content was analyzed. Generated miRNA profiles demonstrated a typical trend for specific miRNA species, with low levels before the transplantation, increased 1 h after the procedure, followed by a steady temporal decline in their levels. miRNA species following this expression trend included hsa-miR-375-3p, hsa-miR-129-5p, miR-200b-5p, and hsa-miR-216b-5p (**Figure 2D** and **Table 4**).

Based on our nT1D miRNA and Langerhans islet transplantation individuals' miRNA profiling results, eight differentially expressed miRNAs were selected in individuals with nT1D with FDR < 0.05 for further *in vitro* miRNAs synthetic vesicles immunomodulation testing.

Extracellular Vesicles' miRNA Immunomodulatory Role in Type 1 Diabetes

The effect of differentially expressed miRNAs in T1D was investigated on the pediatric whole blood specimens from nT1D and HC participants (Characteristics of participants: **Table 2**), with the aim to preserve as much as possible blood immune cells sub-populations and intricate cells' interactions in *in vitro* testing. To specify the effect of differentially expressed miRNA and mimic the EVs miRNAs delivery to the target cells of the immune system without other immunomodulatory EVs components, individual miRNA species were packed with N-[1-(2,3-Dioleoyloxy)propyl]-N,N,N-trimethylammonium methyl-sulfate (DOTAP) synthetic vesicles, entering cells via the endolysosomal pathway. Eight selected miRNAs differentially expressed in people with diabetes and transplantation individuals (hsa-miR-122-5p, hsa-miR-192-5p, hsa-miR-193b-5p, hsa-miR-185-5p, hsa-miR-195-3p, hsa-miR-455-5p, hsa-miR-375-3p, and hsa-miR-129-5p) were tested for their potential effect on early and transient activation as well as cytotoxicity of the effector immune cells. All tested miRNAs, except hsa-miR-193b-5p, substantially induced CD69 early and transient activation of CD4C and CD8C T-cells in whole blood samples, as well as CD107a degranulation (cytotoxicity) of CD56+ NK and CD8+ T-cells in all tested samples (**Figures 3A–D**, **4** and **Tables 5A,B**) ($p < 0.0001$). Interestingly, the stimulation with "naked" miRNAs (not integrated into vesicles to evade endolysosomal path), and empty DOTAP vesicles did not induce any detectable activation or cytotoxic degranulation (**Tables 5A,B**). The DOTAP/miRNAs vesicles delivery was generally associated with lower early transient activation of CD4+ T-cell in nT1D compared to HC (**Figures 4A,B**). Compelling differences in the expression of CD4+ CD69+ between nT1D and HC were observed at stimulation with hsa-miR-122-5p (overexpressed in nT1D),

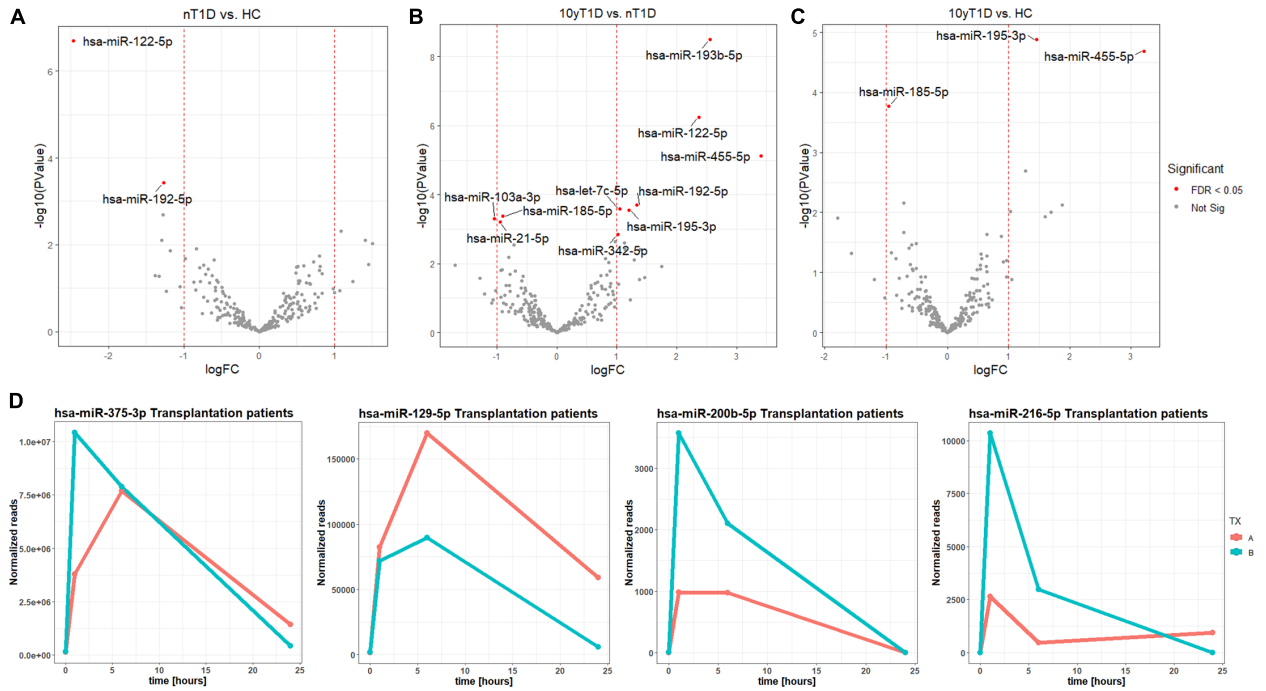

FIGURE 2 | Differentially expressed EVs miRNAs between nT1D, 10yT1D, HC, and Islet transplantation participants. Differential expression Volcano plots of panel **(A)** nT1D and HC, **(B)** 10yT1D and HC, and **(C)** 10yT1D and nT1D (nT1D, new-onset T1D participants, *N* = 10; 10yT1D – 10 years duration T1D participants, *N* = 10; HC, healthy controls, *N* = 10; red dots represent differentially expressed miRNAs with FDR < 0.05). **(D)** Chronological presentation of differentially expressed hsa-miR-375-3p, hsa-miR-129-5p, hsa-miR-200b-5p, and hsa-miR-216-5p in Langerhans islet transplantation participants [TX; **(A,B)** anonymized individuals] before (0 h), and 1, 6, and 24 h after the transplantation.

hsa-miR-455-5p (with higher expression in nT1D and HC), hsa-miR-375-3p, and hsa-miR-129-5p (elevated in Langerhans islet transplantation and associated with beta-cell stress and Langerhans islets' damage) ($p < 0.05$) (**Figure 4A** and **Table 6A**). Tested DOTAP/miRNAs complexes strongly induced CD8+ T-cells proliferation, NK cell (CD56+) and T cell (CD8+) CD107a+ cytotoxic degranulation, however, the difference in activity between nT1D and HC were not observed (**Figures 4B–D** and **Tables 6A,B**).

The stimulation of immune cells with EVs' miRNAs influenced the regulation of the immune system. This potentially contributes to the pathogenesis of T1D with modulated T-cell activation and cytotoxicity. Interestingly, vesicles containing miRNAs modulated T-cell activation more intensively in HC compared to nT1D individuals. These results pawed the way for the next step: the investigation of pathway associated with immune cells' EVs internalization, miRNA interaction, and *in vitro* inhibition of this pathway.

Extracellular Vesicles' Intracellular Accumulation in Phagocytes

miRNA intracellular accumulation in cells of the immune system occurred only if miRNA was transfected with vesicles; bare miRNA did not enter the cells of the immune system (**Figures 5A,B**). The analysis of the DOTAP/miRNA internalization process with fluorescent-labeled miRNA by fluorescence microscopy (**Figure 5E**) and flow cytometry revealed preferential vesicles internalization by monocytes and, to a lesser degree, by granulocytes (**Figures 5B–D**), while lymphocytes internalization of DOTAP/miRNA was negligible. These results indicate the essential role of the endolysosomal antigen-presentation pathway of monocytes and granulocytes, and the internalized miRNAs associated immune system activation.

TLR7/8 miRNA Activation

Monocytes and granulocytes express endosomal TLR7 and TLR8 (TLR7/8), capable of detecting intracellular single-stranded pathogen RNA (ssRNA) in the endolysosomal pathway, where the TLR7/8 activation is RNA structure and sequence (uridine nucleotide accessibility) dependent (Gantier et al., 2008). The comparison of miRNA structures and immune response shows the highest immune activation with hsa-miR-455-5p, likely because of exposed uridines in the loop and prime ends of the sequence. Moderate stimulation response of other studied miRNAs containing accessible uridines was observed. The non-response of hsa-miR-193b-3p was probably the consequence of the inaccessibility of paired uridines in dsRNA stem-loop miRNAs structure (**Figure 6**).

To confirm the involvement of the endolysosomal TLR7/8 in the activation of the immune system and to investigate

TABLE 3 | sRNA toolbox differential expression of nT1D, 10yT1D, HC EVs miRNAs sequencing results.

nT1D– HC	Average nT1D reads	Average HC reads	logFC	logCPM	*P*-value	FDR
hsa-miR-122-5p	**4,832,438.59**	**873,511.46**	**−2.46785**	**16.72597**	**2.01E-07**	**4.96E-05**
hsa-miR-192-5p	**41,257.96**	**17,091.76**	**−1.27135**	**10.25227**	**0.000378**	**0.046676**
hsa-miR-378c	143.27	48.72	−1.55396	2.239277	0.000898	0.073921
hsa-miR-193b-5p	3,945.46	1,625.99	−1.27892	6.671317	0.002011	0.124193
10yT1D - HC	**Average 10yT1D reads**	**Average HC reads**	**logFC**	**logCPM**	***P*-value**	**FDR**
hsa-miR-195-3p	**1,636.58**	**4,503.83**	**1.460336**	**7.339928**	**1.31E-05**	**0.002516**
hsa-miR-455-5p	**61.75**	**573.41**	**3.213685**	**4.404186**	**2.04E-05**	**0.002516**
hsa-miR-185-5p	**107,325.25**	**55,217.37**	**−0.95879**	**11.81067**	**0.000168**	**0.013854**
hsa-miR-193b-5p	670.36	1,625.99	1.277958	6.671317	0.002032	0.125479
10yT1D – nT1D	**Average 10yT1D reads**	**Average nT1D reads**	**logFC**	**logCPM**	***P*-value**	**FDR**
hsa-miR-193b-5p	**670.36**	**3,945.46**	**2.556865**	**6.671317**	**3.12E-09**	**7.72E-07**
hsa-miR-122-5p	**937,326.45**	**4,832,438.59**	**2.366128**	**16.72597**	**5.62E-07**	**6.95E-05**
hsa-miR-455-5p	**61.75**	**657.31**	**3.410471**	**4.404186**	**7.36E-06**	**0.000606**
hsa-let-7c-5p	**19,030.00**	**39,414.73**	**1.050441**	**10.49258**	**0.000263**	**0.011701**
hsa-miR-192-5p	**16,394.18**	**41,257.96**	**1.331473**	**10.25227**	**0.000201**	**0.011701**
hsa-miR-195-3p	**1,636.58**	**3,783.13**	**1.208751**	**7.339928**	**0.000284**	**0.011701**
hsa-miR-185-5p	**107,325.25**	**57,606.27**	**−0.89769**	**11.81067**	**0.000421**	**0.01486**
hsa-miR-103a-3p	**7,893.16**	**3,831.02**	**−1.04276**	**8.13815**	**0.000496**	**0.015299**
hsa-miR-21-5p	**194,384.87**	**100,930.19**	**−0.94556**	**12.83508**	**0.000621**	**0.017045**
hsa-miR-342-5p	**3,763.81**	**7,595.65**	**1.012932**	**8.101386**	**0.001444**	**0.035672**
hsa-miR-193a-5p	1,193.08	2,612.78	1.130626	6.479336	0.002455	0.050524
hsa-miR-99a-5p	6,818.56	13,390.50	0.973615	8.923166	0.002289	0.050524
hsa-miR-26a-5p	53,554.47	32,617.91	−0.71534	11.0815	0.002887	0.054844
hsa-miR-100-5p	1,199.68	2,641.43	1.138557	6.625715	0.003799	0.063369
hsa-miR-483-5p	396.41	1,040.34	1.391449	4.955521	0.003848	0.063369
hsa-miR-20a-5p	2,076.58	1,190.35	−0.80257	6.350269	0.006577	0.101525
hsa-miR-125a-5p	8,138.86	14,308.18	0.813912	9.126002	0.007022	0.102028
hsa-miR-150-3p	1,580.15	3,857.16	1.28739	6.946875	0.00793	0.108823
hsa-miR-1246	517.56	945.83	0.869583	5.027435	0.009174	0.11926
hsa-miR-652-3p	106.61	32.75	−1.69822	1.944765	0.011289	0.139417
hsa-miR-365b-5p	83.10	280.48	1.753845	3.458699	0.012046	0.14168

Differential expression edgeR results of EVs miRNAs results reported as average normalized read counts per miRNAs in groups of participants, log fold-change (logFC), log counts per million (logCPM), P-value and FDR for differentially expressed miRNAs. Only miRNAs with FDR lower than 0.15 are reported in this table, miRNAs with FDR < 0.05 were considered as statistically significant differentially expressed miRNAs and are indicated in bold [nT1D, new-onset T1D, n = 10; 10yT1D, 10 years duration T1D, n = 10; HC, healthy controls, n = 10].

potential molecular therapeutic targets, the activated pathway was inhibited by an endosomal TLR7/8 inhibitor. Chloroquine (CQ) decreases ssRNA binding affinity to the TLR7/8 (Kuznik et al., 2011), thus preventing downstream activation of signaling pathways. The CQ co-application with vesicle-miRNAs resulted in an efficient inhibition of the T-cell activation and less effective inhibition of NK cells (**Figure 7**). This miRNA activation of TLR7/8 did not depend on the synthetic vesicle delivery system: The DOTAP/miRNA vesicle immunomodulation was comparable to Lipofectamine RNAiMAX (**Supplementary Tables S1A,B**).

Cytokine/Chemokine Profiling

The DOTAP/miRNA activation was also associated with the increased cytokine and chemokine release. Vesicle miRNAs immune cell activation was evaluated with the inflammation cytokine profile assessment. The investigated miRNAs hsa-miR-122-5p, hsa-miR-129-5p, hsa-miR-375-3p, and hsa-miR-455-5p delivered with vesicles, but not hsa-miR-193b-5p, resulted in the increase of IFN-alpha, IFN-gamma, TNF-alpha, IL-1beta, IL-10, IL-6, and MCP-1 release (all $p < 0.05$) (**Figure 8A** and **Supplementary Table S2**).

The DOTAP/miRNA transfection did not result in a significant increase of IL-8, IL-17A, IL-18, IL-23, and IL-33 levels, moreover, IL-12p70 and IL-17 levels were below the detection limit. miRNA vesicle transfections with the CQ inhibitor did not differentiate with the cytokine/chemokine release levels compared to negative control (DOTAP), with some exception of MCP-1 and IL-10 (**Figure 8A**).

These data indicate the importance of human self-derived EVs miRNAs as auto-agents, which can modulate the immune system through the TLR7/8 pathway. However, we did not

TABLE 4 | sRNA toolbox differential expression analysis results of transplantation patients EVs miRNAs.

0–1 h	TX-A-0h	TX-B-0h	TX-A-1h	TX-B-1h	logFC	logCPM	*P*-value	FDR
hsa-miR-375-3p	**136,975.67**	**127,121.52**	**4,368,840.55**	**9,970,659.54**	**5.76278**	**15.87156**	**1.69E-10**	**1.02E-07**
hsa-miR-129-5p	**1,702.33**	**1,582.07**	**94,994.24**	**68,848.56**	**5.640418**	**9.850739**	**2.65E-07**	**7.99E-05**
hsa-miR-216b-5p	**3.69**	**6.78**	**3,046.05**	**9,894.10**	**10.23924**	**5.071745**	**7.66E-06**	**0.00154**
hsa-miR-200b-5p	**3.69**	**6.78**	**1,129.48**	**3,414.97**	**8.729792**	**3.849213**	**4.09E-05**	**0.006166**
hsa-miR-148a-3p	**9,998,029.89**	**9,061,974.78**	**35,735,485.55**	**98,568,812.39**	**2.816885**	**18.73319**	**0.000112**	**0.013546**
hsa-miR-122-5p	**1,216,369.54**	**1,502,879.92**	**15,503,699.54**	**4,756,837.30**	**2.897392**	**16.40263**	**0.000305**	**0.030693**
hsa-miR-4433b-3p	**8,357.09**	**14,649.83**	**200.71**	**780.87**	**−4.55107**	**5.750177**	**0.000395**	**0.034015**
hsa-miR-125a-5p	1,070.08	5,163.14	18,243.83	41,876.67	3.269816	7.781954	0.001069	0.080548
hsa-miR-200a-3p	2,311.44	718.73	10,964.20	17,189.51	3.215605	7.092002	0.001227	0.082218
hsa-miR-216a-3p	1.84	3.39	665.09	1,619.78	8.703054	2.902087	0.001504	0.090667
0-6 h	**TX-A-0h**	**TX-B-0h**	**TX-A-6h**	**TX-B-6h**	**logFC**	**logCPM**	***P*-value**	**FDR**
hsa-miR-375-3p	**136,975.67**	**127,121.52**	**6,901,633.47**	**6,653,568.65**	**5.681633**	**15.87156**	**2.6E-10**	**1.57E-07**
hsa-miR-129-5p	**1,702.33**	**1,582.07**	**152,258.22**	**75,867.93**	**6.117951**	**9.850739**	**4.73E-08**	**1.42E-05**
hsa-miR-200b-5p	**3.69**	**6.78**	**878.90**	**1,776.87**	**7.959885**	**3.849213**	**0.000105**	**0.018083**
hsa-miR-216b-5p	**3.69**	**6.78**	**424.64**	**2,510.18**	**8.103809**	**5.071745**	**0.00012**	**0.018083**
0-24h	**TX-A-0h**	**TX-B-0h**	**TX-A-24h**	**TX-B-24h**	**logFC**	**logCPM**	***P*-value**	**FDR**
hsa-miR-129-5p	**1,702.33**	**1,582.07**	**62,388.85**	**6,028.34**	**4.380553**	**9.850739**	**2.25E-05**	**0.013545**
hsa-miR-493-5p	**695.18**	**1,636.30**	**4.52**	**2.99**	**−8.22825**	**3.977484**	**7.36E-05**	**0.0222**
hsa-miR-375-3p	136,975.67	127,121.52	1,503,963.49	444,589.80	2.883261	15.87156	0.000264	0.05316
hsa-miR-216b-5p	3.69	6.78	982.52	5.98	6.532697	5.071745	0.001061	0.099431
hsa-miR-4433b-3p	8,357.09	14,649.83	1,012.36	344.99	−4.08287	5.750177	0.001154	0.099431
hsa-miR-486-3p	81,442.82	34,780.37	306,362.18	502,742.48	2.799422	11.54946	0.000708	0.099431
hsa-miR-654-3p	666.48	1,058.85	2.71	1.99	−8.44209	3.083302	0.000844	0.099431

Langerhans islets transplantation individuals (TX represents a transplantation participant, letters A and B represent an individual A and B) edgeR differential expression EVs miRNAs results before (0 h) and after 1, 6, and 24 h after the transplantation procedure. Differentially expressed miRNAs are reported as miRNAs normalized read count, log fold-change (logFC) and log counts per million (logCPM), the difference of expression is reported with P-value and FDR. Only miRNAs with FDR lower than 0.10 are reported, miRNAs with FDR < 0.05 are considered as significant and are indicated in bold.

test the miRNA immune system activation via miRNA-mRNA interactions.

DISCUSSION

Micro-RNAs are primarily involved in the intracellular regulation of mRNA translation, mRNA degradation, and gene expression (Djuranovic et al., 2012; Cottrell et al., 2017). Furthermore, miRNAs can be packed in EVs released from maternal cells, and can modulate specific cellular processes in the recipient cells (Kosaka et al., 2013). A few studies investigated EVs protein cargo (Cianciaruso et al., 2017; Hasilo et al., 2017; Rutman et al., 2018) and total plasma miRNA in T1D (Garcia-Contreras et al., 2017) so far, however, the immunomodulatory role of EVs miRNA has not been well established. To our knowledge, this is the first EVs study demonstrating beta-cell-released EVs presence in blood plasma using TEM (**Figure 1**), and the potential role of EVs miRNA in the etiology of T1D. The TEM characterization demonstrated the presence of Langerhans islets' EVs in plasma in a non-quantitative manner. We further specified EVs fraction using NGS miRNA profiling, which included EVs miRNA amplification and allowed low count miRNA detection in the samples with limited sample volume.

Using NGS sequencing and comparison of blood plasma EVs profiles of healthy controls, nT1D individuals with an active beta-cell destruction, and 10yT1D participants with non-detectable beta-cell activity or autoimmunity process, we characterized differentially expressed EVs miRNA in T1D (**Figures 2A–C**). The most prominently overexpressed miRNAs in the nT1D cohort was hsa-miR-122-5p, previously associated with liver pathology (Hu et al., 2012), metabolism regulation (Willeit et al., 2017; Barajas et al., 2018), and T1D (Åkerman et al., 2018). Elevated hsa-miR-192-5p and hsa-miR-193b-5p in T1D are reported as markers of prediabetes in the adult population (Párrizas et al., 2015). Additionally, some EVs miRNAs differentially expressed in 10yT1D individuals could indicate the early development of diabetic complications (La Sala et al., 2016). Due to the variability of preserved beta-cell mass at the onset of T1D and differences in the autoimmune process activity, the differentially expressed miRNA profiles in T1D individuals might not be clearly associated with beta-cell damage.

The EVs enriched fraction included EVs from all parts of a human body, including Langerhans islets EVs, EVs of the cells of the immune system and other EVs released as the result

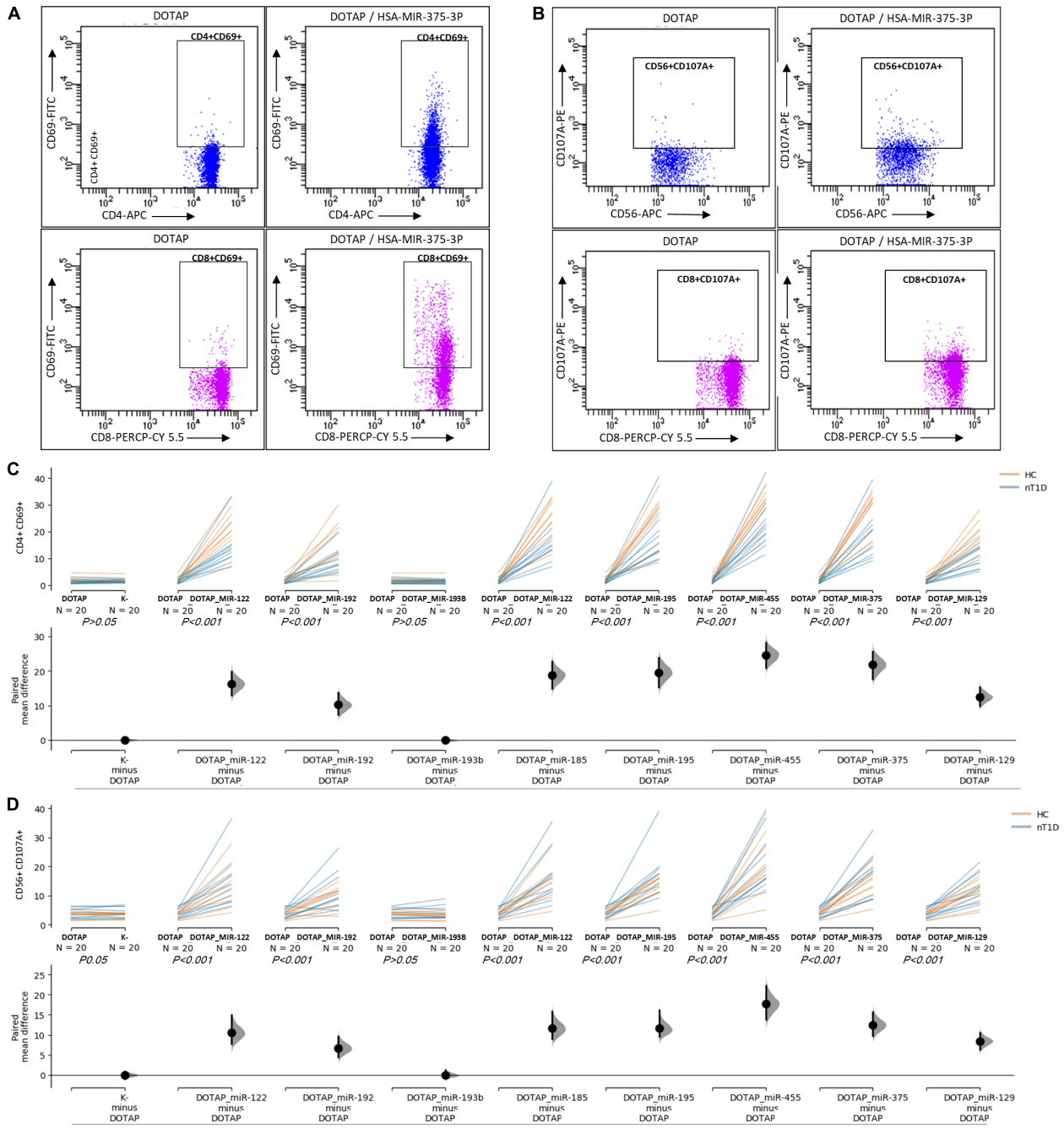

FIGURE 3 | The stimulation effect of endolysosomal delivered miRNAs. **(A)** Representative flow cytometry stimulation effect of DOTAP as a negative control (left scatter plots) and DOTAP/hsa-miR375-3p (right scatter plots) on the upregulated expression of CD69 early activation marker effect on CD4+ (top scatter plots) and CD8+ T-cells (bottom scatter plots). **(B)** The effect of stimulation on the upregulated expression of CD107a marker (cytotoxicity/degranulation) on CD56+ NK cells (top scatter plots) and CD8+ T-cells (bottom scatter plots) after the stimulation with DOTAP – a negative control (left scatter plots) and DOTAP/hsa-miR375-3p (right scatter plots). Paired data analysis plots with effect size are presented for panel **(C)** CD4+ CD69+ results, and **(D)** CD56+ CD107a+. Whole blood samples were treated with different DOTAP/miRNAs and compared to DOTAP and K- (blood sample alone) as negative controls [the observed effects were assessed 21 h after the stimulation; HC and nT1D $N = 20$; P-values represent a paired Hedges' g mean difference analysis significance: $P < 0.001$ significant difference].

of a metabolic imbalance. We cannot declare the miRNAs as beta-cell or other tissue specific. However, some miRNA were differentially expressed in T1D individuals, probably as a result of autoimmunity and metabolic imbalance.

Individuals with Langerhans islets transplantation were additionally included in our study to investigate the miRNA during the active (intensive) beta-cell damage and destruction: beta-cells are exposed to the transplantation stress and

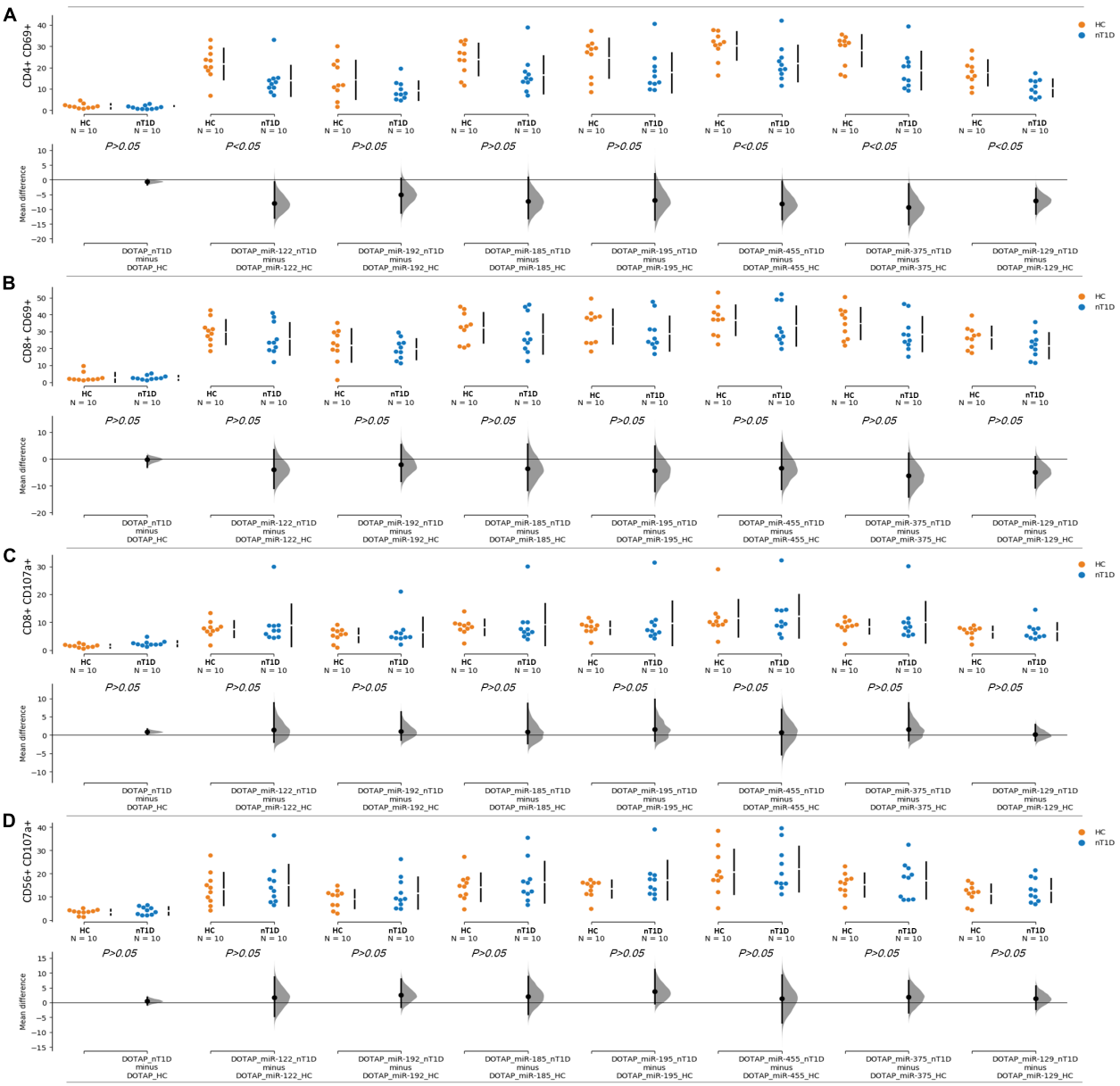

FIGURE 4 | Differences in the stimulation effect between compared HC and nT1D participants. The graphs show the differences in stimulation effect on the upregulated expression of early activation marker CD69 on **(A)** CD4+ T-cells and **(B)** CD8+ T-cells in blood samples of nT1D and HC. The differences between HC and nT1D were significant in the stimulation experiments with DOTAP/hsa-miR-122-5p, DOTAP/hsa-miR-455-5p, DOTAP/hsa-miR-375-3p, and DOTAP/hsa-miR-129-5p ($P < 0.05$). The stimulation effect was not observed in expression of CD107a cytotoxicity/degranulation marker on **(C)** CD8+ T-cells and **(D)** CD56+ NK-cells [the observed effects were assessed 21 h after the stimulation; HC $N = 10$; nT1D $N = 10$; P-values represent an unpaired Hedges' g mean difference analysis significance: $P < 0.05$ significant difference].

partial destruction, which can reflect in stress released EVs. The differential expression analysis of TX patients' EVs miRNA profiles demonstrated increased expression of hsa-miR-375-3p, hsa-miR-129-5p, hsa-miR-200b-5p, and hsa-miR-216b-5p (**Figure 2D**). The most prominent increase was observed for hsa-miR-375-3p, the miRNA with the highest expression in beta-cells (LaPierre and Stoffel, 2017), and associated with beta-cell destruction at the T1D onset, although the published data are not unequivocal (Marchand et al., 2016; Erener et al., 2017). Other miRNAs were also likely released from beta-cells, where hsa-miR-200 regulate beta-cell apoptosis and miR-126 glucose promoted/inhibited proliferation (Belgardt et al., 2015; Tao et al., 2016).

Eight significantly differentially expressed miRNA were selected for further *in vitro* functional testing on

TABLE 5A | Vesicle delivered miRNA effect on CD69+ T-cell activation (paired mean difference analysis).

CD4+CD69+	Control	Difference	*p*-Value paired_students_*t*-test	*q*-Value	Discovery
K-	DOTAP	2.6264E-02	8.6365E-01	5.8758E-01	No
DOTAP/miR-122	**DOTAP**	**2.7464E+00**	**1.6806E-08**	**4.4134E-08**	**Yes**
DOTAP/miR-192	**DOTAP**	**1.8868E+00**	**4.9719E-06**	**8.1600E-06**	**Yes**
DOTAP/miR-193b	DOTAP	−7.4805E-02	5.1846E-01	5.7924E-01	No
DOTAP/miR-185	**DOTAP**	**2.9176E+00**	**8.4219E-09**	**2.7645E-08**	**Yes**
DOTAP/miR-195	**DOTAP**	**2.7709E+00**	**3.4213E-08**	**6.4174E-08**	**Yes**
DOTAP/miR-455	**DOTAP**	**3.9724E+00**	**5.3356E-11**	**7.0056E-10**	**Yes**
DOTAP/miR-375	**DOTAP**	**3.2153E+00**	**2.2949E-09**	**1.5066E-08**	**Yes**
DOTAP/miR-129	**DOTAP**	**2.7410E+00**	**2.2487E-08**	**4.9210E-08**	**Yes**
DOTAP_RNA41	DOTAP	4.2537E-02	7.6026E-01	5.8758E-01	No
miR-455	DOTAP	1.5354E-02	8.9017E-01	5.8758E-01	No
miR-122	K-	−9.7474E-02	6.6254E-01	5.8758E-01	No
miR-192	K-	−1.5876E-01	4.7228E-01	5.7924E-01	No
miR-193b	K-	−1.1766E-01	5.7350E-01	5.7924E-01	No
miR-185	K-	−1.7129E-02	9.3976E-01	5.8758E-01	No
miR-195	K-	−5.9610E-02	7.8414E-01	5.8758E-01	No
miR-455	K-	−1.1846E-02	9.3739E-01	5.8758E-01	No
miR-375	K-	3.6059E-17	1.0000E+00	5.9682E-01	No
miR-129	K-	9.6813E-02	5.3791E-01	5.7924E-01	No
RNA41	K-	−2.5097E-02	8.8383E-01	5.8758E-01	No
TLR7-8	**DOTAP**	**3.0293E+00**	**6.3610E-09**	**2.7645E-08**	**Yes**
TLR3	**DOTAP**	**1.0111E+00**	**5.3732E-04**	**7.8389E-04**	**Yes**
CD8+CD69+	**Control**	**Difference**	***p*-Value paired_students_*t*-test**	***q*-Value**	**Discovery**
K-	DOTAP	−3.5588E-02	7.3354E-01	5.0607E-01	No
DOTAP/miR-122	**DOTAP**	**3.9153E+00**	**9.7819E-12**	**6.4218E-11**	**Yes**
DOTAP/miR-192	**DOTAP**	**3.0016E+00**	**1.4703E-09**	**2.4132E-09**	**Yes**
DOTAP/miR-193b	DOTAP	−1.0218E-01	2.7066E-01	2.5384E-01	No
DOTAP/miR-185	**DOTAP**	**3.6261E+00**	**9.7638E-11**	**2.5640E-10**	**Yes**
DOTAP/miR-195	**DOTAP**	**3.7437E+00**	**2.0622E-10**	**4.5127E-10**	**Yes**
DOTAP/miR-455	**DOTAP**	**4.2105E+00**	**8.4335E-12**	**6.4218E-11**	**Yes**
DOTAP/miR-375	**DOTAP**	**3.8933E+00**	**5.2785E-11**	**1.7327E-10**	**Yes**
DOTAP/miR-129	**DOTAP**	**3.8765E+00**	**2.1802E-11**	**9.5421E-11**	**Yes**
DOTAP_RNA41	DOTAP	2.0586E-02	8.4795E-01	5.0607E-01	No
miR-455	DOTAP	−1.6476E-01	1.2326E-01	1.6184E-01	No
miR-122	K-	−4.3292E-02	7.0370E-01	5.0607E-01	No
miR-192	K-	−1.0950E-01	3.1443E-01	2.7523E-01	No
miR-193b	K-	−2.9184E-02	8.0635E-01	5.0607E-01	No
miR-185	K-	−2.3014E-02	8.4403E-01	5.0607E-01	No
miR-195	K-	−1.7466E-01	1.8840E-01	2.0614E-01	No
miR-455	K-	−1.4118E-01	1.5360E-01	1.8335E-01	No
miR-375	K-	−9.4143E-02	3.3667E-01	2.7628E-01	No
miR-129	K-	−8.4734E-02	4.4671E-01	3.4502E-01	No
RNA41	K-	−1.0715E-01	2.6647E-01	2.5384E-01	No
TLR7-8	**DOTAP**	**3.3806E+00**	**3.3197E-10**	**6.2268E-10**	**Yes**
TLR3	**DOTAP**	**1.6381E+00**	**4.2134E-06**	**6.1470E-06**	**Yes**

Hedges' g correction with 5000 re-samplings and 95% confidence interval was used to predict the effect of miRNA stimulation. Stimulation results with FDR q-Value < 0.05 were considered as significant. DOTAP, DOTAP synthetic vesicles; DOTAP/miRNA, miRNA implicated with DOTAP synthetic vesicles; K-, samples with only blood cells; miR, investigated miRNA alone.

whole blood cells from participants with nT1D and HC. hsa-miR-122-5p, hsa-miR-192-5p, and hsa-miR-193b-5p had higher expression in nT1D, while hsa-miR-185-5p was overexpressed and hsa-miR-195-3p and hsa-miR-455-5p were under-expressed in 10yT1D participants compared to nT1D and HC. Additionally, we also included

TABLE 5B | Vesicle delivered miRNA effect on CD107a+ degranulation (paired mean difference analysis).

CD8+CD107a+	Control	Difference	*p*-Value paired_students_*t*-test	*q*-value	Discovery
K-	DOTAP	−1.0618E-01	2.9950E-01	1.9105E-01	No
DOTAP/miR-122	**DOTAP**	**1.5409E+00**	**1.4560E-05**	**2.5210E-05**	**Yes**
DOTAP/miR-192	**DOTAP**	**1.3375E+00**	**4.7945E-05**	**7.2636E-05**	**Yes**
DOTAP/miR-193b	DOTAP	9.6877E-03	9.5480E-01	5.3277E-01	No
DOTAP/miR-185	**DOTAP**	**1.6789E+00**	**5.2593E-06**	**1.4867E-05**	**Yes**
DOTAP/miR-195	**DOTAP**	**1.6455E+00**	**7.3601E-06**	**1.4867E-05**	**Yes**
DOTAP/miR-455	**DOTAP**	**1.9170E+00**	**2.2720E-06**	**9.1790E-06**	**Yes**
DOTAP/miR-375	**DOTAP**	**1.8501E+00**	**1.3130E-06**	**7.9570E-06**	**Yes**
DOTAP/miR-129	**DOTAP**	**2.4048E+00**	**1.7697E-09**	**2.1448E-08**	**Yes**
DOTAP_RNA41	DOTAP	−5.3420E-03	9.6707E-01	5.3277E-01	No
miR-455	DOTAP	−2.0158E-01	2.7230E-01	1.8335E-01	No
miR-122	K-	−2.1979E-01	8.4525E-02	6.4027E-02	No
miR-192	K-	−2.3455E-01	1.6733E-01	1.1930E-01	No
miR-193b	K-	−3.1049E-01	3.3047E-02	2.8610E-02	No
miR-185	K-	−4.0712E-01	2.5528E-02	2.3800E-02	No
miR-195	K-	−4.4367E-01	2.0979E-02	2.2280E-02	No
miR-455	K-	−8.9528E-02	4.6490E-01	2.8173E-01	No
miR-375	**K-**	**−4.3032E-01**	**2.9780E-04**	**3.6094E-04**	**Yes**
miR-129	K-	−2.8434E-01	8.4272E-02	6.4027E-02	No
RNA41	K-	−2.3236E-01	2.2060E-02	2.2280E-02	No
TLR7-8	**DOTAP**	**1.5650E+00**	**7.3086E-06**	**1.4867E-05**	**Yes**
TLR3	**DOTAP**	**9.4161E-01**	**8.9379E-05**	**1.2036E-04**	**Yes**
CD56+CD107a+	**Control**	**Difference**	***p*-Value paired_students_*t*-test**	***q*-Value**	**Discovery**
K-	DOTAP	−1.3256E-02	9.0796E-01	5.7902E-01	No
DOTAP/miR-122	**DOTAP**	**1.8273E+00**	**2.4102E-06**	**4.5210E-06**	**Yes**
DOTAP/miR-192	**DOTAP**	**1.6059E+00**	**9.7302E-06**	**1.5970E-05**	**Yes**
DOTAP/miR-193b	DOTAP	−1.4613E-02	9.0412E-01	5.7902E-01	No
DOTAP/miR-185	**DOTAP**	**2.1148E+00**	**3.7265E-07**	**8.1548E-07**	**Yes**
DOTAP/miR-195	**DOTAP**	**2.3678E+00**	**5.7913E-08**	**1.5208E-07**	**Yes**
DOTAP/miR-455	**DOTAP**	**2.5599E+00**	**3.8286E-08**	**1.2567E-07**	**Yes**
DOTAP/miR-375	**DOTAP**	**2.5780E+00**	**5.9181E-09**	**2.5901E-08**	**Yes**
DOTAP/miR-129	**DOTAP**	**2.4245E+00**	**5.4724E-09**	**2.5901E-08**	**Yes**
DOTAP_RNA41	DOTAP	2.0922E-01	2.0392E-01	2.4340E-01	No
miR-455	DOTAP	−6.3502E-03	9.7018E-01	5.7902E-01	No
miR-122	K-	1.5036E-01	5.4555E-01	4.7754E-01	No
miR-192	K-	1.1245E-01	7.0847E-01	5.7902E-01	No
miR-193b	K-	1.7812E-01	5.0498E-01	4.7360E-01	No
miR-185	K-	−1.5432E-02	9.5770E-01	5.7902E-01	No
miR-195	K-	2.3277E-01	3.8008E-01	3.8388E-01	No
miR-455	K-	6.2975E-03	9.6463E-01	5.7902E-01	No
miR-375	K-	−1.5547E-02	9.4458E-01	5.7902E-01	No
miR-129	K-	3.4333E-01	3.0670E-01	3.3558E-01	No
RNA41	K-	3.5283E-01	2.0151E-01	2.4340E-01	No
TLR7-8	**DOTAP**	**2.7014E+00**	**1.9012E-09**	**2.4963E-08**	**Yes**
TLR3	**DOTAP**	**9.2900E-01**	**4.3701E-04**	**6.3755E-04**	**Yes**

Hedges' g correction was used with 5000 re-samplings and 95% confidence interval to predict the effect of miRNA stimulation. Stimulation results with FDR q-Value < 0.05 were considered as significant. DOTAP, DOTAP synthetic vesicles; DOTAP/miRNA, miRNA implicated with DOTAP synthetic vesicles; K-, samples with only blood cells; miR, investigated miRNA alone.

hsa-miR-375-3p and hsa-miR-129-5p, which were the most significantly differentially expressed EVs miRNAs in the TX patients. These *in vitro* results were obtained on the complex whole blood samples with preserved immune cells sub-populations and immune system interactions in T1D-affected participants that represent a more reliable model

TABLE 6A | New-onset T1D vs. healthy controls EVs-miRNA *in vitro* CD69+ T-cell activation (unpaired mean difference analysis).

CD4+CD69+	Control	Test	Difference	*p*-Value mann_whitney	*q*-Value	Discovery?
0	K-_HC	K-_nT1D	−0.44444	0.2712	0.2106	No
1	DOTAP_HC	DOTAP_nT1D	−0.59812	0.1397	0.1454	No
2	**DOTAP/miR-122_HC**	**DOTAP/miR-122_nT1D**	**−1.04901**	**0.0190**	**0.0530**	**Yes**
3	DOTAP/miR-192_HC	DOTAP/miR-192_nT1D	−0.68356	0.2123	0.1751	No
4	DOTAP/miR-193b_HC	DOTAP/miR-193b_nT1D	−0.49906	0.3631	0.2663	No
5	**DOTAP/miR-185_HC**	**DOTAP/miR-185_nT1D**	**−0.85531**	**0.0587**	**0.0968**	**Yes**
6	DOTAP/miR-195_HC	DOTAP/miR-195_nT1D	−0.7087	0.1405	0.1454	No
7	**DOTAP/miR-455_HC**	**DOTAP/miR-455_nT1D**	**−1.02069**	**0.0257**	**0.0530**	**Yes**
8	**DOTAP/miR-375_HC**	**DOTAP/miR-375_nT1D**	**−1.08936**	**0.0257**	**0.0530**	**Yes**
9	**DOTAP/miR-129_HC**	**DOTAP/miR-129_nT1D**	**−1.32454**	**0.0091**	**0.0530**	**Yes**
10	**DOTAP_RNA41_HC**	**DOTAP_RNA41_nT1D**	**−1.15444**	**0.0021**	**0.0272**	**Yes**
11	**miR-122_HC**	**miR-122_nT1D**	**−1.24898**	**0.0222**	**0.0530**	**Yes**
12	miR-192_HC	miR-192_nT1D	−0.77725	0.1690	0.1593	No
13	miR-193b_HC	miR-193b_nT1D	−0.85842	0.1992	0.1751	No
14	**miR-185_HC**	**miR-185_nT1D**	**−1.23485**	**0.0281**	**0.0530**	**Yes**
15	**miR-195_HC**	**miR-195_nT1D**	**−1.01682**	**0.0660**	**0.0968**	**Yes**
16	miR-455_HC	miR-455_nT1D	−0.76955	0.1297	0.1454	No
17	miR-375_HC	miR-375_nT1D	−0.63762	0.5219	0.3626	No
18	miR-129_HC	miR-129_nT1D	−0.75303	0.1432	0.1454	No
CD8+CD69+	**Control**	**Test**	**Difference**	***p*-Value mann_whitney**	***q*-Value**	**Discovery?**
0	K-_HC	K-_nT1D	0.111526	0.3073	0.7285	No
1	DOTAP_HC	DOTAP_nT1D	−0.13007	0.4043	0.7285	No
2	DOTAP/miR-122_HC	DOTAP/miR-122_nT1D	−0.45179	0.2565	0.7285	No
3	DOTAP/miR-192_HC	DOTAP/miR-192_nT1D	−0.25269	0.3447	0.7285	No
4	DOTAP/miR-193b_HC	DOTAP/miR-193b_nT1D	−0.24695	0.7332	0.9013	No
5	DOTAP/miR-185_HC	DOTAP/miR-185_nT1D	−0.33599	0.4274	0.7285	No
6	DOTAP/miR-195_HC	DOTAP/miR-195_nT1D	−0.4013	0.4274	0.7285	No
7	DOTAP/miR-455_HC	DOTAP/miR-455_nT1D	−0.30755	0.3847	0.7285	No
8	DOTAP/miR-375_HC	DOTAP/miR-375_nT1D	−0.61642	0.1859	0.7285	No
9	DOTAP/miR-129_HC	DOTAP/miR-129_nT1D	−0.65536	0.1212	0.7285	No
10	DOTAP_RNA41_HC	DOTAP_RNA41_nT1D	−0.41737	0.4490	0.7285	No
11	miR-122_HC	miR-122_nT1D	−0.60098	0.3591	0.7285	No
12	miR-192_HC	miR-192_nT1D	−0.47615	0.7837	0.9100	No
13	miR-193b_HC	miR-193b_nT1D	−0.54299	0.9264	1.0000	No
14	miR-185_HC	miR-185_nT1D	−0.59773	0.5228	0.7285	No
15	miR-195_HC	miR-195_nT1D	−0.6915	0.3153	0.7285	No
16	miR-455_HC	miR-455_nT1D	−0.08925	0.5199	0.7285	No
17	miR-375_HC	miR-375_nT1D	−0.49366	0.4642	0.7285	No
18	miR-129_HC	miR-129_nT1D	−0.57465	0.6466	0.8446	No

Hedges' g correction was used with 5000 re-samplings and 95% confidence interval to predict the effect of miRNA stimulation. Stimulation results with FDR q-Value < 0.1 were considered as significant. DOTAP, DOTAP synthetic vesicles; DOTAP/miRNA, miRNA implicated with DOTAP synthetic vesicles; K-, samples with only blood cells; miR, investigated miRNA alone; HC, healthy controls; nT1D, new onset type 1 diabetes participants.

compared to the one-dimensional experiments on homogenous cell cultures or model organisms with differences in the immune signaling (Brehm et al., 2012). The results of this functional miRNA study revealed significantly increased NK and T-cell early transition proliferation and cytotoxicity when cells were exposed to diabetes-associated EVs miRNAs in vesicular form, but not bare miRNAs alone (**Figure 3**). Furthermore, nT1D participants presented considerably lower CD69+ CD4+ activation response compared to HC, indicating the potential effect of the immune exhaustion and tolerance (Yi et al., 2010; Frenz et al., 2016) as the result of previous exposure to miRNAs involved in the development of T1D autoimmunity and beta-cell destruction. The vesicle delivered miRNA also resulted in the increased release of IFN-alpha, IFN-gamma, TNF-alpha, IL-1beta, IL-6 IL-10, and MCP-1 (**Figure 8A**), which indicates TLR7/8 associated cytokine/chemokine release (Gantier et al., 2008; Salvi et al., 2018; Pluta et al., 2019). The same

TABLE 6B | New-onset T1D vs. healthy controls EVs-miRNA *in vitro* CD107a+ degranulation (unpaired mean difference analysis results).

CD8+CD107a+	Control	Test	Difference	*P*-value mann_whitney	*q*-Value	Discovery?
0	K-_HC	K-_nT1D	0.973031	0.0409	0.4279	No
1	DOTAP_HC	DOTAP_nT1D	1.066027	0.0169	0.3537	No
2	DOTAP/miR-122_HC	DOTAP/miR-122_nT1D	0.230197	0.8500	1.0000	No
3	DOTAP/miR-192_HC	DOTAP/miR-192_nT1D	0.249794	0.7052	1.0000	No
4	DOTAP/miR-193b_HC	DOTAP/miR-193b_nT1D	0.952713	0.0692	0.4823	No
5	DOTAP/miR-185_HC	DOTAP/miR-185_nT1D	0.152561	0.4270	1.0000	No
6	DOTAP/miR-195_HC	DOTAP/miR-195_nT1D	0.259727	0.6229	1.0000	No
7	DOTAP/miR-455_HC	DOTAP/miR-455_nT1D	0.098524	0.9698	1.0000	No
8	DOTAP/miR-375_HC	DOTAP/miR-375_nT1D	0.267454	0.5966	1.0000	No
9	DOTAP/miR-129_HC	DOTAP/miR-129_nT1D	0.06552	0.6225	1.0000	No
10	DOTAP_RNA41_HC	DOTAP_RNA41_nT1D	0.486602	0.3442	1.0000	No
11	miR-122_HC	miR-122_nT1D	0.528305	0.6458	1.0000	No
12	miR-192_HC	miR-192_nT1D	0.490841	1.0000	1.0000	No
13	miR-193b_HC	miR-193b_nT1D	0.479991	0.7827	1.0000	No
14	miR-185_HC	miR-185_nT1D	0.431101	0.6466	1.0000	No
15	miR-195_HC	miR-195_nT1D	0.268122	0.9269	1.0000	No
16	miR-455_HC	miR-455_nT1D	0.716379	0.1109	0.5796	No
17	miR-375_HC	miR-375_nT1D	0.650574	0.2678	1.0000	No
18	miR-129_HC	miR-129_nT1D	0.476454	0.5209	1.0000	No
CD56+CD107a+	**Control**	**Test**	**Difference**	***P*-value mann_whitney**	***q*-Value**	**Discovery?**
0	K-_HC	K-_nT1D	0.569524	0.4956	0.9525	No
1	DOTAP_HC	DOTAP_nT1D	0.343142	0.5447	0.9525	No
2	DOTAP/miR-122_HC	DOTAP/miR-122_nT1D	0.19403	0.7623	0.9525	No
3	DOTAP/miR-192_HC	DOTAP/miR-192_nT1D	0.431914	0.5708	0.9525	No
4	DOTAP/miR-193b_HC	DOTAP/miR-193b_nT1D	0.623708	0.5964	0.9525	No
5	DOTAP/miR-185_HC	DOTAP/miR-185_nT1D	0.263588	0.7054	0.9525	No
6	DOTAP/miR-195_HC	DOTAP/miR-195_nT1D	0.537545	0.3073	0.9525	No
7	DOTAP/miR-455_HC	DOTAP/miR-455_nT1D	0.128074	0.9698	1.0000	No
8	DOTAP/miR-375_HC	DOTAP/miR-375_nT1D	0.272265	0.6230	0.9525	No
9	DOTAP/miR-129_HC	DOTAP/miR-129_nT1D	0.276433	0.7623	0.9525	No
10	DOTAP_RNA41_HC	DOTAP_RNA41_nT1D	0.275529	0.8203	0.9525	No
11	miR-122_HC	miR-122_nT1D	−0.30146	0.5200	0.9525	No
12	miR-192_HC	miR-192_nT1D	−0.508	0.2343	0.9525	No
13	miR-193b_HC	miR-193b_nT1D	−0.69441	0.5219	0.9525	No
14	miR-185_HC	miR-185_nT1D	−0.86097	0.2353	0.9525	No
15	miR-195_HC	miR-195_nT1D	−0.32652	0.5228	0.9525	No
16	miR-455_HC	miR-455_nT1D	0.273825	0.7907	0.9525	No
17	miR-375_HC	miR-375_nT1D	−0.6002	0.1709	0.9525	No
18	miR-129_HC	miR-129_nT1D	−1.23716	0.0828	0.9525	No

Hedges' g correction with 5000 re-samplings and 95% confidence interval was used to predict the effect of miRNA stimulation. Stimulation results with FDR q-Value < 0.1 were considered as significant. DOTAP, DOTAP synthetic vesicles; DOTAP/miRNA, miRNA implicated with DOTAP synthetic vesicles; K-, samples with only blood cells, miR, investigated miRNA alone; HC, healthy controls; nT1D, new onset type 1 diabetes participants.

cytokines/chemokines are reported as increased in the individuals with T1D autoimmunity (Fatima et al., 2016; Waugh et al., 2017).

This difference in the *in vitro* stimulation indicated the potential role of EVs' delivered miRNAs in the regulation of the immune system in T1D-related to beta-cell damage (**Figure 4A**). *In vitro* miRNA tests were performed with approximately ten-times higher miRNA concertations compared to the plasma EVs-RNA concentrations estimated from the total isolated amount of blood plasma EVs RNA (**Supplementary Figure S7**). However, EVs with miRNAs released in affected tissues with prolonged exposure to stress factors might be sufficient to activate the immune system and to drive autoimmunity. The vesicles accumulated in phagocytes (monocytes and granulocytes) (**Figures 5B–D**) where TLR7/8 are expressed and participate in the ssRNA immune activation in the anti-viral innate immunity (Aharon et al., 2008; Cros et al., 2010; Lester and Li, 2014). The

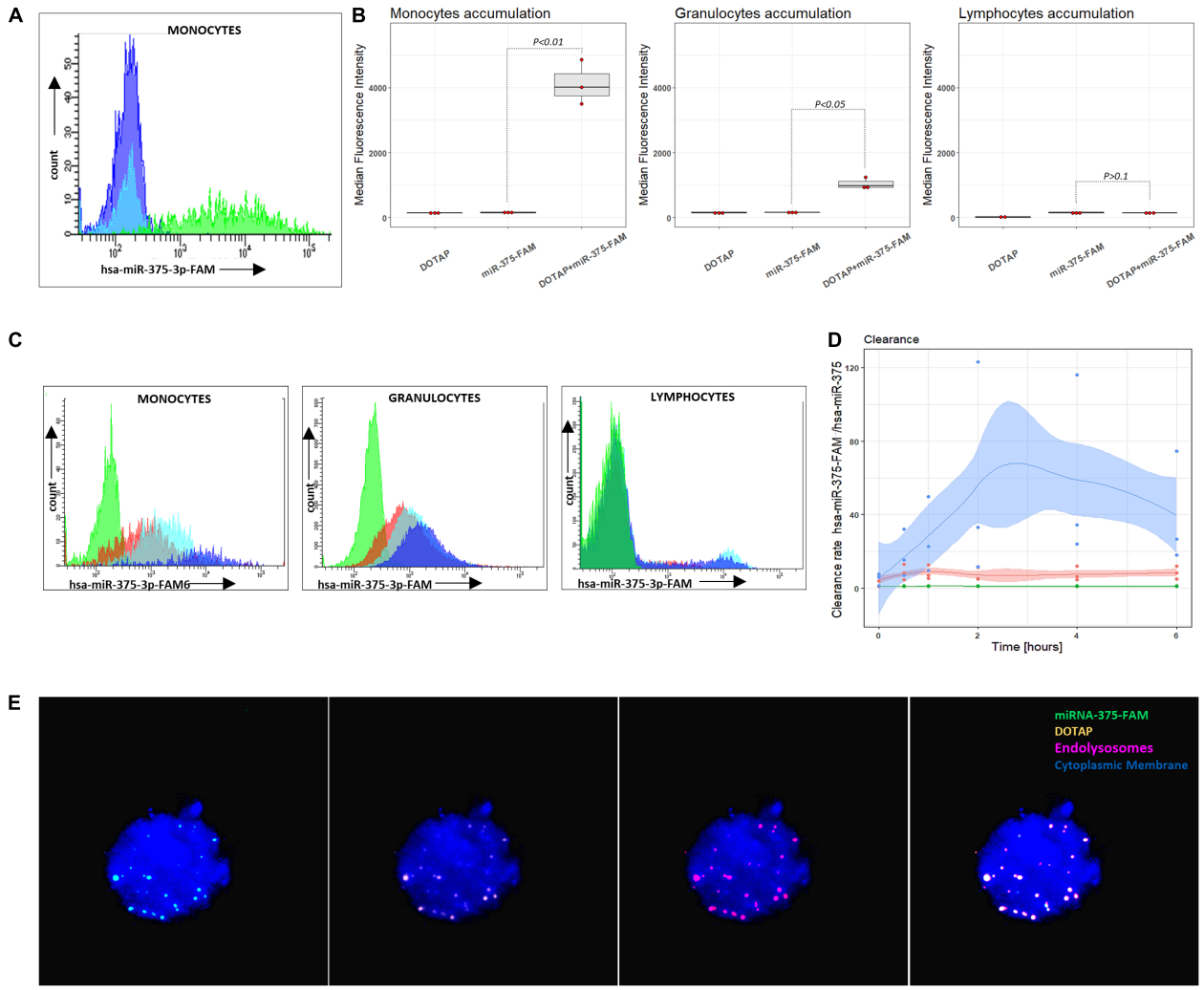

FIGURE 5 | Vesicle internalization and intracellular aggregation. **(A)** Representative results of flow cytometry DOTAP, hsa-miRNA-375-FAM (3'FAM labeled miRNA) and DOTAP/hsa-miRNA-375-FAM transfection in the whole blood samples, detecting miRNA-FAM in monocytes, granulocytes, lymphocytes after [the observed effects were assessed 4h after the stimulation; dark blue: DOTAP, light blue: hsa-miRNA-375-FAM, green peak: DOTAP/hsa-miRNA-375-FAM]. **(B)** Monocytes, granulocytes and lymphocytes median fluorescence intensity regarding the transfected DOTAP, fluorescent-labeled hsa-miRNA-375-FAM and DOTAP/hsa-miRNA-375-FAM [*P*-values represent a paired Hedges' g mean difference between hsa-miRNA-375-FAM and DOTAP/hsa-miRNA-375-FAM: $P < 0.05$ significant difference, $N = 3$]. **(C)** Representative results of flow cytometry increasing monocytes, granulocytes, lymphocytes fluorescence with the time of blood cells exposed to DOTAP formed vesicles with FAM fluorescent-labeled miRNA [green peak: non-labeled hsa-miR-375-3p, 5 min; red color:hsa-miR-375-3p-FAM, 5min; light blue: hsa-miR-375-3p-FAM, 2 h; dark blue: hsa-miR-375-3p-FAM, 6 h]. **(D)** Monocytes, granulocytes and lymphocytes relative mean fluorescence ratio of DOTAP/hsa-miR-375-3p-FAM with DOTAP/hsa-miR-375-3p within 6 h from the beginning of the transfection (DOTAP/hsa-miR-375-FAM / DOTAP/hsa-miR-375) (solid lines: average value, shaded areas: standard deviation; $N = 3$). **(E)** Fluorescent microscopy image of DOTAP/miRNA-375-3p-FAM up-taken vesicles (green) with DOTAP vesicles (orange), located in endolysosomes and lysosomes (red); cytoplasmic membrane (blue).

TLR7/8 innate immunity activation is not T1D specific, but is probably involved in the immune system modulation and autoimmunity (Salvi et al., 2018; Pluta et al., 2019). This is in line with the ssRNA-structure dependent TLR7/8 activation (Gantier et al., 2008), with the accessible uridines in the loop and prime ends of the sequence (**Figure 6**). Additionally, the vesicle miRNAs activation of the TLR7/8 pathway was specified with the utilization of CQ, which inhibited vesicle miRNA immunomodulation and showed strong evidence of TLR7/8 pathway activation (**Figure 7**). However, additional possible direct effects of EVs miRNA content on T-cells (Zhang et al., 2006; Wang et al., 2008) or direct miRNA-mRNA regulation effects were not excluded.

In light of the reported results, we proposed a novel role of EVs' miRNAs in the etiology of T1D, suggesting the immune response modulation via the TLR7/8 activation and EVs miRNAs involvement into inflammation and autoimmunity. Beta-cells-released EVs carrying miRNAs could enter the surrounding tissues where EVs are internalized and accumulated in phagocytes, where they trigger endosomal TLR7/8 mediated

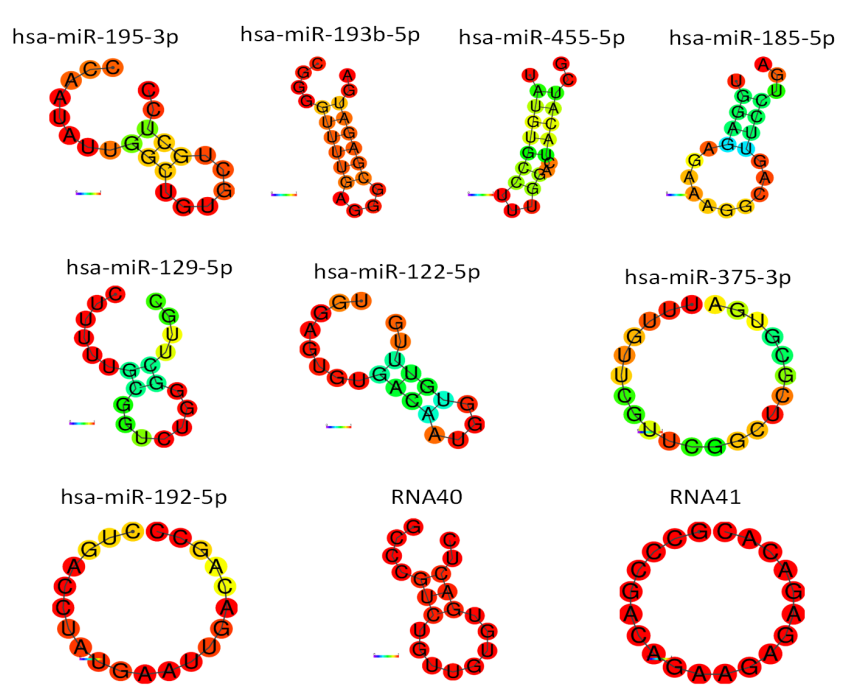

RNAfold web server	The free energy of the thermodynamic ensemble
>hsa-miR-193b-5p MIMAT0004767 CGGGGUUUUGAGGGCGAGAUGA	-2.13 kcal/mol
>hsa-miR-455-5p MIMAT0003150 UAUGUGCCUUUGGACUACAUCG	-1.63 kcal/mol
>hsa-miR-122-5p MIMAT0000421 UGGAGUGUGACAAUGGUGUUUG	-0.96 kcal/mol
>hsa-miR-375-3p MIMAT0000728 UUUGUUCGUUCGGCUCGCGUGA	-0.91 kcal/mol
>hsa-miR-192-5p MIMAT0000222 CUGACCUAUGAAUUGACAGCC	-0.17 kcal/mol
>hsa-miR-129-5p MIMAT0000242 CUUUUUGCGGUCUGGGCUUGC	-1.46 kcal/mol
>hsa-miR-195-3p MIMAT0004615 CCAAUAUUGGCUGUGCUGCUCC	-2.45 kcal/mol
>hsa-miR-185-5p MIMAT0000455 UGGAGAGAAAGGCAGUUCCUGA	-1.94 kcal/mol
>RNA40 GCCCGUCUGUUGUGUGACUC	-2.62 kcal/mol
>RNA41 GCCCGACAGAAGAGAGACAC	-0.00 kcal/mol

FIGURE 6 | miRNA structure prediction with thermodynamics parameters. RNAfold structure prediction of studied miRNA. Red-colored nucleotides in the predicted structure represent a high probability of nucleotide in predicted structure, blue-colored nucleotides low probability. The table shows the thermodynamic data results of the RNAfold server tool for predicted miRNA structures.

response. This in turn led to the release of cytokines in the antigen-independent manner and the activation of other sub-populations of the innate and adaptive immune system, resulting in the increased cell activation, proliferation, cytotoxicity, inflammation and cytokine release (Mohammad Hosseini et al., 2015; Farrugia and Baron, 2017; Salvi et al., 2018). EVs released by other cells can enhance the immune response and contribute to the development of autoimmunity during the inflammation stress and metabolic imbalance (Robbins et al., 2016). The prolonged exposure to EVs miRNA could result in the immune system exhaustion and lower immune activation response to vesicle derived miRNA in nT1D. Immune exhaustion with higher CD8+ T-cell activation compared to CD4+ T-cells could represent the specific autoimmune phenotype (Morawski and Bolland, 2018) which promotes the autoimmune beta-cell destruction and overt T1D (**Figure 8B**).

One of the most common mechanisms proposed in autoimmunity is an innate immune cell hyper-activation, such as dendritic cells (DC), that can overstimulate T lymphocytes (Di Marco et al., 2018). TLR7/8 activation in DC triggers the release of pro-inflammatory cytokines (Morse and Horwitz, 2017; Salvi et al., 2018) and immune cells intercellular interactions, resulting in expanded T-cell-clones and auto-immune risk phenotype, in both mice and humans (Ara et al., 2018; Morawski and Bolland, 2018). The TLR7/8 activation of the downstream immune system and auto-immune risk phenotype contributes to beta-cell destruction, promotes diabetes development, and causes T-cell exhaustion (Lee et al., 2011). Our results are in line with the published miRNA TLR7/8 immunomodulation (Salvi et al., 2018; Pluta et al., 2019), however, we could not link them directly to any specific stage of the T1D development.

TLR7/8 receptors are part of anti-viral innate immunity and can be involved in numerous viral infections as triggering factors associated with T1D (Katsarou et al., 2017; Paschou et al., 2017). Viral infections can also impair and promote cell stress EVs release (Deschamps and Kalamvoki, 2018), impaired EVs cargo loading (de Jong et al., 2012), and contribute to the dysregulation of the immune system, breakdown of self-tolerance, and potential development of autoimmunity (Cianciaruso et al., 2017). Here we showed that differentially expressed human miRNAs in the blood of people with T1D packed into vesicles mimic the action of pathogen ssRNA recognized by TLR7/8. The activation was potentially triggered through the principle of molecular/viral mimicry with pathogenic viral ssRNAs. Additionally, as the immune system is activated in an antigen-independent manner, it also supports the EVs miRNA-induced bystander immune activation and autoimmunity (Pacheco et al., 2019).

The effect of the circulating EVs' miRNAs on blood immune cells in our study indicated the systemic immune response. However, it is reported that ssRNA molecules can promote the monocyte activation and differentiation into tissue macrophages (Krutzik et al., 2005; Saha et al., 2017), which can infiltrate into the affected target tissues (Eng et al., 2018), resulting in an enhanced local immune response. Moreover, Langerhans islets contain resident macrophages that hold an essential role in the local islet immunity, development of acute insulitis, and

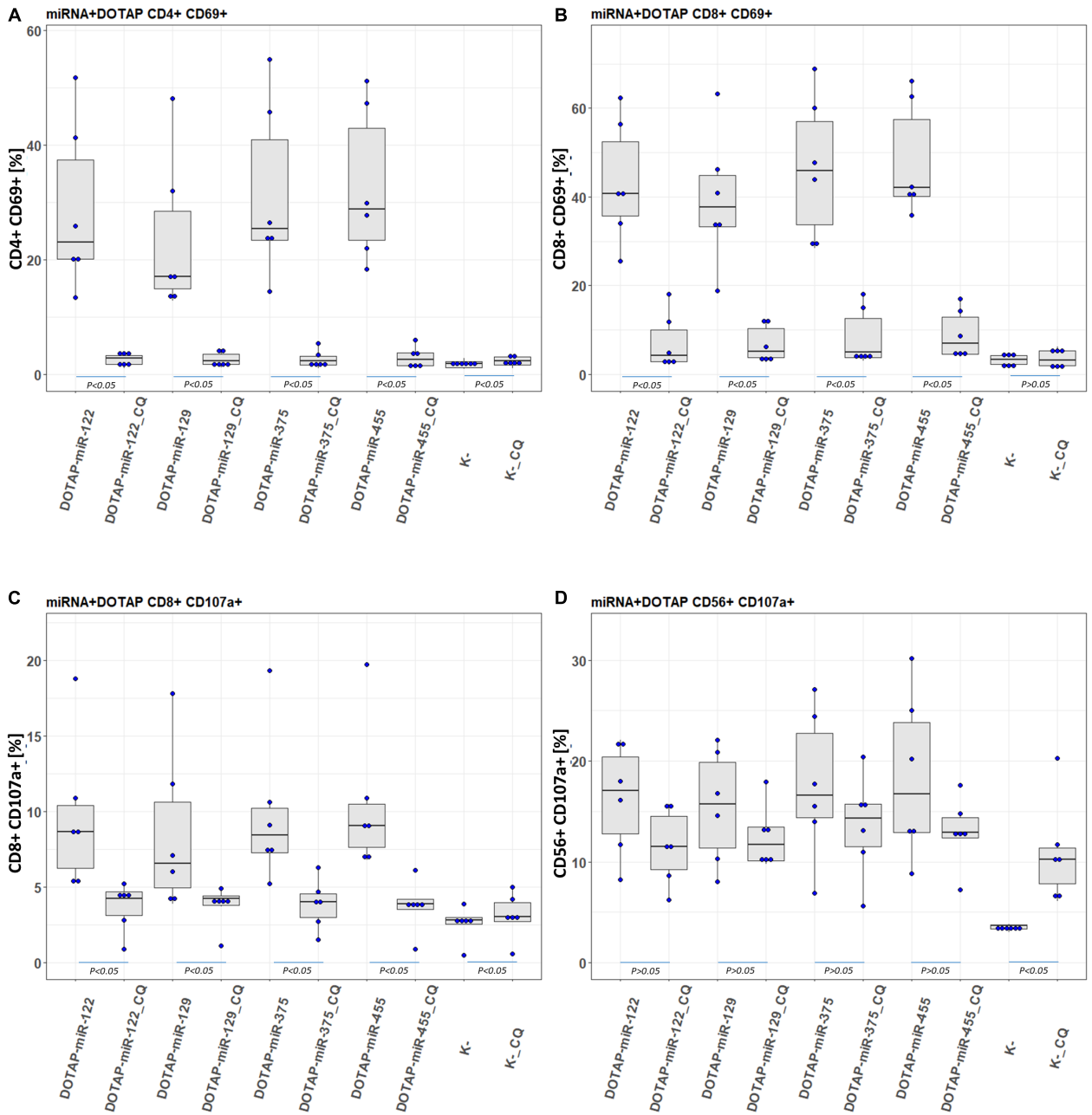

FIGURE 7 | Chloroquine miRNA/DOTAP inhibition. Chloroquine (CQ) inhibition of hsa-miR-122-5p, hsa-miR-455-5p, hsa-miR-375-3p, hsa-miR-129-5p DOTAP vesicle stimulation effect on expression of early transition activation marker (CD69) on panels **(A)** CD4+ and **(B)** CD8+ T-cells and degranulation marker (CD107a) on panels **(C)** CD8+ T-cells and **(D)** CD56+ NK cells after 21h stimulation [box plot: Q1, median, Q3; whisker lines: 1.5 IQR; *N* = 6; K- negative control, *P*-values under blue lines represent a paired Hedges' g mean difference analysis significance: $P < 0.05$ significant difference].

autoimmunity (Carrero et al., 2016, 2017). EVs ssRNA TLR7/8 activation also leads to impaired monocyte differentiation into DC (Assier et al., 2007), DC modulation, T-reactive clone selection, and Treg/Teff equilibrium modulation (Wang et al., 2008; Anz et al., 2010; Dominguez-Villar et al., 2015). Our *in vitro* miRNAs stimulation results indicated a substantial EVs miRNAs' immunoregulatory effect on the systemic innate and adaptive immunity as well as their possible involvement on a local tissue level in the development and progression of autoimmunity and beta-cell loss in T1D.

Collectively, our study provided data describing the importance of a complex involvement of EVs-derived human miRNAs in the regulation of the immune system, and potentially in the development of T1D autoimmunity, with the implications for developing strategies for the prevention and treatment of T1D-related immune processes.

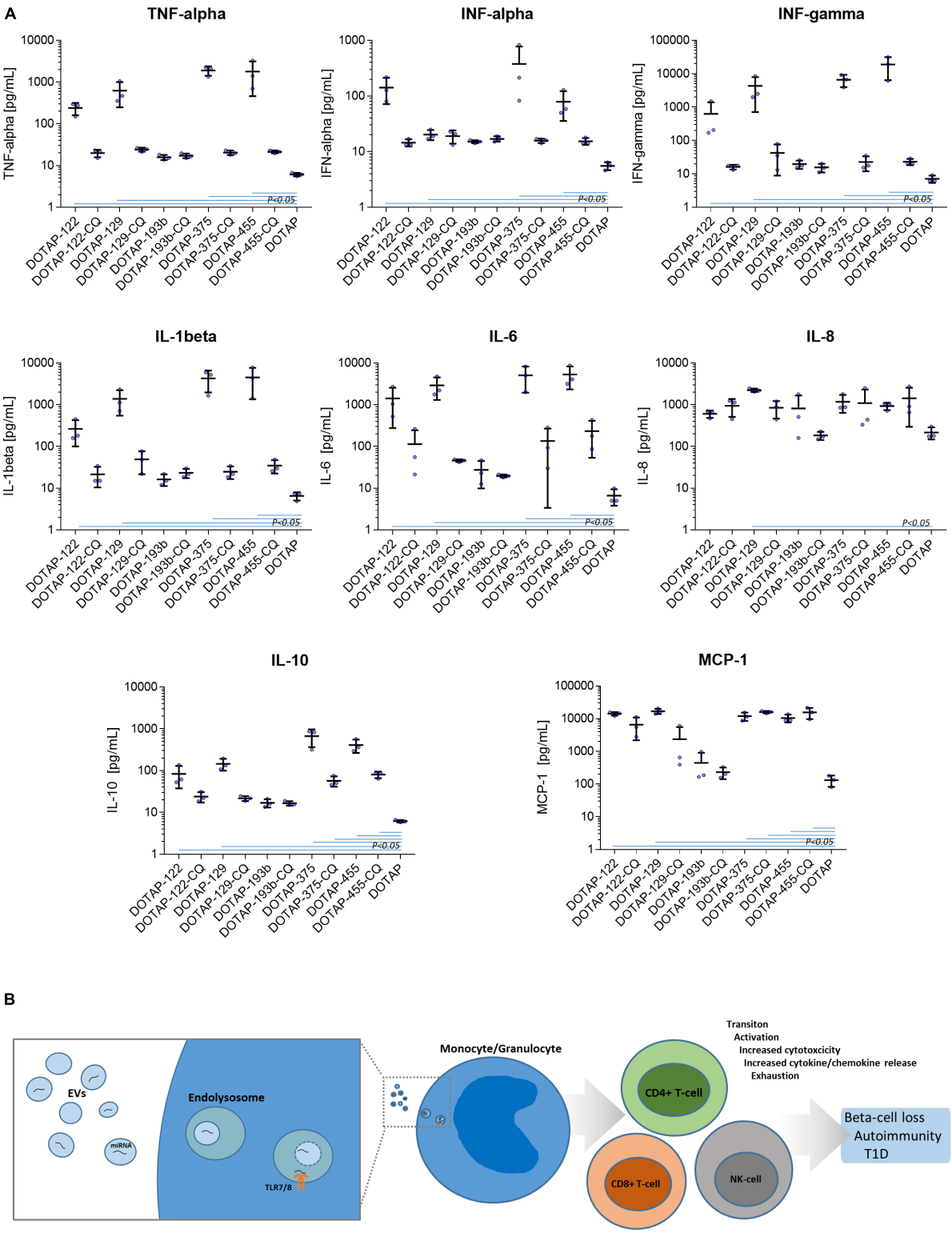

FIGURE 8 | (A) Cytokine/chemokine release response as a result of DOTAP/miRNA transfection. Blue lines in graphs show Kruskal-Wallis ANOVA test *P*-values < 0.05 significant difference of DOTAP/miRNA compared to DOTAP negative control blue dots: cytokine/chemokine assessed levels; mean, error bars SD [$N = 3$]. **(B)** The proposed model of EVs derived miRNAs immune system modulation in type 1 diabetes via TLR7/8. EVs miRNAs immune system activation via TLR7/8 increases proliferation and cytotoxicity of the immune system of effector cells, cytokine/chemokine release and immune system exhaustion, dysregulation, and autoimmunity.

DATA AVAILABILITY STATEMENT

The datasets GENERATED for this study can be found in NCBI http://www.ncbi.nlm.nih.gov/bioproject/591780.

ETHICS STATEMENT

The study protocol was approved by the Republic of Slovenia National Medical Ethics Committee (No. 29/02/2013 and 31/04/2016), and principles of the Declaration of Helsinki were followed. Written informed consent was obtained from the participants or participants' parents prior to the study.

AUTHOR CONTRIBUTIONS

TT developed the hypothesis, designed the experimental approach, performed the experimental work, analyzed the data, coordinated the project, and wrote the manuscript. JK designed the experimental approach, developed the hypothesis, statistically analyzed the data, and wrote the manuscript. KP designed the experiments and performed the flow cytometry studies and analysis. SH performed the TEM sample preparation and imaging. KD and NB provided the diabetes and healthy control samples. KTP and MD read the manuscript and provided the feedback. PV contributed to TEM experimental approach, data interpretation, and characterization. LP and EB designed the experimental approach, provided and prepared the Langerhans islet medium and Langerhans islets transplantation patients' plasma samples. AI discussed the hypothesis, flow cytometry study design, interpreted flow cytometry data, and wrote the manuscript. TB conceived the hypothesis, led the project, coordinated the project, and wrote the manuscript. All authors reviewed and approved the final manuscript.

FUNDING

This work was supported by the Slovenian Research Agency under grant P3-0343, P3-0108, and the University Medical Centre Ljubljana grant 20160161. Human islets were provided by the San Raffaele Diabetes Research Institute, IRCCS Ospedale San Raffaele (Milan), within the European islet distribution program for basic research supported by JDRF (2-RSC-2019-724-I-X). This project received funding from the Innovative Medicines Initiative 2 Joint Undertaking under grant agreement 115797 (INNODIA). This Joint Undertaking receives support from the Union's Horizon 2020 Research and Innovation Programme and the European Federation of Pharmaceutical Industries and Associations, JDRF, and The Leona M. and Harry B. Helmsley Charitable Trust.

ACKNOWLEDGMENTS

We thank prof. Michael Hackenberg and sRNA developer team for their technical support with sRNAtoolBox data analysis. We also thank T1D participants and their families, healthy control participants, Brigita Mali, and nursing team of the University Children's Hospital, Department of Pediatric Endocrinology, Diabetes and Metabolic Diseases.

SUPPLEMENTARY MATERIAL

The Supplementary Material for this article can be found online at: https://www.frontiersin.org/articles/10.3389/fcell.2020.00202/full#supplementary-material

REFERENCES

Aharon, A., Tamari, T., and Brenner, B. (2008). Monocyte-derived microparticles and exosomes induce procoagulant and apoptotic effects on endothelial cells. *Thromb. Haemost.* 100, 878–885. doi: 10.1160/th07-11-0691

Åkerman, L., Casas, R., Ludvigsson, J., Tavira, B., and Skoglund, C. (2018). Serum miRNA levels are related to glucose homeostasis and islet autoantibodies in children with high risk for type 1 diabetes. *PLoS One* 13:e0191067. doi: 10.1371/journal.pone.0191067

Anz, D., Koelzer, V. H., Moder, S., Thaler, R., Schwerd, T., Lahl, K., et al. (2010). Immunostimulatory RNA blocks suppression by regulatory T cells. *J. Immunol. Baltim.* 1950, 939–946. doi: 10.4049/jimmunol.0901245

Ara, A., Ahmed, K. A., and Xiang, J. (2018). Multiple effects of CD40–CD40L axis in immunity against infection and cancer. *Immun. Targets Ther.* 7, 55–61. doi: 10.2147/ITT.S163614

Armstrong, D., and Wildman, D. E. (2018). Extracellular vesicles and the promise of continuous liquid biopsies. *J. Pathol. Transl. Med.* 52, 1–8. doi: 10.4132/jptm.2017.05.21

Assier, E., Marin−Esteban, V., Haziot, A., Maggi, E., Charron, D., and Mooney, N. (2007). TLR7/8 agonists impair monocyte-derived dendritic cell differentiation and maturation. *J. Leukoc. Biol.* 81, 221–228. doi: 10.1189/jlb.0705385

Barajas, J. M., Reyes, R., Guerrero, M. J., Jacob, S. T., Motiwala, T., and Ghoshal, K. (2018). The role of miR-122 in the dysregulation of glucose-6-phosphate dehydrogenase (G6PD) expression in hepatocellular cancer. *Sci. Rep.* 8:9105. doi: 10.1038/s41598-018-27358-5

Battelino, T., Nimri, R., Dovc, K., Phillip, M., and Bratina, N. (2017). Prevention of hypoglycemia with predictive low glucose insulin suspension in children with type 1 diabetes: a randomized controlled trial. *Diabetes Care* 40, 764–770. doi: 10.2337/dc16-2584

Becker, A., Thakur, B. K., Weiss, J. M., Kim, H. S., Peinado, H., and Lyden, D. (2016). Extracellular vesicles in cancer: cell-to-cell mediators of metastasis. *Cancer Cell* 30, 836–848. doi: 10.1016/j.ccell.2016.10.009

Beignon, A.-S., McKenna, K., Skoberne, M., Manches, O., DaSilva, I., Kavanagh, D. G., et al. (2005). Endocytosis of HIV-1 activates plasmacytoid dendritic cells via Toll-like receptor– viral RNA interactions. *J. Clin. Invest.* 115, 3265–3275. doi: 10.1172/JCI26032

Belgardt, B.-F., Ahmed, K., Spranger, M., Latreille, M., Denzler, R., Kondratiuk, N., et al. (2015). The microRNA-200 family regulates pancreatic beta cell survival in type 2 diabetes. *Nat. Med.* 21, 619–627. doi: 10.1038/nm.3862

Benjamini, Y., Krieger, A. M., and Yekutieli, D. (2006). Adaptive linear step-up procedures that control the false discovery rate. *Biometrika* 93, 491–507. doi: 10.1093/biomet/93.3.491

Brehm, M. A., Powers, A. C., Shultz, L. D., and Greiner, D. L. (2012). Advancing animal models of human type 1 diabetes by engraftment of functional human tissues in immunodeficient mice. *Cold Spring Harb. Perspect. Med.* 2:a007757. doi: 10.1101/cshperspect.a007757

Carrero, J. A., Ferris, S. T., and Unanue, E. R. (2016). Macrophages and dendritic cells in islets of Langerhans in diabetic autoimmunity: a lesson on cell interactions in a mini-organ. *Curr. Opin. Immunol.* 43, 54–59. doi: 10.1016/j.coi.2016.09.004

Carrero, J. A., McCarthy, D. P., Ferris, S. T., Wan, X., Hu, H., Zinselmeyer, B. H., et al. (2017). Resident macrophages of pancreatic islets have a seminal role in the initiation of autoimmune diabetes of NOD mice. *Proc. Natl. Acad. Sci. U.S.A.* 114, E10418–E10427. doi: 10.1073/pnas.1713543114

Ceriello, A., and Kilpatrick, E. S. (2013). Glycemic variability: both sides of the story. *Diabetes Care* 36, S272–S275. doi: 10.2337/dcS13-2030

Christoffersson, G., Rodriguez-Calvo, T., and von Herrath, M. (2016). Recent advances in understanding type 1 diabetes. *F1000Res.* 5:F1000FacultyRev–110. doi: 10.12688/f1000research.7356.1

Cianciaruso, C., Phelps, E. A., Pasquier, M., Hamelin, R., Demurtas, D., Alibashe Ahmed, M., et al. (2017). Primary human and Rat β-cells release the intracellular autoantigens GAD65, IA-2, and proinsulin in exosomes together with cytokine-induced enhancers of immunity. *Diabetes* 66, 460–473. doi: 10.2337/db16-0671

Claridge-Chang, A., and Assam, P. N. (2016). Estimation statistics should replace significance testing. *Nat. Methods* 13, 108–109. doi: 10.1038/nmeth.3729

Cottrell, K. A., Szczesny, P., and Djuranovic, S. (2017). Translation efficiency is a determinant of the magnitude of miRNA-mediated repression. *Sci. Rep.* 7:14884. doi: 10.1038/s41598-017-13851-w

Cros, J., Cagnard, N., Woollard, K., Patey, N., Zhang, S.-Y., Senechal, B., et al. (2010). Human CD14dim Monocytes Patrol and Sense Nucleic Acids and Viruses via TLR7 and TLR8 Receptors. *Immunity* 33, 375–386. doi: 10.1016/j.immuni.2010.08.012

Cumming, G. (2014). The new statistics: why and how. *Psychol. Sci.* 25, 7–29. doi: 10.1177/0956797613504966

de Jong, O. G., Verhaar, M. C., Chen, Y., Vader, P., Gremmels, H., Posthuma, G., et al. (2012). Cellular stress conditions are reflected in the protein and RNA content of endothelial cell-derived exosomes. *J. Extracell. Vesicles* 1:18396. doi: 10.3402/jev.v1i0.18396

Deschamps, T., and Kalamvoki, M. (2018). Extracellular vesicles released by herpes simplex virus 1-infected cells block virus replication in recipient cells in a sting-dependent manner. *J. Virol.* 92:e01102-18. doi: 10.1128/JVI.01102-18

Di Marco, M., Ramassone, A., Pagotto, S., Anastasiadou, E., Veronese, A., and Visone, R. (2018). MicroRNAs in autoimmunity and hematological malignancies. *Int. J. Mol. Sci.* 19:3139. doi: 10.3390/ijms19103139

Djuranovic, S., Nahvi, A., and Green, R. (2012). miRNA-mediated gene silencing by translational repression followed by mRNA deadenylation and decay. *Science* 336, 237–240. doi: 10.1126/science.1215691

Dominguez-Villar, M., Gautron, A.-S., de Marcken, M., Keller, M. J., and Hafler, D. A. (2015). TLR7 induces anergy in human CD4+ T cells. *Nat. Immunol.* 16, 118–128. doi: 10.1038/ni.3036

Eng, H.-L., Hsu, Y.-Y., and Lin, T.-M. (2018). Differences in TLR7/8 activation between monocytes and macrophages. *Biochem. Biophys. Res. Commun.* 497, 319–325. doi: 10.1016/j.bbrc.2018.02.079

Erener, S., Marwaha, A., Tan, R., Panagiotopoulos, C., and Kieffer, T. J. (2017). Profiling of circulating microRNAs in children with recent onset of type 1 diabetes. *JCI Insight* 2:e89656. doi: 10.1172/jci.insight.89656

Farrugia, M., and Baron, B. (2017). The role of toll-like receptors in autoimmune diseases through failure of the self-recognition mechanism. *Int. J. Inflamm.* 2017:8391230. doi: 10.1155/2017/8391230

Fatima, N., Faisal, S. M., Zubair, S., Ajmal, M., Siddiqui, S. S., Moin, S., et al. (2016). Role of pro-inflammatory cytokines and biochemical markers in the pathogenesis of type 1 diabetes: correlation with age and glycemic condition in diabetic human subjects. *PLoS One* 11:e0161548. doi: 10.1371/journal.pone.0161548

Freeman, D. W., Hooten, N. N., Eitan, E., Green, J., Mode, N. A., Bodogai, M., et al. (2018). Altered extracellular vesicle concentration. Cargo, and Function in Diabetes. *Diabetes* 67, 2377–2388. doi: 10.2337/db17-1308

Frenz, T., Grabski, E., Buschjäger, D., Vaas, L. A. I, Burgdorf, N., Schmidt, R. E., et al. (2016). CD4+ T cells in patients with chronic inflammatory rheumatic disorders show distinct levels of exhaustion. *J. Allergy Clin. Immunol.* 138, 586.e10–589.e10. doi: 10.1016/j.jaci.2016.04.013

Gantier, M. P., Tong, S., Behlke, M. A., Xu, D., Phipps, S., Foster, P. S., et al. (2008). TLR7 is involved in sequence-specific sensing of single-stranded RNAs in human macrophages. *J. Immunol. Baltim.* 1950, 2117–2124.

Garcia-Contreras, M., Shah, S. H., Tamayo, A., Robbins, P. D., Golberg, R. B., Mendez, A. J., et al. (2017). Plasma-derived exosome characterization reveals a distinct microRNA signature in long duration Type 1 diabetes. *Sci. Rep.* 7:5998. doi: 10.1038/s41598-017-05787-y

Hasilo, C. P., Negi, S., Allaeys, I., Cloutier, N., Rutman, A. K., Gasparrini, M., et al. (2017). Presence of diabetes autoantigens in extracellular vesicles derived from human islets. *Sci. Rep.* 7:5000. doi: 10.1038/s41598-017-04977-y

Ho, J., Tumkaya, T., Aryal, S., Choi, H., and Claridge-Chang, A. (2019). Moving beyond P values: data analysis with estimation graphics. *Nat. Methods* 16:565. doi: 10.1038/s41592-019-0470-3

Hoshino, A., Costa-Silva, B., Shen, T.-L., Rodrigues, G., Hashimoto, A., Tesic Mark, M., et al. (2015). Tumour exosome integrins determine organotropic metastasis. *Nature* 527, 329–335. doi: 10.1038/nature15756

Hu, J., Xu, Y., Hao, J., Wang, S., Li, C., and Meng, S. (2012). MiR-122 in hepatic function and liver diseases. *Protein Cell* 3, 364–371. doi: 10.1007/s13238-012-2036-3

Hudoklin, S., Jezernik, K., Neumüller, J., Pavelka, M., and Romih, R. (2011). Urothelial plaque formation in post-Golgi compartments. *PLoS One* 6:e23636. doi: 10.1371/journal.pone.0023636

Hudoklin, S., Jezernik, K., Neumüller, J., Pavelka, M., and Romih, R. (2012). Electron tomography of fusiform vesicles and their organization in urothelial cells. *PLoS One* 7:e32935. doi: 10.1371/journal.pone.0032935

Kamerkar, S., LeBleu, V. S., Sugimoto, H., Yang, S., Ruivo, C. F., Melo, S. A., et al. (2017). Exosomes facilitate therapeutic targeting of oncogenic KRAS in pancreatic cancer. *Nature* 546, 498–503. doi: 10.1038/nature22341

Katsarou, A., Gudbjörnsdottir, S., Rawshani, A., Dabelea, D., Bonifacio, E., Anderson, B. J., et al. (2017). Type 1 diabetes mellitus. *Nat. Rev. Dis. Primer* 3:17016. doi: 10.1038/nrdp.2017.16

Kosaka, N., Iguchi, H., Hagiwara, K., Yoshioka, Y., Takeshita, F., and Ochiya, T. (2013). Neutral sphingomyelinase 2 (nSMase2)-dependent exosomal transfer of angiogenic microRNAs regulate cancer cell metastasis. *J. Biol. Chem.* 288, 10849–10859. doi: 10.1074/jbc.M112.446831

Krutzik, S. R., Tan, B., Li, H., Ochoa, M. T., Liu, P. T., Sharfstein, S. E., et al. (2005). TLR activation triggers the rapid differentiation of monocytes into macrophages and dendritic cells. *Nat. Med.* 11, 653–660. doi: 10.1038/nm1246

Kuznik, A., Bencina, M., Svajger, U., Jeras, M., Rozman, B., and Jerala, R. (2011). Mechanism of endosomal TLR inhibition by antimalarial drugs and imidazoquinolines. *J. Immunol. Baltim.* 1950, 4794–4804. doi: 10.4049/jimmunol.1000702

La Sala, L., Cattaneo, M., De Nigris, V., Pujadas, G., Testa, R., Bonfigli, A. R., et al. (2016). Oscillating glucose induces microRNA-185 and impairs an efficient antioxidant response in human endothelial cells. *Cardiovasc. Diabetol.* 15:71. doi: 10.1186/s12933-016-0390-9

LaPierre, M. P., and Stoffel, M. (2017). MicroRNAs as stress regulators in pancreatic beta cells and diabetes. *Mol. Metab.* 6, 1010–1023. doi: 10.1016/j.molmet.2017.06.020

Lee, A. S., Ghoreishi, M., Cheng, W. K., Chang, T.-Y. E., Zhang, Y. Q., and Dutz, J. P. (2011). Toll-like receptor 7 stimulation promotes autoimmune diabetes in the NOD mouse. *Diabetologia* 54, 1407–1416. doi: 10.1007/s00125-011-2083-y

Lester, S. N., and Li, K. (2014). Toll-like receptors in antiviral innate immunity. *J. Mol. Biol.* 426, 1246–1264. doi: 10.1016/j.jmb.2013.11.024

Lorenz, R., Bernhart, S. H., Höner zu Siederdissen, C., Tafer, H., Flamm, C., Stadler, P. F., et al. (2011). ViennaRNA Package 2.0. *Algorithms Mol. Biol.* 6:26. doi: 10.1186/1748-7188-6-26

Ludwig, A.-K., Miroschedji, K. D., Doeppner, T. R., Börger, V., Ruesing, J., Rebmann, V., et al. (2018). Precipitation with polyethylene glycol followed by washing and pelleting by ultracentrifugation enriches extracellular vesicles from tissue culture supernatants in small and large scales. *J. Extracell. Vesicles* 7:1528109. doi: 10.1080/20013078.2018.1528109

Marchand, L., Jalabert, A., Meugnier, E., Van den Hende, K., Fabien, N., Nicolino, M., et al. (2016). miRNA-375 a Sensor of glucotoxicity is altered in the serum of children with newly diagnosed type 1 diabetes. *J. Diabetes Res.* 2016:1869082. doi: 10.1155/2016/1869082

Martin, M. (2011). Cutadapt removes adapter sequences from high-throughput sequencing reads. *EMBnet.J.* 17, 10–12. doi: 10.14806/ej.17.1.200

Mohammad Hosseini, A., Majidi, J., Baradaran, B., and Yousefi, M. (2015). Toll-Like receptors in the pathogenesis of autoimmune diseases. *Adv. Pharm. Bull.* 5, 605–614. doi: 10.15171/apb.2015.082

Morawski, P. A., and Bolland, S. (2018). Strong selection of a few dominant CD8 clones in a TLR7-dependent autoimmune mouse model. *bioRxiv* [Preprint]. doi: 10.1101/393819

Morse, Z. J., and Horwitz, M. S. (2017). Innate viral receptor signaling determines type 1 diabetes onset. *Front. Endocrinol.* 8:249. doi: 10.3389/fendo.2017.00249

Pacheco, Y., Acosta-Ampudia, Y., Monsalve, D. M., Chang, C., Gershwin, M. E., and Anaya, J.-M. (2019). Bystander activation and autoimmunity. *J. Autoimmun.* 103:102301. doi: 10.1016/j.jaut.2019.06.012

Párrizas, M., Brugnara, L., Esteban, Y., González-Franquesa, A., Canivell, S., Murillo, S., et al. (2015). Circulating miR-192 and miR-193b are markers of prediabetes and are modulated by an exercise intervention. *J. Clin. Endocrinol. Metab.* 100, E407–E415. doi: 10.1210/jc.2014-2574

Paschou, S. A., Papadopoulou-Marketou, N., Chrousos, G. P., and Kanaka-Gantenbein, C. (2017). On type 1 diabetes mellitus pathogenesis. *Endocr. Connect.* 7, R38–R46. doi: 10.1530/EC-17-0347

Patterson, C. C., Harjutsalo, V., Rosenbauer, J., Neu, A., Cinek, O., Skrivarhaug, T., et al. (2019). Trends and cyclical variation in the incidence of childhood type 1 diabetes in 26 European centres in the 25 year period 1989-2013: a multicentre prospective registration study. *Diabetologia* 62, 408–417. doi: 10.1007/s00125-018-4763-3

Piemonti, L., and Pileggi, A. (2000). "Islet transplantation," in *Endotext*, eds K. R. Feingold, B. Anawalt, A. Boyce, G. Chrousos, K. Dungan, A. Grossman et al. (South Dartmouth, MA: MDText.com, Inc.).

Pluta, L., Yousefi, B., Damania, B., and Khan, A. A. (2019). Endosomal TLR-8 Senses microRNA-1294 Resulting in the Production of NFκB Dependent Cytokines. *Front. Immunol.* 10:2860. doi: 10.3389/fimmu.2019.02860

Rider, M. A., Hurwitz, S. N., and Meckes, D. G. (2016). ExtraPEG: a polyethylene glycol-based method for enrichment of extracellular vesicles. *Sci. Rep.* 6:23978. doi: 10.1038/srep23978

Robbins, P. D., Dorronsoro, A., and Booker, C. N. (2016). Regulation of chronic inflammatory and immune processes by extracellular vesicles. *J. Clin. Invest.* 126, 1173–1180. doi: 10.1172/JCI81131

Rueda, A., Barturen, G., Lebrón, R., Gómez-Martín, C., Alganza, Á, Oliver, J. L., et al. (2015). sRNAtoolbox: an integrated collection of small RNA research tools. *Nucleic Acids Res.* 43, W467–W473. doi: 10.1093/nar/gkv555

Rutman, A. K., Negi, S., Gasparrini, M., Hasilo, C. P., Tchervenkov, J., and Paraskevas, S. (2018). Immune response to extracellular vesicles from human islets of langerhans in patients with type 1 diabetes. *Endocrinology* 159, 3834–3847. doi: 10.1210/en.2018-00649

Saha, B., Kodys, K., Adejumo, A., and Szabo, G. (2017). Circulating and exosome-packaged hepatitis C single-stranded RNA induce monocyte differentiation via TLR7/8 to polarized macrophages and fibrocytes. *J. Immunol. Baltim.* 1950, 1974–1984. doi: 10.4049/jimmunol.1600797

Salam, M., Bao, Y., Herrick, C. J., Mcgill, J. B., and Hughes, J. (2018). Hidden epidemic—half of T1DM is diagnosed in adulthood. *Diabetes* 67, 1699–P. doi: 10.2337/db18-1699-P

Salvi, V., Gianello, V., Busatto, S., Bergese, P., Andreoli, L., D'Oro, U., et al. (2018). Exosome-delivered microRNAs promote IFN-α secretion by human plasmacytoid DCs via TLR7. *JCI Insight* 3:e98204. doi: 10.1172/jci.insight.98204

Schneider, C. A., Rasband, W. S., and Eliceiri, K. W. (2012). NIH image to ImageJ: 25 years of image analysis. *Nat. Methods* 9, 671–675.

Tan, L., Wu, H., Liu, Y., Zhao, M., Li, D., and Lu, Q. (2016). Recent advances of exosomes in immune modulation and autoimmune diseases. *Autoimmunity* 49, 357–365. doi: 10.1080/08916934.2016.1191477

Tao, H., Wang, M., Zhang, M., Zhang, S., Wang, C., Yuan, W., et al. (2016). MiR-126 suppresses the glucose-stimulated proliferation via IRS-2 in INS-1 β Cells. *PLoS One* 11:0149954. doi: 10.1371/journal.pone.0149954 .

Tesovnik, T., Kovač, J., Hovnik, T., Dovč, K., Bratina, N., Battelino, T., et al. (2018). Association of glycemic control and cell stress with telomere attrition in type 1 diabetes. *JAMA Pediatr.* 172, 879–881. doi: 10.1001/jamapediatrics.2018.1175

Thomas, N. J., Jones, S. E., Weedon, M. N., Shields, B. M., Oram, R. A., and Hattersley, A. T. (2018). Frequency and phenotype of type 1 diabetes in the first six decades of life: a cross-sectional, genetically stratified survival analysis from UK Biobank. *Lancet Diabetes Endocrinol.* 6, 122–129. doi: 10.1016/S2213-8587(17)30362-5

Turpin, D., Truchetet, M.-E., Faustin, B., Augusto, J.-F., Contin-Bordes, C., Brisson, A., et al. (2016). Role of extracellular vesicles in autoimmune diseases. *Autoimmun. Rev.* 15, 174–183. doi: 10.1016/j.autrev.2015.11.004

van Niel, G., D'Angelo, G., and Raposo, G. (2018). Shedding light on the cell biology of extracellular vesicles. *Nat. Rev. Mol. Cell Biol.* 19, 213–228. doi: 10.1038/nrm.2017.125

Wang, G.-J., Liu, Y., Qin, A., Shah, S. V., Deng, Z., Xiang, X., et al. (2008). Thymus exosomes-like particles induce regulatory T cells. *J. Immunol. Baltim.* 1950, 5242–5248. doi: 10.4049/jimmunol.181.8.5242

Waugh, K., Snell-Bergeon, J., Michels, A., Dong, F., Steck, A. K., Frohnert, B. I., et al. (2017). Increased inflammation is associated with islet autoimmunity and type 1 diabetes in the diabetes autoimmunity study in the young (DAISY). *PLoS One* 12:e0174840. doi: 10.1371/journal.pone.0174840

Weir, G. C., and Bonner-Weir, S. (2013). Islet β cell mass in diabetes and how it relates to function, birth, and death. *Ann. N. Y. Acad. Sci.* 1281, 92–105. doi: 10.1111/nyas.12031

Wickham, H. (2016). *ggplot2: Elegant Graphics for Data Analysis*, 2nd Edn. Cham: Springer.

Willeit, P., Skroblin, P., Moschen, A. R., Yin, X., Kaudewitz, D., Zampetaki, A., et al. (2017). Circulating MicroRNA-122 Is associated with the risk of new-onset metabolic syndrome and type 2 diabetes. *Diabetes* 66, 347–357. doi: 10.2337/db16-0731

Yáñez-Mó, M., Siljander, P. R.-M., Andreu, Z., Zavec, A. B., Borràs, F. E., Buzas, E. I., et al. (2015). Biological properties of extracellular vesicles and their physiological functions. *J. Extracell. Vesicles* 4:27066. doi: 10.3402/jev.v4.27066

Yi, J. S., Cox, M. A., and Zajac, A. J. (2010). T-cell exhaustion: characteristics, causes and conversion. *Immunology* 129, 474–481. doi: 10.1111/j.1365-2567.2010.03255.x

Yuana, Y., Sturk, A., and Nieuwland, R. (2013). Extracellular vesicles in physiological and pathological conditions. *Blood Rev.* 27, 31–39. doi: 10.1016/j.blre.2012.12.002

Zhang, H.-G., Liu, C., Su, K., Su, K., Yu, S., Zhang, L., et al. (2006). A membrane form of TNF-alpha presented by exosomes delays T cell activation-induced cell death. *J. Immunol. Baltim.* 1950, 7385–7393. doi: 10.4049/jimmunol.176.12.7385

Conflict of Interest: The authors declare that the research was conducted in the absence of any commercial or financial relationships that could be construed as a potential conflict of interest.

frontiers in Genetics

ORIGINAL RESEARCH
published: 23 April 2020
doi: 10.3389/fgene.2020.00321

Identification and Integrated Analysis of MicroRNA and mRNA Expression Profiles During Agonistic Behavior in Chinese Mitten Crab (*Eriocheir sinensis*) Using a Deep Sequencing Approach

Yangyang Pang†, Long He†, Yameng Song, Xiaozhe Song, Jiahuan Lv, Yongxu Cheng and Xiaozhen Yang**

National Demonstration Center for Experimental Fisheries Science Education, Key Laboratory of Freshwater Aquatic Genetic Resources, Ministry of Agriculture, Engineering Research Center of Aquaculture, Shanghai Ocean University, Shanghai, China

OPEN ACCESS

Edited by:
Junjie Xiao,
Shanghai University, China

Reviewed by:
Zhiqiang Xu,
Freshwater Fisheries Research Institute of Jiangsu Province, China
Shu Huang,
Dalian Ocean University, China

***Correspondence:**
Yongxu Cheng
yxcheng@shou.edu.cn
Xiaozhen Yang
xzyang@shou.edu.cn;
zny119@163.com

†These authors have contributed equally to this work

Specialty section:
This article was submitted to RNA, a section of the journal Frontiers in Genetics

Received: *21 September 2019*
Accepted: *18 March 2020*
Published: *23 April 2020*

Citation:
Pang Y, He L, Song Y, Song X, Lv J, Cheng Y and Yang X (2020) Identification and Integrated Analysis of MicroRNA and mRNA Expression Profiles During Agonistic Behavior in Chinese Mitten Crab (Eriocheir sinensis) Using a Deep Sequencing Approach. Front. Genet. 11:321. doi: 10.3389/fgene.2020.00321

As a commercially important species, the Chinese mitten crab (*Eriocheir sinensis*) has been cultured for a long time in China. Agonistic behavior often causes limb disability and requires much energy, which is harmful to the growth and survival of crabs. In this paper, we divided crabs into a control group (control, no treatment) and an experimental group (fight, agonistic behavior after 1 h) and then collected the thoracic ganglia (TG) to extract RNA. Subsequently, we first used a deep sequencing approach to examine the transcripts of microRNAs (miRNAs) and messenger RNAs (mRNAs) in *E. sinensis* displaying agonistic behavior. According to the results, we found 29 significant differentially expressed miRNAs (DEMs) and 116 significant differentially expressed unigenes (DEGs). The DEMs esi-miR-199a-5p, esi-let-7d, esi-miR-200a, and esi-miR-200b might participate in the regulation of agonistic behavior by mediating neuroregulation and energy metabolism. Focusing on the transcripts of the mRNAs, the renin–angiotensin system (RAS) Kyoto Encyclopedia of Genes and Genomes (KEGG) pathway might be involved in the regulation of agonistic behavior through glucose metabolism as this pathway was significantly enriched with DEGs. Besides, an integrated analysis of the miRNA and mRNA profiles revealed that the retinoid X receptor (RXR) was also involved in visual signal transduction, which was important for agonistic behavior. In addition, four vital agonistic behavior-related metabolic pathways, including the cAMP signaling, MAPK, protein digestion and absorption, and fatty acid metabolism pathways, were significantly enriched with the predicted target unigenes. In conclusion, the findings of this study might provide important insight enhancing our understanding of the underlying molecular mechanisms of agonistic behavior in *E. sinensis*.

Keywords: *Eriocheir sinensis*, agonistic behavior, microRNA, mRNA, neurogenesis, energy metabolism

INTRODUCTION

Chinese mitten crab (*Eriocheir sinensis*) has been loved by Chinese people and cultured in many areas of China for a long time (Cheng et al., 2018). Agonistic behavior is a common phenomenon in crustaceans and usually decreases the crabs' integrity, survival, and growth (Laranja et al., 2010; Harlıoğlu et al., 2013; Romano and Zeng, 2016). In our previous studies, we reported the agonistic behavior of *E. sinensis* and further investigated the regulation of serotonin (5-HT) and dopamine (DA) in agonistic behavior through the cAMP signaling pathway (Pang et al., 2019a; Yang et al., 2019). First, we had divided the agonistic behavior in *E. sinensis* into three stages: approach, contact, and fight; and then, we found a sign in the concentration of 5-HT, DA, cAMP, and PKA after agonistic behavior (Yang et al., 2019). Subsequently, we injected the 5-HT, DA, or cAMP to crabs and observed the effect of agonistic behavior after injection. The results showed that 5-HT and DA could regulate the behavior through the cAMP–PKA signaling pathway (Pang et al., 2019a). However, the mechanism underlying agonistic behavior in *E. sinensis* is unclear, and research investigating this topic is lacking. An understanding of the regulatory mechanisms underlying the switching of agonistic behavior is essential for elucidating the behavioral plasticity of animals and ultimately decreasing the occurrence of agonistic behavior.

MicroRNAs (miRNAs) constitute a class of non-coding RNAs with a length of 18–22 nt that can regulate gene expression and usually play an important role in many biological processes (Bartel, 2004; Wang L. et al., 2018). According to reports, miRNAs could mediate neurogenesis at many key steps in vertebrate and invertebrate (Li and Jin, 2010) and regulate animal behaviors through nervous systems (Lane et al., 2018). For example, miR-375 and miR-200b could regulate attraction/aversion behavior via the dopaminergic and GABAergic systems in amphibians (Dulcis et al., 2017). Another study showed that the overexpression of let-7d perfected the anxiolytic and depressant-like behaviors by targeting the DA D3 receptor (Bahi and Dreyer, 2018). Researchers have also found that miR-96, which could inhibit the 5-HT1B receptor, affected aggressive behavior in mice (Jensen et al., 2009). Although many reports described the effects of miRNAs on animal behaviors, studies investigating the effects of miRNAs on aggressive behavior in crustaceans were lacking. Combined with our previous researches, 5-HT and DA as two neurotransmitters played key roles in nervous systems and regulated the agonistic behavior in *E. sinensis*. So to research the relationship between miRNAs and nervous systems would undoubtedly be of great help to understand the regulatory mechanisms of agonistic behavior. In addition, agonistic behavior usually was accompanied by energy metabolism (Briffa and Elwood, 2002). We also found that the glucose level has a significant upregulation after the fight in *E. sinensis* (Yang et al., 2019). There were reports that miRNAs could regulate the energy metabolism in animals; for example, miR-199a-5p could participate in the regulation of glucose metabolism (Wu et al., 2015; Yan et al., 2017; Esteves et al., 2018). Therefore, the relationship between miRNAs and energy metabolism was valued in research on agonistic behavior.

The central nervous system (CNS) plays a major role in regulating several behaviors in some invertebrates, including agonistic behavior (Momohara et al., 2018), reproduction behavior (Thongbuakaew et al., 2019), and phototactic behavior (Rivetti et al., 2018). Besides, the thoracic ganglia (TG) is an important nerve tissue that participates in the formation of the CNS in crustaceans (Mulloney and Smarandache-Wellmann, 2012). The TG is among the many places where many neurotransmitters transfer biological information, such as DA, 5-HT, octopamine (OA), and tyramine (TA) (Vomel and Wegener, 2008). In our previous studies, we had done a lot of research on TG, including *in vitro* culture and RT-qPCR (Pang et al., 2019a). Based on the measurements of the TG, we found that 5-HT and DA could regulate the agonistic behavior of *E. sinensis* through the TG (Pang et al., 2019a; Yang et al., 2019). Therefore, investigating the TG was suitable for analyzing the mechanism underlying agonistic behavior in *E. sinensis*.

In this study, we obtained the transcriptomes of miRNAs and mRNAs after agonistic behavior by using Illumina HiSeq^{TM} 2000 technology. Also, we analyzed the functions of the significant differentially expressed miRNAs (DEMs) and mRNAs in the TG and performed an integrated analysis of their relationships. We aimed to reveal the underlying molecular mechanisms involved in the regulation of agonistic behavior in *E. sinensis*.

MATERIALS AND METHODS

Animals and Sampling

Male Chinese mitten crabs (*E. sinensis*) with a body weight of 25.56 ± 4.73 g were obtained from the Shuxin crab base in Chongming Island, Shanghai (China). The crabs were maintained in separate opaque tanks of 29.0:18.0:19.5 cm (length:width:height) for at least 7 days under single-rearing conditions before the behavioral experiments, and the tanks were filled with thoroughly aerated freshwater to a depth of 12 cm by a circulating system. The intact crabs were reared individually to avoid social contact. A basal diet was used to feed the crabs once daily from 18:30 to 19:00.

The crabs were divided into a control group (control) and an experimental group (fight). In the experimental group, two crabs with a weight difference of 1–4% were paired in a new tank of 20.0:15.5:19.5 cm (length:width:height). The tank was filled with 10 cm of water and divided into equal halves by an opaque partition. Before each pairing, each pair of crabs was placed on either side of the partition. After 10 min, the partition board was removed, and the agonistic behavior of the crabs was observed for 1 h using a high-definition camera (H.264 DVR) based on our previous research (Yang et al., 2019). We ensured that agonistic behavior occurred within 1 h, and then, the TG were collected for deep sequencing. In the control group, the crabs were placed on either side of the partition for 70 min, and then, their TG were harvested.

RNA Extraction and Quality Check

The total RNA was extracted using a TRIzol reagent (Sangon Biotech Co., Ltd.) according to the manufacturer's instructions.

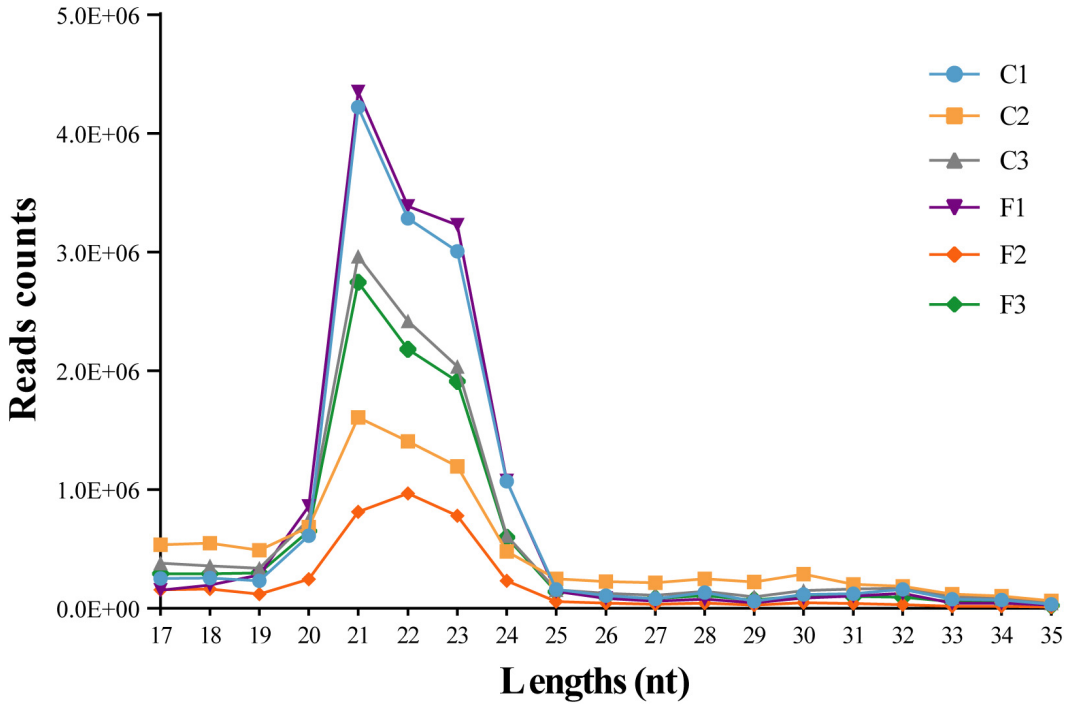

FIGURE 1 | Length distribution of the clean reads from six siRNA libraries. The nucleotide length of the siRNAs is shown on the *X*-axis, and the counts of the different nucleotide lengths are shown on the *Y*-axis.

After RNA extraction, every two crabs which were collected from one pair were mixed as one sample to subsequent detection. Qubit 2.0 (Invitrogen, United States) was used to determine the concentration and purity of the total RNA. The integrity of the RNA and genome contamination were examined by agarose gel electrophoresis.

Small RNA Library Construction and Illumina Sequencing

Based on the above results, three samples from the fight group (named F1, F2, and F3) and another three samples from the control group (named C1, C2, and C3) were used to construct six small RNA libraries. In each library, a 6 μl mixture contained approximately 1 μg or more total RNA, and 1 μL 3′ adapter and DEPC H_2O were used to prepare the RNA mix; then, the mixture was incubated at 72°C for 2 min. Subsequently, 1.8 μl 10 × T4 RNA ligase buffer, 3.5 μl 25 mM $MgCl_2$, 2.2 μl PEG8000 (50%), 0.5 μl RNase inhibitor, and 1 μl ligase 2 were added to the RNA mix. Then, 15 μl of the mixture was incubated at 22°C for 1 h, 1 μl RT primer was added to the above mixture, and the reaction conditions used were as follows: 75°C for 5 min; 37°C for 30 min, and 25°C for 15 min. To ligate with the 5′ adapter, 16 μl of the above hybrid production was opened with a secondary structure at 70°C for 2 min, and then, 1 μl ATP (10 mM), 1 μl 5′ adapter, and 1 μl ligase 1 were added. The obtained reaction solution was incubated for 1 h at 20°C. Then, the adaptor-ligated small RNAs were reverse transcribed to create the complementary DNA (cDNA) constructs. Subsequently, the cDNA constructs were amplified by PCR using an Illumina small RNA primer set and Phusion polymerase under the following conditions: 95°C for 5 min; 15 cycles of 94°C for 10 s, 55°C for 10 s, and 72°C for 15 s; 72°C for 5 min; and 4°C for ∞. The productions of PCR were detected by 12% polyacrylamide (PAGE). The reads were obtained with a single end sequencing pattern at Sangon Biotech Co., Ltd. (Shanghai, China) using Illumina HiSeq™ 2000.

MRNA Library Construction and Sequencing

Simultaneously, we also selected three samples from the fight group (named F4, F5, and F6) and another three samples from the control group (named C4, C5, and C6) to construct six mRNA libraries. The samples used for the mRNA transcriptome analysis were prepared according to a VAHTS™ mRNA-seq V2 Library Prep Kit for Illumina® (Vazyme Biotech Co., Ltd., Nanjing, China). Poly-T oligo-linked magnetic beads were used to purify the PolyA mRNA from the total RNA, and the intact mRNA was broken into fragments with a bead washing buffer and a metal bath. The aforementioned mRNAs were used as templates to synthesize the first-strand cDNA. Then, the second-strand cDNA was synthesized using the second-strand buffer and second-strand enzyme mix. Subsequently, the cDNA was end-repaired, a base was added to the 3′ end, and the cDNA was amplified by PCR. Finally, the constructed cDNA libraries were sequenced with Illumina HiSeq™ 2000.

Analysis of miRNA and mRNA Sequence Data

The adapter sequences (sequence: TGGAATTCTCGGGTGCC AAGGAACTC) were removed from the raw data using the cutadapt software. In addition, the low-quality reads (a base quality less than Q20, the average quality of four consecutive bases less than Q20 and reads shorter than 17 nucleotides) were filtered using trimmomatic (Bolger et al., 2014). Finally, the clean reads of 17–35 nt were used in the subsequent analysis.

The clean reads may contain other small RNAs (rRNAs, sRNAs, snRNAs, and snoRNAs), which were compared using the rfam (Nawrocki et al., 2015) database and blastn. The conditions of the alignment were as follows: gapopen = 0, evalue < 0.01, and mismatch ≤ 1.

For the animal miRNAs, miranda (Betel et al., 2008) was used to predict the target genes. The predicted miRNA targets were based on a threshold value for the parameters as follows: S ≥ 150, $\Delta G \leq -30$ kcal/mol. The target genes were predicted based on the *E. sinensis* mRNA transcriptome sequence obtained in this study as a reference genome.

Regarding the mRNA sequencing, raw reads from Illumina HiSeq^{TM} 2000 may contain sequencing primers and low-quality sequences, which can affect the analytical quality. Therefore, the raw reads were cleaned through the following three steps: (a) linger sequences were discarded; (b) $Q < 20$ ($Q = -10 \log_{10}E$) bases were removed; and (c) read lengths shorter than 25 bp were discarded. Then, the clean reads were used for the *de novo* assembly using Trinity. Regarding the annotation, the assembled final unigenes with screening condition were annotated using the NCBI nucleotide sequence (NT) and NCBI protein nonredundant (Nr) databases. The unigenes were also classified using the Gene Ontology (GO) and Kyoto Encyclopedia of Genes and Genomes (KEGG) databases.

Differential Expression Analysis of miRNAs and mRNAs

The expression levels of the miRNAs were determined by using RPM (normalized to determine the expression in transcripts per million). To identify the significant DEMs between two groups, the read counts of the samples were analyzed as input data using edgeR (Xiaobei et al., 2014). The screening conditions were as follows: p-value < 0.05 and $|\log\text{FoldChange}| > 1$. The expression levels of the genes were determined by using the TPM (transcripts per million) method. An analysis of the differential expression levels across the samples was performed using DEGseq, and the significant differentially expressed genes (DEGs) were identified (q-value < 0.05, $|\text{FoldChange}| > 2$). Then, the significantly enriched terms were obtained by mapping the DEGs to the corresponding KEGG pathways.

Quantitative Real-Time PCR-Verified miRNAs

Five DEMs were randomly chosen for a quantitative real-time PCR (RT-qPCR) analysis to validate the accuracy of the RNA-seq results. The total RNA (500 ng), which was returned after sequencing (three samples per group), was used as a template to synthesize first-strand cDNA with a miRNA 1st Strand cDNA Synthesis Kit (by stem loop: 5′-GTCGTATCCAGTGCAGGGTCCGAGGTA TTCGCACTGGA TACGAC-3′, Vazyme Biotech) according to the manufacturer's instructions (Zhang et al., 2018). Specific primers were designed based on the DEMs with a miRNA design software (Vazyme designed) (**Table 1**).

The RT-qPCR reaction system contained 5 μl of 2 × miRNA Universal SYBR qPCR Master (Vazyme Biotech), 1 μl of diluted first-strand cDNA, 3.6 μl of PCR-grade water, 0.2 μl of specific primers, and 0.2 μl of mQ Primer R (5′-AGTGCAGGGTCCGAGGTA TT-3′) (Zhang et al., 2018). The mixtures were run under the following conditions: 95°C for 5 min; 40 cycles of 95°C for 10 s and 60°C for 30 s; and 95°C for 15 s, 60°C for 1 min, and 95°C for 15 s on an ABI 7500 Real-Time PCR System (Life Technology, United States). We used snRNA as an internal control (Liu et al., 2019). The DEM expression levels were calculated using the $2^{-\Delta\Delta Ct}$ method (Pang et al., 2019b).

STATISTICAL ANALYSIS

The data are expressed as the mean ± SD, and a T-test analysis of variance was used to compare two groups. A P-value < 0.05 indicated a statistically significant difference.

RESULTS

Overview of Small RNA Sequences in *E. sinensis*

To explore the role of miRNAs in the regulation of agonistic behavior in *E. sinensis*, we obtained 34,367,222 clean reads from the control group and 28,150,606 clean reads from the fight group using Illumina HiSeq^{TM} 2000 (**Supplementary Table S1**). The small RNA sequences with lengths of 17–35 nt were the most enriched in 21–23 nt (**Figure 1**). As shown in **Supplementary Table S2**, the clean reads in the six small RNA libraries were composed of rRNAs, tRNAs, snRNAs, snoRNAs, and miRNAs.

Identification of Mature miRNAs

The miRNA clean reads were blasted against the mature sequences of known miRNAs included in the miRbase (Kozomara and Griffiths-Jones, 2014), which revealed a total of

TABLE 1 | Primers selected for evaluating the miRNA expression levels with RT-qPCR.

Primer name	Primer sequence (5′–3′)
esi-miR-194-5p	CGCGTGTAACAGCAACTCCAT
esi-miR-192	GCGCTGACCTATGAATTGACAG
esi-let-7b-3p	GCGCGCTATACAACCTACTGC
esi-lig-miR-750	GCGCGCAGATCTAACTCTTCC
esi-miR-146b-5p	CGCGTGAGAACTGAATTCCA
snRNA	CGTTGGAACGATACAGAGAAGAT

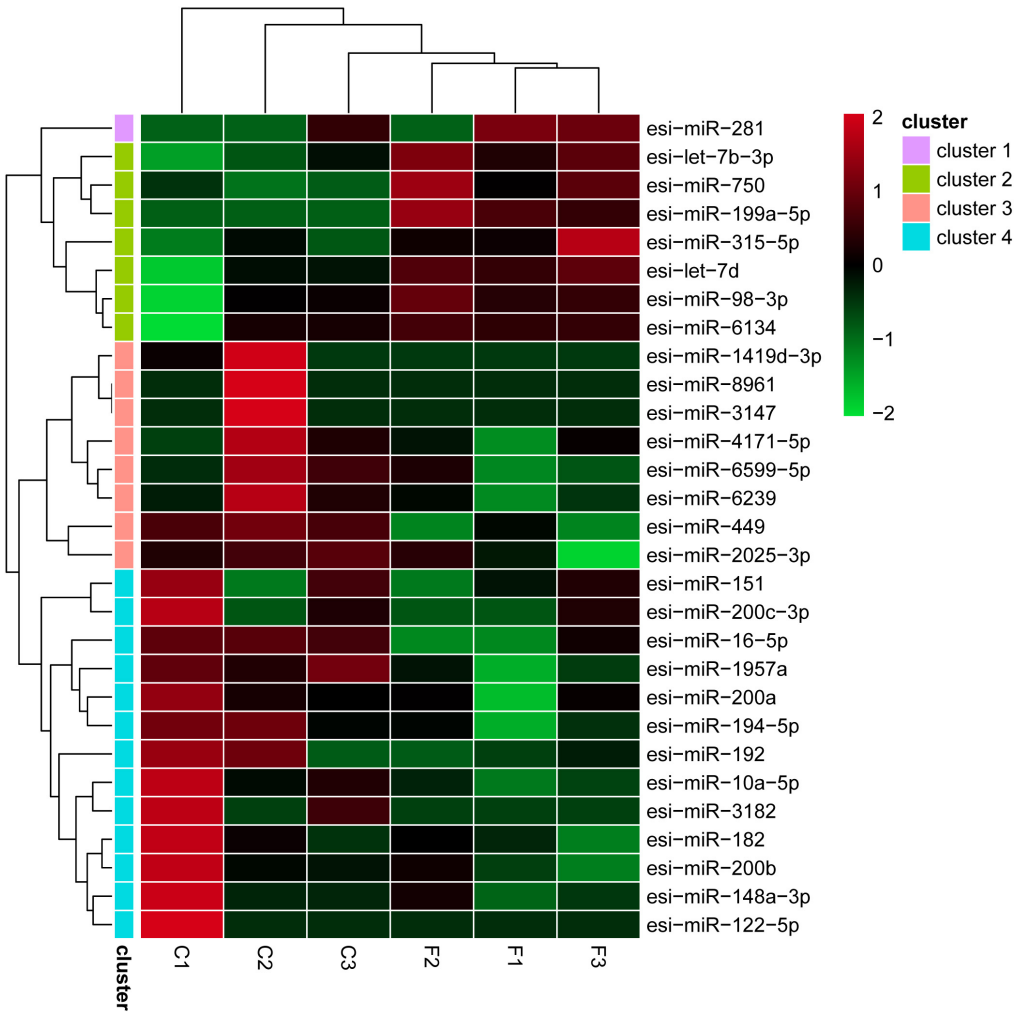

FIGURE 2 | Differential expression of 29 miRNAs using a linkage hierarchical cluster analysis. The color indicates the $\log_2$-fold change from high (red) to low (green) as indicated by the color scale. The names of the miRNAs and the cluster to which they belong are shown on the right side.

893 mature miRNAs in *E. sinensis*, and the number of mature miRNAs in each library is shown in **Supplementary Table S2**. When we summarized the conserved miRNAs, 64 miRNAs were specific to the fight group. While 129 miRNAs did not belong to any family, all remaining miRNAs belonged to 117 known families. The top five miRNA families included miR-10 (69 miRNAs), let-7 (48 miRNAs), miR-9 (30 miRNAs), miR-8 (26 miRNAs), and miR-25 (24 miRNAs).

Most miRNAs had a relatively low expression level, and the RPM of some miRNAs was even below 100 (Wang L. et al., 2018). In this study, eight mature miRNAs, namely, esi-miR-100-5p, esi-miR-263b, esi-let-7-5p, esi-miR-184-3p, esi-miR-100a-5p, esi-miR-276a-3p, esi-miR-7a, and esi-miR-83, had an expression level greater than 10,000 RPM in each library.

DEM Analysis and RT-qPCR Verification

The levels of the DEMs between the control and fight groups were compared according to RPM values $\geq$ 5 as determined by a linkage hierarchical cluster analysis. We obtained 29 DEMs, namely, 8 upregulated and 21 downregulated DEMs, compared to the control group, indicating that these miRNAs might be involved in agonistic behavior-specific regulation (**Figure 3**).

Five DEMs were selected to verify the RNA-Seq results. The results of the RT-qPCR analysis confirmed that esi-miR-194-5p and esi-miR-192 were significantly downregulated in the fight group (**Figure 2**). Additionally, esi-let-7b-3p and esi-miR-750 were significantly upregulated in the fight group. We also found that esi-miR-146b-5p does not exhibit a significant difference in expression between the control and fight groups. Our results confirmed the data from the RNA-Seq.

De novo Assembly and Unigene Functional Annotation

From RNA-Seq, we obtained 145,309,464 raw reads from the fight group and 142,210,006 raw reads from the control group.

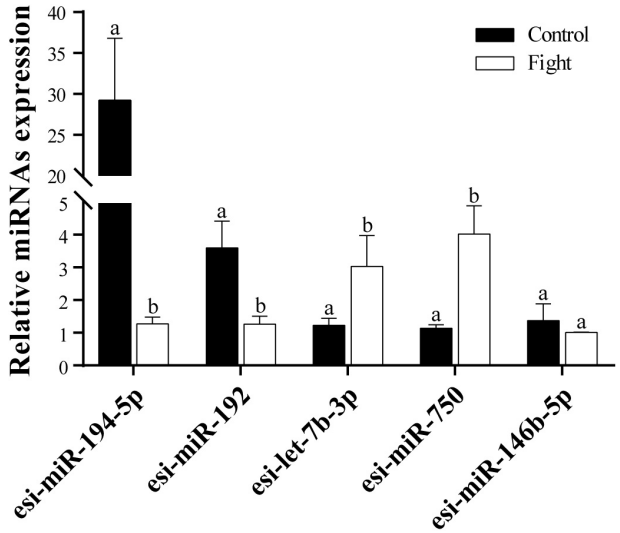

FIGURE 3 | RT-qPCR analysis of five selected DEMs. Relative expression levels of tch-miR-194-5p, efu-miR-192, chi-Let-7b-3p, lgi-miR-750, and gga-miR-146b-5p are shown. The different lowercase letters above the bars indicates significant differences ($P < 0.05$) between the control and fight groups.

The clean reads were selected by excluding reads that did not conform to the requirements. Thus, there were 136,737,066 and 139,889,948 clean reads in the fight and control groups, respectively (**Supplementary Table S1**), and these reads were used for *de novo* assembly. Then, 217,281 unigenes were obtained from six mRNA libraries. In total, 18,950 unigenes had a length greater than 1,000 bp, and 53,333 unigenes were greater than 500 bp in length (**Figure 4**).

Besides, the unigenes were used for further functional analysis. In total, 30,458 unigenes were annotated by the GO database and assigned to the following three groups: molecular function, biological process, and cellular component; these groups were further divided into 57 categories. Most unigenes were concentrated in the binding, cellular process, and cell categories. The signaling pathways of 8,447 unigenes were analyzed using the KEGG KAAS online pathway analysis tool[1]. In addition, all unigenes were mapped to the following five processes: organismal systems (25.64%), metabolism (25.13%), genetic information (16.16%), cellular processes (15.90%), and environmental information processing (15.17%). Most unigenes were associated with signal transduction, translation, transport, and catabolism; carbohydrate metabolism; and endocrine system pathways.

DEG Analysis

We performed an analysis to detect significant differences in expression levels across the samples and found 101 upregulated significant DEGs and 15 significant downregulated DEGs between the fight and control groups. Furthermore, significant DEGs were assigned to KEGG pathways. The significantly enriched pathways (q-value < 0.05) included the renin–angiotensin system (RAS) (**Figure 5**), NOD-like receptor signaling pathway, cytosolic DNA-sensing pathway, renin secretion, and ribosome biogenesis in eukaryotes.

MiRNA Target Gene Prediction and Functional Annotation

Miranda was used to predict the target genes based on the mRNA transcriptome. In our work, in total, 12,819 unigenes were targeted by 647 miRNAs. In addition, 43 miRNAs were predicted to target more than 100 genes; among these, miR-6914-5p was predicted to target 2,258 genes, which is the largest number observed in this study. Also, we found that 3,688 unigenes were targeted by two or more miRNAs. Furthermore, 15 DEGs targeted by 23 miRNAs were predicted (**Table 2**).

In addition, the predicted target unigenes of 29 DEMs were shown in the **Supplementary Material (S1)**.

To analyze the functions of the target genes among the different groups, most genes were classified into 44 different GO terms. The terms male meiosis, apical cortex, and ARF guanyl-nucleotide exchange factor activity were the most highly enriched in the biological process, cellular component, and molecular function categories, respectively, between the control and fight groups. In addition, 259 target genes were assigned to 169 KEGG pathways. The top 20 enriched pathways are shown in **Figure 5** and include the cAMP signaling pathway, MAPK signaling pathway-fly, protein digestion and absorption, and fatty acid biosynthesis.

DISCUSSION

In this study investigating agonistic behavior in *E. sinensis*, we reveal the underlying molecular mechanisms through an analysis of miRNA and mRNA expression profiles using a deep sequencing approach. We found 29 miRNAs and 116 unigenes with significant differential expression in the fight group. In the 29 DEMs, we did not find any that was characterized in crustaceans, but the mse-miR-281 (*Manduca sexta*) (Zhang et al., 2012), lgi-miR-750 (*Lottia gigantea*) (Song et al., 2018), sme-miR-315-5p (*Schmidtea mediterranea*) (da Silva et al., 2015), cin-miR-4171-5p (*Ciona intestinalis*), and nve-miR-2025-3p (*Nematostella vectensis*) were characterized in invertebrates. And then, we analyzed the functions of the DEMs and found that they play some key roles in the regulation of animal behaviors. For example, esi-miR-199a-5p as a DEM could induce neuronal apoptosis by targeting the HIF-1α gene and then affect learning and memory behaviors in rats (Yan et al., 2017). Besides, miR-199a-5p was believed to participate in the regulation of glucose metabolism (Wu et al., 2015; Yan et al., 2017; Esteves et al., 2018). Agonistic behavior usually was accompanied by energy consumption, especially glucose metabolism (Briffa and Elwood, 2002). Due to the high conservation of miRNAs (Lewis et al., 2005), we assumed that miR-199a-5p may

[1]http://www.kegg.jp/blastkoala/

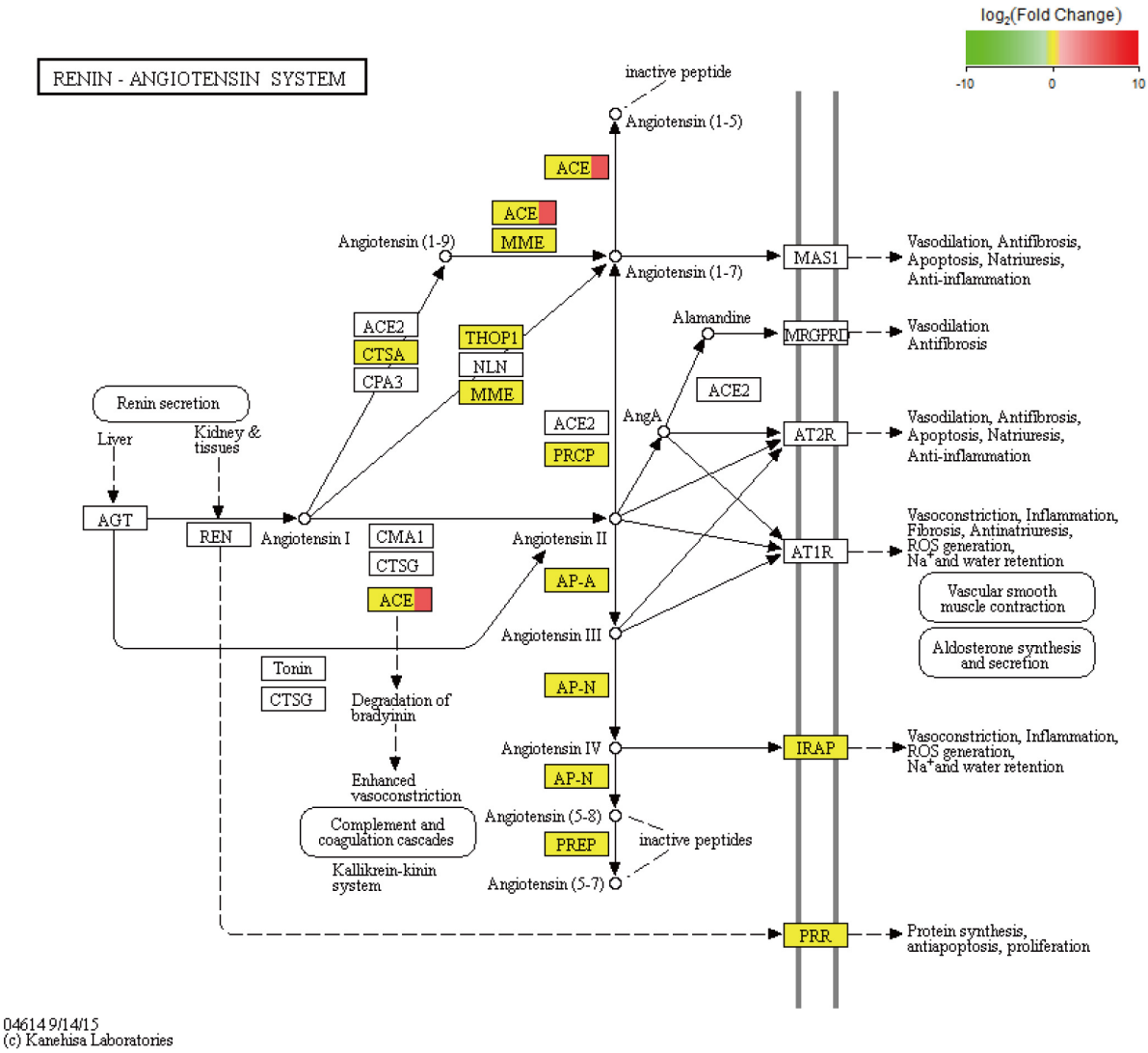

FIGURE 4 | KEGG pathway of the renin–angiotensin system. In addition, the red color indicates upregulated genes, and the yellow color indicates genes with no significant differences in expression. ACE is angiotensin converting enzyme.

regulate crabs' agonistic behavior by mediating neurogenesis and energy metabolism.

Based on the analysis of the mRNA transcripts, we also found some DEGs which could regulate energy metabolism. For example, we observed that the KEGG pathway of the RAS was significantly enriched with DEGs (**Figure 5**). The RAS, which consists of angiotensinogen, angiotensin-converting enzyme (ACE) isoforms, and angiotensin peptides and their receptors, performs many important functions, including glucose homeostasis (Luther and Brown, 2011), electrolyte balance (Jackson et al., 2018), and features of a neurotransmitter (Phillips et al., 1979) in mammals. In the RAS, angiotensinogen is transformed to form angiotensin (Ang) I under renin action and is then cleaved by ACE to form Ang II. Ang II can induce metabolic effects by acting on cell surface G protein-coupled receptors (White et al., 2019). In fact, the RAS has been shown to mediate glucose metabolism (Gamba et al., 2019). As previously discussed, agonistic behavior is usually accompanied by glucose metabolism in crustaceans. Therefore, there is new evidence suggesting that the RAS may participate in the regulation of agonistic behavior in crabs. Based on the above studies, ACE, which was significantly upregulated in our results, plays a key role in the RAS pathway. A series of studies show that ACE is related to glucose and lipid metabolism (Vaughan et al., 2016; Glover et al., 2019). In addition, ACE modulates behavioral and metabolic responses to diet in *Drosophila melanogaster* (Glover et al., 2019). Moreover, ACE may alter anxiety-like behavior (Wang L.A. et al., 2018) and cognitive ability (Gamba et al., 2019) by mediating the RAS. Therefore, we propose that the ACE gene plays a key role in the RAS pathway to alter energy metabolism, thereby affecting agonistic behavior in *E. sinensis*.

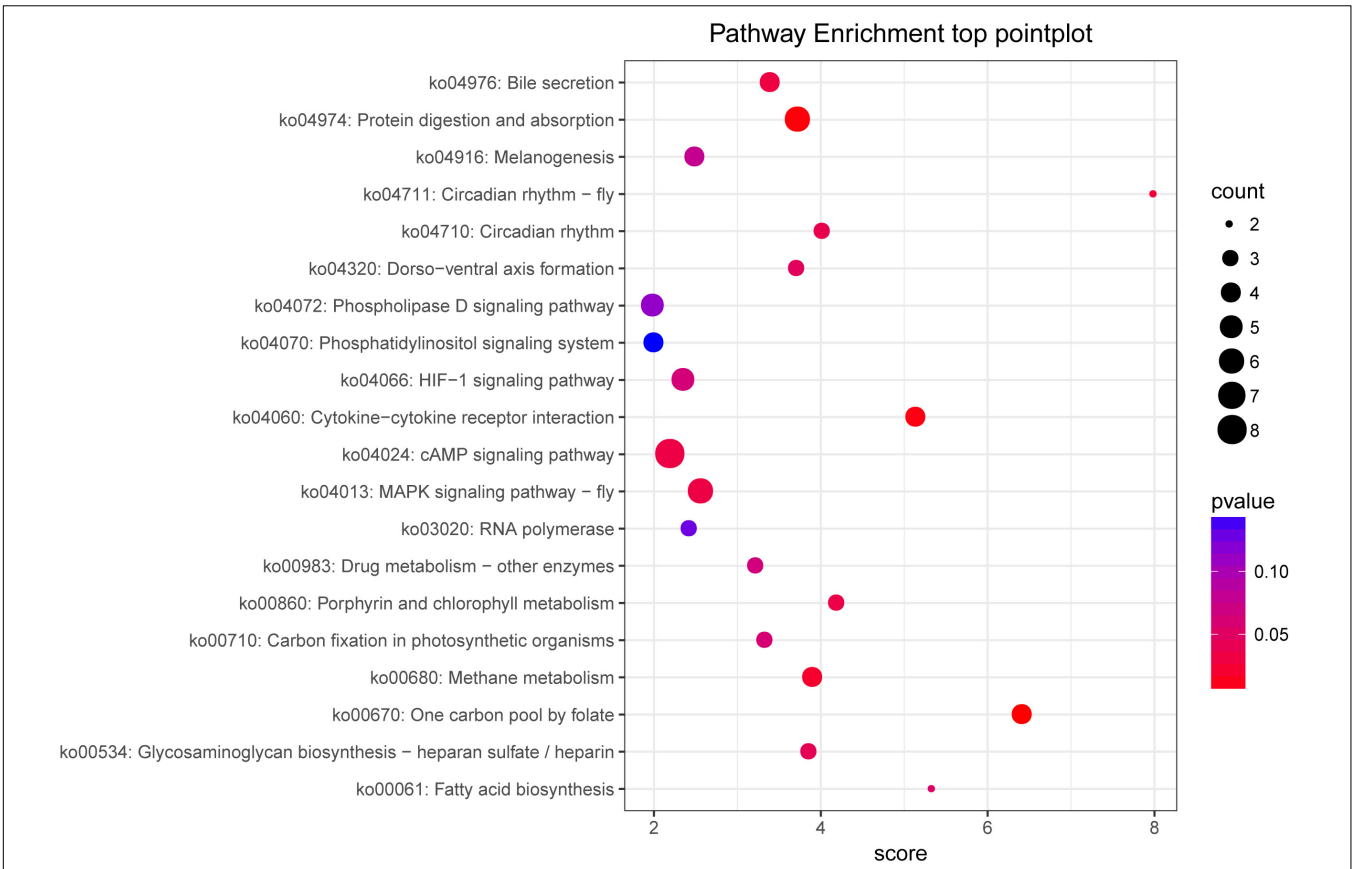

FIGURE 5 | KEGG pathway enrichment of target genes between the control and fight groups. The abscissa represents the pathway enrichment grade. The *P*-value indicates the significance of the enrichment grade, and the circle size indicates the counts of the target genes.

Focusing on the neuroregulation in behavior, research show that let-7d played an important role in regulating the attention deficit hyperactivity disorder; Wu et al. (2010) found that an increased level of let-7d could decrease tyrosine hydroxylase activity by targeting galectin-3 and affect DA metabolism in rats (Wu et al., 2010). A recent study also showed that through a D3R target-mediated mechanism, let-7d improved anxiety and depression disorders (Bahi and Dreyer, 2018). The above evidence suggested that let-7d is involved in the upstream and downstream regulation of DA. According to previous studies, DA is a key neurotransmitter that may affect agonistic behavior in crustaceans. For example, Briffa and Elwood (2002) confirmed that the circulating levels of DA significantly decrease after a fight in *Pagurus bernhardus*, and the same result was found in shore crab (*Carcinus maenas*) (Sneddon et al., 2000). In addition, an injection of DA could improve catechol-*O*-methyltransferase (COMT) gene expression, and COMT might be related to aggressiveness in the swimming crab (*Portunus trituberculatus*) (Zhu et al., 2018). In our previous two studies, we also found that the DA level is significantly decreased during agonistic behavior and suggested that an injection of DA reduced agonistic behavior in *E. sinensis* (Pang et al., 2019a; Yang et al., 2019). In contrast to let-7d, two DEMs, that is, esi-miR-200a and esi-miR-200b, exhibited a significant downregulation in the fight group. However, these DEMs also played important roles in regulating the dopaminergic system (Dulcis et al., 2017; Wu et al., 2018). Wu et al. (2018) proved that miR-200a could influence Parkinson's disease by mediating the DA2 receptor, which regulates the cAMP–PKA signaling pathway. In addition, miR-200b is associated with methamphetamine (METH) addiction, and METH could induce behavioral changes by changing the DA level in rats (Sim et al., 2017). Thus, the significant change in esi-let-7d, esi-miR-200a, and esi-miR-200b indicated that these factors may influence agonistic behavior in *E. sinensis* by mediating the DA regulation mechanism. However, the different expression levels among esi-miR-200a, esi-miR-200b, and esi-let-7d suggest that these factors may play different roles in the regulation of agonistic behavior.

In our results, we predict that the *E. sinensis* retinoid X receptor (RXR) as a DEG was targeted by five miRNAs (**Table 2**). In the eyes, retinoic acid (RA) is responsible for phototransduction through binding the G-protein receptors (Uray et al., 2016). The activity of RA can be regulated by RXR, which is important for the proper function of the retina (Janssen et al., 1999). RXR can regulate the development of cone photoreceptors in many animals, and the first step of the phototransduction of vision requires cone photoreceptors (Hennig et al., 2008). To the best of our knowledge, the visual

TABLE 2 | Predicted significant DEGs were targeted by miRNAs.

Unigene	Length (bp)	Expression (F vs. C)	Accession number	Regulatory miRNAs
Eriocheir sinensis caspase mRNA	2,526	Up	TRINITY_DN67527_c1_g1	esi-miR-6914-5p
Eriocheir sinensis retinoid X receptor (RXR) mRNA	12,562	Up	TRINITY_DN71171_c0_g3	esi-miR-2b, esi-miR-6914-5p, esi-miR-7911c-5p
Eriocheir sinensis C-type lectin mRNA	1,288	Up	TRINITY_DN70126_c0_g1	esi-let-7e-3p
Eriocheir sinensis ecdysteroid receptor (EcR) gene	874	Up	TRINITY_DN60221_c3_g5	esi-miR-6599-5p
Eriocheir sinensis Down syndrome cell adhesion molecule (Dscam) gene	555	Up	TRINITY_DN56196_c7_g1	esi-miR-9277
Eriocheir sinensis clone CX003 microsatellite sequence	417	Up	TRINITY_DN62484_c3_g1	esi-miR-6914-5p
Eriocheir sinensis fatty acid-binding protein 9 (FABP9) gene	936	Up	TRINITY_DN63173_c3_g2	esi-miR-1386
Eriocheir sinensis WAP2	882	Up	TRINITY_DN66360_c1_g1	esi-miR-6914-5p
NFX1-type zinc finger-containing protein 1	1,382	Up	TRINITY_DN73356_c3_g1	esi-miR-3574
Uncharacterized protein	2,212	Up	TRINITY_DN66345_c1_g1	esi-miR-224, esi-miR-133d, esi-miR-133
Uncharacterized protein	285	Up	TRINITY_DN66345_c0_g2	esi-miR-133c-3p, esi-miR-133d, esi-miR-133, esi-miR-133, esi-miR-133b, esi-miR-133a, esi-miR-133-3p, esi-miR-133-3p
Uncharacterized protein	1,018	Up	TRINITY_DN73807_c1_g3	esi-miR-133c-3p, esi-miR-133d, esi-miR-133, esi-miR-133, esi-miR-133b, esi-miR-133, esi-miR-133b, esi-miR-133a, esi-miR-133-3p, esi-miR-133-3p
Uncharacterized protein	266	Up	TRINITY_DN62223_c4_g2	esi-miR-423-5p, esi-miR-423
Uncharacterized protein	3,240	Up	TRINITY_DN68868_c0_g1	esi-miR-276a-5p, esi-miR-378b
–	757	Up	TRINITY_DN67560_c0_g4	esi-miR-3574

systems are widely used for animal communication, including color discrimination (Chiou et al., 2011), individual recognition (Gherardi et al., 2010), and other animal behaviors (Aquiloni and Gherardi, 2010). Undoubtedly, differences in visual signals can also induce changes in the behavioral responses of crustaceans. For example, mantis shrimp (*Squilla empusa*) displayed varying degrees of agonistic behavior according to vision differences (Wortham-Neal, 2002). In summary, we propose that visual signals were produced when the two crabs met, and then, the signals were conducted into the animals' CNS by receptors that may contain RXR. Subsequently, the command for agonistic behavior is issued by the CNS. Of course, the behavior may be regulated by complex physiological processes, such as neurotransmission, energy metabolism, and immunoregulation. Based on our results, genes other than those discussed above exhibited significant expression differences. Due to the length of this paper, we only analyzed the DEGs considered to perform considerable functions in the regulation of agonistic behavior. The other DEGs will be further explored in future studies.

Analyzing the predicted target unigene enrichment KEGG pathways (**Figure 5**), we found that the cAMP signaling pathway is the most enriched. The cAMP is a second messenger that can be activated by neuromodulators and then affect protein kinase A (PKA) activity (Buckley et al., 2016; Momohara et al., 2016). According to reports, the cAMP–PKA signaling pathway was detected to be essential for mediating loser and winner effects in agonistic behavior (Momohara et al., 2016). Our previous studies also showed that an injection of CPT-cAMP into crabs inhibited agonistic behavior in *E. sinensis* (Pang et al., 2019a). Therefore, the results of this study further demonstrate that the cAMP signaling pathway participates in the regulation of agonistic behavior. And the cAMP pathway played an important role in the energy metabolism and the conduction of nerve signals in crustaceans (Pang et al., 2019a; Yang et al., 2019). Also, we found that the MAPK pathway was significantly enriched with unigenes. The MAPK pathway is a three-tiered cascade (MAP3Ks–MAP2Ks–MAPKs), and the MAPK family includes

extracellular signal−regulated kinase (ERK), P38, and c−Jun NH2−terminal kinase (JNK) (Malki et al., 2014). Several studies have reported that the MAPK pathway is linked to highly aggressive behavior (Malki et al., 2014; Malki et al., 2016a,b). In MAPK signaling cascades, ERK seems to be mainly associated with aggression (Malki et al., 2014). ERK is a key factor in the MAPK pathway that has been revealed to be involved in energy metabolism (Kuo et al., 2019). In fact, our results further show that the protein digestion and absorption pathway and fatty metabolism pathway are significantly enriched with DEGs. As previously mentioned, energy metabolism may be regulated by ERK or other key factors involved in agonistic behavior. To sum up, this study suggested that the regulation between miRNAs and genes could mediate the energy metabolism and the neurogenesis to regulate the agonistic behavior in *E. sinensis*.

CONCLUSION

In this paper, we performed an integrated analysis of miRNA and mRNA expression profiles and found that the miRNAs and mRNAs were involved in the behavior by mediating the progress of neurogenesis and energy metabolism in *E. sinensis*. We propose that DEMs and DEGs, mainly including esi-miR-199a-5p, esi-let-7d, the esi-miR-200 family, RXR, and ACE genes, may regulate agonistic behavior. Additionally, the miRNAs and mRNAs mainly focus on the RAS, cAMP, MAPK, and energy metabolism pathways after a fight. These results reveal the underlying molecular mechanisms of agonistic behavior and could guide researchers in investigating behavioral plasticity in the Chinese mitten crab.

DATA AVAILABILITY STATEMENT

The datasets generated for this study can be found in the https://dataview.ncbi.nlm.nih.gov/object/PRJNA565886?reviewer=ugafl4uq46l71e8ro649glsvhh.

ETHICS STATEMENT

The animal study was reviewed and approved by the Animal Experiments Ethics Committee of Shanghai Ocean University.

AUTHOR CONTRIBUTIONS

The experiments of this study were designed by YP and XY. YS, XS, and JL assisted YP and LH to complete several animal experiments. Results analysis and manuscript writing were made by YP, and then were reviewed and edited by XY. The funding resources came from YC. All authors read and approved the final manuscript.

FUNDING

We are grateful for the support by the National Key R&D Program of China (2019YFD0900105), the China Agriculture Research System (CARS-48), the National Natural Science Foundation of China (41876190), the Fishery Science and Technology Projects in Jiangsu Province (d2018_4), the Shandong Joint Fund (U1706209), the Aquaculture Engineering Research Platform in Shanghai established by the Shanghai Science and Technology Commission (16DZ2281200), and the capacity-promoting project of Shanghai Engineering and Technology Center from Shanghai Municipal Science and Technology Commission (19DZ2284300).

SUPPLEMENTARY MATERIAL

The Supplementary Material for this article can be found online at: https://www.frontiersin.org/articles/10.3389/fgene.2020.00321/full#supplementary-material

REFERENCES

Aquiloni, L., and Gherardi, F. (2010). Crayfish females eavesdrop on fighting males and use smell and sight to recognize the identity of the winner. *Anim.l Behav.* 79, 265–269. doi: 10.1016/j.anbehav.2009.09.024

Bahi, A., and Dreyer, J. L. (2018). Lentiviral-mediated let-7d microRNA overexpression induced anxiolytic- and anti-depressant-like behaviors and impaired dopamine D3 receptor expression. *Eur. Neuropsychopharmacol.* 28, 1394–1404. doi: 10.1016/j.euroneuro.2018.09.004

Bartel, D. P. (2004). MicroRNAs: genomics, biogenesis, mechanism, and function. *Cell* 116, 281–297.

Betel, D., Wilson, M., Gabow, A., Marks, D. S., and Sander, C. (2008). The microRNA.org resource: targets and expression. *Nucleic Acids Res.* 36, D149–D153.

Bolger, A. M., Lohse, M., and Usadel, B. (2014). Trimmomatic: a flexible trimmer for Illumina sequence data. *Bioinformatics* 30, 2114–2120. doi: 10.1093/bioinformatics/btu170

Briffa, M., and Elwood, R. W. (2002). Power of shell-rapping signals influences physiological costs and subsequent decisions during hermit crab fights. *Proc.: Biol. Sci.* 269, 2331–2336. doi: 10.1098/rspb.2002.2158

Buckley, S. J., Fitzgibbon, Q. P., Smith, G. G., and Ventura, T. (2016). In silico prediction of the G-protein coupled receptors expressed during the metamorphic molt of *Sagmariasus verreauxi* (*Crustacea*: *Decapoda*) by mining transcriptomic data: RNA-seq to repertoire. *Gen. Comp. Endocrinol.* 228, 111–127. doi: 10.1016/j.ygcen.2016.02.001

Cheng, Y. X., Wu, X. G., and Li, J. Y. (2018). "Chinese mitten crab culture: current status and recent progress towards sustainable development," in *Aquaculture in China*, eds J-F Gui, Q. Tang, L. Zhongjie, S. S. De Silva, and L. Jiashou (Hoboken, NJ: John Wiley & Sons, Limited), 55–69.

Chiou, T. H., Marshall, N. J., Caldwell, R. L., and Cronin, T. W. (2011). Changes in light-reflecting properties of signalling appendages alter mate choice behaviour in a stomatopod crustacean *Haptosquilla trispinosa*. *Mar. Freshw. Behav. Physiol.* 44, 1–11. doi: 10.1080/10236244.2010.546064

da Silva, W., dos Santos, R. A. S., and Moraes, K. C. M. (2015). Mir-351-5p contributes to the establishment of a pro-inflammatory environment in the H9c2 cell line by repressing PTEN expression. *Mol. Cell. Biochem.* 411, 363–371. doi: 10.1007/s11010-015-2598-5

Dulcis, D., Lippi, G., Stark, C. J., Do, L. H., Berg, D. K., and Spitzer, N. C. (2017). Neurotransmitter switching regulated by miRNAs controls changes in social preference. *Neuron* 95, 1319.e5–1333.e5.

Esteves, J. V., Yonamine, C. Y., Pinto, D. C., Gerlinger-Romero, F., Enguita, F. J., and Machado, U. F. (2018). Diabetes modulates microRNAs 29b-3p, 29c-3p, 199a-5p and 532-3p expression in muscle: possible role in GLUT4 and HK2 repression. *Front. Endocrinol.* 9:12. doi: 10.3389/fendo.2018.00536

Gamba, P., Staurenghi, E., Testa, G., Giannelli, S., Sottero, B., and Leonarduzzi, G. (2019). A crosstalk between brain cholesterol oxidation and glucose metabolism in Alzheimer's disease. *Front. Neurosci.* 13:9. doi: 10.3389/fnins.2019.00556

Gherardi, F., Cenni, F., Parisi, G., and Aquiloni, L. (2010). Visual recognition of conspecifics in the American lobster. *Homarus americanus*. Ani. Behav. 80, 713–719. doi: 10.1016/j.anbehav.2010.07.008

Glover, Z., Hodges, M. D., Dravecz, N., Cameron, J., Askwith, H., Shirras, A., et al. (2019). Loss of angiotensin-converting enzyme-related (ACER) peptidase disrupts behavioural and metabolic responses to diet in *Drosophila melanogaster*. *J. Exp. Biol.* 222:jeb194332. doi: 10.1242/jeb.194332

Harlıoğlu, M. M., Harlıoğlu, A. G., Mişe Yonar, S., and Çakmak Duran, T. (2013). Effects of dietary l-tryptophan on the agonistic behavior, growth, and survival of freshwater crayfish *Astacus leptodactylus* Eschscholtz. *Aqu. Int.* 22, 733–748. doi: 10.1007/s10499-013-9702-1

Hennig, A. K., Peng, G. H., and Chen, S. M. (2008). Regulation of photoreceptor gene expression by Crx-associated transcription factor network. *Brain Res.* 1192, 114–133. doi: 10.1016/j.brainres.2007.06.036

Jackson, L., Eldahshan, W., Fagan, S. C., and Ergul, A. (2018). Within the brain: the renin angiotensin system. *Int. J. Mol. Sci.* 19, 876.

Janssen, J. J. M., Kuhlmann, E. D., van Vugt, A. H. M., Winkens, H. J., Janssen, B. P. M., Deutman, A. F., et al. (1999). Retinoic acid receptors and retinoid X receptors in the mature retina: subtype determination and cellular distribution. *Curr. Eye Res.* 19, 338–347. doi: 10.1076/ceyr.19.4.338.5307

Jensen, K. P., Covault, J., Conner, T. S., Tennen, H., Kranzler, H. R., and Furneaux, H. M. (2009). A common polymorphism in serotonin receptor 1B mRNA moderates regulation by miR-96 and associates with aggressive human behaviors. *Mol. Psychiatry* 14, 381–389. doi: 10.1038/mp.2008.15

Kozomara, A., and Griffiths-Jones, S. (2014). miRBase: annotating high confidence microRNAs using deep sequencing data. *Nucleic Acids Res.* 42, D68–D73.

Kuo, Y.-T., Lin, C.-C., Kuo, H.-T., Hung, J.-H., Liu, C.-H., Jassey, A., et al. (2019). Identification of baicalin from bofutsushosan and daisaikoto as a potent inducer of glucose uptake and modulator of insulin signaling-associated pathways. *J. Food Drug Anal.* 27, 240–248. doi: 10.1016/j.jfda.2018.07.002

Lane, B. J., Kick, D. R., Wilson, D. K., Nair, S. S., and Schulz, D. J. (2018). Dopamine maintains network synchrony via direct modulation of gap junctions in the crustacean cardiac ganglion. *Elife* 7:18.

Laranja, J. L. Q., Quinitio, E. T., Catacutan, M. R., and Coloso, R. M. (2010). Effects of dietary l-tryptophan on the agonistic behavior, growth and survival of juvenile mud crab *Scylla serrata*. *Aquaculture* 310, 84–90. doi: 10.1016/j.aquaculture.2010.09.038

Lewis, B. P., Burge, C. B., and Bartel, D. P. (2005). Conserved seed pairing, often flanked by adenosines, indicates that thousands of human genes are microRNA targets. *Cell* 120, 15–20. doi: 10.1016/j.cell.2004.12.035

Li, X. K., and Jin, P. (2010). Roles of small regulatory RNAs in determining neuronal identity. *Nat. Rev. Neurosci.* 11, 329–338. doi: 10.1038/nrn2739

Liu, X., Luo, B. Y., Feng, J. B., Zhou, L. X., Ma, K. Y., and Qiu, G. F. (2019). Identification and profiling of microRNAs during gonadal development in the giant freshwater prawn *Macrobrachium rosenbergii*. *Sci. Rep.* 9:2406.

Luther, J. M., and Brown, N. J. (2011). The renin-angiotensin-aldosterone system and glucose homeostasis. *Trends Pharmacol. Sci.* 32, 734–739.

Malki, K., Du Rietz, E., Crusio, W. E., Pain, O., Paya-Cano, J., Karadaghi, R. L., et al. (2016a). Transcriptome analysis of genes and gene networks involved in aggressive behavior in mouse and zebrafish. *Am. J. Med. Gen. Part B Neuropsychiatr. Gen.* 171, 827–838. doi: 10.1002/ajmg.b.32451

Malki, K., Tosto, M. G., Pain, O., Sluyter, F., Mineur, Y. S., Crusio, W. E., et al. (2016b). Comparative mRNA analysis of behavioral and genetic mouse models of aggression. *Am. J. Med. Gen.Part B Neuropsychiatr. Gen.* 171B, 427–436. doi: 10.1002/ajmg.b.32424

Malki, K., Pain, O., Du Rietz, E., Tosto, M. G., Paya-Cano, J., Sandnabba, K. N., et al. (2014). Genes and gene networks implicated in aggression related behaviour. *Neurogenetics* 15, 255–266. doi: 10.1007/s10048-014-0417-x

Momohara, Y., Aonuma, H., and Nagayama, T. (2018). Tyraminergic modulation of agonistic outcomes in crayfish. *J. Comp. Physiol.Neuroethol. Sens. Neural Behav. Physiol.* 204, 465–473. doi: 10.1007/s00359-018-1255-3

Momohara, Y., Minami, H., Kanai, A., and Nagayama, T. (2016). Role of cAMP signalling in winner and loser effects in crayfish agonistic encounters. *Eur. J. Neurosci.* 44, 1886–1895. doi: 10.1111/ejn.13259

Mulloney, B., and Smarandache-Wellmann, C. (2012). Neurobiology of the crustacean swimmeret system. *Prog. Neurobiol.* 96, 242–267. doi: 10.1016/j.pneurobio.2012.01.002

Nawrocki, E. P., Burge, S. W., Alex, B., Jennifer, D., Eberhardt, R. Y., Eddy, S. R., et al. (2015). Rfam 12.0: updates to the RNA families database. *Nucleic Acids Res.* 43, D130–D137.

Pang, Y. Y., Song, Y. M., Zhang, L., Song, X. Z., Zhang, C., Lv, J. H., et al. (2019a). 5-HT2B, 5-HT7, and DA2 receptors mediate the effects of 5-HT and DA on agonistic behavior of the Chinese mitten crab (*Eriocheir sinensis*). *ACS Chem. Neurosci.* 10, 4502–4510. doi: 10.1021/acschemneuro.9b00342

Pang, Y. Y., Zhang, C., Xu, M. J., Huang, G. Y., Cheng, Y. X., and Yang, X. Z. (2019b). The transcriptome sequencing and functional analysis of eyestalk ganglions in Chinese mitten crab (*Eriocheir sinensis*) treated with different photoperiods. *PloS One* 14:e0210414. doi: 10.1371/journal.pone.0210414

Phillips, M. I., Weyhenmeyer, J., Felix, D., Ganten, D., and Hoffman, W. E. (1979). Evidence for an endogenous brain renin-angiotensin system. *Federation Proc.* 38, 2260–2266.

Rivetti, C., Campos, B., Pina, B., Raldua, D., Kato, Y., Watanabe, H., et al. (2018). Tryptophan hydroxylase (TRH) loss of function mutations induce growth and behavioral defects in *Daphnia magna*. *Sci. Rep.* 8:1518.

Romano, N., and Zeng, C. (2016). Cannibalism of decapod crustaceans and implications for their aquaculture: a review of its prevalence, influencing factors, and mitigating methods. *Rev Fish. Sci. Aqu.* 25, 42–69. doi: 10.1080/23308249.2016.1221379

Sim, M. S., Soga, T., Pandy, V., Wu, Y. S., Parhar, I. S., and Mohamed, Z. (2017). MicroRNA expression signature of methamphetamine use and addiction in the rat nucleus accumbens. *Metab. Brain Dis.* 32, 1767–1783. doi: 10.1007/s11011-017-0061-x

Sneddon, L. U., Taylor, A. C., Huntingford, F. A., and Watson, D. G. (2000). Agonistic behaviour and biogenic amines in shore crabs *Carcinus maenas*. *J. Exp. Biol.* 203, 537–545.

Song, W., Zhu, Y. F., Wang, L. M., Jiang, K. J., Zhang, F. Y., Ma, C. Y., et al. (2018). Identification and profiling of microRNAs of *Euphausia superba* using Illumina deep sequencing. *J. Oceanol. Limnol.* 36, 2278–2287. doi: 10.1007/s00343-019-7229-7

Thongbuakaew, T., Suwansa-ard, S., Sretarugsa, P., Sobhon, P., and Cummins, S. F. (2019). Identification and characterization of a crustacean female sex hormone in the giant freshwater prawn. *Macrobrachium rosenbergii*. Aquaculture 507, 56–68. doi: 10.1016/j.aquaculture.2019.04.002

Uray, I. P., Dmitrovsky, E., and Brown, P. H. (2016). Retinoids and rexinoids in cancer prevention: from laboratory to clinic. *Semin. Oncol.* 43, 49–64. doi: 10.1053/j.seminoncol.2015.09.002

Vaughan, D., Brogioli, M., Maier, T., White, A., Waldron, S., Rittweger, J., et al. (2016). The angiotensin converting enzyme insertion/deletion polymorphism modifies exercise-induced muscle metabolism. *PloS One* 11:20. doi: 10.1371/journal.pone.0149046

Vomel, M., and Wegener, C. (2008). Neuroarchitecture of aminergic systems in the larval ventral ganglion of *Drosophila melanogaster*. *PloS One* 3:18. doi: 10.1371/journal.pone.0001848

Wang, L., Xu, X., Yang, J., Chen, L., Liu, B., Liu, T., et al. (2018). Integrated microRNA and mRNA analysis in the pathogenic filamentous fungus *Trichophyton rubrum*. *BMC Genomics* 19:933. doi: 10.1186/s12864-018-5316-3

Wang, L. A., de Kloet, A. D., Smeltzer, M. D., Cahill, K. M., Hiller, H., Bruce, E. B., et al. (2018). Coupling corticotropin-releasing-hormone and angiotensin converting enzyme 2 dampens stress responsiveness in male mice. *Neuropharmacology* 133, 85–93. doi: 10.1016/j.neuropharm.2018.01.025

White, M. C., Fleeman, R., and Arnold, A. C. (2019). Sex differences in the metabolic effects of the renin-angiotensin system. *Biol. Sex Differ.* 10:31.

Wortham-Neal, J. L. (2002). Intraspecific agonistic interactions of *Squilla empusa* (*Crustacea* : *Stomatopoda*). *Behaviour* 139, 463–486. doi: 10.1163/15685390260135961

Wu, C., Lv, C., Chen, F. Q., Ma, X. Y., Shao, Y., and Wang, Q. Y. (2015). The function of miR-199a-5p/Klotho regulating TLR4/NF-kappa B p65/NGAL pathways in rat mesangial cells cultured with high glucose and the mechanism. *Mol. Cell. Endocrinol.* 417, 84–93. doi: 10.1016/j.mce.2015.09.024

Wu, D. M., Wang, S., Wen, X., Han, X. R., Wang, Y. J., Shen, M., et al. (2018). Inhibition of microRNA-200a upregulates the expression of striatal dopamine receptor D2 to repress apoptosis of striatum via the cAMP/PKA signaling pathway in rats with Parkinson's disease. *Cell. Physiol. Biochem.* 51, 1600–1615. doi: 10.1159/000495649

Wu, L. H., Zhao, Q. L., Zhu, X. C., Peng, M., Jia, C. Y., Wu, W., et al. (2010). A novel function of microRNA Let-7d in regulation of galectin-3 expression in attention deficit hyperactivity disorder rat brain. *Brain Pathol.* 20, 1042–1054. doi: 10.1111/j.1750-3639.2010.00410.x

Xiaobei, Z., Helen, L., and Robinson, M. D. (2014). Robustly detecting differential expression in RNA sequencing data using observation weights. *Nucleic Acids Res.* 42:e91. doi: 10.1093/nar/gku310

Yan, J., Yu, Y., Sun, Y., Hu, R., and Jiang, H. (2017). Ketamine induces neuronal apoptosis and cognitive disorder via miR-199a-5p/HIF-1α in neonatal rats. *Mol. Cell. Toxicol.* 13, 395–404. doi: 10.1007/s13273-017-0044-3

Yang, X. Z., Pang, Y. Y., Huang, G. Y., Xu, M. J., Zhang, C., He, L., et al. (2019). The serotonin or dopamine by cyclic adenosine monophosphate-protein kinase A pathway involved in the agonistic behaviour of Chinese mitten crab, *Eriocheir sinensis*. *Physiol. Behav.* 209:112621. doi: 10.1016/j.physbeh.2019.112621

Zhang, X. F., Zheng, Y., Jagadeeswaran, G., Ren, R., Sunkar, R., and Jiang, H. B. (2012). Identification and developmental profiling of conserved and novel microRNAs in *Manduca sexta*. *Insect Biochem. Mol. Biol.* 42, 381–395. doi: 10.1016/j.ibmb.2012.01.006

Zhang, Y., Yang, L., Ling, C., and Heng, W. (2018). HuR facilitates cancer stemness of lung cancer cells via regulating miR-873/CDK3 and miR-125a-3p/CDK3 axis. *Biotechnol. Lett.* 40, 623–631. doi: 10.1007/s10529-018-2512-9

Zhu, F., Fu, Y. Y., Mu, C. K., Liu, L., Li, R. H., Song, W. W., et al. (2018). Molecular cloning, characterization and effects of catechol-omethyltransferase (comt) mrna and protein on aggressive behavior in the swimming crab *Portunus trituberculatus*. *Aquaculture* 495, 693–702. doi: 10.1016/j.aquaculture.2018.06.055

Conflict of Interest: The authors declare that the research was conducted in the absence of any commercial or financial relationships that could be construed as a potential conflict of interest.

frontiers in Genetics

ORIGINAL RESEARCH
published: 23 July 2020
doi: 10.3389/fgene.2020.00712

Plasma Small Extracellular Vesicles Derived miR-21-5p and miR-92a-3p as Potential Biomarkers for Hepatocellular Carcinoma Screening

Andrei Sorop[1,2†], Razvan Iacob[1,3,4†], Speranta Iacob[1,3,4], Diana Constantinescu[1], Leona Chitoiu[5], Tudor Emanuel Fertig[3,5], Anca Dinischiotu[2], Mihaela Chivu-Economescu[2,6], Nicolae Bacalbasa[1,3], Lorand Savu[1,7], Liliana Gheorghe[1,3,4], Simona Dima[1,4] and Irinel Popescu[1,4,7*]*

[1] Center of Excellence in Translational Medicine, Fundeni Clinical Institute, Bucharest, Romania, [2] Faculty of Biology, University of Bucharest, Bucharest, Romania, [3] "Carol Davila" University of Medicine and Pharmacy, Bucharest, Romania, [4] Digestive Diseases and Liver Transplantation Center, Fundeni Clinical Institute, Bucharest, Romania, [5] Ultrastructural Pathology Laboratory, Victor Babeş National Institute, Bucharest, Romania, [6] Department of Cellular and Molecular Pathology, Stefan S. Nicolau Institute of Virology, Bucharest, Romania, [7] "Titu Maiorescu" University of Medicine and Pharmacy, Bucharest, Romania

Introduction: Liquid biopsy using circulating microvesicles and exosomes is emerging as a new diagnostic tool that could improve hepatocellular carcinoma (HCC) early diagnosis and screening protocols. Our study aimed to investigate the utility of plasma exosomal miR-21-5p and miR-92-3p for HCC diagnosis during screening protocols.

Methods: The study group included 106 subjects: 48 patients diagnosed with HCC during screening, who underwent a potentially curative treatment (surgical resection or liver transplantation), 38 patients with liver cirrhosis (LC) on the waiting list for liver transplantation, and 20 healthy volunteers. The exosomes were isolated by precipitation with a reagent based on polyethylene glycol and were characterized based on morphological aspects (i.e., diameter); molecular weight; CD63, CD9, and CD81 protein markers; and exosomal miR-21-5p and miR-92a-3p expression levels.

Results: We first demonstrate that the exosome population isolated with the commercially available Total Exosome Isolation kit respects the same size ranging, morphological, and protein expression aspects compared to the traditional ultracentrifugation technique. The analysis of the expression profile indicates that miR-21-5p was upregulated ($p = 0.017$), and miR-92a-3p was downregulated ($p = 0.0005$) in plasma-derived exosomes from HCC subjects, independently from the patient's characteristics. AUROC for HCC diagnosis based on AFP (alpha-fetoprotein) was 0.72. By integrating AFP and the relative expression of exosomal miR-21-5p and miR-92a-3p in a logistic regression equation for HCC diagnosis, the combined AUROC of the new exosomal miR HCC score was 0.85—significantly better than serum AFP alone ($p = 0.0007$).

OPEN ACCESS

Edited by:
Junjie Xiao,
Shanghai University, China

Reviewed by:
Alessio Naccarati,
Italian Institute for Genomic Medicine (IIGM), Italy
Marco Maugeri,
University of Skövde, Sweden

***Correspondence:**
Simona Dima
dima.simona@gmail.com
Irinel Popescu
irinel.popescu220@gmail.com

[†] These authors have contributed equally to this work and share first authorship

Specialty section:
This article was submitted to RNA, a section of the journal Frontiers in Genetics

Received: 20 January 2020
Accepted: 11 June 2020
Published: 23 July 2020

Citation:
Sorop A, Iacob R, Iacob S, Constantinescu D, Chitoiu L, Fertig TE, Dinischiotu A, Chivu-Economescu M, Bacalbasa N, Savu L, Gheorghe L, Dima S and Popescu I (2020) Plasma Small Extracellular Vesicles Derived miR-21-5p and miR-92a-3p as Potential Biomarkers for Hepatocellular Carcinoma Screening. Front. Genet. 11:712. doi: 10.3389/fgene.2020.00712

Conclusion: Together with serum AFP, plasma exosomal miR-21-5p and miR-92a-3p could be used as potential biomarkers for HCC diagnosis in patients with LC subjected to screening and surveillance.

Keywords: exosomes, microRNA, serum biomarkers, hepatocellular carcinoma, screening

INTRODUCTION

Hepatocellular carcinoma (HCC) is the fifth most common cancer worldwide and the second most frequent cause of cancer-related death globally. It is closely linked to the presence of an underlying chronic liver disease and has a high clinical and biological heterogeneity (Laurent-Puig et al., 2001; Akinyemiju et al., 2017). Early detection of HCC is critical for a curative treatment and for improving long-term outcomes of patients. HCC detection at an early stage is challenging as the disease usually progresses asymptomatically. Thus, screening programs are used for cancer detection in patients at risk for tumor development and usually include ultrasound (US) with or without serum biomarkers, such as alpha-fetoprotein (AFP) (Galle et al., 2018; Heimbach et al., 2018). Pooled sensitivity of US for any HCC stage in a meta-analysis of 32 studies (Tzartzeva et al., 2018) was good (84%, 95% CI 76–92), but it decreased to a modest value (47%, 95% CI 33–61) for the detection of early stage HCC. Serum AFP levels also exhibit a low sensitivity for early HCC diagnosis, ranging from 20 to 65% (El-Serag and Davila, 2011; Tian et al., 2017).

Biomarker quantification using blood samples is less expensive than radiological imaging and could potentially detect early stage HCC even before it could be identified by conventional imaging (Johnson et al., 2014). The use of other biomarkers, such as AFP isoforms or des-gamma-carboxy prothrombin (DCP), has been proposed to improve the accuracy of AFP in the early detection of HCC and subsequent therapeutic response monitoring (Lim et al., 2016; Cerban et al., 2018; Li and Chen, 2019). The GALAD scoring algorithm, comprising gender, age, AFP-L3, AFP, and DCP, has very good performance for HCC detection in large validation studies, including patients of diverse liver disease etiologies, even for detecting early stage HCC (BCLC 0/A) (Berhane et al., 2016; Best et al., 2019). Advances in genomics and proteomics platforms have resulted in the identification of numerous other novel biomarkers and have improved the diagnostic accuracy of HCC. The study of these biomarkers has contributed to the clarification of mechanisms driving hepatocarcinogenesis, facilitating personalized diagnosis and treatment strategies.

Over the past decade, research on small extracellular vesicles (EVs)–exosomes has made significant advances, highlighting their important role as microRNA (miRNA) carriers, disease biomarkers, and potential therapeutic targets (Ailawadi et al., 2015; Yanez-Mo et al., 2015). MiRNAs are highly conserved small non-coding RNAs, that influence the expression of almost 30% of human protein-coding genes at the posttranscriptional and the translational levels (Fu et al., 2012). Exosomes are a specific population of EVs defined by their diameter, between 40 and 150 nm (Malm et al., 2016).

Exosomes are involved in HCC progression by regulating proliferation, angiogenesis, and invasion of tumor cells. Exosomes may also regulate HCC hypoxia stress and drug resistance. Based on these observations, exosomes are emerging as novel biomarkers for liver diseases including HCC (Cai et al., 2017). Exosomes carry a wide range of components, such as miRNAs, mRNAs, transcription factors, proteins, and lipids. This content is highly variable and depends on cellular origin, thus performing powerful and transmissible functions on recipient cells (Melo et al., 2015; Milane et al., 2015). Many studies have shown that circulating miRNAs derived from exosome species are involved in the development of HCC and can be considered as possible diagnostic or prognostic markers (Xu et al., 2011).

The aim of the present study was to investigate the clinical utility of plasma exosomal miR-21-5p and miR-92a-3p quantification for HCC diagnosis as potential new biomarkers for HCC screening programs.

MATERIALS AND METHODS

Patients and Sample Collection

A total number of 106 subjects were included in this study after written informed consent according to the Guidelines of the Fundeni Clinical Institute Ethics Committee (30884/22.10.2014 and 29435/12.09.2016), which are subject to the Helsinki Declaration on ethical principles for medical research involving human subjects. The patients were divided into three groups: 48 patients diagnosed with HCC during the screening program, who underwent a potentially curative treatment at the Digestive Diseases and Liver Transplantation Center, Fundeni Clinical Institute (all cases had a confirmed HCC diagnosis by pathological examination following the therapeutic procedure); 38 patients included on the waiting list for liver transplantation for liver cirrhosis (LC) and, thus, during the screening program for HCC; and as a control group (C) 20 healthy volunteers. Peripheral blood samples from all the subjects were collected in 5-mL vacutainer (Becton Dickinson) tubes spray-coated with EDTA as anticoagulant and centrifuged at 4200 × rpm for 10 min at room temperature (RT) to separate the plasma fraction. The plasma was transferred to fresh tubes and stored at −80°C until further analysis.

Plasma Exosome Isolation

Exosome isolation was performed by two well-known techniques. The Total Exosome Isolation (TEIp) kit is based on polyethylene glycol precipitation (PEG) and ultracentrifugation (UC). The TEIp kit (Invitrogen, Life Technologies) was used to isolate exosomes (small EVs) from the plasma following the manufacturer's protocol with minor modifications

(Rider et al., 2016; Moon et al., 2019). First, plasma samples were thawed at 37°C for 1 min in a water bath. Exosomes were isolated from approximately 2 mL of cryopreserved plasma by differential centrifugation at 3000 × *g* for 20 min and at 15,000 × *g* for 20 min at 4°C to completely remove the cellular components. Briefly, 0.5 volumes of 1× PBS and 0.05 volumes of Proteinase K were added to the clarified plasma by mixing and incubated at 37°C for 10 min. To the mixed solution, 0.2 volumes of total exosome isolation reagent was added and incubated on ice for 1 h, followed by centrifugation at 10,000 × *g* for 10 min at 4°C. Finally, the exosome pellets were resuspended in the appropriate volume for characterization and RNA isolation.

One milliliter of plasma for characterization methods was ultracentrifuged according to the method previously described (Thery et al., 2006) with some protocol modifications. Briefly, plasma was centrifuged at 3000 × *g*, 30 min, and 4°C to remove cell debris. Then, the supernatants were collected in ultracentrifuge tubes, and 1× PBS was added to up to two thirds of the tubes and centrifuged at 29,500 × *g* for 45 min, 4°C to remove large particles. Next, we filtrated the supernatants with a 0.22-μm filter, and the exosomes were pelleted with ultracentrifugation at 120,000 × *g* for 2 h, 4°C in an SW-40-Ti swinging-bucket rotor, Optima XPN-100 ultracentrifuge instrument (Beckman Coulter, Brea, CA, United States). The exosome pellets were resuspended in appropriate volumes for further experiments.

The characterization of the patient's plasma-derived exosomes was made through the following methods: nanoparticle tracking analysis, negative stain, transmission electron cryomicroscopy (cryoTEM), and western blotting (Tang et al., 2017).

Nanoparticle Tracking Analysis

The size distribution of small EVs was determined using a Delsa Nano Analyzer (DelsaNano, Beckman Coulter, Brea, CA, United States). This instrument utilizes photon correlation spectroscopy (PCS) and electrophoretic light scattering techniques to determine the size distribution and zeta potential of exosomes. The capture data and analysis settings for intensity distribution were performed manually according to the manufacturer's instructions.

Negative Stain

Screening of specimens by negative stain in TEM represented a quick method to analyze the distribution of particles and to select an optimal dilution for cryoTEM. Copper grids (100 mesh) coated with formvar and carbon films were glow discharged to increase the binding of particles to the support film. A volume of 5 μl of sample was incubated for 2 min on grids at RT. Excess sample was removed by blotting. The grids were stained with three successive drops of 2% uranyl acetate with excess stain again removed by blotting. Image acquisition was done at RT using a 200 kV Talos F200C TEM (Thermo Fisher Scientific) under similar imaging conditions as for cryoTEM.

Transmission Electron Cryomicroscopy

Samples were embedded in a thin layer of vitreous ice by rapid plunging in liquid nitrogen (LN_2)-cooled ethane, using a Leica grid plunging system (Leica EM GP, Leica Microsystems, Wetzlar, Germany). Briefly, copper grids (Quantifoil R2/2, Quantifoil Micro Tools, Großlöbichau, Germany) were glow discharged and then incubated for 2 min at 90% humidity with a 5-μl droplet of isolated EVs and finally blotted for 5 s before plunging. The grids were then transferred under liquid LN_2 to the cold stage of a 200 kV Talos F200C TEM (Thermo Fisher Scientific) equipped with a 4 k × 4 k Ceta camera. Specimens were examined in the low-dose mode, at maximum 8 electrons per $Å^2$ and 8–12 μm under focus. Images acquired at 28,000×, 36,000×, and 45,000× nominal magnifications gave a final object sampling of 5.2, 4.1, and 3.2 Å, respectively.

Western Blotting Analysis

The exosome concentration was determined indirectly by quantifying the protein concentration in exosome lysates. Isolated exosomal pellets from the plasma were washed in phosphate-buffered saline, mixed with RIPA lysis buffer containing Complete O^{TM}, Mini, EDTA-free Protease Inhibitor Cocktail (Roche Applied Science). The protein concentration of exosome lysates was determined using BCA protein assay (Pierce, Thermo Fisher Scientific). The absorbance was read at 562 nm using a TriStar^2 S LB 942 plate reader (Berthold). To ascertain the isolation of the exosomes from plasma samples, western blotting analysis was established for the cluster of differentiation 63 (CD63), CD9, and CD81. Whole protein extracts (60 μg) were electrophoretically separated by SDS-PAGE and transferred onto polyvinylidene fluoride (PVDF) membranes that were subsequently blocked in tris-buffer saline (TBS)-0.5% Tween 20 with 2% bovine serum albumin and then incubated with the primary antibodies against proteins of interest at 4°C overnight. The following monoclonal primary antibodies were used: mouse anti-CD63 (ID: 10628D, clone Ts63) (1:250), mouse anti-CD9 (ID: 10626D, clone Ts9) (1:250), and mouse anti-CD81 (MA5-13548, clone 1.3.3.22) (1:250), all from Invitrogen (Life Technologies). Mouse monoclonal anti-β-actin (clone Ac-74) (Sigma-Aldrich) (1:2000) was used as a control. Membranes were then washed with TBS-T (0.5% Tween-20) and incubated 2 h with secondary antibodies anti-mouse conjugated with HRP (RD Systems) (1:2000). Signals were developed using ECL HRP chemiluminescent substrate (Invitrogen) and captured using MicroChemi 4.2 system (Bio Imaging Systems).

Isolation of Exosomal RNA

The RNA was extracted from exosomes that have been isolated with a TEIp kit. Isolation of total RNA from exosomes was performed by the standard method with TRIzol (Invitrogen, Thermo Fisher Scientific) according to manufacturer specifications with several modifications: 1 mL of TRIzol was added to the exosome samples and incubated overnight at −20°C. After incubation, 300 μl of chloroform was added and centrifuged at 12,000 × *g* for 15 min at 4°C to separate a clear upper aqueous layer containing total RNA that precipitates with 1 volume of isopropanol 100% and glycogen (20 mg/mL) as a carrier. Samples were incubated for 1 h on ice to get a maximum recovery of the amount of RNA species from exosomes (including miRNAs).

Exosomal RNA samples were centrifuged at 15,000 × *g*, and the pellet was washed twice in 1 mL of 75% ethanol. Subsequently, the pellet was air-dried and eluted in 15 μl RNase- and DNase-free water. The quantity of the RNA was determined by the concentration and purity (A260/A280 and A260/A230) assessed by NanoDrop ND1000 (NanoDrop Technologies, Waltham, MA, United States). Quality and size distribution pattern of exosomal RNA was analyzed using chip-based capillary electrophoresis Agilent Bioanalyzer 2100 with a Small RNA Chip and Pico RNA Chip (Agilent Technologies, Santa Clara, CA, United States), according to manufacturer protocol.

Assessment of Plasma Exosomal miRNA Levels Using Quantitative Real-Time PCR

MiRNA profiling was performed for the exosome samples isolated by the TEIp kit, and the expression levels were quantified by real-time quantitative PCR (RT-qPCR). TaqMan probes for miR-21-5p (ID: 000397) and miR-92a-3p (ID: 000431) (Applied Biosystems, Thermo Fisher Scientific) were used for quantitative real-time PCR (qRT-PCR). A TaqMan MicroRNA Reverse Transcription Kit (Applied Biosystems, Thermo Fisher Scientific) was used to synthesize cDNA by incubation as follows: 4°C for 5 min, 16°C for 30 min, 42°C for 30 min, and 85°C for 5 min. The amplification step was performed by TaqMan Universal PCR Master Mix, No AmpErase UNG (Applied Biosystems, Thermo Fisher Scientific) with the following thermocycler protocol: 95°C for 10 min + (95°C for 15 s; 60°C for 60 s) for 40 cycles. The ABI PRISM 7300 Sequence Detection System (Applied Biosystems, Thermo Fisher Scientific) was used to analyze miR-21-5p, miR-92a-3p relative expression normalized to miR-16-5p (ID:000391) (Davoren et al., 2008; Matsumura et al., 2015).

The expression level of the three miRNAs are related as fold changes $2^{-\Delta\Delta\ Ct}$ (see section "Materials and Methods" in **Supplementary Data S1**) above to the mean expression level determined by assessing the healthy controls (n = 20), thus providing a quantitative parameter to define the exosomal expression of miRNAs in HCC and LC samples, respectively, that was used in subsequent statistical analyses.

Statistical Analysis

Categorical variables were expressed as percentages of respective populations and compared between study groups using the Chi-square test. Continuous variables, including the expression levels of the analyzed exosomal miRNAs, were compared between study groups using the Mann–Whitney U test or Student's t-test when appropriate. Logistic regression was used to generate a multiparametric predictive score for HCC diagnosis. The characteristics of different diagnostic tests for HCC diagnosis were investigated by the means of receiver operating characteristic (ROC) curves and compared using the empirical non-inferiority test of the AUROCs. A p-value of <0.05 was considered for statistical significance. Statistical analysis was conducted using NCSS 9 and MedCalc 19.0.7 statistical software packages.

TABLE 1 | Patient's demographic and clinical characteristics in the two study groups depicted as percentages of respective categories or mean ± standard deviation (LC and HCC).

Variable	LC	HCC	*p*-Value
Age > 60 years	36.84%	68.75%	0.003
Male	55.26%	56.25%	0.92
HVC etiology	38.89%	52.08%	0.23
HBV etiology	33.33%	33.33%	1
HDV etiology	25%	8.33%	0.07
INR	1.5 ± 0.49	1.12 ± 0.18	<0.0001
Tbil (mg/dl)	2.99 ± 3.13	0.83 ± 0.58	<0.0001
Serum creatinine (mg/dl)	0.88 ± 0.24	0.97 ± 0.31	0.29
Serum albumin (g/dl)	3.34 ± 0.79	3.67 ± 0.72	0.06
MELD score	14.02 ± 5.09	8.83 ± 2.83	<0.0001
Ascites	31.11%	6.25%	0.001
Child Pugh class A	52.63%	91.67%	
Child Pugh class B	28.95%	8.33%	
Child Pugh class C	18.42%	0%	0.0001
Serum AFP (ng/ml)	10.52 ± 18.15	200.55 ± 380.29	0.001
miR-21-5p relative expression	15.17 ± 19.29	47.96 ± 71.31	0.017
miR-92a-3p relative expression	1.24 ± 1.18	0.61 ± 0.99	0.0005

HBV, hepatitis B virus; HCV, hepatitis C virus; HDV, hepatitis D virus; INR, international normalized ratio; Tbil, total bilirubin; MELD score, model for end-stage liver disease score; AFP, alpha-fetoprotein.

RESULTS

Patient's Characteristics

Forty-eight patients with HCC, 38 with LC, and 20 healthy volunteers were included in this study. The therapeutic procedure in the HCC study group was liver resection in 42 patients (87.5%) and liver transplantation in 6 patients (12.5%). The following patient's clinical characteristics were registered: age, gender, etiology of liver disease, liver function parameters (INR, total bilirubin level, serum creatinine, serum albumin), MELD score, Child Pugh class, the presence of ascites, and baseline AFP level (ng/mL). Patient's characteristics are depicted in **Table 1**. HCV etiology was the most prevalent in our patients. There were significantly older patients in the HCC group, whereas liver function parameters were more frequently abnormal in the LC group, in comparison to the HCC study group, explained by the fact that, in the HCC study group, liver resection was conducted more frequently than liver transplantation.

Characterization of Plasma-Derived Exosomes

Exosome isolation and characterization are still major scientific challenges (Lotvall et al., 2014), thus optimizing techniques to isolate exosomes for clinical applications is essential for further biomarker studies.

To validate the exosome isolation methods, the characterization study was performed on samples of a small group of eight patients (four HCC, two LC, two C). The analysis has shown that the exosome population isolated

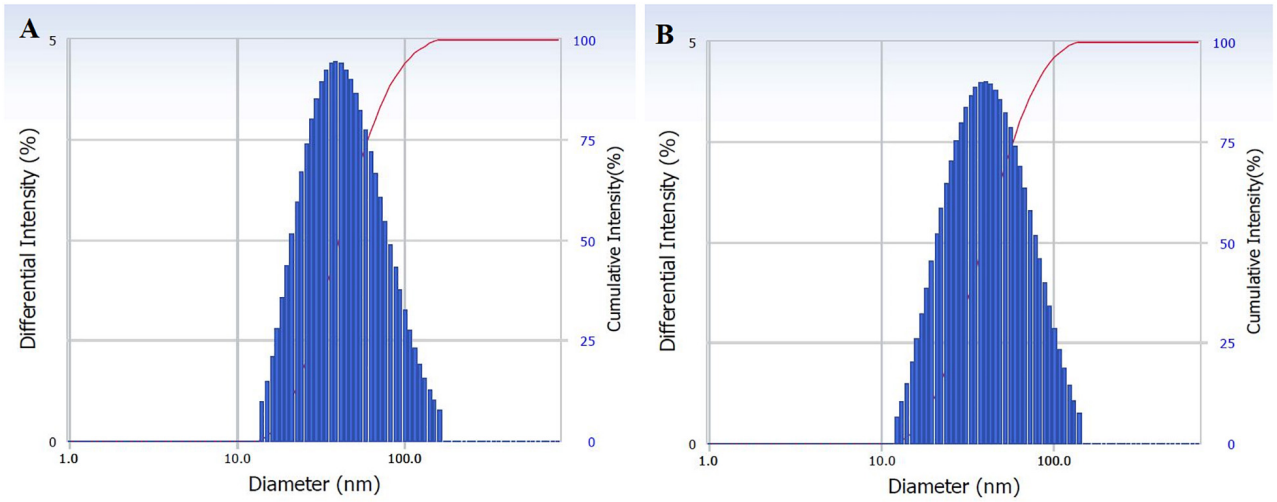

FIGURE 1 | Characterization of isolated exosomes with both methods **(A)** UC and **(B)** TEIp by size distribution of their hydrodynamic diameter using Delsa Nano Analyzer (DelsaNano, Beckman Coulter, Brea, CA, United States). The histograms display the intensity (weighted) size distributions, and the scale of each peak is proportional to the percentage (% amount of the total scattered intensity due to exosome particles).

with the commercial TEIp kit shows the same size ranging, morphological, and protein expression aspects compared to the traditional technique UC. The results of this comparison are reported below.

Nanoparticle Tracking Analysis

The size distribution of hydrodynamic diameters of exosomes was determined in real-time using a DelsaNano C particle analyzer. The average size of exosomes isolated by UC was 62.9 ± 45.6 nm (n = 4) and for exosomes isolated with TEIp was 66.7 ± 45.3 nm (n = 5) (mean ± SD). The overall average size of small EVs varies between 40 and 150 nm; thus, we can observe that the vesicles isolated with both methods have a similar size range (**Figures 1A,B**).

Exosomes were visualized using two electron microscopy (EM) techniques to compare the outcome of the two different EV isolation methods from the blood of HCC patients (TEIp and UC) and validate the presence of EVs in samples for further analysis.

Negative staining of the exosome samples isolated with each of the two methods showed cup-shaped particles within the anticipated size range for exosomes. Moreover, we observed that exosomes isolated with the TEIp kit have a more uniform distribution and a much higher density per grid as compared to the samples obtained by UC at 120,000 × g (**Figure 2**). Even though both types of samples had visible lipid and protein contamination, the EVs isolated by TEIp kit showed significantly reduced levels of membrane and protein aggregates, which were abundant in UC samples (**Figure 2F**).

In addition to negative stain, cryoTEM yielded additional information on exosomes regarding their structure, membrane, and lumen since lipid bilayers and vesicle internal structure could be visualized (Simons and Raposo, 2009).

Transmission Electron Cryomicroscopy

The morphological analysis of small EVs from plasma revealed by cryoTEM showed clearly defined round structures with a visible lipid bilayer, thus confirming the efficiency of isolation of a heterogenous population of EVs, ranging in size between 40 and 150 nm (**Figure 3**). For all samples isolated with both methods, we applied a 10× dilution and a short digestion with proteinase K for 10 min at 37°C, and we observed a higher lipoprotein contamination (**Figure 3B**) and a lower number of vesicles per grid square for samples isolated by ultracentrifugation. To the contrary, TEM showed a far lower concentration of contaminants for samples obtained using the TEIp kit (**Figure 3A**). As compared to negative stain, cryoTEM is a more powerful tool for differentiating membrane-derived vesicles from other lipid contaminants, stemming from substantial advances in contrast enhancement, detector technology and data processing. Because high levels of contaminants may interfere with downstream applications, cryoTEM is essential for sample screening in EV studies. CryoTEM analysis revealed that both techniques successfully isolated exosomes within the expected size range and morphology, consistent with Delsa Nano particle Analyzer results.

Western Blotting Analysis

The presence of exosomes was validated by immunoblotting of specific exosomal protein markers (CD63, CD81, and CD9). Western blot was performed to compare exosome extraction methods through exosome-specific protein analysis with all three different types of antibodies (CD9, CD81, and CD63). As shown in **Figure 4**, there was a fairly similar expression for CD63 for both isolation methods; however, the bands in the CD9 protein were less intense after ultracentrifugation than the corresponding sample bands isolated with the TEIp kit. Only the CD81 protein yield showed better results after UC, its expression showing

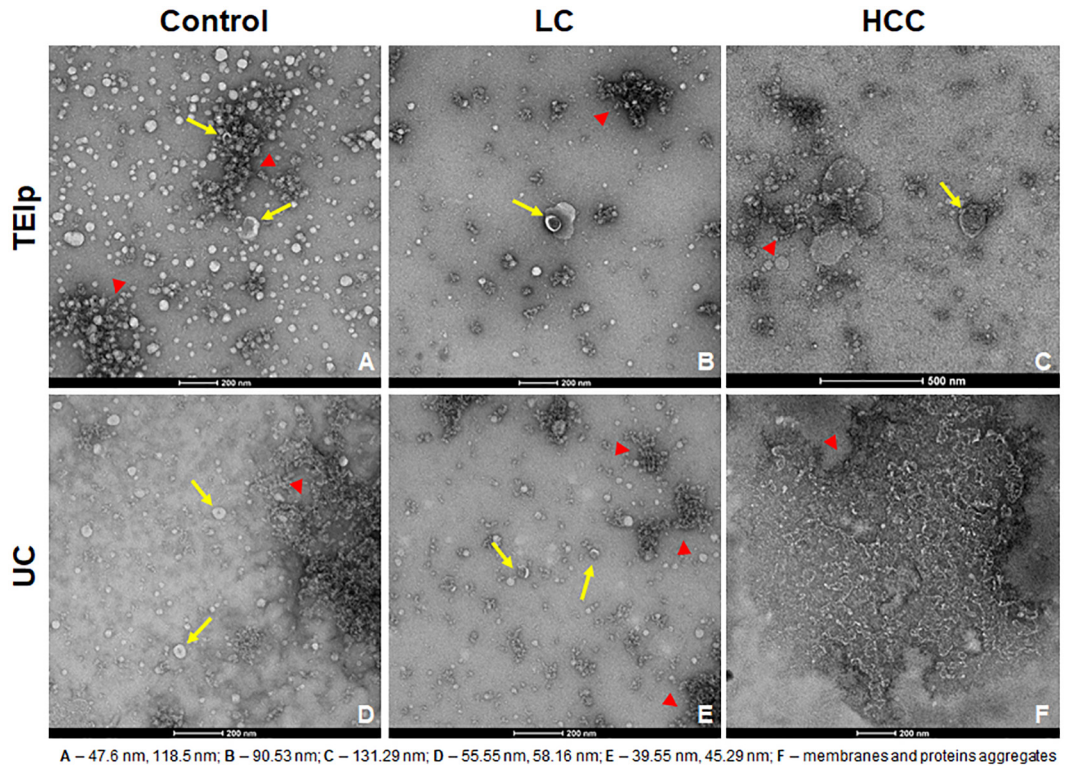

FIGURE 2 | Gallery of negative stain digital micrographs showing cup-shaped exosomes with size ranging in between 40 and 150 nm (yellow arrows) and lipoprotein contamination (red triangles) in samples isolated from patients plasma by TEIp kit **(A–C)** or UC **(D–F)**.

to be strong and uniform across samples with liver pathology compared with controls. The analysis showed that all three exosome-specific proteins are present in the lysate obtained with the TEIp kit. However, looking at pre-equilibrated samples in terms of total amount of protein, we observed less accentuated bands in kit preparations compared with UC. This suggests that there are more non-exosomal proteins in kit preparations that in UC, probably due to precipitation of various other soluble proteins.

The Expression Level of the miR-21-5p and miR-92a-3p in Exosomes Isolated From HCC and Cirrhotic Patients

Bioanalyzer analysis has shown that exosomal RNA is enriched in small RNAs fraction (**Figures 5A–C**), thus it could be used to quantify the expression levels of microRNA species. As expected, there was a statistically significant higher level of baseline AFP in the HCC group ($p = 0.001$; **Figure 6A**). The expression level of the exosomal miR-21-5p was significantly higher in HCC patients in comparison to the LC group ($p = 0.017$; **Figure 6B**), whereas the expression of miR-92a-3p in exosomes was significantly lower in patients with HCC ($p = 0.0005$; **Figure 6C**).

Relative expression levels of miR-21-5p and miR-92a-3p were compared considering different patient characteristics defining demographic features and liver disease severity parameters. There were no statistically significant changes in relative expression identified (**Table 2A**). Furthermore, relative expression levels of miR-21-5p and miR-92a-3p were compared between subgroups defined by significant tumor characteristics: number of tumors, largest tumor diameter, Milan criteria, baseline AFP level with two cutoffs (20 and 100 ng/ml), and no statistically significant differences were noted either (**Table 2B**).

The AUROC for HCC diagnosis for serum AFP in our study group was 0.72.

Using logistic regression, a statistical model to predict HCC diagnosis including baseline serum AFP and relative expression levels of miR-21-5p and miR-92a-3p was generated. Based on the new prediction model, the probability of HCC diagnosis could be calculated as follows: Prob (HCC) = $1/[1 + \text{Exp}(-\text{XB})]$, where XB = $-0.26 - 1.30 \times$ RQ_ miR-92a-3p $+ 0.020 \times$ Serum_AFP $+ 0.025 \times$ RQ_ miR-21-5p.

The AUROC of the new score for HCC diagnosis is 0.85, performing significantly better that AFP alone ($p = 0.0007$) as an HCC screening tool (**Figure 7**).

DISCUSSION

In clinical practice, the most widely used serological markers for HCC screening are serum AFP, Des-gamma carboxyprothrombin (DCP), and human protein-induced vitamin K absence (PIVKA II) (Galle et al., 2018). According to the most recent EASL guidelines, the cutoff value of 20 ng/ml for AFP shows

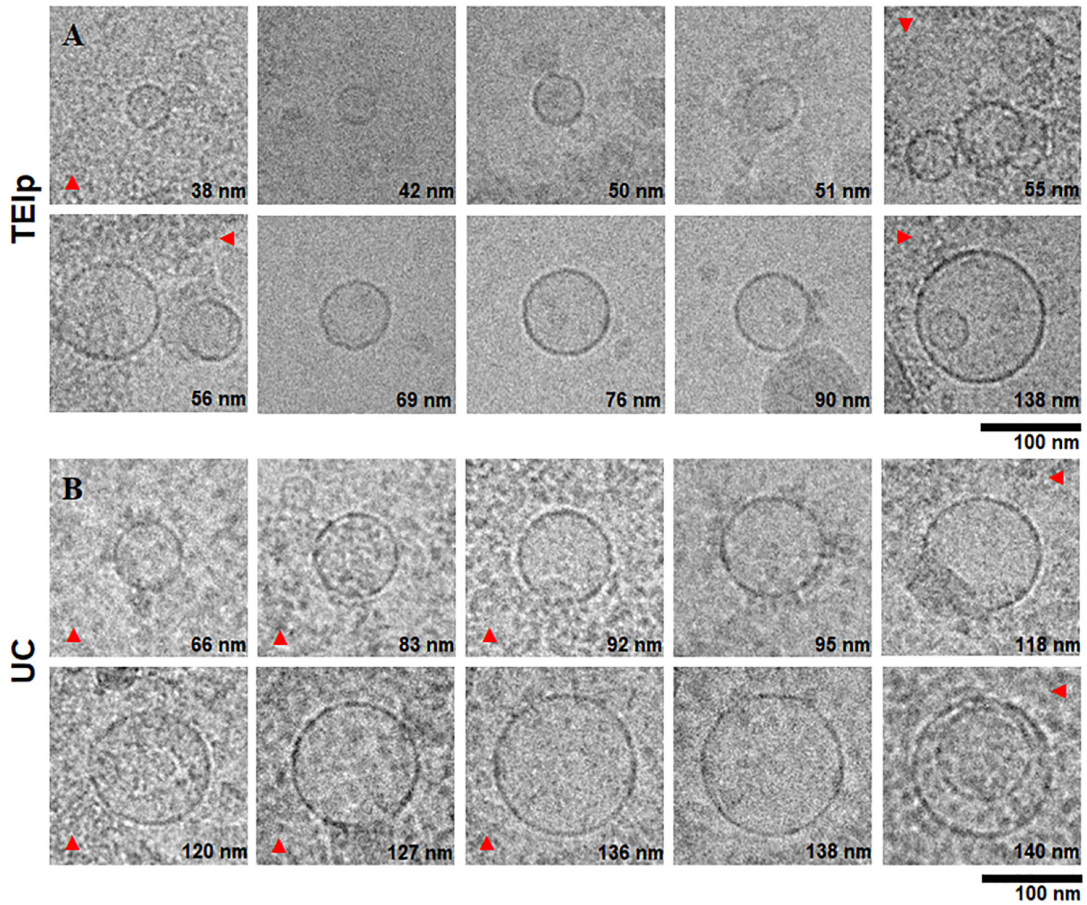

FIGURE 3 | Characterization of small extracellular vesicles by cryo-electron microscopy. Gallery of digital micrographs showing small EVs and lipoprotein contamination (red arrows) in samples isolated from LC patients plasma by exosome isolation TEIp kit **(A)** (top panel) and UC **(B)** (bottom panel).

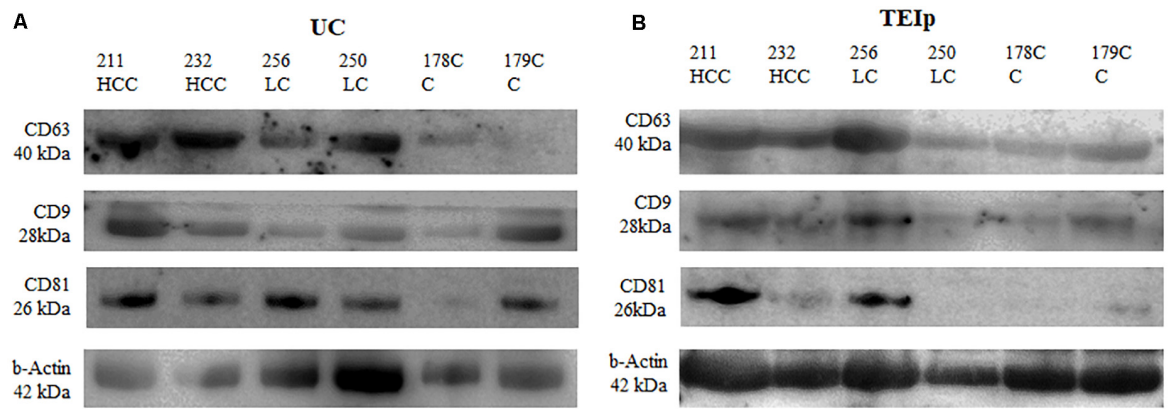

FIGURE 4 | Positive detection for specific exosomal surface markers (CD 63, CD9, and CD81) and for the control-positive marker (b-actin) by immunoblotting. **(A)** exosomes isolated by UC and **(B)** TEIp kit.

good sensitivity for HCC diagnosis while the conventional AFP cutoff value of 200 ng/ml is associated with satisfactory specificity and positive predictive value (i.e., low false positivity) of >97% but at a cost of lower sensitivity and negative predictive value (Galle et al., 2018). Early diagnosis of HCC represents a challenge due to lack of reliable biomarkers, emphasizing the need for new diagnostic tools. Over the past years, the new diagnostic concept known as "liquid biopsy"

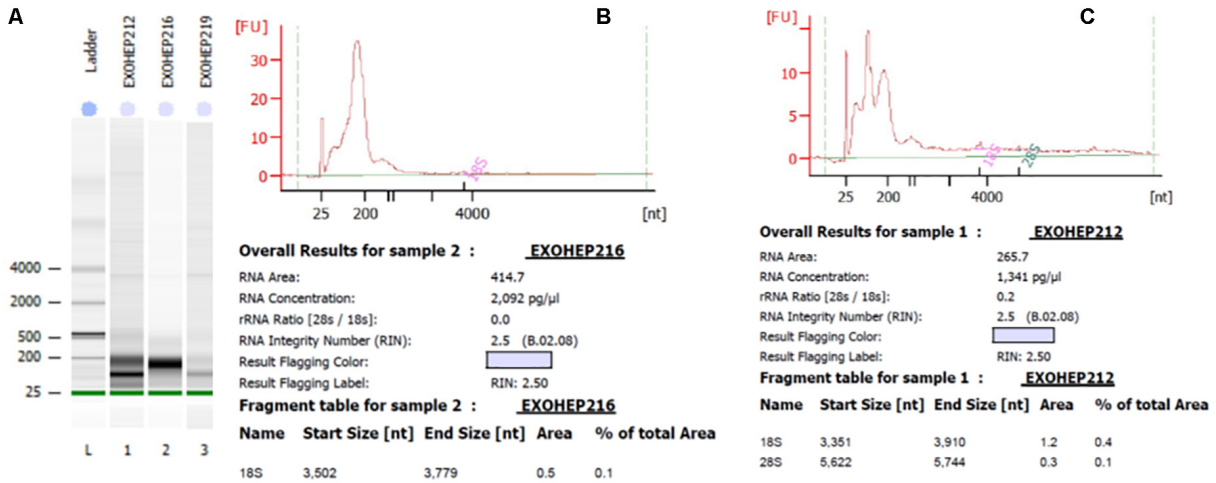

FIGURE 5 | Bioanalyzer analysis of total exosomal RNA by Agilent RNA Pico Chip. The RNA 6000 ladder standard **(A)** first lane contains five RNA fragments between 0.2 and 6 kB. In bands of exosomal RNA from plasma, almost all of the samples revealed a visible band in the small RNA area. **(B,C)** Elecrophoregram for total exosomal RNA.

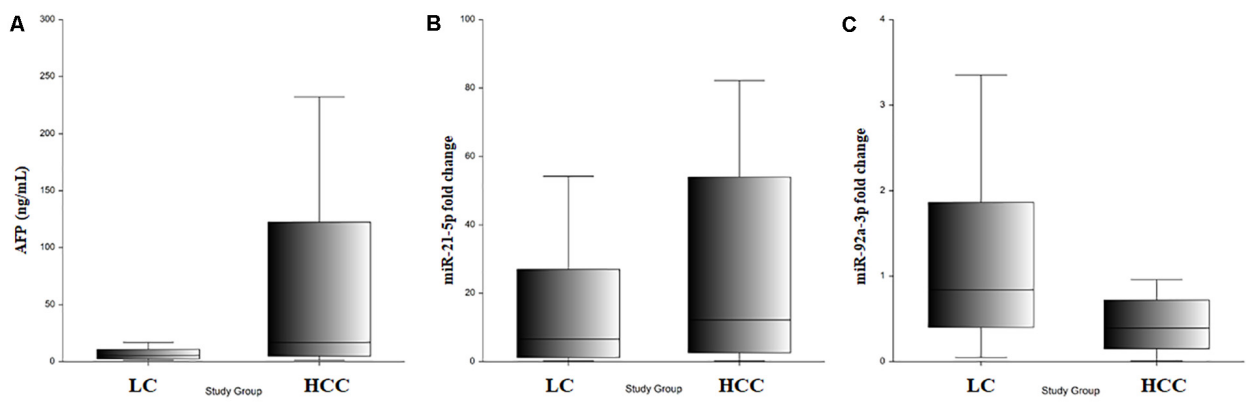

FIGURE 6 | (A) Serum AFP level in LC and HCC. **(B)** Exosomal miR-21-5p relative expression in LC and HCC. **(C)** Exosomal miR-92a-3p relative expression in LC and HCC.

has emerged, and it is also relevant for HCC screening. Circulating tumor cells and circulating tumor DNA are most frequently investigated as liquid biopsy. Exosomes or tumor-educated platelets comprising miRNAs and extracellular RNA are also considered liquid biopsy specimens (Ye et al., 2019). Liquid biopsy has several advantages: non-invasiveness, dynamic monitoring, and the most important of all, overcoming the limit of spatial and temporal tumor heterogeneity. Exosome populations, however, are notoriously heterogeneous and hard to distinguish from spherical lipoproteins when using conventional methods. Therefore, validating the presence of these small EVs in patient samples through imaging methods, prior to other downstream applications, is crucial. In our study, EVs were isolated from plasma samples by precipitation with a reagent based on polyethylene glycol. The presence of EVs in patient's samples was validated using two EM techniques, cryo-electron microscopy and negative stain, and further characterized based on morphological aspects; diameter and molecular weight; CD63, CD9, and CD81 protein markers; and exosomal quality and quantity. The isolation of EVs using a commercially available kit facilitates the workflow in a translational medicine approach, simplifying the diagnostic procedure for clinical practice.

The present work represents a validation trial of two miRNA candidates selected from an miRNA panel obtained following a comprehensive transcriptomic analysis of tissue, serum, and serum exosomes from HCC patients in a previous study by our group (Mjelle et al., 2019). Briefly, paired tissue, serum, and serum exosome sequencing has indicated a correlation of miR-21 between serum exosomes and tumor tissue, supporting the notion that miR-21 could be exported from tissue to circulation via exosomes. On the contrary, tumoral miR-92a-3p was under-expressed, suggesting that it could be less encountered in exosomal fractions. Taken into account their differential expression in our previous work, the aim of the present study

TABLE 2 | Relative gene expression (fold change in gene expression) of miR-21-5p and miR-92a-3p according to different patient's clinical and tumoral characteristics.

Variable	miR-92a-3p	*p*-Value	miR-21-5p	*p*-Value
A: miR relative expression levels according to clinical characteristics (HCC and LC cases)				
Age > 60 years	1.06 ± 1.37		37.12 ± 68.17	
Age < 60 years	0.69 ± 0.67	0.4	29.07 ± 39.86	0.71
Male	0.85 ± 1.07		23.36 ± 34.92	
Female	0.93 ± 1.19	0.74	46.25 ± 74.82	0.64
VHC etiology	0.89 ± 1.32		29.53 ± 52.51	
Non-HCV etiology	0.88 ± 0.91	0.96	36.11 ± 61.66	0.33
HBV etiology	0.69 ± 0.75		38.04 ± 69.54	
Non-HBV etiology	0.98 ± 1.26	0.5	30.56 ± 50.7	0.36
HDV etiology	0.86 ± 0.83		28.6 ± 38.91	
Non-HDV etiology	0.89 ± 1.16	0.34	33.87 ± 60.30	0.68
Abnormal INR (>1.27)	1.15 ± 1.1		20.56 ± 32.47	
Normal INR	0.75 ± 1.11	0.11	40.39 ± 65.69	0.18
Low albumin (<3.5 g/dl)	0.92 ± 0.95		29.29 ± 40.46	
Normal albumin	0.86 ± 1.25	0.12	37.28 ± 68.87	0.86
Abnormal Tbil (>1.2 mg/dl)	1.07 ± 1.1		24.38 ± 59.67	
Normal Tbil	0.79 ± 1.12	0.13	38.34 ± 55.35	0.16
High creatinine (>1.3 mg/dl)	0.65 ± 0.88		30.14 ± 30.79	
Normal creatinine	0.91 ± 1.14	0.43	33.77 ± 58.81	0.98
MELD > 15	1.02 ± 0.93		11.47 ± 14.37	
MELD < 15	0.86 ± 1.15	0.13	37.75 ± 61.07	0.11
Ascites – Yes	0.82 ± 1.02		25.96 ± 39.79	
Ascites – No	0.91 ± 1.16	0.95	35.73 ± 62.79	0.87
B: miR relative expression levels according to tumoral characteristics (HCC cases)				
Single nodule	0.70 ± 1.15		45.35 ± 71.81	
Multiple nodules	0.42 ± 0.30	0.89	57.44 ± 74.30	0.94
Diameter >5 cm	0.63 ± 0.75		45.09 ± 65.48	
Diameter <5 cm	0.62 ± 11.1	0.77	50.55 ± 75.97	1
Outside Milan criteria	0.62 ± 0.74		39.98 ± 63.74	
Within Milan criteria	0.62 ± 1.13	0.77	53.63 ± 76.73	0.47
AFP > 20 ng/ml	0.71 ± 1.26		52.51 ± 85.51	
AFP < 20 ng/ml	0.52 ± 0.65	0.45	43.77 ± 56.73	0.53
AFP > 100 ng/ml	0.92 ± 1.59		34.36 ± 58.05	
AFP < 100 ng/ml	0.49 ± 0.58	0.2	53.56 ± 76.18	0.3

was to investigate the diagnostic utility of these two exosomal miRNAs (miR-21-5p and miR-92a-3p) for HCC diagnosis during a screening program. The present study recruited a different study population directly from the daily clinical practice. All the patients included in present study were subject to the HCC screening protocol that led either to the detection of HCC and a subsequent curative procedure (liver resection or liver transplantation) or were still under the HCC screening protocol while on the waiting list for liver transplantation.

MicroRNAs have been proposed for HCC diagnosis, but most studies are focused on individual miRNAs (Ji et al., 2018). There are, however, some emerging models including multiple miRNAs for HCC diagnosis reported in the literature. The study by Motawi et al. (2015) reveals a serum miRNA panel of miR-19a, miR-146a, miR-195, and miR-192 with high diagnostic accuracy for HCC diagnosis in the context of HCV infection. It has been shown that differentially expressed serum miRNAs, integrated in a 2-miRNA panel according to the regression equation $p = -2.988 + 1.299 \times$ miR-27b-3p $+ 1.245 \times$ miR-192-5p are relevant for HBV-related HCC diagnosis (Zhu et al., 2017).

Other recent studies based on bioinformatics analysis of available data sets show that miRNA panels, including miR-221 and miR-99c, are more effective in HCC diagnosis than the traditional serum marker AFP. This combination has a high diagnostic accuracy with AUROC > 0.9 (Ji et al., 2018). In another study conducted by Zhang et al. (2017), a panel consisting of three serum miRNAs (miR-92-3p, miR-107, and miR-3126-5p) and AFP was significantly better for discriminating the early stage HCC patients and low-level AFP HCC patients from controls (Zhang et al., 2017).

Exosomal miRNAs expression may be used as a serum biomarker instead of serum miRNA expression. Wang et al. (2018) show that serum exosomal levels of miR-122, miR-148a, and miR-1246 are significantly higher in HCC than in LC and normal control subjects. Furthermore, there were no differences in miRNAs expression among studied groups taking into account other variables associated with reduced hepatic synthetic function during liver disease progression (albumin and prothrombin time). This is concordant with our results, showing no difference in miR-21-5p and miR-92a-3p expression according to liver function parameters alone or as defined by MELD score or Child-Pugh class. This finding is significant since it facilitates the use of these miRNA biomarkers irrespective of liver disease severity, during screening and surveillance protocols for HCC.

Liao et al. (2015) show that miRNA-21 is expressed in tumor tissue and derived exosomes. Similarly, we have previously shown a consistent positive correlation of miR-21 between serum exosomes and tumor tissue, indicating that miR-21 could be exported from tissue to circulation via exosomes (Mjelle et al., 2019). Moreover, comparing serum and exosomal levels of the miR-21 in patients with HCC, chronic hepatitis, and healthy controls, Wang et al. (2014) suggest that exosomes are the main vehicle of the miRNAs. In this study, miR-21 expression was significantly higher in exosomes compared to exosome-depleted supernatants and whole serum (Wang et al., 2014). Pu et al. (2018) show that the ratio of miR-144-3p/miR-21-5p investigated in EVs extracted from two groups of patients (HCC and chronic hepatitis B) was significantly higher than in EV-depleted serum. Furthermore, statistical analysis has indicated that the miR-144-3p/miR-21-5p ratio performs better than serum AFP for HCC diagnosis (area under the ROC curve 0.78) (Pu et al., 2018). Our research aimed to demonstrate whether serum exosomal miR-21-5p and miR-92a-3p expression level could distinguish patients with HCC from liver cirrhotic patients as an integrated biomarker panel, irrespective of liver disease etiology.

Fornari et al. (2015) show that HCC-derived exosomes carry miR-519d, miR-21, miR-221, and miR-1228 and that circulating and tissue expression levels are correlated. The authors suggest that miR-519d performs better than AFP for HCC diagnosis. On the contrary, miR-21 and miR-221 had a more heterogenous

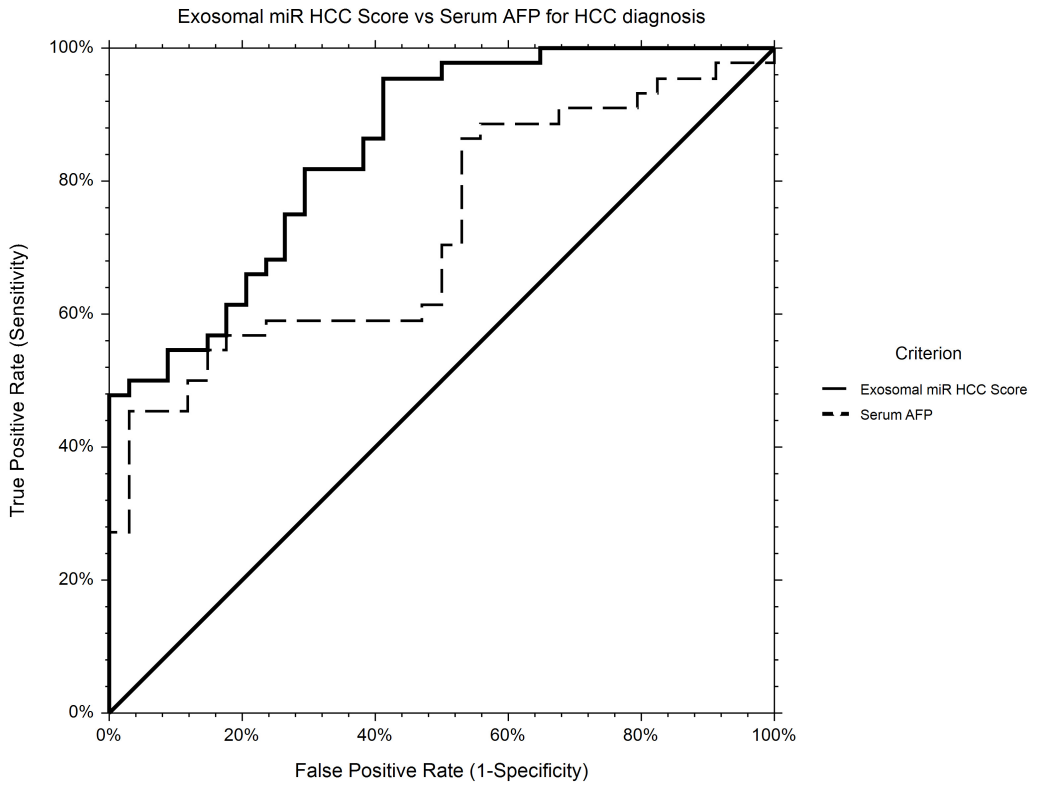

FIGURE 7 | ROC curve for HCC diagnosis for *Exosomal miR HCC Score* in comparison to *Serum AFP*. *Exosomal miR HCC score* (AUROC 0.85) is calculated based on a logistic regression equation including exosomal relative expression of miR-21-5p, miR-92a-3p, and serum AFP level and is significantly better for HCC diagnosis in comparison to AFP alone (AUROC 0.72).

expression in different populations, correlated to viral prevalence and ethnicity (Fornari et al., 2015). This is concordant to our study, which did not show better diagnostic accuracy for miR-21-5p alone in comparison to AFP for diagnosis of HCC (AUROC 0.65 – data not shown).

In other studies, however, serum miR-21 proved to be an independent predictor for tumor recurrence following treatment, stronger than AFP (Tomimaru et al., 2012), raising important physiopathological questions.

Zhou et al. (2018) show that exosomal miR-21 derived from HCC cell lines is increased and promotes cancer progression by activating cancer-associated fibroblasts (CAFs). MiR-21 can be involved in transformation of normal hepatic stellate cells (HSCs) into CAFs by directly targeting the phosphatase and tensin homolog (PTEN) gene, leading to activation of PDK1/AKT signaling pathway in hHSCs and secretion of angiogenic cytokines, including vascular endothelial growth factor (VEGF), matrix metallopeptidase 2 (MMP-2), matrix metallopeptidase 9 (MMP-9), fibroblast growth factor 2 (FGF2), and transforming growth factor (TGF). Experimental data indicates that high levels of serum exosomal miRNA-21 correlate with activation of CAFs and with higher vessel density in patients with HCC. More importantly, the high expression of miR-21 derived from serum exosomes showed a positive correlation with survival rate in patients with HCC. Furthermore these results suggest that miR-21 may be also a potential target for HCC prevention and treatment (Zhou et al., 2018). Recent studies have shown that overexpression of miR-21 could increase the methylation level of the phosphatase and tensin homolog pseudogene 1 (PTENp1) promoter by regulating ten eleven translocation (TET) expression, thereby inhibiting PTENp1 expression, thus leading to downregulation of PTEN and affecting the growth of HCC cells (Cao et al., 2019). MiR-21 can promote the proliferation and metastasis of HCC cells by inhibiting the PTEN expression (Meng et al., 2007), reversion inducing cysteine-rich protein with kazal motifs (RECK) and human sulphatase-1 (Sulf-1) (Bao et al., 2013) and can induce resistance at chemotherapeutic drugs in HCC cells (He et al., 2015). Thus, differentially expressed exosomal miR-21 is an important biomarker for both early detection of HCC and disease progression.

Data related to miR-92a expression in HCC is still controversial. Several authors emphasize that circulating miR-92a is significantly under-expressed in HCC and that the dysregulated pattern is related to cancer development and HCC progression (Ohyashiki et al., 2010; Wang et al., 2017). Expression level of exosome-derived miR-92a, significantly decreased in plasma of HCC patients in comparison to controls, has also been proposed as a potential diagnostic biomarker for HCC (Ohno et al., 2013; Qu et al., 2015). Our results are in concordance with this finding as we also found an under-expression

of miR-92a in plasma exosomes of HCC cases in our study group, in comparison to LC. On the other hand, *in vivo* studies have suggested that the downregulation of miR-92a suppresses the biological processes of tumor growth in HCC and that F-box and WD repeat domain-containing 7 (PBXW7) is a direct target of miR-92a, promoting tumor progression in this setting (Yang et al., 2015). These contradictory results could be explained by several technical aspects, such as miRNA purification/detection protocol, sample storage conditions, and different internal controls and also by the type of analyzed samples: serum or plasma. There is also data suggesting that dysregulation of miR-92a is, in fact, cancer type–specific (Ohno et al., 2013). Overexpression of miR-92a could induce various carcinogenesis processes in different tumors. It has been shown to promote ovarian cancer cell adhesion, proliferation, and invasion by suppressing integrin α5 expression, contrasting the effects observed in HCC (Ohyagi-Hara et al., 2013).

In our study, the diagnostic accuracy for HCC for exosomal relative expression of miR-21-5p, miR-92a-3p, and serum AFP were analyzed individually and combined. The statistical model integrating the two selected miRNAs and AFP could be proposed as a novel screening tool for HCC as it performed best for differentiating HCC from cirrhotic controls in comparison to the individual variables.

The addition of this miRNA panel to traditional serological tumor markers may improve the diagnostic accuracy for HCC detection and, in a translational setting, could be more easily and conveniently performed in comparison to other liquid biopsy techniques, isolating circulating tumor cells or circulating tumor DNA. Model validation in a larger cohort of plasma exosomal samples could improve diagnostic accuracy.

CONCLUSION

In summary, exosome trafficking proteins, miRNAs, and lncRNAs are important emerging diagnostic biomarkers for HCC. Our exosomal miR-HCC score, integrating exosomal miR-21-5p, miR-92a-3p expression, and serum AFP, could provide a novel diagnostic tool for HCC screening in clinical practice.

DATA AVAILABILITY STATEMENT

All datasets generated for this study are included in the article/**Supplementary Material**.

ETHICS STATEMENT

This study, involving human participants, was reviewed and approved by the Ethics Committee of Fundeni Clinical Institute. The patients provided their written informed consent to participate in the study.

AUTHOR CONTRIBUTIONS

AS, RI, AD, and SD contributed to the design of the study. AS, DC, MC-E, LC, and TF performed the experiments. AS, RI, SI, DC, and SD organized the study database. RI performed the statistical analysis and clinical results interpretation. AS and DC wrote the first draft of the manuscript. SD, RI, SI, MC-E, and LC wrote sections of the manuscript. IP, SD, NB, LS, LG, and AD supervised the studies and reviewed the manuscript. All authors contributed to manuscript revision, read and approved the submitted version.

FUNDING

This study was supported by funding from EEA Financial Mechanism 2009–2014 under the project contract number 4SEE/30.06.2014 and by a grant of the Romanian National Authority for Scientific Research and Innovation, CCCDI – UEFISCDI, project number PN-III-P3-3.1-PM-RO-CN-2018-0209, contract number 1 BM/2018.

SUPPLEMENTARY MATERIAL

The Supplementary Material for this article can be found online at: https://www.frontiersin.org/articles/10.3389/fgene.2020.00712/full#supplementary-material

REFERENCES

Ailawadi, S., Wang, X., Gu, H., and Fan, G. C. (2015). Pathologic function and therapeutic potential of exosomes in cardiovascular disease. *Biochim. Biophys. Acta* 1852, 1–11. doi: 10.1016/j.bbadis.2014.10.008

Akinyemiju, T., Abera, S., Ahmed, M., Alam, N., Alemayohu, M. A., Allen, C., et al. (2017). The burden of primary liver cancer and underlying etiologies from 1990 to 2015 at the global, regional, and national level: results from the global burden of disease study 2015. *JAMA Oncol.* 3, 1683–1691.

Bao, L., Yan, Y., Xu, C., Ji, W., Shen, S., Xu, G., et al. (2013). MicroRNA-21 suppresses PTEN, and hSulf-1 expression, and promotes hepatocellular carcinoma progression through AKT/ERK pathways. *Cancer Lett.* 337, 226–236. doi: 10.1016/j.canlet.2013.05.007

Berhane, S., Toyoda, H., Tada, T., Kumada, T., Kagebayashi, C., Satomura, S., et al. (2016). Role of the GALAD and BALAD-2 serologic models in diagnosis of hepatocellular carcinoma and prediction of survival in patients. *Clin. Gastroenterol. Hepatol.* 14, 875.e6–886.e6.

Best, J., Bechmann, L. P., Sowa, J. P., Sydor, S., Dechene, A., Pflanz, K., et al. (2019). GALAD score detects early hepatocellular carcinoma in an international cohort of patients with nonalcoholic steatohepatitis. *Clin. Gastroenterol. Hepatol.* 18, 728.e4–735.e4.

Cai, S., Cheng, X., Pan, X., and Li, J. (2017). Emerging role of exosomes in liver physiology and pathology. *Hepatol. Res.* 47, 194–203. doi: 10.1111/hepr.12794

Cao, L. Q., Yang, X. W., Chen, Y. B., Zhang, D. W., Jiang, X. F., and Xue, P. (2019). Exosomal miR-21 regulates the TETs/PTENp1/PTEN pathway to promote hepatocellular carcinoma growth. *Mol. Cancer* 18:148.

Cerban, R., Ester, C., Iacob, S., Paslaru, L., Dumitru, R., Grasu, M., et al. (2018). Evaluation of tumor response using alpha-fetoprotein and des-gamma-carboxy prothrombin in hepatocellular carcinoma patients who underwent transarterial chemoembolization. *Chirurgia* 113, 524–533.

Davoren, P. A., McNeill, R. E., Lowery, A. J., Kerin, M. J., and Miller, N. (2008). Identification of suitable endogenous control genes for microRNA gene expression analysis in human breast cancer. *BMC Mol. Biol.* 9:76. doi: 10.1186/1471-2199-9-76

El-Serag, H. B., and Davila, J. A. (2011). Surveillance for hepatocellular carcinoma: in whom and how? *Ther. Adv. Gastroenterol.* 4, 5–10. doi: 10.1177/1756283x10385964

Fornari, F., Ferracin, M., Trere, D., Milazzo, M., Marinelli, S., Galassi, M., et al. (2015). Circulating microRNAs, miR-939, miR-595, miR-519d, and miR-494, identify cirrhotic patients with HCC. *PLoS One* 10:e0141448. doi: 10.1371/journal.pone.0141448

Fu, L. L., Wen, X., Bao, J. K., and Liu, B. (2012). MicroRNA-modulated autophagic signaling networks in cancer. *Int. J. Biochem. Cell. Biol.* 44, 733–736. doi: 10.1016/j.biocel.2012.02.004

Galle, P. R., Forner, A., Llovet, J. M., Mazzaferro, V., Piscaglia, F., Raoul, J. L., et al. (2018). EASL clinical practice guidelines: management of hepatocellular carcinoma. *J. Hepatol.* 69, 182–236.

He, X., Li, J., Guo, W., Liu, W., Yu, J., Song, W., et al. (2015). Targeting the microRNA-21/AP1 axis by 5-fluorouracil, and pirarubicin in human hepatocellular carcinoma. *Oncotarget* 6, 2302–2314. doi: 10.18632/oncotarget.2955

Heimbach, J. K., Kulik, L. M., Finn, R. S., Sirlin, C. B., Abecassis, M. M., Roberts, L. R., et al. (2018). AASLD guidelines for the treatment of hepatocellular carcinoma. *Hepatology* 67, 358–380. doi: 10.1002/hep.29086

Ji, J., Chen, H., Liu, X. P., Wang, Y. H., Luo, C. L., Zhang, W. W., et al. (2018). A miRNA combination as promising biomarker for hepatocellular carcinoma diagnosis: a study based on bioinformatics analysis. *J. Cancer* 9, 3435–3446. doi: 10.7150/jca.26101

Johnson, P. J., Pirrie, S. J., Cox, T. F., Berhane, S., Teng, M., Palmer, D., et al. (2014). The detection of hepatocellular carcinoma using a prospectively developed and validated model based on serological biomarkers. *Cancer Epidemiol. Biomarkers Prev.* 23, 144–153. doi: 10.1158/1055-9965.epi-13-0870

Laurent-Puig, P., Legoix, P., Bluteau, O., Belghiti, J., Franco, D., Binot, F., et al. (2001). Genetic alterations associated with hepatocellular carcinomas define distinct pathways of hepatocarcinogenesis. *Gastroenterology* 120, 1763–1773. doi: 10.1053/gast.2001.24798

Li, Y., and Chen, J. (2019). Serum des-gamma-carboxy prothrombin for diagnosis of adult primary cancer in liver. *J. Coll. Phys. Surg. Pak.* 29, 972–976. doi: 10.29271/jcpsp.2019.10.972

Liao, Q., Han, P., Huang, Y., Wu, Z., Chen, Q., Li, S., et al. (2015). Potential role of circulating microRNA-21 for hepatocellular carcinoma diagnosis: a meta-analysis. *PLoS One* 10:e0130677. doi: 10.1371/journal.pone.0130677

Lim, T. S., Kim, D. Y., Han, K. H., Kim, H. S., Shin, S. H., Jung, K. S., et al. (2016). Combined use of AFP, PIVKA-II, and AFP-L3 as tumor markers enhances diagnostic accuracy for hepatocellular carcinoma in cirrhotic patients. *Scand. J. Gastroenterol.* 51, 344–353. doi: 10.3109/00365521.2015.1082190

Lotvall, J., Hill, A. F., Hochberg, F., Buzas, E. I., Di Vizio, D., Gardiner, C., et al. (2014). Minimal experimental requirements for definition of extracellular vesicles and their functions: a position statement from the International society for extracellular vesicles. *J. Extracell. Vesicles* 3:26913. doi: 10.3402/jev.v3.26913

Malm, T., Loppi, S., and Kanninen, K. M. (2016). Exosomes in Alzheimer's disease. *Neurochem. Int.* 97, 193–199.

Matsumura, T., Sugimachi, K., Iinuma, H., Takahashi, Y., Kurashige, J., Sawada, G., et al. (2015). Exosomal microRNA in serum is a novel biomarker of recurrence in human colorectal cancer. *Br. J. Cancer* 113, 275–281. doi: 10.1038/bjc.2015.201

Melo, S. A., Luecke, L. B., Kahlert, C., Fernandez, A. F., Gammon, S. T., Kaye, J., et al. (2015). Glypican-1 identifies cancer exosomes and detects early pancreatic cancer. *Nature* 523, 177–182. doi: 10.1038/nature14581

Meng, F., Henson, R., Wehbe-Janek, H., Ghoshal, K., Jacob, S. T., and Patel, T. (2007). MicroRNA-21 regulates expression of the PTEN tumor suppressor gene in human hepatocellular cancer. *Gastroenterology* 133, 647–658. doi: 10.1053/j.gastro.2007.05.022

Milane, L., Singh, A., Mattheolabakis, G., Suresh, M., and Amiji, M. M. (2015). Exosome mediated communication within the tumor microenvironment. *J. Control Release* 219, 278–294. doi: 10.1016/j.jconrel.2015.06.029

Mjelle, R., Dima, S. O., Bacalbasa, N., Chawla, K., Sorop, A., Cucu, D., et al. (2019). Comprehensive transcriptomic analyses of tissue, serum, and serum exosomes from hepatocellular carcinoma patients. *BMC Cancer* 19:1007. doi: 10.1186/s12885-019-6249-1

Moon, S., Shin, D. W., Kim, S., Lee, Y. S., Mankhong, S., Yang, S. W., et al. (2019). Enrichment of exosome-like extracellular vesicles from plasma suitable for clinical vesicular miRNA biomarker research. *J. Clin. Med.* 8:1995. doi: 10.3390/jcm8111995

Motawi, T. K., Shaker, O. G., El-Maraghy, S. A., and Senousy, M. A. (2015). Serum MicroRNAs as potential biomarkers for early diagnosis of hepatitis c virus-related hepatocellular carcinoma in egyptian patients. *PLoS One* 10:e0137706. doi: 10.1371/journal.pone.0137706

Ohno, S., Ishikawa, A., and Kuroda, M. (2013). Roles of exosomes, and microvesicles in disease pathogenesis. *Adv. Drug Deliv. Rev.* 65, 398–401. doi: 10.1016/j.addr.2012.07.019

Ohyagi-Hara, C., Sawada, K., Kamiura, S., Tomita, Y., Isobe, A., Hashimoto, K., et al. (2013). miR-92a inhibits peritoneal dissemination of ovarian cancer cells by inhibiting integrin alpha5 expression. *Am. J. Pathol.* 182, 1876–1889. doi: 10.1016/j.ajpath.2013.01.039

Ohyashiki, J. H., Umezu, T., Kobayashi, C., Hamamura, R. S., Tanaka, M., Kuroda, M., et al. (2010). Impact on cell to plasma ratio of miR-92a in patients with acute leukemia: in vivo assessment of cell to plasma ratio of miR-92a. *BMC Res. Notes* 3:347. doi: 10.1186/1756-0500-3-347

Pu, C., Huang, H., Wang, Z., Zou, W., Lv, Y., Zhou, Z., et al. (2018). Extracellular Vesicle-Associated mir-21, and mir-144 are markedly elevated in serum of patients with hepatocellular carcinoma. *Front. Physiol.* 9:930. doi: 10.3389/fphys.2018.00930

Qu, Z., Jiang, C., Wu, J., and Ding, Y. (2015). Exosomes as potent regulators of HCC malignancy and potential bio-tools in clinical application. *Int. J. Clin. Exp. Med.* 8, 17088–17095.

Rider, M. A., Hurwitz, S. N., and Meckes, D. G. Jr. (2016). ExtraPEG: a polyethylene glycol-based method for enrichment of extracellular vesicles. *Sci. Rep.* 6:23978.

Simons, M., and Raposo, G. (2009). Exosomes–vesicular carriers for intercellular communication. *Curr. Opin. Cell Biol.* 21, 575–581. doi: 10.1016/j.ceb.2009.03.007

Tang, Y. T., Huang, Y. Y., Zheng, L., Qin, S. H., Xu, X. P., An, T. X., et al. (2017). Comparison of isolation methods of exosomes and exosomal RNA from cell culture medium and serum. *Int. J. Mol. Med.* 40, 834–844. doi: 10.3892/ijmm.2017.3080

Thery, C., Amigorena, S., Raposo, G., and Clayton, A. (2006). Isolation and characterization of exosomes from cell culture supernatants and biological fluids. *Curr. Protoc. Cell Biol.* 3:22.

Tian, M. M., Fan, Y. C., Zhao, J., Gao, S., Zhao, Z. H., Chen, L. Y., et al. (2017). Hepatocellular carcinoma suppressor 1 promoter hypermethylation in serum. A diagnostic and prognostic study in hepatitis B. *Clin. Res. Hepatol. Gastroenterol.* 41, 171–180. doi: 10.1016/j.clinre.2016.10.003

Tomimaru, Y., Eguchi, H., Nagano, H., Wada, H., Kobayashi, S., Marubashi, S., et al. (2012). Circulating microRNA-21 as a novel biomarker for hepatocellular carcinoma. *J. Hepatol.* 56, 167–175. doi: 10.1016/j.jhep.2011.04.026

Tzartzeva, K., Obi, J., Rich, N. E., Parikh, N. D., Marrero, J. A., Yopp, A., et al. (2018). Surveillance imaging and alpha fetoprotein for early detection of hepatocellular carcinoma in patients with cirrhosis: a meta-analysis. *Gastroenterology* 154, 1706.e1–1718.e1.

Wang, H., Hou, L., Li, A., Duan, Y., Gao, H., and Song, X. (2014). Expression of serum exosomal microRNA-21 in human hepatocellular carcinoma. *Biomed. Res. Int.* 2014:864894.

Wang, S., Wang, J. Q., and Lv, X. W. (2017). Exosomal miRNAs as biomarkers in the diagnosis of liver disease. *Biomark. Med.* 11, 491–501. doi: 10.2217/bmm-2017-0011

Wang, Y., Zhang, C., Zhang, P., Guo, G., Jiang, T., Zhao, X., et al. (2018). Serum exosomal microRNAs combined with alpha-fetoprotein as diagnostic markers of hepatocellular carcinoma. *Cancer Med.* 7, 1670–1679. doi: 10.1002/cam4.1390

Xu, Y., Xia, F., Ma, L., Shan, J., Shen, J., Yang, Z., et al. (2011). MicroRNA-122 sensitizes HCC cancer cells to adriamycin and vincristine through modulating expression of MDR and inducing cell cycle arrest. *Cancer Lett.* 310, 160–169.

Yanez-Mo, M., Siljander, P. R., Andreu, Z., Zavec, A. B., Borras, F. E., Buzas, E. I., et al. (2015). Biological properties of extracellular vesicles and their physiological functions. *J. Extracell. Vesicles* 4:27066.

Yang, W., Dou, C., Wang, Y., Jia, Y., Li, C., Zheng, X., et al. (2015). MicroRNA-92a contributes to tumor growth of human hepatocellular carcinoma by targeting FBXW7. *Oncol. Rep.* 34, 2576–2584. doi: 10.3892/or.2015.4210

Ye, Q., Ling, S., Zheng, S., and Xu, X. (2019). Liquid biopsy in hepatocellular carcinoma: circulating tumor cells and circulating tumor DNA. *Mol. Cancer* 18:114.

Zhang, Y., Li, T., Qiu, Y., Zhang, T., Guo, P., Ma, X., et al. (2017). Serum microRNA panel for early diagnosis of the onset of hepatocellular carcinoma. *Medicine* 96:e5642. doi: 10.1097/md.0000000000005642

Zhou, Y., Ren, H., Dai, B., Li, J., Shang, L., Huang, J., et al. (2018). Hepatocellular carcinoma-derived exosomal miRNA-21 contributes to tumor progression by converting hepatocyte stellate cells to cancer-associated fibroblasts. *J. Exp. Clin. Cancer Res.* 37:324.

Zhu, H. T., Liu, R. B., Liang, Y. Y., Hasan, A. M. E., Wang, H. Y., Shao, Q., et al. (2017). Serum microRNA profiles as diagnostic biomarkers for HBV-positive hepatocellular carcinoma. *Liver Int.* 37, 888–896. doi: 10.1111/liv.13356

Conflict of Interest: The authors declare that the research was conducted in the absence of any commercial or financial relationships that could be construed as a potential conflict of interest.

Advantages of publishing in Frontiers

OPEN ACCESS
Articles are free to read for greatest visibility and readership

FAST PUBLICATION
Around 90 days from submission to decision

HIGH QUALITY PEER-REVIEW
Rigorous, collaborative, and constructive peer-review

TRANSPARENT PEER-REVIEW
Editors and reviewers acknowledged by name on published articles

Frontiers
Avenue du Tribunal-Fédéral 34
1005 Lausanne | Switzerland

Visit us: www.frontiersin.org
Contact us: info@frontiersin.org | +41 21 510 17 00

REPRODUCIBILITY OF RESEARCH
Support open data and methods to enhance research reproducibility

DIGITAL PUBLISHING
Articles designed for optimal readership across devices

FOLLOW US
@frontiersin

IMPACT METRICS
Advanced article metrics track visibility across digital media

EXTENSIVE PROMOTION
Marketing and promotion of impactful research

LOOP RESEARCH NETWORK
Our network increases your article's readership